Department of Energy Responses to the Nuclear Regulatory Commission Request for Additional Information on the Draft Waste Incidental to Reprocessing Evaluation for Vitrification of Low Activity Waste

Prepared for the U.S. Department of Energy
Assistant Secretary for Environmental Management

Office of River Protection

P.O. Box 450
Richland, Washington 99352

Department of Energy Responses to the Nuclear Regulatory Commission Request for Additional Information on the Draft Waste Incidental to Reprocessing Evaluation for Vitrification of Low Activity Waste

D. B. Darling
Washington River Protection Solutions

D. J. Swanberg
Washington River Protection Solutions

K. P. Lee
ORANO

L. H. Cree
Washington River Protection Solutions

Date Published
July 2021

Prepared for the U.S. Department of Energy
Assistant Secretary for Environmental Management

Office of River Protection

**P.O. Box 450
Richland, Washington 99352**

APPROVED
By Janis Aardal at 6:39 am, Aug 17, 2021

_____   _____
Release Approval   Date

TRADEMARK DISCLAIMER

Department of Energy Responses to the Nuclear Regulatory Commission Request for Additional Information on the Draft Waste Incidental to Reprocessing Evaluation for Vitrification of Low Activity Waste (Revision 1, Consolidated Response)

July 2021

This page intentionally left blank.

TABLE OF CONTENTS

TABLE OF ATTACHMENTS

TABLE OF FIGURES

TABLE OF TABLES

LIST OF TERMS

Acronyms and Abbreviations

2-D	two dimensional
3-D	three-dimensional
ADT	Advective-Diffusive Transport
asl	above sea level
BBI	Best-Basis Inventory
CA	composite analysis
CAB	carbon adsorber bed
CCU	Cold Creek Unit
CCUg	CCU gravel unit
CDF	Cumulative Distribution Function
CERCLA	*Comprehensive Environmental Response, Compensation, and Liability Act of 1980*
CFR	*Code of Federal Regulations*
CHEM	Chemical
CHPRC	CH2M HILL Plateau Remediation Company
COPC	constituent of potential concern
CPGWM	Central Plateau Groundwater Model
CPM	Central Plateau Model/Central Plateau Groundwater flow model
CPVZ	Central Plateau Vadose Zone
Cs	cesium
CST	crystalline silicotitanate
CY	calendar year
DFLAW	Direct-Feed Low-Activity Waste
DIW	de-ionized water
DOE	U.S. Department of Energy
DOE M	DOE Manual
DOE O	DOE Order
DWS	drinking water standard
ECF	environmental calculation file
ECKEChem	Equilibrium-Conservation-Kinetic Equation Chemistry
Ecology	Washington State Department of Ecology
EIS	Environmental Impact Statement
EMF	Effluent Management Facility

EPA	U.S. Environmental Protection Agency
ERDF	Environmental Restoration Disposal Facility
ETF	Effluent Treatment Facility
EWG	enhanced waste glass
FFTF	Fast Flux Test Facility
FLTF	Field Lysimeter Test Facility
FRR	fractional release rate
FY	fiscal year
GAC	granular activated carbon
GFM	geologic framework model
GWB	The Geochemists Workbench®
H2	Hanford formation sand unit
H3/Hf3	Hanford formation gravel unit
HCZ	high conductivity zone
HDW	Hanford Defined Waste model
HEIS	Hanford Environmental Information System
HEPA	high-efficiency particulate air
HLW	high-level radioactive waste
HMS	Hanford Meteorological Station
HSU	hydrostratigraphic unit
HTWOS	Hanford Tank Waste Operations Simulator
I	iodine
IDF	Integrated Disposal Facility
IDF PA	RPP-RPT-59958, *Performance Assessment for the Integrated Disposal Facility, Hanford Site, Washington*
ILAW	immobilized low-activity waste (synonymous with VLAW)
IX	ion exchange
LAW	low-activity waste or Low-Activity Waste Vitrification Facility
LDR	Land Disposal Restrictions
LERF	Liquid Effluent Retention Facility
LFRG	Low-Level Waste Disposal Facility Federal Review Group
LLBG	low-level burial ground
LLNL	Lawrence Livermore National Laboratory
LLW	low-level radioactive waste
LSW	liquid secondary waste
MCC	moisture characteristic curve

MCL	maximum contaminant level
MDA	moisture-dependent anisotropy
MPR	model package report
NRC	U.S. Nuclear Regulatory Commission
ORP	DOE Office of River Protection
OU	operable unit
P2R	Plateau to River Groundwater Model
PA	Performance Assessment
PA-TCT	power averaged tensorial-connectivity-tortuosity
PCT	product consistency test
PNNL	Pacific Northwest National Laboratory
PT	Pretreatment
R&D	research and development
RAI	request for additional information
RCRA	*Resource Conservation and Recovery Act of 1976*
RL	DOE Richland Operations Office
RLD	Radioactive Liquid Waste Disposal
Rtf	Ringold Taylor Flats unit
Rwie	Ringold Unit E
RWMB	Radioactive Waste Management Basis
SBS	submerged bed scrubber
SCR	selective catalytic reducer
SMRN	secondary mineral reaction network
SPFT	single-pass flow-through
SRCA	Stirred Reactor Coupon Analysis
Sr	strontium
SSW	solid secondary waste
STLP	Supplemental Treated LAW Evaporation Process
STOMP	Subsurface Transport Over Multiple Phases
TBR	WHC-SD-WM-TI-699, *Technical Basis for Classification of Low-Activity Waste Fraction from Hanford Site Tanks*
Tc	technetium
TC&WM EIS	Tank Closure and Waste Management Environmental Impact Statement
TED	total effective dose
TLP	Treated LAW Evaporation Process
TSCR	Tank-Side Cesium Removal

TST	transition-state theory
UDQE	unreviewed disposal question evaluation
U.S.	United States
VLAW	vitrified low-activity waste (synonymous with ILAW)
VSL	Vitreous State Laboratory
WAC	Waste Acceptance Criteria
WESP	wet electrostatic precipitator
WIR	Waste Incidental to Reprocessing
WMA	Waste Management Area
WTP	Hanford Tank Waste Treatment and Immobilization Plant; Waste Treatment Plant
VZPW	vadose zone pore water

Units

µg	microgram
Ci	curie
cm	centimeter
ft	foot
ft2	square foot
ft3	cubic foot
g	gram
gal	gallon
in	inch
kg	kilogram
km	kilometer
L	liter
m	meter
m3	cubic meter
mrem	millirem
nCi	nanocurie
pCi	picocurie
psi	pounds per square inch
psig	pounds per square inch gauge pressure
yr	year

1.0   INTRODUCTION

In accordance with DOE Order (O) 435.1, *Radioactive Waste Management* and its accompanying manual, DOE M 435.1-1, *Radioactive Waste Management Manual*, the U.S. Department of Energy (DOE) manages radioactive waste in a manner that protects the public, workers and the environment, and that complies with applicable federal, state and local laws. Certain waste resulting from reprocessing of spent nuclear fuel that is incidental to reprocessing is not high-level radioactive waste (HLW) and is managed in accordance with the requirements for low-level radioactive waste (LLW). In April 2020, DOE issued the *Draft Waste Incidental to Reprocessing Evaluation for Vitrified Low-Activity Waste Disposed Onsite at the Hanford Site, Washington* (herein referred to as the Draft WIR Evaluation) (DOE/ORP-2020-01).

By means of an interagency agreement between DOE and the U.S. Nuclear Regulatory Commission (NRC), NRC is conducting a consultative technical review of DOE's Draft WIR Evaluation. Prior to preparation of the Draft WIR Evaluation, DOE prepared the *Performance Assessment for the Integrated Disposal Facility, Hanford Site, Washington* (herein referred to as the IDF PA) (RPP-RPT-59958), which is a technical reference document for the Draft WIR Evaluation. The IDF PA has undergone independent review by DOE's Low Level Waste Disposal Facility Review Group (LFRG). DOE also engaged in extensive discussions and scoping meetings, including discussions with states and Tribal Nations, regarding the fundamental technical bases, approaches, and key parameter values to be used in developing the IDF PA. The IDF PA was issued in 2019, and the Draft WIR Evaluation was subsequently issued for NRC consultation and comments by states, Tribal Nations, and the public in April 2020.

DOE and NRC staff have engaged in a series of public meetings to clarify the approaches and rationales documented in the Draft WIR Evaluation and IDF PA. DOE, NRC and Washington River Protection Solutions, LLC, participated in public meetings that were held on September 28 and October 6, 2020 to review and get clarifications on the NRC List of Topics that was provided regarding potential questions on the Draft WIR Evaluation. On November 6, 2020, NRC staff submitted requests for additional information (RAIs) (External letter "Request for Additional Information on the Draft Waste Incidental to Reprocessing Evaluation for Vitrified Low-Activity Waste Disposed Onsite at the Hanford Site, Washington" [NRC 2020]).

This Revision 1, Consolidated Response document provides DOE's responses to all of the NRC RAIs, to facilitate NRC's completion of a Technical Evaluation Report (TER) on the Draft WIR Evaluation.[1]   For each of the 26 RAIs, the NRC comment, basis information, and proposed path forward is quoted directly as received from NRC (with minor typographical corrections and the addition of 508 compliant graphics explanations). These are followed by DOE's technical response to the RAIs. The topics discussed herein are technical in nature. The RAIs and responses are part of the ongoing interaction between DOE and NRC staff regarding the review

---

[1]By letter dated June 21, 2021, DOE provided responses to 20 of the RAIs. This Revision 1, Consolidated Response includes DOE's prior responses (without change) to those 20 RAIs and also includes DOE's responses to the remaining six RAIs (RAI 2-2, RAI 2-4, RAI 2-6, RAI 2-8, RAI 2-12, and RAI 2-13).

of the Draft WIR Evaluation and its references, including the IDF PA, and can only be understood in that context; a working knowledge of those documents is assumed.

The RAIs were organized by NRC according to the three criteria contained in DOE Manual (M) 435.1-1, Section II.B(2)(a). Those criteria provide, in relevant part, that the wastes:

"(1) Have been processed, or will be processed, to remove key radionuclides to the maximum extent that is technically and economically practical; and

(2) Will be managed to meet safety requirements comparable to the performance objectives set out in 10 CFR 61 Subpart C, *Performance Objectives*; and

(3) Are to be managed, pursuant to DOE's authority under the *Atomic Energy Act of 1954*, as amended, and in accordance with the provisions of Chapter IV of this Manual *[DOE M 435.1-1]*, provided the waste will be incorporated in a solid physical form at a concentration that does not exceed the applicable concentration limits for Class C low-level waste as set out in 10 CFR 61.55, *Waste Classification[.]*"

The RAIs responses are organized according to applicable categories based upon these criteria, as presented in Sections 3.0, 4.0, and 5.0 below.

2.0   NRC'S INTRODUCTORY STATEMENT IN THE REQUEST FOR ADDITIONAL INFORMATION RELATED TO SECONDARY WASTE

NRC's Introductory Statement in the Request for Additional Information Related to Secondary Waste

NRC stated in the last paragraph on page 1 and continuing onto page 2 of the Request for Additional Information (RAI), under "Structure of Comments": "DOE indicated that the scope for the VLAW draft waste incidental to reprocessing (WIR) evaluation was limited to vitrified waste generated as part of the Direct Feed Low Activity Waste (DFLAW) process (DOE-ORP-2020-01, 2020). Secondary solid wastes (SSW) generated by the process were not within the scope of the draft waste evaluation though those secondary wastes were evaluated in the PA as they would be disposed in the same facility as the VLAW. NRC evaluated the scope of the evaluation in the acceptance review and determined that the DOE approach was not consistent with the intent of the incidental waste process. DOE's election of vitrification as the primary waste production process results in some key radionuclides that are volatized and effectively separated from the waste (e.g., ^{129}I), or are removed in other processing steps. If the majority of that activity that is separated or removed will be disposed in near-surface disposal (i.e., as other than high-level waste), then the resulting waste forms and waste streams are within the scope of the draft waste evaluation, especially for DOE M 435.1-1 Criterion 2 as the key radionuclides drive the long-term risk for the disposal. As a result, NRC has included secondary SSW within the scope of the review."

DOE Response to NRC's Introductory Statement Related to Secondary Waste

Because several of the NRC's RAIs involve secondary waste, DOE is providing the following comments and observations here as a matter of convenience, to avoid repeating the same information in the applicable RAI responses. As NRC notes, the scope of the *Draft Waste Incidental to Reprocessing Evaluation for Vitrified Low-Activity Waste Disposed Onsite at the Hanford Site* (Draft WIR Evaluation) focuses on the separated, pretreated and vitrified low activity waste (VLAW). DOE has not included other wastes, including solid secondary waste (SSW), within the scope of the Draft WIR Evaluation.

As background, the Hanford Site currently stores radioactive waste in underground storage tanks. The waste was generated, in part, by the prior reprocessing of spent nuclear fuel. DOE is retrieving waste from the Hanford tanks, and has decided to separate the tank waste into a low-activity waste stream and a high-level radioactive waste stream.[2]

The Draft WIR Evaluation concerns the low-activity waste from some of the Hanford tanks. For the low-activity waste at issue in the Draft WIR Evaluation, DOE has decided to use the direct-feed low-activity waste (DFLAW) pretreatment approach.[3] The DFLAW pretreatment approach is a two-phased approach (Phase 1 and Phase 2, described below) that will separate and pretreat

[2] See "Record of Decision: Final Tank Closure and Waste Management Environmental Impact Statement for the Hanford Site, Richland, Washington", 78 FR 75913 (Dec. 31, 2013).
[3] See "Amended Record of Decision for the Direct-Feed Low-Activity Waste Approach at the Hanford Site, Washington", 84 FR 424 (Jan. 28, 2019).

supernate (essentially the upper-most layer of tank waste that contains low concentrations of long-lived radionuclides) from the applicable tanks.

The DFLAW pretreatment approach will entail in-tank settling, decanting, filtration, and cesium ion exchange removal, using the Tank Side Cesium Removal (TSCR) System for Phase 1 and either a second TSCR unit or a filtration and cesium removal facility for Phase 2. As explained in the Draft WIR Evaluation, the DFLAW pretreatment process will remove over 99% of the cesium, as well as other key radionuclides. After pretreatment using the DFLAW approach, the resulting, pretreated waste stream – called Low Activity Waste or LAW-- will be vitrified in the Low Activity Waste Vitrification Facility.[4] LAW from which key radionuclides have been removed to the maximum extent technically and economically practical during the pretreatment process, will be managed and disposed of as LLW, subject to the analysis and commitments of the Final WIR Evaluation and WIR Determination. The vitrified LAW (also called VLAW) will meet the performance objectives and measures for LLW disposal, as demonstrated in the Draft WIR Evaluation,[5] and be disposed of in the Integrated Disposal Facility (IDF).

During vitrification of the LAW, some radionuclides, including ^{99}Tc and ^{129}I, will volatize. The LAW Vitrification Facility will, by design, maximize the capture of the volatized ^{99}Tc and ^{129}I into the VLAW. Since the completion of the *Performance Assessment for the Integrated Disposal Facility, Hanford Site, Washington* (IDF PA), the latest flowsheet modeling shows that approximately 98% of the ^{99}Tc and approximately 96% of the ^{129}I will be captured into the VLAW, and approximately 99% of all radioactivity in the pretreated LAW will be incorporated into the VLAW.[6] In sum, the vast majority of all radionuclides in the LAW, including ^{99}Tc and ^{129}I, will be captured in the VLAW and will not be entrained in secondary waste.

The SSW and other secondary solid waste[7] – including HEPA filters, carbon bed adsorbers, a submerged bed scrubber, a wet electrostatic precipitator, and certain solidified evaporator waste -

---

[4] The LAW will meet the waste acceptance criteria for the Low Activity Waste Vitrification Facility, which has been designed to meet the applicable requirements in DOE regulations, Orders and standards.

[5] In addition, the VLAW will be in a solid physical form that does not exceed Class C LLW concentrations, as shown in Section 6 of the Draft WIR Evaluation.

[6] The latest flowsheet modeling discussed above, RPP-RPT-57991, 2019, *One System River Protection Project Integrated Flowsheet*, Revision 3, Washington River Protection Solutions, LLC, Richland, Washington and MR-50461 - 00, *2019 Flowsheet Integration Joint Scenarios*, were prepared after the IDF PA and will be appropriately considered as part of maintenance of the IDF PA. ^{3}H and ^{14}C are volatile radionuclides which will not be captured in the VLAW and are considered in the IDF PA to the extent those radionuclides are entrained in secondary waste. It bears emphasizing that after pretreatment using the DFLAW approach, the pretreated LAW stream will contain approximately 1% of the radioactivity from the applicable tank waste, and the VLAW will capture approximately 99% of all radioactivity in the pretreated LAW. See e.g., responses to RAIs 1-2, 2-1, 2-10 and 2-17.
  The response to RAI 2-17 compares the revised VLAW inventory (based on the latest flowsheet modeling) to the disposal concentration limits developed to protect an inadvertent intruder (IDF-00002, *Waste Acceptance Criteria for the Integrated Disposal Facility,* Table G-1). The evaluation demonstrates that the updated VLAW inventory will meet DOE's performance measures for inadvertent intrusion into the VLAW.

[7] SSW, which is discussed in the Draft WIR Evaluation for additional background information, is radioactive solid waste derived from Waste Treatment Plant (WTP) operations and will include a wide variety of wastes from routine maintenance activities, non-routine maintenance activities, and day-to-day operating activities. The SSW includes carbon bed adsorbers and HEPA filters generated by the off gas system at the LAW Vitrification Facility, as well as Effluent Treatment Facility-Generated (ETF- Generated) SSW. For additional information, and as

- will be generated by, or derived from, the off gas system associated with the vitrification of the pretreated LAW. Importantly, after pretreatment using the DFLAW approach, the pretreated LAW stream will contain approximately 1% of the radioactivity from the applicable tank waste, and the VLAW will capture approximately 99% of all radioactivity in the pretreated LAW.[8] Otherwise put, the relevant secondary wastes, in combination, will contain approximately 1% of 1% (.0001) of the radioactivity initially in the reprocessing waste from the applicable tanks.

If DOE issues a Final WIR Evaluation and WIR Determination in the future, then the pretreated LAW—from which key radionuclides will have been removed to the maximum extent technically and economically practical – may be appropriately managed and disposed of as LLW, subject to the analysis and commitments of the Final WIR Evaluation and WIR Determination. Secondary waste generated from processes associated with further treatment, stabilization, solidification, storage, transport or disposal of this pretreated LAW must necessarily continue to be managed and disposed of as LLW and cannot be considered HLW.[9] This secondary waste can be disposed of in the IDF, if it is properly characterized and meets the waste acceptance criteria (WAC)[10] for the IDF, including radionuclide concentration limits to ensure protection of a hypothetical inadvertent intruder.[11]

DOE notes that the IDF PA correctly includes SSW because SSW is planned to be disposed of at IDF. This does not mean, however, that the SSW should be included within the scope of the Draft WIR Evaluation.

Several of NRC's RAIs pertain to secondary waste. DOE has responded to such RAIs to provide additional information and clarification.

---

described in sections 2.5.1.4 and 2.5.3 and in footnotes 33 and 40 of the Draft WIR Evaluation, the liquid off-gas system condensate generated by the LAW Vitrification Facility will be sent to the Effluent Management Facility, where evaporator liquid concentrate will be recycled to the LAW stream for vitrification and the evaporator overheads will be sent to ETF, which in turn will generate treated and solidified ETF liquid secondary waste (ETF-LSW). For convenience here, the above-mentioned wastes are collectively referred to as secondary waste, except as otherwise noted. The secondary waste will be properly characterized and classified prior to disposal, and must meet the waste acceptance criteria for the disposal facility (currently planned as the IDF).

[8] See e.g., responses to RAIs 1-2, 2-1, 2-10 and 2-17.

[9] DOE has previously determined that such secondary waste is not HLW. The citation WIR determinations for Hanford, DOE-ORP-PPD-EM-50168 Waste Incidental to Reprocessing Determinations, Revision 2 (Dec. 9, 2020), encompassed secondary waste, and explains that such waste is not from the reprocessing of spent nuclear fuel. Alternatively, a citation WIR could be based on the factual situation that the relevant secondary wastes, in combination, will contain approximately 1% of 1% (.0001) of the radioactivity initially in the reprocessing waste from the applicable tanks as explained above, and thus such waste is akin to "contaminated job wastes including laboratory items such as clothing, tools, and equipment" described in Chapter II.B.(1) of DOE Manual 435.1-1 concerning citation WIR determinations. Under either approach, the result is the same: the secondary waste is not HLW.

[10] IDF-00002, 2019, *Waste Acceptance Criteria for the Integrated Disposal Facility*, Rev. 0, CH2M HILL Plateau Remediation Company, Richland, Washington.

[11] As demonstrated in the IDF PA base case, potential doses attributable to secondary waste will be well-below the performance objectives and performance measures for LLW disposal. See also the response to RAI 2-17.

3.0   REMOVAL OF KEY RADIONUCLIDES TO THE MAXIMUM EXTENT PRACTICAL

RAI 1-1   (Removal of ^{90}Sr to the Maximum Extent Practicable)

Comment

Additional information is needed on the amount of soluble ^{90}Sr expected to be in the waste processed for Direct-Feed Low-Activity Waste (DFLAW) and the technologies that may be used to remove it to the maximum extent practical.

Basis

In the draft WIR evaluation, DOE states that most of the ^{90}Sr is insoluble but strontium can be soluble in some tanks with higher organic concentrations. Tanks with soluble ^{90}Sr are not currently planned to be part of the DFLAW campaigns and therefore are not discussed in the draft WIR evaluation. DOE indicated there would likely be a separate WIR evaluation for the tanks beyond DFLAW. However, in the draft WIR evaluation, DOE stated that the Integrated Disposal Facility (IDF) PA includes VLAW from tanks with soluble ^{90}Sr (see footnote 51). The NRC is reviewing the total risk from the disposal of waste in the IDF, including the potential for soluble ^{90}Sr to be part of the inventory for IDF, as within the scope of this evaluation, and therefore is requesting additional information on what amount of soluble ^{90}Sr is expected in the tanks and the technologies that may be used to remove soluble ^{90}Sr to the maximum extent practical.

Table 3-29 of the PA document[12] shows that nearly 100% of the ^{90}Sr is assumed to remain in the high-level waste (HLW) (i.e., not listed as waste going to IDF) under Case 7, 8B, 9, 10A, and 10B. It is unclear if any of these cases include the processing of the tanks with the soluble ^{90}Sr waste.

Waste Form	Case 7	Case 8B	Case 9	Case 10A	Case 10B
Non-IDF (HLW)	99.46%	99.61%	99.71%	99.54%	99.63%
ILAW Glass	0.54%	0.39%	0.29%	0.45%	0.36%
LAW Melters	0.00%	0.00%	0.00%	0.00%	0.00%
ETF-Generated Secondary Solid Waste	0.00%	0.00%	0.00%	0.00%	0.00%
Secondary Solid Waste	0.00%	0.00%	0.00%	0.00%	0.00%
IDF Total	**0.54%**	**0.39%**	**0.29%**	**0.46%**	**0.37%**

Path Forward

Please provide additional information on what percentage of the ^{90}Sr is estimated to be soluble versus insoluble in the tanks. Please provide additional basis for what percentage of the soluble ^{90}Sr DOE estimates can be extracted using the ion exchange columns, or other technologies planned to be used.

---

[12] The PA document is RPP-RPT-59958 Rev. 1A, *Performance Assessment for the Integrated Disposal Facility, Hanford Site, Washington*, Department of Energy, Richland, WA, July 2019. The PA consists of computer files (models) as well as a supporting document.

DOE Response

In the total inventory of tank waste stored in the Hanford Tank Farms single-shell and double-shell tanks, it is estimated that 4% of the ^{90}Sr is soluble (demonstrated in "Calculation" below). Under the DFLAW approach, nearly all of the ^{90}Sr that is not soluble is expected to be removed from the tank waste via the settle and decant process combined with the filter within the Tank Side Cesium Removal (TSCR) unit for Phase 1, and either a second TSCR unit or a filtration and cesium removal facility for Phase 2. With respect to soluble ^{90}Sr, process modeling in support of the IDF PA and the VLAW WIR, (described in RPP-ENV-58562, *Inventory Data Package for the Integrated Disposal Facility Performance Assessment* and RPP-RPT-57991, *River Protection Project Integrated Flowsheet*, respectively) conservatively assumed that all soluble ^{90}Sr present in staged DFLAW campaigns (19% of the total tank farms soluble ^{90}Sr, or less than 1% of the total tank farms inventory of ^{90}Sr) would remain in the DFLAW feed. However, there is recent laboratory data showing that almost all of the soluble ^{90}Sr will be removed by the crystalline silicotitanate (CST) within the TSCR unit (PNNL-28945, *Characterization of Cs-Loaded CST Used for Treatment of Hanford Tank Waste in Support of Tank-Side Cesium Removal*). Nevertheless, to bound the analysis, DOE assumed no ^{90}Sr is removed by CST ion exchange.

DOE intends to characterize the amount of ^{90}Sr in the low-activity waste (LAW) feed/VLAW after startup by sampling and analyzing every batch received in the LAW Vitrification Facility concentrate receipt vessels (24590-LAW-PL-PENG-17-0001, *ILAW Product Compliance Plan*) and tracking it through the vitrification process. Characterization of strontium in the LAW feed will be used to reduce the conservatism in the assumption that CST does not remove ^{90}Sr.

Furthermore, each waste package destined for the IDF will have a certified waste profile that is prepared by the waste generator. The radionuclide concentrations in the shipment cannot exceed the concentrations in the certified waste profile. The IDF waste acceptance team will review the certified waste profile to ensure each profile meets the requirements in the IDF Waste Acceptance Criteria (WAC) (IDF-00002, *Waste Acceptance Criteria for the Integrated Disposal Facility*). Annually, the IDF will prepare a report that summarizes waste receipts from the past fiscal year together with all past receipts (DOE M 435.1-1). The intent is to compare actual waste receipt volumes and inventories to the volume and activity levels evaluated in the IDF PA to ensure the continued adequacy of the PA and also provide an indication for the remaining capacity (volume and/or activity) of the IDF.

DOE plans to track the radionuclides, including strontium, in the VLAW, as well as other wastes, disposed of at the IDF to provide information for future closure of the IDF, including updated PA analyses. Prior to IDF closure, a revision to the IDF PA, using data provided by the LAW Vitrification Facility and other waste generators, will evaluate whether there is reasonable expectation that the performance objectives and performance measures are met for protection of the member of the public and inadvertent intruder from dose consequences from ^{90}Sr and other radionuclides in the VLAW, as well as all other waste streams, disposed of in the IDF.

Calculation

The amount of soluble strontium, and insoluble strontium present in the Hanford tank waste was estimated using data directly from RPP-RPT-57991. Due to the assumptions used in the flowsheet, explained in the response to RAI 1-1, all soluble strontium present in the Hanford Tank Farms is assumed to be routed as feed to the LAW Vitrification Facility[13] and assumed supplemental LAW[14] treatment facilities, and all insoluble strontium is routed as feed to the HLW Vitrification Facility during the full-scale mission. Thus, the concentration information for ^{90}Sr, combined with the stream volume for the representative streams from Table 6-7 of RPP-RPT-57991, can be used to calculate the percentage of soluble ^{90}Sr in the tank waste, as demonstrated below:

$$Total\ soluble\ ^{90}Sr\ inventory\ (Ci)$$
$$= \left[C_{28}^{^{90}Sr}\left(\frac{Ci}{L}\right) * V_{28}(gal) + C_{41}^{^{90}Sr}\left(\frac{Ci}{L}\right) * V_{41}(gal) + C_{45}^{^{90}Sr}\left(\frac{Ci}{L}\right) * V_{45}(gal) \right.$$
$$\left. + C_{46}^{^{90}Sr}\left(\frac{Ci}{L}\right) * V_{46}(gal) \right] * 3.785\left(\frac{L}{gal}\right) = 8.2E+05\ Ci$$

$$Total\ insoluble\ ^{90}Sr\ inventory\ (Ci) = \left[C_{35}^{^{90}Sr}\left(\frac{Ci}{L}\right) * V_{35}(gal) \right] * 3.785\left(\frac{L}{gal}\right)$$
$$= 1.9E+07\ Ci$$

$$\%\ soluble\ ^{90}Sr = \frac{Total\ soluble\ ^{90}Sr\ inventory}{\left(Total\ soluble\ ^{90}Sr\ inventory + Total\ insoluble\ ^{90}Sr\ inventory\right)}$$
$$= 4\%$$

where,

$$C_X^{^{90}Sr} = concentration\ of\ ^{90}Sr\ in\ stream\ X, Ci/L$$

$$V_X = total\ volume\ of\ stream\ X, gal$$

X = Stream number from Table 6-7 of RPP-RPT-57991

---

[13] Vitrification at the Hanford Tank Waste Treatment and Immobilization Plant (WTP) LAW Vitrification Facility includes DFLAW operations as well as vitrification in the WTP LAW Vitrification Facility following pre-treatment at the WTP Pre-Treatment Facility after the DFLAW mission is completed. Vitrification in the WTP LAW Vitrification Facility following the DFLAW mission is provided for additional information and completeness, and is outside the scope of the Draft WIR Evaluation.

[14] Information concerning supplemental LAW is provided in this RAI response for additional information and completeness, and is outside the scope of both the Draft WIR Evaluation and DOE decisions concerning supplemental LAW treatment. DOE has not made decisions concerning the potential path forward for supplemental LAW treatment, as explained in footnote 7 of the Draft WIR Evaluation and 78 FR 75913, "Record of Decision: Final Tank Closure and Waste Management Environmental Impact Statement for the Hanford Site, Richland, Washington." As explained in section 1.2 of the Draft WIR Evaluation, the Draft WIR Evaluation does not address or include in its scope supplemental LAW. To bound the IDF PA analysis, the IDF PA assumed that supplemental LAW may potentially be vitrified and disposed of in the IDF, although, as explained above, DOE has made no decisions concerning the potential path forward for supplemental LAW treatment.

Table 1-1-1. Values from Table 6-7 of RPP-RPT-57991.

	Stream Number, X				
	28[a]	35[b]	41[c]	45[d]	46[e]
$C_X^{^{90}Sr}$ (Ci/L)	2.00E-03	3.17E-01	1.45E-03	1.50E-03	1.59E-03
V_X (gal)	2.35E+07	1.54E+07	6.33E+07	3.00E+07	2.06E+07

[a] Stream 28 represents the treated low-activity waste (LAW) waste stream sent to the LAW Vitrification Facility, used during the Direct-Feed Low-Activity Waste mission. This stream contains only soluble ^{90}Sr.

[b] Stream 35 represents the treated high-level radioactive waste (HLW) waste stream sent from the Hanford Tank Waste Treatment and Immobilization Plant (WTP) Pretreatment facility to the HLW Vitrification Facility. This stream contains only ^{90}Sr that is not soluble.

[c] Stream 41 represents the treated LAW waste stream sent from the WTP Pretreatment facility to the LAW Vitrification Facility. This stream contains only soluble ^{90}Sr.

[d] Stream 45 represents the treated LAW waste stream sent from the WTP Pretreatment facility to the potential supplemental LAW facility (see footnote 13). This stream contains only soluble ^{90}Sr.

[e] Stream 46 represents the treated LAW waste stream sent to the potential supplemental LAW facility (see footnote 13). This stream contains only soluble ^{90}Sr.

Reference: RPP-RPT-57991, *River Protection Project Integrated Flowsheet*.

References

78 FR 75913, 2013, "Record of Decision: Final Tank Closure and Waste Management Environmental Impact Statement for the Hanford Site, Richland, Washington," *Federal Register*, Vol. 78, pp. 75913–75919 (December 13).

24590-LAW-PL-PENG-17-0001, 2021, *ILAW Product Compliance Plan*, Rev. 2, Bechtel, River Protection Project Waste Treatment Plant, Richland, Washington.

DOE M 435.1-1, 2011, *Radioactive Waste Management Manual*, Change 2, U.S. Department of Energy, Washington, D.C.

IDF-00002, 2019, *Waste Acceptance Criteria for the Integrated Disposal Facility*, Rev. 0, CH2M HILL Plateau Remediation Company, Richland, Washington.

PNNL-28945, 2019, *Characterization of Cs-Loaded CST Used for Treatment of Hanford Tank Waste in Support of Tank-Side Cesium Removal*, RPT-TCT-005, Rev. 0, Pacific Northwest National Laboratory, Richland, Washington.

RPP-ENV-58562, 2016, *Inventory Data Package for the Integrated Disposal Facility Performance Assessment*, Rev. 3, Washington River Protection Solutions, LLC, Richland, Washington.

RPP-RPT-57991, 2019, *River Protection Project Integrated Flowsheet*, 24590-WTP-RPT-MGT-14-023, Rev. 3, Washington River Protection Solutions, LLC, Richland, Washington.

RPP-RPT-59958, 2019, *Performance Assessment for the Integrated Disposal Facility, Hanford Site*, Rev. 1A, Washington River Protection Solutions, LLC and INTERA, Inc., Richland, Washington.

RAI 1-2 (Percentage of Key Radionuclide Removal)

Comment
Additional information is needed on the percentage of key radionuclides removed from the waste that will be disposed in the integrated disposal facility.

Basis
Table 3-29 in the PA document lists the wasteform distributions resulting from the five cases considered to potentially be disposed of in IDF for 11 of the 25 key radionuclides identified by DOE. The 14 key radionuclides that are not listed in Table 3-29 are ^{60}Co, ^{59}Ni, ^{63}Ni, ^{228}Rn, ^{229}Th, ^{232}Th, ^{238}Pu, ^{241}Pu, ^{242}Pu, ^{241}Am, ^{243}Am, ^{242}Cm, ^{243}Cm, ^{244}Cm. (Note that ^{233}U and ^{235}U are listed in Table 3-29 but they are not listed as a key radionuclide in the draft WIR evaluation.)

In Table 2-3 of the draft WIR evaluation DOE lists the estimated total radioactivity in the 177 underground waste tanks, broken down by how much radioactivity is in the supernate, saltcake, and sludge for certain radionuclides (Note that key radionuclides ^{228}Rn, ^{232}Th are not listed in Table 2-3 of the draft WIR evaluation). For 12 of the 14 key radionuclides that are not listed in Table 3-29, Table 2-3 of the draft WIR evaluation shows that there is some percentage of these radionuclides that remains in the supernate or saltcake. For example, more than 80% of the ^{59}Ni and ^{63}Ni is in the saltcake or supernate, and about 45% of the ^{60}Co is in the saltcake or supernate. About 20-25% of the ^{238}Pu, ^{241}Pu, ^{242}Pu, ^{241}Am, ^{243}Am, ^{242}Cm, ^{243}Cm, and ^{244}Cm are not in the sludge. In the draft WIR evaluation, DOE states that ^{59}Ni is present in very low concentrations in the vitrified LAW and is an insignificant contributor to dose after IDF closure. However, it is unclear what percentage of these radionuclides may be present in the various waste forms that will be disposed of at IDF and what was removed by processing.

Figure 1-2-1. Data from Table 2-3 in the Draft Waste Incidental to Reprocessing Evaluation.
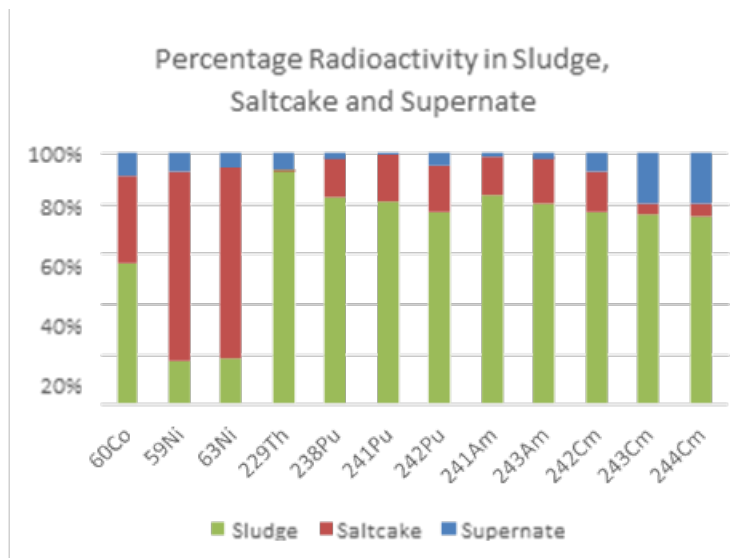
Path Forward
Please provide the percentages of key radionuclides removed for those key radionuclides (see Table 4-3 of the draft WIR evaluation) that are not already included in Table 3-29.

DOE Response
Table 4-3 in the Draft WIR Evaluation identifies key radionuclides. The second and third columns of Table 4-3 identify as key radionuclides those radionuclides listed in Title 10, *Code of Federal Regulations* (CFR), Part 61, "Licensing Requirements for Land Disposal of Radioactive Waste," Subpart D—Technical Requirements for Land Disposal Facilities, §61.55, "Waste Classification" (10 CFR 61.55)[15], and the last column identifies those radionuclides important to the IDF PA (RPP-RPT-59958)[16].

The DFLAW approach is currently planned for waste from tanks without significant soluble ^{90}Sr, as explained in the Draft WIR Evaluation in footnote 51. For the applicable tanks, the DFLAW pretreatment approach will use settling, decanting, filtration and ion exchange, which will remove over 99% of the ^{137}Cs as well as other key radionuclides, as shown in the Draft WIR Evaluation Section 4 and Table 1-2-1 below.

The curies in the supernate, saltcake, sum of saltcake and supernate, and sludge in the applicable tanks are identified in Columns 1, 2, 3 and 4 of Table 1-2-1, respectively. Column 5 of Table 1-2-1 is the total curies in the applicable tanks. Column 6 of Table 1-2-1 is the curies that will remain in the pretreated LAW during the DFLAW approach. In general, column 6 is that portion of Column 3 treated during DFLAW approach with more than 99.9% reduction in Cs (RPP-CALC-63643, *Sum of Fractions Calculations for DFLAW Immobilized LAW Glass*)[17]. The expected removal of each key radionuclide using the DFLAW approach is provided in Column7 of Table 1-2-1. Under the DFLAW approach, the total curies in the pretreated LAW are anticipated to be approximately 1% of the initial total curies in the applicable tanks, as shown in the last row of Column 7 of Table 1-2-1.

The expected inventory in the VLAW glass from RPP-CALC-63643 is provided in Column 8. For the DFLAW approach, approximately 99% of the radionuclides in the pretreated LAW will be captured in the VLAW, as shown in Column 9 of Table 1-2-1. Approximately 96% of the ^{129}I and approximately 98% of the ^{99}Tc in the pretreated LAW sent to the LAW Vitrification Facility will be captured in the VLAW.[18] The VLAW will contain approximately 99% of the total curies in the pretreated LAW as provided in the last row of Column 9 of Table 1-2-1.

---

[15] Some are of lesser importance due to their low concentrations in the waste, their small dose conversion factors, short half-life, or both.

[16] To provide a bounding radiological risk analysis in the IDF PA, no credit is taken in flowsheet modeling for removal of key radionuclides other than ^{137}Cs by the ion exchange media. However, other radionuclides are expected to be removed by the ion exchange media. As explained in Section 4.2.2.1 of the Draft WIR Evaluation, the DFLAW approach includes "Passing through crystalline silicotitanate (CST) ion exchange media to remove ^{137}Cs, and large fractions of Ca, U, ^{90}Sr, Np and Pu if present in soluble form (PNNL-28783, *Dead-End Filtration and Crystalline Silicotitanate Cesium Ion Exchange with Hanford Tank Waste AW-102*)."

[17] In general, sludge is separated through decanting and filtration prior to cesium removal during the DFLAW approach. The percentage of ^{137}Cs removed per DFLAW campaign is 99.95% or greater per RPP-CALC-63643. Table 1-2-1 rounds this value to three significant figures.

[18] ^{3}H and ^{14}C are volatile radionuclides which will not be captured in the VLAW.

Table 1-2-1. Radionuclide Content in Supernate, Saltcake, Sludge and Vitrified Low-Activity Waste.[1] (2 sheets)

Radionuclide	Supernate (Ci) (1)	Saltcake (Ci) (2)	Supernate + Saltcake (Ci) (3)	Sludge (removed via settle / decant) (Ci) (4)	Total in DFLAW Tanks (Ci) (5)	Radionuclide Content in Pretreated LAW Sent to LAW Vit Facility (Ci) (6)	Percent Removed by DFLAW Approach (7)	Radionuclide Content in VLAW Glass (Ci) (8)	Percent of LAW Radionuclides in VLAW Glass (9)
Column Formula	BBI	BBI	(1)+(2)	BBI	(3)+(4)	RPP-CALC-63643	[1-(6)/(5)]*100	RPP-CALC-63643	(8)/(6)*100
^{3}H	1.27E+02	2.09E+02	3.36E+02	8.81E+01	4.24E+02	1.37E+02	67.7%	0.00E+00	0%
^{14}C	6.47E+01	1.64E+02	2.29E+02	8.63E+00	2.38E+02	1.43E+02	39.7%	0.00E+00	0%
^{60}Co	9.30E+01	9.92E+01	1.92E+02	5.41E+02	7.33E+02	2.44E+01	96.7%	2.44E+01	99.9%
^{59}Ni	4.44E+01	1.93E+02	2.37E+02	9.77E+01	3.35E+02	3.17E+01	90.5%	3.17E+01	99.9%
^{63}Ni	2.52E+03	1.69E+04	1.94E+04	8.83E+03	2.83E+04	2.01E+03	92.9%	2.01E+03	99.9%
^{90}Sr	4.72E+04	1.15E+06	1.20E+06	1.49E+07	1.61E+07	2.12E+05	98.7%	2.12E+05	99.8%
^{94}Nb[2]	NA	NA	NA	NA	NA	—	—	—	—
^{99}Tc	9.44E+03	6.70E+03	1.61E+04	5.86E+02	1.67E+04	7.48E+03	55.2%	7.36E+03	98.4%
^{126}Sn	1.34E+02	7.79E+01	2.12E+02	1.73E+01	2.30E+02	5.47E+01	76.2%	5.46E+01	99.9%
^{129}I	1.15E+01	5.33E+00	1.68E+01	7.67E-01	1.76E+01	9.71E+00	45.0%	9.34E+00	96.2%
^{137}Cs	1.58E+07	6.12E+06	2.19E+07	1.06E+06	2.30E+07	1.47E+03	100%	1.46E+03	99.2%
^{229}Th	1.81E-01	3.19E-03	1.84E-01	2.63E-03	1.87E-01	1.14E-01	39.1%	1.14E-01	99.9%
^{233}U	6.55E-01	4.16E+01	4.23E+01	7.33E+00	4.96E+01	8.01E-01	98.4%	7.99E-01	99.8%
^{234}U	4.96E-01	1.34E+01	1.39E+01	2.91E+01	4.30E+01	5.68E-01	98.7%	5.67E-01	99.8%
^{235}U	6.55E-01	4.16E+01	4.23E+01	7.33E+00	4.96E+01	2.12E-02	98.7%	2.12E-02	99.8%
^{238}U	3.82E-01	1.16E+01	1.20E+01	2.14E+01	3.33E+01	4.45E-01	98.7%	4.44E-01	99.8%
^{237}Np	1.92E+00	2.48E+01	2.67E+01	4.02E+01	6.70E+01	2.82E+00	95.8%	2.82E+00	99.8%
^{238}Pu	9.11E+00	1.12E+02	1.21E+02	1.02E+03	1.14E+03	6.79E+00	99.4%	6.78E+00	99.9%
^{239}Pu	5.95E+01	1.92E+03	1.98E+03	9.56E+03	1.15E+04	9.20E+01	99.2%	9.19E+01	99.9%
^{240}Pu	1.36E+01	4.44E+02	4.58E+02	2.45E+03	2.91E+03	2.06E+01	99.3%	2.06E+01	99.9%

Table 1-2-1. Radionuclide Content in Supernate, Saltcake, Sludge and Vitrified Low-Activity Waste.[1] (2 sheets)

Radionuclide	Supernate (Ci) (1)	Saltcake (Ci) (2)	Supernate + Saltcake (Ci) (3)	Sludge (removed via settle / decant) (Ci) (4)	Total in DFLAW Tanks (Ci) (5)	Radionuclide Content in Pretreated LAW Sent to LAW Vit Facility (Ci) (6)	Percent Removed by DFLAW Approach (7)	Radionuclide Content in VLAW Glass (Ci) (8)	Percent of LAW Radionuclides in VLAW Glass (9)
^{241}Pu	1.30E+02	2.49E+03	2.62E+03	2.40E+04	2.66E+04	9.07E+01	99.7%	9.06E+01	99.9%
^{242}Pu	9.44E-02	3.49E-02	1.29E-01	3.45E-01	4.74E-01	7.09E-02	85.0%	7.09E-02	99.9%
^{241}Am	7.18E+01	5.94E+03	6.01E+03	8.39E+04	9.00E+04	9.76E+01	99.9%	9.75E+01	99.9%
^{243}Am	3.15E-02	3.58E+00	3.61E+00	3.86E+01	4.22E+01	4.78E-02	99.9%	4.77E-02	99.9%
^{242}Cm	1.87E-01	1.56E+01	1.58E+01	6.98E+01	8.57E+01	2.21E+00	97%	2.20E+00	99.8%
^{243}Cm	3.54E-02	2.09E+00	2.13E+00	7.51E+00	9.63E+00	1.46E-01	98.5%	1.45E-01	99.8%
^{244}Cm	6.63E-01	4.13E+01	4.20E+01	1.49E+02	1.91E+02	2.63E+00	98.6%	2.62E+00	99.8%
Others[3]	1.52E+07	7.36E+06	2.26E+07	1.67E+07	3.93E+07	3.51E+05	99.1%	3.50E+05	99.8%
Totals	**3.11E+07**	**1.47E+07**	**4.58E+07**	**3.28E+07**	**7.85E+07**	**5.75E+05**	**99.3%**	**5.73E+05**	**99.8%**

Source: RPP-CALC-63643, *Sum of Fractions Calculations for DFLAW Immobilized LAW Glass*, Rev. 4 and associated Excel® (a registered trademark of Microsoft Corporation in the U.S. and other countries) file.

Note: Numbers are rounded to three significant figures.

[1] The Draft WIR Evaluation (DOE/ORP-2020-01, *Draft Waste Incidental to Reprocessing Evaluation for Vitrified Low-Activity Waste Disposed Onsite at the Hanford Site, Washington*) uses the term vitrified low-activity waste (VLAW) which is also called immobilized low-activity waste (ILAW). Reference documents may use ILAW and as such this is synonymous with VLAW.

[2] As noted in the Draft WIR Evaluation, Table 4-3 Footnote c, "^{94}Nb is a key radionuclide identified in 10 CFR 61.55 that is not applicable to Hanford tank waste. The total amount of ^{94}Nb created from 1944 to 1989 in all Hanford reactors is about 0.1 Ci. ^{94}Nb is primarily produced in reactors from activation of natural niobium in stainless steel and Inconel® (a registered trademark of Special Metals Corporation, New Hartford, New York), neither of which were used at Hanford in the fuels that were reprocessed. Therefore, ^{94}Nb is not a key radionuclide in vitrified LAW (RPP-13489, *Activity of Fuel Batches Processed Through Hanford Separations Plants, 1944 Through 1989*, Table H-1)." It is not a standard analyte for the Best-Basis Inventory (BBI) and thus content information is not available.

[3] Others are identified in Table 1-2.2.

DFLAW = Direct-Feed Low-Activity Waste

The information in Table 1-2-1 will be added to the final WIR Evaluation. ^{233}U and ^{235}U are also included in Table 1-2-1, but were omitted from Table 4-3 in the Draft WIR Evaluation. These radionuclides will be added to Table 4-3 of the final WIR evaluation.

The following Table 1-2-2 provides the list of radionuclides included in the row Others of Table 1-2-1.

Table 1-2-2. Radionuclides in Others of Table 1-2.1.

^{106}Ru
^{113m}Cd
^{125}Sb
^{134}Cs
^{137m}Ba
^{151}Sm
^{152}Eu
^{154}Eu
^{155}Eu
^{226}Ra
^{227}Ac
^{228}Ra
^{231}Pa
^{232}Th
^{232}U
^{236}U
^{79}Se
^{90}Y
^{93m}Nb
^{93}Zr

It bears emphasizing that the vast majority of the curies in the tanks will not be disposed of in the IDF. For the entire Hanford cleanup mission[19], the Table 1-2-3 provides Base Case 7 modelling

---

[19] The entire Hanford cleanup mission encompasses the storage, retrieval, treatment, and disposal of approximately 56 million gallons of radioactive waste contained in the Hanford Site waste tanks and closure of all the tanks and associated equipment (ORP-11242, *River Protection System Plan*, Rev. 8).

percentages of radionuclides that do not end up in LLW planned to be disposed at IDF[20], i.e., Non-IDF versus the tank waste contents (Best-Basis Inventory [BBI]).

Table 1-2-3. Run Case 7 Radionuclides. (2 sheets)

Radionuclide	Non-IDF	BBI	Portion of BBI Not in IDF*
106-Ru	-2.14E-03	1.20E+01	—
113m-Cd	5.04E+02	3.89E+03	13.0%
125-Sb	1.51E+00	4.13E+03	0.0%
126-Sn	1.58E-01	3.91E+02	0.0%
129-I	5.98E-01	2.94E+01	2.0%
134-Cs	7.11E+02	7.13E+02	99.7%
137-Cs	3.87E+07	3.90E+07	99.2%
137m-Ba	3.65E+07	3.68E+07	99.2%
14-C	8.24E+02	5.51E+02	149.5%**
151-Sm	3.15E+06	3.57E+06	88.2%
152-Eu	7.91E+02	9.07E+02	87.2%
154-Eu	4.82E+04	5.30E+04	90.9%
155-Eu	2.41E+04	2.55E+04	94.5%
226-Ra	1.18E-05	9.95E-03	0.1%
227-Ac	-9.32E+00	4.14E+00	—
228-Ra	-2.89E+02	6.77E+00	—
229-Th	1.42E+00	1.48E+00	95.9%
231-Pa	4.73E+00	5.16E+00	91.7%
232-Th	6.61E+00	6.77E+00	97.6%
232-U	8.17E+00	8.87E+00	92.1%
233-U	6.37E+02	6.82E+02	93.4%
234-U	2.14E+02	2.37E+02	90.3%
235-U	8.75E+00	9.71E+00	90.1%
236-U	6.05E+00	6.50E+00	93.1%
237-Np	9.02E+01	1.15E+02	78.4%

---

[20] LLW planned to be disposed at IDF includes Fast Flux Test Facility (FFTF) decommissioning waste, waste management facility-generated (secondary) waste, and onsite non-CERCLA non-tank waste, as mentioned in DOE/EIS-0391, *Final Tank Closure and Waste Management Environmental Impact Statement for the Hanford Site, Richland, Washington.*

Table 1-2-3. Run Case 7 Radionuclides. (2 sheets)

Radionuclide	Non-IDF	BBI	Portion of BBI Not in IDF*
238-Pu	2.25E+03	2.63E+03	85.6%
238-U	1.94E+02	2.15E+02	90.2%
239-Pu	4.30E+04	4.94E+04	87.0%
240-Pu	9.10E+03	1.08E+04	84.3%
241-Am	1.42E+05	1.57E+05	90.4%
241-Pu	7.15E+04	8.38E+04	85.3%
242-Cm	8.22E-02	1.22E+02	0.1%
242-Pu	6.78E-01	8.26E-01	82.1%
243-Am	6.38E+01	7.23E+01	88.2%
243-Cm	5.04E-03	1.35E+01	0.0%
244-Cm	1.07E-01	2.98E+02	0.0%
3-H	2.81E+03	2.82E+03	99.6%
59-Ni	1.41E+03	1.62E+03	87.0%
60-Co	3.71E+03	4.10E+03	90.5%
63-Ni	1.26E+05	1.44E+05	87.5%
79-Se	4.51E-02	1.44E+02	0.0%
90-Sr	4.27E+07	4.76E+07	89.7%
90-Y	4.27E+07	4.76E+07	89.7%
93-Zr	3.37E+03	3.73E+03	90.3%
93m-Nb	2.85E+03	3.17E+03	89.9%
99-Tc	2.14E+01	2.65E+04	0.1%
Totals	**1.64E+08**	**1.75E+08**	**93.7%**

Adapted from Table A-1. Run Case 7 Radionuclides. of RPP-ENV-58562, *Inventory Data Package for the Integrated Disposal Facility Performance Assessment*, Rev. 3. Table data was drawn from the 2014 Best-Basis Inventory (BBI) which was the basis of the Integrated Disposal Facility (IDF) Performance Assessment (RPP-RPT-59958, *Performance Assessment for the Integrated Disposal Facility, Hanford Site*).
*Column added.
**Includes 222S laboratory sources -, i.e. sources are not in the BBI.

The Hanford Tank Waste Operations Simulator (HTWOS) reports certain radionuclides (i.e., [227]Ac, [228]Ra, [93m]Nb) as negative inventory values, which is due to the fact that HTWOS has four second-order decay chains; parent to daughter to granddaughter isotope. None of the radionuclides reporting negative inventories are considered major risk drivers and therefore will have a negligible impact on the overall performance of the IDF (see Section 2.7.7 in RPP-17152, *Hanford Tank Waste Operations Simulator (HTWOS) Version 8.1 Model Design Document*).

References

DOE/EIS-0391, 2012, *Final Tank Closure and Waste Management Environmental Impact Statement for the Hanford Site, Richland, Washington*, U.S. Department of Energy, Washington, D.C.

DOE/ORP-2020-01, 2020, *Draft Waste Incidental to Reprocessing Evaluation for Vitrified Low-Activity Waste Disposed Onsite at the Hanford Site, Washington*, U.S. Department of Energy, Office of River Protection, Richland, Washington.

ORP-11242, 2017, *River Protection System Plan*, Rev. 8, U.S. Department of Energy, Office of River Protection, Richland, Washington.

PNNL-28783, 2019, *Dead-End Filtration and Crystalline Silicotitanate Cesium Ion Exchange with Hanford Tank Waste AW-102*, RPT-TCT-003, Rev. 0, Pacific Northwest National Laboratory, Richland, Washington.

RPP-13489, 2002, *Activity of Fuel Batches Processed Through Hanford Separations Plants, 1944 Through 1989*, Rev. 0, Fluor Hanford, Inc., Richland, Washington.

RPP-17152, 2015, *Hanford Tank Waste Operations Simulator (HTWOS) Version 8.1 Model Design Document,* Rev. 12, Washington River Protection Solutions, LLC/AEM Consulting, LLC, Richland, Washington.

RPP-CALC-63643, *Sum of Fractions Calculations for DFLAW Immobilized LAW Glass*, Rev. 4, Washington River Protection Solutions, LLC, Richland, Washington.

RPP-ENV-58562, 2016, *Inventory Data Package for the Integrated Disposal Facility Performance Assessment*, Rev. 3, Washington River Protection Solutions, LLC, Richland, Washington.

RPP-RPT-59958, 2019, *Performance Assessment for the Integrated Disposal Facility, Hanford Site, Washington*, Rev. 1A, Washington River Protection Solutions, LLC, Richland, Washington.

RAI 1-3 (Percentage of ^{99}Tc and ^{129}I Recycled versus Removed)

Comment
Additional information is needed on the percent of the ^{99}Tc and ^{129}I that could potentially be removed from the waste versus remaining in either the VLAW or the SSW. (See also RAI 2-10).

Basis
In the draft WIR evaluation, DOE stated on page 4-12 that, "with respect to ^{99}Tc and ^{129}I, the LAW Vitrification Facility is designed to maximize the capture of these radionuclides in the vitrified waste form. The LAW Vitrification Facility off gas system is designed to recycle and/or capture that portion of volatile radionuclides (including ^{99}Tc and ^{129}I) which are not vitrified (see Section 2.5.3)." During the LAW vitrification process, the volatile components will be drawn off through the melter offgas treatment system, will go through a submerged bed scrubber (SBS) and Wet Electrostatic Precipitator (WESP), two stages of high-efficiency particulate air (HEPA) filters, as well as two carbon adsorber beds, which remove the ^{129}I.

The draft WIR evaluation states that the ^{99}Tc and ^{129}I in the liquid condensate resulting from the offgas system (from the SBS and WESP) can potentially be routed in three ways:

1. recycle back to the LAW Vitrification Facility for blending with incoming DFLAW feed;
2. return back to the Hanford tank farms; and
3. purge via a tanker truck load-out station ((RPP-RPT-58971, Effluent Management Facility Evaporator Concentrate – Purge Alternatives Evaluation).

Table 3-29 in the PA document provides the summary of radionuclide inventories and wasteform distributions for five cases. As shown below, the majority of the ^{99}Tc and ^{129}I does not remain in the HLW tanks. In Case 7, Case 8B, and Case 9, about 40% of the Best Basis Inventory (BBI) of ^{129}I ends up in the Secondary Solid Waste (SSW). In Case 10A and Case 10B, nearly 80% of the ^{129}I ends up in either the Effluent Treatment Facility-Generated (ETF- Generated) SSW or the SSW. A negligible amount of the ^{129}I remains in the HLW in any of cases.

In Case 7, over 99% of the ^{99}Tc is assumed to end up in the Immobilized Low-Activity Waste (ILAW) glass. In Case 8B, as a result of removing ^{99}Tc from the LAW off-gas stream, 16,500 Ci of ^{99}Tc accumulates over the course of the waste treatment and immobilization plant mission.

The footnote on Table 3-29 states that "these curies would likely be processed in High-Level Waste and would not end up at the IDF". In the PA document, DOE further describes Case 8B as follows: "a ^{99}Tc removal unit operation has been added after the submerged bed scrubber (SBS) wet electrostatic precipitator (WESP) to remove ^{99}Tc at an efficiency of 99% from the LAW liquid off-gas steam prior to being recycled back to pretreatment. This inventory would not be disposed of at IDF and represents the lower range of ^{99}Tc inventory in glass and grout waste forms."

Figure 1-3-1. Iodine-129 Distribution across Waste Forms as Percent of Best-Basis Inventory by Case.
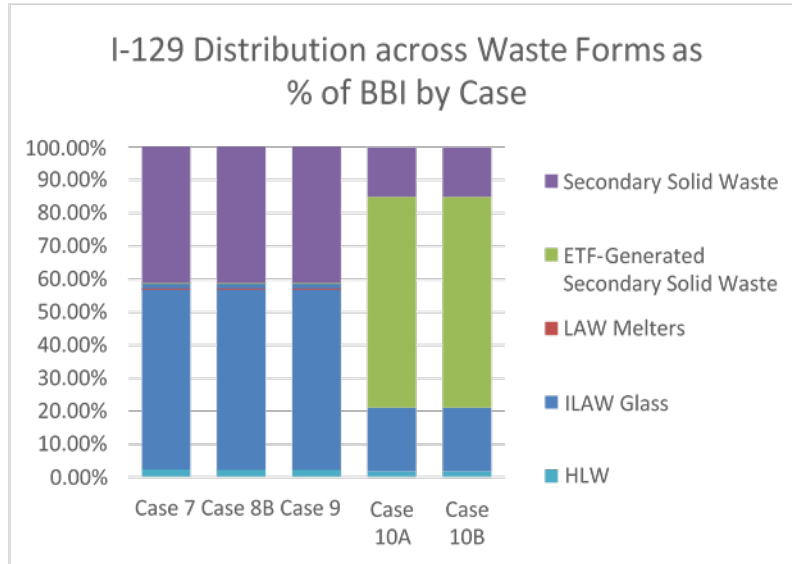
Adapted from data in Table 3-29 of RPP-RPT-59958, *Performance Assessment for the Integrated Disposal Facility, Hanford Site, Washington*.

Figure 1-3-2. Technetium-99 Distribution across Waste Forms as Percent of Best-Basis Inventory by Case.
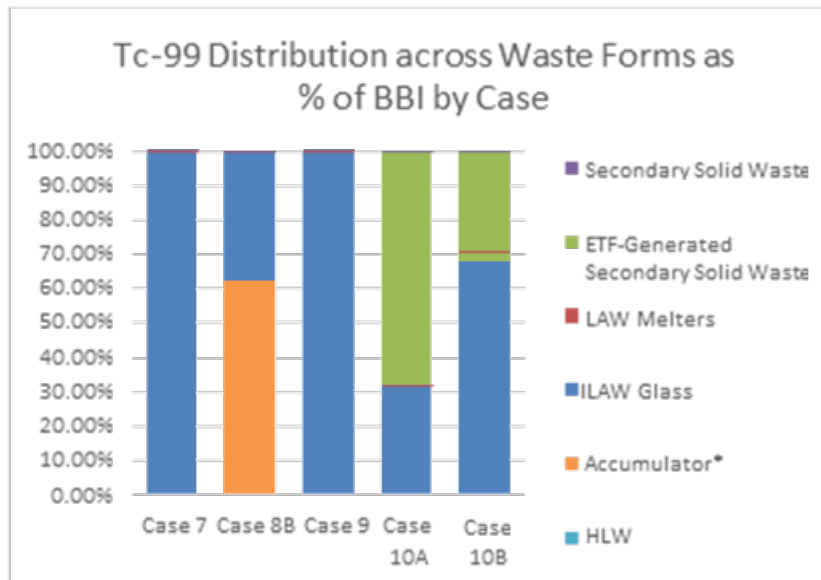
Adapted from data in Table 3-29 of RPP-RPT-59958, 2019, *Performance Assessment for the Integrated Disposal Facility, Hanford Site, Washington*.

Path Forward

Please provide additional information on the percentage of ^{99}Tc and ^{129}I that is expected to be recycled back to the DFLAW feed, percent returned to the tank farm to be disposed of as HLW, and percent purged via the Effluent Management Facility (EMF) evaporator concentrate.

Please provide additional information about the accumulator mentioned in Table 3-29 of the PA document. Please specify if the ^{99}Tc is assumed to be accumulating in one component or in multiple parts of the waste treatment plant (WTP). Please provide the hypothetical plan for disposal of the accumulator waste under this scenario.

DOE Response

In the time since the IDF PA study was performed, the DFLAW flowsheet has matured and the EMF design (used only during DFLAW) has been finalized. In the current flowsheet configuration (RPP-RPT-57991), all ^{99}Tc and ^{129}I in the liquid concentrate resulting from the off-gas system (from the SBS and WESP) will be recycled internally back to the concentrate receipt vessels of the LAW Vitrification Facility. By recycling the liquid concentrate internally, it is estimated that 98.4% of the ^{99}Tc and 96.2% of the ^{129}I that is sent to the LAW Vitrification Facility as feed will be incorporated into the VLAW during DFLAW (RPP-CALC-63643; see also Table 1-2-1 of the response to RAI 1-2). No ^{99}Tc or ^{129}I will be returned to the tank farm to be disposed of as HLW, or purged via the EMF evaporator concentrate. The Final WIR Evaluation will be updated to reflect the current flowsheet configuration. Cases 10A and 10B were hypothetical scenarios that investigated alternatives to recycling all EMF concentrate back to the concentrate receipt vessels in the LAW Vitrification Facility. With finalization of the DFLAW flowsheet, Cases 10A and 10B are no longer potential scenarios and will be withdrawn from the analyses performed for the IDF PA for its next revision, as part of PA maintenance. In the event of an extended outage of the EMF evaporator and continued tank waste treatment through the LAW melters, the dilute EMF evaporator feed will be returned to the tank farms. If that were to occur, the ^{99}Tc and ^{129}I would eventually be fed back to the LAW Vitrification Facility in a larger recycle loop, due to the soluble nature of both isotopes.

The accumulator[21] mentioned in Table 3-29 of the IDF PA document for Case 8B is a modeling tool used to symbolize an undefined ^{99}Tc removal operation for mass balance purposes. Case 8B was developed for the IDF PA to align with a hypothetical scenario that removed 99% of ^{99}Tc in the LAW Vitrification Facility liquid off-gas system for incorporation into HLW. In Case 8B this removal process is a hypothetical process to align with the conditions of the scenario. Case 8B is no longer a potential scenario and will be withdrawn from the analyses performed for the IDF PA for its next revision as part of PA maintenance. Due to the volatility and soluble nature of ^{99}Tc, if it were to be collected and fed to the HLW Vitrification Facility (which is not possible during DFLAW operations since the HLW Vitrification Facility is under construction and not available), only a fraction of it would be retained in the immobilized high-level waste glass. The remaining ^{99}Tc would be collected in HLW off-gas condensates, returned to the Pretreatment Facility and routed to the LAW Vitrification Facility to be incorporated into the VLAW glass. The much larger recycle loop and technical challenges that this situation would create make this scenario not technically feasible.

---

[21] No accumulator is included as part of the draft VLAW WIR. The accumulator was included in the IDF PA as a hypothetical scenario.

The inventory sensitivity cases (Cases 8B, 10A, and 10B) were deterministic cases used to demonstrate dose impacts for different LAW Vitrification Facility operating scenarios. The cases were hypothetical, but confirmed a strong correlation between waste stream inventory and waste stream dose using the PA models. Subsequent to the completion of the IDF PA, a spreadsheet was developed to track inventories and forecast the impacts to groundwater due to changes in inventory. This spreadsheet is referred to as the Risk Budget Tool and was developed in RPP-CALC-63176, *Integrated Disposal Facility Risk Budget Tool Analysis*. The calculations demonstrate that changes to the groundwater concentrations and dose to a member of the public in the future from a specific waste stream are proportional to a change in the inventory in that waste stream. Inventory changes or "what if" scenarios can be rapidly evaluated using the Risk Budget Tool and these evaluations are consistent with equivalent analyses that could be conducted with the IDF PA system model. In future revisions of the IDF PA, DOE will consider using probabilistic methods to evaluate inventory uncertainty instead of deterministic sensitivity studies.

References

DOE/ORP-2020-01, 2020, *Draft Waste Incidental to Reprocessing Evaluation for Vitrified Low-Activity Waste Disposed Onsite at the Hanford Site, Washington*, U.S. Department of Energy, Office of River Protection, Richland, Washington.

RPP-CALC-63176, 2020, *Integrated Disposal Facility Risk Budget Tool Analysis*, Rev. 0A, Washington River Protection Solutions, LLC, Richland, Washington.

RPP-CALC-63643, *Sum of Fractions Calculations for DFLAW Immobilized LAW Glass*, Rev. 4, Washington River Protection Solutions, LLC, Richland, Washington.

RPP-RPT-57991, 2019, *River Protection Project Integrated Flowsheet*, 24590-WTP-RPT-MGT-14-023, Rev. 3, Washington River Protection Solutions, LLC, Richland, Washington.

RPP-RPT-58971, 2020, *Effluent Management Facility Evaporator Concentrate – Purge Alternatives Evaluation*, Rev. 1, Washington River Protection Solutions, LLC, Richland, Washington.

RAI 1-4   (Alternative Technology Evaluation Impacting ^{99}Tc and ^{129}I)

Comment

Additional information is needed on the alternative technologies considered for removal of ^{129}I and ^{99}Tc.

Basis

Depending on the processes used and separation that may occur, a moderate to significant amount of ^{129}I and ^{99}Tc may end up in the SSW (See the previous figures in RAI 1-3). If these key radionuclides in the SSW ultimately are disposed of in IDF, the NRC staff considers those secondary waste streams within the scope of the draft WIR evaluation and therefore considers the impact of the secondary waste and the alternative technologies considered for the wasteforms. The NRC staff note that in discussions with the DOE, the DOE has stated that the scope of the draft WIR evaluation is limited to the vitrified waste. DOE has stated that the SSW is a newly generated waste stream and will include a wide variety of waste (HEPA filters, or carbon filters) that will be generated after the low activity waste has been vitrified. Therefore, DOE considers SSW to be outside the scope of the WIR evaluation, but DOE has included the SSW as part of IDF PA analysis and the SSW will be classified to ensure it meets the Waste Acceptance Criteria (WAC) for IDF.

DOE has conducted previous studies to compare alternative technologies for removal of radionuclides from the Hanford tank wastes. These studies are summarized in the Technical Basis Summary Report (WHC-SD-WM-TI-699) completed in 1996. In the draft WIR evaluation DOE summarized the findings of the report, but DOE did not discuss alternative technologies considered for the SSW waste forms or technologies that would selectively drive the ^{99}Tc and ^{129}I back into the HLW.

Path Forward

As a result of high operating temperatures, the vitrification process appears to selectively partition the ^{99}Tc and ^{129}I to the SSW waste stream during processing of the waste. Given that ^{99}Tc and ^{129}I are key risk drivers, please provide information regarding potential technologies that may have been considered to connect the offgas system to other waste treatments that would result in those key radionuclides being incorporated into HLW compared to the VLAW or SSW.

DOE Response

The Draft WIR Evaluation focuses on the WIR criteria for separated and pretreated VLAW using the DFLAW approach. Other wastes, including secondary waste such as the carbon adsorber beds (CABs), are outside the scope of the Draft WIR Evaluation, as explained in the Draft WIR Evaluation and DOE's Response to NRC's Introductory Statement Related to Secondary Waste. To bound the analysis, the IDF PA correctly includes all wastes potentially disposed of in the IDF, including the CABs and other secondary wastes, for demonstrating compliance with performance objectives and performance measures. The following is being provided for additional information and completeness, although it is outside the scope of the Draft WIR Evaluation.

As a result of high operating temperatures in the LAW melter, volatile constituents present in the LAW feed (including ^{99}Tc and ^{129}I) will non-selectively partition to the melter off-gas system. The LAW vitrification melter off-gas system has operations (i.e., an SBS and a WESP) to recover volatile constituents. These constituents are incorporated back into the LAW vitrification feed stream via the EMF for eventual incorporation into VLAW.[22]

As provided in more detail in the answers to RAI 1-2 and RAI 1-3, approximately 98% of the ^{99}Tc, 96% of the ^{129}I, and 99% of all radionuclides from the pretreated LAW are now projected to be incorporated into the VLAW during the DFLAW approach.[23] Revisions of the IDF PA will incorporate changes per required PA maintenance activities as required in DOE M 435.1-1 Chapter IV Section (P) (4).

DOE will monitor all waste as it is disposed to ensure that the IDF WAC is met and that the IDF PA is maintained.

References

78 FR 75913, 2013, "Record of Decision: Final Tank Closure and Waste Management Environmental Impact Statement for the Hanford Site, Richland, Washington," *Federal Register*, Vol. 78, pp. 75913–75919 (December 13).

DOE M 435.1-1, 2011, *Radioactive Waste Management Manual*, Change 2, U.S. Department of Energy, Washington, D.C.

DOE/ORP-2020-01, 2020, *Draft Waste Incidental to Reprocessing Evaluation for Vitrified Low-Activity Waste Disposed Onsite at the Hanford Site, Washington*, U.S. Department of Energy, Office of River Protection, Richland, Washington.

RPT-RPT-59958, 2019, *Performance Assessment for the Integrated Disposal Facility, Hanford Site*, Rev. 1A, Washington River Protection Solutions, LLC and INTERA, Inc., Richland, Washington.

WHC-SD-WM-TI-699, 1996, *Technical Basis for Classification of Low-Activity Waste Fraction from Hanford Site Tanks*, Rev. 2, Westinghouse Hanford Company, Richland, Washington.

---

[22] The EMF is planned to be used only during the DFLAW approach.

[23] DOE is not pursuing other potential processes that would divert volatized Tc and I to non-VLAW (non-ILAW) waste streams (see 78 FR 75913, "Record of Decision: Final Tank Closure and Waste Management Environmental Impact Statement for the Hanford Site, Richland, Washington").

RAI 1-5   (Removal and Disposal of Separated ^{129}I)

Comment
In the draft WIR evaluation, DOE indicated that they did not identify a technology that could practically remove ^{129}I from tank wastes. It isn't clear why the ^{129}I that is separated very efficiently by the vitrification process could not be disposed as HLW.

Basis
DOE identified ^{129}I as a key radionuclide with respect to protection of an offsite member of the public. Iodine-129 is present in tank waste in very low concentrations and therefore it is difficult to remove. Iodine-129 is very long-lived and mobile in the environment. The vitrification process operates at very high temperatures and volatizes nearly all of the ^{129}I present in the waste streams. This ^{129}I then goes into the offgas system and is captured or recycled back to the glass melters. Even with recycling the capture of ^{129}I in the glass is less than 50%.

Section 4.2.2.6 of the draft WIR evaluation states that "DOE has also explored whether there is an available technology to remove ^{129}I. However, the ^{129}I concentration in the tank wastes is typically 1,000 to 10,000 times lower than would exist in commercial fuel dissolver solutions for which an available iodine removal technology was developed. Iodine-129 removal is not considered to be technically practical because no technology has been demonstrated for the relatively low concentrations in the Hanford Site tank waste (WHC-SD-WM-TI-699, *Technical Basis for Classification of Low-Activity Waste Fraction from Hanford Site Tanks*)."

In section 2.5.3 of the draft WIR evaluation DOE stated that the "The volatile components will be drawn off through the melter offgas treatment system, go through a submerged bed scrubber (SBS) and Wet Electrostatic Precipitator (WESP). The LAW melter offgas system consists of two stages of high-efficiency particulate air (HEPA) filters for the purpose of removing radioactive particulates from the offgas, in order to achieve compliance with both environmental and occupational dose limits. Downstream of the HEPA filters are two carbon adsorber beds filled with granular activated carbon media. By design, the purpose of these beds is to remove mercury, halides, and acid gases as well as ^{129}I." It was not clear whether DOE evaluated the disposal of the ^{129}I separated by the vitrification process as HLW.

Path Forward
Please provide information as to whether DOE evaluated the disposal of the ^{129}I that would be adsorbed by the two carbon adsorber beds filled with granular activated carbon media as HLW. Please also describe what percentage of the ^{129}I can technically and practically be removed using the carbon adsorber beds.

DOE Response
The Draft WIR Evaluation focuses on the WIR criteria for separated and pretreated VLAW using the DFLAW approach. Other wastes, including secondary waste such as the CABs, are outside the scope of the Draft WIR Evaluation, as explained in the Draft WIR Evaluation and DOE's Response to NRC's Introductory Statement Related to Secondary Waste. To bound the analysis, the IDF PA[24] correctly includes all wastes potentially disposed of in the IDF, including the

---

[24] The IDF PA is titled *Performance Assessment for the Integrated Disposal Facility, Hanford Site, Washington.*

CABs and other secondary wastes, for compliance with performance objectives and performance measures. The following is being provided for additional information and completeness, although it is outside the scope of the Draft WIR Evaluation.

The LAW Vitrification Facility's melter off-gas system has a primary system and a secondary system. The primary system consists of the SBS to remove particulates and cool the off-gas, an SBS Condensate Vessel to maintain SBS liquid level, and a WESP to remove aerosols and micron-sized particulates. The secondary system consists of the Vessel Ventilation Subsystem, Off-Gas HEPA Preheaters, HEPA Filters, Activated CABs, Catalyst Skid, Catalytic Oxidizer Heat Recovery Exchanger, Catalytic Oxidizer Electric Heater, Thermal Catalytic Oxiders, Selective Catalytic Reducer (SCR), Caustic Collection Tank, Caustic Scrubber, and Exhausters.

The CABs are used to remove mercury, halides, and acid gases, including iodine, for the control of air emissions to meet EPA air discharge limits and reduce occupational doses. The CABs are not designed or relied upon in the Draft WIR Evaluation as a treatment process for removing ^{129}I to meet the first WIR criterion under DOE M 435.1-1 (concerning removal of key radionuclides to the maximum extent technically and economically practical).

The CABs will be properly characterized and classified, and if characterized as LLW, treated, and disposed of in the IDF in accordance with IDF-00002. The CABs are identified as a future newly-generated LLW in the LAW Vitrification Facility Radioactive Waste Management Basis (RWMB).[25]

The LAW Vitrification Facility off-gas system in combination with the EMF and recycling the EMF bottoms back to the LAW Vitrification facility will, by design, maximize the capture of the volatized ^{129}I in the VLAW glass. Approximately 96% of the ^{129}I will be captured in the VLAW as explained in the response to RAI 1-2, compared to 57.51% assumed in the IDF PA[26]

---

[25] In addition, the CABs will be replaced periodically. The CABs are expected to be below 10 CFR 61.55 Class C concentration limits.

[26] Since the time of the preparation of DOE/EIS-0391, *Final Tank Closure and Waste Management Environmental Impact Statement for the Hanford Site, Richland, Washington* and the IDF PA, there have been two major changes in modeling assumptions: 1) It is no longer assumed that the EMF bottoms will be recycled to the Tank Farms, and 2) Single-pass iodine incorporation is increased from 20% to 58.33%. These are more fully explained as follows. When the modeling was performed for the IDF PA, the flowsheet assumption was that some of the EMF bottoms would be returned to Tank Farms. At that time, it was assumed that only 67% of the bottoms would be recycled back to the WTP LAW Vitrification Facility, and the other 33% would be returned to Tank Farms to be processed again through the WTP LAW Vitrification Facility at a later time. There is no return to the Tank Farms in the latest flowsheet modeling. Additionally, to be consistent with DOE/EIS-0391, the single-pass iodine incorporation rate was originally set at 20% (RPP-ENV-58562 Rev. 3, page 49) per State of Washington Department of Ecology direction (*Mass Balance Revision, 17546 Revision of PCAL 17284-2 Mass Balance*, WT-ST-056 Rev. 2 Attachment 4). This resulted in about 56.64% of the iodine being incorporated in the VLAW. Latest modeling (RPP-RPT-57991 Rev. 3) is now consistent with the WTP *Flowsheet Bases, Assumptions, and Requirements* (24590-WTP-RPT-PT-02-005 Rev, 8), which has 58.33% single pass incorporation. The combination of no returns to the Tank Farms and higher first pass incorporation now projects 96.2% of the iodine will be incorporated into VLAW. See Responses to RAI 1-2 and RAI 2-17 (which incorporates the updated modeling assumptions).

References

24590-WTP-RPT-PT-02-005, 2016, *Flowsheet Bases, Assumptions, and Requirements*, Rev. 8, Bechtel, River Protection Project, Waste Treatment Plant, Richland, Washington.

DOE/ORP-2020-01, 2020, *Draft Waste Incidental to Reprocessing Evaluation for Vitrified Low-Activity Waste Disposed Onsite at the Hanford Site, Washington*, U.S. Department of Energy, Office of River Protection, Richland, Washington.

IDF-00002, 2019, *Waste Acceptance Criteria for the Integrated Disposal Facility*, Rev. 0, CH2M HILL Plateau Remediation Company, Richland, Washington.

RPP-ENV-58562, 2016, *Inventory Data Package for the Integrated Disposal Facility Performance Assessment*, Rev. 3, Washington River Protection Solutions, LLC, Richland, Washington.

RPP-RPT-57991, 2019, *River Protection Project Integrated Flowsheet*, 24590-WTP-RPT-MGT-14-023, Rev. 3, Washington River Protection Solutions, LLC, Richland, Washington.

WHC-SD-WM-TI-699, 1996, *Technical Basis for Classification of Low-Activity Waste Fraction from Hanford Site Tanks*, Rev. 2, Westinghouse Hanford Company, Richland, Washington.

WT-ST-056, 2007, *Mass Balance Revision, 17546 Revision of PCAL 17284-2 Mass Balance*, Rev. 2, Columbia Energy & Environmental Services, Inc., Richland, Washington.

4.0   RADIONUCLIDE INVENTORY AND RELEASE RATES

RAI 2-1 (Scope of PA Compared to Scope of Draft WIR Evaluation)

Comment
The results from the PA that are directly applicable to the scope of the draft WIR evaluation are not clear. One factor could have been the timing of the completion of the PA and draft WIR evaluation.

Basis
The performance assessment was completed before the draft WIR evaluation. The performance assessment was completed in 2018 while the draft WIR evaluation was completed in 2020. Although DOE evaluated a number of different scenarios associated with waste volumes and the fraction of key radionuclides that would end up in different waste streams, the translation of the PA results to the scope of the draft waste evaluation is not clear. The inventory in the PA was larger and encompasses the smaller inventory associated with DFLAW. For example, in the PA, DOE evaluated disposal of 130,000 canisters of vitrified waste whereas the DFLAW approach is estimated to generate 13,500 canisters. The impacts associated with some wastes do not scale linearly with volume or radioactivity. Intruder impacts generally scale linearly with activity whereas impacts to an offsite intruder through all-pathways generally scale linearly with volume. In order to properly risk-inform the review process, the baseline results are needed consistent with assumptions in the draft waste evaluation.

DOE did not include secondary wastes generated as part of waste processing within the scope of the draft waste evaluation. However, as discussed previously, if significant fractions of key radionuclides are separated or partitioned as a result of waste processing (e.g. volatilization) and those radionuclides are ultimately disposed as non-HLW then those waste streams would be within the scope of the evaluation according to NRC practice and regulation. The cumulative impact of all radioactive material disposed of at IDF needs to be considered when evaluating the performance objectives of 10 CFR Part 61.

Path Forward
Please ensure that the cumulative impact of all radioactive material disposed of at IDF is considered when evaluating the performance objectives of 10 CFR Part 61, including the doses resulting from the DFLAW inventory and the associated secondary wastes generated from processing the DFLAW inventory. If significant portions of key radionuclides end up in processing components, such as the off-gas system and those components are disposed as non-HLW, then they should be included in the results. Please also provide the waste classification results for all relevant waste streams and a demonstration that those streams will be incorporated into a solid physical form.

DOE Response
The Draft WIR Evaluation focuses on the separated and pretreated LAW that has been pretreated using the DFLAW approach and vitrified (VLAW), as explained in the Draft WIR Evaluation and DOE's Response to NRC's Introductory Statement Related to Secondary Waste. The

following information is provided for additional information and completeness, outside the scope of the Draft WIR Evaluation.

To bound the analysis and provide the "cumulative impact" of all waste potentially disposed in the IDF, the IDF PA correctly analyzes all LLW that potentially may be disposed of at the IDF, including VLAW and secondary waste, for compliance with performance objectives and performance measures, as discussed in the IDF PA.

It bears emphasizing that the IDF is planned to receive LLW generated from a variety of sources as analyzed in the IDF PA, including: DFLAW approach-generated VLAW, additional VLAW from continued Hanford Waste Treatment and Immobilization Plant (WTP) LAW Vitrification Facility operation, assumed potential supplemental VLAW[27], VLAW glass melters, and solid secondary waste (SSW) generated by routine WTP operations and other site operations. Additional waste streams would be generated that are not a result of the WTP process, including encapsulated Fast Flux Test Facility (FFTF) decommissioning debris waste, encapsulated secondary waste management waste, and encapsulated onsite non-CERCLA[28] non-tank debris LLW. WTP processing components are not planned to be disposed in the IDF other than maintenance-related items.[29]

The secondary waste that will be generated by, or derived from, the off-gas system associated with the vitrification of the pretreated LAW using the DFLAW approach will not contain significant quantities of key radionuclides. Per RPP-CALC-63643 Rev. 4, approximately 1% of the total key radionuclides after pretreatment during the DFLAW approach will be in such secondary waste, with approximately 4% of the ^{129}I and approximately 2% of the ^{99}Tc in SSW. See also RAI 1-2 response.

All LLW, including secondary waste, disposed at the IDF will be properly characterized and classified, will undergo applicable treatment, and must be compliant with IDF-00002, which requires solid waste forms for disposal. Additionally, wastes emplaced in the IDF must meet the *Washington Administrative Code* 173-303-140, "Land Disposal Restrictions," which only allows wastes not containing free liquids in a landfill.

---

[27] Information concerning potential supplemental LAW treatment is provided in the IDF PA and, by reference, in this RAI response for additional information and completeness, and is outside the scope of both the Draft WIR Evaluation and DOE decisions concerning supplemental LAW treatment. DOE has not made decisions concerning the potential path forward for supplemental LAW treatment, as explained in footnote 7 of the Draft WIR Evaluation and 78 FR 75913, "Record of Decision: Final Tank Closure and Waste Management Environmental Impact Statement for the Hanford Site, Richland, Washington". As explained in section 1.2 of the Draft WIR Evaluation, the Draft WIR Evaluation does not address or include in its scope supplemental LAW. To bound the IDF PA analysis, the IDF PA assumed that supplemental LAW may potentially be vitrified and disposed of in the IDF, although, as explained above, DOE has made no decisions concerning the potential path forward for supplemental LAW treatment. Changes to the actual disposed inventory of LLW assumed in the IDF PA will be appropriately evaluated through PA revisions or Supplemental Analysis per the PA maintenance and change control program.

[28] *Comprehensive Environmental Response, Compensation, and Liability Act of 1980*, 42 USC 9601 et seq.

[29] No decision has been made as to where WTP equipment will be disposed upon its mission completion and are not included in the IDF PA.

Radionuclides will be identified as required in 24590-WTP-ICD-MG-01-003, *ICD 03 - Interface Control Document for Radioactive Solid Waste*, Section 3.3.1.2, which states:

"The WTP Contractor shall characterize RSW[30] streams to:

1. Determine the physical characteristics and chemical characterization of the waste with sufficient accuracy and detail to properly designate and manage waste in accordance with state and federal regulations, and

2. Ensure the requirements for major radionuclides and the concentration of each major radionuclide are established with sufficient sensitivity and accuracy to properly classify and manage the waste as required by DOE M 435.1-1.

3. Ensure all RSW streams being transported to applicable Treatment, Storage, and Disposal (TSD) facility(s) are certified in accordance with DOE M 435.1-1."

References

10 CFR 61, "Licensing Requirements for Land Disposal of Radioactive Waste," *Code of Federal Regulations,* as amended.

24590-WTP-ICD-MG-01-003, 2019, *ICD 03 - Interface Control Document for Radioactive Solid Waste*, Rev. 7, Bechtel, River Protection Project, Waste Treatment Plant, Richland, Washington.

78 FR 75913, 2013, "Record of Decision: Final Tank Closure and Waste Management Environmental Impact Statement for the Hanford Site, Richland, Washington," *Federal Register*, Vol. 78, pp. 75913–75919 (December 13).

Comprehensive Environmental Response, Compensation, and Liability Act of 1980, 42 USC 9601 et seq.

DOE M 435.1-1, 2011, *Radioactive Waste Management Manual*, Change 2, U.S. Department of Energy, Washington, D.C.

DOE/ORP-2020-01, 2020, *Draft Waste Incidental to Reprocessing Evaluation for Vitrified Low-Activity Waste Disposed Onsite at the Hanford Site, Washington*, U.S. Department of Energy, Office of River Protection, Richland, Washington.

IDF-00002, 2019, *Waste Acceptance Criteria for the Integrated Disposal Facility*, Rev. 0, CH2M HILL Plateau Remediation Company, Richland, Washington.

RPP-CALC-63643, *Sum of Fractions Calculations for DFLAW Immobilized LAW Glass*, Rev. 4, Washington River Protection Solutions, LLC, Richland, Washington.

WAC 173-303-140, "Land Disposal Restrictions," *Washington Administrative Code*, as amended.

---

[30] Radioactive Solid Waste (RSW).

RAI 2-2 (Model Support for the Performance Assessment)

Comment
Additional information is needed related to demonstrate whether the conceptual and numerical models used in the performance assessment (PA) were adequately supported over the range of projected future conditions.

Basis
DOE used performance assessment modeling to integrate the results of process models and other numerical representations. The resultant system-level model was developed with the GoldSim software package. The system model was used to transfer information between models, to propagate uncertainties, and to integrate the results. The performance assessment modeling represented the present-day IDF and was used to estimate the releases of radioactivity to the environment for thousands of years into the future. Though performance assessment models cannot be validated in the traditional manner of other numerical models, performance assessment models must have adequate support of the results for the models intended purpose.

DOE presented the information used to develop the modeling in the PA report (RPP-RPT-59958, Rev. 1, 2018). The PA report was very extensive. Technical studies have been completed for decades at the Hanford site on a wide range of topics (e.g., infiltration, waste release, hydrology). Though studies have been completed to evaluate the performance of systems (e.g., engineered cover performance, unsaturated zone hydrology) and other studies are planned (e.g., glass lysimeter studies), most of the technical work has been used to develop parameter values for input to the various models, rather than to develop confirmatory information supporting the results of the PA models or the underlying conceptual models. DOE provided limited support that the conceptual models were implemented appropriately with the numerical models in the PA or that the model projections would likely bound anticipated impacts.

The IDF in its current configuration has been in existence for almost 15 years, with initial construction completed much earlier. DOE has completed numerous iterations of performance assessment calculations over the years, with the current calculations being performed prior (2018) to the recent WMA-C performance assessment that NRC reviewed (2019). In the IDF PA, DOE could not incorporate lessons learned or address recommendations made by NRC on WMA-C, one of which was for increased model support. Model support is an essential element of numerical modeling, especially of complex systems. Key intermediate results of the PA modeling include, but are not limited to, the secondary minerals that form during glass corrosion, the amount of water that contacts the wasteforms (capillary effects included), the transport time of radionuclides to the underlying aquifer, and the amount of dilution in the aquifer. Support should be provided for the key intermediate results of the numerical modeling. For example, on page 3-170 of the PA document a discussion of groundwater contaminants on the Central Plateau is provided. One of those contaminants listed is ^{90}Sr. The PA model, with appropriate changes to inputs to represent operating conditions, should be able to produce a travel time of ^{90}Sr to the water table in the approximately 40 years that was observed. It isn't clear that the existing model could generate the observed result, suggesting some aspect of infiltration, geology and properties of the unsaturated zone, unsaturated zone hydrology, or unsaturated zone geochemistry may not

be appropriate. The potential non-uniqueness of calibrated inputs places greater importance on confidence-building activities.

Because of the importance of model support to the decision-making process, a dedicated plan, strategy, and document summarizing model support for the VLAW PA could enhance confidence that the numerical models adequately project or bound future impacts.

Path Forward
Please provide a summary of model confidence-building activities for the VLAW PA model or provide DOE's strategy and plan for future verification activities that are anticipated to be completed. Describe activities that have been included in the PA maintenance plan. Complete modeling with the PA model used for the VLAW PA that shows that transport of ^{90}Sr to the aquifer can be generated in the modeling results under reasonable historical operating conditions.

DOE Response
The models used in the calculations used in the IDF PA have been supported by intermediate results of the numerical modeling as identified in the basis for RAI 2-2 as well as other model confidence-building activities. Additional model confidence-building studies have been identified and included in the IDF Maintenance Plan (CHPRC-03348, *Performance Assessment Maintenance Plan for the Integrated Disposal Facility*). This response is organized into the following topics:

- Summary of model confidence-building activities

- Summary of intermediate results of numerical modeling:

    o Secondary minerals formed during glass corrosion
    o Water contacting waste forms
    o Radionuclide transport time in the vadose zone
    o Transport of ^{90}Sr in the vadose zone
    o Dilution in the saturated zone

- Summary of maintenance activities planned to verify the representativeness of models.

Summary of Model Confidence-Building Activities
The confidence-building activities conducted for the component models used in the IDF PA are summarized in the model package reports (MPRs) developed as part of the implementation of the quality assurance program. For each of the component models (i.e., [i] the near-field hydrology model, [ii] the VLAW glass release model, [iii] the cementitious waste release model, [iv] the vadose zone flow and transport model, [v] the saturated zone flow and transport and [vi] the receptor dose model), an important part of the model confidence-building activities was to compare the model assumptions and predictions developed in the 2017 IDF PA to model assumptions and predictions developed in previous analyses that had been subject to regulatory review and acceptance, importantly including those developed in the Tank Closure and Waste Management Environmental Impact Statement (TC&WM EIS, DOE/EIS-0391, *Final Tank*

Closure and Waste Management Environmental Impact Statement for the Hanford Site, Richland, Washington).

The process of developing model confidence in the IDF PA models by comparison with the models developed and used as part of the TC&WM EIS analysis started with the scoping meetings held with stakeholders that are summarized in Section 2.5.4 of RPP-RPT-59958. The proposed modeling approach and model assumptions eventually adopted for the IDF PA is based in part on the TC&WM EIS modeling approach and assumptions, and the general regulatory acceptance of the adequacy of TC&WM EIS for its intended purpose. Of particular note are observations made by the Washington State Department of Ecology (Ecology) in the forward to DOE/EIS-0391:

> "Ecology understands the methods and formulas used for the waste form release calculations (for all waste types). *After reviewing the analysis approaches and contaminant release results for the waste forms identified above, Ecology agrees with most of the approaches used.* The one area where Ecology has concerns is the steam reforming waste form release rates. Based on the limited test data available, the results in this final EIS may overestimate the contaminant retention in the steam reforming waste form." (Ecology forward to DOE/EIS-0391, emphasis added)

> "This *Final TC & WM EIS* uses the STOMP [Subsurface Transport Over Multiple Phases][31] modeling code for vadose zone modeling. *Based on its current review, Ecology believes that the Hanford parameters used with this code are adequate for the purposes served by this EIS.* Ecology notes that the TC & WM EIS STOMP modeling code parameters are based on a regional scale and may need to be adjusted for site-specific closure decisions or other Hanford assessments. Use of STOMP in other assessments requires careful technical review and consideration of site-specific parameters. Ecology supports the process that DOE used for the Waste Management Area C performance assessment workshops in determining appropriate site-specific parameters[32]. These workshops included a broad level of participation with other agencies, tribal nations, and stakeholders." (Ecology forward to DOE/EIS-0391, emphasis added)

In addition to the above areas of agreement, Ecology noted several areas of further agreement in its forward to DOE/EIS-0391, including:

- Overall modeling approaches for vadose zone and groundwater.
- Release mechanisms for contaminants from various waste forms.

---

[31] Subsurface Transport Over Multiple Phases (STOMP) has been developed and distributed by Battelle Memorial Institute, Richland, Washington.

[32] The process used in the Waste Management Area C PA workshops in determining appropriate site-specific parameters was the same as the process adopted in the IDF PA workshops summarized in Section 2.5.4 of RPP-RPT-59958.

Ecology's forward to the TC&WM EIS noted that "Ecology's agreement on these issues and parameters is specifically for the purposes of this *Final TC & WM EIS* and is based on Ecology's current knowledge and best professional judgment". As a result, the planning, scoping and implementation process used in the development of the 2017 IDF PA (summarized in Section 2.1.2 of RPP-RPT-59958) included stakeholder workshops where potential changes to the models, assumptions and parameters to be used in the 2017 IDF PA were discussed. Comparisons between the models and assumptions used in the 2017 IDF PA and the TC&WM EIS are summarized in Section 2.5.4 and Tables 2-8 and 2-9 of RPP-RPT-59958. The results of the 2017 IDF PA calculations and TC&WM EIS are compared in Section 8.3 of RPP-RPT-59958.

Summary of Intermediate Results of Numerical Modeling

In part, model confidence is provided by the comparison of models and assumptions with previously developed and reviewed models and assumptions, including the TC&WM EIS models. Model confidence (i.e., model support) is further provided by comparing the numerical modeling intermediate results to relevant observations. Examples of these comparisons are summarized below.

Secondary Minerals Formed During Glass Corrosion

As noted in the basis for RAI 2-2, one of the key intermediate results to which the IDF PA models could be compared relates to the secondary minerals formed during glass corrosion. Model support for the selection of the base-case secondary mineral reaction network (SMRN) adopted in the PA is described in PNNL-21812, *Integrated Disposal Facility FY 2012 Glass Testing Summary Report* and references cited therein. For example, a geochemical model was used in those investigations to infer the existence of secondary minerals that formed in Product Consistency Tests (PCTs) at 90 °C. This confirmatory identification is based on comparisons between model predictions with observed changes in solution chemistry as a function of an assumed amount of glass corrosion. This provided guidance for the selection of the SMRN adopted in the IDF PA to simulate glass corrosion and calculate fractional release rates (FRRs). In addition, research studies conducted at Pacific Northwest National Laboratory (PNNL) and the Vitreous State Laboratory (VSL) use different techniques (e.g., x-ray diffraction, scanning electron microscopy, and energy dispersive X-ray spectroscopy) to identify the secondary minerals that are formed during the corrosion experiments.

A related confidence-building activity in the IDF PA involved comparisons of calculated FRRs from the glass waste forms that were calculated using both The Geochemist's Workbench®[33] (GWB) and STOMP. Several sensitivity cases defined by different initial and boundary conditions in the disposal facility were used for these comparisons. The GWB and STOMP models are independent insofar as to how time is treated differently in the two modeling approaches (based on residence time versus absolute time, respectively). In all other ways, they share a common conceptual and parameter basis. There is general good agreement obtained between GWB and STOMP results. This agreement enhances confidence that the complex reactive-transport processes controlling fractional releases from VLAW glass are being simulated in a consistent manner in the two modeling approaches over the range of initial and boundary conditions considered in the different sensitivity cases.

---

[33] The Geochemist's Workbench® is a registered trademark of Aqueous Solutions LLC, Champaign, Illinois.

Water Contacting Waste Form

The RAI basis notes that it may be possible to use the intermediate result of the water contacting the waste form to support the model confidence. The IDF PA assumed that all the water that percolates through the surface cover enters the waste trenches and can contact the waste form. The waste release models assume that some fraction of the water seeping through the backfilled trenches can enter the fractured ILAW glass, grouted SSW or Effluent Treatment Facility (ETF)-liquid secondary waste (LSW) waste forms depending on the hydraulic characteristics of the waste form. The remaining fraction of the percolating water is assumed to flow in the backfill around the waste forms. There are no direct observations of the moisture content in the waste form or backfill with which to compare the model predicted values. Because there is uncertainty in the hydraulic characteristics of the waste forms and the backfill, sensitivity analyses were conducted to determine the extent to which the water contacting the waste impacted the release rates and associated performance. Additional sensitivity analyses are conducted as part of the response to RAI 2-12.

Vadose Zone Transport

Support for the natural system models used in the IDF PA is possible using different observations of fate and transport of water and contaminants in the vadose zone and saturated zone in the Central Plateau of the Hanford Site. One such comparison is that of observed and predicted ^{99}Tc concentrations associated with releases from a past tank leak in the 241-C Tank Farm documented in RPP-RPT-59197, *Analysis of Past Tank Waste Leaks and Losses in the Vicinity of Waste Management Area C at the Hanford Site, Southeast Washington*. The comparison was used as a basis for updating the activity of ^{99}Tc released from the tank leak and confirming that the results of the vadose zone fate and transport model ^{99}Tc released could predict ^{99}Tc transport time to the water table in the decades following the release event. The vadose zone fate and transport model for the 241-C Tank Farm is similar to that adopted for the IDF PA documented in RPP-RPT-59958.

Comparisons of observed and predicted vadose zone transport have also occurred in areas of past discharge of liquid wastes to cribs and trenches in the Central Plateau. For example, comparisons of observed and model-predicted ^{99}Tc concentrations near the BC cribs and trenches have been documented in PNNL-14907, *Vadose Zone Contaminant Fate-and-Transport Analysis for the 216-B-26 Trench*. While the one-dimensional (1-D) vadose zone flow and transport model used in PNNL-14907 is not the same as that adopted in the 2017 IDF PA, it uses similar assumptions of vadose zone hydraulic and transport properties.

Observed contaminant migration in areas of past liquid discharge can also provide partial support for the vadose zone fate and transport models used in the 2017 IDF PA. However, it is important to caveat that general conclusion by recognizing that the vadose zone flow regime beneath past liquid discharge sites is characterized by focused high volumes of liquid discharged as well as background net infiltration rates that are much greater than the long-term average steady-state recharge rate in the area near the IDF.[34]

---

[34] Many liquid discharge events occurred during past practices in the Central Plateau of the Hanford Site. These discharge events range from volumetric discharge events of thousands to millions of cubic meters of liquid waste applied over periods of years to decades to areas of 100's to 1,000's of m². A common way of characterizing

The moisture content predicted using the vadose zone flow and transport model is another example of an intermediate result that can be used to support the model. The moisture content of sediments in the vadose zone has been measured in boreholes drilled in undisturbed and disturbed surface areas near the IDF. Comparisons of observed and predicted vadose zone moisture contents in undisturbed and disturbed areas near the IDF are presented in the response to RAI 2-15.

Transport of Strontium-90 in the Vadose Zone
The basis for RAI 2-2 notes the following example of the type of model support that may be possible with the vadose zone component of the IDF PA model:

> "The PA model, with appropriate changes to inputs to represent operating
> conditions, should be able to produce a travel time of 90Sr to the water table in
> the approximately 40 years that was observed. It isn't clear that the existing model
> could generate the observed result, suggesting some aspect of infiltration, geology
> and properties of the unsaturated zone, unsaturated zone hydrology, or
> unsaturated zone geochemistry may not be appropriate."

The hypothesis that the vadose zone model should be able to produce transport times for ^{90}Sr of about 40 years to reproduce the observed ^{90}Sr concentrations in the groundwater illustrated in Figure 3-93 on page 3-170 of RPP-RPT-59958 is not unreasonable. The proposed path forward suggested in the RAI to use the PA model to show that the transport of ^{90}Sr is reasonable given assumed historic operating conditions is also not unreasonable.

Strontium-90 contamination in the groundwater in the 200 East Area of the Central Plateau is observed at two discrete locations in the saturated zone illustrated in Figure 3-93 of RPP-RPT-59958. It is reasonable to presume that the source of this observed contamination in the saturated zone is the result of ^{90}Sr released to the vadose zone from past waste disposal practices and subsequent transport of ^{90}Sr through the vadose zone to the water table. If that were the case, then one would expect that the vadose zone fate and transport model used for the IDF PA, with appropriate changes to represent the different ^{90}Sr source inventory and liquid volume discharged, should be able to reproduce the timing and magnitude of ^{90}Sr flux to the water table that would generate the observed ^{90}Sr plume in the underlying saturated zone. There are several reasons why such a comparison would be uncertain, including the uncertainty in the inventory of ^{90}Sr released and liquid volume discharged. As summarized below, the explanation for the observed ^{90}Sr plumes in the 200 East Area is not consistent with a solid waste disposal

---

these events is the use of the "pore volume" concept, where one pore volume is equal to the volume of liquid waste discharged divided by the footprint area of the discharge site divided by the pore volume of the sediments between the base of the discharge site and the water table (see for example ECF-200EA1-17-0066, *Pore Volume Calculation – 200-EA-1 Operable Unit Liquid Waste Disposal Sites,* Rev. 1). Pore volumes that range from less than one to over 1,000 are common at discharge sites in the Central Plateau. Given that the discharge events commonly occur within a single year, a pore volume of 1.0 corresponds to a net infiltration (or recharge) rate of about 35 m/yr (given a vadose zone thickness of about 100 m and a porosity of about 0.35), a factor 10,000 times greater than the long-term average steady-state recharge rate of 3.5 mm/yr beneath the IDF liner system assumed in the IDF PA. While the vertical Darcy flux associated with the liquid discharge events dissipates with depth in the vadose zone, the different recharge conditions between liquid discharge sites and the IDF need to be considered in any comparisons of model predictions with observed vadose zone contamination.

scenario, so the fate and transport of ^{90}Sr in the vadose zone developed for a covered solid waste disposal facility placed several hundred feet above the aquifer is not likely to reproduce the observed plumes.

The details of the observed ^{90}Sr plume are summarized in DOE/RL-2019-66, *Hanford Site Groundwater Monitoring Report for 2019* (Section 9.6) which explains the source of the two ^{90}Sr plumes observed in the 200-BP-5 Operable Unit of the Central Plateau as follows.

> "Strontium-90 exceeds the 8 pCi/L DWS *[drinking water standard]* near the former Gable Mountain Pond (inactive and dry since the mid- to late 1980s) and near the 216-B-5 reverse well (Figure 9-19 *[reproduced here as Figure 2-2-1]*). About 179 Ci of strontium-90 was discharged to Gable Mountain Pond, with most of it associated with the 1964 PUREX Plant unplanned release (UPR-200-E-34)[35]. About 7.5 Ci of strontium-90 were injected into the 216-B-5 reverse well between 1945 and 1947[36]. Because strontium-90 tends to bind to vadose zone sediments, it reached groundwater only at locations where the vadose zone is relatively thin (e.g., <12 m [39 ft] at Gable Mountain Pond) or where waste was injected into the aquifer (216-B-5 reverse well).
>
> …
>
> The strontium-90 plume exceeding the DWS beneath the eastern half of the former Gable Mountain Pond is located within a thin narrow saturated channel of Hanford formation gravels bounded by the Ringold mud unit and Elephant Mountain basalt.
>
> …
>
> Well 699-53-47B has historically had the highest strontium-90 concentration and continued to have the highest concentration in 2019 (Figure 9-20 *[reproduced here as Figure 2-2-2]*). Strontium-90 at well 699-53-47B has ranged between 220 and 281 pCi/L since 2012, with an average concentration of 250 pCi/L. In 2019, the strontium-90 concentration at well 699-53-47B was 262 pCi/L. The stable strontium-90 concentrations at well 699-53-47B, indicating a continuing source of contamination, may be present from the vadose zone.
>
> Farther west at well 699-54-49, located beneath the central portion of the former Gable Pond, the strontium-90 concentration has declined from 180 to 158 pCi/L between 2012 and 2019 (Figure 9-20 *[reproduced here as Figure 2-2-2]*). The decline in concentration is consistent with radioactive decay. The Hanford

---

[35] The ^{90}Sr inventory of 179 Ci discharged to the Gable Mountain Pond reported in DOE/RL-2019-66 is based on SIM-v1 (RPP-26744, *Hanford Soil Inventory, Rev. 1*) which assumed the ^{90}Sr was decayed to January 1, 2001. Most of the ^{90}Sr inventory is related to the discharge of about 59 Ci of liquid and 367 Ci of entrained solids in 1964 (activity decayed to the 1964 discharge date) with about 1.2×10^7 m^3 of liquid waste [ECF-HANFORD-17-0079, *Hanford Soil Inventory Model (SIM-v2) Calculated Radionuclide Inventory of Direct Liquid Discharges to Soil in the Hanford Site's 200 Areas*, Appendix E].

[36] The ^{90}Sr inventory of 7.5 Ci discharged to the 216-B-5 reverse well reported in DOE/RL-2019-66 is based on SIM-v1 (RPP-26744) which assumed the ^{90}Sr was decayed to January 1, 2001. The reported injection of liquid waste to the 216-B-5 reverse well in the current version of SIM-v2 (ECF-HANFORD-17-0079) is 9,180 m^3 and 7.0 Ci in 1945, 13,700 m^3 and 10.4 Ci in 1946 and 9,180 m^3 and 10.3 Ci in 1947 (inventory decay corrected to the discharge dates).

formation gravel aquifer thickness at this well is approximately 3.7 m (12 ft), or twice as thick as beneath the east end of Gable Mountain Pond.

Near the western end of the former Gable Mountain Pond at well 699-55-50C, the aquifer thickness is estimated at 12 m (39 ft), and strontium-90 concentration continues to be less than detection (Figure 9-20 *[reproduced here as Figure 2-2-2]*). Well 699-52-55, located 1.4 km (0.87 mi) west of Gable Mountain Pond, also has detectable strontium-90 (14 pCi/L in 2019). The source of contamination is not currently known.

Five wells (299-E28-2, 299-E28-7, 299-E28-23, 299-E28-24, and 299-E28-25) define the strontium-90 plume near the former 216-B-5 reverse well. Wells 299-E28-2 and 299-E28-7 define the northwest and southeast portion of the plume, respectively. Well 299-E28-2 is currently upgradient of the 216-B-5 reverse well, but prior to 2011 it was downgradient. Well 299-E28-7 is currently downgradient of the 216-B-5 reverse well. Strontium-90 concentrations continue to decline at all five wells faster than the decay rate (Figure 9-21 *[reproduced here as Figure 2-2-3]*). The highest strontium-90 concentration in 2019 was at well 299-E28-24, located <4 m (13 ft) downgradient from the former 216-B-5 reverse well, with a concentration of 337 pCi/L. Strontium-90 concentrations at downgradient well 299-E28-4, located 290 m (950 ft) from well 299-E28-7, continue to be less than detection."

In summary, the ^{90}Sr groundwater plumes are not the result of transport through a thick vadose zone, such as exists beneath the IDF, but instead are the result of two discrete sources, the Gable Mountain Pond (216-A-25) and direct injection in the 216-B-5 reverse well.

Saturated Zone Dilution

The amount of dilution afforded by the saturated zone beneath the IDF is a function of the specific discharge (i.e., the hydraulic conductivity times the hydraulic gradient) with the groundwater regime beneath the IDF. The hydraulic conductivity in the high-conductivity zone beneath the IDF has been inferred from hydraulic tests conducted in this zone to the north of the IDF as well as the calibrated hydraulic properties in the Central Plateau groundwater flow model as summarized in Section 4.4.2.2 of RPP-RPT-59958. Additional information on the hydraulic properties of this zone is summarized in the response to RAI 2-16.

The current model of groundwater flow in the Central Plateau is documented in CP-57037, *Model Package Report: Plateau to River Groundwater Model Version 8.3*, Rev. 2. The current model has hydraulic properties of the high-conductivity zone similar to those used in the 2017 IDF PA, 15,000 m/day vs. 17,000 m/day. The current model has used comparisons of model-predicted and observed plumes of tritium and ^{129}I to support the confidence in the model. Example comparisons of predicted and observed plumes are presented in Figure 2-2-4. While these comparisons provide general support to the flow model in the Central Plateau area of the Hanford Site, they are not resolved sufficiently to provide confidence in the flow regime immediately beneath and downgradient of the IDF. Therefore, additional maintenance activities are planned to confirm the saturated zone model and parameters used in the IDF PA.

Figure 2-2-1. Strontium-90 Plumes in the 200 East Area.
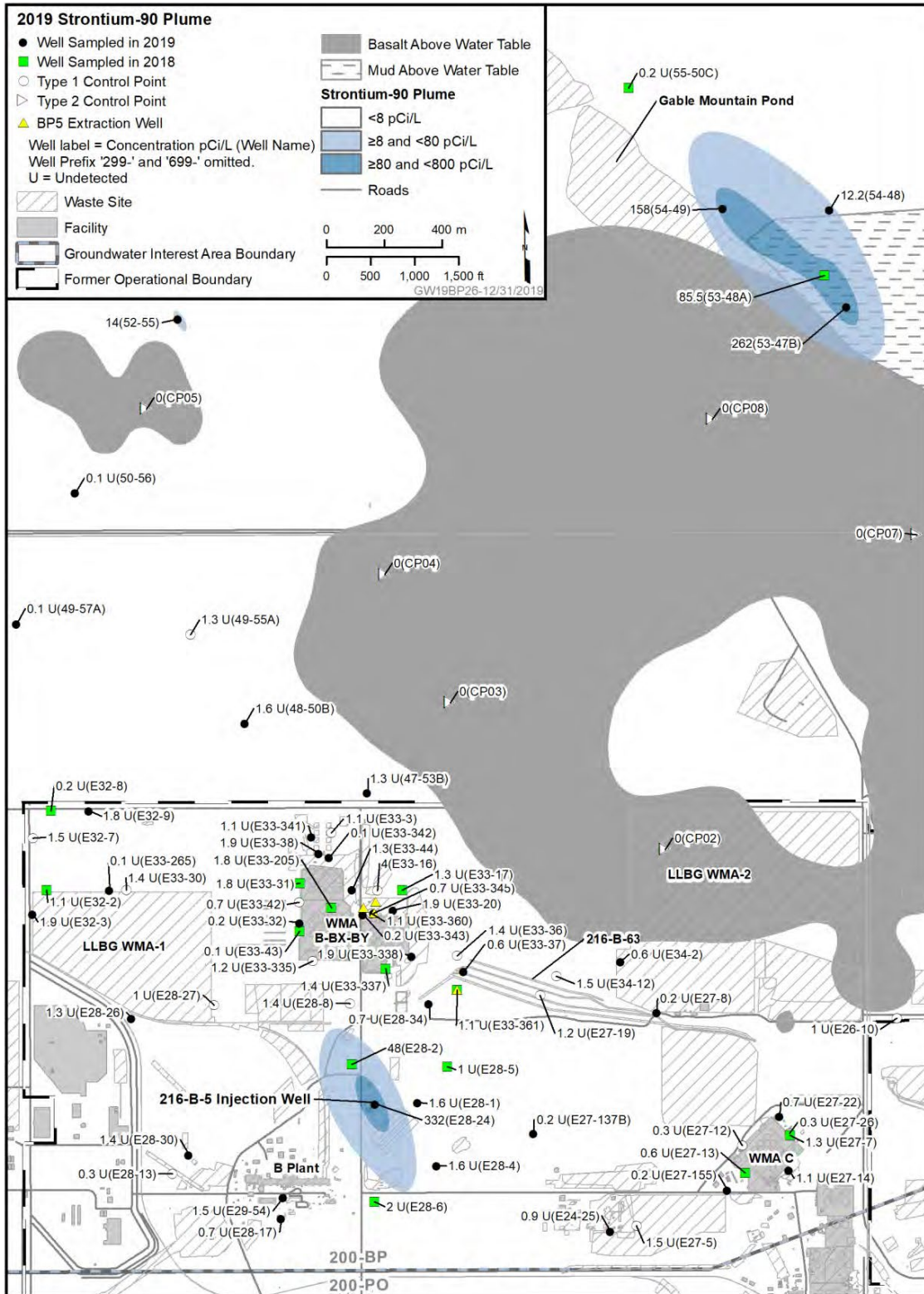
LLBG = low-level burial ground   WMA = waste management area

Source: DOE/RL-2019-66, *Hanford Site Groundwater Monitoring Report for 2019*, Figure 9-19.

Figure 2-2-2. Strontium-90 Concentrations in Wells near the Gable Mountain Pond.
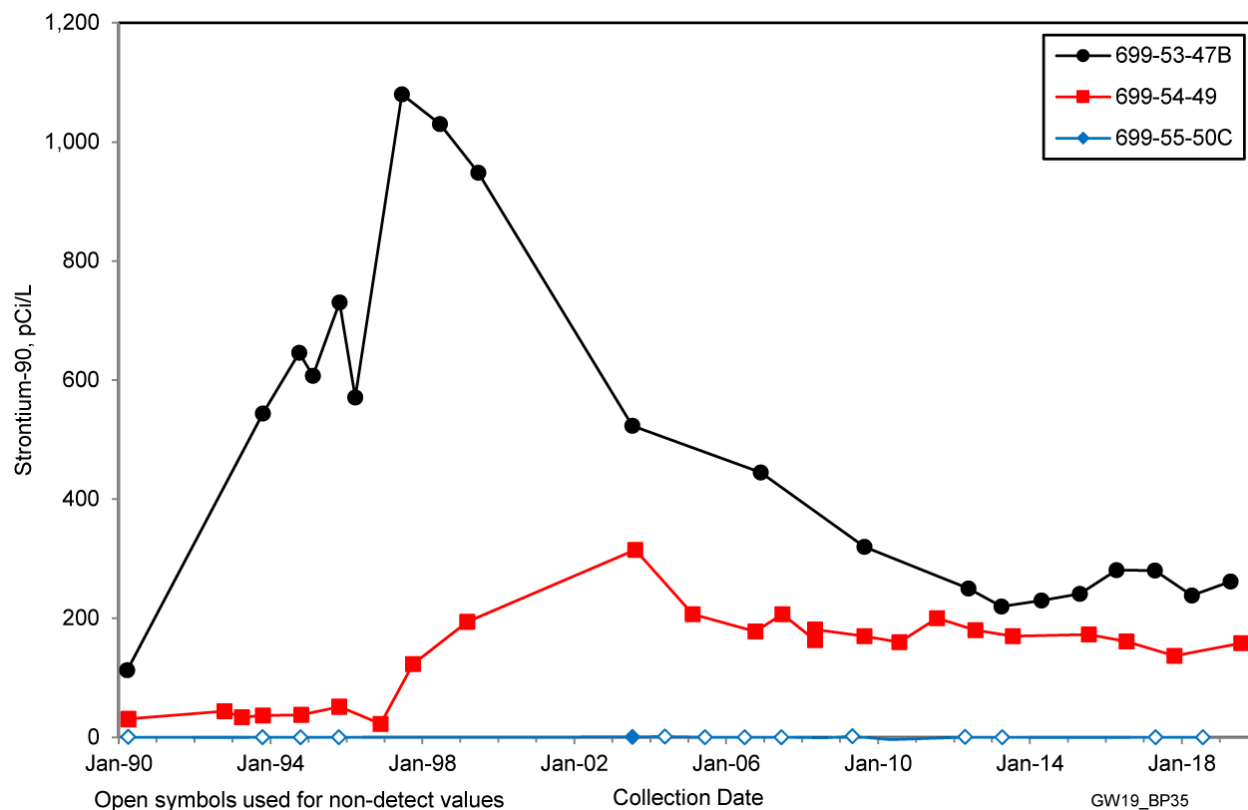
Source: DOE/RL-2019-66, *Hanford Site Groundwater Monitoring Report for 2019*, Figure 9-20.

Note: As reported in DOE/RL-2019-66, the source of the Sr-90 observed in wells near the Gable Mountain Pond was the release of about 179 Ci of Sr-90 to the Gable Mountain Pond (216-A-25). Most of the Sr-90 inventory is related to the discharge of about 59 Ci of liquid and 367 Ci of entrained solids in 1964 (activity decayed to the 1964 discharge date) with about 1.2E07 m^3 of liquid.

Plans for Additional Verification Activities

Subsequent to the development and application of the models used in the IDF PA, additional activities were identified that define DOE's strategy and plan for future verification activities. These activities are presented in the IDF PA Maintenance Plan (CHPRC-03348). The activities identified in the maintenance plan are those developed to confirm and improve the technical basis for the key assumptions made in the IDF PA. The key assumptions and uncertainties are summarized in Section 2.8 and 8.4 of RPP-RPT-59958. The most safety-significant assumptions are summarized in Table 2-2-1 (based on Table 8-6 of RPP-RPT-59958).

Figure 2-2-3. Strontium-90 Concentration in Wells near the 216-B-5 Reverse (Injection) Well.
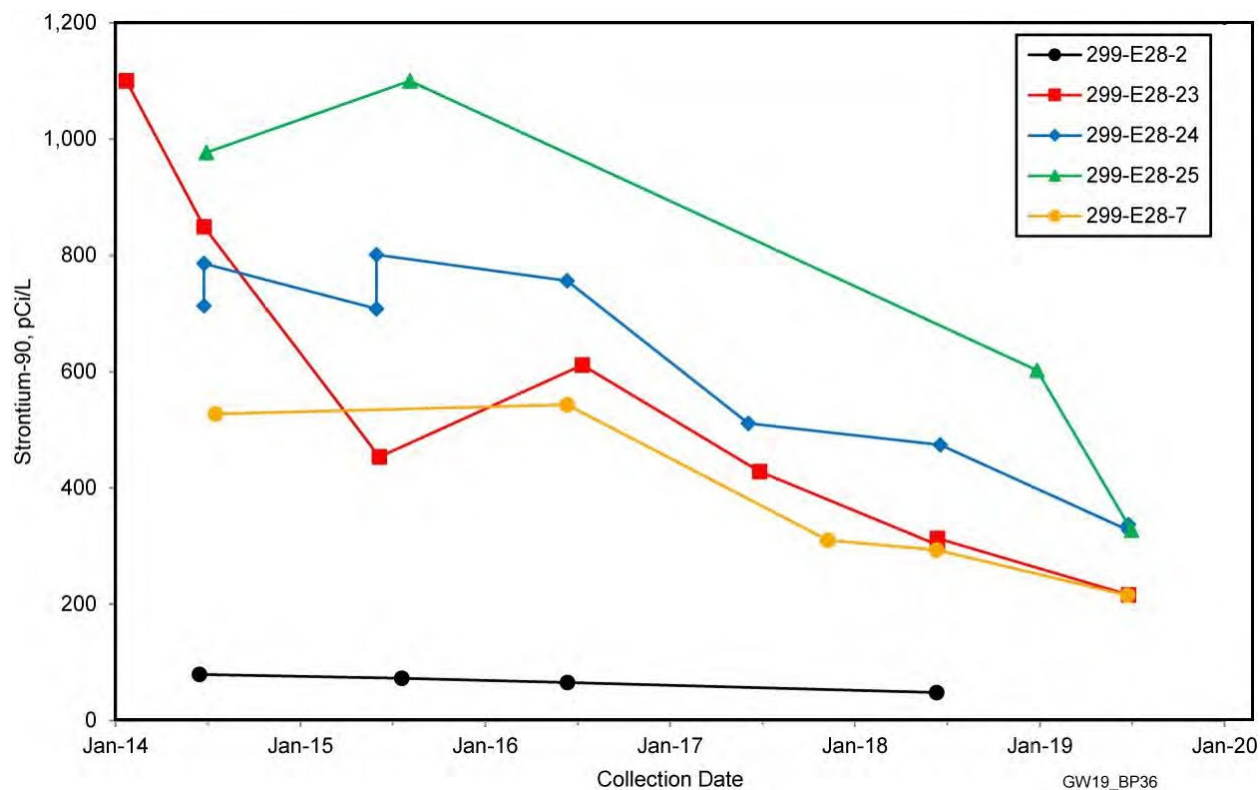
Source: DOE/RL-2019-66, *Hanford Site Groundwater Monitoring Report for 2019*, Figure 9-21.

Note: As reported in DOE/RL-2019-66, about 7.5 Ci of Sr-90 was injected into the 216-B-5 reverse well between 1945 and 1947. The reported value in DOE/RL-2019-66 is based on a decay date of January 1, 2001. The reported injection in the current version of SIM-v2 [ECF-HANFORD-17-0079, *Hanford Soil Inventory Model (SIM-v2) Calculated Radionuclide Inventory of Direct Liquid Discharges to Soil in the Hanford Site's 200 Areas*] is 9,180 m^3 and 7.0 Ci of Sr-90 in 1945, 13,700 m^3 and 10.4 Ci of Sr-90 in 1946 and 9,180 m^3 and 10.3 Ci of Sr-90 in 1947 (inventory decay corrected to the respective discharge dates). The highest observed Sr-90 concentration in 2019 was at well 299-E28-24, located <4 m (13 ft) downgradient from the former 216-B-5 reverse well, with a concentration of 337 pCi/L. The observed Sr-90 concentrations have declined at rates faster than the Sr-90 decay rate due to lateral transport of the Sr-90 plume.

The maintenance activities identified in the IDF PA Maintenance Plan (CHPRC-03348) have been categorized by technical area and then into two groups of research and development (R&D) activities: (1) activities planned to continue the evaluation of assumptions related to the design basis used for the IDF PA and the related scientific studies of waste form and site characteristics and (2) activities planned to conduct focused testing on key assumptions related to the conceptual models and parameter values used in the forecasts of the IDF performance. Several of the R&D activities relate to RAIs identified in the NRC review of the draft WIR evaluation and the IDF PA. A mapping of the planned R&D activities to the NRC RAIs is provided in Table 2-2-2.

Figure 2-2-4. Comparison of Observed and Predicted Tritium and Iodine-129 Plumes.
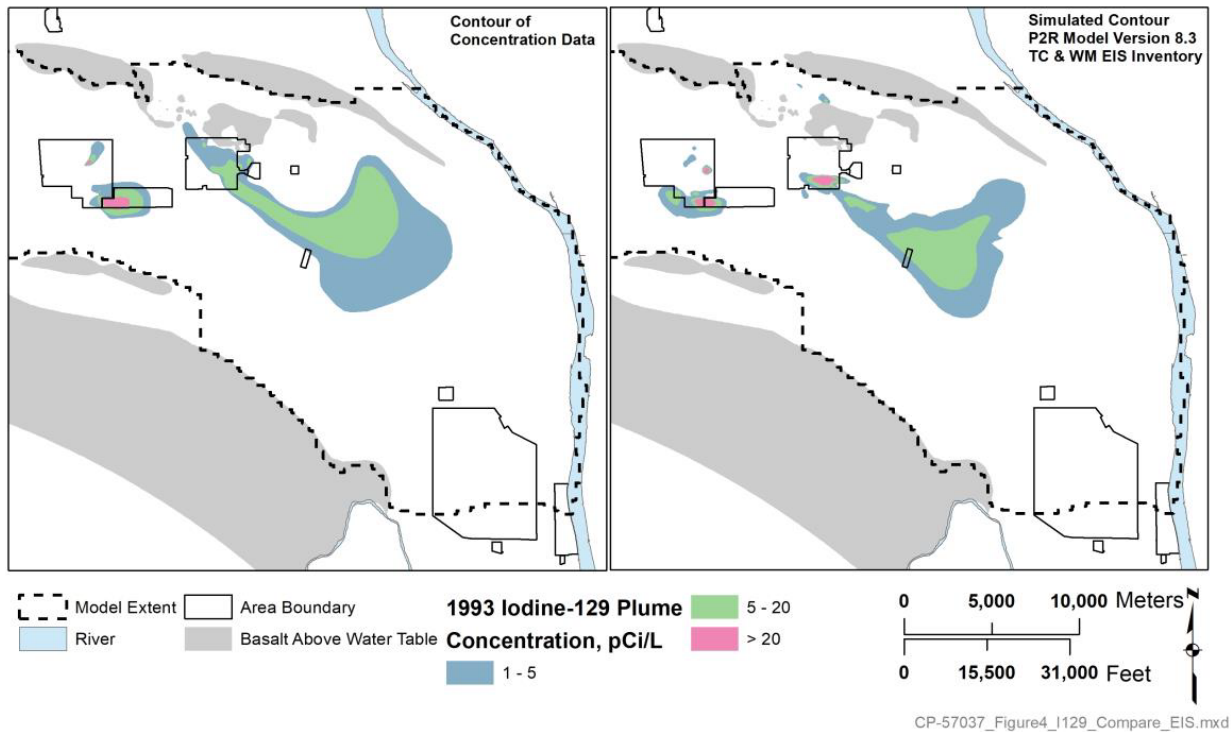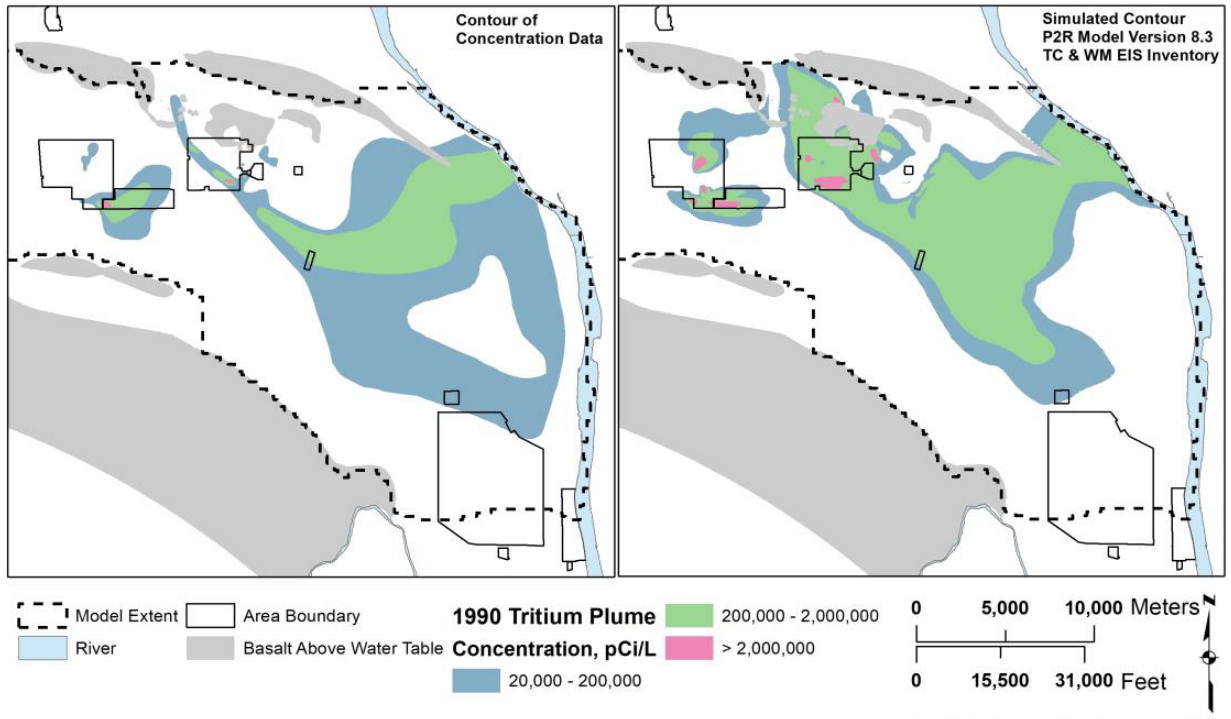
Source: CP-57037, *Model Package Report: Plateau to River Groundwater Model Version 8.3*, Rev. 2 (P2R Model Version 8.3), Figure 4-92 and 4-93.

Note: Simulations assume inventory release based on TC&WM EIS (DOE/EIS-0391, *Final Tank Closure and Waste Management Environmental Impact Statement for the Hanford Site, Richland, Washington*).

Table 2-2-1. Summary of Highly Significant Safety Functions of Features of Engineered and Natural Barriers Assumed in the Integrated Disposal Facility Performance Assessment. (2 sheets)

Barrier – Feature	Safety Function Type	Safety Function Description	Significance
Institutional Control – Natural Environment	Climate – Meteorology	The natural environment in the area is characterized by semi-arid conditions with low annual precipitation and high potential evapotranspiration, which limits the availability of water to infiltrate below the root zone of the native vegetation.	Highly Significant. Recharge to the vadose zone is directly dependent on the semi-arid conditions that exist at Hanford.
Engineered System – Cap and Backfill	Hydraulic – Flow	The final design of the cover has not yet been established but is believed to be able to produce very low initial flow rates. Over some period, this function may deteriorate. The inclined cover functions to divert infiltrating water even after the asphalt layer has degraded.	Highly Significant. The flow rate into the surface barrier equals the recharge rate under the Integrated Disposal Facility (IDF). This recharge rate affects the release rate from cementitious waste forms and controls the transport time though the vadose zone to the water table.
Source Term – Glass Waste Form	Chemical	The chemical properties of the glass limit fractional release rates of constituents of potential concern (COPCs) from the waste form through controls on the overall glass reaction rate resulting from matrix dissolution and hydration (due to alkali-H$^+$ ion exchange).	Highly Significant. The dissolution of glass directly affects the COPC release rate.
Source Term – Cementitious Waste Form	Chemical	The composition of the grout can enhance reducing conditions in the grout, as well as hydraulic characteristics (i.e., paste vs. mortar, cement/water ratio). The hydrochemical conditions of the waste form may create reducing conditions, for which certain COPCs (i.e., ^{99}Tc) show significant sorption capacity or solubility limitations, while others (i.e., ^{129}I) lose sorption capacity or become more soluble.	Highly Significant. The sorption of COPCs on the grout and other substrate materials in the solid secondary waste affect the COPC release rate from cementitious waste forms.
	Transport – Diffusion	The cementitious grouts have low effective diffusion limiting the diffusive transport of COPCs out of the waste form.	Highly Significant. The effective diffusion coefficient affects the COPC release rate from cementitious waste forms.

Table 2-2-1. Summary of Highly Significant Safety Functions of Features of Engineered and Natural Barriers Assumed in the Integrated Disposal Facility Performance Assessment. (2 sheets)

Barrier – Feature	Safety Function Type	Safety Function Description	Significance
Engineered System – Facility and Liner	Hydraulic – Flow	Maintaining low hydraulic conductivity during the operational period allows any COPCs released from waste forms to be retained and removed from sump.	Highly Significant. Lateral flow above the liner which can occur at higher surface barrier infiltration rates can focus the recharge to the vadose zone under the liner, which in turn decreases the COPC transport time to the water table.
Natural Barrier – Vadose Zone	Hydraulic – Flow	The rate of water flow through the vadose zone is slow due to both low net infiltration rate and hydraulic properties of Hanford sand and gravel units, leading to long transport times in the vadose zone.	Highly significant. The flow rate through the vadose zone and the hydraulic properties of the vadose zone materials directly determine whether COPCs released from the IDF will reach the water table (and hence compliance boundary) within 1,000 years.
	Transport – Sorption	Vadose zone materials sorb some of the COPCs, delaying their arrival at the water table. However, several key contaminants are not believed to sorb significantly.	Highly significant. Sorption can significantly delay the arrival of COPCs at the water table and a K_d greater than about 2.0 mL/g can delay arrival by more than 10,000 years.
Natural Barrier – Saturated Zone	Hydraulic – Flow	Advective groundwater flow in the saturated zone leads to contaminant dilution.	Highly significant. The high groundwater flow rate in the saturated Hanford formation significantly dilutes COPCs that reach the water table.

Source: RPP-RPT-59958, *Performance Assessment for the Integrated Disposal Facility, Hanford Site, Washington*, Table 8-6 also repeated in CHPRC-03348, *Performance Assessment Maintenance Plan for the Integrated Disposal Facility*, Table 2-4.

Note: The degree of significance is based on the results of sensitivity analyses using detailed process models described in Section 5.0 of RPP-RPT-59958 as well as sensitivity and uncertainty analyses using the integrated system model described in Sections 6.2 and 6.3, respectively of RPP-RPT-59958.

Table 2-2-2. Integrated Disposal Facility Performance Assessment Maintenance Activities and Related Requests for Additional Information.

Category of Maintenance Activity	Maintenance Plan Activity	Related RAIs
Waste Inventory and inventory allocation (see CHPRC-03348, Section 4.2)	Evaluate the evolution of constituent of potential concern (COPC) inventory based on revisions to tank inventories.	—
	Evaluate the evolution of COPC inventory allocation among different waste forms.	RAI 1-3
	Evaluate the evolution of COPC inventory allocation among different solid secondary waste (SSW) streams.	RAI 2-21
	Evaluate the evolution of plans, including designs, for treatment and disposal of SSW waste streams.	RAI 2-21
	Evaluate the evolution of information related to the waste stream loading efficiency in immobilized low-activity waste (ILAW), Effluent Treatment Facility-liquid secondary waste (LSW) and SSW.	RAI 1-3
Near-Field Chemistry (and effect on ILAW glass dissolution) (see CHPRC-03348, Section 4.3)	Evaluate ongoing studies of pH-buffering controls on ILAW glass corrosion.	—
	Evaluate ongoing studies on effects of steel corrosion on glass corrosion.	—
	Evaluate ongoing studies on microbial effects on glass corrosion.	—
Near-Field Hydrology (see CHPRC-03348, Section 4.4)	Evaluate ongoing studies of Hanford closure cap designs and other closure cap studies in semi-arid environments.	—
	Evaluate ongoing engineering studies supporting the evolution of design and properties of backfill materials.	—
	Evaluate ongoing studies of the properties of the different materials used in liner system.	—
	Evaluate ongoing development of conceptual plans for backfill emplacement.	—
Glass Corrosion and COPC Release (see CHPRC, Section 4.5)	Evaluate ongoing national and international research on glass corrosion mechanisms and rates.	RAI 2-7 RAI 2-8
	Evaluate ongoing national and international research on secondary mineral reaction networks.	RAI 2-12
	Evaluate the potential for Stage III corrosion of ILAW glass under Integrated Disposal Facility (IDF)-relevant environmental conditions.	RAI 2-9
	Evaluate the evolution of glass compositions and loading with enhanced glass formulations.	RAI 2-6 RAI 2-10
	Develop metrics to compare contractual durability test results to data used in glass corrosion models.	RAI 2-7
Cementitious Waste Forms COPC Release (see CHPRC-03348, Section 4.6)	Evaluate ongoing national and international research on grout properties and release models.	—
	Evaluate ongoing international research on natural analogs of cementitious and glass materials.	—
	Evaluate ongoing research on transport characteristics of cementitious materials using accelerated tests to approximate the effects of aging/alteration/weathering –	RAI 2-19

Table 2-2-2. Integrated Disposal Facility Performance Assessment Maintenance Activities and Related Requests for Additional Information.

Category of Maintenance Activity	Maintenance Plan Activity	Related RAIs
Cementitious Waste Forms COPC Release (see CHPRC-03348, Section 4.6) (continued)	Evaluate ongoing research on the effects of getters to enhance retention of key COPCs on cementitious materials.	RAI 2-21
	Evaluate ongoing research on corrosion in highly alkaline environment surrounded by dry backfill.	—
	Evaluate ongoing research on microbial effects on transport processes in cementitious materials.	—
	Evaluate transport characteristics (sorption and diffusion) of cementitious materials exposed to partially saturated conditions for both LSW formulations and SSW formulations.	RAI 2-19 RAI 2-20
	Evaluate bulk (i.e., average) transport properties (notably Kd) of solidified non-debris waste streams, with special focus on the retention of ^{129}I on the granular activated carbon and Ag mordenite substrate materials.	RAI 2-19 RAI 2-20
	Evaluate scale dependency of diffusive properties of paste materials used to encapsulate debris waste, with special focus on the diffusivity of ^{129}I and ^{99}Tc in the encapsulating grout used for the high-efficiency particulate air filter waste stream.	RAI 2-21
Vadose Zone and Saturated Zone Flow and COPC Transport (see CHPRC-03348, Section 4.7)	Evaluate vadose zone model results and parameter values used in ongoing Central Plateau remediation or related activities.	RAI 2-15
	Evaluate undisturbed present-day soil moisture profiles determined from ongoing studies of other Central Plateau areas near the IDF.	RAI 2-15
	Evaluate ongoing research and testing related to characterization of present-day natural infiltration, with focus on the Central Plateau area.	RAI 2-15
	Evaluate saturated zone flow model results and parameter values used in ongoing Central Plateau remediation or related activities.	RAI 2-14 RAI 2-16
	Evaluate assumptions and analyses used in the ongoing Hanford Composite Analysis and other ongoing performance assessments (including the Waste Management Area A-AX performance assessment).	RAI 2-16
	Evaluate saturated zone flow properties and hydrostratigraphy at the IDF.	RAI 2-14 RAI 2-16
Human receptor exposure pathways and routes (see CHPRC-03348, Section 4.8)	Evaluate ongoing national and international research and guidance on models and parameters used to evaluate human receptor exposure pathways and routes.	—
	Evaluate ongoing Hanford risk and other related analyses that include models and parameters used to evaluate human receptor exposure pathways and routes.	—
	Evaluate potential effects of COPC accumulation in soil due to irrigation.	—

Source: CHPRC-03348, *Performance Assessment Maintenance Plan for the Integrated Disposal Facility*, Section 4.0.

RAI = Request for Additional Information

The implementation of the maintenance activities following the release of RPP-RPT-59958 has been summarized in the 2019 Annual Status Report (DOE/ORP-2020-02, *Fiscal Year 2019*

Annual Summary Report for the Integrated Disposal Facility, Hanford Site, Washington).
Additional aspects of the maintenance activities that are relevant to related RAI responses are
included in the individual RAI responses, for example:

- Additional information on the corrosion rates for possible ILAW glasses is presented in
  the response to RAI 2-7

- Additional information on the possibility of Stage III glass corrosion is presented in the
  response to RAI 2-9

- Additional information on the hydrostratigraphy and hydraulic characteristics of the
  saturated zone sediments near the IDF is presented in the responses to RAI 2-14 and
  2-16, respectively

- Additional information on *in-situ* moisture contents observed in the vadose zone near the
  IDF is presented in the response to RAI 2-15

- Additional information on ^{129}I and ^{99}Tc sorption on granular activated carbon (GAC) and
  silver mordenite is presented in the response to RAI 2-20.

As additional information is developed, it will be evaluated as part of the IDF change-control
process using the unreviewed disposal question evaluation (UDQE) process and the results
summarized in annual status reports in accordance with the IDF PA Maintenance Plan.

The IDF Maintenance Plan also includes Section 4.9, which discusses the use of lysimeters to
collect waste form release data that can be used to validate waste form release models. The
lysimeters include laboratory-prepared samples for both vitrified and cement waste forms.
Leachate collected from the lysimeters will be used to validate the release models. At the end of
the lysimeter test period, the samples will be retrieved and characterized to document the
corrosion that is observed. The plan to collect data from the lysimeters is discussed in RAI 2-9.

References

CHPRC-03348, 2019, *Performance Assessment Maintenance Plan for the Integrated Disposal
        Facility*, Rev. 1, INTERA, Inc./CH2M HILL Plateau Remediation Company, Richland,
        Washington.

CP-57037, 2020, *Model Package Report: Plateau to River Groundwater Model, Version 8.3*,
        Rev. 2, CH2M HILL Plateau Remediation Company, Richland, Washington. Available
        at: https://pdw.hanford.gov/document/AR-03674.

DOE/EIS-0391, 2012, *Final Tank Closure and Waste Management Environmental Impact
        Statement for the Hanford Site, Richland, Washington*, U.S. Department of Energy,
        Washington, D.C.

DOE/ORP-2020-02, 2020, *Fiscal Year 2019 Annual Summary Report for the Integrated Disposal Facility, Hanford Site, Washington*, Rev. 0, U.S. Department of Energy, Office of River Protection, Richland, Washington.

DOE/RL-2019-66, 2020, *Hanford Site Groundwater Monitoring Report for 2019*, Rev. 0, U.S. Department of Energy, Richland Operations Office, Richland, Washington. Available at: https://pdw.hanford.gov/document/AR-04023.

ECF-HANFORD-17-0079, 2018, *Hanford Soil Inventory Model (SIM-v2) Calculated Radionuclide Inventory of Direct Liquid Discharges to Soil in the Hanford Site's 200 Areas*, Rev. 0, CH2M HILL Plateau Remediation Company, Richland, Washington.. Available at: https://www.osti.gov/servlets/purl/1441375.

ECF-200EA1-17-0066, 2019, *Pore Volume Calculation – 200-EA-1 Operable Unit Liquid Waste Disposal Sites*, Rev. 1, CH2M HILL Plateau Remediation Company, Richland, Washington. Available at: https://pdw.hanford.gov/document/AR-02618

PNNL-14907, 2004, *Vadose Zone Contaminant Fate-and-Transport Analysis for the 216-B-26 Trench*, Pacific Northwest National Laboratory, Richland, Washington. Available at: http://www.pnnl.gov/main/publications/external/technical_reports/PNNL-14907.pdf.

PNNL-21812, 2013, *Integrated Disposal Facility FY 2012 Glass Testing Summary Report*, Rev. 1, Pacific Northwest National Laboratory, Richland, Washington. Available at: https://www.pnnl.gov/main/publications/external/technical_reports/PNNL-21812Rev1.pdf.

RPP-26744, 2005, *Hanford Soil Inventory Model, Rev. 1*, Rev. 0, CH2M HILL Hanford Group, Inc., Richland, Washington. Available at: https://pdw.hanford.gov/document/0081114H

RPP-RPT-59197, 2016, *Analysis of Past Tank Waste Leaks and Losses in the Vicinity of Waste Management Area C at the Hanford Site, Southeast Washington*, Rev. 1, INTERA, Inc./ CH2M HILL Plateau Remediation Company/Washington River Protection Solutions, LLC/TecGeo, Inc., Richland, Washington. Available at: https://pdw.hanford.gov/document/0072362H.

RPP-RPT-59958, 2018, *Performance Assessment for the Integrated Disposal Facility, Hanford Site*, Rev. 1, Washington River Protection Solutions, LLC and INTERA, Inc., Richland, Washington.

RPP-RPT-59958, 2019, *Performance Assessment for the Integrated Disposal Facility, Hanford Site, Washington*, Rev. 1A, Washington River Protection Solutions, LLC, Richland, Washington.

RAI 2-3 (PA Modeling Discretization)

Comment
From the information provided, it isn't clear that the numerical model utilized had a discretization sufficient to ensure acceptable accuracy.

Basis
STOMP modeling was used to estimate the flow of water through the different materials in the system (e.g., engineered cover, wasteforms, unsaturated zone) and to calculate the flux rates of radionuclides from the wasteforms to the unsaturated zone. Numerical modeling of materials with very different properties, especially moisture characteristic curves which describe the unsaturated flow processes, must use a discretization of the model that is fine enough such that the numerical modeling results have converged and are sufficiently precise.

Figure 4-22 from the PA document (shown below), provided the numerical grid and material properties assigned for near-field flow. It appears that some layers are not continuous in the model. It is not clear how the discretization was fine enough to ensure proper precision. The text of the PA document describes the stair-stepped discretization but does not explain how it was determined that the model discretization was sufficient. The potential impact is shown in Figure 5-11 from the PA document (partial figure provided below) where the saturation values and liquid flux rates appear to have large variations as a result of the numerical grid selection.

DOE described the discretization of the model for glass degradation on page 5-49 of the PA document. An attempt was made to strike a balance between computational time and accuracy. Modeling with a 2 cm by 2 cm grid spacing resulted in execution times of over a month per simulation. The resultant fractional release rate (FRR) from the glass was 26% higher than the coarser grid, which DOE did not believe was significant in the context of performance assessment uncertainties. A 2 cm grid spacing is extremely coarse to represent the processes occurring at the glass/engineered system interface. Layers that are tens of microns thick can significantly influence the ingress and egress of species at the interface. With only two data points with respect to the influence of grid discretization, it is unknown how much the FRR's will increase as the grid spacing is further refined and at what point further refinement will have a minimal impact.

Figure 2-3-1. Two-Dimensional Vertical Cross-Section Model of Integrated Disposal Facility Showing Numerical Grid and Surface Barrier Materials.
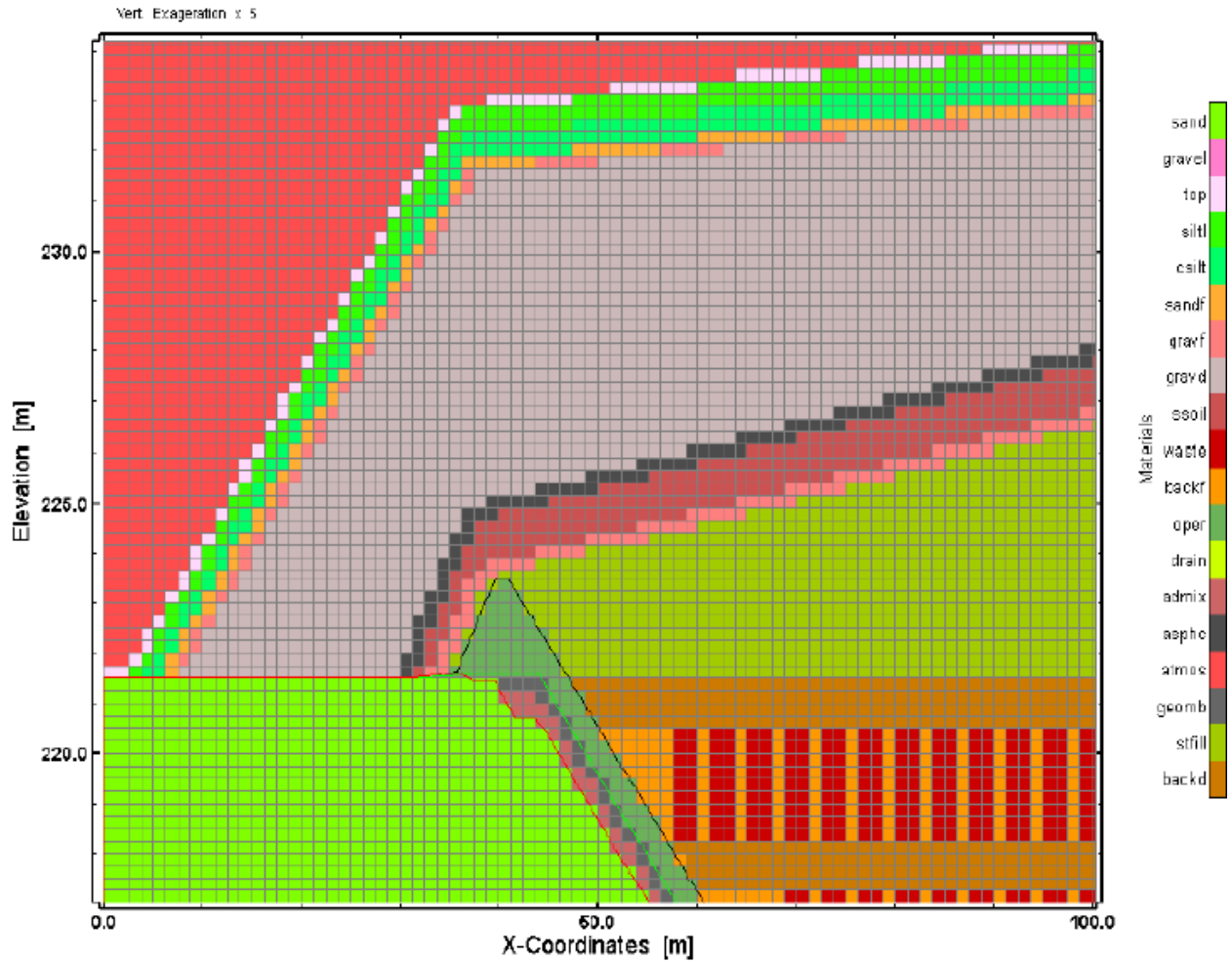
Source: Figure 4-22 of RPP-RPT-59958, *Performance Assessment for the Integrated Disposal Facility, Hanford Site, Washington.*

Figure 2-3-2. CLD3-Infiltration: 33.0 mm/yr Spatial Distribution of Saturation (Top) and Magnitude of Water Fluxes (Middle), and Vertical Fluxes (Bottom) at 750 years [After Cover/Liner Degradation].
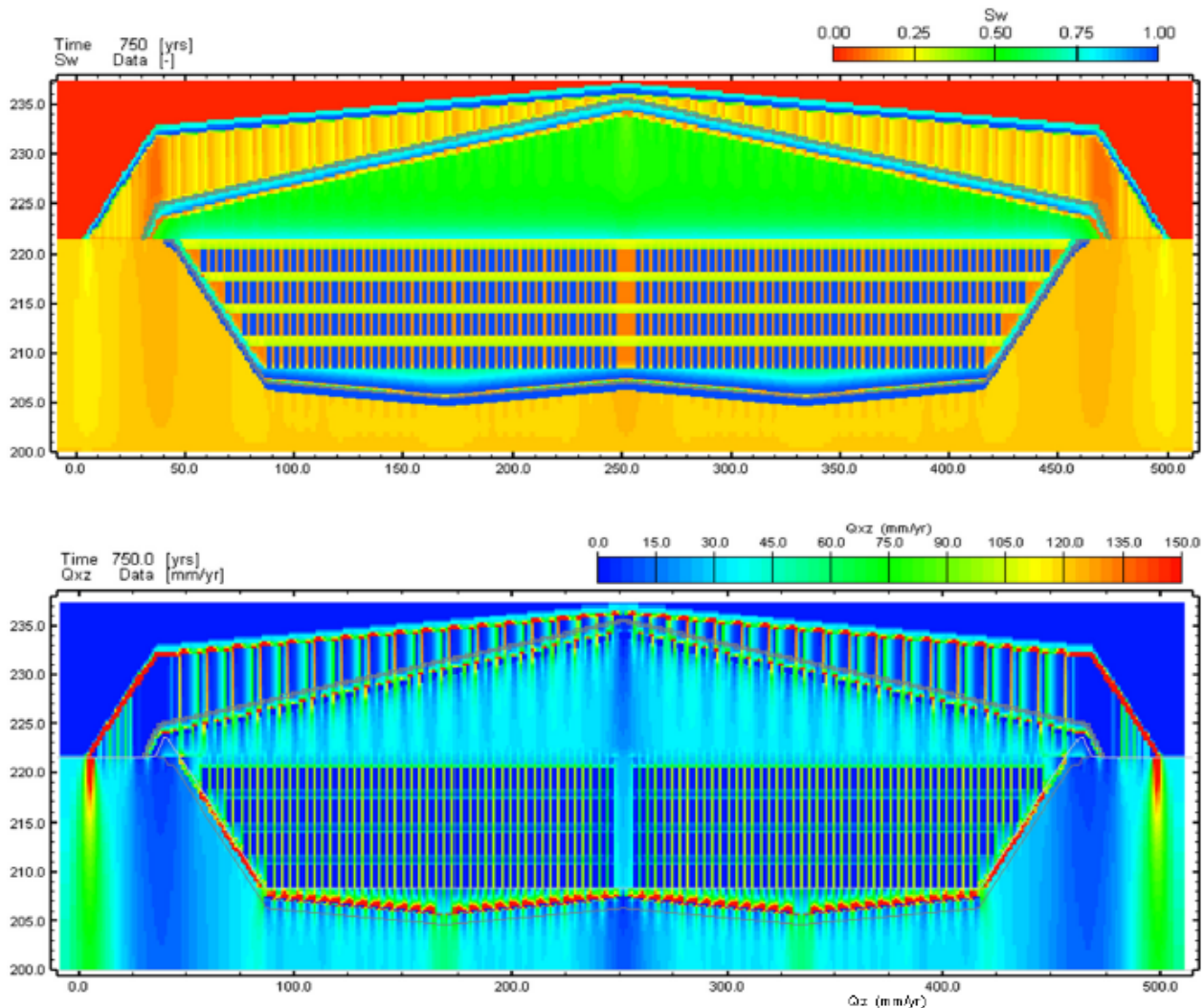
Source: Figure 5-11 of RPP-RPT-59958, *Performance Assessment for the Integrated Disposal Facility, Hanford Site, Washington.*

Path Forward

Please provide additional basis for the discretization of the numerical models used in the PA to simulate near-field flow, release, and transport. Demonstrate that the simulated releases were not artificially biased by the stair-stepped grid representation of the slopes of the engineered cover and liner system. Provide a basis for the amount of increase, at the limit, on the FRR's from the glass as a function of refined numerical grids for release, and how the model should appropriately account for the uncertainty of a coarser numerical grid.

DOE Response

Grid Discretization in the Two-Dimensional Near-Field Flow Model:
DOE acknowledges that the discontinuous layers of the engineered surface barrier in the two-dimensional (2D) near-field flow model depicted in RPP-RPT-59958, Figure 4-22 do not physically represent the continuous layers that would be constructed in the barrier above the IDF. The discontinuous nature of the model layers in the surface barrier are a result of the selected grid size used to represent the engineered surface barrier, but DOE believes that the grid size was adequate for the intended purpose of the model, which was to investigate moisture distribution in the vicinity of the waste containers and through the IDF liner system. The simulation results were then used to develop boundary conditions for radionuclide fate and transport simulations; the near-field flow model was not used to simulate radionuclide fate and transport.

The numerical grid in the near-field flow model of the IDF simulates flow in the surface barrier, through and around the IDF waste region, and through the liner system into the vadose zone beneath the IDF. The model was used to verify a flow boundary condition for the waste form release models; the model was not used to simulate radionuclide release and transport from the waste forms to the bottom of the IDF. Similarly, the near-field flow model was also used to develop a flow boundary condition for the vadose zone flow and transport model that simulated flow and radionuclide transport from the top of the vadose zone just below the liner system down to the groundwater. The near-field flow model was not used to simulate transport of radionuclides to the groundwater.

The 2D representation of the Modified *Resource Conservation and Recovery Act of 1976* (RCRA) Subtitle C barriers focused on the capillary barrier effect of the different layers having different hydraulic and unsaturated flow properties. Simplifications in terms of discretization and assigned hydraulic properties based on the data package report PNNL-23711, *Physical, Hydraulic, and Transport Properties of Sediments and Engineered Materials Associated with Hanford Immobilized Low-Activity Waste* were biased toward conservative properties with regard to vertical flow through the different layers. This was done by increasing the hydraulic conductivity of the asphalt layer and decreasing the hydraulic conductivity of the gravel drain layers compared to the values given in the data package report (Table 4-7 in RPP-RPT-59958). The simplified discretization using a rectangular finite difference grid resulted in discontinuous sand- and gravel-filter layers overlying the gravel drain layer, resulting in non-uniform vertical flow. The capillary barrier effect of the gravel drain layer and associated lateral flow in the overlying layers is somewhat diminished, due to the reduced hydraulic and unsaturated flow properties of the gravel drain.

Except where additional resolution was a priori believed to be necessary, the vertical thickness of each node in the near-field flow model is predominantly 0.25 m. Near the apex of the asphalt layer of the surface barrier, the node thickness reduces to 0.15 m for three node layers; the thicknesses of the nodes containing the liner system are 0.125 m; and the top of the vadose zone below two 0.25-m thick grid cells at the bottom of the liner system has a node thickness of 0.5 m. A single 0.15-m thick node is also included at the elevation for the top of the berm used to raise the liner above present-day ground surface.

The discontinuous appearance of the engineered layers in the model of the cover system occurs because the thickness of the engineered layers may be less than the thickness of the nodes representing each layer (0.25 m). For instance, the design basis for the Modified RCRA Subtitle C cover (described in the IDF Facility Data package RPP-20691, *Facility Data for the Hanford Integrated Disposal Facility Performance Assessment*, Section 5.0) includes a 10-cm thick asphalt base layer, a 15-cm thick asphalt layer, a gravel drainage layer with a variable thickness that has a minimum value of 15-cm, a 15-cm thick gravel filter layer, and a 15-cm thick sand filter layer. Each of these layers is angled with a 2° to 5° slope to promote drainage while minimizing erosion. Due to the slope of the layers, multiple node layers smaller than 15-cm thickness would have been needed to form a continuous layer across the width of the barrier or a complex gridding scheme would have been necessary. DOE decided to forego this refinement because the engineered surface barrier was not being modeled to predict its performance to reduce precipitation to net infiltration. Net infiltration rates have been negotiated between DOE and the Washington State Department of Ecology. The prescribed net infiltration rates (0.5 mm/yr under an intact surface barrier and 3.5 mm/yr under a degraded surface barrier) are used as a boundary condition for the waste form release models, not the rates simulated using the near-field flow model.

The near-field flow model was also used to develop estimates of saturations in the backfill and waste forms in the absence of long-term data and evaluate the distribution of moisture into the vadose zone in the presence of an intact and a degraded liner system.

The near-field flow modeling was limited to unsaturated flow through the IDF including the preliminary design of the surface barrier above the IDF waste area and the existing liner system at the base of the trench. Moreover, the representation of the different components of the surface barrier and liner system was simplified to evaluate moisture distribution throughout the IDF and the potential for the liner system to distribute flow into the top of the vadose zone below the IDF. The examination of the model results distributing flow into the vadose zone was used to identify distinct zones associated with the IDF footprint, where the recharge rates are enhanced or reduced compared to the ambient recharge rate at land surface. This redistribution of moisture provided the flow boundary condition at the top of the vadose zone for far-field flow and transport modeling. This was done for different ambient recharge rates, and for different time periods, as described in detail in Section 4.4.2.1.4 in RPP-RPT-59958. A key finding of the near-field flow model was that even with degraded properties of the liner system, the liner system caused moisture to flow laterally towards the sumps. Eventually, saturations above the sumps would result in a head pressure that was sufficient to cause flow through the liner system into the vadose zone. This resulted in a vadose zone flow profile that is much different than if the liner system were not present. This observation also reduces the potential flow consequences of the stair stepping imposed by the coarse gridding in the engineered surface cover layers.

In addition to the distributed infiltration scenario, which was considered as the base case, a uniform infiltration scenario that distributed all the flow into the IDF across the top of the vadose zone below the IDF was used as the other end-member scenario. The mapping of the simulated flow rates computed using the 2D near-field flow model to the top of the three-dimensional (3D) model required averaging over the different grid sizes between the detailed 2D cross section grid for the near-field flow model and the coarser 3D surface grid for the vadose zone flow and

transport model. The resulting distributed infiltration rates are mapped in a simplified manner as prescribed recharge rate distribution in the 3D vadose zone model as described in Section 5.1.1.5 in RPP-RPT-59958. This resulted in distributed infiltration cases with net infiltration rates of 1.7 mm/yr, 3.5 mm/yr, and 5 mm/yr. These three net infiltration rates were also used as flow boundary conditions for the advective-diffusive transport models simulating release of constituents of potential concern (COPCs) from the cementitious waste forms and VLAW in RPP-CALC-61030, *Cementitious Waste Form Release Calculations for the Integrated Disposal Facility Performance Assessment* and RPP-CALC-61031, *Low-Activity Waste Glass Release Calculations for the Integrated Disposal Facility Performance Assessment*. No distributed infiltration scenario was considered for sensitivity cases that applied ambient infiltration rates of 0.9 mm/yr and 33 mm/yr; near-field flow models for these conditions indicated reduced or negligible variations in the distribution of flow into the top of the vadose zone across the footprint of the IDF.

Simplifications in the near-field model in representing the different components of the surface barrier and liner combined with limited sensitivity cases in terms of material properties were based on the fact that the cover represented a preliminary design concept. The maintenance plan (CHPRC-03348, *Performance Assessment Maintenance Plan for the Integrated Disposal Facility*) includes future studies on barrier performance based on information learned from historical and current studies on surface barrier concepts at other Hanford sites, including the Prototype Hanford Barrier (DOE/RL-2016-37, *Prototype Hanford Barrier 1994 to 2015*). The hydraulic properties and flow through the surface barrier are listed as a key assumption in the IDF PA (Table 8-6 in RPP-RPT-59958) and potential maintenance approaches include review of as-constructed information from similar barriers at other closed facilities at Hanford (i.e., Environmental Restoration Disposal Facility [ERDF] or Waste Management Area [WMA] C). As performance data is collected on similarly constructed barriers, DOE will evaluate these key assumptions included in the IDF PA.

Grid Discretization in the Vitrified Waste Release Model:
Simulating corrosion of vitrified waste did not investigate grid spacing finer than 2 cm. As indicated in the IDF PA (RPP-RPT-59958 Section 5.1.2.2), simulations of LAWA44 glass using a 2-cm grid spacing required one and a half months to run to completion. The resultant fractional release rate (2.04E-07 yr-1) was 51% higher than a simulation with 15-cm grid spacing (1.35E-07 yr-1). By the time the 2-cm run was complete and the results were evaluated, there was not enough time and computational resources to both investigate finer grid spacing and complete the suite of analyses planned for the IDF PA. Additional evaluations around the grid spacing were not performed. Instead, the simulated corrosion rate used in the PA base case was fixed at a value, 2.5E-07 yr-1, that is 40% higher than the highest corrosion rate calculated for a single waste package using the 15-cm spacing for either LAWA44 glass (1.35E-07 yr-1), LAWB45 glass (8.27E-09 yr-1) or LAWC22 glass (1.78E-07 yr-1) (RPP-CALC-61031 Tables 6-2, 6-3, and 6-4) and 22.5% higher than calculated for a single LAWA44 waste package using the 2-cm spacing. The result is comparable to the highest corrosion rate calculated for four stacked waste containers using a 15-cm grid spacing [LAWC22 STOMP(c)[37] rate was 2.52E-07 yr-1].

---

[37] Subsurface Transport Over Multiple Phases (STOMP) is developed and distributed by Battelle Memorial Institute.

In the release calculations for the 2005 PA (PNNL-15198, *Waste Form Release Calculations for the 2005 Integrated Disposal Facility Performance Assessment*), the investigators used a 2-cm grid spacing to simulate vitrified waste corrosion with the STORM[38] code (Subsurface Transport Over Reactive Multiphases) and compared the results to a simulation that used 1-cm grid spacing. They concluded that the results were not significantly different from each other (PNNL-15198 Section 2.2.2). Similar conclusions were made for the 2001 PA when grid spacing at 5 cm and 2.5 cm were compared (PNNL-13369, *Waste Form Release Calculations for the 2001 Immobilized Low-Activity Waste Performance Assessment*, page 5). No additional uncertainty was applied to the 2.5E-07 yr^{-1} corrosion rate applied in the PA to account for grid size resolution. The vitrified waste corrosion rate is applied to all containers of vitrified waste, even those whose corrosion rate based on the glass type is expected to be lower than the corrosion rate for Envelope C glass. Therefore, there is already some pessimism included in the vitrified waste releases in the base case. Furthermore, the uncertainty analysis includes multiple sources of uncertainty that increase the vitrified waste corrosion rate by up to a factor of 30 times higher than the base case rate (additional discussion is presented in response to RAI 2-7). In the uncertainty analysis, DOE's limit on dose was not exceeded in 1,000 or 10,000 years.

---

[38] Subsurface Transport Over Reactive Multiphases was developed by Pacific Northwest National Laboratory, Richland, Washington.

References

CHPRC-03348, 2019, *Performance Assessment Maintenance Plan for the Integrated Disposal Facility*, Rev. 1, INTERA, Inc./CH2M HILL Plateau Remediation Company, Richland, Washington.

DOE/RL-2016-37, 2016, *Prototype Hanford Barrier 1994 to 2015*, Rev. 0, U.S. Department of Energy, Office of River Protection, Richland, Washington.

PNNL-13369, 2001, *Waste Form Release Calculations for the 2001 Immobilized Low-Activity Waste Performance Assessment*, Pacific Northwest National Laboratory, Richland, Washington.

PNNL-15198, 2005, *Waste Form Release Calculations for the 2005 Integrated Disposal Facility Performance Assessment*, Pacific Northwest National Laboratory, Richland, Washington.

PNNL-23711, 2015, *Physical, Hydraulic, and Transport Properties of Sediments and Engineered Materials Associated with Hanford Immobilized Low-Activity Waste*, RPT-IGTP-004, Rev. 0, Pacific Northwest National Laboratory, Richland, Washington.

Resource Conservation and Recovery Act of 1976, 42 USC 6901, et seq.

RPP-20691, 2015, *Facility Data for the Hanford Integrated Disposal Facility Performance Assessment*, Rev. 1, CH2M HILL Plateau Remediation Company, Richland, Washington.

RPP-CALC-61030, 2017, *Cementitious Waste Form Release Calculations for the Integrated Disposal Facility Performance Assessment*, Rev. 0, INTERA, Inc. for Washington River Protection Solutions, LLC, Richland, Washington.

RPP-CALC-61031, 2017, *Low-Activity Waste Glass Release Calculations for the Integrated Disposal Facility Performance Assessment*, Rev. 0, INTERA, Inc. for Washington River Protection Solutions, LLC, Richland, Washington.

RPP-RPT-59958, 2019, *Performance Assessment for the Integrated Disposal Facility, Hanford Site, Washington*, Rev. 1A, Washington River Protection Solutions, LLC, Richland, Washington.

RAI 2-4 (Near-field and UZ Modeling Approach)

Comment
Use of uniform properties and discrete layers may not yield accurate contaminant flux rates primarily for near-field flow.

Basis
DOE assigned uniform hydrologic properties for different material layers in the simulation domain. Moisture characteristic curves (MCC's) are used to describe the relationships between saturations, pore pressures, and hydraulic conductivity. MCC's can take different forms, with some of the most common being Van Genuchten and Brooks/Corey. These relationships are derived by the fitting of empirical data to mathematical expressions. The data are generally uncertain and therefore the derived parameters are also uncertain. DOE recognized this uncertainty. For the unsaturated zone, a number of measurements were available to derive the parameters. Data on particle-size distribution, moisture retention, and saturated hydraulic conductivity (Ks) were cataloged for over 284 samples from throughout the Hanford Site, including locations in the 200 East and West Areas (PNNL-13672, "A Catalog of Vadose Zone Hydraulic Properties for the Hanford Site"). By comparison, very limited samples were available to define MCC's for the hydrologic layers within the boundaries of the engineered disposal facility.

Throughout the PA document (for example page 5-19), DOE indicated that highly permeable layers, such as the drainage layers, act as capillary barriers under most conditions. In addition, Table 5-14 showed that the simulated flux of water through the wasteform is approximately ten times less than the infiltration rate. Adequate model support was not provided for the simulated capillary barrier effects provided by the modeling. The figure below (Figure 5-1 from RPPCALC-61031) show the coarse discretization and discrete layers used in the near-field modeling. It isn't clear how much of the observed reduction in flow through the wasteform is a result of the modeling approach selected.

In the real system, a fractured glass surrounded by soil will have some of the fine-grained soil that infills the fractures at the boundary of the glass (NRC notes that the glass is contained in a stainless steel canister and DOE has elected to ignore the effects of the canister). When finer scale modeling is used, water that flows along the surface of the unfractured glass will enter the fractures and saturations can build up locally resulting in dynamic rivulets of flow which otherwise would not be observed in the coarse-scale modeling with large timesteps. In addition, the MCC parameters have natural variability which is not represented in the DOE modeling approach where uniform properties are prescribed for every cell of a given material type. Modeling of the capillary barrier effect using heterogeneous properties showed much earlier breakthrough of moisture than would be estimated using homogeneous properties (Ho and Webb, 1998).

Figure 2-4-1. Grids for Alternative Disposal Configurations Involving One Waste Package or Four Vertically Stacked Waste Packages.
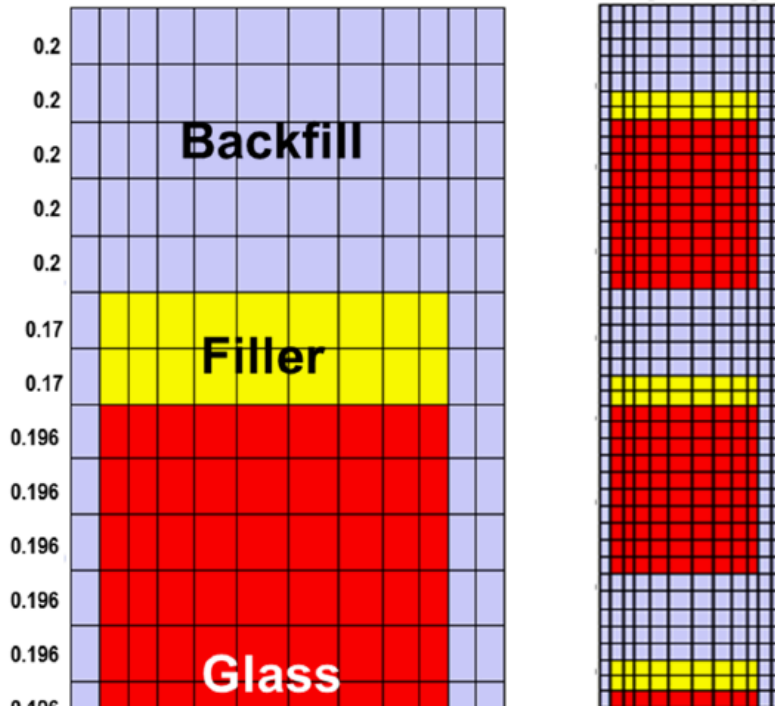
Source: Figure 5-1 of RPP-CALC-61031, *Low-Activity Waste Glass Release Calculations for the Integrated Disposal Facility Performance Assessment.*

Path Forward

Please provide information that demonstrates that the numerical grids used for near-field flow were sufficient to evaluate performance. This could include performing numerical modeling of near-field flow and transport using refined spatial and temporal representations with natural heterogeneity. . Please provide additional support for the numerical model results.

DOE Response

The RAI basis correctly notes the uncertainty associated with modeling the near-field hydrologic conditions for flow both into and through the engineered facility as well as flow through the partially saturated waste forms. The RAI basis notes that while the vadose zone beneath the engineered facility liner has testing results and data to define the moisture characteristic curves (MCCs) of the vadose zone sediments, such information is limited for the layers included in the engineered facility near-field hydrology model described in Sections 4.4.1.1 and 5.1.1 of RPP-RPT-59958 and the glass release model described in Sections 4.4.1.2 and 5.1.2 of RPP-RPT-59958. Both of these models and the impact of uncertain MCCs and model discretization are discussed below.

<u>Near-Field Hydrology Model</u>

The near-field hydrology model is principally used to evaluate the flow through the liner system on the floor of the IDF. Although the surface cover, waste container and backfill layers of the facility are included with the liner system in the near-field hydrology model, the net infiltration rate through the surface cap has been assumed to be 0.5 mm/yr for the first 500 years of the

57

design life of the surface cover and then immediately increase to 3.5 mm/yr at 500 years after closure and remain at 3.5 mm/yr for the duration of the 10,000-year time period modeled. While it is possible to perform more precise modeling of the role of the surface cover in minimizing flow into the facility, such modeling was not performed due in part to the uncertainty in the properties of the surface cover layers as noted in the RAI as well as the observation that the final design and identification of the hydraulic properties of the surface cover layers has not been completed. The values of 0.5 mm/yr and 3.5 mm/yr and the design life of 500 years are assumed values, consistent with values used for the TC&WM EIS and the WMA C PA (see DOE/EIS-0391 and RPP-ENV-58782, *Performance Assessment of Waste Management Area C, Hanford Site, Washington*, respectively)[39]. The impact the uncertainty in these values has on the predicted performance of the IDF and the associated engineered and natural barriers was evaluated in sensitivity and uncertainty analyses presented in the IDF PA document.

ILAW Glass Release Model
The ILAW glass release model consists of two different models: (a) a 2-D unsaturated flow and transport model coupled to a reactive geochemistry model based on transition-state theory of glass corrosion developed with STOMP and the Equilibrium-Conservation-Kinetic Equation Chemistry (ECKEChem) module (illustrated in Figure 2-4-1 [Figure 5-1 of RPP-CALC-61031] presented in the RAI basis) and (b) a 1-D reactive transport model assuming stationary state within the fractured glass developed with GWB. The stationary state assumption in the GWB model allowed the flow regime calculated using STOMP to be implemented with a residence time based on the flow properties of the glass and backfill and the assumed net infiltration rate as summarized in Table 5-14 (referenced in the RAI basis).

DOE acknowledged the uncertainty in the flow properties of the glass and backfill as well as the uncertainty in the net infiltration rate through the surface cover that could lead to a range of advective-diffusive transport with the STOMP model and a range of possible residence times in the GWB model and therefore a range in predicted FRRs.[40] Sensitivity analyses presented in Section 5.1.2 of RPP-RPT-59958 explored a range of near-field hydrology conditions in the fractured glass that were designed to evaluate the impact of the uncertain hydrologic conditions along with other parameters affecting the dissolution of the ILAW glass and release of mobile radionuclides.

The RAI questions whether the predicted reduction in flow through the fractured ILAW glass waste form is representative or whether it is a result of the modeling approach. The RAI basis

---

[39] The base-case net infiltration rate through the surface cover used for the IDF-East barrier in the TC&WM EIS was 0.9 mm/yr, based in part on the recommended value in PNNL-14744, *Recharge Data Package for the 2005 Integrated Disposal Facility Performance Assessment*. All other Central Plateau surface barriers modeled in the TC&WM EIS assumed a post-design life net infiltration rate of 3.5 mm/yr. Sensitivity analyses were performed using a net infiltration rate of 3.5 mm/yr for the IDF-East barrier in the TC&WM EIS. During scoping meetings for the IDF PA, it was determined that the IDF PA would use the 3.5 mm/yr post-design life net infiltration rate as the base case and evaluate the impact of this value by using alternative values of between 0.5 and 5.2 mm/yr.

[40] As noted in the RAI basis, it is relevant to note that DOE does not currently take any performance credit for degradation of the vitrified waste containers, and the potential distribution of inter-granular stress corrosion cracks of the canisters, which would delay water from contacting the waste form. The aperture of the cracks of the stainless steel canister are expected to be sufficiently small and filled with corrosion products that fine-grained soils would not enter through the potentially-failed canister to potentially infill fractures of the glass.

speculates on alternative processes that may affect the flow rate (and by extension the moisture content and thus the residence time) in the fractured glass, including (a) the potential for fine-grained soil to infill fractures at the glass/backfill contact, thus allowing the saturation to build up locally with dynamic rivulets of flow, and (b) natural variability or heterogeneity in MCC parameters affecting the local flow regime and potentially allowing earlier breakthrough of mobile radionuclides.[41]

DOE acknowledged that uncertainty exists in the processes acting on the fractured ILAW glass and that this uncertainty could affect the flow regime (both Darcy flux and moisture content) in the fractured glass and resulting residence time and release of mobile radionuclides from the glass waste form. However, both of the hypothesized scenarios (i.e., the potential for fine-grained soil to infill fractured glass and the heterogeneity in fracture properties) would be expected to result in more rapid flow through the glass and also shorter residence times and smaller surface area for interacting with the glass, reducing the radionuclide and chemical concentrations in the pore fluid in the glass and thus reducing the FRR.

Analyses were performed to ensure that the numerical grids were of sufficient resolution to provide a reasonable estimate of the hydraulic conditions in the fractured glass. These analyses consisted of refining the grid from 264 cells used in the nominal model representation illustrated in Figure 5-1 of RPP-RPT-59958 to 16,340 cells (using a mesh with a minimum cell size of 2 cm × 2 cm instead of the 10 cm × 19.6 cm used for the nominal model). The resulting increase in FRR of about 26% between the finer resolution mesh and the coarser mesh used for the nominal model was not believed to be significant and the increased computational time from 12 hours to 1.5 months was not believed appropriate given the other uncertainties (such as the ILAW Transition State Theory corrosion model parameters and other near-field hydrogeochemical environmental conditions that are more significant (RPP-CALC-61031, Section 7), including the hydraulic conditions and SMRN addressed in the response to RAI 2-12.

DOE does not believe that additional detailed process modeling (i.e., modeling using the multi-dimensional flow and reactive chemistry representation in the STOMP-ECKEChem model) of the potential effects of fracture infilling or natural heterogeneity that may be postulated for the ILAW glass or backfill would yield meaningful results, without defining a basis for the postulated changes in MCC or fracture characteristics. A wide range of possible scenarios could be envisioned that lead to different hydraulic conditions in the fractured glass (not to mention the unknown evolution of these conditions as the glass degrades after the closure of the facility). DOE believes that it is more appropriate to evaluate the impact of the uncertainty in the hydraulic conditions in the fractured glass in order to determine the extent to which the uncertain hydraulic conditions can impact the predicted release rates from the glass. The uncertainty in the hydraulic conditions was analyzed in several sensitivity cases presented in

---

[41] The predicted breakthrough of mobile radionuclides, such as ^{99}Tc, is dependent on the net infiltration rate and associated vertical Darcy flux into and through the fractured ILAW glass (see Figures 2-4-1 and 2-4-2 and Table 2-4-1). However, the IDF PA assumes that the steady-state FRR is applied to the ILAW waste form immediately after closure of the facility and does not take credit for any delay in release associated with the advective transport time through the engineered barriers or the effect of the pour canister in delaying the contact of water with the fractured glass surface.

Section 5.1.3 of RPP-RPT-59958 and additional sensitivity analyses presented in the response to RAI 2-12.

The principal effect the uncertainty in the hydraulic properties and conceptual model of the fractured ILAW glass have on the predicted release rates is the result of their effect on the hydraulic conditions (i.e., Darcy flux and moisture content) in the fractured glass (see Table 2-4-1). The hydraulic conditions in the fractured glass control the pore water velocity through the glass and the associated residence time (see Figures 2-4-2 and 2-4-3 and Table 2-4-1). As illustrated with the GWB results presented in the IDF PA, increasing the residence time results in an increase in the concentration which results in an increase in the release rate for a given Darcy flux.

Figure 2-4-2. Predicted Residence Time and Technetium Concentration for Different Background Net Infiltration Rates for LAWA44.
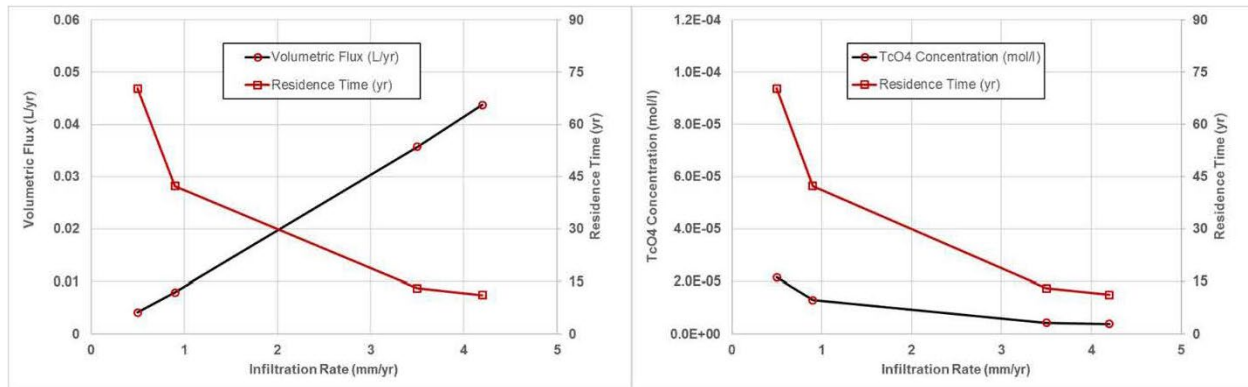
Source: RPP-RPT-59958, *Performance Assessment for the Integrated Disposal Facility, Hanford Site, Washington*, Figure 5-43 (derived from RPP-CALC-61031, *Low-Activity Waste Glass Release Calculations for the Integrated Disposal Facility Performance Assessment*, Figure 7-16).

Note: The decrease in technetium concentration with increased net infiltration rates is the result of the decrease in the residence time. The residence time is inversely related to the pore velocity, where the pore velocity is equal to the Darcy flux divided by the moisture content. The technetium flux is the product of the technetium concentration and the Darcy flux (which increases as the net infiltration rate increases). As indicated in Table 2-4-1, for a net infiltration rate of 3.5 mm/yr, the vertical Darcy flux is 0.357 mm/yr and the moisture content is 0.00238, so the pore velocity is 15.0 cm/yr and the residence time (for a 196 cm glass canister) is 13.1 years.

To address the impact of uncertainty in the hydraulic characteristics of the fractured ILAW glass, additional sensitivity analyses have been performed. These additional sensitivity analyses are presented in the response to RAI 2-12 because they also relate to uncertainty in the MCC used to describe the fractured glass.[42] These sensitivity analyses are also relevant to address the uncertainty in ILAW glass hydraulic conditions identified in the basis for RAI 2-4.

---

[42] Although uncertainty also exists in the MCC of the backfill around the fractured glass and the corrosion products of the stainless steel pour canister, the sensitivity analyses performed using the 2-D STOMP model of ILAW glass release indicate that the uncertainty in the hydraulic properties of the glass is more significant than the uncertainty in the hydraulic properties and flow conditions in the backfill around the glass containers. Therefore, the additional sensitivity analyses focus on the hydraulic properties of the fractured glass.

Figure 2-4-3. Fractional Release Rates from LAWA44 Immobilized Low-Activity Waste Glass Predicted using Two-Dimensional STOMP Model and Base Case Glass Parameters for Different Infiltration Rates.
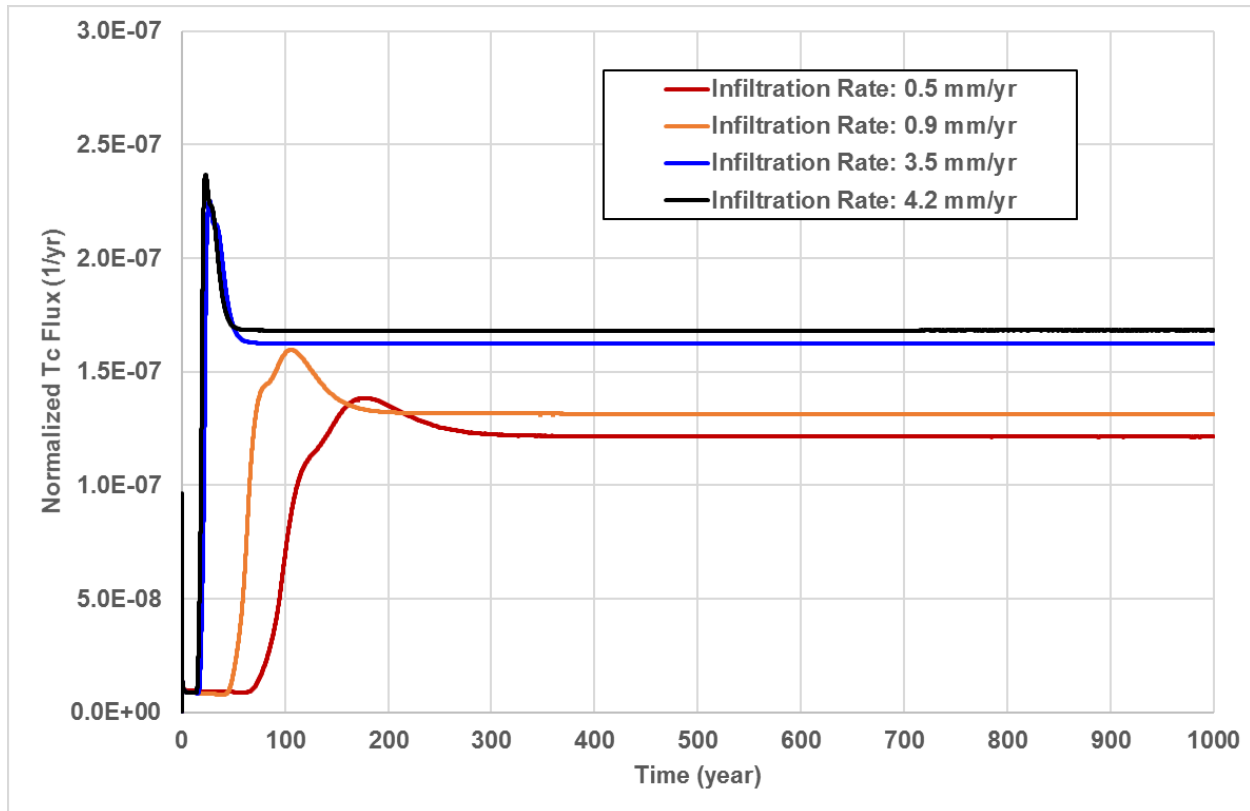
Source: RPP-RPT-59958, *Performance Assessment for the Integrated Disposal Facility, Hanford Site, Washington*, Figure 5-40 (derived from RPP-CALC-61031, *Low-Activity Waste Glass Release Calculations for the Integrated Disposal Facility Performance Assessment*, Figure 7-13).

Note: The time to reach a steady-state fractional release rate increases as the infiltration rate (and associated Darcy flux through the fractured immobilized low-activity waste glass) decreases while the predicted steady-state fractional release rate increases as the infiltration rate increases. The predictions illustrated assume a constant infiltration rate starting at time zero. The actual disposal system is assumed to have an infiltration rate of 0.5 mm/yr for the first 500 years after closure and then increase to 3.5 mm/yr. There is no credit taken for the pour canister causing a delay in the time it takes for infiltrating water to contact the fractured glass waste form. The Integrated Disposal Facility Performance Assessment uses the steady-state fractional release rate and assigns that fractional release rate starting at closure. This assumes that the delay in reaching the steady-state value as well as the initial short-term transient increase in the fractional release rate are not significant to the predicted release rate and resulting groundwater concentration and dose.

Subsurface Transport Over Multiple Phases (STOMP) has been developed and distributed by Battelle Memorial Institute, Richland, Washington.

Table 2-4-1. The Geochemist's Workbench®-Predicted Fractional Release Rates from LAWA44 for Different Background Percolation Fluxes and the Base Case Glass and Backfill Hydraulic Properties.

Background Net Infiltration Rate (mm/yr)	Q (glass) (cm³/yr)	Vertical Darcy Flux (cm/yr)	Moisture Content	Pore Velocity (cm/yr)	Residence Time (years)	Concentration (mol TcO4/L)	Release Rate (mol TcO4/yr)	Fractional Release Rate (yr⁻¹)
0.5	4.16	4.16E-03	0.00149	2.79	70.3	8.82E-05	3.66E-07	1.71E-07
0.9	7.96	7.96E-03	0.00172	4.63	42.3	4.36E-05	3.47E-07	1.62E-07
3.5	35.7	3.57E-02	0.00238	15.0	13.1	9.59E-06	3.43E-07	1.60E-07
4.2	43.7	4.37E-02	0.00250	17.5	11.2	7.98E-06	3.49E-07	1.63E-07

Source: RPP-CALC-61031, *Low-Activity Waste Glass Release Calculations for the Integrated Disposal Facility Performance Assessment*, Tables 7-8 and 7-9.

Note: Q(glass) represents the volumetric flux through a 0.1-m wide section of glass. The background net infiltration rate equals the percolation flux through the surface cover. The base case net infiltration rate during the design life of the surface cover is 0.5 mm/yr and increases to either 0.9 mm/yr (for the Tank Closure and Waste Management Environmental Impact Statement base case) or 3.5 mm/yr (for the Integrated Disposal Facility Performance Assessment base case) after the 500-yr design life of the surface cover.

The volumetric flux (Q), vertical Darcy flux and moisture content are derived from a STOMP two-dimensional model run using the base case glass and backfill moisture characteristic curves. They represent a single cell that is 0.1 m wide and has a thickness of 1.0 m. The predicted vertical Darcy flux in the fractured glass is about 10% of the net infiltration rate for the assumed hydraulic properties of the glass and backfill. Residence time is based on a vertical height of glass in a single container of 196 cm.

Although the moisture content values presented in Table 7-8 of RPP-CALC-61031 are reported to two significant figures, the number of significant figures was increased to three for consistency with the other values.

The concentration values are presented in GWB result files along with the fractional release rate. The concentrations differ from the STOMP example results illustrated in the RAI 2-12 DOE Response.

Fractional release rate values are in Table 7-9 of RPP-CALC-61031 based on a GWB model file which assumes 2.14 mol of TcO4 for LAWA44 in GWB.

Subsurface Transport Over Multiple Phases (STOMP) has been developed and distributed by Battelle Memorial Institute, Richland, Washington.
The Geochemist's Workbench® (GWB) is a registered trademark of Aqueous Solutions LLC, Champaign, Illinois.

References:
DOE/EIS-0391, *Final Tank Closure and Waste Management Environmental Impact Statement for the Hanford Site, Richland, Washington.*
RPP-RPT-59958, *Performance Assessment for the Integrated Disposal Facility, Hanford Site, Washington.*

Summary
The spatial resolution of the numerical grids used in the near-field hydrology and glass release models is sufficient for the intended purpose of defining the Darcy flux and moisture content in the backfill sediments, the liner system and the fractured ILAW glass. The impact of uncertainty in the near field and ILAW glass hydraulic conditions has been evaluated in sensitivity analyses presented in Sections 5.1.1 and 5.1.3 of RPP-RPT-59958, respectively. The effect of uncertainty in the hydraulic characteristics of the fractured glass is evaluated in additional sensitivity analyses presented in the response to RAI 2-12.

References

DOE/EIS-0391, 2012, *Final Tank Closure and Waste Management Environmental Impact Statement for the Hanford Site, Richland, Washington*, U.S. Department of Energy, Washington, D.C.

Ho, C. K., and S. W. Webb, 1998, "Review of Porous Media Enhanced Vapor-Phase Diffusion Mechanisms, Models, and Data-Does Enhanced Vapor-Phase Diffusion Exist?," *Journal of Porous Media*, Vol. 1, No. 1, pp. 71–92.

PNNL-13672, 2001, *A Catalog of Vadose Zone Hydraulic Properties for the Hanford Site,* Pacific Northwest National Laboratory, Richland, Washington.

PNNL-14744, 2004, *Recharge Data Package for the 2005 Integrated Disposal Facility Performance Assessment*, Pacific Northwest National Laboratory, Richland, Washington.

RPP-CALC-61031, 2017, *Low-Activity Waste Glass Release Calculations for the Integrated Disposal Facility Performance Assessment*, Rev. 0, INTERA, Inc. for Washington River Protection Solutions, LLC, Richland, Washington.

RPP-ENV-58782, 2016, *Performance Assessment of Waste Management Area C, Hanford Site, Washington*, Rev. 0, INTERA, Inc./CH2M HILL Plateau Remediation Company/ Ramboll Environ, Inc./Washington River Protection Solutions, LLC/TecGeo, Inc., Richland, Washington.

RPP-RPT-59958, 2019, *Performance Assessment for the Integrated Disposal Facility, Hanford, Washington*, Rev. 1A, Washington River Protection Solutions, LLC, Richland, Washington.

RAI 2-5 (Disposition of Nitrate)

Comment
Previous evaluations by DOE had a large amount of nitrate ($9x10^6$ kg) that would be disposed of in IDF. The current inventory cases have values ranging from $1.6x10^5$ kg to $2.2x10^6$ kg. It is not clear how the nitrate is being removed or where it will be disposed.

Basis
Previous studies identified high nitrate feed as a potential problem for the productions of high performance glass (RPP-54130, 2012). The Environmental Impact Statement (EIS) had about nine million kilograms of nitrate in the waste feed whereas the present PA for IDF has about $1.6x10^5$ to $2.2x10^6$ kg depending on the inventory case (DOE/EIS-0391, 2012). It wasn't clear to the staff how the nitrate is being removed or where and how it will be disposed.

Path Forward
Please describe the removal and disposition of nitrate from the waste feed for VLAW.

DOE Response
Nitrate is the most prominent anion present in LAW feed. Nitrite is also present but typically at lower concentrations. There is a total of 9.6E+05 kilogram-moles (kmol) (5.9E+07 kg) of nitrate and 3.7E+05 kmol (1.7E+07 kg) of nitrite in the pretreated LAW, which will be vitrified in the Hanford LAW Vitrification Facility. The majority of nitrates (nitrate + nitrite) fed to LAW vitrification are converted to nitrogen gas and ammonia in the melter and the melter off-gas system. A small fraction of the nitrates accumulate in the off-gas condensate evaporator overheads and caustic scrubber liquid effluent. Those streams are routed to the Liquid Effluent Retention Facility (LERF)/Effluent Treatment Facility (ETF) where they are incorporated into the liquid secondary waste (LSW) and immobilized in grout for disposal in the IDF.

Nitrates can cause deleterious effects during vitrification. Of greatest concern, as noted in RPP-54130, *Technetium Retention in WTP LAW Glass with Recycle Flow-Sheet: DM10 Melter Testing, VSL-12R2640-1, Rev. 0*, is the potential for foaming in the melt. This will be controlled by adding sucrose as a reductant to react with the nitrates (NO_3^-/NO_2^-) as described in Section 2.3 of RPP-54130. The exothermic reactions of sucrose with nitrates also provide heat, which enhances conversion of feed and glass formers to oxides in the cold cap and increases melt rate. The amount of sucrose added is less than what would be needed to convert all of the nitrate/nitrite to nitrogen gas to avoid over-reducing the melt. Too much reductant can lead to formation of sulfides and molten metals.

A summary material balance for nitrates and nitrogen compounds across the LAW Vitrification system, expressed in kmol, for the IDF PA (RPP-RPT-59958) base case is presented in Figure 2-5-1. The material balance is from the HTWOS model run performed to support the IDF PA (RPP-RPT-23412, *Hanford Tank Waste Operations Simulator Model Data Package for the Development Run for the Refined Target Case*). The material balance calculations are based on reactions described in 24590-WTP-RPT-PT-02-005, *Flowsheet Bases, Assumptions, and Requirements*, Rev. 7, which in turn are based on data from melter runs with simulants performed at the Vitreous State Laboratory (VSL).

Figure 2-5-1. Low-Activity Waste/Supplemental Low-Activity Waste Nitrogen Balance in Kmol by Contributor.
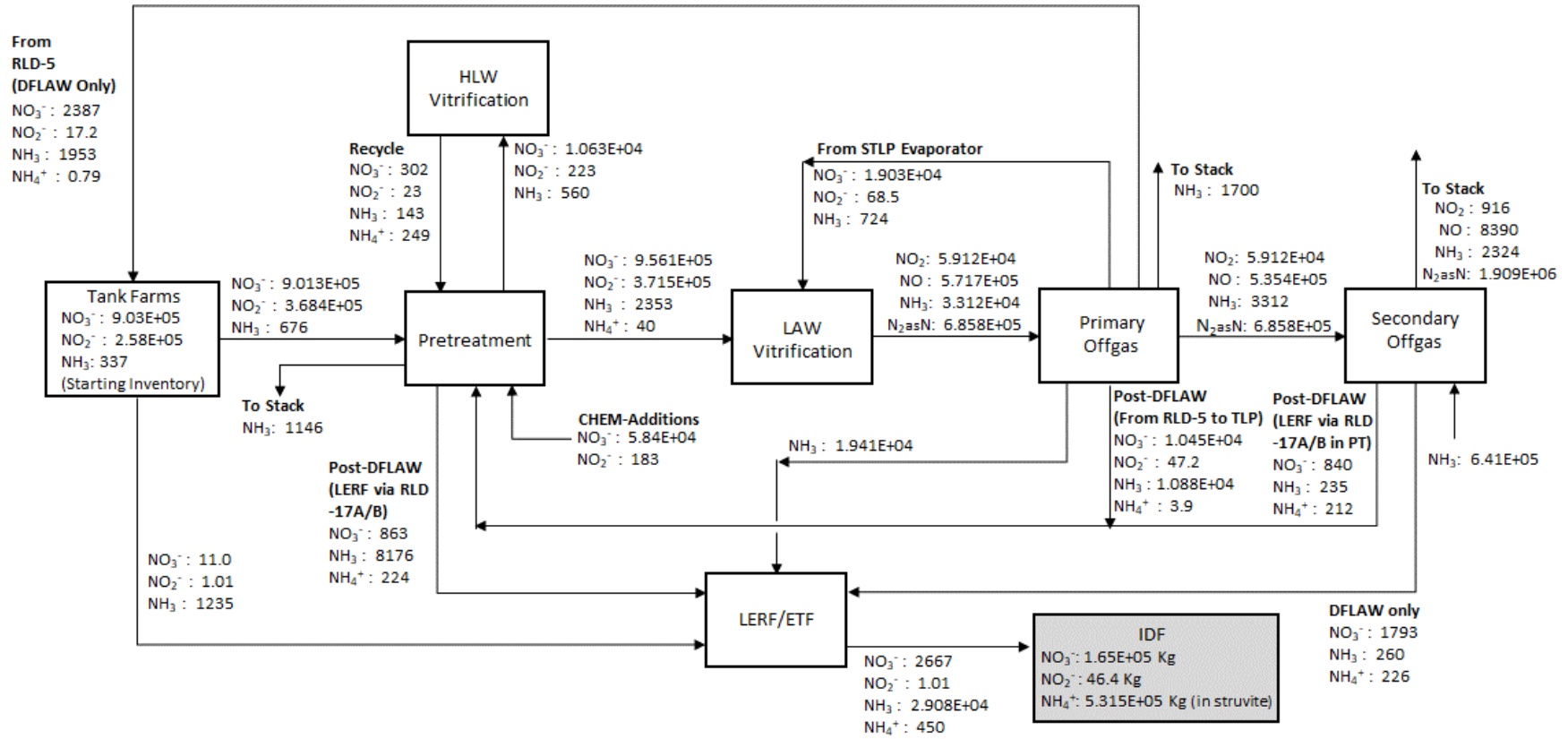
CHEM   = Chemical
DFLAW = Direct-Feed Low-Activity Waste
ETF   = Effluent Treatment Facility
HLW   = high-level radioactive waste

IDF   = Integrated Disposal Facility
LAW   = low-activity waste
LERF   = Liquid Effluent Retention Facility
PT   = Pretreatment

RLD   = Radioactive Liquid Waste Disposal
STLP   = Supplemental Treated LAW Evaporation Process
TLP   = Treated LAW Evaporation Process

Pretreated LAW is fed to the melters where nitrate/nitrite are converted to NO_2, NO, N_2, and NH_3 gases by reduction with sucrose. Approximately 50% of the nitrate/nitrite in the LAW feed is converted to N_2 gas (reported as kmol N in Figure 2-5-1) in the melter. Small amounts of the NO_2 and NO that remain in the melter off-gas are removed, converted to NO_3^- in the primary off-gas system, and recycled for blending with LAW feed. The secondary off-gas system includes an SCR designed to reduce most of the remaining NO_2 and NO to N_2 gas in order to minimize airborne emissions of regulated NOx compounds. The SCR is followed by a caustic scrubber that captures about 20% of the residual NO_2/NO exiting the SCR as aqueous NO_3^-. During DFLAW the liquid effluent from the caustic scrubber is routed directly to the LERF/ETF. All streams entering the LERF/ETF are summed to determine the total nitrate/nitrite for disposal in the IDF. The main contribution to the IDF inventory will be secondary waste from the caustic scrubber during DFLAW. Following DFLAW operations, the main contribution will be condensate from evaporation of liquid effluents from both the LAW and supplemental LAW vitrification off-gas treatment systems.[43] The total nitrate, to be disposed of in the IDF from LSW streams as a result of treating LAW waste both during and post-DFLAW, is estimated to be about 1.6E+05 kg for the IDF PA base case.

The estimated inventory of nitrate present in the grouted ETF SSW used for the Tank Closure and Waste Management Environmental Impact Statement (TC&WM EIS)[44] analysis is based on an HTWOS model run that was performed in 2005 (RPP-RPT-23412) which predates the model runs performed to support the IDF PA by a decade. The model results were further interpreted by the EIS analysts and preparers and the nitrate inventory may have been chosen to represent a bounding case for impact analysis purposes. The inventory of 9E+06 kg of nitrates ($NO_3^- + NO_2^-$ expressed as NO_3^- to simplify the analysis) represents about 13% of the tank waste inventory used for the EIS analysis. Since that time the understanding of the technology and the waste treatment flowsheet have matured substantially, and it is reasonable to project that only a small fraction of nitrate will survive the LAW vitrification and off-gas treatment processes and be incorporated in the grouted ETF LSW assumed to be disposed of in the IDF.

---

[43] Information concerning the secondary waste associated with the supplemental LAW is provided in this RAI response for additional information and completeness only, and is outside the scope of both the Draft WIR Evaluation and DOE decisions concerning supplemental LAW treatment. DOE has not made decisions concerning the potential path forward for supplemental LAW treatment, as explained in footnote 7 of the Draft WIR Evaluation and 78 FR 75913, "Record of Decision: Final Tank Closure and Waste Management Environmental Impact Statement for the Hanford Site, Richland, Washington." As explained in Section 1.2 of the Draft WIR Evaluation, the Draft WIR Evaluation does not address or include in its scope supplemental LAW. To bound the IDF PA analysis, the IDF PA assumed that supplemental LAW may potentially be vitrified and disposed of in the IDF, although, as explained above, DOE has made no decisions concerning the potential path forward for supplemental LAW treatment.

[44] DOE/EIS-0391, *Final Tank Closure and Waste Management Environmental Impact Statement for the Hanford Site, Richland, Washington.*

References

24590-WTP-RPT-PT-02-005, 2013, *Flowsheet Bases, Assumptions, and Requirements*, Rev. 7, Bechtel, River Protection Project, Waste Treatment Plant, Richland, Washington.

78 FR 75913, 2013, "Record of Decision: Final Tank Closure and Waste Management Environmental Impact Statement for the Hanford Site, Richland, Washington," *Federal Register*, Vol. 78, pp. 75913–75919 (December 13).

DOE/EIS-0391, 2012, *Final Tank Closure and Waste Management Environmental Impact Statement for the Hanford Site, Richland, Washington*, U.S. Department of Energy, Washington, D.C.

RPP-54130, 2012, *Technetium Retention in WTP LAW Glass with Recycle Flow-Sheet: DM10 Melter Testing, VSL-12R2640-1, Rev. 0*, Vitreous State Laboratory, The Catholic University of America/EnergySolutions, Federal EPC, Inc./Washington River Protection Solutions LLC, Richland, Washington.

RPP-RPT-23412, 2005, *Hanford Tank Waste Operations Simulator Model Data Package for the Development Run for the Refined Target Case*, Rev. 1, CH2M HILL Hanford Group, Inc., Richland, Washington.

RPP-RPT-59958, 2019, *Performance Assessment for the Integrated Disposal Facility, Hanford Site, Washington*, Rev. 1A, Washington River Protection Solutions, LLC and INTERA, Inc., Richland, Washington.

RAI 2-6 (Glass Wasteform and Volatile Species Distribution)

Comment

Additional information is necessary to demonstrate that volatile species would be uniformly distributed in the glass inside a canister after cooling.

Basis

Volatilization of certain radionuclides (^{99}Tc, ^{129}I, ^{137}Cs) during glass production is well-known but also presents a challenge. DOE's assessment of glass performance in the VLAW PA assumed that volatile species retained in the glass will be uniformly distributed throughout the glass matrix. Volatilization and subsequent deposition of certain radionuclides during the cooling process may result in a non-uniform distribution of activity (e.g., ^{99}Tc) within the waste canister. Deposited radionuclides at the surface of the glass or on the walls of the canister would be available for more rapid release than the 1x10-7 to 1x10-8 1/yr fractional release rates calculated in the PA.

The volatilization temperature of ^{99}Tc is well below the glass melting point (Tc_2O_7 boils at 311C) such that after production and prior to solidification, ^{99}Tc may be volatized during the cooling of the glass wasteform. In addition, the glass may have a significant temperature gradient from the centerline to the walls of the canister for production-scale canisters creating complex dynamics in terms of gas and liquid flows. Experiments on the laboratory-scale demonstrated that up to 20% of volatile species were deposited on the walls of crucibles and ampules during testing (Kim, 2017). Experiments completed to examine the impact of a fire on a solidified glass canister showed that not only could cesium that had been immobilized in a glass matrix be volatized but that it ended up as a gas in the head space of the canister (PNNL-11052, 1996).

In RPP-54130, the distribution of Tc was estimated throughout a glass production system with recycle of the off-gas. Sulfate salt phases were observed on the melt pool surfaces. The salt phases showed an approximate fifty-fold enrichment in concentrations of Tc compared to the concentration in the glass suggesting that the distribution of Tc throughout the solidified glass may not be uniform.

Path Forward

Please provide additional basis that ^{99}Tc will be uniformly distributed in the glass of production scale canisters and that deposition on the canister surfaces will not occur. If information is not available, provide plans that describe how the assumed distribution of ^{99}Tc will be verified prior to full-scale production, or show that the results of the performance assessment, including uncertainties, are not sensitive to the distribution of ^{99}Tc within the glass wasteform.

DOE Response

Technetium Incorporation and Homogeneity Within Glass

From VSL-11R2260-1, *Improving Technetium Retention in Hanford LAW Glass – Phase 2*, it was found that technetium retention in the waste glass varied widely over different compositions.

However, the glass was found to be homogeneous over the length of the pour. The report states the following.

> "The glass was discharged from the melters periodically into square steel cans, five gallon pales *[sic]*, and 55 gallon drums using airlift systems. The discharged product glass was sampled from each can by removing sufficient glass from the top of the cans for technetium and total inorganic analysis, as well as iron oxidation state determination. In these tests no secondary phases were observed in the discharged glass. … Glass samples were also obtained by dipping a rod into the glass pool at the beginning and end of each DM10 and DM100 test. … These "dip samples" were analyzed in the same manner as the discharge samples and also underwent visual examination to detect the presence of a separate sulfate phase on the glass pool surface. … All discharge and most dip samples were counted for ^{99m}Tc to determine the technetium retention for each feed composition and set of test conditions. … In the majority of the tests, the concentration of ^{99m}Tc in the discharged glass increased over the course of each test, reaching a steady-state concentration in most of these tests. Also, for the vast majority of the tests, the dip sample taken at the end of each test and the last glass discharges are very close in ^{99m}Tc activity, indicating uniformity of concentration throughout the glass pool."

Figure 2-6-1 shows the relative agreement between poured glass and melt pool dip samples in terms of ^{99m}Tc concentration in the glass at the end of a series of DM10 test sequences reported in VSL-11R2260-1. The average agreement between dip and discharged glass samples in this series of tests was within 6%.

In similar tests conducted with the DM100 melter system, also reported in VSL-11R2260-1, agreement between poured glass and melt pool samples was within 2.5%.

Deposition of Volatiles on Canister Walls
Deposition or accumulation of significant amounts of volatile or semi-volatile constituents on the inner walls of the LAW glass containers is not expected for a variety of reasons. Immediately after pouring, the glass begins to cool rapidly. At the same time, the container walls are being heated by conductive and radiative heat transfer from the glass as it cools. The container is maintained under active ventilation as it is being filled and for several hours after filling.

The source of potential release of volatile constituents would be the exposed surface of the hot glass. Once poured, the surface of the glass will cool rather rapidly to below 1,000 °C in about 15 minutes, then to 900 °C in about one hour and to 800 °C in about four hours. Any volatile constituents that were somehow incorporated into the bulk glass would have to first diffuse to the surface in order to be released into the air space above the glass, then come in contact with a container wall surface cool enough to condense the material before being swept away by the active ventilation system.

Figure 2-6-1. Comparison of Bulk Glass and Melt Pool Dip Samples.
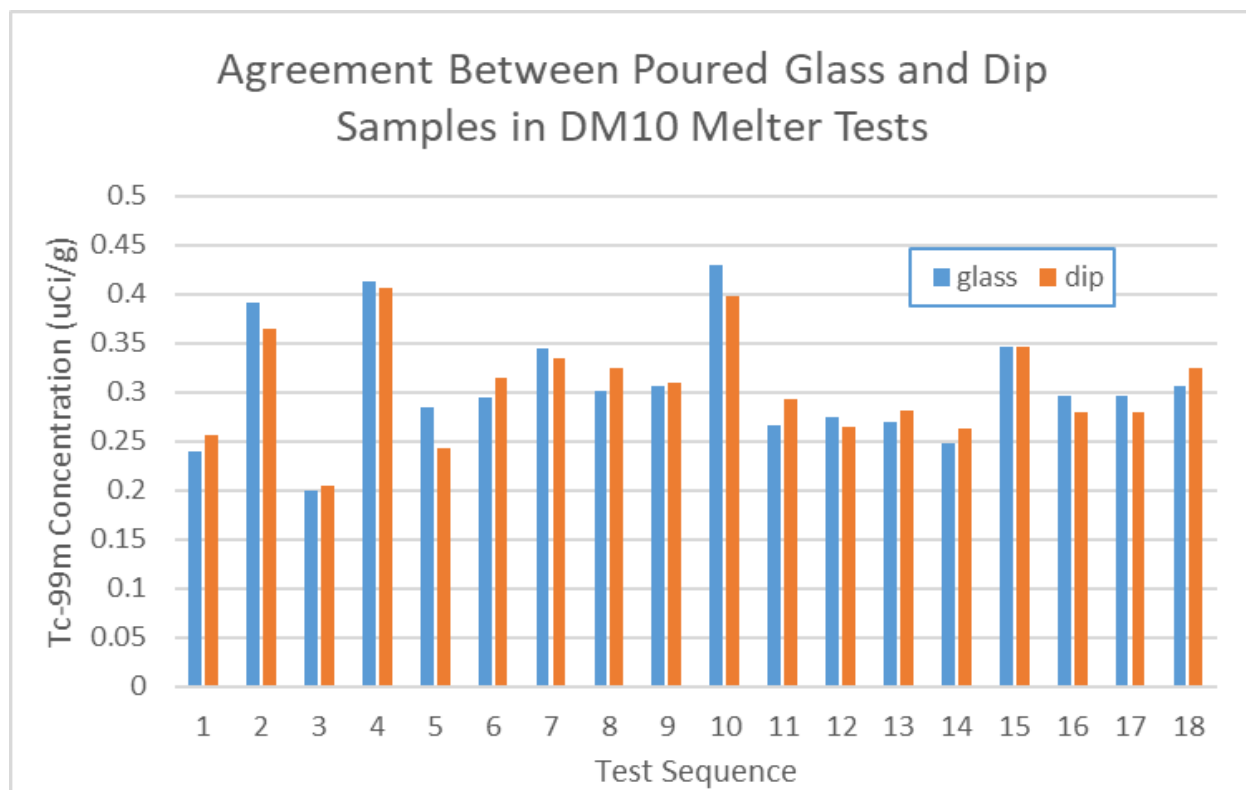
A Duratek report (24590-101-TSA-W000-0009-101-00007, *RPP Pilot Melter Prototypic LAW Container and HLW Canister Glass Fill Test Results Report*) investigating the temperature profiles of prototypic LAW containers during and after glass pouring shows that after an initial temperature spike, the glass cools rapidly (about 300 °C decrease) in the first four hours, followed by slower cooling over the next several days (see Figures 42 through 68 of the referenced report). Three fully-instrumented LAW containers had thermocouples placed on the interior, outside surface, and top flange of containers. During the pouring and cooling period, the temperatures along the centerline and at 4-in. and 10-in. radial offset locations were nearly identical at all heights within the container. At the end of the cooling period, the centerline temperature was between 70 and 110 °C higher than a 16-in. offset location and between 300 and 330 °C higher than the container surface temperature. An example of the temperature profiles from one of the instrumented containers is provided in Figure 2-6-2. The glass pool was also dip sampled before and after each container pour and the composition was analyzed with X-ray fluorescence. The results showed no significant changes in glass composition over the course of the test.

The NRC reviewers cited a study summarized in PNNL-11052, *Volatility Literature of Chlorine, Iodine, Cesium, Strontium, Technetium, and Rhenium; Technetium and Rhenium Volatility Testing*, Section 3.3.5 where investigators reported on cesium volatility from waste glass in a stainless steel container during reheating. The purpose of the study was to simulate the event of a fire in a storage facility. This represents an accident scenario with extreme conditions (reheating cooled canisters to temperatures between 400 °C and 1,000 °C) that would not be

experienced by a LAW glass waste canister under normal operating or disposed conditions. Despite reheating the canister to as high as 1,000 °C, the authors reported the concentration of cesium in the headspace of the canister to be the equivalent of 1.1 mCi (4×10^7 Bq) for an initial glass inventory of 811 Ci (3×10^{13} Bq). This corresponds to a very small fraction, nearly 10^{-6} times the initial glass inventory of cesium that was volatilized. As a side note, the distribution of cesium after the initial glass pouring and cooling was found to be homogeneous in the glass using a gamma scanning method.

As the NRC reviewers noted, some forms of technetium (e.g., Tc_2O_7) are volatile at vitrification temperatures. With a boiling point of 311 °C this species of technetium would be driven off in the cold cap above the glass and not retained in the melt pool at 1,150 °C. This is consistent with observed data wherein a significant fraction of the technetium present in the waste feed is volatilized to the melter offgas and later captured for recycle. In LAW vitrification, reductants are added in part to reduce Tc(VII) to Tc(IV) as TcO_2 which is much less volatile than Tc_2O_7. Volatilization of pure TcO_2 has been reported to occur at about 930 °C (UCRL-53440, *Critical Review of the Chemistry and Thermodynamics of Technetium and Some of its Inorganic Compounds and Aqueous Species*). The retention of less volatile forms of technetium in the final glass product is consistent with results of small scale melter tests using LAW simulants spiked with ^{99m}Tc and large scale melter tests spiked with rhenium as a surrogate for technetium (VSL-11R2260-1).

In a separate study ("X-ray Absorption Fine Structure Studies of Speciation of Technetium in Borosilicate Glasses" [Lukens et.al. 2003]), samples of borosilicate glass were prepared from simulated Hanford waste spiked with pertechnetate and analyzed via X-ray absorption spectroscopy. The two major species identified were TcO_4^-, present as low-volatile alkaline pertechnetate, and TcO_2, both of which were homogeneously distributed throughout the glass. The presence of small amounts of organic reductant favored the formation of TcO_2 species in the glass.

The NRC reviewers also referred to the study "Volatile species of technetium and rhenium during waste vitrification" (Kim and Kruger 2018, cited by NRC as "Kim 2017") wherein up to 20% of volatile species were deposited on the walls of crucibles and ampules during testing. The cited volatilization data from the crucible tests are not directly applicable to future glass canisters poured from a production scale LAW melter. The crucible tests were performed by melting glass frit or calcined waste simulant spiked with perrhenate and pertechnetate salts at a range of temperatures and hold times to investigate the volatilization behavior of technetium and rhenium. The crucible tests also did not include reductants. It is interesting to note the authors did conclude that the results provide convincing evidence that technetium and rhenium volatilize as alkali perrhenates and alkali pertechnetates during vitrification of Hanford LAW instead of decomposing into alkali oxides and Tc_2O_7 or Re_2O_7.

Figure 2-6-2. Temperature Profile for a Low-Activity Waste Glass Container During Filling and Cooling.

Figure 57 – LT002 42" Elevation Temperatures
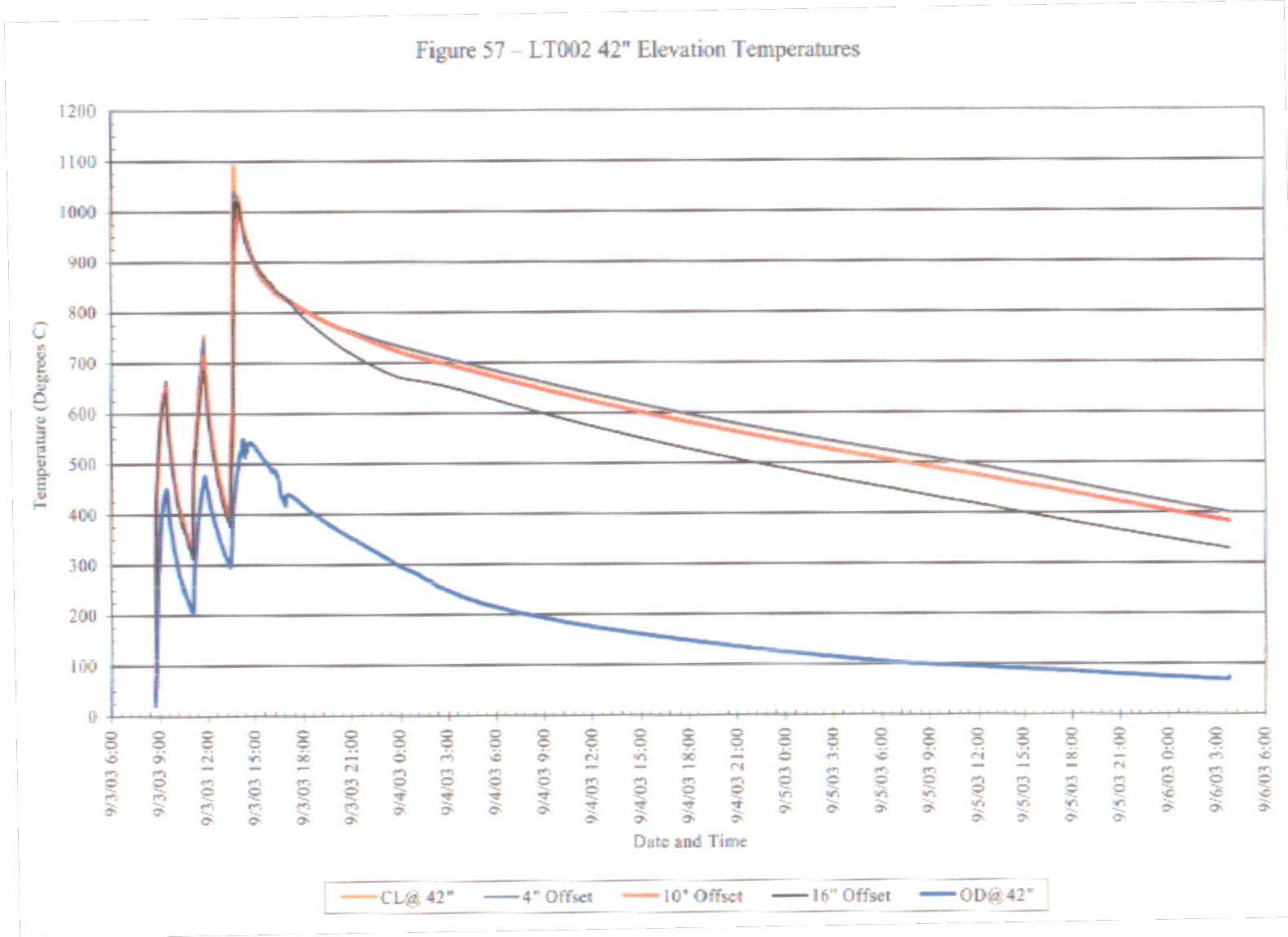
Two major differences between crucible tests and vitrification in melters are the presence of a cold cap and the addition of reductants. In the melter, a cold cap is purposefully formed by feeding the waste through the top of the melter onto the surface of the glass melt pool. An excerpt from VSL-11R2260-1 states: "In the cold cap, it is likely that technetium species are first incorporated into low-melting salt phases, which, for LAW feeds are primarily nitrates (sodium nitrate, for example, melts at ~320°C)."

Additionally, sugar will be added as a chemical reductant during operations of the WTP melter. The reductant, along with the formation of the cold cap in a melter (versus a crucible), decreases volatilization from the melt pool. An excerpt about reductants and their function in the cold cap from VSL-11R2260-1 states:

> "Sugar and other reductants can also be used to promote the formation of more reducing conditions in the cold cap in order to favor the IV oxidation state and thereby increase technetium retention. As the feed material travels downward through the cold cap and the temperature rises, the molten nitrates react exothermically with any reductants that are present; any excess reductants would then tend to reduce technetium to its less volatile oxidation state."

Sulfate Salt Phases

The formation of sulfate salt phases on melt pool surfaces has been recognized as a problem in past glass studies, and will be mitigated with process controls to prevent the formation or accumulation of sulfate salts. From the program plan for ILAW glass testing (RPP-PLAN-60520, *Program Plan for Immobilized Low Activity Waste (ILAW) Glass Testing*), the loading of LAW in glass was found to be limited by several factors, including "molten salt formation in the melter that is promoted by elevated sulfate concentration". For the baseline ILAW glass formulations, "the SO_3 concentration in glass must be at or below 0.77 wt% to avoid the formation or accumulation of a salt layer on the surface of the melt pool." For enhanced waste glass (EWG), the maximum target is 1.5 wt% SO_3 to still meet process and product performance requirements. The glass property-composition models developed in VSL-07R1230-1, *Final Report ILAW PCT, VHT, Viscosity, and Electrical Conductivity Model Development* were used to confirm that the resulting glass meets WTP contract performance requirements after accounting for uncertainties.

In addition, from the report RPP-PLAN-60520 it was determined that "higher sulfur loadings [can be] achieved by increasing the concentrations of glass former additives such as CaO and Li_2O and introducing V_2O_5 as a new additive". The IDF PA RPP-RPT-59958 discusses the plan for lithium to be added to Envelope B[45] waste "as a glass-forming additive to decrease the viscosity of the molten LAWB45 glass and to improve incorporation of sulfate in the glass matrix" and to Envelope C waste "to increase the loading of sulfate in LAWC22 glass."

---

[45] At Hanford the LAW has been classified into "Envelopes" according to the composition of the waste for vitrification purposes. Briefly, Envelope A is generally high in sodium content while Envelope B has elevated sulfate that limits waste loading in the glass. Envelope C contains organic complexants with elevated levels of soluble strontium and transuranic elements. The specific composition ranges for each of the Envelopes are described in Specification 7 of the Waste Treatment and Immobilization Plant Contract between DOE-ORP and Bechtel National, Inc.

The references above show the development of understanding of the sulfate solubility limit in LAW glass and glass formulation algorithms which are designed to be conservatively below that limit. Without the formation of the separate sulfate salt phase, technetium will not be able to concentrate in the salt phase as described in the basis section of this RAI.

The appearance of sulfate salt phases on the surface of the melt pool after two of the tests reported in RPP-54130, *Technetium Retention in WTP LAW Glass with Recycle Flow-Sheet: DM10 Melter Testing, VSL-12R2640-1, Rev. 0* was unexpected but could be attributed to sulfate content in the melter feed that was ~10% higher than in previous tests and at or near the sulfate solubility limit for those specific glass compositions. From the report, "the secondary [sulfate] phases observed in the present tests are therefore attributable to the higher concentrations of sulfur, chlorine, and potassium which exceeded both the target concentrations and the nominal amounts processed in previous tests in which secondary phases were not observed." LAW glasses are formulated to be below the sulfate solubility limit and the data are incorporated in glass formulation algorithms to minimize the potential for sulfate salt phase formation (PNNL-25835, *2016 Update of Hanford Glass Property Models and Constraints for Use in Estimating the Glass Mass to be Produced at Hanford by Implementing Current Enhanced Glass Formulation Efforts*). It is of particular concern during operations to avoid the formation of a sulfate salt layer as this would be highly corrosive to the melter refractory liner as well as Inconel® (a registered trademark of Special Metals Corporation, New Hartford, New York) components such as bubblers. It is of lesser concern for glass poured from the melter because the glass pour spout is fed from a location near the bottom of the melt pool and would not draw off material from the salt phase floating on top of the melt pool. Despite the fact that a salt phase on the surface of the melt pool would be unlikely to affect the quality of the glass product, the potential for salt phase formation is of considerable concern for sustained melter operations, so the information from these tests—along with other considerations such as melter scale, melt pool temperature, cold cap coverage, etc.—are used to evaluate whether adjustments to sulfate solubility models and/or glass formulation model constraints would be warranted during DFLAW operations.

References

24590-101-TSA-W000-0009-101-00007, 2004, *RPP Pilot Melter Prototypic LAW Container and HLW Canister Glass Fill Test Results Report*, Rev. 00A, Duratek, Inc., Columbia, Maryland.

Kim, D. and A. A. Kruger, 2018, "Volatile species of technetium and rhenium during waste vitrification," *Journal of Non-Crystalline Solids*, Vol. 481, No. 1, pp. 71–92.

Lukens, W. W., D. K., Shuh, I. S. Muller, and D. A. McKeown, 2003, "X-ray Absorption Fine Structure Studies of Speciation of Technetium in Borosilicate Glasses," *MRS Online Proceedings Library Archive*, Vol. 802, pp. 99–104.

PNNL-11052, 1996, *Volatility Literature of Chlorine, Iodine, Cesium, Strontium, Technetium, and Rhenium; Technetium and Rhenium Volatility Testing*, Pacific Northwest National Laboratory, Richland, Washington.

PNNL-25835, 2016, *2016 Update of Hanford Glass Property Models and Constraints for Use in Estimating the Glass Mass to be Produced at Hanford by Implementing Current Enhanced Glass Formulation Efforts*, Pacific Northwest National Laboratory, Richland, Washington.

RPP-54130, 2012, *Technetium Retention in WTP LAW Glass with Recycle Flow-Sheet: DM10 Melter Testing, VSL-12R2640-1, Rev. 0*, Vitreous State Laboratory, The Catholic University of America/Energy*Solutions*, Federal EPC, Inc./Washington River Protection Solutions LLC, Richland, Washington.

RPP-PLAN-60520, 2020, *Program Plan for Immobilized Low Activity Waste (ILAW) Glass Testing*, Rev. 1, Washington River Protection Solutions, LLC, Richland, Washington.

RPP-RPT-59958, 2019, *Performance Assessment for the Integrated Disposal Facility, Hanford Site*, Washington, Rev. 1A, Washington River Protection Solutions, LLC and INTERA, Inc., Richland, Washington.

UCRL-53440, 1983, *Critical Review of the Chemistry and Thermodynamics of Technetium and Some of its Inorganic Compounds and Aqueous Species*, Lawrence Livermore National Laboratory, Livermore, California.

VSL-07R1230-1, 2007, *Final Report ILAW PCT, VHT, Viscosity, and Electrical Conductivity Model Development*, Rev. 0, Pacific Northwest National Laboratory/Vitreous State Laboratory, The Catholic University of America, Washington, D.C.

VSL-11R2260-1, 2011, *Improving Technetium Retention in Hanford LAW Glass – Phase 2*, Rev. 0, Vitreous State Laboratory, The Catholic University of America/Energy*Solutions*, Federal EPC, Inc./Washington River Protection Solutions LLC, Richland, Washington.

RAI 2-7 (Glass Wasteform Fractional Release Rate)

Comment

The development of the fractional release rate expressions to represent glass degradation may not adequately reflect all significant sources of uncertainty.

Basis

DOE developed expressions to represent the fractional release rate from glass as a function of different variables for different glass compositions. The expressions were based on the results of reactive transport calculations using process-level models (RPP-CALC-61031 and RPP-CALC-61192). Uncertainties were then represented in the expressions by performing regression on glass-type-specific kinetic dissolution parameters.

It isn't clear that the derived expressions reflect all important sources of uncertainty. The process for developing the expressions derived parameters from experimental data to then parameterize glass degradation expressions. However, the experimental data was in some cases highly uncertain and the uncertainty associated with fitting curves to the experimental data was not carried forward or was more limited than suggested by the data. In addition, some parameters, arguably the most important parameters, were set constant when the data do not suggest they should be fixed.

The figure below from PNNL-24615 shows the empirical data for determining the sodium ion exchange rate for LAWABP1 glass. The value was estimated to be 5.3x10-11 mol/m2 s by extrapolating the data to 15 °C and assuming the value was constant in the PA (draw a line horizontally from the best fit slope at 15 °C to the y-axis). The fractional release rates are sensitive to this parameter and based on the four data points, their uncertainty, and the extrapolation of the data the basis provided by DOE was not adequate for fixing this value as a constant.

Figure 2-7-1. Sodium Ion Exchange Rate vs. Reciprocal Temperature for LAWABP1 Glass.
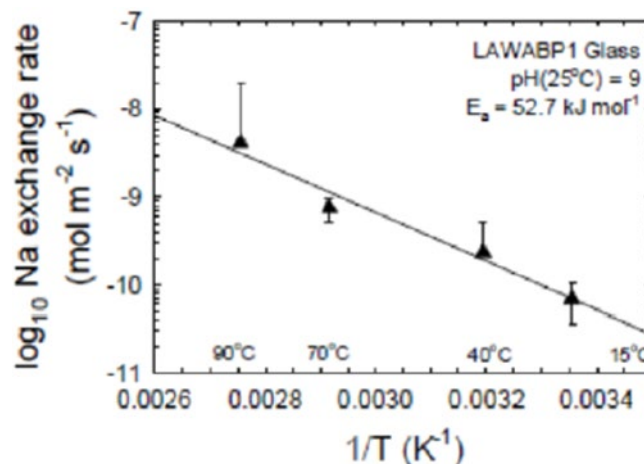
Source: Figure 4.6 of PNNL-24615, *Immobilized Low-Activity Waste Glass Release Data Package for the Integrated Disposal Facility Performance Assessment.*

Figure 4-7 from PNNL-24615 has a relatively poor fit of the data at 40 °C, which impacts the uncertainty assigned to the coefficients. When NRC staff attempted to use a broader range for activation energy in the FRR regression equations in order to understand the significance of the uncertainty the expression yielded non-physical results. Table 4-1 from PNNL shows the derived parameters for the different glass compositions. As implemented in the PA, the three most important parameters (the forward rate constant (ko), the glass apparent equilibrium constant (a), the Na ion-exchange rate (rIEX)) were all fixed as constants. Even if the previously discussed shortcomings are dismissed, some of the derived parameters have R2 of only 0.78 on a logarithmic scale.

Figure 2-7-2. Normalized Glass Dissolution Rate, Based on Boron, as a Function of pH(T) for LAWA44.
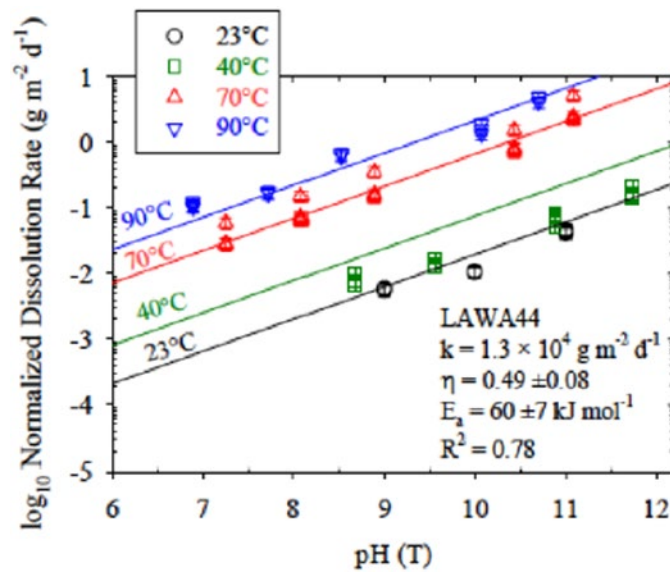
Source: Figure 4.7 of PNNL-24615, *Immobilized Low-Activity Waste Glass Release Data Package for the Integrated Disposal Facility Performance Assessment.*

Table 2-7-1. Summary of Rate Law Parameters for LD6-5412, LAWABP1, LAWA44, LAWB45, and LAWC22 at 15 °C.

Table 4.1. Summary of Rate Law Parameters for LD6-5412, LAWABP1, LAWA44, LAWB45, and LAWC22 at 15 °C

	$\bar{k}_0$		K_g (a)	η	E_a	σ	r_{IEX}	
Glass	Reported Forward Rate Constant (g/[m² d])	Converted[b] Forward Rate Constant (mol/[m² s])	Glass Apparent Equilibrium Constant Based on Activity Product $a[SiO_2(aq)]$	pH Power Law Coefficient	Glass Dissolution Activation Energy (kJ/mol)	Temkin Coefficient	Na Ion-Exchange Rate (mol/[m² s])	Refer
LD6-5412	9.7×10^6	1.8×10^0	1.14×10^{-4}	0.40 ± 0.03	74.8 ± 1.0	1	$1.74 \times 10^{-11(c)}$	McGrail et
LAWABP1	3.4×10^6	5.7×10^{-1}	4.90×10^{-4}	0.35 ± 0.03	68 ± 3.0	1	3.4×10^{-11}	McGra (200
LAWA44	1.3×10^4 $(R^2 = 0.78)$	2.2×10^{-3}	1.87×10^{-3} $(R^2 = 0.95)$	0.49 ± 0.08	60 ± 7	1	5.3×10^{-11}	Pierce et a
LAWB45	1.6×10^4 $(R^2 = 0.96)$	3.0×10^{-3}	1.79×10^{-3} $(R^2 = 0.78)$	0.34 ± 0.03	53 ± 3	1	$0.0 \times 10^{0(d)}$	Pierce et a
LAWC22	1.0×10^5 $(R^2 = 0.96)$	1.8×10^{-2}	1.80×10^{-3} $(R^2 = 0.94)$	0.42 ± 0.02	64 ± 2	1	1.2×10^{-10}	Pierce et a

Source: Table 4.1 of PNNL-24615, *Immobilized Low-Activity Waste Glass Release Data Package for the Integrated Disposal Facility Performance Assessment.*

Additional uncertainties not reflected in the empirical FRR expressions include the assumption that the properties of laboratory-scale produced glass will be identical to production-scale glass, the Temkin coefficient was assumed to be one without empirical data to justify the selection, and the uncertainties associated with assumed secondary mineral formation in the process modeling (i.e., the need to assume Chalcedony formation without it being empirically observed).

In the PA, DOE properly took the information from the underlying technical reports, however it is not clear that in the underlying technical reports DOE properly characterized and reflected the uncertainties in the empirical data and the assumed theoretical degradation expressions.

Path Forward

Please address the treatment of the uncertainties described in the basis portion of this comment with respect to development of glass fractional release rate expressions for the PA. If necessary, revise the expressions and generate new PA results that reflect the full range of uncertainty in the glass degradation rates. NRC staff understands that a variety of sensitivity cases were examined by DOE for various uncertainties associated with glass degradation. However, most of those examinations were one-at-a-time evaluations that can be mathematically compounded but may not yield a fair assessment of the importance of these uncertainties combined with other uncertainties raised by this RAI package. If appropriate, the expressions used in the system model uncertainty analyses should be revised.

The uncertainty associated with the performance of production-scale glass may be addressed by providing DOE's performance verification plan to assure the quality and performance of production-scale glass.

DOE Response

Technical Validity of the Glass Dissolution Model Framework – In 1998, PNNL-11834, *A Strategy to Conduct an Analysis of the Long-Term Performance of Low-Activity Waste Glass in a Shallow Subsurface Disposal System at Hanford* asserted the following statement in the strategy document that has served as the basis for Hanford ILAW glass dissolution modeling for the past 22 years:

> "…of all the models that have been developed to describe glass dissolution behavior, the general kinetic rate law proposed by Aagaard and Helgeson (Aagaard and Helgeson 1982) and later adapted by Grambow (Grambow 1985), best describes the majority of the experimental data that has been gathered over 35 years of studying glass/water reaction processes."

The current relevance of the choice in PNNL-11834 to model the dissolution of Hanford LAW glass using Grambow's transition state theory-based model coupled with alkali ion-exchange and the formation of secondary minerals is evident in the opening statement made by Fournier et al. in their 2018 paper titled "Application of GRAAL model to the resumption of International Simple Glass alteration":

> "The methodology developed for predicting nuclear waste behavior under disposal conditions combines experimental approaches and modeling. A waste glass canister placed in contact with water undergoes irreversible chemical processes leading to its degradation into more stable phases. This transformation occurs in three kinetic stages: the initial alteration rate (stage I), the residual rate (stage II), and, in some cases, a resumption of alteration (stage III) related to zeolites precipitation. Affinity effects based on the transition state theory are used to account for the rate drop from stage I to stage II."

Note that Fournier et al. are asserting that, in 2018, the state of the art for predicting glass dissolution was consistent with rapid alteration which slows based on affinity effects according to transition state theory (as predicted by the Grambow model). Again, this is the model framework for glass dissolution identified in PNNL-11834 and currently used in the IDF PA (RPP-RPT-59341, *Integrated Disposal Facility Model Package Report: ILAW Glass Release*; PNNL-20781, *Integrated Disposal Facility FY 2011 Glass Testing Summary Report*).

Glass Dissolution Model Parameterization for the 2017 PA – Laboratory testing was used to assess the temperature and pH dependency of the rate-controlling parameters detailed in PNNL-11834. This assessment was completed on a set of prototypic ILAW glasses based on projections of glass compositions that could be produced at the WTP. Glasses were formulated for each of the original A, B, and C operating envelopes. The dissolution rate parameters measured in these tests were, excluding the Temkin coefficient (σ) which is assumed to be 1:

k_o = Dilute rate coefficient
η = pH power low coefficient
E_a = Dilute rate dissolution activation energy
K_g = Pseudo-equilibrium constant
r_{iex} = Ion exchange rate

As the NRC reviewer correctly noted, there is uncertainty associated with estimating model parameters from individual tests and this uncertainty was represented in the IDF PA modeling process by evaluating PA response over a range of properties larger than those observed experimentally (see the discussion in the next section). Since the 2017 IDF PA, a more robust uncertainty assessment using principal component analysis has been developed where instead of extracting uncertainties on individual parameters, the uncertainties of the correlated parameters are determined simultaneously, which allows for a more realistic analysis of uncertainty space.

The NRC reviewer also questioned the assumption of using a Temkin coefficient equal to one in the chemical affinity term. A Temkin coefficient not equal to unity would be used to account for non-ideal behavior in ionic solutions. McGrail originally proposed a method to measure both K_g and σ using single-pass flow-through (SPFT) tests with varying flow rates (DOE/RL-97-69, *Hanford Immobilized Low-Activity Tank Waste Performance Assessment* [see page G-10]; PNNL-11834). However, attempts to implement the method to measure both K_g and σ proved to be inadequate and it was decided to use the approach of others and assume $\sigma=1$ and determine K_g empirically ("Measurement of kinetic rate law parameters on a Na–Ca–Al borosilicate glass for low-activity waste" [McGrail et al. 1997]). It has also been argued that σ must equal to one for the transition-state theory (TST)-based model to be fundamentally valid ("Chemical Weathering Rates of Silicate Minerals," Chapter 2. Fundamental approaches in describing mineral dissolution and precipitation rates [Lasaga 1995]). It should be noted that work subsequent to completing the 2017 IDF PA has assessed K_g values for a much wider range of glasses and the range represented by new values will be incorporated into the PA through the PA maintenance process.

Another issue raised by the NRC reviewer was that there are "…uncertainties associated with assumed secondary mineral formation in the process modeling (i.e., the need to assume Chalcedony formation without it being empirically observed)." There are many different mineral phases observed when water is allowed to contact ILAW glass for extended periods (c.f. VSL-20R4820-1, *Final Report FY 2020, Long-Term PCT of ILAW Glasses* and the references cited in this document). For the 2017 IDF PA, because the suite of weathering products that will form as a consequence of the glass-water reactions cannot be determined a priori, results from existing (The Catholic University of America/VSL and Pacific Northwest National Laboratory [PNNL]) long-term product consistency tests (PCTs) conducted at 90 °C

were compared to thermodynamic equilibrium predictions (PNNL-20781). Modeling of PCT results for 128 glass samples was conducted using the secondary-phase reaction network reported in PNNL-14805, *Waste Form Release Data Package for the 2005 Integrated Disposal Facility Performance* for LAWA44. Comparison between measured and predicted results for the concentrations of major glass-forming components in solution for the 128 PCTs were in agreement (PNNL-20781). As noted by the NRC reviewer, the secondary reaction product network used in PNNL-20781 (and subsequently in the IDF PA) were not all observed experimentally, and some that were observed were excluded (compare Tables 5.1, 5.2, and 5.3 in PNNL-20781). These substitutions were done to match temporal trends in dissolved species data using species for which thermodynamic data were available (PNNL-20781). Chalcedony is used as a generalized representation of amorphous silica species that are observed experimentally and known to be more soluble than the corresponding crystalline species. Thus, it facilitates better fit of empirical results in the TST model framework.

Current work is collecting data on secondary mineral reaction networks (SMRNs) formed by dissolution of a wide range of ILAW glasses and this information will be used to update the SMRN used in the IDF PA to account for differences that may arise from the enhanced waste loading glass compositions. This work will follow the approach detailed in PNNL-20781, but more emphasis will be given to including frequently-measured compounds and providing a quantitative assessment of fitting quality for the phases selected.

Efforts to Bound Uncertainty in the 2017 IDF PA – The IDF PA uncertainty analysis (evaluated using the IDF PA system model implemented in GoldSim[©46]) included assessment of the uncertainty in the glass dissolution rate. The included uncertainties resulted in simulated fractional dissolution rates that spanned more than three orders of magnitude from $5.77\text{E-}09 \text{ yr}^{-1}$ to $1.78\text{E-}05 \text{ yr}^{-1}$. At these fractional dissolution rates, the VLAW lifetimes (corresponding to VLAW that is ~99.9% corroded) range from 400,000 years to more than 10 million years, with a range of 0.2% to 18% corroding in 10,000 years.

Although the compliance case simulates vitrified waste corrosion using a fixed dissolution rate without variability or uncertainty, the system model includes multiple aspects of uncertainty (but not variability). The system model includes the capability to include uncertainty in the glass type (as a surrogate for evaluating glass variability), kinetic dissolution rate parameters, and dissolution model regression coefficients.

The system model does not simulate the physical processes involved in glass dissolution but instead uses a regression model to calculate an applied dissolution rate. The system model abstraction includes the capability to simulate glass type uncertainty. With this capability, all vitrified waste could be simulated using the dissolution rate parameters developed in the laboratory for representative glasses from envelopes A (LAWA44), B (LAWB45), and C (LAWC22).

The system model abstraction also includes the capability to evaluate uncertainty in the dissolution rate model parameters for each glass type. Uncertainties in these parameters were

---

[46] GoldSim© simulation software is copyrighted by GoldSim Technology Group LLC of Issaquah, Washington (see http://www.goldsim.com).

developed from laboratory experiments for the four parameters used in the rate model (η - the pH power law coefficient, E_a - the glass dissolution activation energy, K_g - the glass apparent equilibrium constant, and R_{IEX} - the sodium ion exchange rate constant). Uncertainties for η and E_a were developed by the principal investigators that used laboratory experiments to develop the parameter values. However, uncertainties for K_g and R_{IEX} were not reported. The lead PA modeler evaluated the data and determined that a factor of 3 for K_g and a factor of 10 for R_{IEX} were appropriate to represent error or uncertainty that could be introduced by the parameter development process (RPP-CALC-61194, *System Model Calculations for the Integrated Disposal Facility Performance Assessment*, Section 4.3.1.2). More recent evaluations of glasses studied after the 2017 PA provide uncertainties based on experimental data for K_g and R_{IEX} (PNNL-26169, *FY2016 ILAW Glass Corrosion Testing with the Single-Pass Flow-Through Method* and PNNL-27098, *FY2017 ILAW Glass Corrosion Testing with the Single-Pass Flow-Through Method*).

These parameters, including uncertainty, are applied to a regression model that was developed from multiple process model runs simulating glass dissolution for the four glass types using different values for the rate parameters. The different values for K_g in the simulations used to develop the abstraction ranged from 1E-04 to 5E-03, which is a factor of 4.9 lower than the lowest value for the four included glass types and a factor of 2.7 higher than the highest value for the four included glass types. The different values for R_{IEX} in the modeling used to develop the abstraction ranged from 5E-16 mol/cm^2/s to 1E-12 mol/cm^2/s, which is a factor of 6.8 lower than the lowest rate value for the four included glass types and a factor of 83 higher than the highest rate value for the four included glass types. The range for the pH power law coefficient ranged from 0.25 to 0.55, which does not extend across the full range of values in the data package (0.31 to 0.57) when uncertainty is included in the laboratory-developed parameters. The range of values for the rate constant, which accounts for the intrinsic forward rate constant and the activation energy, ranged from 1E-19 mol/cm^2/s to 5E-15 mol/cm^2/s. This range extends across the full range of values for the four glass types when uncertainty in the activation energy is included, which extends from 1.6E-19 mol/cm^2/s to 2.6E-16 mol/cm^2/s. Up to 126 rate parameter combinations were simulated with the process model for each glass. A regression model was fit to the process model output to generate a representative equation that could be used to calculate the dissolution rate in the PA model without incorporating the process model simulations into the system model. The system model abstraction included uncertainty in the estimates of the regression coefficients when calculating the applied dissolution rate.

These uncertainties in the regression model coefficients and estimates of the parameter values were included in the IDF PA uncertainty evaluation. Uncertainty in the glass type was not included in the PA uncertainty analysis. Only rate parameters for the envelope A glass were included in the uncertainty analysis; simulating LAWABP1 glass was excluded because it is no longer a glass formulation planned for production at the WTP. In addition, LAWB45 was not simulated because it tended to have lower dissolution rates than envelope A and envelope C glass types. Envelope C was not simulated because the dissolution rates for envelope A and envelope C glasses are similar so that simulating one is representative of the other.

Figures 2-7-3 and 2-7-4 below show the distribution of fractional dissolution rates from the applied uncertainties for LAWA44 glass and LAWC22 glass. The ratio of the 99.9-percentile

value to the 0.1-percentile value is about 3,000 for LAWA44 glass and about 1,600 for LAWC22 glass, illustrating that either type would provide an uncertainty range that spans more than three orders of magnitude.

In summary, to account for different uncertainties in both the dissolution model and the parameter values, the corrosion rates evaluated in the PA uncertainty analysis spanned more than three-order-of-magnitude range. This range was from 44x below to 70x above the rate used in the compliance case for LAWA44. None of the realizations in the uncertainty analysis exceeded the 25 mrem/yr dose limit in 1,000 years or in 10,000 years.

Figure 2-7-3. Distribution of Fractional Dissolution Rates from the Applied Uncertainties for LAWA44 Glass.
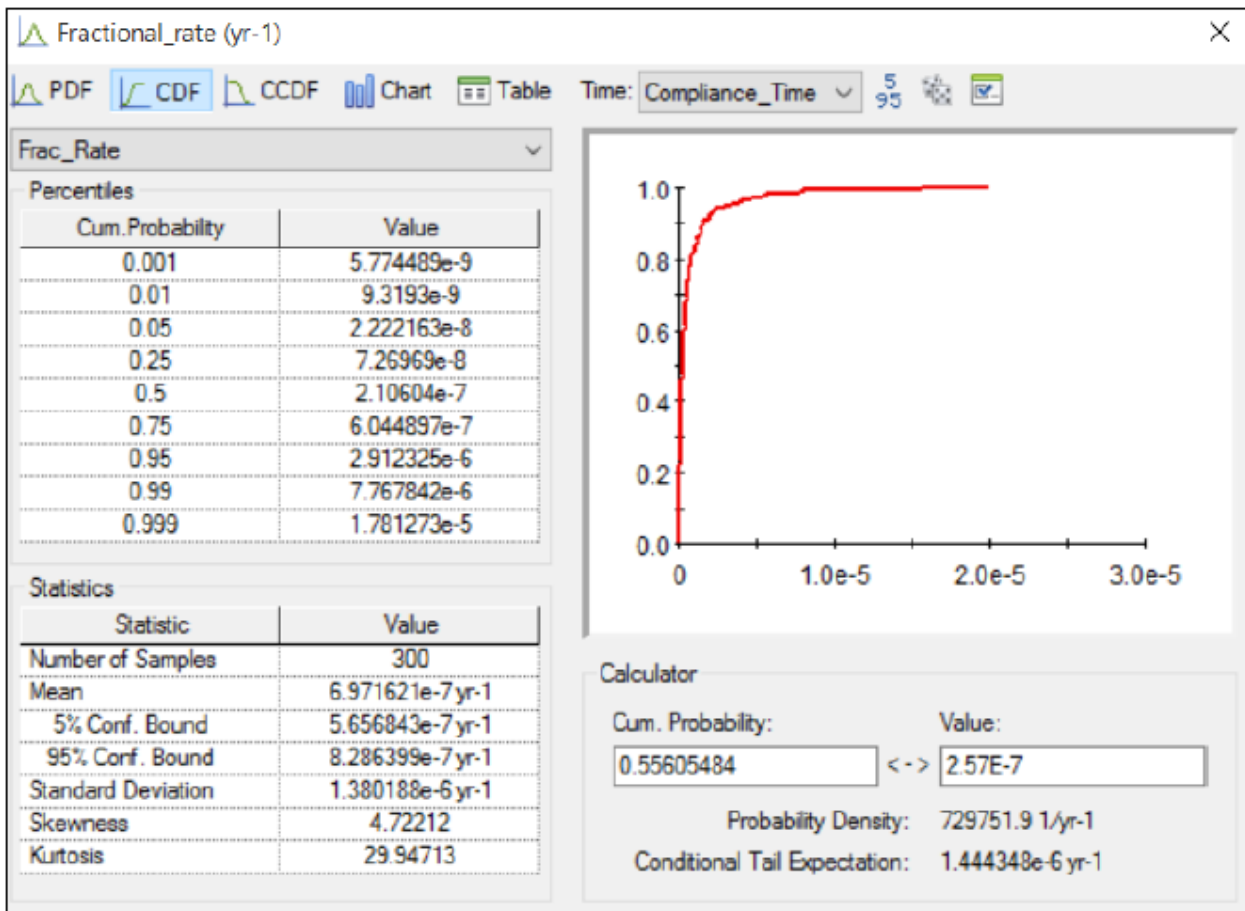
Source: RPP-CALC-61194, *System Model Calculations for the Integrated Disposal Facility Performance Assessment*, Rev. 1A, Figure 7.3-45(a).

Correlating Laboratory-Scale and Production-Scale Glass Performance – It is not practical or necessary to verify the performance characteristics of VLAW glass made from real waste at the production scale through laboratory-scale testing of actual VLAW glass samples. Glass durability as determined via methods such as the Product Consistency Test (ASTM C1285) and Vapor-phase Hydration Test (ASTM C1663) for nuclear waste glasses has been correlated with glass composition to demonstrate compliance with Waste Acceptance Product Specifications for

high-level waste and WTP contract specifications for VLAW glass (PNNL-22631, *Glass Property Models and Constraints for Estimating the Glass to be Produced at Hanford by Implementing Current Advanced Glass Formulation Efforts*; PNNL-25835). The detailed strategies for demonstrating compliance with glass durability requirements for all DOE vitrification facilities are described in the waste form compliance plans for those facilities, and the data and test results demonstrating compliance are found in the waste form qualification reports for those facilities. All rely on laboratory-scale testing of glasses made from simulated waste to cover a range of compositions of glasses to be made from real waste. The composition of nuclear waste glass during actual production operations is then controlled within the pre-qualified glass composition region and the performance of any glass produced can be predicted from models that correlate glass performance with glass composition, after accounting for uncertainties in composition and performance (PNNL-22631, PNNL-25835).

Figure 2-7-4. Distribution of Fractional Dissolution Rates from the Applied Uncertainties for LAWC22 Glass.
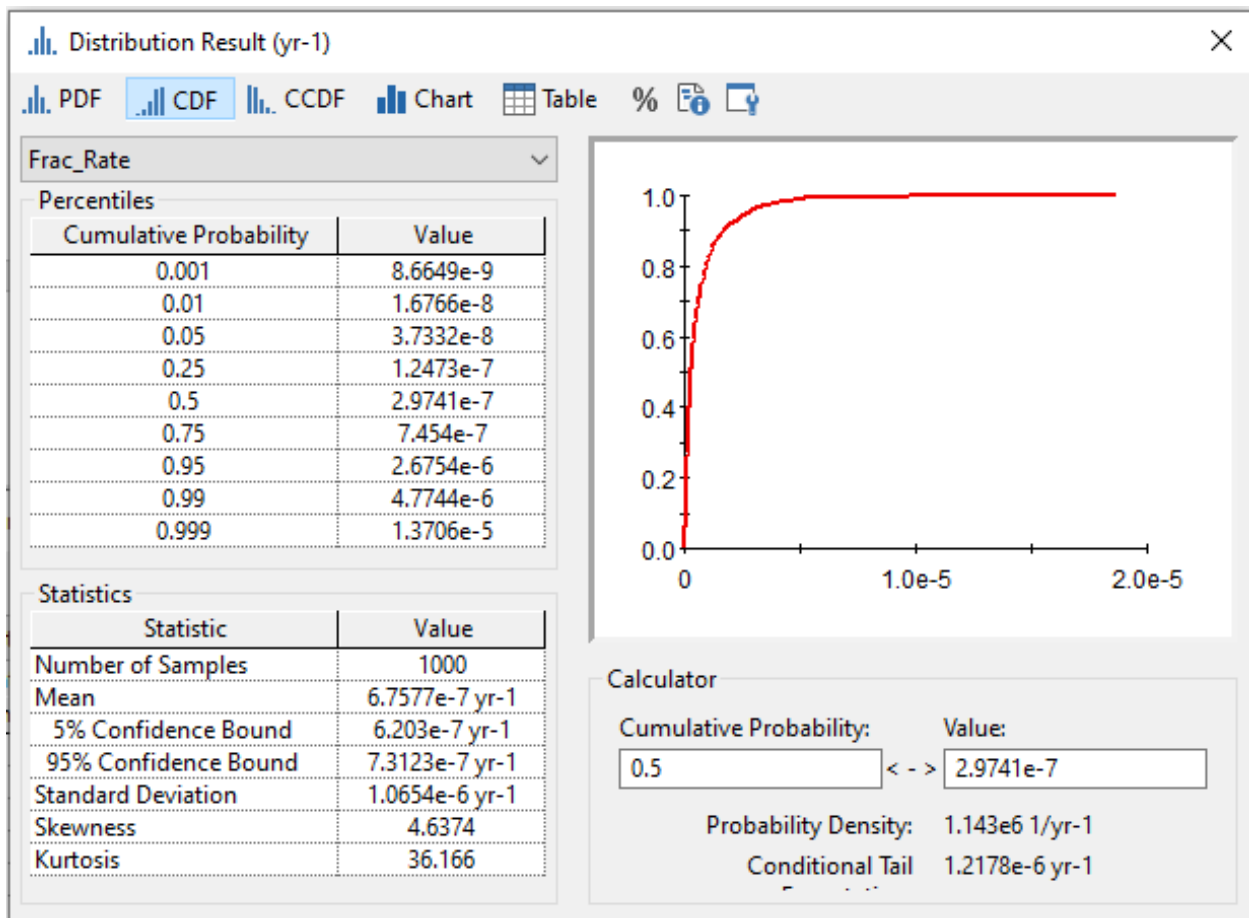
This same approach is utilized to determine the projected long-term performance of VLAW glass under IDF disposal conditions. As described in the section below titled "**Ongoing and Future Work to Improve Representation of Uncertainty in Glass Dissolution Rates**," glass dissolution parameters are correlated, where possible, with glass composition. Conservative or bounding values will be implemented for parameters that do not show definitive correlation with

glass composition. Statistical analyses of the data will provide the basis for establishing ranges of variation and uncertainty.

There is a large body of data collected over decades demonstrating the relationships between glass composition and glass properties and performance for nuclear waste borosilicate glasses. There are numerous reports of tests and demonstrations of VLAW glass production with simulated waste at scales ranging from crucible scale (hundreds of grams) to a 1/3 scale pilot melter system producing greater than 5 metric tons of glass per day. Excellent agreement in glass properties was observed across the full range of scales (c.f. VSL-07R1130-1, *Final Report – Enhanced LAW Glass Formulation Testing* [also referenced as ORP-56293, *Final Report – Enhanced LAW Glass Formulation Testing, VSL-07R1130-1, Rev. 0, dated 10/05/07*]; VSL-06R6480-1 [also referenced as ORP-56324, *Final Report – DuraMelter 100 Tests to Support LAW Glass Formulation Correlation Development, VSL-06R6480-1, Rev. 0*]; VSL-01R3501-2, *Final Report – Melter Tests with LAW Envelope A and C Simulants to Support Enhanced Sulfate Incorporation* [also referenced as ORP-63503, *Final Report – Melter Tests with LAW Envelope A and C Simulants to Support Enhanced Sulfate Incorporation, VSL-01R3501-2, Rev. 0*]). Finally, properties of glass made from real waste at crucible scale were found to be in excellent agreement with VLAW glass made from simulated waste in melter runs at a range of scales (PNNL-13372, *Vitrification and Product Testing of AW-101 and AN-107 Pretreated Waste*).

Ongoing and Future Work to Improve Representation of Uncertainty in Glass Dissolution Rates – The IDF PA is evaluated annually as relevant new information is made available. There are on-going efforts funded by DOE to address several areas of uncertainty associated with ILAW glass dissolution, including the issues raised by the NRC reviewer. The details of the testing approach can be found in RPP-PLAN-60520, *Program Plan for Immobilized Low Activity Waste (ILAW) Glass Testing*. The following is a brief description of the items relevant to the NRC reviewer's comments on the need to better define uncertainty.

- **Dilute Rate Parameters (η, E_a, k_0)**: The NRC reviewer specifically identified uncertainty in dilute rate parameters reported for LAWA44 in PNNL-14805. Since the time of issuance of the ILAW data package, further insight has been gained into the uncertainty and relationship of the dilute rate model parameters. In recent years, analyses have been carried out that have shown that the three dilute rate model parameters are correlated with one another ("The dissolution behavior of borosilicate glasses in far-from equilibrium conditions" [Neeway et al. 2018]). Principal component analysis showed that, as a result of this correlation, the 95% confidence interval volume on the magnitude of the three dilute rate model parameters adopts a flattened ellipsoidal shape in the 3-D space defined by the three model parameters (Figure 2-7-5). Therefore, independently varying the three parameters in sensitivity analyses can result in highly inaccurate estimates and appropriate uncertainties for the three parameters should be determined from this ellipsoid representation instead. This observation was first made using glass dissolution data collected using the SPFT technique, including data on the glasses used in the 2017 IDF PA.

Figure 2-7-5. Example of Principal Component Analysis of the Dilute Rate Model Parameters for a Borosilicate Glass.
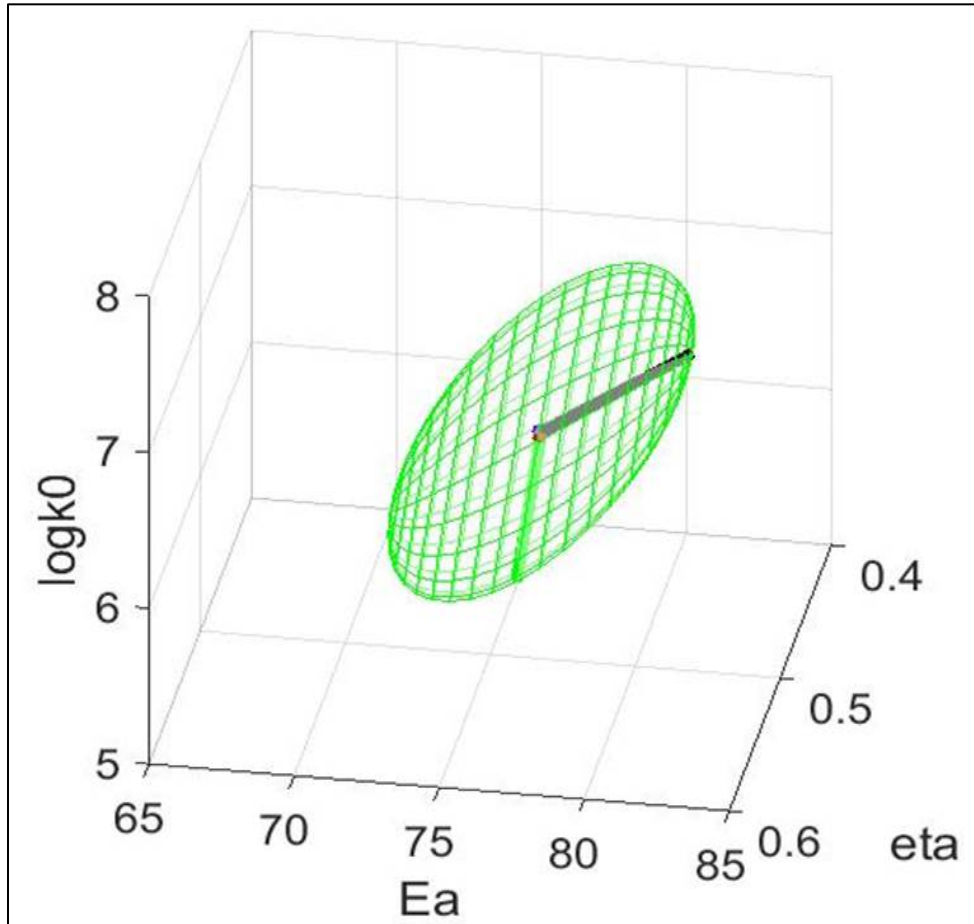
Note: The measured dilute rate model parameters are the center point and the flattened ellipsoid space (Green mesh) represents the 95% confidence interval around the correlated parameters.

More recently this correlation was confirmed based on data collected using a novel technique termed the Stirred Reactor Coupon Analysis (SRCA). This technique was applied to a statistically designed matrix of glasses that were designed to represent the EWG composition space, which in itself covers a majority of the composition ranges allowed in the baseline models (Figure 2-7-6). SRCA relies on the use of a physical measurement of the amount of glass removed from the surface of a coupon sample relative to an area that was protected (masked) from dissolution. The difference between corroded and protected portions of the glass coupon generates a "step" that can be measured (e.g., using optical profilometry). Multiple measurements of this step provide experimental uncertainty that is applied to the corrosion rate. The traditional SPFT method uses crushed glass and analysis of glass components in the leachate solution (e.g., boron) to determine corrosion rates with error derived from analytical uncertainty and test variables (e.g., assumed glass surface area). The SRCA technique enables high test throughput resulting in 24 new glass compositions being analyzed in a single year, compared to only 2 to 4 per year with traditional SPFT testing.

Figure 2-7-6. Scatter Plot of Individually Varied Glass Components (in mass fractions) in the Statistically-Designed Glass Formulations Representative of the Enhanced Low-Activity Waste Glass Compositional Region.
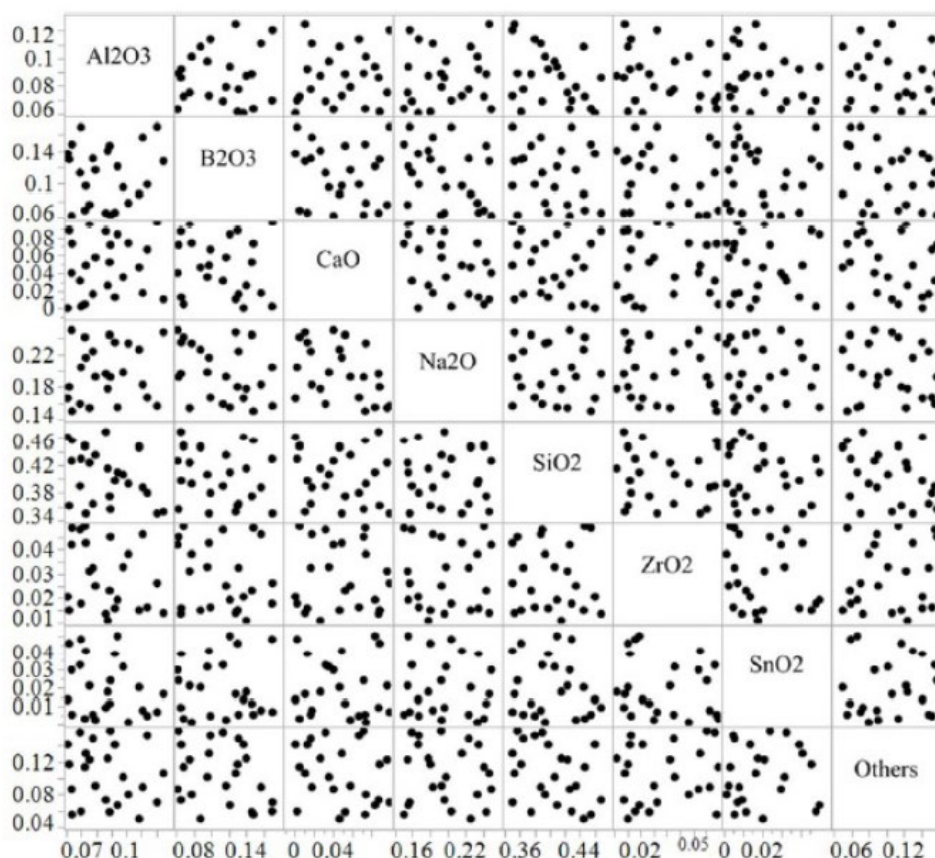
Dilute rate parameters (k_0, E_a, η) results for the 24 glasses tested in fiscal year (FY) 2020 are expected to provide a statistically valid representation of the range for these parameters for all LAW glasses to be produced at the WTP using current process flowsheet algorithms. In addition, composition–parameter correlation modeling is being completed to determine if individual constituents, or combinations of glass constituents, dictate the magnitude and uncertainty of the dilute rate model parameters or if a range of valid values of the dilute rate model parameters can be represented by a single ellipsoid. Final results are expected to be made available to the IDF PA maintenance effort in FY 2022.

- **Pseudo-equilibrium Coefficient**: Data mining and experimental efforts have been ongoing since FY 2019 to assess K_g values for EWGs. In testing of enhanced waste loading glasses, irregularities were observed in SPFT tests used to determine K_g where the glass dissolution rate did not slow with increased silicon addition to solution as one would expect from the TST rate model. A data mining effort was initiated to assess the source of this irregularity using a plethora of SPFT and PCT data sets on ILAW glass available at both PNNL and the VSL and other borosilicate glass data available in the ALTGlass database from SRNL and PNNL. The data mining effort concluded that the

irregularity arose from the application of test method to determine K_g and was not a characteristic of the glass type or composition.

An alternate test method, termed the q/S sweep method, where the expected response of the glasses to increasing silicon concentrations was observed, was identified to measure K_g using existing data. Unlike tests where silicon is added to the reactor feed to suppress glass dissolution, the q/S sweep method relies on adjusting the flowrate and glass surface area to increase the solution concentration of silicon and other glass components. Additionally, unlike the baseline method where only the influence of orthosilicic acid is used to determine K_g, in the q/S sweep method all glass components are dissolved in solution so the effect of orthosilicic acid on the rate is not isolated. Experimental testing was also carried out on the alternate test method and K_g values were obtained successfully. This data set of K_g values will be subjected to statistical analysis to determine if there are primary and secondary glass composition dependencies. These dependencies can then be used to determine how to represent K_g for the expected range of EWG glass compositions. Due to the nature of the K_g value a single, conservative bounding value may be used to represent all EWG compositions or the magnitude of K_g may be tied to glass composition.

In addition, a rate model verification effort is being executed in which the K_g values determined for individual glasses are being combined with independently-measured dilute rate parameters and used to model theoretical response of the glass in a PCT. These responses are then being compared to experimental data sets to determine how well the independently-measured parameters describe the complete time dependence response as a validation of the rate model. The impact of the K_g value used in the validation model on the degree of deviation between the predicted and actual response is being explored to support the definition of K_g values selected for IDF PA uncertainty analysis. Final results are expected to be available to the IDF PA maintenance effort in FY 2022.

- **Alkali Ion Exchange**: The NRC reviewer noted the uncertainty associated with estimates of alkali ion exchange rates as demonstrated in Figure 4.6 from PNNL-13043, *Waste Form Release Data Package for the 2001 Immobilized Low-Activity Waste Performance Assessment*. The alkali ion-exchange process within borosilicate glass has long been recognized as being a diffusion-based process that involves the exchange of hydronium ions with alkali ions within the glass matrix ("A glass dissolution model for the effects of *S/V* on leachate pH" [Feng and Pegg 1994], "The ion exchange phase in corrosion of nuclear waste glasses" [Ojovan et al. 2006]). However, until recently testing methods have not focused on extracting the time and pH dependency that results from these mechanistic phenomena. Not accounting for these effects may be one of the reasons for variation in experimentally-derived ion-exchange rates.

  To circumvent this limitation, work at VSL and PNNL has been ongoing since FY 2017 to gather information on the time, temperature, and pH dependence of alkali ion exchange in ILAW glasses to better represent the ion-exchange process in the rate model (PNNL-26594, *A Critical Review of Ion Exchange in Nuclear Waste Glasses to Support*

the Immobilized Low-Activity Waste Integrated Disposal Facility Rate Model). Initial results indicate the time-dependent ion-exchange rates rapidly fall below the time-invariant constant rate values utilized for the 2017 PA analysis. This program includes work using an alternate test method to measure time-dependent ion-exchange rates, the Pulse Flow Tests developed by VSL (VSL-19R4620-2, *Final Report FY 2019 ILAW Glass Ion Exchange Rate Testing*) and analysis of data from surface area:volume variable (known as q/S) SPFT tests at PNNL in FY 2021. The equation being parameterized is:

$$r_{IEX} = \frac{1}{2} k_{d0} exp\left(-\frac{E_{ad}}{RT}\right)\left(\frac{[H^+]}{[H^+]_0}\right)^\alpha t^{-\gamma}$$

Note: Υ is a positive number (theoretically 0.5) and the model conceptually accounts for ion-exchange rate diminishing with time as the outer layer of glass becomes depleted of alkali ions. To date, data has been collected and analyzed for 17 glasses and data for at least 4 more glasses will be available in FY 2021. These 21 glasses represent a large portion of the compositional region for both baseline and enhanced waste loading glasses, especially for the alkali and alkali-earth species that are pertinent to the ion-exchange process (Figure 2-7-7). Results for the ion-exchange time-dependent rate parameters are being evaluated for correlations with glass composition (as individual constituents, or combinations of constituents). This approach will define how best to represent the parameters for the time-dependent ion-exchange rate equation for the full ILAW glass compositions and the associated uncertainty (e.g., a single set of conservative parameters, or parameters whose magnitude are tied to glass composition). Initial results indicate that once a glass starts to corrode in the disposal environment, within a year, the predicted time-dependent ion-exchange rates fall below the time-invariant constant rate values utilized for the 2017 PA analysis. Finally, data from long-term dissolution tests are being evaluated to determine whether the ion-exchange rates eventually reach steady state as the glass dissolution front recedes at the same rate as the ion-exchange front is receding into the glass. Final results are expected to be available to the IDF PA maintenance effort in FY 2022.

- **Potential for, and Effect of, Stage III Behavior**: This topic is more fully addressed in the response to RAI 2-09. The following discussion is a summary of the recent work being conducted for the IDF PA maintenance program to address the potential impacts of Stage III behavior.

The potential uncertainty in the glass dissolution rate that results from Stage III dissolution behavior is being addressed through zeolite seeding experiments using 24 statistically-designed glasses that span the possible composition space for the enhanced waste loading glasses, which in itself covers a majority of the composition ranges of components included in the baseline models. In summary, samples of the 24 glasses are being incubated in aqueous solutions, at multiple temperatures, both with and without zeolite seeding. In the static test, zeolite seeds can initiate an acceleration of glass dissolution (Stage III) (PNNL-28898, *FY2019 Status Report: Seeded ILAW Glass*

Stage III Static Dissolution Rate Measurements; "In-situ monitoring of seeded and unseeded stage III corrosion using Raman spectroscopy" [Ryan et al. 2019]). Initial results indicate that the magnitude and onset of Stage III behavior can vary with composition with some glasses showing no evidence of rate increase. Dissolved glass component concentrations are being measured in periodically-collected liquid samples to assess the dissolution rate with time. At the conclusion of the tests, the secondary solid phases that are formed are also being analyzed and the results used to compare to phases identified in unseeded static tests of the same glasses. The unseeded test data will support defining the secondary mineral network to be used in the IDF PA. The glasses being tested provide statistical coverage of the VLAW glass composition region (see the next section). The seeded test solids analysis will provide comparison of changes to the phases upon Stage III occurrence and in the artificial presence of zeolite phases.

Figure 2-7-7. Scatterplot of 15 Glass Compositions for Which Sodium Ion Exchange Was Measured by Single-Pass Flow-Through (12 red full circles), by Single-Pass Flow-Through and Pulse Flow Test (3 black diamonds), and by Pulse Flow Test Only (3 blue triangles).
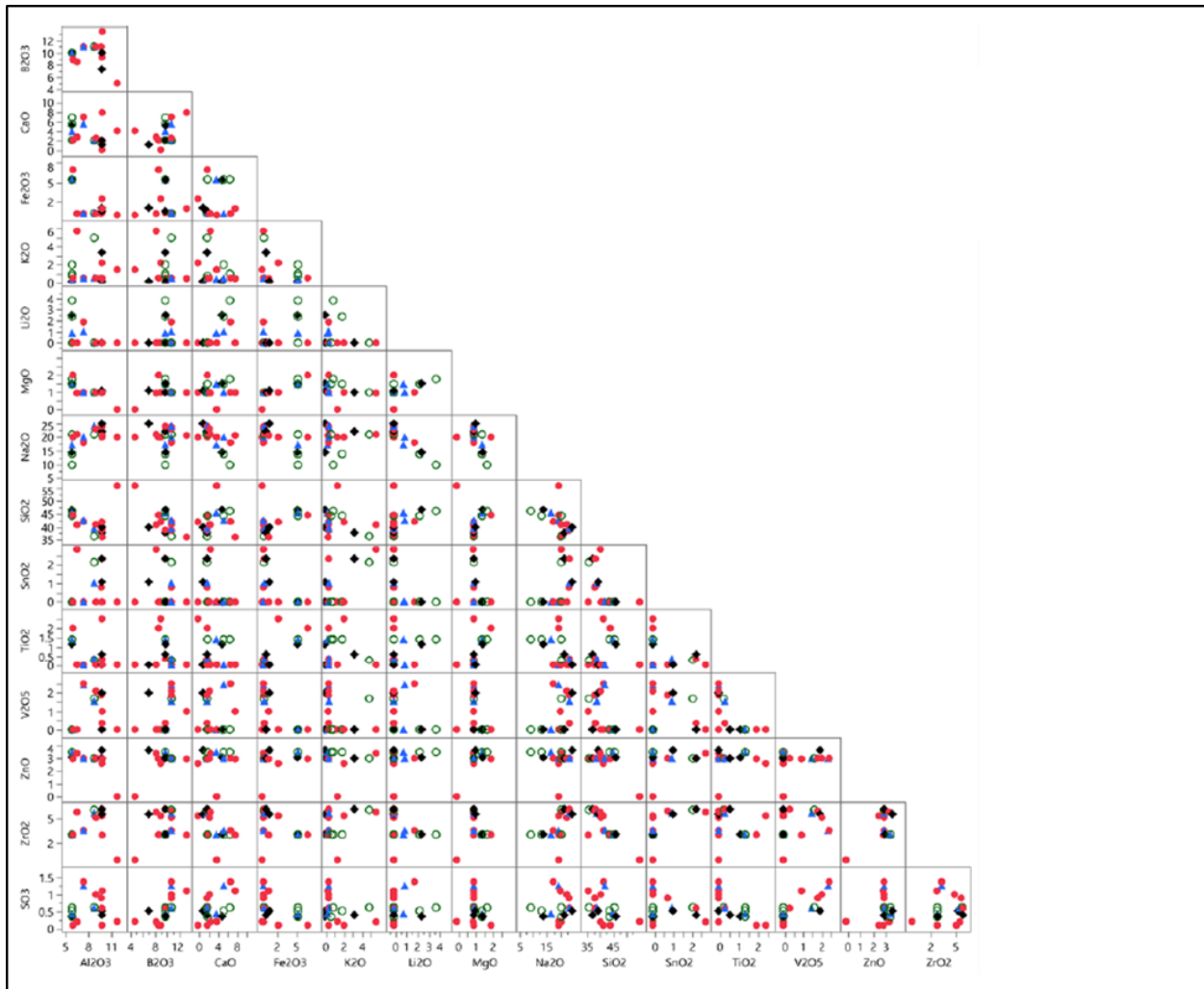
Note: Glasses to be measured by Pulse Flow Test in fiscal year 2021 are shown in the green open circles.

The dissolution rates in seeded tests (Stage III rates) are also being correlated with glass composition to determine if individual constituents, or combinations of constituents, dictate the magnitude of the Stage III rates and subsequent behavior. The range of the measured Stage III rates will be evaluated as part of the IDF PA uncertainty evaluation to determine: 1) if the occurrence of Stage III in the IDF using a conservative Stage III rate can still meet performance objectives, or 2) if compositional constraints could be imposed to assure Stage III rates for the full ILAW glass inventory would fall within performance objective limits. Final results are expected to be available for the IDF PA maintenance effort in FY 2022.

- **Secondary Mineral Reaction Network**: The SMRN employed in the IDF PA requires an update to encompass the EWG composition region, to provide technical defense in depth for the mineral phases used in the PA, and to evaluate any potential correlation between the secondary mineral phases formed and the glass composition. Thus far, efforts on secondary minerals for EWGs have only focused on their impact on Stage III behavior. However, additional relevant secondary phases, which are instrumental in predicting long-term glass dissolution rates in the IDF PA, have not been fully identified for EWG glasses. The SMRN used in IDF PA modeling is being revised in FY 2021 and FY 2022 based on solids analysis conducted at VSL in long-term PCTs (c.f. VSL-20R4820-1) and at PNNL for the unseeded and seeded Stage III tests. Geochemical modeling will be used to assess the ability of the SMRN to match glass dissolution data using the existing SMRN, any updated SMRN for EWG, and phases observed in the long-term tests. This work will follow the approach detailed in PNNL-20781, but more emphasis will be given to including frequently measured compounds and those with greatest potential to influence dissolution behavior in the IDF environment. This information will be available to the IDF PA maintenance effort in FY 2022.

- **Corroboration of IDF PA Prediction and Field Lysimeter Results**: Work is being conducted to validate predictions of ILAW glass dissolution rates in the Hanford Site IDF using the Field Lysimeter Test Facility (FLTF). As shown in Figure 2-7-8, the FLTF has a series of field lysimeter tubes (most extend to a depth of 3 m) that can be filled with various waste forms, including glass and cementitious materials, and back filled with IDF soils. Water infiltration rate is controlled within each lysimeter tube. Water samples will be collected at various depths within the lysimeters over the next several years, along with measurements of the *in situ* distribution of moisture.

  Prior to initiation of the lysimeter test, a modeling effort was performed using the same simulation style as the IDF PA to predict the behavior of the emplaced waste forms and corresponding contaminant release, using ^{99}Tc and ^{127}I as tracers for the cementitious waste forms and molybdenum and rhenium as tracers for the glass waste forms (PNNL-27394, *Field-Scale Lysimeter Studies of Low-Activity Waste Form Degradation Implementation Plan*). As data are collected from the tests, comparisons will be made against the initial modeling that will serve as validation of the model and determine the extent to which the laboratory-based parameters are applicable to waste form behavior in the field. Water analysis and *in situ* soil moisture data from these tests will start to be

available in FY 2021 but data from solids analysis will not be available until the tests conclude, which depending on the test may be 5 years to 25 years in the future.

Figure 2-7-8. Images of the Field Lysimeter Test Facility a) Aerial Photograph of the Facility, b) Artist Three-Dimensional Drawing of the Facility, c) Depiction of the Layout of Buried Waste Forms and Sampling Devices Within a Single Lysimeter Tube, d) Photograph of the Lower Level of Buried Cementitious Waste Forms, and e) Photograph of the Underground Sampling Bay Showing the Two Rows of Lysimeter Tubes.

With the two glass formulations selected, Stage III behavior may not be observed over the duration of the lysimeter test. However, post-experimental characterization of the excavated waste forms and backfill will also be completed at the test conclusion to evaluate the evolution of mineral phases and to determine if any zeolite phases have been formed. Note that the presence of zeolites does not indicate that Stage III behavior is inevitable, but their presence does suggest Stage III may occur. As stated under the discussion of Stage III (above), data is also being collected in laboratory tests to assess the magnitude of the impact of Stage III rate behavior on contaminant release from the IDF to the surrounding environment.

Conclusion – The IDF PA model used an abstraction of a rate model that has a development history that has been documented in peer-reviewed literature for decades. The IDF PA model includes uncertainty in the parameters that are associated with the rate model and accounts for additional uncertainties in the development of an abstraction of that rate model. The IDF PA model also includes multiple conservatisms about the propensity of the dissolution rate to be a continuous process despite recent observations that the ion-exchange process (which controls glass dissolution at long time frames) might not be constant and is expected to decrease with time. DOE continues to evaluate the mechanisms associated with borosilicate glass dissolution,

which includes the development of additional glass formulations, models to correlate dissolution rate parameters with glass composition, and additional processes that may accelerate (Stage III) or reduce (diffusion of sodium ions across an expanding layer of alteration products) the VLAW dissolution rate.

In accordance with the PA maintenance plan, advancements in borosilicate glass science are evaluated in the PA on an annual basis as new information is gained.

References

Aagaard, P. and H. C. Helgeson, 1982, "Thermodynamic and kinetic constraints on reaction rates among minerals and aqueous solutions I. Theoretical considerations," *American Journal of Science*, vol. 282, pp. 237–285.

DOE/RL-97-69, 1998, *Hanford Immobilized Low-Activity Tank Waste Performance Assessment*, Rev. 0, U.S. Department of Energy, Richland, Washington.

Feng, X. and I. L. Pegg, 1994, "A glass dissolution model for the effects of *S/V* on leachate pH," *Journal of Non-Crystalline Solids*, vol. 175, Issues 2–3, pp. 281–293.

Fournier, M., P. Frugier, and S. Gin, 2018, "Application of GRAAL model to the resumption of International Simple Glass alteration," *npj Materials Degradation*, vol. 2, Article number 21, pp. 1–9.

Grambow, B., 1985, "A General Rate Equation for Nuclear Waste Glass Corrosion" in *Materials Research Society Symposium Proceedings 44*, pp. 15–27, Cambridge University Press, Cambridge, United Kingdom.

Lasaga A. C., 1995, "Chemical Weathering Rates of Silicate Minerals," Chapter 2. Fundamental approaches in describing mineral dissolution and precipitation rates, in Reviews in Mineralogy and Geochemistry, vol. 31, No. 1, pp. 23–86.

McGrail, B. P., W. L. Ebert, A. J. Bakel, and D. K. Peeler, 1997, "Measurement of kinetic rate law parameters on a Na–Ca–Al borosilicate glass for low-activity waste," *Journal of Nuclear Materials*, vol. 249, pp. 175–189.

Neeway, J. J., P. C. Rieke, B. P. Parruzot, J. V. Ryan, and M. R. Asmussen, 2018, "The dissolution behavior of borosilicate glasses in far-from equilibrium conditions," *Geochimica et Cosmochimica Acta*, vol. 226, pp. 132–148.

Ojovan, M. I., A. Pankov, and W. E. Lee, 2006, "The ion exchange phase in corrosion of nuclear waste glasses," *Journal of Nuclear Materials*, vol. 358, pp. 57–68.

PNNL-11834, 2000, *A Strategy to Conduct an Analysis of the Long-Term Performance of Low-Activity Waste Glass in a Shallow Subsurface Disposal System at Hanford*, Rev. 1, Pacific Northwest National Laboratory, Richland, Washington.

PNNL-13043, 2001, *Waste Form Release Data Package for the 2001 Immobilized Low-Activity Waste Performance Assessment*, Rev. 2, Pacific Northwest National Laboratory, Richland, Washington.

PNNL-13372, 2000, *Vitrification and Product Testing of AW-101 and AN-107 Pretreated Waste*, WTP-RPT-003, Rev. 0, Pacific Northwest National Laboratory, Richland, Washington.

PNNL-14805, 2004, *Waste Form Release Data Package for the 2005 Integrated Disposal Facility Performance*, Pacific Northwest National Laboratory, Richland, Washington.

PNNL-20781, 2011, *Integrated Disposal Facility FY 2011 Glass Testing Summary Report*, Pacific Northwest National Laboratory, Richland, Washington.

PNNL-22631, 2013, *Glass Property Models and Constraints for Estimating the Glass to be Produced at Hanford by Implementing Current Advanced Glass Formulation Efforts*, Rev. 1, ORP-58289, Pacific Northwest National Laboratory, Richland, Washington.

PNNL-24615, 2015, *Immobilized Low-Activity Waste Glass Release Data Package for the Integrated Disposal Facility Performance Assessment*, RPT-IGTP-005, Pacific Northwest National Laboratory, Richland, Washington.

PNNL-25835, 2016, *2016 Update of Hanford Glass Property Models and Constraints for Use in Estimating the Glass Mass to be Produced at Hanford by Implementing Current Enhanced Glass Formulation Efforts*, Pacific Northwest National Laboratory, Richland, Washington.

PNNL-26169, 2017, *FY2016 ILAW Glass Corrosion Testing with the Single-Pass Flow-Through Method*, RPT-IGTP-013, Rev. 0.0, Pacific Northwest National Laboratory, Richland, Washington.

PNNL-26594, 2017, *A Critical Review of Ion Exchange in Nuclear Waste Glasses to Support the Immobilized Low-Activity Waste Integrated Disposal Facility Rate Model*, RPT-IGTP-018, Rev 0.0, Pacific Northwest National Laboratory, Richland, Washington.

PNNL-27098, 2018, *FY2017 ILAW Glass Corrosion Testing with the Single-Pass Flow-Through Method*, RPT-IGTP-015, Rev. 0, Pacific Northwest National Laboratory, Richland, Washington.

PNNL-27394, 2018, *Field-Scale Lysimeter Studies of Low-Activity Waste Form Degradation Implementation Plan*, RPT-IGTP-017, Rev 0.0, Pacific Northwest National Laboratory, Richland, Washington.

PNNL-28898, 2019, *FY2019 Status Report: Seeded ILAW Glass Stage III Static Dissolution Rate Measurements*, Pacific Northwest National Laboratory, Richland, Washington.

RPP-CALC-61031, 2017, *Low-Activity Waste Glass Release Calculations for the Integrated Disposal Facility Performance Assessment*, INTERA, Inc. for Washington River Protection Solutions LLC, Richland, Washington.

RPP-CALC-61192, 2017, *Integrated Disposal Facility Performance Assessment: Sensitivity Calculations for ILAW Glass Dissolution Rate Parameters*, Rev. 0, AEM Consulting, LLC for Washington River Protection Solutions LLC, Richland, Washington.

RPP-CALC-61194, 2018, *System Model Calculations for the Integrated Disposal Facility Performance Assessment*, Rev. 1A, INTERA, Inc. for Washington River Protection Solutions, LLC, Richland, Washington.

RPP-PLAN-60520, 2020, *Program Plan for Immobilized Low Activity Waste (ILAW) Glass Testing*, Rev. 1, Washington River Protection Solutions, LLC, Richland, Washington.

RPP-RPT-59341, 2016, *Integrated Disposal Facility Model Package Report: ILAW Glass Release*, Rev. 0A, Washington River Protection Solutions, LLC, Richland, Washington.

RPP-RPT-59958, 2019, *Performance Assessment for the Integrated Disposal Facility, Hanford Site, Washington*, Rev. 1A, Washington River Protection Solutions, LLC, Richland, Washington.

Ryan, J. V., B. Parruzot, A. M. Lines, S. A. Bryan, L. M. Seymour, J. F. Bonnett, and R. K. Motkuri, 2019, "In-situ monitoring of seeded and unseeded stage III corrosion using Raman spectroscopy," *npj Materials Degradation*, vol. 3, Article number 34, pp. 1–7.

VSL-01R3501-2, 2001, *Final Report – Melter Tests with LAW Envelope A and C Simulants to Support Enhanced Sulfate Incorporation*, Vitreous State Laboratory, The Catholic University of America, Washington, D.C. (ORP-63503, 2001, *Final Report – Melter Tests with LAW Envelope A and C Simulants to Support Enhanced Sulfate Incorporation, VSL-01R3501-2, Rev. 0*, Rev. 0, U.S. Department of Energy, Office of River Protection, Richland, Washington).

VSL-06R6480-1, 2006, *Final Report – DuraMelter 100 Tests to Support LAW Glass Formulation Correlation Development*, Vitreous State Laboratory, The Catholic University of America, Washington, D.C. (ORP-56324, 2006, *Final Report – DuraMelter 100 Tests to Support LAW Glass Formulation Correlation Development, VSL-06R6480-1, Rev. 0*, Rev. 0, U.S. Department of Energy, Office of River Protection, Richland, Washington).

VSL-07R1130-1, 2007, *Final Report – Enhanced LAW Glass Formulation Testing*, Vitreous State Laboratory, The Catholic University of America, Washington, D.C. (ORP-56293, 2007, *Final Report – Enhanced LAW Glass Formulation Testing, VSL-07R1130-1, Rev. 0, dated 10/05/07*, Rev. 0, U.S. Department of Energy, Office of River Protection, Richland, Washington).

VSL-19R4620-2, 2019, *Final Report FY 2019 ILAW Glass Ion Exchange Rate Testing*, Vitreous State Laboratory, The Catholic University of America, Washington, D.C.

VSL-20R4820-1, 2020, *Final Report FY2020, Long-Term PCT of ILAW Glasses*, Vitreous State Laboratory, The Catholic University of America, Washington, D.C.

RAI 2-8 (Glass Cracking)

Comment
Additional information is needed on the basis for the assumed factor of 10 increase in specific surface area of the glass to account for cracking.

Basis
Glass release rates for many glass formulations, although not all, are directly proportional to the specific surface area (m2/g). To account for potential cracking of the glass during cooling and handling, DOE increase the geometric surface area of the glass by a factor of 10. In sensitivity cases (termed RSA) examined in the PA document, DOE further increased the specific surface area by a factor of 10 and showed a proportional increase in the fractional release rate for two do not address what the value will be for production-scale glass canisters which will have different glass compositions.

Many of the reports dealing with cracking of glass are older (e.g., PNL-5947) but do have useful information to try to evaluate the DOE assumed value of 10. PNL-5947 had a maximum adjusted relative surface area of 65 with many of the reported values greater than 10. Table 1 show below (from ML040130177) provides some observed values from the literature (including values from PNL-5947).).

Table 2-8-1. Summary of Studies Examining Surface Area Increases Due to Thermal Fracturing.

Glass Composition	Glass block size (relative)	Surface Area Increase (relative to unfractured glass)	Reference
SRL211	large-scale	2 - 40	Smith and Baxter 1981
SRL211, SRL131	large-scale	7 - 18	Peters and Slate 1981
SRL211, SRL131	small-scale	0 - 18	Peters and Slate 1981
borosilicate	large-scale	9.0 - 16.3	Laude et al. 1982
SRL165	large-scale	25 - 35	Bickford and Pellarin 1987
borosilicate	small- to large scale	1.1 - 86	Faletti and Ethridge 1988
borosilicate	medium-scale	2.0 - 10	Lutze et al. 1986
R7T7	small-scale, 1:10	10 -12	Vernaz and Godon 1991
PNL76-375	large-scale	8 - 45	Martin 1985
PNL76-375	small-scale	1.1 - 12	Martin 1985
borosilicate	medium-scale	not measured	Keinzler 1989
BRET HLW borosilicate glass	medium-scale	not measured	Farnsworth et al. 1985

Source: Table 1 of Section 2.2.1.5 of UCRL-ID-108314, *Preliminary Waste Form Characteristics Report Version 1.0*, Rev. 1.

NRC staff were not able to determine the canister filling and cooling procedures that DOE would use to determine the appropriateness of the assumed factor of 10. Rapid cooling can contribute to more significant crack formation, however slow cooling can impact the quality and performance of glass that is produced. NRC staff were also not able to identify verification plans for the specific surface area in production-scale glass canisters.

Path Forward
Please provide additional technical basis for the assumed effect of cracking on glass specific surface area, utilize a bounding value, or provide plans to verify the assumed value in production-scale glass canisters. Please describe the cooling cycles anticipated to be used during glass production.

DOE Response

Source of 10X Estimate for Increased Reactive Surface Area Due to Cracking
The reactive surface area increase of 10 times (10X) to account for cracking was introduced in the first ILAW PA in 2001, where it is stated on page 5 of PNNL-13369 that "Fracturing is expected to increase the glass surface area a maximum of 10X over its geometric surface area." The evidence provided to support this value was the statement that there is a "sparse degree of

glass fracturing in the waste package based on prior experience with high-level waste glasses (Farnsworth et al. 1985; Peters and Slate 1981)." This same language is repeated to support a fractured glass surface area equal to 10 times the external waste package surface area in the data package produced for a 2005 update of the IDF PA (PNNL-15198) and also the 2017 IDF PA (RPP-RPT-59958). The 2017 IDF PA also cites RPP-17657, *Risk Assessment Supporting the Decision on the Initial Selection of Supplemental ILAW Technologies*, but that document does not add any new information to support the value of 10X. Rather, RPP-17657 again states "Stresses induced from differential rates of cooling are expected to induce stress fractures in the glass. Our baseline assumption is that available glass surface area is 10X greater than geometric surface area (PETERS and SLATE, 1981; FARNSWORTH et al., 1985)." In summary, the current and historic IDF PAs have based the assumption of an increase in reactive surface area in VLAW of 10 times over the waste package external surface area and two cited references are given to support this assumption.

Of the two references listed in the various IDF PA documents, only "Fracturing of Simulated High-Level Waste Canisters" (Peters and Slate 1981) directly reports estimated surface area increases due to cracking. "The Effect of Radial Temperature Gradients on Glass Fracture in Simulated High-Level Waste Canisters" (Farnsworth et al. 1985) reports data on the distribution of particle sizes for fractured nuclear waste glasses cooled under different conditions; no measurements of surface area increases are provided. The upper value for the surface area increase in Peters and Slate (1981) is 18 times the external surface area. It is important to note that the surface area estimates provided by these authors were generated from visual inspection of fracturing, and, as will be discussed below, are not an estimate of the changes in *reactive* surface area, but rather are estimates of the changes in *total* surface area.

Factors Affecting Estimates of Reactive Surface Area for Nuclear Waste Glasses
The increase in surface area available for glass corrosion due to cracking depends on two independent properties; the degree of cracking and the susceptibility of the cracks to corrosion. The degree of cracking in nuclear waste glass is largely driven by the cooling profile through the annealing range (DP-1629, *An Assessment of Savannah River Borosilicate Glass in the Repository Environment*) and the properties of the container in contact with the cooling glass ("A Method for Predicting Cracking in Waste Glass Canisters" [Faletti and Ethridge 1988]). The susceptibility of the cracks to corrosion is governed by factors such as the location of the cracks in the monolith, the geometric properties of the cracks, and the rate of corrosion and corrosion product diffusion. Cracks that are completely internal to the waste form are not accessible to water infiltration. In narrow cracks that are accessible to water infiltration, corrosion of the glass will form alteration products that can fill the cracks and result in self-sealing ("A fractured roman glass block altered for 1800 years in seawater: Analogy with nuclear waste glass in a deep geological repository" [Verney-Carron et. al 2008]). If the rate of glass dissolution is rapid compared with the diffusive or advective movement of the dissolved glass components through a crack, then the accumulation of glass components in the pore fluid will slow the dissolution reactions (see description of transition-state-theory model in the response to RAI Comment 2-7). Hence, not all cracks visually observed in tests, such as those reported by Peters and Slate (1981) and Farnsworth et al. (1985) and those in the table provided with this comment, will increase dissolution rates in direct proportion to the increased surface area.

ORP-59015-00, *Glass Formulations and Testing with TWRS LAW Simulants, Final Report* expressed the relationship between external surface area of a glass and the reactive surface area available for dissolution due to cracking by the following equation:

$$S_g = \alpha \cdot \beta \cdot A_g \tag{1}$$

Where:

S_g = Surface area available to water for dissolution reaction (termed the "reactive surface area" [cm^2])
α = Ratio of total surface area (external + cracks) to the external surface area (unitless)
β = Fraction of crack surface area available to water for dissolution reaction (unitless)
A_g = External surface area of the ILAW glass waste package (cm^2).

Testing such as that reported in the table provided in this comment provide measurements of α, but do not suggest the impacts of β on dissolution rates. Unfortunately, there has been little direct research to quantify β for nuclear waste glasses. "Effects of Cracks on Glass Leaching" (Perez and Westsik 1981) report the results of glass dissolution experiments using uniform glass pucks separated by platinum wires to simulate cracks. The experimental apparatus is shown in Figure 2-8-1 (a reproduction of Figure 1 from Perez and Westsik [1981]).

Figure 2-8-1. Schematic of Clamp-Pellet Assembly.

FIGURE 1. Schematic of clamp-pellet assembly.
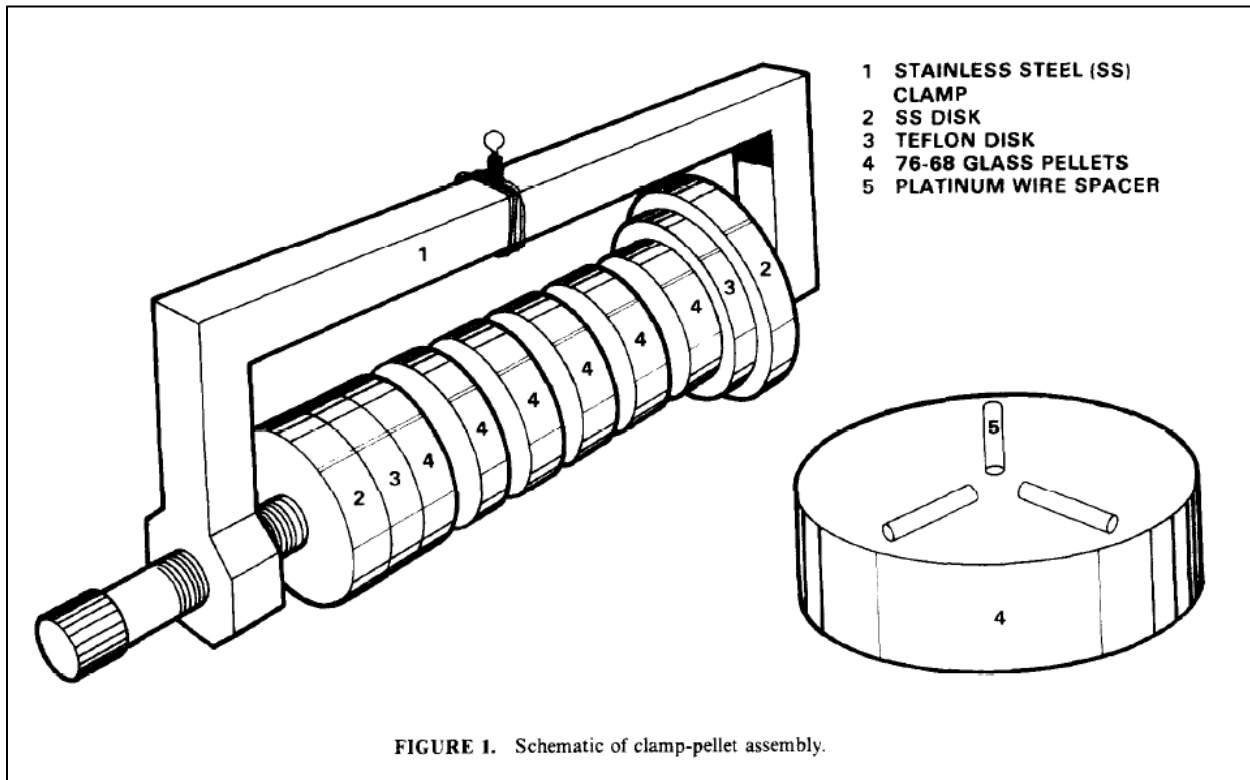
Gaps with widths of "infinite," 0.038 cm, "nominally zero," and "zero" were tested. The "infinite" condition was represented by incubating well-spaced samples in water. The 0.038-cm condition used platinum wire as shown above to separate the glass pucks that were then held together with the clamp. The "nominally zero" condition used pucks clamped together with no spacing wire. The "zero" condition used a glass monolith rather than separate pucks clamped together. All samples were incubated in water at 98 °C and the concentrations of glass components (silicon, sodium, cesium, and boron) were measured for 92 days. The results showed little to no reaction within the nominally zero cracks and that the external surface glass reacted faster than the glass within the 0.038-cm cracks. The ratio of the estimated crack reaction rate (based on the 0.038-cm cracks) to the surface reaction rate ranged from 0.4 (based on sodium release) to 0.2 (based on silicon release). These results affirm the assertion that 1) not all observed cracks provide reactive surface area for hydrolysis, and 2) slow diffusive and advective processes within the cracks may lead to the accumulation of glass components in the pore fluid and slower dissolution reactions. Both phenomena will contribute to lowering the value of β.

In an analysis of a fractured archaeological glass block altered for 1,800 years in seawater, Verney-Carron et al. (2008) report that if all surface area (including cracks) had reacted at the rate of the exposed outer surface the samples would have a total altered volume of 88.4%. However, the measured percentage of altered glass was only 12.2%. These values equate to an average β value of 0.14, which is below the range reported by Perez and Westsik (1981).

A β value of 0.13 can be derived from the estimated dissolution rates for R7T7-type nuclear waste glass provided in "Archaeological analogs and the future of nuclear waste glass" (Verney-Carron et al. 2010). This work compared simulated dissolution of R7T7-type glass under two hypothetical conditions. The first condition simulated all surface area (external and cracks) undergoing transformation at the residual rate (that considers the effects of saturation in solution, the passivating role of the alteration layer and the slow precipitation of secondary crystalline phases), but without diffusion limitations within cracks. The second condition accounted for diffusion limitations within cracks. The former condition resulted in a predicted alteration volume of 40% after 100,000 years of simulated time, while the latter conditions resulted in a predicted alteration volume of only 5% after the same simulated duration.

Finally, DP-1629 reports that the relative increase in surface area observed for large containers of high-level nuclear waste glass was about 25 times the unfractured surface area. However, the leaching rate only increased by a factor of 5 which implies a β value of 0.2.

Review of the Possible Range for α for VLAW Glasses

Faletti and Ethridge (1988) provide a summary of measured values of α for nuclear waste glasses formed in canisters of differing sizes (from 17 to 60 cm in diameter) and materials (carbon and stainless steel), and cooled under a variety of conditions. The experimentally-measured α values summarized by these authors range from 1 to 97 (see the "Source" column in Table 1 of Faletti and Ethridge [1988]).

Note that this is a slightly larger range than what is reported for these authors in the table provided in UCRL-ID-108314, *Preliminary Waste Form Characteristics Report Version 1.0*,

cited in the Basis as ML040130177. If data for canisters that were cooled by water quenching are excluded from the analysis[47], then the values range from 1 to 48. This reduced range is similar to the range observed from all the other test results reported in Table 1 of UCRL-ID-108314. It is also similar to the value of 40 for SON68 nuclear waste glass quoted in Verney-Carron et al. (2008).

Faletti and Ethridge (1988) suggest the need for an adjustment factor to account for the fact that the values were measured using either radial or longitudinal slices of the waste forms and both methods underestimate the cracking that occurs perpendicular to the slices. A factor of 1.58 for values measured using radial slices and 1.36 for values measured from longitudinal sections is proposed. Application of these factors yields a range of α for the air cooled canisters of 1 to 65 (see the "Adjusted" column in Table 1 of Faletti and Ethridge [1988]).

This adjusted data, along with temperature cooling profiles for the associated test, were used to suggest a correlation between the center line temperature and surface temperature when the centerline temperature is equal to 500 °C (termed ΔT_r) and α. For carbon steel canisters the suggested correlation is:

$$RA = 1.0 \text{ for } \Delta T_r \leq 30 \text{ °C}$$
$$RA = 1.0 + 0.10 \, \Delta T_r \text{ for } \Delta T_r \geq 30 \text{ °C}$$

and for stainless steel canisters the correlation is:

$$RA = 1.0 \text{ for } \Delta T_r \leq 30 \text{ °C}$$
$$RA = 1.0 + 1.23 \, \Delta T_r \text{ for } \Delta T_r \geq 30 \text{ °C}$$

The order-of-magnitude difference in the slopes of the two correlations was suggested to be the result of the greater propensity of glass to adhere to stainless steel. The reference temperature of 500 °C was chosen because it is slightly below the glass transition temperature of most nuclear waste glasses, and so below this temperature the glass no longer has the ability to absorb residual stresses due to changes in density as the glass cools. It should be noted that the equation for stainless steel containers was developed from only two data points extracted from NUREG/CR-4198, *Fracture in Glass/High Level Waste Canisters Final Report* and the authors, Faletti and Ethridge (1988), indicated that additional data would be needed to confirm the validity of the correlation.

Ignoring the uncertainty associated with the limited data, and applying the equation for stainless steel containers using the predicated cooling profile for the Hanford ILAW canisters, gives an estimate of 74 for the average α (Table 2-8-2). Data for the canister cooling profiles were taken from CALC-ILAW-ME-0003, *ILAW Transporter Project, ILAW Container Cooling Profiles from WTP ILAW Shipping through Two Weeks on the IDF Cooling Pad*, Rev. 2 (see Figure 2-8-2). Results are given for three simulated canisters that are placed in proximity to one another. Heat profiles are slightly different for each canister as a result of their relative locations and the sequence they leave the cooling area. The predicted average α value is slightly higher

---

[47] Note that water cooling can create greater thermal gradients and increased cracking over air cooling and the WTP VLAW canisters will be air cooled (Farnsworth et al. 1985).

than the maximum of the range of the adjusted values reported by Faletti and Ethridge (1988) for air cooled containers (i.e. $\alpha = 65$).

Table 2-8-2. Temperature Profile Data and the Corresponding Predicted α Values.

Location	Canister	F	C	Delta-T (C)	α
Centerline	All	932	500	—	—
Surface	1	355	179	321	74.7
Surface	2	360	182	318	74.1
Surface	3	365	185	315	73.5
Average -->					74.1

Figure 2-8-2. Predicted Maximum Centerline and Surface Temperatures for Hanford Vitrified Low-Activity Waste Containers Cooling in the Transport Pallet.
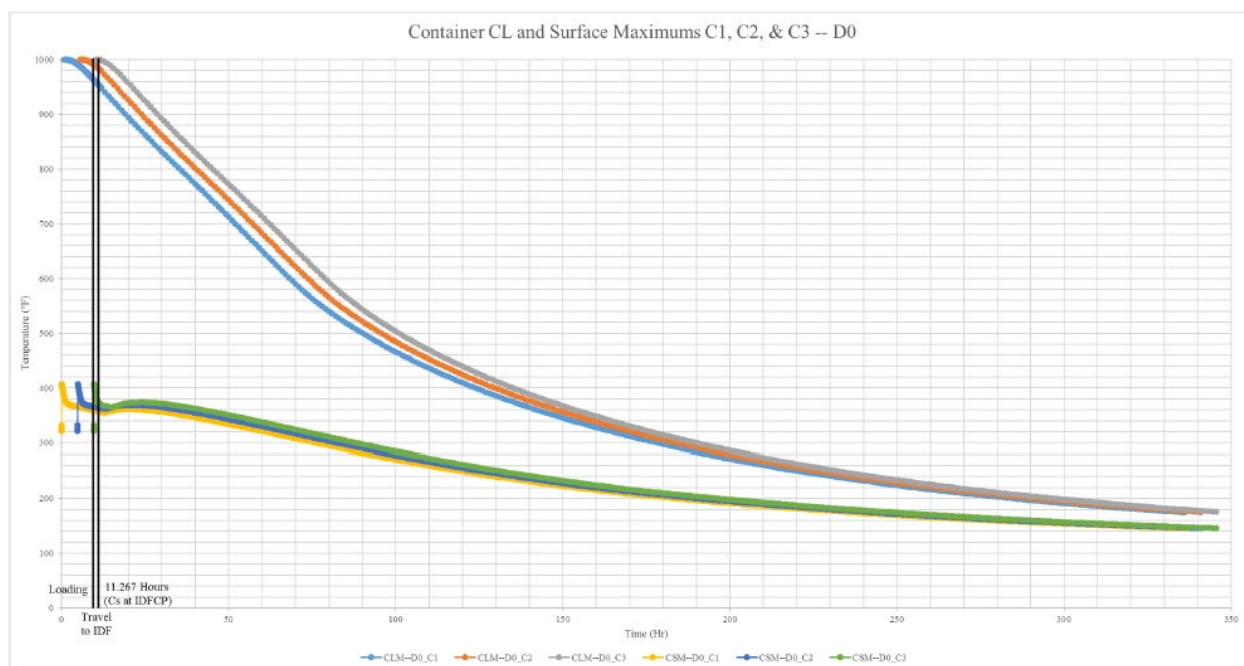
Source: CALC-ILAW-ME-0003, *ILAW Transporter Project, ILAW Container Cooling Profiles from WTP ILAW Shipping through Two Weeks on the IDF Cooling Pad*, Figure 6-1.

In summary, data for air-cooled nuclear waste glasses suggests that the ratio of total surface area (external + cracks) to the external surface area (i.e., α) could be as much as 74 for Hanford VLAW containers, but that the range of measured values is from 1 to 48 (unadjusted values), or 1 to 65 (adjusted values).

Table 2-8-3 summarizes the range of values for the ratio of reactive surface area (S_g) to external surface area (A_g) that is derived by combining the maximum α values described in the preceding paragraph with the range of estimated β values (0.13 to 0.4). Results using an average of the α values reported by Faletti and Ethridge (1988) for results in air-cooled stainless steel containers is also included in the table. It is of note that the average α value of 27 is close to the value of 25 reported in DP-1629 for air-cooled stainless steel containers of HLW glass. In addition, DP-1629 reports a product of α and β equal to 5 which is within the range (3.6 to 11) calculated using the average α value reported by Faletti and Ethridge (1988) for air-cooled stainless steel containers.

Table 2-8-3. Range of Predicted Reactive Surface Area to External Surface Area (S_g/A_g).

Data Set	Maximum α	S_g/A_g
Faletti and Ethridge (1988), unadjusted data	48	6.2 to 19
Faletti and Ethridge (1988), adjusted data	65	8.5 to 26
Estimated based on Faletti and Ethridge (1988) correlation and Hanford VLAW cooling profiles	74	9.6 to 30
Faletti and Ethridge (1988), average of adjusted values for air-cooled stainless steel containers (see from their Table 1)	27*	3.6 to 11

*The value is an average rather than a maximum.

Reference: Faletti, D. W. and L. J. Ethridge, 1998, "A Method for Predicting Cracking in Waste Glass Canisters," *Nuclear and Chemical Waste Management*, vol. 8, Issue 2, pp. 123–133.

As is evident from the table, the value of 10 times that was used for the IDF PA analysis is within the range of results for each case listed. In addition, the maximum predicted value of reactive surface area for all cases only exceeds the 10 times value by a factor of 3. A factor of 3 increase is within the range of uncertainty evaluated in the PA in sensitivity studies and in the uncertainty analysis. Furthermore, RPP-CALC-61031 (Tables 6-2 and 6-4) shows a nearly proportional relationship between the reactive surface area and the glass dissolution rate. Also, the Risk Budget Tool (RPP-CALC-63176 Rev. 0A) demonstrates that peak groundwater and dose results in the PA scale linearly with the dissolution rate so the PA results would change by at most a factor of 3 over the base case. Since the peak groundwater concentration from ^{99}Tc in glass is approximately a factor of 10 below the EPA maximum contaminant level (MCL), and the dose is well below 4 mrem/yr, a change in dose by a factor of 3 would not change the conclusions of the PA.

Description of the Estimated Cooling Profile for Hanford VLAW Glass Containers
The VLAW glass disposal containers are stainless steel, 4 ft in diameter and 7.5 ft tall right circular cylinders. To allow the glass to flow uniformly to the periphery of the container, the glass is poured into the container at a rate of about 2.7 times the average glass production rate of 15 MT glass/day per melter (24590-WTP-RPT-PT-02-005, Rev. 8). The glass is poured periodically in batch mode, while slurry feeding to the melter is continuous. The design temperature of the glass pour is 1,150 °C. The nominal glass pour is 1,420 kg over a period of

51 minutes to minimize melt pool level change. About four pours are required to fill a VLAW container (24590-WTP-RPT-PT-02-005, Rev. 8).

Filled containers remain in the WTP facility with forced-air cooling for up to 42 hours from the start of the pour (CALC-ILAW-ME-0003). The containers will then be placed in pallets, a shielded structure that allows the containers to be safely transported from the WTP to the IDF. The thermal analysis results shown in Figure 2-8-2 describe the predicted temperature response at the centerline and surface of the container once it leaves the area of active cooling and is placed in the pallet. Results are given for three simulated canisters that are placed in proximity to one another. Heat profiles are slightly different for each canister as a result of their relative locations and the sequence they leave the cooling area. Data sets in the figure beginning with "CLM" represent maximum centerline temperatures and those beginning with "CSM" represent maximum surface temperatures.

References

24590-WTP-RPT-PT-02-005, 2016, *Flowsheet Bases, Assumptions, and Requirements*, Rev. 8, Bechtel, River Protection Project, Waste Treatment Plant, Richland, Washington.

CALC-ILAW-ME-0003, 2017, *ILAW Transporter Project, ILAW Container Cooling Profiles from WTP ILAW Shipping through Two Weeks on the IDF Cooling Pad*, Atkins, Richland, Washington.

DP-1629, 1982, *An Assessment of Savannah River Borosilicate Glass in the Repository Environment*, E. I. du Pont de Nemours & Co., Savannah River Laboratory, Aiken, South Carolina.

Farnsworth, R. K., M. K. W. Chan, and S. C. Slate, 1985, "The Effect of Radial Temperature Gradients on Glass Fracture in Simulated High-Level Waste Canisters," *Materials Research Society Symposium Proceedings*, vol. 44, pp. 831–838.

Faletti, D. W. and L. J. Ethridge, 1998, "A Method for Predicting Cracking in Waste Glass Canisters," *Nuclear and Chemical Waste Management*, vol. 8, Issue 2, pp. 123–133.

NUREG/CR-4198, 1985, Fracture in Glass High Level Waste Canisters, NUREG/CR-4198, Iowa State University for U.S. Nuclear Regulatory Commission, Washington DC (1985).

UCRL-ID-108314, 1994, *Preliminary Waste Form Characteristics Report Version 1.0*, Rev. 1, Lawrence Livermore National Laboratory, Livermore, California (ML040130177).

ORP-59015-00, 1998, *Glass Formulations and Testing with TWRS LAW Simulants, Final Report*, Rev. 0, Vitreous State Laboratory at The Catholic University of America, Washington, D.C.

Perez, J. M. and J. H. Westsik, 1981, "Effects of Cracks on Glass Leaching," *Nuclear and Chemical Waste Management*, vol. 2, Issue 2, pp. 165–168.

Peters, R. D., and S. C. Slate, 1981, "Fracturing of Simulated High-Level Waste Canisters," *Nuclear Engineering and Design*, vol. 67, Issue 3, pp. 425–445.

PNL-5947, 1986, *A Method for Predicting Cracking in Waste Glass Canisters*, Pacific Northwest Laboratory, Richland, Washington.

PNNL-13369, 2001, *Waste Form Release Calculations for the 2001 Immobilized Low-Activity Waste Performance Assessment*, Pacific Northwest National Laboratory, Richland, Washington.

PNNL-15198, 2005, *Waste Form Release Calculations for the 2005 Integrated Disposal Facility Performance Assessment*, Pacific Northwest National Laboratory, Richland, Washington.

RPP-17657, 2003, *Risk Assessment Supporting the Decision on the Initial Selection of Supplemental ILAW Technologies*, Rev. 0, CH2M HILL Hanford Group, Inc./Pacific Northwest National Laboratory/Fluor Federal Services, Inc., Richland, Washington.

RPP-CALC-61031, 2017, *Low-Activity Waste Glass Release Calculations for the Integrated Disposal Facility Performance Assessment*, INTERA, Inc. for Washington River Protection Solutions, LLC, Richland, Washington.

RPP-CALC-63176, 2020, *Integrated Disposal Facility Risk Budget Tool Analysis*, Rev. 0A, Washington River Protection Solutions, LLC, Richland, Washington.

Verney-Carron, A., S. Gin, and G. Libourel, 2008, "A fractured roman glass block altered for 1800 years in seawater: Analogy with nuclear waste glass in a deep geological repository," *Geochimica et Cosmochimica Acta*, vol. 72, Issue 22, pp. 5372–5385.

Verney-Carron, A., S. Gin, and G. Libourel, 2010, "Archaeological analogs and the future of nuclear waste glass," *Journal of Nuclear Materials*, vol. 406, Issue 3, pp. 365–370.

RAI 2-9 (Glass Stage III)

Comment

Additional information is needed to support the basis that Stage III glass corrosion will not occur for disposal of vitrified waste at IDF.

Basis

Stage III behavior in glass corrosion or degradation is believed to occur late in the reaction sequence as a result of the formation of zeolites and other phases which deplete silicon and other species in solution faster than which those species are added to solution. The phenomenon is not well-understood but has been associated with higher temperatures and closed systems. DOE indicated that Stage III conditions are not likely at IDF because it will be low temperature (15°C) and an open system. The temperature of the system is fairly certain unless degrading organic matter or heat-generating waste were to be disposed in the facility. The openness of the system is more uncertain. The impermeable asphalt layer combined with the Geosynthetic Composite Layer (GCL) liner under the facility can result in very low flow rates and conditions that could approximate a closed system. In addition, the fluid that reacts with the glass in the simulations was not a fluid that had reacted with the overlying engineered barriers but was a Hanford groundwater composition.

The modeling of glass degradation used Chalcedony as a kinetic control because the results of chemical reaction progress modeling were found to agree reasonably well with experimental results involving several different glass types at 90°C if chalcedony was assumed to form (PNNL-20781, 2011); however, chalcedony has not been directly detected as an alteration product of glass corrosion (PNNL-24615, 2015). In other words, Chalcedony and the assumed kinetic controls is a calibration parameter used by DOE to fit the empirical data. That does not justify the assumption of the absence of Stage III behavior. In the assessment of different secondary mineral formation, DOE didn't consider minerals that could conceivably generate Stage III glass corrosion because such behavior was considered unlikely under IDF-relevant conditions (PNNL-24615, 2015).

Path forward

Please demonstrate Stage III behavior is unlikely taking into consideration the potential temperature ranges and degrees of openness of the disposal system. This may be done by performing geochemical modeling or generating experimental data using relevant fluid compositions and appropriate minerals. PA calculations could be used to address the significance of the formation of Stage III behavior.

DOE Response

DOE maintains that Stage III conditions are not likely at the IDF because it will be low temperature (15 °C) and an open system. However, DOE recognizes the point raised by the NRC review:

> "The openness of the system is more uncertain. The impermeable asphalt
>   layer combined with the Geosynthetic Composite Layer (GCL) liner under

the facility can result in very low flow rates and conditions that could approximate a closed system."

Hence, work to assess the potential impacts of Stage III rate acceleration in Hanford VLAW glasses is an ongoing part of the IDF PA Maintenance Program. Laboratory-based efforts are addressing two questions: 1) If the IDF acts more like a closed system, then is there experimental evidence that Stage III behavior, or the formation of zeolites, occurs at the IDF temperature (approximately 15 °C)?, and 2) Are induced Stage III glass dissolution rates high enough at the IDF temperature to cause contaminant releases to exceed IDF performance objectives? As the NRC reviewer noted, the temperature of the IDF system is fairly certain since no significant sources of heat will be part of the waste buried in the facility. In addition to the laboratory efforts, a long-term field study in the Hanford Site FLTF is underway to observe the behavior of glass waste forms under conditions that more closely represent those of waste buried in the IDF.

Laboratory Testing to Address Question 1
Long-term testing at the VSL has been observing the dissolution behavior of numerous ILAW glass samples in a closed system containing glass in an aqueous solution. These glass samples have been incubating for as long as ten years. As has been reported by numerous authors, Stage III rate acceleration is observed at temperatures at, or above, 90 °C for samples with high surface area-to-liquid volume ratios (i.e., conditions that promote concentrated aqueous solutions) (VSL-20R4820-1; "Resumption of alteration at high temperature and pH: rates measurements and comparison with initial rates" [Fournier et al. 2014]). It should be noted that a vast majority of the historical glass corrosion data available, as a whole, has been obtained from tests performed at 90 °C. Figure 2-9-1 (extracted from VSL-20R4820-1) shows results for ten Hanford ILAW glasses (and a reference glass ANL-LRM-2) incubated in water for 10 years. Clearly, several of the glasses have accelerated from a low rate to a high rate indicating Stage III behavior (c.f. IDF9A187, IDF6D6, IDF3F7, IDF7E12, IDF8A125, IDF4A15, IDF1B2, IDF5A20, ANL-LRM-2). Similar behavior is also observed in glasses in the ALTGlass database ("Accelerated Leach Testing of GLASS (ALTGLASS): I. Informatics approach to high level waste glass gel formation and aging" [Jantzen et al. 2017]).

In contrast, the glasses represented in Figure 2-9-1 showed much less alteration when tested at 40 °C (see Figure 2-9-2) than at 90 °C, and rate resumption is not as evident. Note that in both figures the data are presented as the normalized *cumulative* release of boron, so the slope of each curve approximates the dissolution rate for that glass[48]. VSL asserts that none of the glasses tested at 40 °C have reached an accelerated Stage III rate over the 10-year testing period (VSL-20R4820-1). The highest initial rate was for IDF8A125, with 11% of the glass reacted at 900 days with little alteration occurring since then. PNNL evaluated the data represented in Figure 2-9-2 and suggested that four glasses (IDF8A125, IDF9A187, IDF5A20, and IDF2G9) may show onset times of Stage III glass dissolution (PNNL-28898). However, as the data shows, if Stage III behavior is occurring, it is not sustained in all glasses.

---

[48] Note that the data shown in these figures represents tests where 4% of the liquid volume is removed and replaced with deionized water at each sampling interval so any estimates of reaction rates should account for this slight departure from purely static test conditions.

Figure 2-9-1. PCT-B (static dissolution) Results (90 °C and S/V of 2,000 m⁻¹) for the Ten Integrated Disposal Facility Glasses (Total available normalized boron release is 100 g/L at S/V of 2,000 m⁻¹).
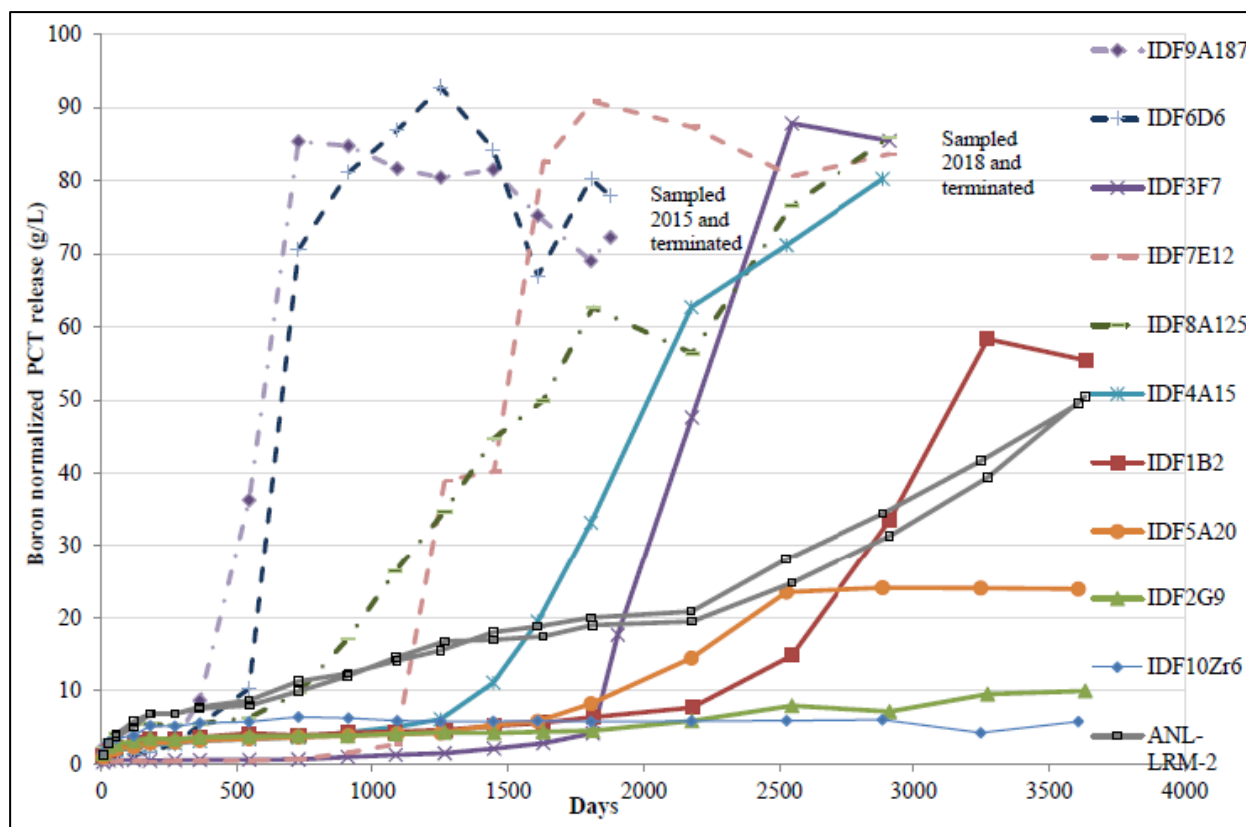
Source: VSL-20R4820-1, *Final Report FY2020, Long-Term PCT of ILAW Glasses*.

Evidence for Stage III rate increase in ILAW glasses at temperatures below 90 °C has been reported by Ryan et al. (2019). These researchers observed dissolution rate increase in an ILAW glass (LAWA76) in tests at 70 °C. LAWA76 was chosen since it exhibited a rapid transition to Stage III at 90 °C, and it was thought that this system may be susceptible to the same processes at lower temperatures. After approximately 75 days, Stage III behavior was observed and continued in a constant fashion for the remainder of the test period (approximately 4 months).

Laboratory Testing to Address Question 2

It is difficult to show through testing that ILAW glass would not undergo Stage III rate acceleration at IDF conditions due to the slow dissolution rates at lower temperatures and uncertainty regarding nucleation time of zeolite phases that can promote Stage III. Testing has been undertaken at PNNL to determine the range of dissolution rates that could be expected **IF** Stage III were to occur by seeding with zeolites known to promote Stage III (PNNL-28898). The logic associated with these tests is as follows:

- If Stage III rates are experimentally measured at multiple temperatures for a glass, an apparent activation energy can be used to determine a Stage III rate at the IDF

temperature of 15 °C (Note: experimental data are available at 22 °C, which is only a 7 °C difference)

- This Stage III rate can then be used in a sensitivity case in a PA calculation to assess the impact of Stage III behavior in the IDF PA

- If the result of the PA calculation where Stage III is assumed to occur is below compliance limits, it would provide technical defensibility for a minimal risk of Stage III adversely impacting IDF performance objectives.

Figure 2-9-2. PCT-B Results (40 °C and S/V of 2,000 m-1) for the Ten Integrated Disposal Facility Glasses (Total available normalized boron release is 100 g/L at S/V of 2,000 m^{-1}).
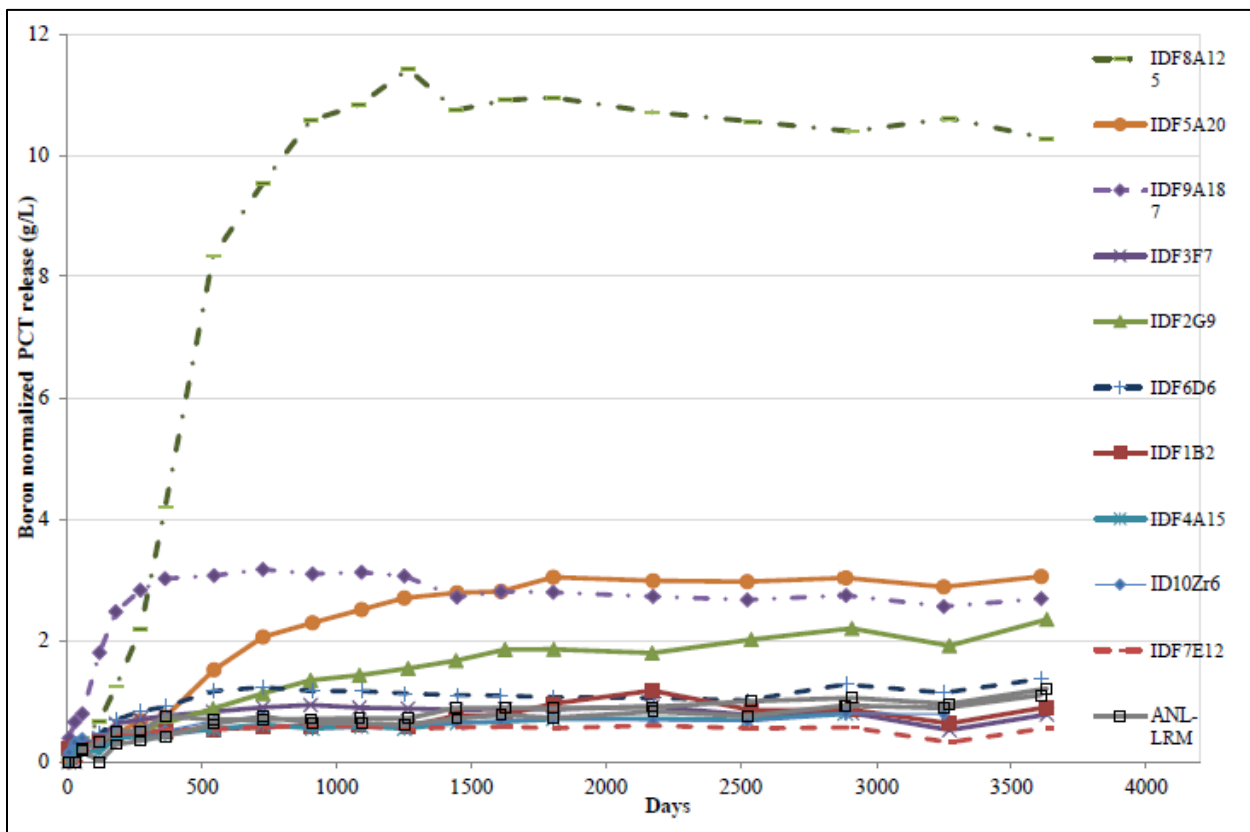
Note the 8 times difference in the Y-axis scales between Figures 1 and 2.

Source: VSL-20R4820-1, *Final Report FY2020, Long-Term PCT of ILAW Glasses.*

To support this analysis, Stage III data on glasses that cover the full range of ILAW glass compositions is needed. A method has been developed at PNNL wherein long-term PCTs are seeded with zeolites once the glasses have reached the Stage II residual rate, then monitored for onset and magnitude of Stage III behavior. This work at PNNL is being conducted on 24 statistically-designed glasses (Figure 2-9-3) that span the possible composition space for enhanced waste loading ILAW glasses. This composition space also covers a majority of the processible baseline glasses ("Acceleration of glass alteration rates induced by zeolite seeds at

controlled pH" [Neeway et al. 2020]; "Multi-glass investigation of Stage III glass dissolution behavior from 22 to 90 °C triggered by the addition of zeolite phases" [Parruzot et al. 2019]; Ryan et al. 2019; PNNL-28898).

Figure 2-9-3. Scatter Plot of Individually Varied Glass Components (in mass fractions) in the Statistically-Designed Glass Formulations Representative of the Enhanced Immobilized Low-Activity Waste Glass Compositional Region.
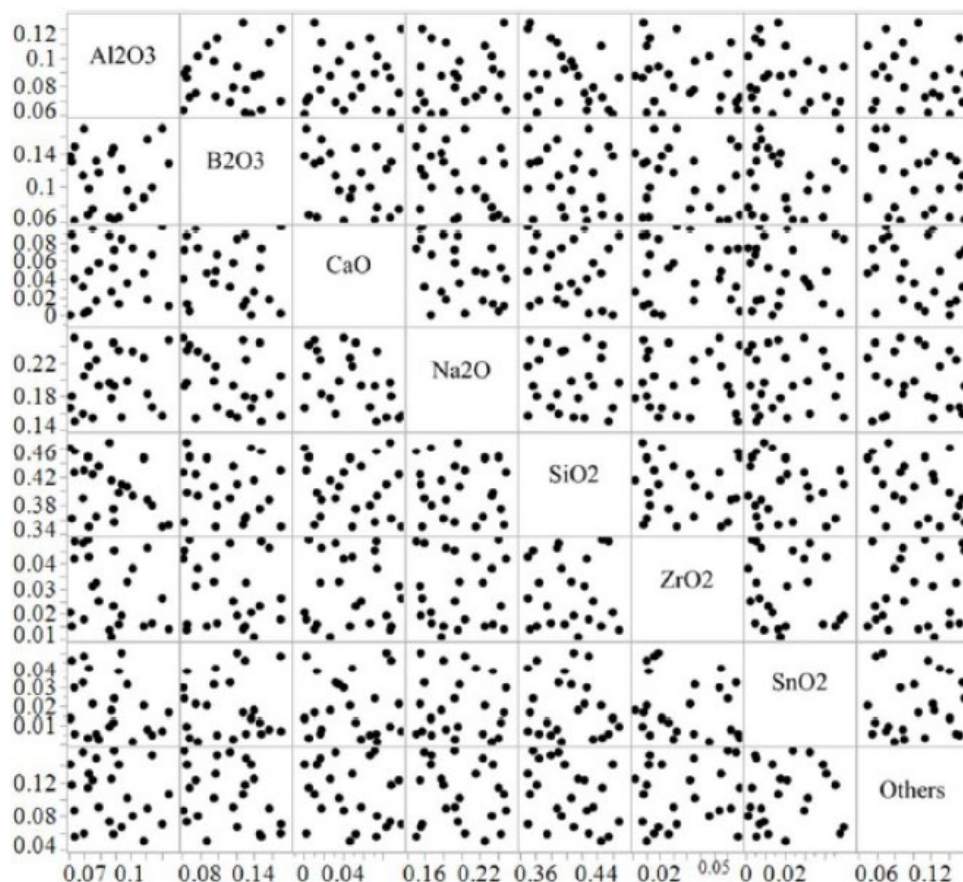
In these tests at PNNL, samples of the 24 glasses are being incubated in aqueous solutions at multiple temperatures (90 °C, 70 °C, 40 °C, and room temperature, ~22 °C), both with and without zeolite seeding. Dissolved glass components are measured in periodically-collected liquid samples to assess dissolution rate with time. At the conclusion of the tests the secondary solid phases that are formed are also being analyzed and the results used to reassess the SMRN to be used in the IDF PA glass dissolution model. Results to date have shown that most of the 24 glasses have shown an increase in rate after zeolite seeds were added to the system at all four temperatures. The responses to the introduction of seeds can be binned into four different behavior types. Figure 2-9-4 summarizes these four types of responses to zeolite seeding for the test duration along with the apparent relationship between the response and the composition of certain elements in the glass. It should be noted that these observations are primarily based on data from tests at 90 °C ("Seeded Stage III Glass Dissolution Behavior of a Statistically Designed Glass Matrix" [Crum et al. *Under Review*]).

Figure 2-9-4. Graphical Depiction of the Four Types of Responses Measured for Hanford Immobilized Low-Activity Waste Glasses Exposed to an Aqueous Solution and Seeded with Zeolite P2.
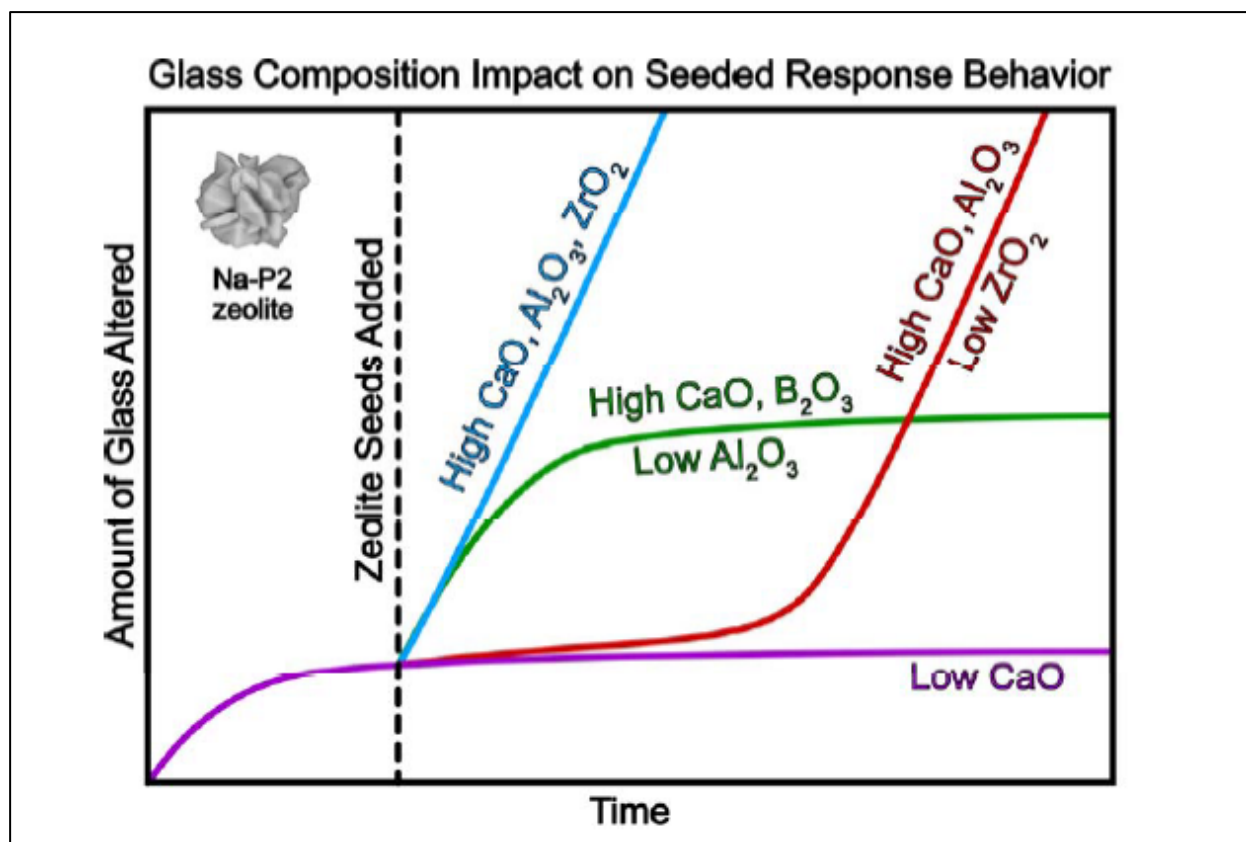
Note: The observed relationship to composition for each of the four responses is also indicated.

Source: "Seeded Stage III Glass Dissolution Behavior of a Statistically Designed Glass Matrix" (Crum et al. *Under Review*).

The ratio of the preliminary predicted dissolution rates for seeded to unseeded tests (i.e., [seeded Stage III rate]/[rate prior to seeding]) at 15 °C reported in PNNL-28898 ranges from 0.9 to 470 with a geometric mean[49] of 5.7. IDF PA predictions indicate that a glass dissolution rate increase of less than approximately 9 times over the nominal Stage II glass dissolution rate would not result in contaminant releases exceeding regulatory limits at the point of compliance (RPP-CALC-63176). Eighteen of the 24 glasses tested had ratios at, or below, 9 times and only one glass had a ratio greater than 11 (eLAW 17) as shown in Figure 2-9-5, which summarizes the rate ratio based on data extracted from Tables 5-4 and 5-5 in PNNL-28898. It should be noted that these results are based predominantly on data collected at 90 °C and 70 °C and will be updated with data collected at lower temperatures in FY 2021. While the Stage III/Stage II ratio may be a useful metric for demonstrating compliance, the ultimate criterion will be whether the potential Stage III rate for any specific glass composition would exceed the IDF PA performance

---

[49] The geometric mean is used rather than the arithmetic mean since the data spans two orders of magnitude with one possible outlier (see Figure 2-9-5). Use of the arithmetic mean would produce a result heavily weighed by the high value measured for eLAW17.

objective. As a defense-in-depth measure, it is expected that glass composition constraints could be implemented to ensure potential Stage III dissolution rates at IDF conditions would be well below a rate that would exceed IDF performance objectives.

Figure 2-9-5. Ratio of Predicted Stage III Rates (from seeded tests) to Stage II Rates (using the rate prior to seeding) at 15 °C.
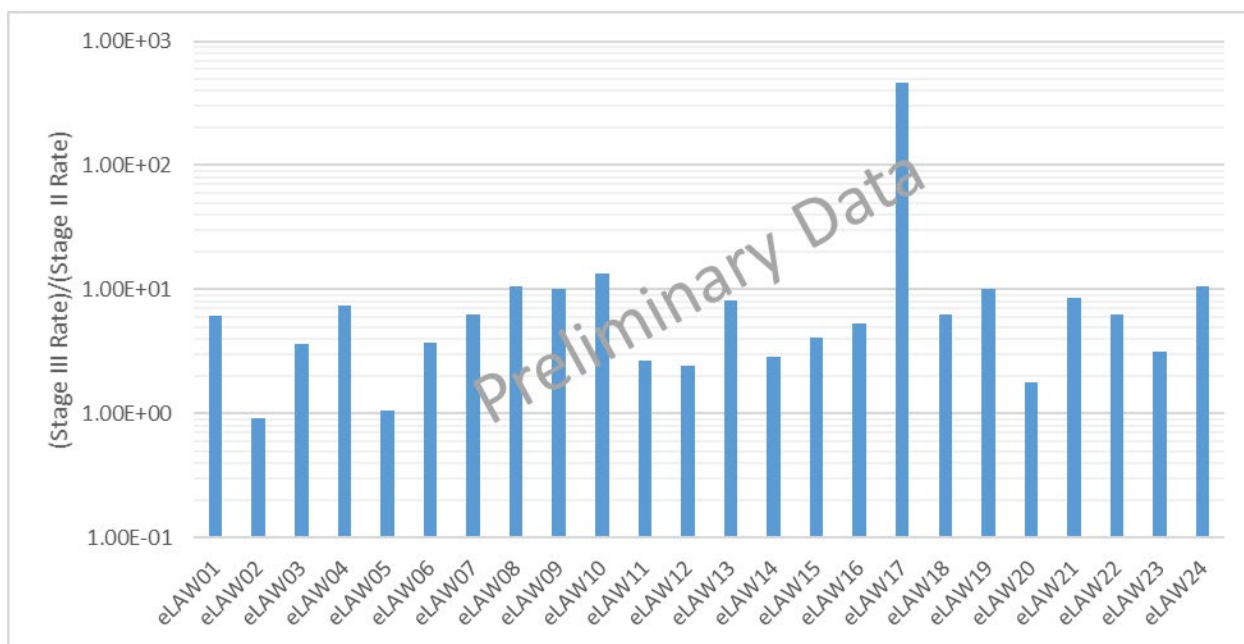
Note: This data is marked as preliminary since it is based on estimates of the Stage II rate that will be updated in fiscal year 2021.

Data in this figure were extracted from Tables 5-4 and 5-5 in PNNL-28898, *FY2019 Status Report: Seeded ILAW Glass Stage III Static Dissolution Rate Measurements*.

Assessing Waste Form Degradation Under Field Conditions

The final area of work being conducted to support validating predictions of ILAW glass dissolution rates within the IDF is a lysimeter field demonstration in the Hanford Site FLTF. As shown in Figure 2-9-6, the FLTF has a series of field lysimeter tubes (most extend to a depth of 3 m) that can be filled with various waste forms, including glass and cementitious materials, and back filled with IDF soils. Water infiltration rate is controlled within each lysimeter tube. Water samples will be collected at various depths within the lysimeters over the next several years, along with measurements of the *in situ* distribution of moisture.

Prior to initiation of the lysimeter test, a modeling effort was performed using the same simulation methods as the IDF PA to predict the behavior of the emplaced waste forms and corresponding contaminant releases, using ^{99}Tc and ^{127}I as tracers for the cementitious waste forms and molybdenum and rhenium as tracers for the glass waste forms (PNNL-27394). As data are collected from the test, comparisons will be made against the initial modeling that will serve as a validation of the model and determine the extent to which the laboratory-based parameters are applicable to waste form behavior in the field. Water analysis and *in situ* soil moisture data from these tests will start to be available in FY 2021 but data from solids analysis

will not be available until the tests conclude, which depending on the test may be 5 years to 25 years in the future.

Figure 2-9-6. Images of the Field Lysimeter Test Facility a) Aerial Photograph of the Facility, b) Artist Three-Dimensional Drawing of the Facility, c) Depiction of the Layout of Buried Waste Forms and Sampling Devices Within a Single Lysimeter Tube, d) Photograph of the Lower Level of Buried Cementitious Waste Forms, and e) Photograph of the Underground Sampling Bay Showing the Two Rows of Lysimeter Tubes.

With the two glass formulations selected, Stage III behavior may not be observed over the duration of the lysimeter test. However, post-experimental characterization of the excavated waste forms and backfill will also be completed at the test conclusion to evaluate the evolution of mineral phases and to determine if any zeolite phases have been formed. Note that the presence of zeolites does not indicate that Stage III behavior is inevitable, but the presence of zeolites has been correlated to Stage III behavior in laboratory testing. As stated under the discussion of Stage III (above), data is also being collected in laboratory tests to assess the magnitude of the impact of Stage III rate behavior on contaminant release from the IDF to the surrounding environment.

References

Crum, J. V., T. J. Reiser, B. P. Parruzot, J. J. Neeway, J. F. Bonnett, S. N. Kerisit, S. K. Cooley, J. V. Ryan, G. L. Smith, R. M. Asmussen, *Under Review*, "Seeded Stage III Glass Dissolution Behavior of a Statistically Designed Glass Matrix," *Journal of the American Ceramic Society*.

Fournier, M., P. Fruiger, and S. Gin, 2014, "Resumption of alteration at high temperature and pH: rates measurements and comparison with initial rates," *Procedia Materials Science*, vol. 7, Issue 14, pp. 202–208.

Jantzen, C. M., C. L. Trivelpiece, C. L. Crawford, J. M. Pareizs, and J. B. Pickett, 2017, "Accelerated Leach Testing of GLASS (ALTGLASS): I. Informatics approach to high level waste glass gel formation and aging," *International Journal of Applied Glass Science*, vol. 8, Issue 1, pp. 69–83.

Neeway, J. J., B. P. Parruzot, J. F. Bonnett, J. T. Reiser, S. N. Kerisit, J. V. Ryan, and J. V. Crum, 2020, "Acceleration of glass alteration rates induced by zeolite seeds at controlled pH," *Applied Geochemistry*, vol. 113, PNNL-SA-148595.

Parruzot, B., J. V. Ryan, J. L. George, R. K. Motkuri, J. F. Bonnett, L. M. Seymour, and M. A. Derewinski, 2019, "Multi-glass investigation of Stage III glass dissolution behavior from 22 to 90 °C triggered by the addition of zeolite phases," *Journal of Nuclear Materials*, vol. 523, pp. 490–501, PNNL-SA-138413.

PNNL-20781, 2011, *Integrated Disposal Facility FY 2011 Glass Testing Summary Report*, Pacific Northwest National Laboratory, Richland, Washington.

PNNL-24615, 2015, *Immobilized Low-Activity Waste Glass Release Data Package for the Integrated Disposal Facility Performance Assessment*, RPT-IGTP-005, Pacific Northwest National Laboratory, Richland, Washington.

PNNL-27394, 2018, *Field-Scale Lysimeter Studies of Low-Activity Waste Form Degradation Implementation Plan*, RPT-IGTP-017, Rev 0.0, Pacific Northwest National Laboratory, Richland, Washington.

PNNL-28898, 2019, *FY2019 Status Report: Seeded ILAW Glass Stage III Static Dissolution Rate Measurements*, RTP-IGTP-021, Rev 0.0, Pacific Northwest National Laboratory, Richland, Washington.

RPP-CALC-63176, 2020, *Integrated Disposal Facility Risk Budget Tool Analysis*, Rev. 0A, Washington River Protection Solutions, LLC, Richland, Washington.

Ryan, J. V., B. Parruzot, A. M. Lines, S. A. Bryan, L. M. Seymour, J. F. Bonnett, and R. K. Motkuri, 2019, "In-situ monitoring of seeded and unseeded stage III corrosion using Raman spectroscopy," *npj Materials Degradation*, vol. 3, Article number 34, pp. 1–7.

VSL-20R4820-1, 2020, *Final Report FY2020 Long-Term PCT of ILAW Glasses*, Vitreous State Laboratory, The Catholic University of America, Washington, D.C.

RAI 2-10 (Volatile Species and Glass)

Comment

One of the most important aspects of uncertainty associated with the VLAW PA appears to be the assumed partitioning of various species, especially volatile species, between different waste types. Additional information is needed to support the amount of volatile species that will be retained in glass (Case 7 – the base case).

Basis

Initial testing of glass production determined a low retention rate of volatile species (Tc, I, Cs). The glass process was modified to recycle the off gas back into the glass feed to increase the loading of volatile species in the glass. The modifications were effective in increasing Tc retention percentages from generally less than 50% to approximately 75% (Pegg, 2015). The Tc retention in the glass assumption in the base case PA is approximately 99.9% - essentially all of the Tc ultimately is disposed in the glass waste form.

Detailed evaluation of Tc recycle was completed by Catholic University's Vitreous State Laboratory (RPP-54130, 2012). The glass production system uses a wet electrostatic precipitator (WESP) among other components. By measuring the amount of Tc in the WESP effluents, DOE estimated that the Tc retention was 99.8%. The Case 7 inventory partitioning of Tc is consistent with the WESP emissions. The amount of Tc observed in the glass was 68%. In addition, the mass balance of Tc across all tests averaged approximately 90%. DOE indicated that a significant amount of technetium was held up in the system during testing, particularly in the WESP internals, the film cooler, and the transition line. This material was therefore not available for recycle and incorporation into the glass. All of the Tc that gets deposited and retained in the various processing equipment eventually has to be disposed and those components are not going to be disposed as glass. Sulfate salt phases were observed on the melt pool surface after two of the tests. The salt phase showed an approximate fifty-fold enrichment in technetium over the glass; rhenium and halides also showed significant enrichments. These phases may be considered as being "retained" by the glass but would not likely have the same release properties as the glass.

DOE's assumed retention of Tc in glass for Case 7 would appear to be unrealistically optimistic. Case 10A had approximately 32% of the Tc in the glass reflecting no recycling of the off gas, which is likely to be unrealistically pessimistic if recycling is used. As discussed above, the mass balance was limited to approximately 90% and the amount of Tc observed to be in the glass was approximately 70%. Appropriate base case values for Tc retention in glass would appear to be in the 70 to 95% range.

The design, operation, and especially the reliability of the off-gas system with recycle would appear to be extremely important to justify the assumed Tc retention in the glass. Staff did not identify information to support the assumed 100% reliability of the off-gas system. System downtime would significantly contribute to not being able to achieve extremely high Tc retention in the glass.

Path forward

Please provide additional basis for the base case inventory or revise the base case inventory to be consistent with the observed testing data. For the base case inventory, DOE should observe mass balance, glass concentrations of volatile species, concentration of species in salt phases, and reliability of the off-gas system. For the base case inventory DOE should also account for the disposal of volatile species that build up in the system components and in what form they will be disposed.

DOE Response

Nuclear chemical processing systems are designed utilizing the principles of redundant capabilities and defense in depth for nuclear safety and environmental protection purposes. Therefore, 100% reliability is the ultimate goal of the design and operating procedures for such systems. The LAW Vitrification Facility off-gas system is designed with multiple unit operations, each having a specific function for controlling the quantities and composition of gaseous, liquid, and solid effluents from the process. The fundamental engineering concept of recycling is employed within the off-gas system design to control emissions of hazardous and radioactive constituents.

The NRC reviewers cited results from scaled melter tests with simulants as indicative of the efficiency and effectiveness that could be expected from the full-scale production system. Those studies provide valuable insight into specific aspects of volatile constituent behavior and performance of the off-gas system and its components. With proper consideration of the test system's limitations and realistic interpretation of the results, the data support the expectation that the full-scale production system will function as designed and will be capable of achieving very high recycle efficiency and incorporation of volatile constituents into the glass.

The NRC reviewers noted the extensive evaluation of technetium recycle in small-scale melter tests by the VSL (RPP-54130). The melter system included several of the major components of a prototypic LAW vitrification off-gas system (e.g., SBS, WESP, and vacuum evaporator) to facilitate simulating full off-gas condensate recycle. Nine separate melter runs were performed with different simulated feed compositions spiked with ^{99m}Tc. The authors reported 68% of technetium observed in the glass with an average mass balance closure of about 90%. In a subsequent analysis of the analytical technique used (VSL-13R2800-1, *Final Report Wet Electrostatic Precipitator Performance and Technetium-Rhenium Behavior in LAW Recycle Flow-Sheet*), VSL determined that the results of solid sample analyses for those tests were biased low by about 8.2%. Applying a correction to the melter test results would raise the average technetium in glass to about 74% and average mass balance closure to 95%.

In 2016, modifications were made to the VSL DM-10 melter system to further investigate the retention of ^{99}Tc and other volatile species in the LAW glass with recycling of the off-gas condensate. Specifically, modifications were made to decrease the hold-up of constituents in the off-gas system and reduce the time required to reach steady-state concentrations in the glass. In particular, reduction of the evaporator sump volume and periodic rinses of the WESP and evaporator head space combined to achieve 100% closure of the technetium mass balance and

near 100%[50] incorporation into the glass (VSL-16R3840-1, *Tracking the Key Constituents of Concern of the WTP LAW Stream*). These results confirmed the effectiveness of recycle and the ability to achieve a high percentage of incorporation of technetium in the glass product. The results also show the base case inventory is consistent with observed testing data.

In tests conducted with ^{99m}Tc, the interpretation of the results is constrained by the short 6-hour half-life of this isotope. Testing with actual ^{99}Tc is not economically practical as the entire melter system would be irreversibly contaminated and all the products generated would need to be managed as radioactive waste. Technetium-99m is readily available from nuclear pharmacies at reasonable cost but due to the rapid decay, the maximum melter run time that can be achieved with reasonable isotope detection limits is about 72 hours. A significant fraction of the run time is required for the system to reach steady state, so the time available for data collection at steady-state operations is limited to between 24 and 48 hours.

It is largely for this reason that the results from these melter tests should be carefully analyzed to determine their applicability to sustained steady-state operations in a production environment. A particularly valuable use of the results is to collect data on the partitioning of key constituents across the melter and off-gas system components and the performance of those components relative to their design specifications and operating parameters. In this regard, it is useful to evaluate performance of the off-gas system at points where key radionuclides and hazardous constituents will be purged from the system and therefore not recycled for incorporation into the glass product.

Major purge points in the off-gas system during DFLAW operations include components located downstream from the WESP (HEPA filters, Carbon Absorber Beds, and the Caustic Scrubber) and overhead condensate from the primary off-gas system evaporator. For example, analysis of the data from DM-10 melter runs showed that only a small fraction of feed technetium, 0.02 to 0.04%, exited the off-gas system through the WESP exhaust (VSL-13R2800-1). Results also showed that virtually all of this remaining small fraction technetium exiting the WESP will accumulate on HEPA filters downstream of the WESP during DFLAW operations. Quantities of technetium in the evaporator overhead condensates ranged from <0.0001 to 0.0004% in DM-10 melter runs conducted in 2016 (VSL-16R3840-1). During DFLAW, the evaporator overhead stream will be directed to LERF/ETF for treatment and solidification in grout for disposal at the IDF.

The NRC reviewers correctly noted that significant percentages of ^{99m}Tc accumulated in off-gas system components during DM-10 melter tests with off-gas recycle. Certain accumulations are expected due to hold-up of process liquids and residual solids at the end of a melter run. This

---

[50] Actual incorporation of technetium into the glass during the third run of this series of tests was 95%. This value represents the average composition over the entire run which included glass produced at the beginning of the run that contained very little technetium. There is no technetium in the glass pool at the start of a run and the technetium increases gradually as technetium in the fresh feed and recycle streams are fed to the melter and the system approaches steady state. After accounting for small amounts of technetium held up in lines and sumps at the end of the test, essentially 100% of the technetium not exiting the system via the WESP exhaust and evaporator overhead condensate during steady-state operation was accounted for in the glass product. The authors also noted in their conclusions that the results helped explain the lower technetium concentrations measured in product glasses in previous tests with recycle reported in RPP-54130/VSL-12R2640-1.

can be considered essentially a snapshot of the system configuration at any given point in time. Such data are useful for comparison to process model predictions as described in Section 9 of VSL-12R2640-1 (RPP-54130) which provide a more realistic representation of steady-state operations. For example, significant accumulations of ^{99m}Tc in the WESP, film cooler, and transition line during the DM-10 melter tests were measured for the primary purpose of closing the technetium mass balance. During steady-state operations, these components will be periodically rinsed or deluged to flush accumulated solids and residuals into the off-gas liquids to be recycled back to LAW vitrification for incorporation into the glass.

The appearance of sulfate salt phases on the surface of the melt pool after two of the tests reported in RPP-54130 was unexpected but could be attributed to sulfate content in the melter feed that was ~10% higher than in previous tests and at or near the sulfate solubility limit for those specific glass compositions. LAW glasses are formulated to be below the sulfate solubility limit and the data are incorporated in glass formulation algorithms to minimize the potential for sulfate salt phase formation (PNNL-25835). It is of particular concern during operations to avoid the formation of a sulfate salt layer as this would be highly corrosive to the melter refractory liner as well as Inconel® (a registered trademark of Special Metals Corporation, New Hartford, New York) components such as bubblers. It is of lesser concern for glass poured from the melter because the glass pour spout is fed from a location near the bottom of the melt pool and would not draw off material from the salt phase floating on top of the melt pool. Despite the fact that a salt phase on the surface of the melt pool would be unlikely to affect the quality of the glass product, the potential for salt phase formation is of considerable concern for sustained melter operations, so the information from these tests – along with other considerations such as melter scale, melt pool temperature, cold cap coverage, etc. – is used to evaluate whether adjustments to sulfate solubility models and/or glass formulation model constraints would be warranted during DFLAW operations.

References

Pegg, I. L., 2015, "Behavior of technetium in nuclear waste vitrification processes," *Journal of Radioanalytical and Nuclear Chemistry*, Vol. 305, No. 1, pp. 287–292.

PNNL-25835, 2016, *Update of Hanford Glass Property Models and Constraints for Use in Estimating the Glass mass to be Produced at Hanford by Implementing Current Enhanced Glass Formulation Efforts*, Pacific Northwest National Laboratory, Richland, Washington.

RPP-54130, 2012*, Technetium Retention in WTP LAW Glass with Recycle Flow-Sheet: DM10 Melter Testing, VSL-12R2640-1, Rev. 0*, Vitreous State Laboratory, The Catholic University of America/Energy*Solutions*, Federal EPC, Inc./Washington River Protection Solutions LLC, Richland, Washington.

VSL-13R2800-1, 2013, *Final Report Wet Electrostatic Precipitator Performance and Technetium-Rhenium Behavior in LAW Recycle Flow-Sheet*, Rev. 0, Vitreous State Laboratory, Catholic University of America, Washington, D.C.

VSL-16R3840-1, 2016, *Final Report Tracking the Key Constituents of Concern of the WTP LAW Stream*, Rev. 0, Vitreous State Laboratory, Catholic University of America, Washington, D.C.

RAI 2-11 (Comparison of STOMP and GWB)

Comment
Additional information is needed to support why some comparison cases for glass release rates generated with STOMP and Geochemist's Workbench (GWB) have not applicable (NA) entries.

Basis
In the evaluation of sensitivity cases for release from the glass wasteform, DOE used both STOMP and GWB to estimate fractional release rates. In most cases the agreement between the two programs was reasonable (see Table 5-4 and Table 5-9 of the PA document). However, in a number of entries in the table results were only provided for one model. Because these types of calculations can have large uncertainties it is good practice to calculate results with two models. Additional information should be provided to provide the basis for only using one model for certain entries.

Path Forward
In the evaluation of sensitivity cases for release from the glass wasteform, DOE used both STOMP and GWB to estimate fractional release rates. In most cases the agreement between the two programs was reasonable (see Table 5-4 and Table 5-9 of the PA document).

DOE Response
DOE used reactive transport models in two different software applications, STOMP and GWB, to evaluate releases from vitrified LAW disposed of in the IDF. Models in both software applications were used to simulate glass corrosion under the expected conditions in the IDF for each simulated glass type (Envelops A, B, and C). The STOMP model is a dynamic model that starts with initial conditions and evolves over time to represent the long-term, steady-state corrosion rate associated with Stage II glass corrosion. The GWB model is an equilibrium model used only to estimate the Stage II corrosion rate. One or both software applications were used to evaluate the sensitivity of the developed models to alternative conditions and parameter values. The reference case conditions were simulated for the three glass types using models for both software applications and the results from the model runs were compared to each other to build confidence that the models developed in each application produced long-term corrosion rates that were comparable. Subsequently, the models in each application were used to investigate corrosion rates under different conditions. In many cases, the alternative conditions were run in both applications, but in others only one or the other model was used. The decision to simulate a prescribed alternative condition using just one software application or both software applications considered model capability and availability of computational resources[51] and time available to perform the simulations before the results were needed in a downstream calculation to support the IDF PA. None of the instances when only a single model was used for a sensitivity case were attributable to a lack of numerical convergence or similar modeling issues.

---

[51] The available resources capable of running STOMP simulations were simultaneously doing simulations for near-field flow, vitrified waste releases, cementitious waste form releases, and far-field (vadose and saturated zone) flow and transport modeling as well as performing similar calculations for the Hanford WMA C performance assessment.

The EIS case (RPP-RPT-59958 Table 5-3) used STOMP to replicate as closely as possible STORM simulations that supported the TC&WM EIS (DOE/EIS-0391). Additional evaluations using GWB were considered unnecessary because this calculation case involved only a comparison of STOMP and STORM results.

Calculation cases that were evaluated using only STOMP (VFLUX, HYDRL, BACK, COMB4) (RPP-RPT-59958 Table 5-3) involved changes in hydraulic properties (porosity, hydraulic conductivity, permeability) of the glass waste form and/or backfill. These properties were not explicitly accounted for in GWB models. The GWB models were instead constrained by STOMP results at steady/stationary state pertaining to the volumetric flow rate, moisture content, and residence time of water infiltrating the waste form.

Calculation cases that were evaluated using only GWB (RSA, SMRN, ICHEM, COMB2, COMB3) (RPP-RPT-59958 Table 5-3) were intended to illustrate the sensitivity of model results to alternative assumptions and/or model parameter values. GWB was considered adequate for this purpose and was also preferred because run times were expected to be much shorter than for comparable STOMP models. The opportunity to run more than 100 STOMP simulations was constrained by the very long run times required to simulate corrosion and the finite amount of time available to perform the simulations, document the analysis, and provide the inputs to downstream modeling projects, such as development of the IDF PA system model. The long STOMP model runs times were discovered once the model was up and running. It became apparent that computational time and required resources would limit the opportunity to perform all of the sensitivity cases that were planned to demonstrate how the corrosion model responds to each parameter. For this reason, the GWB model was developed to complement and augment the limited number of STOMP analyses that could be performed. Whenever possible, both models were used and compared to enhance the confidence in the results reported by the GWB model.

The "N/A" entries in RPP-RPT-59958 Table 5-9 (see also RPP-RPT-59958 Tables 5-4 and 5-6) refer to two STOMP models for the IEX case that could not be evaluated because run times were excessively long. These models were based on assumed upper bounds on the ion-exchange rate constant for LAWA44 and LAWC22 glass. Time steps, which were adjusted automatically in the STOMP simulations, were reduced significantly in these models causing run times to become excessively long. Although these simulations were started, the runs were terminated before completion because it was evident that waiting for the models to complete would delay the completion of the calculation report and jeopardize the completion of the work that used results of the glass release modeling as input. For the runs shown in Table 5-9 that were simulated with both GWB and STOMP, the two models both showed proportional changes to the corrosion rate when the ion-exchange rate was changed. Since the GWB runs for LAWA44 with an ion-exchange rate of 5.3×10^{-10} mol/m^2/s and for LAWC22 with an ion-exchange rate of 1.2×10^{-9} mol/m^2/s showed the same trends as the other cases that were run with both models, it is not believed that stopping the STOMP simulations for these conditions affects the technical validity of PA results.

References

DOE/EIS-0391, 2012, *Final Tank Closure and Waste Management Environmental Impact Statement for the Hanford Site, Richland, Washington*, U.S. Department of Energy, Washington, D.C.

RPP-RPT-59958, 2019, *Performance Assessment for the Integrated Disposal Facility, Hanford Site, Washington*, Rev. 1A, Washington, Department of Energy, Richland, Washington.

RAI 2-12 (Sensitivity and Uncertainty Analyses)

Comment
The sensitivity and uncertainty analyses presented by DOE did not include some aspects that may be important to risk-inform the review process and to determine if the relevant criteria are likely to be met.

Basis
In section 5.2.3 of the PA document, DOE described the uncertainty and sensitivity analyses completed for the draft waste evaluation for VLAW (disposal in the near surface at IDF). Key uncertainties identified by DOE included release rates, recharge rates, vadose zone hydraulic properties, vadose zone transport properties, saturated zone hydraulic properties, and waste loading configuration in the disposal facility. Sensitivity and uncertainty analyses were completed with the deterministic process models as well as the probabilistic system model. The types of uncertainties examined were reasonable and consistent with NRC's understanding of the system. However, there were some uncertainties that were not included within the scope of the evaluation that may be important to understand in order to risk-inform the review and determine if the criteria will be met with reasonable expectation (DOE) or reasonable assurance (NRC).

In section 5.1 of the PA document, DOE described a number of different analyses cases completed to evaluate near-field flow and source-term release. The computational results were presented in RPP-CALC-61029. DOE examined the timing of engineered layer "failures" by examining a case where the surface cover and liner had a step change in properties at 500 years post-closure. While this is an appropriate case to examine, given the uncertainties being addressed, the evaluation is incomplete. The performance of the engineered cover is reliant to a large extent on an asphalt layer whereas the performance of the liner is reliant on a GCL. Because of numerical difficulties, the hydraulic conductivity of the asphalt layer was only increased an order of magnitude in a step manner. The properties of fresh, intact asphalt compared to aged, cracked asphalt would be expected to differ by much more than an order of magnitude. In addition, because of the different materials involved, there is limited expectation that the different layers would "fail" at the same time or same rate. In general, engineered layers closer to the land surface experience a more diverse set of processes and events that lead to more rapid alteration by nature. It would be reasonable to examine a case with a degraded cover and an indefinitely performing liner system. NRC was not able to find information describing the drain and sump systems to evaluate their propensity for plugging or decrease in performance.

In section 5.1.2 of the PA document, DOE examined sensitivity of glass release rates to various parameters. One case, termed HYDRL, examined the effect of changes to hydraulic properties of the glass wasteform. Moisture characteristic curves (MCC's) can have a significant impact on release rates if differing materials are present and simulation of capillary barrier effects occurs. The HYDRL and combined cases should be expanded to include the impact of uncertainties in MCC's. There may be reduced sensitivity of the results to changes in some inputs, such as recharge, due to the masking effect of the asphalt layer performance and the MCC's assigned. The SRMN cases evaluated the impact of the secondary mineral formation network. The SRMN cases showed a large impact from uncertainty in what minerals form and therefore their thermodynamic properties. The SRMN cases should be expanded and, if possible, supported by

information from experiments and the literature. The discussion in the PA indicates that selection of chalcedony (see RAI 2-7) was essentially a calibration as it was used to match empirical results, and actual phases observed in experiments were not used because acceptable glass degradation rates could not be achieved. This is a source of uncertainty within the modeling and the simulated degradation rates in the PA are essentially an extrapolation of short-term empirical observations. This type of uncertainty should be reflected in the base case results, or the potential impact on the base case results communicated to decisionmakers, otherwise a false sense of confidence may be assigned to the assurance as to whether the regulatory criteria will be achieved.

DOE indicated that when considered together, multiple sources of conceptual and parameter uncertainty with respect to glass release modeling may thus have a cancelling effect in predictive models of glass corrosion. The overall impact of these uncertainties on fractional releases may consequently be relatively small. It is unclear how this conclusion was arrived at unless inverse correlations between the relevant uncertainties were observed (and this is not common). Uncertainties will propagate and expand the potential range of outcomes. A probabilistic assessment of glass release rate uncertainties would help better define the range of uncertainty in glass release rates.

A large source of uncertainty in the performance of the IDF is from the inventory splits, or the fraction of key radionuclides that end up in different waste streams. DOE's base case (Case 7) has a very high percentage of the ^{99}Tc that ends up in the glass wasteform because of recycling. By comparison, cases 10A and 10B have a low percentage of ^{99}Tc that ends up in the glass wasteform as a result of volatilization during processing. This uncertainty is the only uncertainty discussed that by itself that can swing the results from compliance to noncompliance. This uncertainty was not included in the global uncertainty analyses completed with the system model. The significance of an individual uncertainty depends on all other uncertainties, how they impact the results, and how close the results are to the regulatory standards. If a key uncertainty is identified but left out of the comprehensive uncertainty analyses the importance of individual uncertainties may be misinterpreted.

DOE examined some types of inventory uncertainties through special cases. The magnitude of the inventory in the base case did not reflect the uncertainty in the inventory that would be generated and processed into the various waste types. NRC had made various comments on the development of inventory values for WMA-C, some of which are also relevant to this draft WIR evaluation (ML20128J832). While it is true that this type of uncertainty has a relatively linear impact on the dose results and can be easily projected, this type of uncertainty directly compounds with other types of uncertainties in the PA and increases the range of potential outcomes thereby decreasing the certainty with which demonstration of compliance with the criteria can be achieved.

Path Forward
Please expand the sensitivity and uncertainty analyses to include the items discussed above in the basis part of this comment (e.g., additional glass release uncertainties, inventory splits, inventory uncertainties).

DOE Response
As noted in the RAI basis, a significant amount of effort was devoted in the IDF PA to evaluate the impact of a range of alternative conceptual models and parameter values on the predicted release and transport of radionuclides and the associated groundwater concentration and dose. The impact was assessed using sensitivity analyses with the detailed process models presented in Sections 5.1.1.4, 5.1.2, 5.1.3.3, 5.2.3, 5.2.4 and 5.2.5 of RPP-RPT-59958, as well as sensitivity and uncertainty analyses using the system models that are presented in Sections 6.2 and 6.3 of RPP-RPT-59958. The purpose of the sensitivity and uncertainty analyses was to evaluate the key uncertainties that could lead to significant increases in the predicted dose to a potential future receptor and to identify the types of R&D activities and related design decisions that could be the focus of future maintenance activities. To that end, DOE believes the range of sensitivity and uncertainty analyses performed are sufficient to evaluate the confidence in demonstrating a reasonable expectation (or reasonable assurance) of compliance with the performance objectives and to identity the activities that are included in the PA maintenance plan (CHPRC-03348).

The RAI path forward recommends that additional sensitivity or uncertainty analyses be performed to evaluate some other uncertainties that were not evaluated as part of the IDF PA. This response provides additional sensitivity analyses to evaluate other uncertainties related to ILAW glass release that were not evaluated as part of the IDF PA.

The specific items raised in the basis part of the RAI are addressed in the following discussion. This discussion addresses the assertion in the RAI that some uncertainties that may be important were not included within the scope of the sensitivity and uncertainty analyses and that the impact of these uncertainties are important to understand in order to determine if the criteria will be met with reasonable expectation (DOE) or reasonable assurance (NRC). The additional uncertainties of particular note in the basis for RAI 2-12 involve the following components of the PA:

- Near-field hydrology and effect of the surface barrier degrading faster than the liner system

- Hydraulic characteristic, notably the MCC, effects on ILAW glass release

- SMRN effects on ILAW glass release

- Other sources of uncertainty effects on ILAW glass release

- Inventory split effect on groundwater pathway concentration and dose

- Inventory effect on groundwater pathway concentration and dose.

The RAI response includes additional sensitivity analyses on the predicted FRR of mobile radionuclides from ILAW glass. These analyses expand on the sensitivity analyses for the HYDRL, SMRN, RSA and COMBX cases presented in Section 5.1.3 of RPP-RPT-59958. For completeness, additional sensitivity analyses are presented on the predicted FRR from ILAW

glasses including the effects of uncertainty in the glass corrosion parameters, reactive surface area and the possible effects of Stage III glass corrosion[52].

The sensitivity analyses presented use LAWC22 as a representative ILAW glass. New information on other ILAW glasses, such as the information presented in recent PNNL and VSL testing summarized in the responses to RAIs 2-7 and 2-9, is not evaluated as part of this RAI response, but will be addressed as appropriate per the PA change control process involving UDQEs and Special Analyses. The new analyses included in this RAI response will be formally documented using the PA change control process and become part of the technical basis for the PA. Additional information related to the identification of an erroneous *riex* value (see PNNL-26594) that was used in the IDF PA (based on an erroneous value recommended in PNNL-24615, *Immobilized Low-Activity Waste Glass Release Data Package for the Integrated Disposal Facility Performance Assessment* from an erroneous value reported in PNNL-14805) is also addressed in the additional sensitivity analyses.

<u>Near-Field Hydrology – Effect of Hydraulic Properties of Cover and Liner Systems</u>
The near-field hydrology model and associated calculations using the near-field hydrology model (described in Sections 4.4.1.1 and 5.1.1, respectively, in RPP-RPT-59958) were used to define the water flux through the IDF liner system to the underlying vadose zone. Although the model included the layers of the surface cover to calculate the fraction of infiltrating water that would be shed to the margins of the cover, the role of the surface cover materials did not affect the flux into the facility because it was assumed that during the assumed 500-yr design life of the surface cover the average annual percolation flux into the facility was 0.5 mm/yr and after the assumed 500-yr design life of the surface cover the average annual percolation flux into the facility was 3.5 mm/yr.

This assumption was made for consistency with the assumptions used in other PAs (notably the WMA C PA described in RPP-ENV-58782) and the TC&WM EIS (DOE/EIS-0391). While it is acknowledged that the evolution of the hydraulic properties of the layers comprising the surface cover would impact the percolation flux, this uncertainty was not specifically modeled but was rather assumed for consistency with the post-design life net infiltration rate (3.5 mm/yr). The impact of uncertainty in the assumed net infiltration rate through the surface cover was evaluated in RPP-RPT-59958, in process-model sensitivity analyses presented in Sections 5.1.2.10, 5.2.3.2 and 5.2.4.2; in system model sensitivity analyses presented in Section 6.2.1.4.1; and in system model uncertainty analyses presented in Section 6.3.3.1.

The RAI basis notes that "It would be reasonable to examine a case with a degraded cover and an indefinitely performing liner system." Such a case, commonly referred to as the "bathtub scenario" as it evaluates the potential for water to fill the facility prior to the liner system degrading, was analyzed with case CLD4 in Section 5.1.1.4 of RPP-RPT-59958. The CLD4

---

[52] RAIs 2-7, 2-8, 2-9 and 2-10 relate to other aspects of the ILAW glass release model that are not explicitly noted in the basis for RAI 2-12. However, because the goal is to provide a complete assessment of the impact of uncertainty on the predicted glass release rates, the additional sensitivity analyses presented in this RAI response have been expanded to address the potential effect of compounded uncertainties related to glass release. This is to address the observation in RAI 2-7 that one-at-a-time evaluations "can be mathematically compounded but may not yield a fair assessment of the importance of these uncertainties combined with other uncertainties raised by this RAI package".

sensitivity analysis assumed the liner system continued to perform its function for 1,000 years after the closure of the facility and that the surface cover ceased performing its function 500 years after closure. The results indicate that while the lowermost operational layer becomes saturated (RPP-RPT-59958, Figure 5-17) during the 1,000-year performance of the liner, the resulting water level changes above the liner do not rise into the lowermost waste layer.

This change in saturated conditions above the liner in this sensitivity case is a combined result of:

- a relatively low net infiltration rate assumed for the surface cover (0.5 mm/yr) for the first 500 years

- the sump is assumed to be operating and removing any leachate for the first 100 years and

- a higher net infiltration rate assumed for the surface cover (3.5 mm/yr) thereafter.

Although there is an initial pulse of water into the vadose zone when the liner system is assumed to instantaneously degrade for this representation of the "bathtub scenario," within a few hundred years the vadose zone flow regime returns to the base case predicted flow regime (RPP-RPT-59958, Figure 5-20).

While it is imaginable to speculate that the liner system performs indefinitely (i.e., the liner system continues to perform its design function and does not degrade until times much greater than 1,000 years), it is not believed such conjecture provides a representative scenario. However, if this assumption is made, the backfill in the facility would be expected to take about 1,300 years to become fully saturated given a backfill porosity of 0.35 for the operational layers and an infiltration rate through the surface cover of 0.5 mm/yr for the first 500 years and then 3.5 mm/yr after the 500-yr design life of the surface cover.[53]

After the trench backfill materials are presumed to have become fully saturated, and assuming the liner system continues to perform its design function, the volumetric flow rate through the surface cover would equal the volumetric flow rate to the underlying vadose zone along the lowest points of the outer margins of the liner system, i.e., 720 m³/yr. The surface area to which this volumetric flow rate is applied is not known; however, it may be considered to represent a fraction of the total perimeter of the surface cover. Although this potential scenario was not analyzed in the IDF PA, assuming the area is small (e.g., several hundred square meters), one might conjecture that the net infiltration rate is large (e.g., greater than 1.0 m/yr) and that the transport time from the surface through the vadose zone to the water table would be small (e.g., less than 100 years). The resulting groundwater concentration would be controlled by the

[53] Assuming the IDF is built out to its maximum areal extent, the total volume of the IDF cells would be 2.93×10⁶ m³ (based on an upper surface area of 420 m × 487 m, a floor surface area of 330 m × 422 m and a height of 17 m), of which it is assumed that 900,000 m³ is a low porosity waste and the remaining volume of 2.03×10⁶ m³ is backfill with a porosity of about 0.35. The annual volumetric flow into the facility would be about 100 m³/yr for the first 400 years after the 100-year institutional control period and then increase to about 720 m³/yr starting after the 500-year design life of the surface barrier.

concentration of the radionuclides released from the waste forms and diluted in the pore water in the bathtub as summarized below.

The concentration in the groundwater from the "bathtub" scenario can be approximated by taking the concentration of a risk-significant radionuclide, e.g., ^{99}Tc, that would build up in the "bathtub" and dividing that by the dilution of the "bathtub" concentration by the lateral groundwater flow in the saturated zone into which the "bathtub" water would be discharged. The concentration in the "bathtub" can be calculated by dividing the activity released from the waste over the time that it takes the "bathtub" to fill by the water volume in the "bathtub." For example, the activity of ^{99}Tc released from ILAW glass when the "bathtub" is filled in 1,300 years is about 9.4 Ci (2.5E-07 yr^{-1} × 1,300 years × 28,800 Ci) and the activity of ^{99}Tc released from SSW when the "bathtub" is filled is about 7.2 Ci[54]. The ^{99}Tc concentration in the "bathtub" would then be about 8,300 pCi/L (16.6 Ci/2×10^6 m^3).

The "bathtub" concentration would get diluted in the saturated zone by the lateral groundwater flow in the saturated zone beneath the facility. Considering the nominal groundwater specific discharge of 70 m/yr, a 5-m high well screen and a flow width of 200 m (about half of the north-south length of the IDF), the volumetric flow rate in the saturated zone would be about 70,000 m^3/yr and the resulting ^{99}Tc groundwater concentration would be about 85 pCi/L (8,300 pCi/L × 720 m^3/yr/70,000 m^3/yr). This is about 25% of the peak ^{99}Tc groundwater concentration of 350 pCi/L calculated for the nominal performance in the IDF PA (see RPP-RPT-59958, Figure 5-98). Therefore, the effect of the postulated scenario with a degraded cover and an indefinitely performing liner system would likely result in a lower peak concentration (and associated groundwater pathway dose) than the base case analyzed in the IDF PA.

ILAW Glass Release – Effect of Glass Hydraulic Property Uncertainty

The ILAW glass release rate is dependent on the hydraulic flow regime through the fractured glass, in that the Darcy flux through the fractured glass and the associated moisture content and pore velocity affect the residence time for aqueous fluids to react with the glass. Higher residence times in the fractured glass lead to higher aqueous concentrations of mobile radionuclides (e.g., dissolved technetium as TcO$_4^-$), and thus an increase in the release rate for a given Darcy flux because the release rate is the product of the aqueous concentration times the Darcy flux. However, there are competing synergistic effects between Darcy flux and moisture content, as increases in Darcy flux result in an increase in moisture content. The Darcy flux through the glass is also dependent on the background infiltration flux through the facility and the properties of the backfill around the glass containers. Because of these coupled relationships of these factors and associated uncertainties, different sensitivity analyses were performed that

[54] The FRR from ILAW glass is 2.5E-07 yr^{-1} and the ILAW ^{99}Tc inventory is 28,800 Ci, yielding a cumulative release of ^{99}Tc from ILAW glass of about 9.4 Ci in 1,300 years. The three most significant SSW waste streams contributing to ^{99}Tc release are HEPA filters, ion-exchange resins and non-CERCLA waste streams. The cumulative 1,000-year FRR from HEPA filters, ion-exchange resins and non-CERCLA waste streams is 0.26, 0.26 and 0.34, respectively (RPP-RPT-59958, Table 5-27). The ^{99}Tc inventory in HEPA filters, ion-exchange resins and non-CERCLA SSW waste streams is 17.43, 2.36 and 1.21 Ci, respectively (RPP-RPT-59958, Table 3-27). Therefore, assuming the 1,000-year cumulative FRR is extended to 1,300 years, the cumulative release of ^{99}Tc from SSW is about 7.2 Ci in 1,300 years (5.9 Ci from HEPA filters, 0.8 Ci from ion-exchange resin and 0.5 Ci from non-CERCLA wastes).

examined these parameters as part of the IDF PA.

The ILAW glass release model and associated calculations (described in Sections 4.4.1.2 and 5.1.2 of RPP-RPT-59958, respectively) consider the effects of uncertainty in the vertical Darcy flux and moisture content through fractured ILAW glass. This was accomplished by modifying the background infiltration rate (from 0.5 to 4.2 mm/yr) as well as the saturated hydraulic conductivity and porosity of fractured glass. Although the impact of uncertainty in the fractured glass saturated hydraulic conductivity and porosity were evaluated, the potential impact of uncertainty in the MCCs, in particular the residual moisture content and van Genuchten parameters alpha and n, has not been evaluated. As noted in the RAI basis, "moisture characteristic curves (MCC's) can have a significant impact on release rates if differing materials are present and simulation of capillary barrier effects occurs". As a result, the RAI basis recommended that "the HYDRL and combined cases should be expanded to include the impact of uncertainties in MCC's".

DOE agrees that the hydraulic characteristics of fractured glass are uncertain and that the effect of the uncertainty in MCCs on the predicted vertical Darcy flux and moisture content should be evaluated. Of particular relevance is the potential impact of the uncertain van Genuchten-Mualem parameter values—namely the saturated hydraulic conductivity, porosity, residual moisture content, and van Genuchten parameters alpha and n—used in the STOMP ILAW glass release model.

The base case glass release model and all sensitivity analyses related to the MCCs, presented in Section 5.1.2 of RPP-RPT-59958, assumed the same parameter values recommended in PNNL-23711 (as previously recommended in PNNL-14700, *Near-Field Hydrology Data Package for the Integrated Disposal Facility 2005 Performance Assessment*), as follows:

- Saturated hydraulic conductivity of 3.1×10^{-5} cm/s
- Porosity of 0.02
- Residual moisture content of 6.0×10^{-5} (residual saturation: 0.003)[55]
- van Genuchten alpha of 0.044 1/cm
- van Genuchten n of 1.88.

The reported best-estimate values of the assumed parameter values above reflect the geometric mean values derived from laboratory tests on three fractured glass samples and fitting a van Genuchten model to the observed pressure-saturation data as summarized in PNNL-14700. Other studies of glass corrosion and associated release modeling reported in RPP-17675, *Risk Assessment Supporting the Decision on the Initial Selection of Supplemental ILAW Technologies* (Table 3-4), PNNL-15198 (Table 3), PNNL-20781 (Table 7.3) and PNNL-21812 (Table 7.3) recommended a saturated hydraulic conductivity of 1.0×10^{-2} cm/s, a residual moisture content of 4.6×10^{-4}, a van Genuchten alpha of 0.2 1/cm, and a van Genuchten n of 3.0.

---

[55] Although PNNL-23711 and PNNL-14700 recommended a residual saturation of 0.03 (i.e., a residual moisture content of 6.0×10^{-4}), the STOMP model file used as the starting case for the calculation a residual saturation of 0.003. This value was maintained in the base case and all sensitivity analyses conducted using the 2-D STOMP reactive transport model.

The recommended hydraulic property values from these PNNL studies provide a useful base case value because these values result in predicted fractional glass release rates that are similar to those used as the base case in the TC&WM EIS, i.e., 2.8E-08 yr^{-1} [56]. However, there is uncertainty in the hydraulic properties of the ILAW glass. As a result, consistent with the RAI basis it is relevant to evaluate the impact of the uncertainty in the ILAW glass hydraulic properties on the predicted release rate of radionuclides from the ILAW glass.

As summarized in Table 2-12-1, for the base case hydraulic (van Genuchten-Mualem) parameter values used in STOMP, increasing the background net infiltration rate results in an increase in the vertical Darcy flux through the fractured glass and also increases the moisture content in the fractured glass. Increasing the vertical Darcy flux through the glass decreases the residence time, while increasing the moisture content increases the residence time. For the base case hydraulic (van Genuchten-Mualem) parameter values, the increased background net infiltration rate reduces the residence time which in turn reduces the predicted concentration calculated using GWB. Therefore, an increased background net infiltration rate has little impact on the release rate or FRR (which is the product of the increased Darcy flux times the reduced concentration).

Different hydraulic (van Genuchten-Mualem) parameter values can affect the fraction of background net infiltration rate that enters the fractured glass versus flowing around the glass and also could result in a different moisture content and resulting residence time. The uncertainty in the hydraulic flow regime around and through the fractured glass was investigated in the IDF PA by conducting sensitivity analyses on the impact of uncertain hydraulic conditions in the ILAW glass on the predicted FRR as documented in Section 5.1.2 of RPP-RPT-59958. The hydraulic conditions varied in these sensitivity analyses included: (a) background infiltration rate (IFLUX cases), (b) temporal variation in background infiltration rate (VFLUX cases), (c) saturated hydraulic conductivity and porosity of ILAW glass (HYDRL cases), and (d) saturated hydraulic conductivity and porosity of backfill (HYDRL cases). The IFLUX cases addressed a range of background infiltration flux values (from 0.5 to 4.2 mm/yr). The HYDRL cases addressed impacts of changing backfill saturated hydraulic conductivities and porosity values, as well as glass saturated hydraulic conductivities and porosity values.

---

[56] The properties of the ILAW glass used in the TC&WM EIS were based on the LAWABP1 glass and the base case net infiltration rate of 0.9 mm/yr. The EIS comparison case for LAWABP1 and a net infiltration rate of 0.9 mm/yr resulted in a predicted fraction release rate of 6.0E-08 yr^{-1} (RPP-CALC-61031 and RPP-RPT-59958, Section 5.1.2.3) compared to the value of 2.8E-08 yr^{-1} reported in RPP-17675 and DOE/EIS-0391.

Table 2-12-1. The Geochemist's Workbench® Predicted Fractional Release Rates from LAWA44 for Different Background Net Infiltration Rates and the Base Case Glass and Backfill Hydraulic Properties.

Background Net Infiltration Rate (mm/yr)	Q (glass) (cm³/yr)	Vertical Darcy Flux (cm/yr)	Moisture Content	Pore Velocity (cm/yr)	Residence Time (yr)	Concentration (mol TcO₄/L)	Release Rate (mol TcO₄/yr)	Fractional Release Rate (yr⁻¹)
0.5	4.16	4.16E-03	0.00149	2.79	70.3	8.82E-05	3.66E-07	1.71E-07
0.9	7.96	7.96E-03	0.00172	4.63	42.3	4.36E-05	3.47E-07	1.62E-07
3.5	35.7	3.57E-02	0.00238	15.0	13.1	9.59E-06	3.43E-07	1.60E-07
4.2	43.7	4.37E-02	0.00250	17.5	11.2	7.98E-06	3.49E-07	1.63E-07

Source: RPP-RPT-59958, *Performance Assessment for the Integrated Disposal Facility, Hanford Site, Washington*, Table 5-14 (derived from RPP-CALC-61031, *Low-Activity Waste Glass Release Calculations for the Integrated Disposal Facility Performance Assessment*, Tables 7-8 and 7-9).

Note: Q(glass) represents the volumetric flux through a 0.1-m wide section of glass. The background net infiltration rate equals the percolation flux through the surface cover. The base case net infiltration rate during the design life of the surface cover is 0.5 mm/yr and increases to either 0.9 mm/yr (for the Tank Closure and Waste Management Environmental Impact Statement base case) or 3.5 mm/yr (for the Integrated Disposal Facility Performance Assessment base case) after the 500-yr design life of the surface cover.

The volumetric flux (Q), vertical Darcy flux and moisture content are derived from a STOMP two-dimensional model run using the base case glass and backfill moisture characteristic curves. They represent a single cell that is 0.1 m wide and has a thickness of 1.0 m. The predicted vertical Darcy flux in the fractured glass is about 10% of the net infiltration rate for the assumed hydraulic properties of the glass and backfill. Residence time is based on a vertical height of glass in a single container of 196 cm.

Although the moisture content values presented in Table 7-8 of RPP-CALC-61031 are reported to two significant figures, the number of significant figures was increased to three for consistency with the other values.

The concentration values are presented in GWB result files along with the fractional release rate. The concentrations differ from the STOMP example results illustrated in Figure 2-12-1.

Fractional release rate values are in Table 7-9 of RPP-CALC-61031 based on GWB model file which assumes 2.14 mol of TcO₄ for LAWA44 in GWB.

The Geochemist's Workbench® (GWB) is a registered trademark of Aqueous Solutions LLC, Champaign, Illinois.
Subsurface Transport Over Multiple Phases (STOMP) has been developed and distributed by Battelle Memorial Institute, Richland, Washington.

Figure 2-12-1. Subsurface Transport Over Multiple Phases IFLUX Results for LAWA44 Glass Showing Variations in Volumetric Flux, Residence Time, and Technetium Concentrations in Effluent Solutions as a Function of Infiltration Rate.
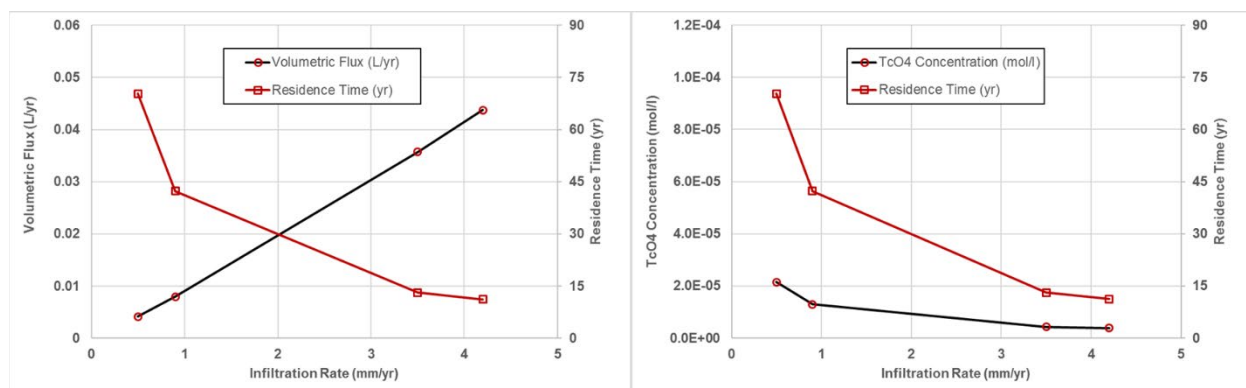
Source: RPP-RPT-59958, *Performance Assessment for the Integrated Disposal Facility, Hanford Site, Washington*, Figure 5-43 (from RPP-CALC-61031, *Low-Activity Waste Glass Release Calculations for the Integrated Disposal Facility Performance Assessment*, Figure 7-16).

Note: The predicted volumetric flux and TcO_4 concentration is for a representative cell located at the base of the immobilized low-activity waste glass at steady state. The cell is 0.1 m wide × 0.196 m high × 1.0 m deep. The residence time is calculated using the predicted volumetric flux (and associated vertical Darcy flux) and the predicted moisture content in the representative cell to calculate a pore velocity that is used over the 1.96-m high glass waste form as presented in Table 2-12-1. It is not appropriate to multiply the single-cell volumetric flux (L/yr) by the TcO_4 concentration (mol/L) to calculate the TcO_4 flux rate (mol/yr) because these values do not include the spatial distribution of TcO_4 releases from the two-dimensional (2-D) STOMP model. The 2-D STOMP model TcO_4 fluxes for all 12 cells across the base of the model domain are summed to provide the total TcO_4 flux, which is then divided by the initial TcO_4 inventory of 26.17 mol for the LAWA44 glass to yield the fractional release rate. The reported values are the steady-state fractional release rate. The one-dimensional stationary-state GWB model calculates the TcO_4 flux based on the residence time, which is dependent on the vertical Darcy flux and moisture content. The vertical Darcy flux and moisture content used in the calculation of the residence time used in the GWB model are based on the 2-D STOMP model for the hydraulic conditions modeled in STOMP, which include: (a) background infiltration rate, (b) glass cross-sectional area, (c) backfill cross-sectional area, (d) glass hydraulic properties (i.e., saturated hydraulic conductivity, porosity, residual saturation, van Genuchten alpha, and van Genuchten n) and (e) backfill hydraulic properties.

The Geochemist's Workbench® (GWB) is a registered trademark of Aqueous Solutions LLC, Champaign, Illinois. Subsurface Transport Over Multiple Phases (STOMP) has been developed and distributed by Battelle Memorial Institute, Richland, Washington.

While the IFLUX and HYDRL sensitivity cases evaluated the impact of changing hydraulic conditions (notably the predicted moisture content and Darcy flux and associated pore velocity and residence time in the glass), these cases did not evaluate the impact that uncertain MCCs could have on the predicted Darcy flux and moisture content. That is, although the saturated hydraulic conductivity and porosity were varied, they were varied using the same residual moisture content and van Genuchten alpha and n parameter values. Changes in saturated hydraulic conductivity and porosity may have little effect on the predicted steady-state Darcy flux through the fractured glass and the corresponding moisture content. This is because the hydraulic properties of the glass are more dependent on the unsaturated hydraulic properties,

i.e., the relative permeability associated with moisture contents closer to the residual moisture content than the saturated moisture content.[57]

The uncertainty analyses conducted as part of the IDF PA (RPP-RPT-59958, Section 6.3.2.2) assumed that the most significant uncertainty was associated with the glass corrosion properties, notably parameters η, RC, K_g and $riex$, where η is the pH power law coefficient, RC is the dissolution model rate constant, K_g is the apparent equilibrium constant, and $riex$ is the rate constant of the ion-exchange reaction. As a result of the perceived significance of these parameters in affecting the predicted FRR, a regression model was developed to correlate these parameters to predicted FRRs using GWB-predicted results using nominal estimates of the reactive surface area, SMRNs and hydraulic properties. The uncertainty analyzed included the uncertainty in values of the glass corrosion parameters and the uncertainty in the regression model fitting constants.

As illustrated in the IDF PA uncertainty analyses (Figure 2-12-2), the predicted groundwater dose is not sensitive to ILAW release parameters at early times (e.g., 1,000 to 3,000 years) of the post-closure analysis, but they do become significant at later times (e.g., 6,000 to 10,000 years after closure). This is because of the greater significance the predicted release of the more mobile ^{99}Tc from the SSW has at early times. The importance of the ILAW release on the predicted groundwater dose at later times is also indicated by the relative increase in the importance of the uncertain parameters that affect the ILAW FRR on the groundwater dose indicated in RPP-RPT-59958, Table 6-42 (reproduced here as Table 2-12-2).[58]

The RAI basis notes that the uncertainty in the glass moisture retention characteristic curves (MCCs) was not evaluated as part of the sensitivity and uncertainty analyses presented in RPP-RPT-59958. The ILAW glass MCCs consist of five parameters, namely the saturated hydraulic conductivity, the porosity, the residual moisture content (or residual saturation), and the van Genuchten alpha and n parameters. While the sensitivity analyses performed did evaluate the impact of the uncertainty in the saturated hydraulic conductivity and porosity for both the ILAW glass and the backfill, the other MCC parameter values were kept at their reference case values, as recommended in PNNL-23711 based on information presented in PNNL-14700.[59] Therefore, it is relevant to evaluate the impact of other uncertain hydraulic

---

[57] The base case predicted moisture content in the fractured glass for the base case net infiltration rate of 3.5 mm/yr and the base case van Genuchten-Mualem parameter values is 0.0024. This corresponds to a saturation of 0.12 (12%) given the assumed base case porosity of 0.02 (2%). The relative hydraulic conductivity at this saturation is orders of magnitude less than the saturated hydraulic conductivity. Therefore, the predicted moisture content (and associated residence time and release rate) is not significantly affected by the saturated hydraulic conductivity or porosity, but may be impacted by the assumed residual moisture content or van Genuchten alpha or n.

[58] The importance of the $riex$ parameter indicated in Table 2-12-2 is based on the assumed uncertainty around the base case value for LAWA44 glass used in the 2017 IDF PA. As summarized in PNNL-26594, the base case $riex$ value (derived from information in PNNL-24615 and PNNL-14805) is erroneous and should be reduced by a factor of 7 which would reduce the predicted FRR from ILAW glass by the same factor. Therefore, conclusions regarding the importance of parameters that affect the predicted ILAW FRR need to consider the pessimistic ILAW glass release assumed for the base case in the 2017 IDF PA.

[59] Other PNNL reports have used different values of saturated hydraulic conductivity, residual moisture content, van Genuchten alpha and van Genuchten n. For example, PNNL-15198, PNNL-20781 and PNNL-21812

(van Genuchten-Mualem) properties of the ILAW glass on the predicted FRR. These analyses are presented in the next section.

Figure 2-12-2. Scatter Plots of Immobilized Low-Activity Waste Fractional Release Rate Against Groundwater Pathway Dose at (a) 1,000 Years, (b) 3,000 Years, (c) 6,000 Years, and (d) 10,000 Years after Closure. (sheet 1 of 2)

(a)

(b)
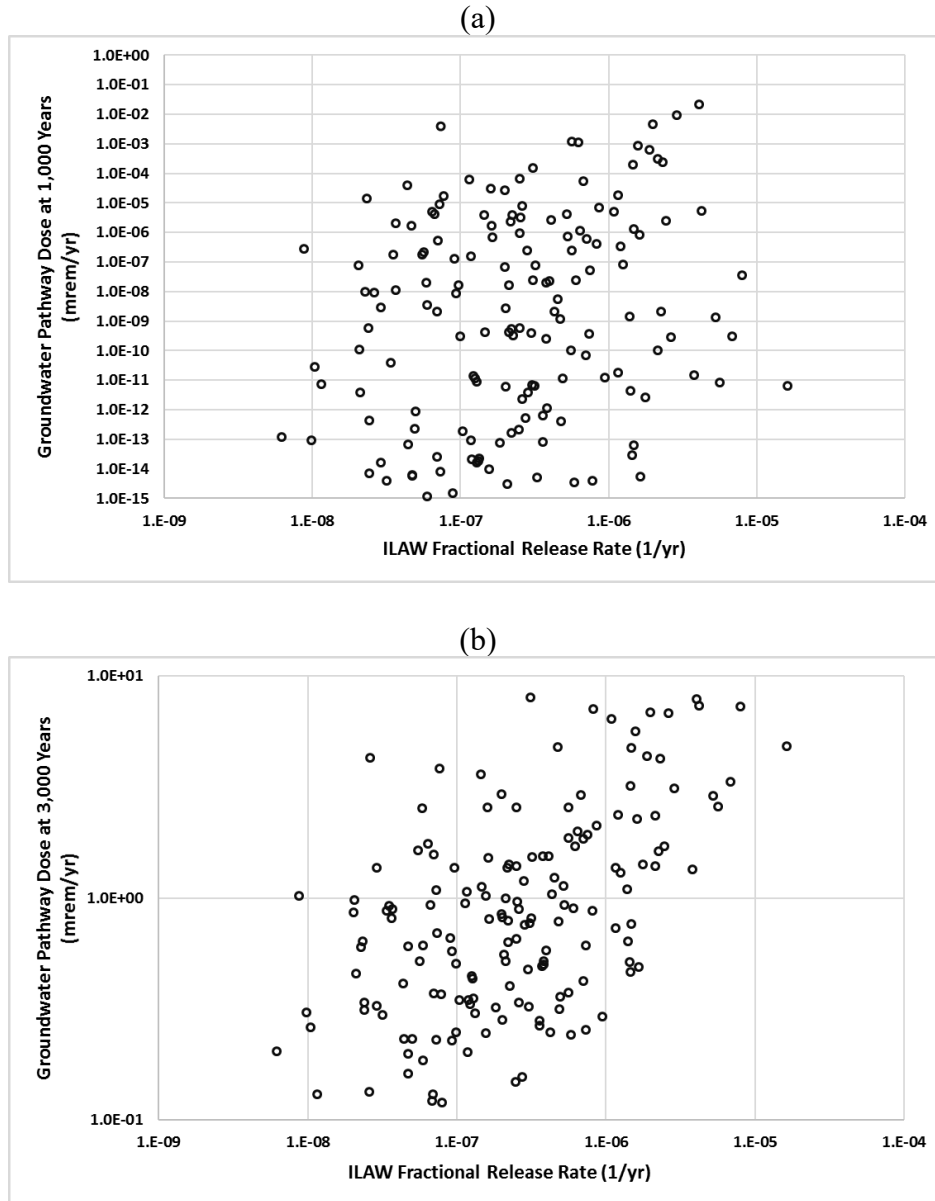
assumed a saturated hydraulic conductivity of fractured glass of 1.0×10^{-2} cm/s (compared to a reference case value of 3.1×10^{-5} cm/s), a residual moisture content of 4.6×10^{-4} (compared to a reference case value of 6.0×10^{-4}), a van Genuchten alpha of 0.2 (compared to the reference case value of 0.044) and a van Genuchten n of 3.0 (compared to a reference case value of 1.88).

Figure 2-12-2. Scatter Plots of Immobilized Low-Activity Waste Fractional Release Rate Against Groundwater Pathway Dose at (a) 1,000 Years, (b) 3,000 Years, (c) 6,000 Years, and (d) 10,000 Years after Closure. (sheet 2 of 2)
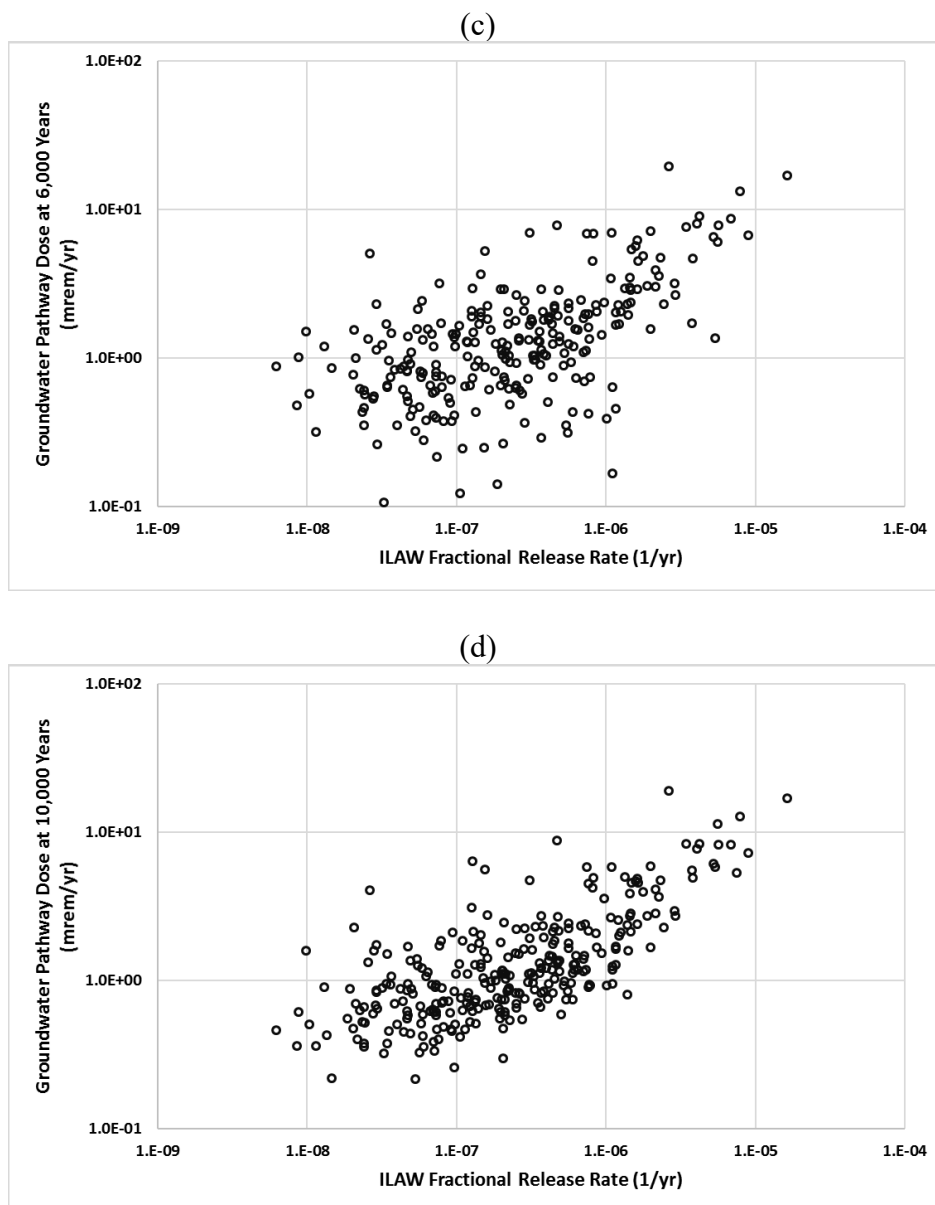
Source: RPP-RPT-59958, *Performance Assessment for the Integrated Disposal Facility, Hanford Site, Washington*, Figure 6-147 (derived from RPP-CALC-61194, *System Model Calculations for the Integrated Disposal Facility Performance Assessment*, Rev. 1, Figure 7.3-44).

Note: The groundwater pathway dose is the total dose from all waste sources: immobilized low-activity waste (ILAW) glass, solid secondary waste (SSW) and Effluent Treatment Facility liquid secondary waste and all radionuclides, importantly both ^{99}Tc and [129]I. The total dose at early times (i.e., 1,000 years) is more significantly affected by ^{99}Tc, which is predominantly derived from SSW sources at early times; therefore, uncertainty in the ILAW FRR does not significantly affect the predicted dose. At later times (e.g., 6,000 or 10,000 years), the dose is derived from both SSW and ILAW sources of [99]Tc (and to a lesser extent [129]I); therefore, uncertainty in the ILAW FRR does significantly affect the predicted dose. These results are based on the uncertainty for engineered and natural barrier performance summarized in RPP-RPT-59958, Section 6.3. The highest dose in the uncertainty analysis was 19.6 mrem/yr.

Table 2-12-2. Uncertain Parameters Important to Groundwater Pathway Total Dose at (a) End of Compliance Time Period (1,000 Years after Closure) (b) 3,000 Years after Closure (c) 6,000 Years after Closure and (d) 10,000 Years after Closure. (2 sheets)

Stochastic Parameter ID	Description	Correlation Coefficient Based on Ranks	Standardized Regression Coefficient Based on Ranks	Partial Correlation Coefficient Based on Ranks	Importance Measures Based on Ranks
(a) 1,000 years after Closure
Irate_bg	Background infiltration rate	0.898	0.915	0.968	0.779
H2_Kd[Tc]	^{99}Tc Kd in H2 Sand	-0.309	-0.345	-0.810	0.120
C2_RateCon_LAWA44	Regression Model Fitting Constant	0.122	0.028	0.121	0.048
SZ_DF_multiplier	Saturated zone Darcy flux multiplier	-0.070	-0.022	-0.089	0.041
(b) 3,000 years after Closure
Irate_bg	Background infiltration rate	0.895	0.901	0.951	0.770
H2_Kd[Tc]	^{99}Tc Kd in H2 Sand	-0.209	-0.227	-0.594	0.072
SZ_DF_multiplier	Saturated zone Darcy flux multiplier	-0.176	-0.127	-0.386	0.068
H3_Kd[Tc]	^{99}Tc Kd in H3 Gravel	0.039	-0.018	-0.061	0.048
C2_RateCon_LAWA44	Regression Model Fitting Constant	0.106	0.007	0.024	0.047
Kg_LAWA44_pdf	apparent equilibrium constant	0.098	0.043	0.144	0.042
(c) 6,000 years after Closure
Irate_bg	Background infiltration rate	0.561	0.499	0.697	0.319
SZ_DF_multiplier	Saturated zone Darcy flux multiplier	-0.44	-0.399	-0.601	0.217
Riex_LAWA44_pdf	Rate of the ion-exchange reaction	0.291	0.221	0.368	0.109
C0_Intercept_LAWA44	Regression Model Fitting Constant	0.289	0.202	0.361	0.089
Kg_LAWA44_pdf	apparent equilibrium constant	0.199	0.148	0.272	0.067
Eta_LAWA44	pH power law coefficient	0.137	0.069	0.132	0.067

Table 2-12-2. Uncertain Parameters Important to Groundwater Pathway Total Dose at (a) End of Compliance Time Period (1,000 Years after Closure) (b) 3,000 Years after Closure (c) 6,000 Years after Closure and (d) 10,000 Years after Closure. (2 sheets)

Stochastic Parameter ID	Description	Correlation Coefficient Based on Ranks	Standardized Regression Coefficient Based on Ranks	Partial Correlation Coefficient Based on Ranks	Importance Measures Based on Ranks
(d) 10,000 years after Closure
SZ_DF_multiplier	Saturated zone Darcy flux multiplier	-0.518	-0.493	-0.721	0.286
Riex_LAWA44_pdf	Rate of the ion-exchange reaction	0.453	0.410	0.636	0.221
C0_Intercept_LAWA44	Regression Model Fitting Constant	0.345	0.276	0.510	0.130
Irate_bg	Background infiltration rate	0.295	0.182	0.368	0.091
C4_logRiex_LAWA44	Regression Model Fitting Constant	-0.268	-0.292	-0.524	0.083
Kg_LAWA44_pdf	apparent equilibrium constant	0.212	0.177	0.353	0.079
Eta_LAWA44	pH power law coefficient	0.085	0.019	0.042	0.063

Source: RPP-RPT-59958, *Performance Assessment for the Integrated Disposal Facility, Hanford Site, Washington*, Table 6-42 (derived from RPP-CALC-61194, *System Model Calculations for the Integrated Disposal Facility Performance Assessment*, Rev. 1, Table 7.3.2-1).

Note: The yellow highlighted values are parameters and regression model fitting constants related to the regression model for immobilized low-activity waste fractional release rates. At early times (i.e., 1,000 or 3,000 years after closure), the most significant uncertainty is related to the background infiltration rate as this controls whether unretarded risk-significant radionuclides, e.g., ^{99}Tc, reach the water table within the time period. The transport time to the water table is most significantly affected by the background infiltration rate. While the transport time is also dependent on the moisture content, the uncertainty in the moisture content was assumed to be a triangular distribution with the minimum of 0.5 times the base case value. As shown in the response to RAI 2-15, the minimum moisture content value is more representative of the observed average moisture content in the H2 sand in areas with undisturbed surfaces near the Integrated Disposal Facility.

DOE/ORP-2021-02, Rev. 1

GWB vs STOMP for Evaluating Effect of Uncertain Hydraulic Properties
The impact of uncertain ILAW glass hydraulic (van Genuchten-Mualem) properties can be
directly evaluated using the 2-D STOMP model by using alternative values for the
five van Genuchten-Mualem parameters that include saturated hydraulic conductivity, porosity,
residual moisture content, van Genuchten alpha and van Genuchten n. However, there is limited
information with which to define the uncertainty in these properties for fractured glass. In
addition, as noted in RAI 2-4, even if one could define a range of van Genuchten-Mualem
parameter values for a representation of hydraulic properties of fractured glass, other
uncertainties related to heterogeneity of the fractured glass and the possibility of fractures
becoming partially filled with fine-grained soils and secondary minerals would further
complicate the interpretation of the analysis and the possible impact on facility performance.

For the purposes of analyzing the impact of uncertain glass hydraulic conditions related to the
uncertain MCCs, the approach taken to address RAI 2-12 is to use a range of plausible hydraulic
conditions related to the vertical Darcy flux and the moisture content using GWB. The
comparison of the results between GWB and STOMP indicate that for the same hydraulic
conditions (notably for the same moisture contents and vertical Darcy fluxes) and the same
ILAW glass corrosion parameters, the two models provide similar results and GWB can be used
for more efficient evaluation of the impacts of these parameter sensitivities on FRRs (see also the
response to RAI 2-11 related to the justification of the use of GWB in addition to STOMP for
sensitivity analyses).

The results of calculated FRRs using the stationary-state assumptions in GWB with the results
calculated using the 2-D STOMP model for assumed steady-state conditions for a range of
different modeling cases are similar (Figure 2-12-3). The GWB runs can be rapidly performed
over a wide range of conditions to explore the impact of uncertainties in the dissolution and
release of mobile radionuclides from the ILAW glass. The GWB model was used as a basis for
developing the regression model fit employed in the uncertainty analyses summarized in
Section 6.3.2.2 of RPP-RPT-59958. The GWB model also has greater flexibility in evaluating
the potential impact of SMRNs conditions, an additional area of uncertainty raised in RAI 2-12.
Therefore, the approach taken for the additional sensitivity analyses to evaluate the impact of
uncertainties in fractured ILAW glass hydraulic conditions was to expand on the use of the GWB
model reference case.

The GWB model was run over a range of conditions in the IDF PA. These GWB modeling cases
are summarized in RPP-RPT-59958 Tables 5-4, 5-5 and 5-6 for representative ILAW glasses
LAWA44, LAWB45 and LAWC22[60]. The range of predicted results for the different glasses
was most affected by changes in corrosion characteristics associated with the TST and
ion-exchange rate-related parameters (i.e., η, RC, K_g and $riex$). The hydraulic conditions in the
three glasses analyzed for the cases when using both STOMP and GWB were assumed to be the
same.

---

[60] Additional glass formulations have been developed and tested by researchers at PNNL and VSL with the results
of the testing and associated TST and *riex* parameters and parameter uncertainty summarized in the response to
RAI 2-7. Additional information related to the possibility of Stage III corrosion of ILAW glasses and associated
corrosion rates is summarized in the response to RAI 2-9. The additional information will be evaluated as part of
the UDQE process when the information is available.

Figure 2-12-3. Comparison of Fractional Release Rates Calculated for Different Sensitivity Analysis Cases Using Subsurface Transport Over Multiple Phases and The Geochemist's Workbench®.
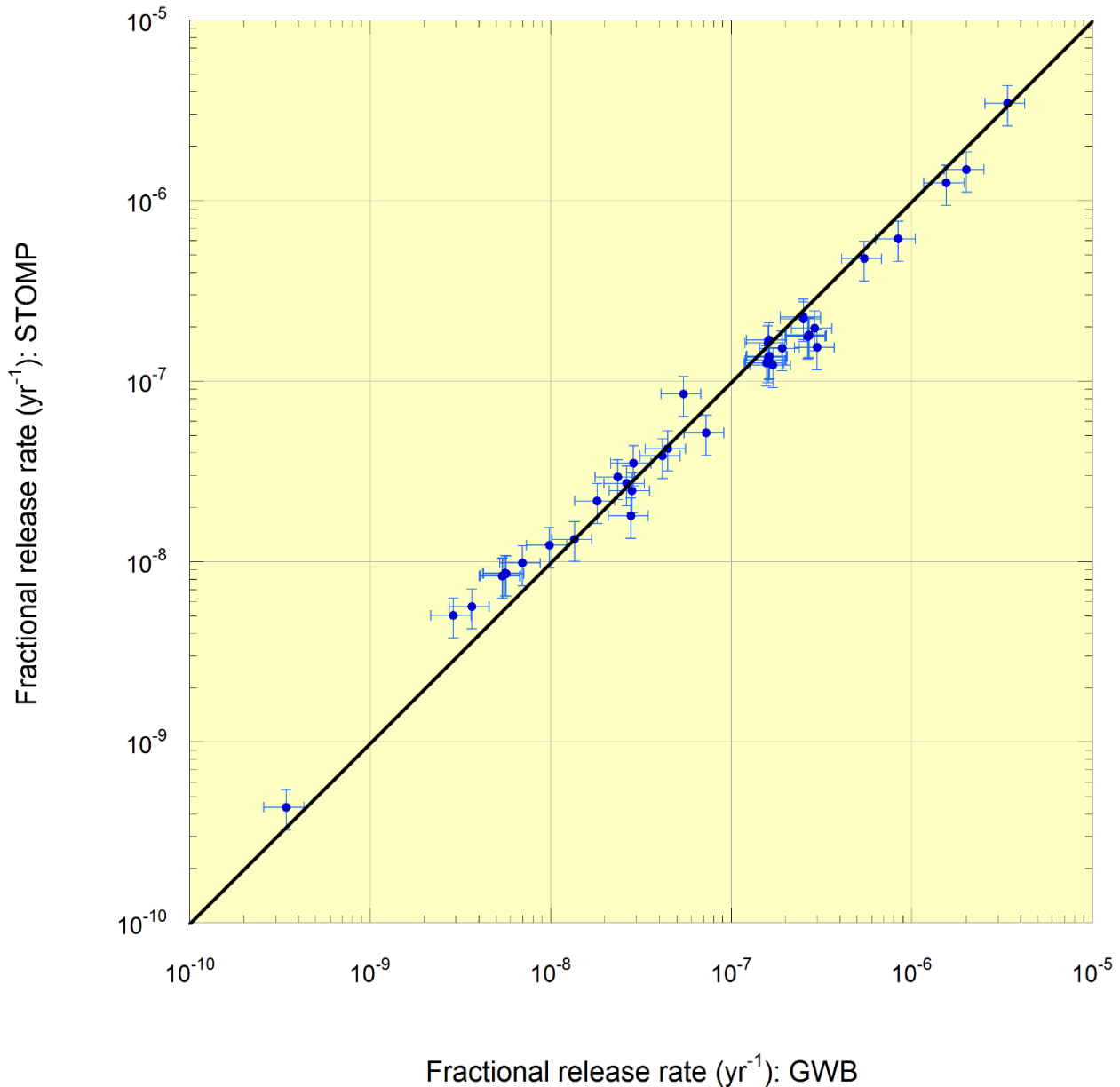
Source: RPP-RPT-59958, *Performance Assessment for the Integrated Disposal Facility, Hanford Site, Washington*, Figure 5-50 (from RPP-CALC-61031, *Low-Activity Waste Glass Release Calculations for the Integrated Disposal Facility Performance Assessment*, Figure 8-1).

Note: The half-lengths of vertical and horizontal bars on the symbols represent +/- 25% of calculated values.

Subsurface Transport Over Multiple Phases (STOMP) has been developed and distributed by Battelle Memorial Institute, 1996. The Geochemist's Workbench (GWB)® is a registered trademark of Aqueous Solutions LLC, Champaign, Illinois.

The glass release sensitivity cases analyzed in the IDF PA (Section 5.1.2 of RPP-RPT-59958) included a number of cases run to evaluate the impact of uncertain glass hydraulic properties and

other uncertain flow conditions in the backfill around the glass that could affect the predicted release rates. The VFLUX, HYDRL and BACK cases that analyze the effect of a time-varying net infiltration rate and the effects of uncertain hydraulic properties of ILAW glass and backfill were only run with the 2-D STOMP model because these cases were designed to evaluate the flow and transport of mobile radionuclides through the fractured glass. The IFLUX cases—which evaluated the effect of the uncertainty in the background long-term average steady-state infiltration rate through the degraded surface cover ranging from a lower bound estimate of 0.5 mm/yr, to the reference case value of 0.9 mm/yr, to the base value of 3.5 mm/yr, to an upper bound value of 4.2 mm/yr—used both STOMP and GWB. The IFLUX results using GWB evaluated the predicted vertical Darcy flux and moisture content from the 2-D STOMP model for each of the four cases analyzed. The vertical Darcy flux and moisture content were used to calculate an average pore velocity and residence time through the 1.96-m high glass waste form that was used as an input to GWB. As summarized in Section 5.1.2.10 and Table 5-15 (reproduced here as Table 2-12-3) of RPP-RPT-59958, the GWB and STOMP FRR results are similar. This comparison provides additional basis for the use of GWB for the additional sensitivity analyses.

The impact that uncertain hydraulic (van Genuchten-Mualem) properties (i.e., saturated hydraulic conductivity, porosity, residual moisture content, and van Genuchten alpha and n parameters) have on the predicted FRR is the result of the impact these property values have on the predicted vertical Darcy flux and moisture content in the fractured ILAW glass. The moisture content also can affect the inert volume (i.e., the volume of the pore space that is not occupied by an aqueous solution and thus does not enter into the calculation of glass corrosion) in the GWB calculation. Therefore, the approach to evaluate and simulate the impact of such hydraulic uncertainty is to evaluate a range of possible vertical Darcy fluxes and a range of possible moisture content values and associated inert volumes[61].

The base case predicted vertical Darcy flux and moisture content are based on the best estimate of the hydraulic (van Genuchten-Mualem) property values used for the ILAW glass and backfill recommended in PNNL-23711 (based on PNNL-14700) as well as the assumed base case infiltration rate of 3.5 mm/yr. It is reasonable to assume that the base case predicted FRR represents the central tendency of the results for the different glasses analyzed, i.e., LAWA44, LAWB45 and LAWC22. The uncertainty in the hydraulic conditions in the fractured glass can then be evaluated by increasing or decreasing the base case values of the vertical Darcy flux and moisture content, which are 0.346 mm/yr and 0.00238, respectively and the associated residence time of 13.1 years.

---

[61] The moisture content can affect both the calculated residence time and the calculated inert volume. The inert volume is also a function of the assumed porosity of the fractured ILAW glass. If one assumes the fracture porosity of the ILAW glass is fixed, then an increase in moisture content results in a decrease in the inert volume. However, if one assumes that the porosity is also uncertain, then one can assume that the inert volume would also be uncertain. Rather than independently varying the residence time (due to moisture content changes) and inert volume, two different end members were used, one in which the inert volume changed with moisture content and one in which the inert volume was fixed and did not change with moisture content.

Table 2-12-3. Summary of Results for the IFLUX Cases Analyzed in the Integrated Disposal Facility Performance Assessment.

Glass	Background Infiltration Rate (mm/yr)	Fractional Release Rate (yr⁻¹)	
		The Geochemist's Workbench®	STOMP
LAWA44	0.5	1.71E-07	1.22E-07
	0.9 (reference case)	1.62E-07	1.35E-07
	3.5 (base case)	1.60E-07	1.62E-07
	4.2	1.63E-07	1.68E-07
LAWB45	0.5	2.90E-09	5.02E-09
	0.9 (reference case)	5.40E-09	8.27E-09
	3.5 (base case)	2.36E-08	2.93E-08
	4.2	2.89E-08	3.50E-08
LAWC22	0.5	3.00E-07	1.53E-07
	0.9 (reference case)	2.70E-07	1.78E-07
	3.5 (base case)	2.51E-07	2.20E-07
	4.2	2.51E-07	2.26E-07

Source: RPP-RPT-59958, *Performance Assessment for the Integrated Disposal Facility, Hanford Site, Washington*, Table 5-15.

Note: The base case ILAW fractional release rate used in the IDF PA was 2.5E-07 yr⁻¹. The STOMP results are for the single ILAW glass container using the reference case values for glass corrosion and hydraulic properties of the ILAW glass and backfill.

Subsurface Transport Over Multiple Phases (STOMP) has been developed and distributed by Battelle Memorial Institute, 1996.

The Geochemist's Workbench® is a registered trademark of Aqueous Solutions LLC, Champaign, Illinois.

The additional sensitivity analyses performed to evaluate the impact of uncertainty in the fractured glass hydraulic conditions make use of the LAWC22 glass as representative of the expected glass composition and corrosion rates and assumes the reference case values for the TST parameters and *riex* [62] as well as the reference case values of $p_{CO2(g)}$. The choice of LAWC22 was based on the observation that the predicted FRR for LAWC22 is greater than the predicted FRR from either LAWA44 or LAWB45 for the reference case (Table 2-12-3). The

---

[62] The reference case value of *riex* for LAWC22 is 1.20×10^{-10} mol Na/m²-s based on the recommended value reported in PNNL-24615 as presented in PNNL-14805. As noted in PNNL-26594, this value is erroneous due to a unit conversion error and should be reduced to 1.28×10^{-11} mol Na/m²-s. To allow comparison to other sensitivity analysis results presented in RPP-RPT-59958, the erroneous value is used for the additional sensitivity analyses presented in this section. The use of the corrected value of *riex* is expected to reduce the predicted FRRs by about a factor of 10 as demonstrated in the IEX sensitivity analysis reported in Section 5.1.2.5 of RPP-RPT-59958.

additional sensitivity analyses cases have the following hydraulic characteristics in the fractured glass:

- Darcy flux = 0.357 mm/yr, moisture content = 2 × Base Case value of 0.00237 (therefore residence time = 2 × Base Case value of 13.1 years, i.e., 26.2 years)

- Darcy flux = 0.357 mm/yr, moisture content = 1/2 × Base Case value

- Darcy flux = 0.357 mm/yr, moisture content = 5 × Base Case value

- Darcy flux = 0.357 mm/yr, moisture content = 1/5 × Base Case value

- Darcy flux = 0.0796 mm/yr, moisture content = 2 × Reference Case value of 0.00172 (therefore residence time = 2 × Reference Case value of 42.3 years, i.e., 84.6 years)

- Darcy flux = 0.0796 mm/yr, moisture content = 1/2 × Reference Case value

- Darcy flux = 0.0796 mm/yr, moisture content = 5 × Reference Case value

- Darcy flux = 0.0796 mm/yr, moisture content = 1/5 × Reference Case value.

Results of Additional Sensitivity Analyses on the Impact of Alternative Glass Hydraulic Properties

The additional sensitivity analyses results are presented in Table 2-12-4. These results started with the reference case values for all TST-corrosion and ion-exchange parameters as summarized in RPP-RPT-59958, Section 5.1.2.1 and varied the moisture content and Darcy flux to evaluate the impact of alternative glass hydraulic properties[63]. The calculations were all performed with GWB by varying the residence time, inert volume, and Darcy flux.

The sensitivity analyses used two different approaches to evaluate changes in the inert volume with changes in moisture content. One approach assumed that the fracture porosity was fixed at the reference case value (0.02) and the inert volume changed as the moisture content changed (i.e., an increased moisture content resulted in a reduction in the inert volume as more of the pore space was occupied by aqueous solution). The other approach assumed that the fracture porosity was also variable and the inert volume was fixed as the moisture content was changed (i.e., an increase in the moisture content did not result in a reduction in the inert volume). In both cases, the pore velocity and associated residence time were changed with the changed moisture content.

---

[63] The reference case values of TST-corrosion and ion-exchange rate parameter values were chosen for these sensitivity analyses to assist in an evaluation of the impacts of the changed parameter on the results presented in Section 5.1.3 of RPP-RPT-59958. It is recognized that there is an error in the *riex* values used to model the LAWA44 and LAWC22 glasses used in the 2017 IDF PA. The values used in the IDF PA were based on recommended values reported in PNNL-24615 based on earlier values reported in PNNL-14805. The corrected values reported in PNNL-26594 would result in a reduction in the FRR by about a factor of ten for LAWC22.

Table 2-12-4. Additional HYDRL Sensitivity Analysis Cases for LAWC22.

Infiltration Rate (mm/yr)	Case	Darcy Flux (cm/yr)	Moisture Content (-)	Seepage Velocity (cm/yr)	Residence Time (years)	Inert Volume (vol.%)	Volumetric Flow Rate (l/yr)	FRR1 (1/yr)	FRR2 (1/yr)
3.5	BC	0.0357	0.00237	15.0	13.1	1.761	0.0357	2.51E-07	2.51E-07
	1a	0.0357	0.00474	7.53	26.03	1.526	0.0357	2.50E-07	5.04E-07
	1b	0.0357	0.001185	30.13	6.51	1.882	0.0357	2.51E-07	1.28E-07
	1c	0.0357	0.01185	3.013	65.1	0.815	0.0357	2.49E-07	1.35E-06
	1d	0.0357	0.00047	75.96	2.58	1.953	0.0357	2.55E-07	6.05E-08
0.9	RC	0.00796	0.00172	4.6	42.35	1.828	0.00796	2.70E-07	2.70E-07
	1e	0.00796	0.00344	2.3	84.70	1.656	0.00796	2.69E-07	5.77E-07
	1f	0.00796	0.00086	9.2	21.18	1.914	0.00796	2.72E-07	1.28E-07
	1g	0.00796	0.0086	0.93	211.66	1.140	0.00796	2.68E-07	1.51E-06
	1h	0.00796	0.00034	23.41	8.37	1.966	0.00796	2.77E-07	4.96E-08

All calculations performed using The Geochemist's Workbench® (a registered trademark of Aqueous Solutions LLC, Champaign, Illinois).

RC = Reference Case (see RPP-RPT-59958, *Performance Assessment for the Integrated Disposal Facility, Hanford Site, Washington*, Rev. 1). The Reference Case assumed a background infiltration rate of 0.9 mm/yr.

BC = Base Case (assumes all the same values as the Reference Case except the background infiltration rate of 3.5 mm/yr).

Moisture Content = volume of water per unit volume of waste form.

Seepage (pore) Velocity = Darcy Flux/Moisture Content.

Residence Time = Flow Length (196 cm – RPP-RPT-59958; Table 5-14)/Seepage Velocity.

Inert Volume = Porosity - Moisture Content. This represents the gas content, i.e., volume of gas per unit volume of waste form. The gas phase does not react directly with the glass and is considered inert.

Volumetric Flow Rate = Darcy Flux (cm^3/cm^2-yr) * Cross-sectional Area (1,000 cm^2) (RPP-RPT-59958; Table 5-14).

Fractional Release Rate (FRR) = [Tc concentration in effluent (mol/L) * Vol. Flow Rate (L/yr)]/Tc inventory (mol).

- FRR1 assumes Inert Volume is controlled by Moisture Content.
- FRR2 assumes no change in Inert Volume from the reference case (RC). This represents a hypothetical bounding case in which changes in moisture content are assumed to be compensated by changes in porosity such that the inert volume remains unchanged.

Tc inventory in a single LAWC22 glass container = 0.215 mol (RPP-RPT-59958; Table 5-14).

To normalize the glass corrosion rate to a 1-liter reference volume of water reacting with the glass, the surface area, A, = [[volumetric specific surface area (0.5 cm^2/cm^3; RPP-RPT-59958; Table 5-14) * glass volume fraction (0.98; RPP-RPT-59958; Table 5-14)]/Moisture Content]*1,000 cm^3/L].

The corresponding STOMP model results for the single LAWC22 glass container using the reference case values for glass corrosion and hydraulic properties of the immobilized low-activity waste (ILAW) glass and backfill is 1.78E-07 yr^{-1} and for the base case value of background infiltration rate is 2.20E-07 yr^{-1}. The corresponding STOMP model results for a column of four LAWC22 glass containers and the base case background infiltration rate is 2.52E-07 yr^{-1}. The Base Case ILAW FRR value of 2.5E-07 yr^{-1} was used for the compliance case in RPP-RPT-59958.

Subsurface Transport Over Multiple Phases (STOMP) has been developed and distributed by Battelle Memorial Institute, Richland, Washington.

The results presented in Table 2-12-4 illustrate that when the inert volume changes with the moisture content, there is no impact of the changed moisture content (and residence times) on the predicted FRR for a given Darcy flux. This is because although an increase in moisture content increases the residence time and hence the amount of TcO4 released to the aqueous solution, that amount of TcO4 released is diluted by the larger amount of solution present in the system, as represented by the increased moisture content. However, if the moisture content change is assumed to be independent of the inert volume in the fracture glass, then a change in moisture content for a given Darcy flux results in a change in residence time (for example an increase in moisture content results in an increase in residence time and an increase in the amount of TcO4 released to the aqueous solution and a corresponding increase in the FRR).

All of the results presented in Table 2-12-4 use the erroneous value of *riex* for the LAWC22 glass as recommended in PNNL-24615 based on information reported in PNNL-14805, which was issued after the PA was completed. As noted in PNNL-26594, the erroneous value of *riex* is about 10 times greater than the value used in the IDF PA for LAWC22. This facilitates traceability to all of the other sensitivity analyses presented in RPP-RPT-59958 which also use the erroneous *riex* value. The use of the corrected value would result in a decrease in the FRR by about a factor of 10 as is apparent in the IEX sensitivity analysis case presented in Section 5.1.3.5 of RPP-RPT-59958. The impact of the use of this erroneous value is evaluated in the additional sensitivity analyses presented below.

Immobilized Low-Activity Waste Glass Release – Effect of Uncertain Secondary Mineral Reaction Networks
The ILAW glass release model and associated calculations (described in Sections 4.4.1.2 and 5.1.2 of RPP-RPT-59958, respectively) consider the effects of uncertainty in the SMRN by modifying the presence or absence of minerals that may be expected to control the dissolution rate of the glass. The SMRN cases evaluated the impact of the secondary mineral formation network. Some of the SMRN cases analyzed for both LAWA44 and LAWC22 (specifically case SMRN-3) showed a large impact from uncertainty in what minerals form and therefore their thermodynamic properties and the resulting effect on the predicted dissolution rate of glass and release rate of mobile radionuclides from the ILAW glass.

The RAI basis asserts that actual secondary minerals observed in experiments were not used in the PA because acceptable glass degradation rates could not be achieved and therefore recommends that the SMRN cases be expanded and, if possible, supported by information from experiments and the literature. As noted in Section 5.1.2.11 of the PA report, the reference-case SMRN was selected based on the consistency of results from a geochemical model with observed solution chemistry data from PCTs at 90 °C (PNNL-20781; PNNL-24615). The geochemical model was a non-kinetic, reaction-path type model (PNNL-20781) that was not used to simulate glass degradation rates. Data characterizing actual secondary minerals observed in experiments were not definitive for purposes of defining the SMRN. The secondary mineral phases are typically amorphous rather than crystalline with uncertain and variable compositions and thermodynamic properties that inhibit exact determination (PNNL-20781).

The importance of the uncertainty associated with SMRN was noted as a significant uncertainty that warranted additional study. As a result, the IDF PA Maintenance Plan, CHPRC-03348,

noted the need for continued R&D investigations aimed at characterizing the mineralogy, mineral chemistry, paragenesis, and crystallinity of secondary solids that form during the corrosion of analogs to ILAW glass. Based on these characterization data, it may be necessary to either estimate or measure relevant thermodynamic properties (e.g., equilibrium constants for hydrolysis reactions) for the key minerals identified so the impact of these observations can be evaluated in ILAW corrosion and release models.

The current status of the implementation of the glass corrosion testing maintenance program is summarized in RPP-PLAN-605201. Although identification of the SMRN has been conducted in the ongoing glass testing program, this testing has focused on EWG compositions rather than the representative glasses analyzed in the IDF PA (LAWA44, LAWB45 and LAWC22).

To address the effect that alternative SMRNs may have on the predicted glass release rates, additional COMBX sensitivity analyses were performed using the alternative hydraulic conditions cases developed to address the effect of MCC uncertainty in response to this RAI. These cases use the SMRN-3 and SMRN-4 representations using the LAWC22 reference case corrosion and ion-exchange parameters.

Correction of *riex* Error

After completing the final draft of the IDF PA, the ILAW glass researchers at PNNL identified an error in the values of *riex* that had been reported in the data package used to support the IDF PA, PNNL-24615 and the key references cited therein, notably PNNL-14805. This error in *riex* reported in PNNL-26594 was the result of an improper calculation of the *riex* values due to an incorrect unit conversion. This error affects the *riex* values used for both LAWA44 and LAWC22 glasses and does not affect the *riex* value for LAWB45, which was 0.0. The error correction results in a reduction of the *riex* by about a factor of 7 for LAWA44 and a factor of 10 for LAWC22 are summarized in Table 2-12-5.

Table 2-12-5. Corrected Values of *riex*.

Glass	Reported *riex* values (Mol Na/m^2-s)	Corrected *riex* values (Mol Na/m^2-s)	Reduction Factor
LAWA44	5.30E-11	7.86E-12	0.148
LAWC22	1.20E-10	1.28E-11	0.107
LAWABP1	3.40E-11	5.04E-12	0.148

Source: PNNL-26594, *A Critical Review of Ion Exchange in Nuclear Waste Glasses to Support the Immobilized Low-Activity Waste Integrated Disposal Facility Rate Model*, Table 4.1.

Note: *riex* values are at 15 °C. Original *riex* values are reported in PNNL-24615 based on values originally presented in PNNL-14805, *Waste Form Release Data Package for the 2005 Integrated Disposal Facility Performance Assessment*. The values for LAWABP1 are shown for interest because this glass was the reference glass used in DOE/EIS-0391, *Final Tank Closure and Waste Management Environmental Impact Statement for the Hanford Site, Richland, Washington*. The *riex* value for LAWB45 is 0.0 mol Na/m^2-s.

The impact of assuming a lower *riex* value was examined in sensitivity analyses presented in Section 5.1.2.5 of RPP-RPT-59958 where it is illustrated that changes in *riex* for LAWA44 and

LAWC22 glasses result in a corresponding change in the FRR for predictions using either STOMP or GWB. A factor of 10 increase or decrease in *riex* results in a factor of 10 increase or decrease in the FRR. The relationship is more complicated for LAWB45 glass because the reference *riex* value for LAWB45 is 0.0 mol Na/m^2-s.

Prior to performing additional sensitivity analyses to address other aspects of the RAI, the corrected values of *riex* are used for both LAWA44 and LAWC22 with all other reference case values kept fixed. The result of these additional sensitivity analyses are presented in the following section.

Additional Sensitivity Analyses
The proposed path forward for RAI 2-12 requested that the sensitivity and uncertainty analyses be expanded to include the evaluation of the impact of additional glass release uncertainties. The previous discussion contains expanded sensitivity analyses on one aspect of glass release uncertainty, related to the HYDRL cases, that was partially evaluated in the IDF PA (RPP-RPT-59958). As noted in the RAI basis, other sources of uncertainty can impact the predicted FRR of radionuclides from the ILAW glass. The sensitivity of the predicted FRR to the uncertainty in environmental- and glass corrosion-related parameters was presented in Section 5.1.2 of RPP-RPT-59958.[64]

This section presents expanded sensitivity analyses, including additional combined cases, for the LAWC22 glass.[65] The additional sensitivity analyses are based on using the GWB model summarized in Section 4.4.1.2.3 of RPP-RPT-59958 and the LAWC22 reference case parameter values summarized in Sections 4.4.1.2.4 and 5.1.2 of RPP-RPT-59958. The reference case values were changed to first develop a new reference case, from which the additional sensitivity analyses were performed.

The first change in the reference case values was to increase the background net infiltration rate from 0.9 mm/yr to 3.5 mm/yr to reflect the long-term average steady-state base case value

---

[64] The ILAW glass release uncertainty analysis presented in Section 6.3.2.2 of RPP-RPT-59958 assumed that the key sources of uncertainty impacting the FRR of radionuclides from ILAW glass were related to uncertainty in the TST corrosion parameters and the sodium ion-exchange rate. The regression model for ILAW glass release presented in Section 6.3.2.2 does not include the effects of uncertainty in other parameters such as (a) the hydraulic properties in the glass and backfill (addressed in the HYDRL and BACK sensitivity cases and the additional MCC cases addressed in this RAI response), (b) the partial pressure of $CO_2(g)$ in the disposal trenches (addressed in the GAS sensitivity cases), (c) the reactive surface area (addressed in the RSA sensitivity cases), and (d) the SMRN (addressed in the SMRN sensitivity cases). While the other factors could have been included in the regression model, it was assumed that their importance had been addressed in the sensitivity analyses and the effects of the uncertainty in these other parameters did not need to be included in the uncertainty analysis.

[65] The LAWA44 glass was used as the representative ILAW glass in the uncertainty analyses presented in Section 6.3.2.2 of RPP-RPT-59958. The use of LAWA44 was based on the observation that the FRR for LAWA44 was similar to LAWC22. The LAWC22 glass was used to define the base case ILAW glass FRR (i.e., 2.5E-07 yr^{-1}) used for the compliance case calculation of the groundwater pathway concentration and dose for comparison to the all-pathways performance objective of DOE M 435.1-1 as presented in Section 5.2.1 of RPP-RPT-59958. The use of LAWC22 for the compliance case fractional release rate was based on the fact that the predicted value of 2.5E-07 yr^{-1} represented the most pessimistic value among the three glasses analyzed (LAWA44, LAWB45, and LAWC22) based on STOMP(c) calculations using reference case corrosion and release parameter values including a net infiltration rate of 3.5 mm/yr and a stack of four ILAW glass cylinders (see RPP-RPT-59958, Section 5.1.2).

assumed in the IDF PA. As summarized in Table 2-12-4, the increased background infiltration rate results in an increase in the vertical Darcy flux in the fractured glass from 0.0796 to 0.357 mm/yr and an increase in the moisture content from 0.00172 to 0.00237 and therefore a decrease in the residence time from 42.35 to 13.1 years.[66] Using the other reference case values and the base case net infiltration rate resulted in the GWB-predicted FRR of 2.51E-07 yr^{-1}. This compares to the equivalent STOMP-predicted FRR of 2.20E-07 yr^{-1} when assuming a single ILAW glass waste container and 2.52E-07 yr^{-1} when assuming a stack of four ILAW glass waste containers (see Table 5-6 of RPP-RPT-59958).[67]

Based on new information on ILAW glass corrosion parameters summarized in the responses to RAI 2-7 and RAI 2-8, two other reference case parameter values were changed to develop a new, updated reference case FRR for LAWC22. These two parameters are *riex* (the sodium ion-exchange rate constant) and the reactive surface area S_{wf}.

As summarized in PNNL-26594, an erroneous value of *riex* was used in the 2017 IDF PA. The erroneous value of 1.20E-10 mol/m^2-sec should have been 1.28E-11 mol/m^2-sec. Using the correct *riex* value resulted in a decrease in the predicted FRR from 2.51E-07 yr^{-1} to 4.26E-08 yr^{-1}.[68]

The response to RAI 2-8 indicates that the multiplication factor for reactive surface area has a range from 10 to 30 times the nominal glass surface area. The reference case value assumed in the IDF PA for each of the ILAW glass was 10 times. Assuming that the range of 10 to 30 is representative and that the geometric mid-point of this range can be used to represent a new reference case, the reactive surface area reference case value is increased from 0.19 cm^2/g to 0.32 cm^2/g. The effect of this increased S_{wf} resulted in an increase in the predicted FRR from 4.26E-08 yr^{-1} to 5.75E-08 yr^{-1}. This represents the new reference value to which the other sensitivity analysis results can be compared.

Starting with the new reference case, additional one-at-a-time sensitivity analyses are performed varying the following parameters:

- *riex*

---

[66] The vertical Darcy flux and moisture content are based on STOMP calculations assuming the base case hydraulic properties, including the MCCs for the fractured glass and backfill materials. The impact of the uncertainty in these values due to the uncertainty in the MCCs is discussed in this RAI response.

[67] The FRR values calculated using GWB and the reference case parameter values represent the effects of Stage II glass corrosion. The potential for initiation and maintenance of Stage III glass corrosion is not included in the reference case model analyzed in the 2017 IDF PA. Based on preliminary information summarized in the response to RAI 2-9, it is possible that Stage III glass corrosion may initiate and persist at relevant temperatures for the ILAW glasses considered in the 2017 IDF PA. If one assumes Stage III glass corrosion does occur and persist, then all FRRs should be multiplied by a factor of about 5.7 as summarized in the response to RAI 2-9. Additional R&D is planned to confirm the applicability of this new information and additional UDQEs will be performed to evaluate the impact of Stage III glass corrosion on the IDF PA.

[68] The sensitivity analyses reported in Table 5-6 of RPP-RPT-59958 indicated that a 10 times reduction in *riex* resulted in about a 10 times reduction in the FRR. The present result is that a 10 times reduction in *riex* resulted in about a 6 times reduction in the FRR. This difference is the result of the different residence times used in the two calculations, with the previous reference case having a residence time of 42.35 years and the current revised reference case having a residence time of 13.1 years.

- Swf
- SMRN
- K_g
- Residence time
- Chalcedony reaction rate
- $p_{CO2(g)}$.

These additional sensitivity analyses consider the effects of Stage I and Stage II corrosion of ILAW glass. The potential effects of Stage III corrosion are not included in these additional calculations due to the lack of information on the probability and rates of Stage III corrosion as summarized in the response to RAI 2-9. If the corrosion enhancement factor identified in the current Stage III testing is reasonable, then the FRRs developed based on Stage I and Stage II rates should be increased by this same factor of 5.7.

Although the sensitivity analyses reported in Section 5.1.2 and Table 5-6 of RPP-RPT-59958 also evaluated the impact of uncertainty in other TST glass corrosion parameters (e.g., η, E_a, and k_0), these parameters were identified as being less sensitive to the predicted FRR and therefore, the uncertainty in these parameter values was not included in the additional sensitivity analyses. A matrix of cases to evaluate the impact of uncertainty in these individual parameters by varying each parameter one at a time was developed as follows:

- *riex cases*: Reference Case value (= 1.28E-11 mol Na/m²-s), 2 × Reference Case value and 1/2 × Reference Case value

- Swf cases: Reference Case value (= 0.32 cm²/g), 3 × Reference Case value and 1/3 × Reference Case value

- SMRN cases: Reference Case value SMRN (= Analcime+Anatase+Baddeleyite+Calcite+Clinochlore-14A+Fe(OH)₃+Gibbsite+Zn(OH)₂(gamma)), SMRN-3 and SMRN-4[69]

- Kg cases: Reference Case value (=1.8E-03 mol/L)[70], 2 × Reference Case value and ½ × Reference Case value

- Residence time cases: Reference Case value (= 13.1 yr), 5 × Reference Case value, ⅕ × Reference Case value

- Chalcedony reaction rate cases: Reference Case value (= 7.32E-13 mol/m²-s), 10 times Reference Case value, 1/10 times Reference Case value

---

[69] SMRN-4 represent the final stage of the alternative SMRNs, i.e., at this stage the solution is no longer supersaturated with respect to plausible secondary minerals (notably clay minerals or zeolites).
[70] The reference case Kg of 1.8E-03 mol/L is maintained even though recent R&D testing results reported in VSL-19R4620-2 recommend a value of 2.0E-03 mol/L for LAWC22 and two similar glasses.

- $p_{CO2(g)}$ cases: Reference Case value (= $10^{-3.5}$ atm), 10 times Reference Case value and ¹⁄₁₀ times Reference Case value (i.e., $10^{-2.5}$ and $10^{-4.5}$).

The increase and decrease in the reference case values were assumed to be the same as adopted in the sensitivity analyses summarized in Table 5-6 of RPP-RPT-59958.[71]

In addition to the one-at-a-time parameter variations, additional COMBX cases were developed to address the potential combined affect if some of the above parameters are assumed to be either at the pessimistic or optimistic end of the range of values[72]. Two different COMBX cases were run. In the first case the residence time was fixed at the updated reference case value of 13.1 years (similar to the approach taken in the IDF PA where the residence time was fixed in the COMBX cases) and, in the second case, the residence time was also varied to represent the pessimistic and optimistic values.

Additional COMBX cases were also developed to illustrate cases where an *ad hoc* mixture of pessimistic and optimistic parameter values was assumed. The COMB-MX1 case assumed optimistic values for parameters controlling the ion-exchange rate and pessimistic values for parameters controlling the glass matrix dissolution rate. The COMB-MX2 case assumed pessimistic values for parameters controlling the ion-exchange rate and optimistic values for parameters controlling the dissolution rate. A comparison of results from these two cases provides insights concerning the relative importance of ion exchange and matrix dissolution on the overall corrosion rate and FRRs. The COMB-MX3 case is like the COMB3 case discussed in RPP-RPT-59958 except that the waste form hydraulic conductivity, and related parameters such as the residence time, were not varied from the reference case.

The results of the additional sensitivity analyses are summarized in Tables 2-12-6 and 2-12-7. The impact of uncertainty in individual parameter values presented in Table 2-12-6 on the predicted FRR is analogous to the results presented in Table 5-6 of RPP-RPT-59958. For example, an increase in the *riex* value results in an increase in the FRR. However, the magnitude of the impact is different because of the different reference case residence times (i.e., 13.1 vs. 42.35 years) and *riex* value (i.e., 1.28×10^{-11} vs. 1.20×10^{-10} mol/m²-sec).

---

[71] Additional information on *riex* variation with time and other new information on other ILAW glasses, such as the information presented in recent PNNL and VSL testing summarized in the responses to RAIs 2-7 and 2-9, will be addressed in appropriate UDQEs and Special Analyses.

[72] Pessimistic values are those values which result in an increase in the predicted FRR while optimistic values are those values which result in a decrease in the predicted FRR. The range of values assumed in the COMBX cases are the same as adopted in sensitivity analyses presented in the 2017 IDF PA (Table 5-6 of RPP-RPT-59958).

Table 2-12-6. Additional Fractional Release Rate Sensitivity Analyses for LAWC22 Glass for Stage II Corrosion.

Case	IR	θ_{glass}	Darcy Flux	MC	Res. Time	r_{IEX}	η	Ea	K_g	Swf	$p_{CO2(g)}$	CR	SMRN	FRR (yr^{-1})
Previous RC	0.9	0.02	7.96E-02	1.72E-03	42.35	1.20E-10	0.42	64	1.80E-03	0.19	$10^{-3.5}$	7.32E-13	-RC	2.70E-07
RC_Rev1	3.5	RC	3.57E-01	2.37E-03	13.1	1.20E-10	RC	RC	RC	0.19	RC	RC	-RC	2.51E-07
RC_Rev2	3.5	RC	3.57E-01	2.37E-03	13.1	1.28E-11	RC	RC	RC	0.19	RC	RC	-RC	4.26E-08
New RC	3.5	RC	3.57E-01	2.37E-03	13.1	1.28E-11	RC	RC	RC	0.32	RC	RC	-RC	5.75E-08
riex	3.5	RC	3.57E-01	2.37E-03	13.1	6.40E-12	RC	RC	RC	0.32	RC	RC	-RC	3.94E-08
riex	3.5	RC	3.57E-01	2.37E-03	13.1	2.56E-11	RC	RC	RC	0.32	RC	RC	-RC	9.71E-08
S_{wf}	3.5	RC	3.57E-01	2.37E-03	13.1	1.28E-11	RC	RC	RC	0.11	RC	RC	-RC	3.39E-08
S_{wf}	3.5	RC	3.57E-01	2.37E-03	13.1	1.28E-11	RC	RC	RC	0.96	RC	RC	-RC	1.39E-07
SMRN	3.5	RC	3.57E-01	2.37E-03	13.1	1.28E-11	RC	RC	RC	0.32	RC	RC	SMRN-3	1.92E-07
SMRN	3.5	RC	3.57E-01	2.37E-03	13.1	1.28E-11	RC	RC	RC	0.32	RC	RC	SMRN-4	1.95E-07
K_g	3.5	RC	3.57E-01	2.37E-03	13.1	1.28E-11	RC	RC	9.00E-04	0.32	RC	RC	-RC	2.87E-08
K_g	3.5	RC	3.57E-01	2.37E-03	13.1	1.28E-11	RC	RC	3.60E-03	0.32	RC	RC	-RC	1.16E-07
Residence Time	3.5	RC	3.57E-01	4.74E-04	2.62	1.28E-11	RC	RC	RC	0.32	RC	RC	-RC	2.96E-08
Residence Time	3.5	RC	3.57E-01	1.19E-02	65.5	1.28E-11	RC	RC	RC	0.32	RC	RC	-RC	2.27E-07
CR	3.5	RC	3.57E-01	2.37E-03	13.1	1.28E-11	RC	RC	RC	0.32	RC	7.32E-14	-RC	5.74E-08
CR	3.5	RC	3.57E-01	2.37E-03	13.1	1.28E-11	RC	RC	RC	0.32	RC	7.32E-12	-RC	5.93E-08
$p_{CO2(g)}$	3.5	RC	3.57E-01	2.37E-03	13.1	1.28E-11	RC	RC	RC	0.32	$10^{-4.5}$	RC	-RC	1.55E-07
$p_{CO2(g)}$	3.5	RC	3.57E-01	2.37E-03	13.1	1.28E-11	RC	RC	RC	0.32	$10^{-2.5}$	RC	-RC	2.94E-08

Previous RC is the reference case used in RPP-RPT-59958, _Performance Assessment for the Integrated Disposal Facility, Hanford Site, Washington_, Table 5-6.

Highlighted row is the new reference case (New RC) based on starting with the reference case in RPP-RPT-59958 by first increasing the infiltration rate (IR) to 3.5 mm/yr (RC_Rev1), then correcting the _riex_ value (RC_Rev2) and finally updating the S_{wf} value based on the information in the response to RAI 2-8. See text.

All results based on The Geochemist's Workbench® (a registered trademark of Aqueous Solutions LLC, Champaign, Illinois) calculations, see Sections 4.4.1.2.3, 4.4.1.2.4 and 5.1.2 of RPP-RPT-59958.

Results do not consider the possible effect of Stage III corrosion (see response to RAI 2-9).

CR	=	Chalcedony Reaction Rate Constant (mol/m^2-s);
Darcy Flux	=	Vertical Darcy flux through fractured glass (mm/yr);
Ea	=	Glass Dissolution Activation Energy (kJ/mol);
FRR	=	Fractional Release Rate (1/yr)
IR	=	Infiltration Rate (mm/yr);
K_g	=	Glass Apparent Equilibrium Constant Based on Activity Product $a_{[SiO2(aq)]}$;
MC	=	Moisture Content at Steady State (dimensionless);
η	=	pH Power Law Coefficient;
$p_{CO2(g)}$	=	Partial Pressure of CO$_2$(g) (bar);
θ_{glass}	=	Porosity of Glass;
RC	=	Reference Case;

Res. Time	=	Residence Time (yr);
r_{IEX}	=	Na Ion-exchange rate constant (mol Na/m^2-s);
SMRN	=	Secondary Mineral Reaction Network;
SMRN-3	=	SMRN-RC+Antigorite+Nontronite-Na+ Clinoptilolite-Na-Clinochlore-14A-Fe(OH)$_3$-Analcime
SMRN-4	=	SMRN-RC+Nontronite-Na+Clinoptilolite-Na+ Saponite-Na-Clinochlore-14A-Fe(OH)$_3$-Analcime
SMRN-RC	=	Analcime+Anatase+Baddeleyite+Calcite+ Clinochlore-14A+Fe(OH)$_3$+Gibbsite+Zn(OH)$_2$(gamma)
S_{wf}	=	Specific Surface Area of Glass (cm^2/g);

Table 2-12-7. Additional Fractional Release Rate Sensitivity Analysis Cases for LAWC22 Glasses for Different Combinations of Pessimistic and Optimistic Assumptions.

Case	IR	θ_{glass}	Darcy Flux	MC	Residence Time (years)	r_{IEX}	η	Ea	K_g	S_{wf}	$p_{CO2(g)}$	CR	SMRN	FRR (yr^{-1})
New RC	3.5	0.02	3.57E-1	2.37E-03	13.1	1.28E-11	0.42	64	1.80E-03	0.32	$10^{-3.5}$	7.32E-13	-RC	5.75E-08
COMB-OPT1	RC	RC	RC	4.74E-04	2.62	6.40E-12	RC	RC	9.00E-04	0.11	$10^{-3.0}$	RC	-RC	1.22E-08
COMB-PES1	RC	RC	RC	1.19E-02	65.5	2.56E-11	RC	RC	3.60E-03	0.96	$10^{-4.0}$	RC	SMRN-4	2.41E-05
COMB-OPT2	RC	RC	RC	RC	13.1	6.40E-12	RC	RC	9.00E-04	0.11	$10^{-3.0}$	RC	-RC	1.28E-08
COMB-PES2	RC	RC	RC	RC	13.1	2.56E-11	RC	RC	3.60E-03	0.96	$10^{-4.0}$	RC	SMRN-4	3.80E-06
COMB-MX1	RC	RC	RC	RC	13.1	6.40E-12	RC	RC	3.60E-03	0.11	$10^{-2.5}$	RC	-RC	5.00E-08
COMB-MX2	RC	RC	RC	RC	13.1	2.56E-11	RC	RC	9.00E-04	0.96	$10^{-4.5}$	RC	-RC	4.33E-07
COMB-MX3	RC	RC	RC	RC	13.1	1.28E-11	RC	RC	1.80E-04	0.64	$10^{-4.5}$	7.32E-14	-RC	2.98E-08

New RC is the new reference case (see Table 2-12.6) based on the previous reference case and correcting the *riex* value and updating the Swf value (see text).
All results based on The Geochemist's Workbench® (a registered trademark of Aqueous Solutions LLC, Champaign, Illinois) calculations, see Sections 4.4.1.2.3, 4.4.1.2.4 and 5.1.2 of RPP-RPT-59958, *Performance Assessment for the Integrated Disposal Facility, Hanford Site, Washington*.

CR	= Chalcedony Reaction Rate Constant (mol/m²-s)		η	= pH Power Law Coefficient
Darcy Flux	= Vertical Darcy flux through Glass Waste Form = (mm/yr)		θ_{glass}	= Porosity of Glass Waste Form
Ea	= Glass Dissolution Activation Energy (kJ/mol)		RC	= Reference Case; IR = Infiltration Rate (mm/yr)
FRR	= Fractional Release Rate (1/yr)		Res. Time	= Residence Time (yr)
K_g	= Glass Apparent Equilibrium Constant Based on Activity Product $a_{[SiO2(aq)]}$		r_{IEX}	= Na Ion-exchange rate constant (mol/m²-s)
MC	= Moisture Content at Steady State (dimensionless)		SMRN	= Secondary Mineral Reaction Network
$p_{CO2(g)}$	= Partial Pressure of $CO_2(g)$ (bar)		S_{wf}	= Specific Surface Area of Glass (cm²/g)

SMRN-RC = Analcime+Anatase+Baddeleyite+Calcite+Clinochlore-14A+Fe(OH)₃+Gibbsite+Zn(OH)₂(gamma)
SMRN-4 = SMRN-RC+Nontronite-Na+Clinoptilolite-Na+Saponite-Na-Clinochlore-14A-Fe(OH)₃-Analcime
Green   = optimistic value
Yellow   = pessimistic value
White   = reference case value

The COMBX cases indicate a total range of FRR results from 1.28E-08 to 3.80E-06 yr^{-1} for the cases when the residence time was fixed at the reference case value of 13.1 years (i.e., from COMB-OPT2 to COMB-PES2, respectively) and from 1.22E-08 to 2.41E-05 yr^{-1} when the residence time was assumed to be either 5 times or 1/5 times the reference case value (i.e., from COMB-OPT1 to COMB-OPT2, respectively). The maximum (pessimistic) predicted FRRs are a factor of 66 and 420 greater than the reference case FRR of 5.75E-08 yr^{-1} while the minimum (optimistic) predicted FRRs are a factor of 4.5 and 4.7 less than the reference case FRR. This non-symmetric distribution reflects the observation that the total corrosion rate is controlled both by the dissolution rate of the glass matrix, in accordance with the TST-based rate law, and by the rate of the ion-exchange reaction controlling glass hydration, i.e., *riex*. In the optimistic cases (COMB-OPT1 and COMB-OPT2), *riex* is too low to significantly affect the aqueous-speciation of silica, i.e., consumption of H$^+$ and production of Na$^+$ by the exchange reaction does not significantly affect the formation of species HSiO$_3^-$ and NaHSiO$_3$(aq). The chemical affinity term in the TST rate law is, therefore, unaffected by *riex* and the glass matrix dissolves at a relatively slow rate. Because parameters in the TST rate law were chosen in the optimistic cases to also minimize the dissolution rate, FRR values are minimized and are essentially insensitive to the assumed residence times. Conversely, the *riex* value significantly affects silica speciation in the pessimistic cases (COMB-PES1 and COMB-PES2). This increases the dissolution rate of the glass matrix due to continuous changes in the concentration of species SiO$_2$(aq), which controls the chemical affinity. Because parameters in the TST rate law were chosen in the pessimistic cases to maximize the dissolution rate, FRR values are also maximized and are sensitive to the assumed residence times.

It is noted that the total range of results in the uncertainty analysis presented in Section 6.3.2.2 of RPP-RPT-59958 is from 5.8E-09 to 1.8E-05 yr^{-1}, and is not significantly different than the range of results determined in the additional COMBX sensitivity analyses presented in this RAI response.

Possible Cancelling Effect of Multiple Sources of Parameter Uncertainty on Predicted Glass Release

The RAI basis noted that the IDF PA concluded that, when considered together, multiple sources of conceptual and parameter uncertainty with respect to glass release modeling may have a cancelling effect in predictive models of glass corrosion and, therefore, that the overall impact of these uncertainties on predicted fractional releases may be relatively small (see discussion of the COMBX cases in Section 5.1.2.16 of RPP-RPT-59958).

The RAI basis questioned how this conclusion was determined. Unless inverse correlations between the relevant uncertainties were observed, it was noted that uncertainties will propagate and expand the potential range of outcomes. It was suggested that probabilistic assessment of glass release rate uncertainties would help better define the range of uncertainty in glass release rates.

Glass release sensitivity analyses are presented in Section 5.1.2 and glass release uncertainty analyses are presented in Section 6.3.2.2 to evaluate the impact of parameter uncertainty on glass release rates using two different process models (STOMP and GWB) and an abstracted regression model within the systems model (GoldSim$^©$). The goal of these sensitivity and

uncertainty analyses was to define the range of uncertainty in the predicted glass release rates. Based on the sensitivity analyses summarized in Section 5.3.1 and presented in Tables 5-4, 5-5 and 5-6 for LAWA44, LAWB45 and LAWC22, respectively, the range of predicted FRRs is about a factor of 30 above and below the base case value of 2.5E-07 yr^{-1}. Based on the uncertainty analyses presented in Section 6.3.2.2, the range of results for LAWA44 is between a minimum of 5.8E-09 yr^{-1} and a maximum of 1.8E-05 yr^{-1} with a 5th to 95th percentile range from 2.2E-08 yr^{-1} to 2.9E-06 yr^{-1} (Figure 2-12-4)[73].

Figure 2-12-4. Cumulative Probability of Immobilized Low-Activity Waste Glass Fractional Release Rate Due to Uncertainty in LAWA44 Glass Corrosion Parameters.
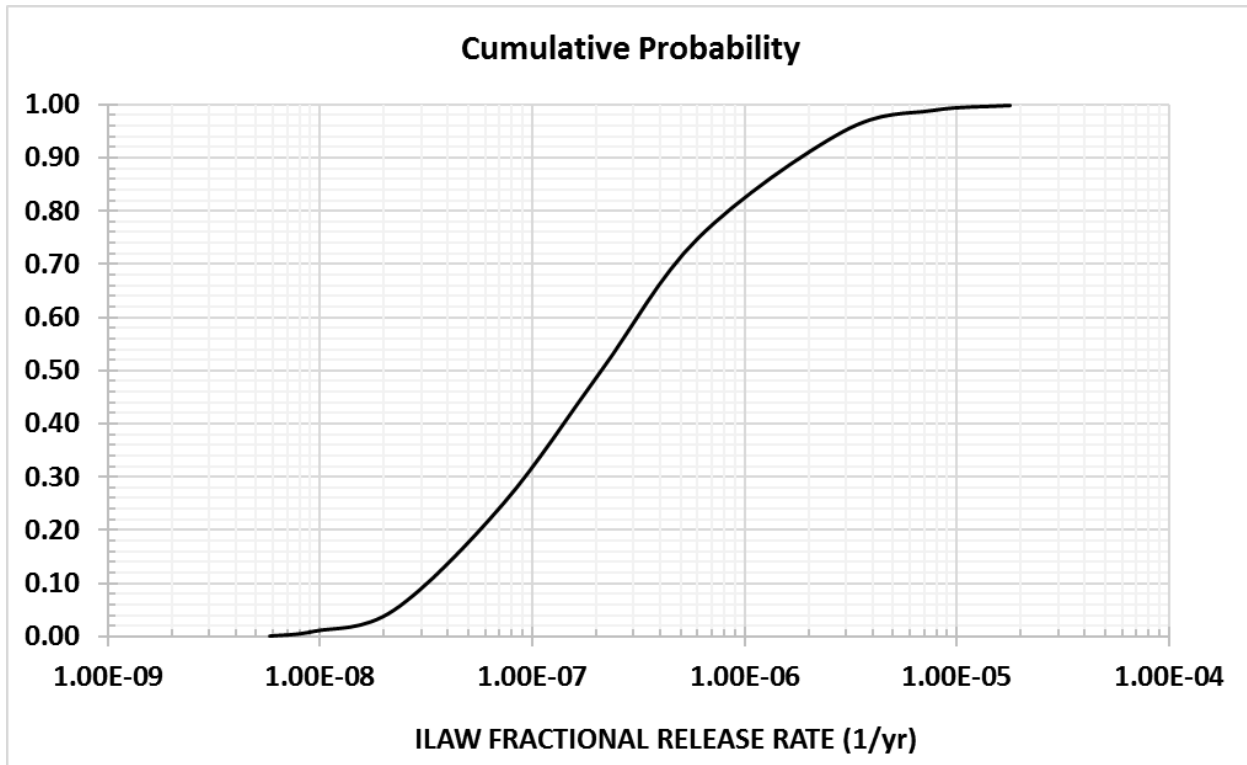
Source: RPP-CALC-61194, *System Model Calculations for the Integrated Disposal Facility Performance Assessment*, Rev. 1, Figure 7.3-45.

Note: The results in this figure are based on 300 realizations sampling only the uncertainty in the parameters related to glass dissolution using the regression model and sampled uncertainty in glass corrosion parameters (i.e., K_g, Ea, η) and ion-exchange parameter, *riex*, for LAWA44. The system model results in RPP-RPT-59958, *Performance Assessment for the Integrated Disposal Facility, Hanford Site, Washington* combined the effects of immobilized low-activity waste (ILAW), solid secondary waste and Effluent Treatment Facility liquid secondary waste release on the total dose at the point of assessment for 300 realizations. The minimum, 5th percentile, 25th percentile, mode (50th percentile), 75th percentile, mean, 95th percentile and maximum values of the fractional release rate are 5.8E-09, 2.2E-08, 7.3E-08, 2.1E-07, 6.0E-07, 7.0E-07, 2.9E-06 and 1.8E-05 yr^{-1}, respectively. These may be compared to the base case value of 2.5E-07 yr^{-1} which is about the 55th percentile of the cumulative distribution of ILAW fractional release rates.

---

[73] The uncertainty analyses included the effect of uncertainty in the LAWA44 glass corrosion properties, specifically the TST parameter values and *riex*. Other properties that could also impact the predicted fractional release were kept at their reference case values. The complete range of predicted glass release rates should consider both the sensitivity and uncertainty analyses.

Most of the sensitivity analyses were conducted varying a single parameter at a time to identify the more significant properties affecting the predicted glass release rates. In addition, combinations of individual sensitivity cases, called the COMBX cases, were analyzed to evaluate the potential impact of combined pessimistic assumptions, combined optimistic assumptions or a combination of both pessimistic and optimistic assumptions. Using the LAWA44 glass as an example, the following COMBX cases were run.

- COMB1 represents a pessimistic case in which the parameter values for chalcedony rate constant, $p_{CO2(g)}$, *riex*, K_g, Kglass and S_{wf} (reactive surface area) were all varied in a direction that leads to an increase in the predicted FRR.

- COMB2 represents a very pessimistic combination case in which the parameter values for $p_{CO2(g)}$, *riex*, K_g and S_{wf} were varied in a direction that leads to an even larger increase in the predicted FRR.

- COMB3 represents an intermediate case with a combination of pessimistic values for S_{wf}, glass hydraulic conductivity and $p_{CO2(g)}$, and optimistic values for K_g and chalcedony rate constant. Given the combination of pessimistic and optimistic assumptions, there is a minimal effect on the predicted FRR as the optimistic and pessimistic assumptions cancel each other.

- COMB4 represents an optimistic case in which parameter values for $p_{CO2(g)}$, *riex*, K_g, Kglass and S_{wf} were varied in a direction that leads to a decrease in the predicted FRR.

The input parameters and associated results of these COMBX cases are summarized in Table 2-12.8.

The COMBX cases are representative examples illustrative of the effect of combined parameter uncertainty. Because it is unlikely that the parameter uncertainty includes only pessimistic values (such as the examples in COMB1 or COMB2) or only optimistic values (such as the example in COMB4), a more insightful perspective can be gained by considering a case in which some values are optimistic and some values are pessimistic, as assumed in the example in COMB3. When a random selection of optimistic and pessimistic input assumptions is made, the result is close to the reference case and the effects of the optimistic and pessimistic assumptions effectively balance or compensate each other.

**Table 2-12-8. Parameter Values and Predicted Fractional Release Rates Using The Geochemist's Workbench®
and STOMP for the Reference Case and COMBX Cases for LAWA44.**

Parameter	Reference Case (RC)		COMB1		COMB2	COMB3	COMB4
	GWB	STOMP	GWB	STOMP	GWB	GWB	STOMP
Infiltration rate (mm yr^{-1})	0.9		3.5		3.5	3.5	3.5
K_g	1.87E-03		2 × RC		5 × RC	0.1 × RC	0.5 × RC
$riex = k_{Na-H}$ (mol Na m^{-2} s^{-1})	5.3E-11		2 × RC		5 × RC	RC	0.5 × RC
Glass specific surface area (cm^2 g^{-1})	0.17		3 × RC		5 × RC	2 × RC	0.33 × RC
Glass saturated hydraulic conductivity (cm s^{-1})	3.1E-5		10 × RC		10 × RC	10 × RC	0.1 × RC
Chalcedony rate constant (mol m^{-2} s^{-1})	7.32E-13		10 × RC		10 × RC	0.1 × RC	RC
$p_{CO2(g)}$ (bar)	$10^{-3.5}$		$10^{-4.0}$		$10^{-4.5}$	$10^{-4.5}$	$10^{-3.0}$
Fractional Release Rate (yr^{-1})	1.62E-07	1.35E-07	3.40E-06	3.44E-06	5.75E-05	1.07E-07	6.71E-09

Source: RPP-RPT-59958, *Performance Assessment for the Integrated Disposal Facility, Hanford Site, Washington*, Tables 5-22, 5-24 and 5-25 (based on RPP-CALC-61031, *Low-Activity Waste Glass Release Calculations for the Integrated Disposal Facility Performance Assessment*, Tables 7-16, 7-18 and 7-19).

K_g = Glass Apparent Equilibrium Constant Based on Activity Product a[SiO$_2$(aq)]
$riex$ = k_{Na-H} = Sodium ion-exchange rate

The cases are as follows:

- COMB1 represents a pessimistic case in which all parameters were varied in a direction that leads to an increase in the predicted fractional release rate
- COMB2 represents a very pessimistic case in which all parameters were varied in a direction that leads to a greater predicted fractional release rate than evaluated in COMB1 case
- COMB3 represents an intermediate case with a combination of pessimistic values for waste form surface area, waste form hydraulic conductivity and $p_{CO2(g)}$ and optimistic values for K_g and chalcedony rate constant
- COMB4 represents an optimistic case in which all parameters were varied in a direction that leads to a decrease in the predicted fractional release rate.

GWB = The Geochemist's Workbench (GWB)® is a registered trademark of Aqueous Solutions LLC, Champaign, Illinois.
STOMP = Subsurface Transport Over Multiple Phases (STOMP)© is copyrighted by Battelle Memorial Institute, 1996.

The discussion in Section 5.1.2.16 of the PA report that describes the COMBX cases considered the apparent additive relationship between changes relative to reference case values in parameters controlling glass corrosion behavior and FRRs. The analysis led to the conclusion that assumed pessimistic changes in one or more parameters might be offset in terms of FRRs by optimistic changes in other parameters. This conclusion was based on the results of the COMB3 case. This conclusion was not meant to imply that the optimistic and pessimistic parameters are inversely correlated such that an "average" release rate results for a single prediction. Instead, it implies that for a range of uncertain input values as might be used in a probabilistic assessment, such as the probabilistic uncertainty analysis presented in Section 6.3.2.2 of RPP-RPT-59958 based on analyses presented in RPP-CALC-61192, *Integrated Disposal Facility Performance Assessment: Sensitivity Calculations for ILAW Glass Dissolution Rate Parameters*, the likelihood of always sampling the more pessimistic values or the more optimistic values is small and it is more likely that the sampling will appropriately sample from the range of values based on the assumed uncertainty distribution. The distribution of predicted results would include the small number of cases for sampling all optimistic values or all pessimistic values.

Similar conclusions with respect to cases which assume a combination of both optimistic and pessimistic assumptions are possible from the additional COMBX cases of COMB-MX1, COMB-MX2 and COMB-MX3 conducted as part of the additional sensitivity analyses presented in Table 2-12-7. *Ad hoc* combinations of optimistic and pessimistic assumptions in these three cases illustrate that the predicted FRR is close to the nominal reference case value, similar to the observation made in the COMBX cases presented in RPP-RPT-59958.

The effect of sampling from a range of values that includes both optimistic and pessimistic values is illustrated in the uncertainty analyses presented in RPP-RPT-59958, Section 6.3.2.2. The resulting cumulative distribution function of predicted FRR results based on 300 realizations is illustrated in Figure 2-12-4. Most of the predicted values are centered around the median value. For example, 50% of the calculated values are FRRs of between 7.3E-08 and 6.0E-07 yr^{-1} (a range of less than 10 times) while 90% of the calculated values are FRRs of between 2.2E-08 and 2.9E-06 yr^{-1} (a range of about 100 times). However, it is possible to have a high FRR (e.g., the maximum value of 1.8E-05 yr^{-1}) or a low FRR (e.g., the minimum value of 5.8E-09 yr^{-1}) for some realizations that sample from either the more pessimistic or more optimistic end of the distributions, respectively. As indicated by the regression analyses, the most significant glass corrosion parameter affecting the predicted FRR is the *riex* (Na-ion-exchange rate) and to a lesser extent the K_g.

In summary, the intent of the statement in the IDF PA that there may be a "cancelling effect" when assuming an *ad hoc* combination of optimistic and pessimistic assumptions was not meant to imply the correlation between the different assumptions. The statement was meant to be an observation that the entire range of possible ILAW glass predicted FRRs can be broad with the maximum and minimum extremes of the distribution resulting when multiple pessimistic assumptions or multiple optimistic assumptions are employed. However, the central tendency of the predicted results are in a narrower range because of the likelihood that there are offsetting factors. This narrower range is exemplified by the probabilistic assessment of FRRs presented in Section 6.3.2.2 of RPP-RPT-59958.

Identification of Risk-Significant ILAW Glass Release Uncertainties
The IDF PA conducted a range of sensitivity and uncertainty analyses to explore the potential significance of uncertain ILAW glass properties and near-field environment conditions on the predicted FRR of radionuclides from the ILAW glass. These analyses were aimed to focus the planned IDF PA maintenance activities on those aspects of the glass performance that were most significant.[74]

The ILAW glass release rate sensitivity analyses, conducted as part of the IDF PA (Section 5.1.2 of RPP-RPT-59958) as well as the additional sensitivity analyses conducted in response to this RAI, illustrate the significance of uncertain glass corrosion and ion-exchange parameters as well as the hydraulic conditions in the fractured glass and other aspects of the near-field hydrogeochemical environment on the predicted FRR from the ILAW glass. These analyses are used as a basis to identify the risk-significant uncertainties in Section 8.4 of RPP-RPT-59958 that were recommended in Section 8.5 of RPP-RPT-59958 as potential candidates for further research for the IDF PA Maintenance Program.

The IDF PA Maintenance Plan (CHPRC-03348) identified these uncertainties as areas for ongoing R&D studies. The specific activities noted in the IDF PA Maintenance Plan include the following.

- **Evaluate ongoing national and international research on glass corrosion mechanisms and rates** – This topic includes: (1) an evaluation of whether the range of parameters used in kinetic (specifically, TST-based) models of glass dissolution are appropriate for the range of glass compositions that will be disposed of in the IDF; (2) characterization or refinement of uncertainty ranges in TST parameters at the IDF temperature of 15°C (41°F); (3) refinement of uncertainty ranges in the reactive surface area of glass waste forms that account for cooling-induced fracturing during production, and possible stress-induced fracturing after emplacement; (4) an evaluation of improvements to kinetic models of the alkali-H+ exchange reaction; and (5) an evaluation of uncertainties in kinetic parameters for the precipitation of secondary reaction products of glass corrosion (e.g., chalcedony/amorphous silica).

- **Evaluate ongoing national and international research on SMRNs** – This topic includes review of ongoing national and international R&D investigations aimed at characterizing the mineralogy, mineral chemistry, paragenesis, and crystallinity of secondary solids that form during the corrosion of analogs to ILAW glass. Based on these characterization data, it may be necessary to either estimate or measure relevant thermodynamic properties (e.g., equilibrium constants for hydrolysis reactions) for the key minerals identified so the impact of these observations can be evaluated in ILAW corrosion and COPC release models.

---

[74] The uncertainty associated with the predicted glass corrosion has been recognized in previous analyses. To evaluate the importance of this uncertainty, previous analyses evaluated a range of FRRs. For example, the TC&WM EIS (DOE/EIS-0391) used a range of values from 10 times to 1/10 times the nominal value of $2.8E-08$ yr^{-1}. The nominal value used in the TC&WM EIS is about 10 times less than the base case value of $2.5E-07$ yr^{-1} used in the IDF PA. This difference is the result of the glass used as the reference glass in the TC&WM EIS, LAWABP1, having different corrosion and ion-exchange rate parameters.

- **Evaluate the potential for Stage III corrosion in the IDF** – This topic includes review of ongoing national and international investigations of Stage III effects on glass corrosion and will assess the extent to which the R&D results may be relevant to IDF performance. Numerical geochemical models of the nucleation, growth, and precipitation kinetics of glass alteration phases in open versus closed aqueous systems as a function of temperature will be used to support the assessments.

- **Evaluate the evolution of glass compositions and loading with enhanced glass formulations** – To provide a basis for comparing the alternative glasses to the baseline ILAW glasses (LAWA44, LAWB45, and LAWC22) evaluated in the IDF PA (RPP-RPT-59958), additional TST-relevant data will be collected and analyzed using SPFT tests. Examples of this have recently been completed by PNNL (PNNL-26169 and PNNL-27098) where the results of testing IDF18-A161, ORPLG9, and other glasses are presented. Prior to making a design decision, it is necessary to confirm that the alternative glass performs adequately to meet the performance objectives analyzed in the IDF PA.

Additional sensitivity and uncertainty analyses evaluating the combined effect of uncertainties associated with releases from the ILAW, SSW and ETF-LSW waste forms as well as uncertainties in the performance of the natural barrier will be conducted as part of the ongoing UDQE process.[75]

Inventory Allocation

The RAI basis noted that a large source of uncertainty in the performance of the IDF is from the inventory splits, or the fraction of key radionuclides that end up in different waste streams. DOE's base case (Case 7) has a very high percentage of the ^{99}Tc that ends up in the glass wasteform because of assumptions about recycling the off-gas condensate back into the LAW feed. By comparison, cases 10A and 10B have a low percentage of ^{99}Tc that ends up in the glass wasteform as a result of volatilization during processing without recycling the off-gas condensate back into the LAW feed. As noted in the RAI basis, this uncertainty by itself can swing the results from compliance to non-compliance and asserts that the importance of individual uncertainties may be misrepresented.

While the above observations are correct, the difference between Case 7 and Cases 10A and 10B is not uncertainty, as asserted in the RAI basis. Cases 10A and 10B were run as hypothetical alternative scenarios. As noted in the IDF PA (RPP-RPT-59958), Cases 10A and 10B are included to help establish waste acceptance criteria for specific waste forms, and should not be

---

[75] Although DOE believed the range of sensitivity and uncertainty analyses summarized in RPP-RPT-59958 encompassed the expected range of outcomes, additional information has become available since the completion of the IDF PA models and calculations in 2016 and 2017 that in some cases extends the range of possible outcomes. Two risk-significant examples of this are (1) the new information on ^{129}I retention (i.e., Kd) on solidified carbon bed media (SSW-GAC) that impacts the release rate of ^{129}I from the SSW-GAC waste stream (see RAI 2-20) and (2) the information on observed average moisture content in the H2 sand that indicate the long-term steady-state moisture content in the H2 sand is overpredicted for the base case assumptions of vadose zone hydraulic properties, resulting in an underprediction of the base case pore velocity and an overprediction of the base case transport time in the vadose zone (see RAI 2-15). The impact of these differences will be evaluated in the ongoing UDQE process and associated Special Analyses.

incorrectly construed as probable, or even potential alternative inventory-allocation cases. These cases were only run to evaluate potential inventory loading constraints of the ETF-LSW. Operating the WTP without recycling the off-gas condensate to the LAW feed is not expected as a part of the current WTP flow sheet models and the WTP would not be operated under this scenario. Therefore, it is not appropriate to include this "uncertainty" in the global uncertainty analysis as suggested by the RAI basis.

Additional sensitivity cases were run using different ^{99}Tc and ^{129}I inventory and inventory allocations. The different inventory and allocation cases illustrated only a limited significance, except for Case 7b. Case 7b was run to provide a comparison with the assumptions used in the TC&WM EIS (DOE/EIS-0391). Case 7b was based on the inventory estimates in the 2002 Best-Basis Inventory (BBI) instead of the updated 2014 BBI and assumed inventory allocations between the ILAW glass, SSW and ETF-LSW based on the same assumptions used in the TC&WM EIS (DOE/EIS-0391). Specifically, Case 7b assumes the ^{99}Tc inventory in the SSW was increased from the base case value of 19.9 Ci to 430.9 Ci (with 377.5 Ci of the SSW inventory on HEPA filters). The Case 7b doses were predicted to exceed the 25 mrem/yr performance objective based on the higher inventory and inventory allocation in the SSW.

The inventory and inventory allocation assumptions used in the TC&WM EIS and assumed in Case 7b is not representative of the expected operations of the WTP and have been updated with more recent information that was used as a basis for the Case 7 inventory and inventory allocation. Therefore, while the Case 7b inventory and inventory allocation provides a useful comparison back to the TC&WM EIS, it should not be characterized as "uncertainty" as it is not representative of expected operating conditions of the WTP.

Subsequent to the completion of the PA, DOE evaluated the impact of waste stream inventory changes on simulated groundwater concentrations using the IDF PA system model, RPP-CALC-63176. The report demonstrated that the waste form release rate and impact to the groundwater from each waste stream was proportional to the inventory in each waste stream. Consequently, a spreadsheet application was developed to scale the impact to groundwater simulated with the PA system model according to proposed or realized changes in inventory. The tool does not consider uncertainty in other parameters related to waste form release, transport through the natural system, or exposure factors, but produces an immediate, PA-based estimate of impacts to groundwater based on alternative inventory allocation information. This tool will not identify the importance of PA parameters that might become more important had inventory uncertainty been included in the PA uncertainty analysis.

A potential change in the inventory allocation that has been evaluated using the tool developed in RPP-CALC-63176 concerns radionuclide inventory in SSW associated with the WTP LAW Vitrification Facility. A change to the flow sheet that may impact the SSW inventory was recently identified in RPP-RPT-61370, *WTP Wet Electrostatic Precipitator Wash Cycle Down Time Effects.* The change included a 30-min daily deluge of the WESPs in the LAW Facility of the WTP. This deluge leads to increases in the quantities of radionuclide constituents that are sent to the off-gas treatment system. The potential implications of this daily deluge of the WESP on radionuclide loading on SSW waste streams and LSW were evaluated in RPP-RPT-61370. RPP-RPT-61370 evaluated the increased radionuclide loading on HEPA filters, carbon

adsorption bed media and in the liquid waste sent to the Hanford ETF for treatment. Higher concentrations in SSW and LSW were reported for the following radionuclides included in the 2017 IDF PA and analyzed in RPP-RPT-59958: ^{90}Sr, ^{99}Tc, ^{129}I, ^{137}Cs, ^{239}Pu, and ^{240}Pu.

The impact of changes in concentrations in the impacted waste streams was analyzed using the spreadsheet application developed in RPP-CALC-63176. The results of the analysis are documented in UDQ-IDF-2020-001-SA, *Special Analysis: Impacts of WESP Daily Deluge from SSW Disposed of at IDF*. The special analysis concluded that the potential increase in ^{99}Tc allocation to HEPA filter SSW could exceed the disposal limit reported in the IDF WAC, which would control the placement and acceptance of the waste into the IDF and ensure that the potential dose to an inadvertent intruder would not exceed the performance objectives and performance measures. The HEPA filter SSW would not cause the dose to exceed performance objectives, but could result in groundwater concentrations that exceed 4 mrem/yr drinking water standard approximately 1,500 years after closure.

Summary
The proposed path forward for RAI 2-12 by NRC staff was to expand the sensitivity and uncertainty analyses related to glass release, inventory splits and inventory uncertainty. This RAI response provides the results of additional sensitivity analyses performed related to the combined effect of uncertainty in the fractured glass hydraulic properties (including MCC uncertainty), SMRN, reactive surface area and glass corrosion characteristics. Additional sensitivity analyses were not performed for inventory splits and inventory uncertainty because the uncertainty analyses presented in Section 6.2.1.4.3 of RPP-RPT-59958 are sufficient to illustrate the importance of these factors in the projected dose to a hypothetical receptor[76].

The additional sensitivity analyses presented in this RAI response focus on the potential effect of MCC uncertainty and the combined effect of ILAW glass release parameter uncertainty on the predicted FRR of mobile radionuclides from ILAW glass. The significance of the uncertainty in the ILAW glass FRR on the overall performance prediction was evaluated in the importance analysis presented in Section 6.3.4.2 of RPP-RPT-59958. These results indicate that at early times in the post-closure period (e.g., 1,000 to 3,000 years after closure of the facility), the uncertainty in the FRR from the ILAW glass is not a significant contributor to the predicted groundwater concentration and total dose. This is because of the higher early release rate of mobile ^{99}Tc from the SSW waste form, specifically the HEPA filter waste stream. However, at late times in the post-closure time period (e.g., 6,000 to 10,000 years after closure of the facility) the uncertainty in the FRR from ILAW glass is one of the more significant uncertainties. This is illustrated by the significant correlation between peak dose and ILAW FRR illustrated in Figure 2-12-2. The increased significance of uncertainty of ILAW glass release at later time is

---

[76] With the exception of Cases 10A and 10B, which are hypothetical cases run to develop information for use in the development of waste acceptance criteria and are not related to uncertainty in the operation of the WTP and related facilities, only Case 7b yielded results that are significantly different from the other analyzed inventory cases. Case 7b is a case that uses the previous (2002) estimate of the BBI and the inventory split between ILAW, SSW and ETF-LSW used in the TC&WM EIS (DOE/EIS-0391). The higher doses predicted for Case 7b are related to the significant increase in the ^{99}Tc inventory in SSW and ETF-LSW (from 19.9 and 0.229 Ci of ^{99}Tc to 430.9 and 86.29 Ci of ^{99}Tc, respectively) and the significant increase in ^{129}I inventory in ETF-LSW (from 0.0642 to 33.6 Ci of ^{129}I). The SSW and ETF-LSW provide a larger fractional and total release rate and the associated dose from these mobile radionuclides than the ILAW waste form (see Section 6.2.1.4.3 of RPP-RPT-59958).

also evident in the observation that most of the significant parameter uncertainties that affect the predicted dose are related to the corrosion of ILAW glass as summarized in Table 6-42 of RPP-RPT-59958 (repeated here as Table 2-12-2). This conclusion is also apparent in the evaluation of the significant factors contributing to the peak doses for the two highest peak dose realizations as summarized in Section 6.3.4.3 of RPP-RPT-59958.

When using the range of predicted ILAW FRRs in the global uncertainty analyses, which includes other sources of engineered system and natural system uncertainty, the impact is that none of the 300 realizations exceeded the 25 mrem/yr performance objective even within the 10,000-year post closure time period. The highest dose realization of the 300 realizations (realization # 47) was 19.6 mrem/yr (Table 6-41 of RPP-RPT-59958). This realization used an ILAW FRR of 2.64E-06 yr^{-1}, about the 94th percentile of the uncertainty distribution and similar to the FRR calculated for pessimistic assumptions in the COMBX sensitivity analyses, when using the erroneous *riex* values for LAWA44 reported in PNNL-24615 and RPP-RPT-59958. Had the correct *riex* values been used, the ILAW FRR would have been about a factor of 10 lower and the corresponding dose from both SSW and ILAW would be expected to be dominated by SSW sources.

Confirming that the FRR from ILAW glass is best represented by the nominal value of 2.5E-07 yr^{-1} or lower when the corrected *riex* value is used, and that FRRs at the higher end of the expected range of possible values (i.e., about 20 to 30 times the nominal value) are unlikely, remains an important consideration in the IDF PA maintenance program. This includes the continued evaluation of the likelihood and consequences associated with the potential for Stage III glass corrosion as discussed in the response to RAI 2-9. The current status of the additional testing of possible ILAW glasses is discussed in the responses to RAIs 2-7 and 2-9.

References

CHPRC-03348, 2019, *Performance Assessment Maintenance Plan for the Integrated Disposal Facility*, Rev. 1, INTERA, Inc./CH2M HILL Plateau Remediation Company, Richland, Washington.

DOE/EIS-0391, 2012, Final Tank Closure and Waste Management Environmental Impact Statement for the Hanford Site, Richland, Washington, U.S. Department of Energy, Washington, D.C.

DOE M 435.1-1, 2011, *Radioactive Waste Management Manual*, Change 2, U.S. Department of Energy, Washington, D.C.

ML20128J832, 2020, *Technical Evaluation Report, Draft Waste Incidental to Reprocessing Evaluation for Closure of Waste Management Area C, Hanford Site, Washington*, U.S. Nuclear Regulatory Commission, Rockville, Maryland.

PNNL-14700, 2004, *Near-Field Hydrology Data Package for the Integrated Disposal Facility 2005 Performance Assessment*, Pacific Northwest National Laboratory, Richland, Washington. Available at: https://www.pnnl.gov/main/publications/external/technical_reports/PNNL-14700.pdf.

PNNL-14805, 2004, *Waste Form Release Data Package for the 2005 Integrated Disposal Facility Performance Assessment*, Pacific Northwest National Laboratory, Richland, Washington. Available at: https://www.pnnl.gov/main/publications/external/technical_reports/PNNL-14805.pdf.

PNNL-15198, 2005, *Waste Form Release Calculations for the 2005 Integrated Disposal Facility Performance Assessment*, Pacific Northwest National Laboratory, Richland, Washington. Available at: https://www.pnnl.gov/main/publications/external/technical_reports/PNNL-15198.pdf.

PNNL-20781, 2011, *Integrated Disposal Facility FY2011 Glass Testing Summary Report*, Pacific Northwest National Laboratory, Richland, Washington. Available at: https://www.pnnl.gov/main/publications/external/technical_reports/PNNL-20781.pdf.

PNNL-21812, 2013, *Integrated Disposal Facility FY 2012 Glass Testing Summary Report*, Rev. 1, Pacific Northwest National Laboratory, Richland, Washington. Available at: https://www.pnnl.gov/main/publications/external/technical_reports/PNNL-21812rev1.pdf.

PNNL-23711, 2015, *Physical, Hydraulic, and Transport Properties of Sediments and Engineered Materials Associated with Hanford Immobilized Low-Activity Waste*, RPT-IGTP-004, Rev. 0, Pacific Northwest National Laboratory, Richland, Washington. Available at: https://www.pnnl.gov/main/publications/external/technical_reports/PNNL-23711.pdf.

PNNL-24615, 2015, *Immobilized Low-Activity Waste Glass Release Data Package for the Integrated Disposal Facility Performance Assessment*, RPT-IGTP-005, Pacific Northwest National Laboratory, Richland, Washington. Available at: https://www.pnnl.gov/main/publications/external/technical_reports/PNNL-24615.pdf.

PNNL-26169, 2017, *FY2016 ILAW Glass Corrosion Testing with the Single-Pass Flow-Through Method*, RPT-IGTP-013, Pacific Northwest National Laboratory, Richland, Washington. Available at: https://www.pnnl.gov/main/publications/external/technical_reports/PNNL-26169.pdf.

PNNL-26594, 2017, *A Critical Review of Ion Exchange in Nuclear Waste Glasses to Support the Immobilized Low-Activity Waste Integrated Disposal Facility Rate Model*, RPT-IGTP-018, Rev 0.0, Pacific Northwest National Laboratory, Richland, Washington. Available at: https://www.pnnl.gov/main/publications/external/technical_reports/PNNL-26594.pdf.

PNNL-27098, 2018, *FY2017 ILAW Glass Corrosion Testing with the Single-Pass Flow-Through Method*, RPT-IGTP-015, Pacific Northwest National Laboratory, Richland, Washington. Available at: https://www.pnnl.gov/main/publications/external/technical_reports/PNNL-27098.pdf.

RPP-17675, 2003, *Risk Assessment Supporting the Decision on the Initial Selection of Supplemental ILAW Technologies*, Rev. 0, CH2M HILL Hanford Group, Inc./Pacific Northwest National Laboratory/Fluor Federal Services, Inc., Richland, Washington. Available at: https://www.osti.gov/servlets/purl/816325.

RPP-CALC-61029, 2017, *Two-Dimensional, Two-Phase Flow Model Calculations for the Integrated Disposal Facility Performance Assessment*, Rev. 0, INTERA, Inc. for Washington River Protection Solutions, LLC, Richland, Washington.

RPP-CALC-61031, 2017, *Low-Activity Waste Glass Release Calculations for the Integrated Disposal Facility Performance Assessment*, Rev. 0, INTERA, Inc. for Washington River Protection Solutions, LLC, Richland, Washington.

RPP-CALC-61192, 2017, *Integrated Disposal Facility Performance Assessment: Sensitivity Calculations for ILAW Glass Dissolution Rate Parameters*, Rev. 0, AEM Consulting, LLC for Washington River Protection Solutions, LLC, Richland, Washington.

RPP-CALC-61194, 2018, *System Model Calculations for the Integrated Disposal Facility Performance Assessment*, Rev. 1, INTERA, Inc. for Washington River Protection Solutions, LLC, Richland, Washington.

RPP-CALC-63176, 2020, *Integrated Disposal Facility Risk Budget Tool Analysis*, Rev. 0A, Washington River Protection Solutions, LLC, Richland, Washington.

RPP-ENV-58782, 2016, *Performance Assessment of Waste Management Area C, Hanford Site, Washington*, INTERA, Inc./CH2M HILL Plateau Remediation Company/Ramboll Environ, Inc./Washington River Protection Solutions, LLC/TecGeo, Inc., Richland, Washington.

RPP-PLAN-60520, 2020, *Program Plan for Immobilized Low Activity Waste (ILAW) Glass Testing*, Rev. 1, Washington River Protection Solutions, LLC, Richland, Washington.

RPP-RPT-59958, 2019, *Performance Assessment for the Integrated Disposal Facility, Hanford Site, Washington*, Rev. 1A, Washington River Protection Solutions, LLC, Richland, Washington.

RPP-RPT-61370, 2019, *WTP Wet Electrostatic Precipitator Wash Cycle Down Time Effects*, Rev. 0, Washington River Protection Solutions, LLC, Richland, Washington.

UDQ-IDF-2020-001-SA, 2021, *Special Analysis: Impacts of WESP Daily Deluge from SSW Disposed of at IDF*, Washington River Protection Solutions, LLC, Richland, Washington.

RAI 2-13 (Quality Assurance)

Comment
Some aspects of the quality assurance program were not clear from the documentation provided.

Basis
DOE provided detailed information on most aspects of the quality assurance program applied to the development of the analyses supporting the draft waste evaluation for VLAW. However, a few aspects of the quality assurance program were not clear. The quality assurance status and controlled use of the major software or computer programs was demonstrated (e.g., GoldSim, STOMP). The quality assurance status or verification activities for ancillary software was not provided in all instances. For example, the Hanford Defined Waste model (HDW) was used as part of the inventory development process. Some components of the HDW were previously assessed and found to contain significant errors, but other components of the HDW were not verified (ML20128J832). The thermodynamic database used in the geochemical modeling for glass degradation (thermo.com.V8.R6+.tdat) came from Lawrence Livermore National Laboratory. The qualification status of that database was not clear.

Verification information was provided for STOMP verification and test cases that demonstrated select aspects of the software. However, it wasn't clear from the documentation provided how those verification activities demonstrate or verify the correct functioning of the software for the key aspects of the performance assessment, namely the glass degradation an release rate calculations and the unsaturated flow phenomena especially the capillary barrier effects. Verification of unsaturated flow phenomena in general is not the same as verifying that STOMP correctly produces results for very dissimilar materials using a coarse numerical grid.

Path Forward
Please provide the qualification status of software and databases that supply information to the performance assessment calculations, or the plans to determine the qualification status of the referenced software and databases. Please provide the verification results or plans for verification of the release rate and unsaturated flow phenomena simulated by STOMP for glass degradation as applicable to the performance assessment.

DOE Response

Hanford Defined Waste Model
The HDW was revised in 2004 from version 4.0 (LA-UR-96-3860, *Hanford Tank Chemical and Radionuclide Inventories: HDW Model Rev. 4*) to version 5.0 (RPP-19822, *Hanford Defined Waste Model – Revision 5.0*). During that revision, updates and significant improvements to the model were made which simplified the HDW model from four separate workbooks to one workbook. Verification of the remaining workbook was completed by an engineer using the spreadsheet verification process that was approved by CH2M HILL Hanford Group, Inc. at the time of revision. The verification process included a spot check of all electronically-copied input data, 100% comparison of hand-entered data, an inspection of all unique formulas, and verification of the resulting units. No plans are currently in place to put the HDW model through any additional qualification exercises or updates. Additional qualification of the HDW model

spreadsheets is of limited value because the HDW estimates that are used in the BBI are being replaced as sample information becomes available.

With regard to the draft WIR evaluation (DOE-ORP-2020-01) in particular, the HDW estimates are being used for planning and screening purposes only. All tank waste that will be incorporated into the VLAW waste product will undergo extensive sampling and characterization (RPP-RPT-59314, *Integrated DFLAW Feed Qualification Program Description*) prior to being transferred to the LAW Vitrification Facility. Additionally, DOE intends to characterize every batch of tank waste received in the LAW Vitrification Facility (24590-LAW-PL-PENG-17-0001) and track it through the vitrification process. For more information, see the response to RAI 1-1 (Removal of ^{90}Sr to the Maximum Extent Practicable).

Thermodynamic Database
The thermodynamic database, thermo.com.V8.R6+.tdat, used to simulate the corrosion of vitrified waste in GWB is based on the geochemical database from Lawrence Livermore National Laboratory (LLNL) (combined dataset version 8 release 6). A copy of the database that had been formatted to work with the software was downloaded from the software vendor. This dataset included additional modifications to organic species that are not part of the vitrified waste corrosion reaction. The LLNL database is available to the public and is a standard reference for geochemical modeling throughout the geochemical modeling community. Consistent with DOE's position regarding geochemical databases on the Yucca Mountain Project (Letter LLYMP0004056 E, "Data Files Utilized by the Geochemical Community"), DOE treats the data included in the database as accepted data that do not require qualification.

Augmenting the database with additional information necessary to simulate glass corrosion and track the formation of additional minerals was necessary. The database was augmented to include library information for: LAWA44, LAWA44_H, LAWA44_SiO2, LAWABP1, LAWABP1_H, LAWABP1_SiO2, LAWB45, LAWB45_H, LAWB45_SiO2, LAWC22, LAWC22_H, and LAWC22_SiO2. The fictive _SiO2 species were added to track the progress of the glass corrosion reaction toward a hypothetical state of equilibrium. The added species for each simulated glass type (e.g., LAWA44) and hydrolyzed glass type (e.g., LAWA44_H) were necessary to simulate the corrosion reaction. The molar volume and molecular weight of these components were developed from laboratory experiments testing the performance of the different glasses. The reaction stoichiometry for each glass type was determined based on laboratory data characterizing the mole fractions of individual glass constituents. Charge balance was used as a constraint to determine the stoichiometry of H$^+$ in these reactions. The values of pseudo-equilibrium constants for each reaction were included in the database but were not used in the simulations because the pseudo-equilibrium constants were already specified as parameters in the respective kinetic rate laws governing glass corrosion.

Model Verification
Work is being conducted to validate predictions of ILAW glass dissolution rates in the Hanford Site IDF using the FLTF. The FLTF has a series of field lysimeter tubes (most extend to a depth of 3 m) that can be filled with various waste forms, including glass and cementitious materials, and backfilled with IDF soils. Water infiltration rate is controlled within each lysimeter tube.

Water samples will be collected at various depths within the lysimeters over the next several years, along with measurements of the *in situ* distribution of moisture.

Prior to initiation of the lysimeter test, a modeling effort was performed using the same simulation style as the IDF PA to predict the behavior of the emplaced waste forms and corresponding contaminant release, using ^{99}Tc and ^{127}I as tracers for the cementitious waste forms and molybdenum and rhenium as tracers for the glass waste forms (PNNL-27394). As data are collected from the tests, comparisons will be made against the initial modeling that will serve as validation of the model and determine the extent to which the laboratory-based parameters are applicable to waste form behavior in the field. Water analysis and *in situ* soil moisture data from these tests will start to be available in FY21 but data from solids analysis will not be available until the tests conclude, which depending on the test may be 5 years to 25 years in the future.

With the two glass formulations selected, Stage III behavior may not be observed over the duration of the lysimeter test. However, post-experimental characterization of the excavated waste forms and backfill will also be completed at the test conclusion to evaluate the evolution of mineral phases and to determine if any zeolite phases have been formed. Note that the presence of zeolites in the lysimeter tests would not necessarily indicate that Stage III behavior occurred, but their presence would indicate that Stage III may have occurred. Data are also being collected in separate laboratory tests to further assess the potential magnitude of the impact of Stage III rate behavior on contaminant release from the IDF to the surrounding environment.

References

24590-LAW-PL-PENG-17-0001, 2021, *ILAW Product Compliance Plan*, Rev. 2, Bechtel, River Protection Project Waste Treatment Plant, Richland, Washington.

DOE/ORP-2020-01, 2020, *Draft Waste Incidental to Reprocessing Evaluation for Vitrified Low-Activity Waste Disposed Onsite at the Hanford Site, Washington*, Rev. 0, U.S. Department of Energy, Office of River Protection, Richland, Washington.

LA-UR-96-3860, 1997, *Hanford Tank Chemical and Radionuclide Inventories: HDW Model Rev. 4*, Los Alamos National Laboratory, Los Alamos, New Mexico.

LLYMP0004056 E, 2000, "Data Files Utilized by the Geochemical Community" (letter from S. P. Mellington to H. A. Benton, Waste Package Department, Civilian Radioactive Waste Management System Management and Operating Contractor - FCF, March 30), U.S. Department of Energy, Office of Civilian Radioactive Waste Management, Yucca Mountain Site Characterization Office, North Las Vegas, Nevada.

ML20128J832, 2020, *Technical Evaluation Report, Draft Waste Incidental to Reprocessing Evaluation for Closure of Waste Management Area C, Hanford Site, Washington*, U.S. Nuclear Regulatory Commission, Rockville, Maryland.

PNNL-27394, 2018, *Field-Scale Lysimeter Studies of Low-Activity Waste Form Degradation Implementation Plan*, RPT-IGTP-017, Rev. 0, Pacific Northwest National Laboratory, Richland, Washington.

RPP-19822, 2005, *Hanford Defined Waste Model – Revision 5.0*, Rev. 0-A, CH2M HILL Hanford Group, Inc./Technical Resources International, Inc., Richland, Washington.

RPP-RPT-59314, 2021, *Integrated DFLAW Feed Qualification Program Description*, 24590-WTP-PD-RAEN-EN-0008, Rev. 2, Washington River Protection Solutions, LLC/ Waste Treatment Completion Company, LLC, Richland, Washington.

RAI 2-14 (Geologic Uncertainty)

Comment
The basis for the interpretation of the geology underlying the footprint of the IDF that removed the Ringold E formation is not clear.

Basis
DOE's previous interpretation of the geology underlying the IDF had a layer termed the Ringold E present in the northwest corner of the footprint of the facility (see the figures below). DOE explained that some geologic information was reinterpreted, and the geologic framework model was revised. The data shows quantitative information to suggest the boundary of the layer is somewhere between the boreholes (see Figure 2-14-1). If the modeling was revised, it isn't clear how the change in the boundary of the unit was validated in the absence of additional data. The significance of the unit is that the Ringold E is much less permeable than the Hanford unit such that fluxes of contaminants into the unit experience lower dilution and therefore result in higher concentrations. If groundwater protection standards apply to all geologic units, then it may be more difficult to demonstrate that groundwater protection standards have been met.

Figure 2-14-1. Hanford South Geologic Framework Model Ringold E Well Control.
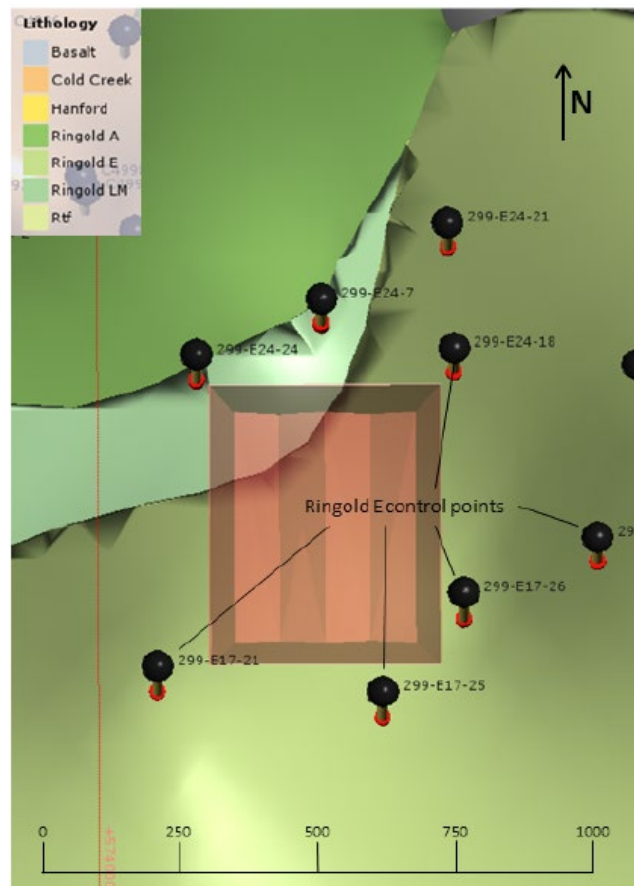
Source: Figure 3-53 of RPP-RPT-59958, *Performance Assessment for the Integrated Disposal Facility, Hanford Site, Washington*.

Figure 2-14-2. Plan View Comparison of Central Plateau and Integrated Disposal Facility Geologic Framework Models at 114.5 Meters.
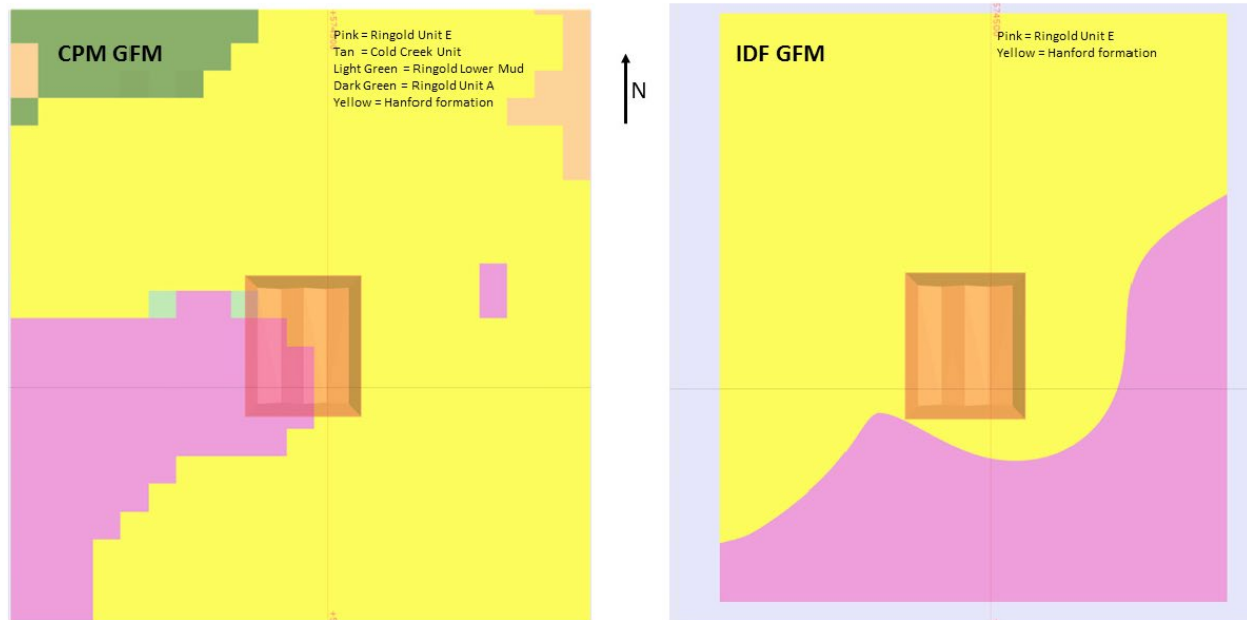
Source: Figure 3-63 of RPP-RPT-59958, *Performance Assessment for the Integrated Disposal Facility, Hanford Site, Washington.*

Path Forward
Please provide additional basis for the reinterpretation of the location of the Ringold E and indicate whether groundwater protection standards apply to this unit.

DOE Response
DOE acknowledges that there is uncertainty in the geologic framework model (GFM) describing the sediments underneath the IDF. Borehole characterization is the main technique that is used to delineate the contact locations between different hydrostratigraphic layers across the Hanford Site. The geologic framework models built from borehole logs are subject to re-interpretation each time a new borehole is drilled into the subsurface and each time a groundwater model is calibrated to existing conditions. Often times the professional staff developing the refinements to the GFMs are different, which can lead to the use of different techniques to interpret contacts points away from boreholes and can also result in alternative contact points being developed from borehole logs based on professional judgement. Working groups are utilized to minimize the changes that can be made by a single individual.

Interpretation of the location of the contact between the Ringold Unit E (Rwie) and Hanford formation hydrostratigraphic units (HSUs) near the IDF has evolved over time as additional boreholes have been drilled and logged. According to well construction and soil boring records in the Hanford Environmental Information System (HEIS) database, between 2000 and the end of 2020 more than 1,000 groundwater wells and 1,600 soil borings have been drilled on the Hanford Site. Since 2014, nearly 300 groundwater wells and 100 soil borings have been drilled. Geologic framework models are coupled to a database of HSU contact points that is regularly

updated with new boring information. The interpretations have been included in the GFMs of the area of the Central Plateau that include the area near the IDF. As noted in the RAI, the location of that contact can make a significant difference in the dilution afforded by the saturated zone beneath the IDF depending on the hydraulic conductivity of the two HSUs beneath the IDF (see RAI 2-16 for additional discussion of the basis for the base case hydraulic conductivity for the Hanford and Rwie HSUs beneath the IDF).[77]

The groundwater protection standards apply to the point-of-compliance, which is defined as the point of maximum predicted groundwater concentration along the groundwater flow path at a boundary located 100 m from the disposed of waste, which is approximated as the edge of the IDF. The groundwater specific discharge between the edge of the IDF and the 100-m boundary controls the amount of dilution contributed by the saturated zone in the IDF PA and therefore controls the predicted groundwater concentration that is compared to the groundwater protection standards. The groundwater specific discharge is determined by the hydraulic conductivity and hydraulic gradient in the HSU beneath and downgradient of the edge of the IDF. Therefore, the groundwater specific discharge is dependent on the hydraulic characteristics of the HSU beneath and within 100 m of the edge of the IDF.

To address the RAI, the response is organized into the following sections:

- Evolution of the Location of the Ringold Unit E in GFMs near the IDF
- Current Interpretation of the Location of the Ringold Unit E near the IDF
- Current Interpretation of the Hydraulic Conductivity of HSUs near the IDF.

Evolution of Location of the Ringold Unit E in GFMs near the IDF
The interpreted location of the Rwie near the IDF has evolved over time as additional boreholes have been drilled and characterized and additional data sources have been interpreted by different subject matter experts to distinguish between the poorly-cemented gravels of the Hanford formation and the Cold Creek Unit (CCU), which comprise the paleochannel deposits in the high-conductivity zone beneath the 200 East Area, and the cemented gravels of the Rwie. The history of the different interpreted GFMs developed for the area is summarized in Table 2-14-1.

At the time of the initial ILAW PA[78] completed in 1998 (DOE/RL-97-69, *Hanford Immobilized Low-Activity Tank Waste Performance Assessment*), it was assumed that the water table beneath the ILAW site was in the Rwie (equivalent to the mapped Ringold Unit 5). This assumption was made given the lack of site-specific information on the lateral extent of the Hanford formation gravel and uncertainty in the location of the Hanford paleochannel near the location of the ILAW site. Prior to 1998, very few boreholes were drilled near the IDF. As a result of this assumption, the dilution of radionuclides released from the ILAW facility and transported to the saturated

---

[77] The importance of the characteristics of the HSUs beneath the IDF, in particular the location of the Rwie/Hanford contact, was noted as a key assumption in Section 8.4.3 of the IDF PA (RPP-RPT-59958). Additional characterization of the hydrostratigraphy in the saturated zone beneath the IDF was identified as maintenance activity in Section 4.7 of the IDF Maintenance Plan (CHPRC-03348).

[78] The Immobilized Low-Activity Waste (ILAW) disposal facility was renamed the Integrated Disposal Facility (IDF).

aquifer beneath the ILAW site was limited by the lower specific discharge in the Rwie (due to the lower hydraulic conductivity of the Rwie compared to the Hanford formation gravels).

Table 2-14-1. Evolution of Geologic Framework Models in the Vicinity of the Integrated Disposal Facility. (5 sheets)

GFM Document ID (Date)	Basis for Interpretation of Hydrostratigraphic Unit Contacts
TC&WM EIS DOE/EIS-0391 (December 2012)	DOE/EIS-0391 Appendix L: The TC&WM EIS groundwater flow model has been encoded with hydrogeologic data for the entire model domain developed from Hanford well borings completed as of September 2009. Approximately 5,000 boring logs from Hanford and its surroundings were reviewed to determine whether the geologic units and discrete hydrostratigraphic layers could be recognized from the geologic descriptions. When multiple logs existed for a borehole, higher credibility was given to those descriptions recorded by a professional geologist. Logs were reviewed for specific identification of the Elephant Mountain basalt, Hanford and Ringold Formations, and Cold Creek and Plio-Pleistocene Units. The logs were further examined to discern textural types among the sedimentary units: mud, silt, sand, and gravel. Each of the resulting hydrogeologic units is encoded with unique properties (see DOE/EIS-0391 Section L.4.4). DOE/EIS-0391 Appendix N: Subsurface geology for the set of STOMP models was determined using field data from over 5,000 boring logs. Soil types for each model domain were assigned based on individual borehole interpretations. Examination of single or multiple cross sections were used to specify the three-dimensional (3-D) spatial distribution of soil types in row/column views.
Hanford South GFM ECF-HANFORD-13-0029, Rev. 0 (July 2014)	To define and construct geologic unit layers within the Hanford South Model, two primary data sets were utilized, 1) best-estimate depth to geologic unit contacts (in feet below ground surface), and 2) ground surface elevations (at the time of drilling in meters above mean sea level). These data are selected based on professional judgment by professional or registered geologists and hydrogeologists, reviewed and approved by general technical consensus for model input. Anomalies in the geologic model and the related borehole data (e.g., elevations) with high variability for specific unit contacts were reevaluated to verify or revise best-estimate geologic unit contacts or ground surface elevations relative to raw and interpreted borehole or other related data. For the Hanford South Model, best estimates of geologic unit contacts were compiled for 1,396 wells and boreholes within, and adjacent to, the Hanford South Model domain. In summary, the technical approach for this work was to assemble a regional stratigraphic model of the southern Hanford Site using previously published interpretations of the geologic units. These geologic units are managed, periodically updated as new well data become available, and maintained in an Excel® spreadsheet at CH2M HILL Plateau Remediation Company (CHPRC) (GeoContacts Hanford revision date). The GeoContacts_Hanford_2014-06-26 data set used for this model is located on the internal link maintained by CHPRC.
Hanford South GFM ECF-HANFORD-13-0029, Rev. 1 (May 2015)	This revision provides the 2014 updated 3-D model results which utilized the GeoContacts_Hanford_2015-02-24 data set. This data set includes the addition of nine new boreholes to the model (none of which are in the 200 East area) and refinements to the surfaces based on input from project staff.

Table 2-14-1. Evolution of Geologic Framework Models in the Vicinity of the Integrated Disposal Facility. (5 sheets)

GFM Document ID (Date)	Basis for Interpretation of Hydrostratigraphic Unit Contacts
Central Plateau GFM, Version 6.3.3 CP-47631, Rev. 2 (July 2015)	Freestone Environmental Services, Inc. provided borehole data for the entire model domain in the form of a geodatabase (NearFieldGeoElevations_7_16_09.mdb) as described in ECF-200PO1-09-2074, *200-PO-1 Groundwater Operable Unit Remedial Investigation Report - Geologic Cross Sections*. A total of 56 wells in the 200-BP-5 Groundwater operable unit (OU) area have undergone elevation adjustments after receiving the hydrostratigraphic unit (HSU) database from Freestone Environmental Services, Inc. Most of these involve the bottom elevation of the Hanford formation. A number of issues led to the reevaluation of HSU elevations in the 200-BP-5 Groundwater OU area including: • Discrepancies in the Pacific Northwest National Laboratory (PNNL) tops database (Geologic Contact Depths_2009_12_03.xls) identified by inspection and review of specific well logs by a geologist • Discrepancies in entries in the database compiled by Freestone Environmental Services, Inc. identified by comparison to the PNNL tops database • Gaps of missing elevations between units identified by inspection • Errors/reinterpretation based on review of well logs. The Hanford formation bottom elevations were lowered to the top of basalt for 49 wells located in the paleochannel area extending from 200 East and through the Gable Gap (between Gable Mountain and Gable Butte). This modification was justified based on the review of well logs that reported the Cold Creek unit beneath the Hanford formation in 200-BP-5 Groundwater OU area to be of large grain size, indicating that it may behave hydraulically much like the Hanford formation. Furthermore, a subset of wells had information gaps where no units were specified below the Hanford formation, and the gap between the bottom of the Hanford unit and the basalt surface needed to be filled for developing a 3-D model.
Hanford South GFM ECF-HANFORD-13-0029, Rev. 2 (December 2015)	This revision provides the 2014 updated 3-D model results which utilized the Leapfrog Geo® modeling software and used the most current GeoContacts_Hanford_2015-02-24 data set. This data set includes the nine 2014 boreholes added in Revision 1 of this environmental calculation file (ECF) and refinements to the surfaces based on input from subject matter experts and project staff. For this version of the Hanford South Geologic Framework Model, best estimates of geologic unit contacts were compiled for 1,405 wells and boreholes within, and adjacent to the Hanford South Geologic Framework Model domain.

Table 2-14-1. Evolution of Geologic Framework Models in the Vicinity of the Integrated Disposal Facility. (5 sheets)

GFM Document ID (Date)	Basis for Interpretation of Hydrostratigraphic Unit Contacts
Integrated Disposal Facility (IDF) GFM RPP-RPT-59343 (July 2016)	Interpretations for Hanford formation sub-unit lithology were made by examining borehole geologic and geophysical logs obtained from the Hanford Environmental Information System (HEIS). HEIS is a quality-controlled database maintained by CHPRC and was accessed for the geologic and geophysical borehole logs needed for interpretation. GeoContacts_Hanford_2015-02-24.xlsx was also accessed for existing interpretations and is the best estimate at the time of drilling for the geologic contact depths for the sedimentary units underlying the Hanford Site. All boreholes identified to exist within the IDF GFM domain were considered for interpretation. However, log information for some of the boreholes existing within the IDF GFM domain was insufficient for use in a high-confidence interpretation and therefore these boreholes were omitted from the facies model. This decision is based on the professional judgment of experienced geologists; when a contact location could be determined it was entered into the database, when there was insufficient information or the quality of the records were poor no contact elevation was determined for that location. It should be noted that saturated flow and transport simulation for IDF utilizes the established Central Plateau Groundwater Model (CPGWM), which incorporated a GFM developed independently of any Hanford South GFM version (CP-47631, *Model Package Report: Central Plateau Groundwater Model, Version 6.3.3*). Therefore, a comparison of the IDF and CPGWM GFM's was needed in order to gauge any possible effects that differences between the two models would have on flow and transport simulations. Data sources include: • PNNL-14586, *Geologic Data Package for 2005 Integrated Disposal Facility Performance Assessment* • PNNL-15237, *Geology of the Integrated Disposal Facility Trench* • PNNL-17913, *Hydrogeology of the Hanford Site Central Plateau – A Status Report for the 200 West Area*, Rev. 1 • ECF-Hanford-13-0029, *Development of the Hanford South Geologic Framework Model, Hanford Site Washington* • HEIS is a controlled database from which borehole geologic and geophysical logs used in IDF GFM geologic interpretations were accessed.
Hanford South GFM ECF-HANFORD-13-0029, Rev. 3 (January 2017)	This revision provides the 2015 updated 3-D model that utilizes the Leapfrog Geo® modeling software and uses the most current GeoContacts_Hanford_2016-05-10.xlsx data set. This data set includes the addition of 64 boreholes drilled or interpreted in fiscal year 2015 and six boreholes with recently revised stratigraphic contacts to the model. After borehole data is input, there are refinements made to the stratigraphic surfaces based on input from subject matter experts and project staff. This version of the Hanford South GFM (HS_051016_EXP.lfvw) has been updated to expand the outer boundary of the model. The expanded domain boundaries are to the expanded to the west, east and south by 7,312, 2,183 and 7,197 meters, respectively, from the previous versions. This expansion was made to accommodate numerical modeling needs.

Table 2-14-1. Evolution of Geologic Framework Models in the Vicinity of the Integrated Disposal Facility. (5 sheets)

GFM Document ID (Date)	Basis for Interpretation of Hydrostratigraphic Unit Contacts
Hanford South GFM ECF-HANFORD-13-0029, Rev. 4 (January 2017)	This revision provides a 2016 update to the Hanford South GFM, which utilizes the Leapfrog Geo® modeling software and uses the most current GeoContact_Hanford_2017-01-12.xlsx data set. This data set includes the boreholes utilized in Revision 3 and 17 boreholes drilled or interpreted in fiscal year 2016. One older borehole (699-38-70) was removed from the 2016 input file because a new borehole (299-W 19-116) was drilled immediately adjacent and has higher data quality available. After borehole data is input, there are refinements made to the stratigraphic surfaces based on input from subject matter experts and project staff.
Central Plateau Vadose Zone (CPVZ) GFM, Rev. 0 CP-60925, Rev. 0 (March 2018)	The technical approach for creating the CPVZ GFM included using the existing Hanford South GFM (ECF-HANFORD-13-0029, Rev. 4) and previously-published interpretations of the major geologic units to refine and update a database of major vadose zone stratigraphic contacts. In addition, an evaluation of available and applicable borehole data was included to interpret vadose contacts where none were previously recorded. During this process, comparisons to the existing GeoContacts data set and area-specific type logs were made to guide, verify, and ultimately select the best-estimate contacts for use in the model. The best-estimate contacts and ground surface elevations were then selected, based on professional judgment and general consensus, to develop two-dimensional (2-D) interpretations, structure and isopach maps, and geologic cross sections. These interpretations were used to further evaluate vadose zone stratigraphic continuity, boundary extents and conditions, and correlation of the units between boreholes across the Composite Analysis domain. Data anomalies identified in the geologic interpretations and boreholes were re-evaluated to verify the best-estimate GeoContacts relative to the raw borehole data and type logs. Changes were made as necessary; the corrected and updated contacts data were defined, through an iterative process, and the final best-estimate contacts data set was used to complete the 2-D interpretations.
Hanford South GFM ECF-HANFORD-13-0029, Rev. 5 (May 2018)	In this revision of this ECF (Revision 5), 96 boreholes were added, seven boreholes were deleted, and the stratigraphy of 16 existing boreholes was revised. Other changes to the model – adjustments in control data and slight changes in model extent – are discussed. The deleted boreholes either contradicted other nearby data or belonged in the 100-Area GFM north of Gable Mountain and Gable Butte.

Table 2-14-1. Evolution of Geologic Framework Models in the Vicinity of the Integrated Disposal Facility. (5 sheets)

GFM Document ID (Date)	Basis for Interpretation of Hydrostratigraphic Unit Contacts
CPVZ GFM, Rev. 1 ECF-HANFORD-18-0035, Rev. 0 (March 2020)	The purpose of this revision includes the following: – Integrate updated saturated zone surfaces from the Hanford South GFM (ECF-HANFORD-13-0029) – Include new geologic data from boreholes drilled after 2016 – Utilize numerical grain-size distribution data stored in the Hanford Virtual Library's ROCSAN database to evaluate existing interpretations based on geologic modified Folk-Wentworth classification and geophysics – Expand the model domain to encompass the Treated Effluent Disposal Facility – Add a light detection and ranging topography surface as the top of the GFM – Correct inconsistencies in the original revision of the CPVZ Rev. 0 (CP-60925) This current revision of the CPVZ GFM contains tops from 1,216 boreholes within the domain boundary compared to the 1,092 boreholes utilized in CP-60925. Twenty-four of the wells from the original 1,092 were removed while 148 boreholes were added in this revision. New boreholes were added in this revision of the CPVZ GFM for the following reasons: a. Recent drilling b. Changes in the model domain boundary c. Site-specific models within the GFM domain providing new information d. New interpretations of older borehole data – Information that makes the hydrostratigraphic interpretation more consistent with the rest of the GFM.

GFM = Geologic Framework Model
TC&WM EIS = Tank Closure and Waste Management Environmental Impact Statement

References:
CP-47631, *Model Package Report: Central Plateau Groundwater Model Version 6.3.3*, Rev. 2.
CP-60925, *Model Package Report: Central Plateau Vadose Zone Geoframework Version 1.0*, Rev. 0.
DOE/EIS-0391, *Final Tank Closure and Waste Management Environmental Impact Statement for the Hanford Site, Richland, Washington.*
ECF-HANFORD-13-0029, *Development of the Hanford South Geologic Framework Model, Hanford Site Washington*, Rev. 0.
ECF-HANFORD-13-0029, *Development of the Hanford South Geologic Framework Model, Hanford Site, Washington*, Rev. 1.
ECF-HANFORD-13-0029, *Development of the Hanford South Geologic Framework Model, Hanford Site, Washington*, Rev. 2.
ECF-HANFORD-13-0029, *Development of the Hanford South Geologic Framework Model, Hanford Site, Washington*, Rev. 3.
ECF-HANFORD-13-0029, *Development of the Hanford South Geologic Framework Model, Hanford Site, Washington Fiscal Year 2016 Update*, Rev. 4.
ECF-HANFORD-13-0029, *Development of the Hanford South Geologic Framework Model, Hanford Site, Washington*, Rev. 5.
ECF-HANFORD-18-0035, *Central Plateau Vadose Zone Geoframework*, Rev. 0.
RPP-RPT-59343, *Integrated Disposal Facility Model Package Report: Geologic Framework*, Rev. 0.

Excel® is a registered trademark of Microsoft Corporation in the U.S. and other countries.
Leapfrog Geo® is a registered trademark of ARANZ Geo Limited, LLC of Christchurch, New Zealand.
Subsurface Transport Over Multiple Phases (STOMP) is developed and distributed by Battelle Memorial Institute.

Between the initial ILAW PA in 1998 and the 2001 version completed in 2001 (DOE/ORP-2000-24, *Hanford Immobilized Low-Activity Waste Performance Assessment: 2001 Version*), additional boreholes were drilled (e.g., 299-E17-21 was constructed in April 1998 and 299-E24-21 was constructed in March 2001) and characterized near the IDF. The new information resulted in a reinterpretation of the location and thickness of the gravels in the Hanford paleochannel and the contact between the Rwie and Hanford gravel. This reinterpretation resulted in there being an increase in the lateral extent of the Hanford gravel beneath the IDF which resulted in an increase in the assumed dilution afforded by the higher specific discharge in the Hanford gravel of about a factor of 7 and a corresponding reduction in peak concentration by a factor of 0.14 (Table ES-8 of DOE/ORP-2000-24). Hydraulic properties of the Rwie and Hanford formation gravels were still based on measurements made from locations throughout the footprint of the Hanford Site.

The basis for the location of the contact of the Rwie and Hanford gravel used to develop the GFM used in the IDF PA is taken from the Hanford South GFM, which uses an HSU contact points database dated in February 24, 2015. By comparison, the Central Plateau Groundwater Model (CPGWM) was based on a contact database developed by PNNL in 2009 (Geologic Contact Depths_2009_12_03.xls) and refined to correct discrepancies identified during a data review before the data were used. No new wells in the vicinity of the IDF were installed to groundwater between December 2009 and February 2015. Therefore, the differences between contact points between the Rwie and Hanford gravel are attributed to grid scale and the technique and rules used to assign HSUs to each grid node.

The HSU contact points away from the well control points for the GFM in CPGWM Version 6.3.3 are interpolated using 100-m grid blocks with varying thicknesses near the water table. The upper and lower HSU surfaces between adjacent layers were developed independently of each other using standard kriging (CP-47631, *Model Package Report: Central Plateau Groundwater Model, Version 6.3.3*, Rev. 2, Section 4.2.6). When the bottom of an upper HSU overlapped with the top of an underlying HSU, preferential assignment was given to the upper HSU in the GFM because the upper units tend to be more permeable and more important to the modeling representation of flow in the aquifer. This decision would tend to substitute Hanford formation gravel where Rwie might be present away from a characterized borehole. The newer Hanford South GFM was developed by another team using different techniques to assign HSU contact points. The Hanford South GFM developed in ECF-HANFORD-13-0029, *Development of the Hanford South Geologic Framework Model, Hanford Site, Washington*, Rev. 2, which is the basis of the IDF GFM, used a different kriging algorithm (the proprietary radial basis interpolation function built into Leapfrog Geo®[79]) that considered the HSU elevation in the nearby boreholes when assigning a grid block to a specific HSU. Because of the different grid scales and interpolation techniques away from borehole control points, the GFMs from two representations near the IDF have different HSU contact points between the Hanford formation and Rwie. The most recent version of the CPGWM (CP-47631, *Model Package Report: Central Plateau Groundwater Model, Version 8.4.5*, Rev. 4) uses the Hanford South GFM.

---

[79] Leapfrog Geo® is a registered trademark of ARANZ Geo Limited, LLC of Christchurch, New Zealand.

The cited figure in the RAI (Figure 3-62 of RPP-RPT-59958), compares the location of the contact of the Rwie and Hanford gravel as interpreted in the CPGWM GFM (documented in CP-47631, Rev. 2) current at the time the IDF PA model was completed and the interpreted contact in the IDF GFM (documented in RPP-RPT-59343, *Integrated Disposal Facility Model Package Report: Geologic Framework*) at an elevation of 119.5 m above sea level (asl) (corresponding to the elevation of the long-term steady-state water table near the IDF). The difference in interpreted surfaces was ascribed to the different GFMs used, with the GFM used in the CPGWM GFM (CP-47631, Rev. 2) based on a predecessor to the Hanford South GFM (see Table 2-14-1) while the interpreted surface in the IDF GFM (RPP-RPT-59343) was based on a more recent version of the Hanford South GFM (ECF-HANFORD-13-0029, Rev. 2). The boreholes used to define the location of the Rwie/Hanford contact are illustrated in Figure 3-53 of RPP-RPT-59958 (which is included in the RAI; see Figure 2-14-1).

The reason for the changing interpretation is that the physical and compositional differences between the Hanford, CCU gravel unit (CCUg) and Rwie are subtle. Traditionally, the key difference used to distinguish the Rwie and the Hanford gravels has been the composition of the gravel. At the time of Ringold deposition the basalt highlands such as Rattlesnake Mountain did not exist, so there were fewer basalt clasts in the gravel. In addition, at that time the ancestral Columbia River was flowing through mountain ranges in Canada that provided abundant quartzite and micas to the sediments. As a result, the Ringold gravels are generally characterized by an increase in quartzite pebbles and a decrease in basalt pebbles compared to the Hanford gravels, with the CCUg gravels having intermediate quartzite and basalt pebble fractions between the Rwie and Hanford end members. In addition, because the Ringold sediments are older, they are characterized by having greater cementation and lithification than the younger CCUg and Hanford formation gravel unit (H3) gravels. The identification of the presence of and contact elevation between HSUs of similar physical and compositional appearance many years after a borehole is drilled is dependent on the quality of the characterization reported in the borehole log and a subjective judgement made by the interpreter(s). In some areas of 200 East, like WMA C, trying to separate these units is very challenging because lower gravel units have been reworked in the main channel areas and interpretations in some local areas have treated these gravel units as a combined undifferentiated H3, CCUg and Rwie unit.

Current Interpretation of the Location of the Ringold Unit E near the IDF

As summarized in Table 2-14-1, the GFMs in the area near the IDF have continued to be updated as new information has been developed and interpreted. The most current version of the Central Plateau Vadose Zone (CPVZ) GFM is documented in ECF-HANFORD-18-0035, *Central Plateau Vadose Zone Geoframework*. Table 2-14-2 summarizes the HSU contacts for the key HSUs (H3 gravel, CCUg and Rwie) that define the location and thickness of these HSUs near the IDF. Figures illustrating the most recent interpretation of the contact are included as Figure 2-14-3 based on the boreholes with interpreted contacts of the Rwie illustrated in Figure 2-14-4 (derived from ECF-HANFORD-18-0035).

Table 2-14-2. Formation Tops and Elevations in Boreholes near the Integrated Disposal Facility. (2 sheets)

Well Name	Hanford ID	Depth (m)	Elevation (m)	H3 Depth (m)	CCU Depth (m)	CCU Elevation (m asl)	CCUg Depth (m)	CCUg Elevation (m asl)	Rtf Depth (m)	Rwie Depth (m)	Rwie Elevation (m asl)	Comment
299-E17-21	B8500	146.3	224.3	75.3	96.7	*127.6*	97.2	*127.1*	97.8	98.5	*125.8*	These boreholes are located to the south or southeast of the Integrated Disposal Facility (IDF). The long-term steady-state water table, assumed to be at an elevation of 119.5 m asl, is in the Rwie for these boreholes consistent with the interpretation in the IDF geologic framework model (RPP-RPT-59343).
299-E17-22	C3826	109.3	220.6	65.9	77.8	*142.8*	86.5	*134.1*	—	93.2	*127.4*	
299-E17-23	C3827	112.8	223.8	77.3	99.5	*124.3*	99.5	*124.3*	99.6	99.7	*124.1*	
299-E17-24	C3828	116.7	224.8	84.6	98.5	*126.3*	99.3	*125.5*	—	100.2	*124.6*	
299-E17-25	C3926	113.9	225.0	83.8	98.8	*126.2*	99.5	*125.5*	—	100.1	*124.9*	
299-E17-26	C4648	115.5	224.4	77.7	85.7	*138.7*	86.9	*137.5*	—	97.9	*126.5*	
299-E24-18	A4753	100.6	219.4	67.4	90.3	*129.1*	90.9	*128.5*	—	—	*<118.8*	These boreholes are located to the north or northeast of the IDF. The long-term steady-state water table, assumed to be at an elevation of 119.5 m asl, is in the CCUg for these boreholes (with the exception of 299-E17-57) in contrast to the interpretation in the IDF geologic framework model (RPP-RPT-59343) which has the water table in the H3 gravel. The CCUg has hydraulic properties equivalent to the H3.
299-E24-21	C3177	101.8	217.8	80.9	82.6	*135.2*	83.0	*134.8*	—	—	*<116.0*	
299-E24-24	C4647	110.9	220.5	67.1	91.2	*129.3*	91.7	*128.8*	—	—	*<109.6*	
299-E24-7	A4757	137.2	218.7	65.1	89.0	*129.7*	89.9	*128.8*	—	115.2	*103.5*	
299-E17-56	D0038	111.2	220.0	—	88.4	*131.6*	89.9	*130.1*	—	103.6	*116.4*	
299-E17-57	D0041	108.4	220.8	—	—	—	—	—	—	—	*<112.4*	
299-E24-164	D0040	106.7	219.1	—	85.3	*133.8*	89.9	*129.2*	—	—	*<112.4*	

Table 2-14-2. Formation Tops and Elevations in Boreholes near the Integrated Disposal Facility. (2 sheets)

Well Name	Hanford ID	Depth (m)	Elevation (m)	H3 Depth (m)	CCU Depth (m)	CCU Elevation (m asl)	CCUg Depth (m)	CCUg Elevation (m asl)	Rtf Depth (m)	Rwie Depth (m)	Rwie Elevation (m asl)	Comment

Source: Modified from ECF-HANFORD-18-0035, *Central Plateau Vadose Zone Geoframework*, Rev. 0, Table C-1.

Reference: RPP-RPT-59343, *Integrated Disposal Facility Model Package Report: Geologic Framework*, Rev. 0.

Note: Blank cells indicate that the stratigraphic unit has not been interpreted in that borehole. The borehole could either be too shallow or the stratigraphic unit itself is not present at that location. CCU depth corresponds to the base of the H3. Elevation tops for CCU, CCUg and Rwie are calculated by taking the surface elevation minus the reported depths from Table C-1 of ECF-HANFORD-18-0035. Because the Rwie is not identified as present in boreholes 299-E24-18, 299-E24-21, 299-E24-24, 299-E17-57 and 299-E24-164, the Rwie depth is greater than the total depth of the borehole and the elevation is less than the elevation of the bottom of the borehole. Geology from boreholes 299-E17-56, 299-E17-57 and 299-E24-164 is reported in SGW-63813, *Borehole Summary Report for the Installation of Six M-24 Wells in the 200-PO-1, 200-UP-1 and 300-FF-5 Operable Units, FY2019*. These interpretations were made in 2019 in parallel to the completion of ECF-HANFORD-18-0035. Borehole 29-E17-57 is noted as being in the Hanford formation for its entire depth.

CCU = Cold Creek unit   Rtf = Ringold Formation member of Taylor Flat
CCUg = Cold Creek unit gravel   Rwie = Ringold Formation member of Wooded Island – unit E
H3   = Hanford formation unit 3

Figure 2-14-3. Ringold Formation Member of Wooded Island – Unit E Structure Elevation (feet) in 200 East Area with Extent Limiting Polygon in Orange.
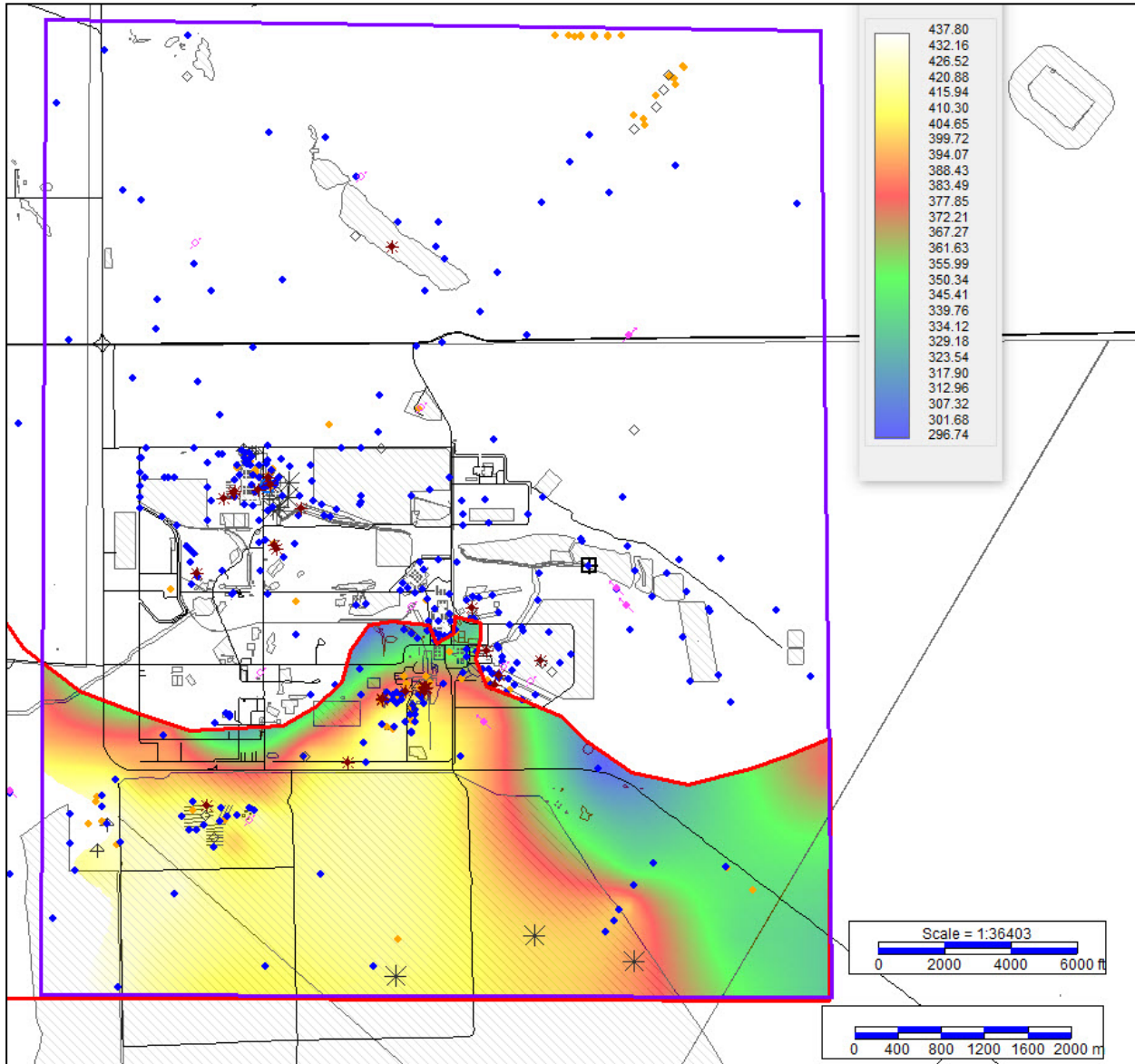
Source: ECF-HANFORD-18-0035, *Central Plateau Vadose Zone Geoframework*, Rev. 0, Figure G-17.

Note: The elevation of the top of the Ringold Unit E (Rwie) varies from about 350 ft (about 107 m) above sea level (asl) in the northwest corner of the Integrated Disposal Facility (IDF) footprint to about 400 ft (about 122 m) asl in the southeast corner of the IDF footprint and averages about 375 ft (about 114 m) asl across the center of the IDF footprint from the southwest corner to the northeast corner. The long-term steady-state water table is at an elevation of about 119.5 m asl, implying that in the southeast corner of the IDF footprint, the steady-state water table is within the Rwie.

Figure 2-14-4. Boreholes near the Integrated Disposal Facility Used to Develop Structural Contours of Hydrostratigraphic Unit Tops.
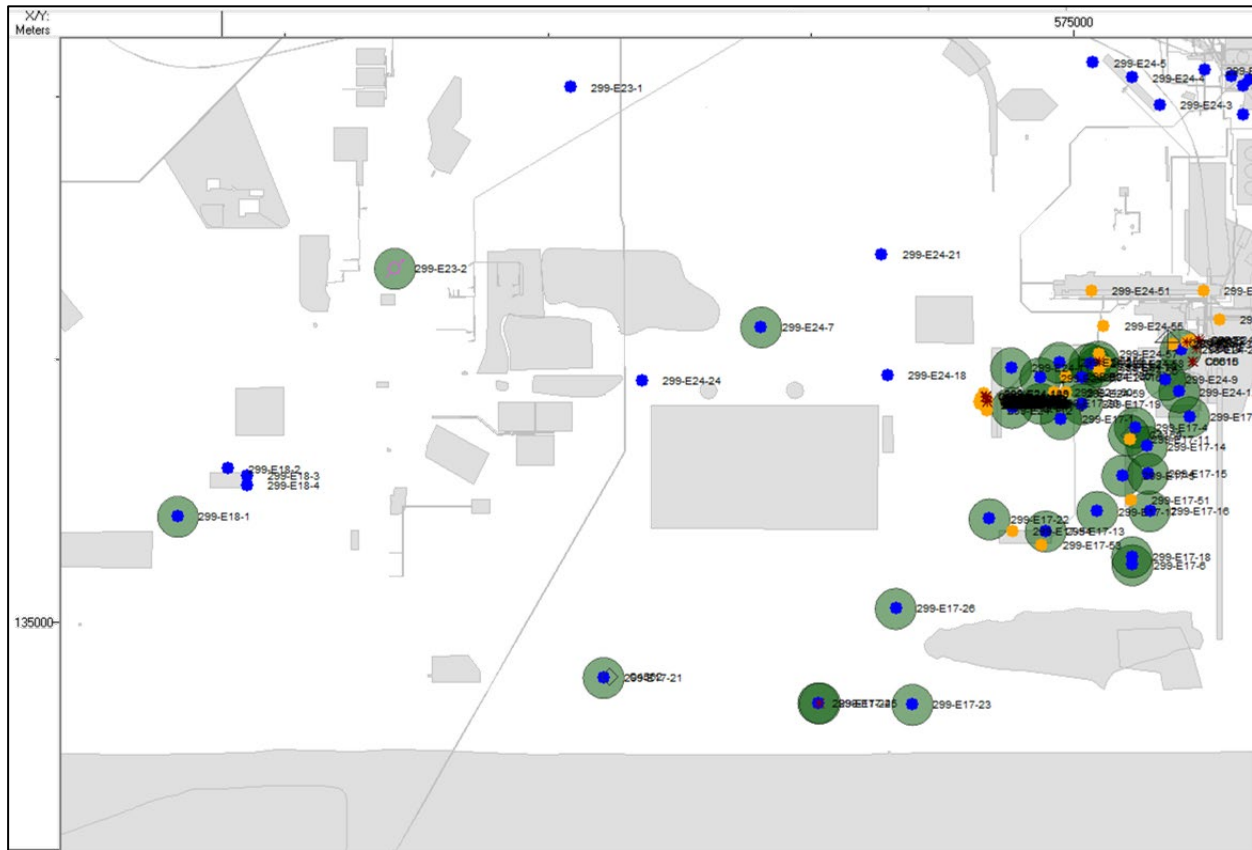
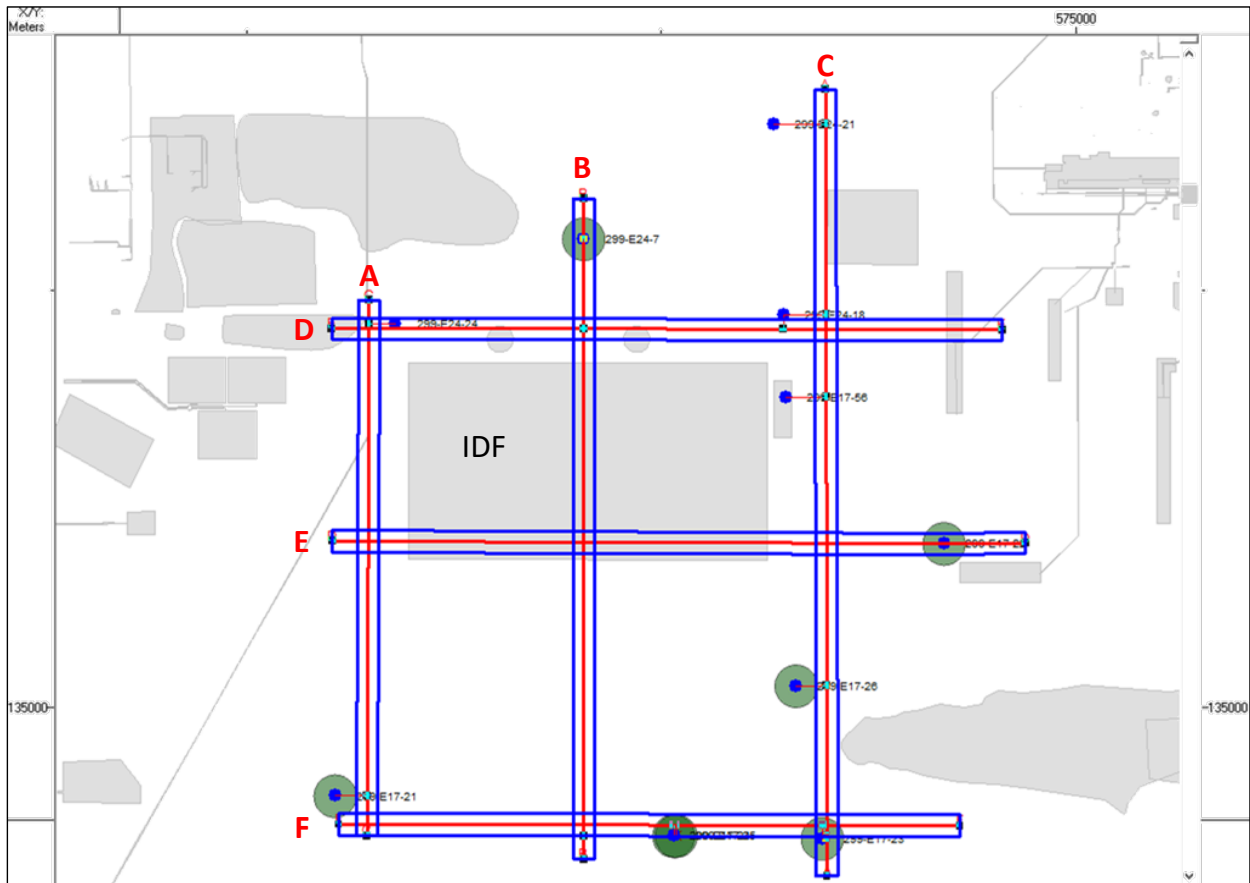Source: Derived from ECF-HANFORD-18-0035, *Central Plateau Vadose Zone Geoframework*.

Note: Green circles indicate boreholes which intersect the Ringold Unit E (Rwie) and were used to develop the top of Rwie structural map.

To provide a more detailed examination of the hydrostratigraphy near the IDF, a series of north-south and west-east cross sections (Figure 2-14-5) have been developed based on the current version of the CPVZ GFM (ECF-HANFORD-18-0035) and are provided in Figures 2-14-6 and 2-14-7. These cross sections illustrate that the vadose zone near the IDF has been reinterpreted (again) to include a thin CCU sand unit between the H3 gravel and the CCU gravel, and that the long-term steady-state water table (at an elevation of 119.5 m asl) is in the CCU gravel instead of the H3 gravel beneath the IDF. This difference is not significant because as summarized in the most recent version of the CPGWM (Plateau to River Groundwater Model [P2R] Version 8.3, described in CP-57037, *Model Package Report: Plateau to River Groundwater Model Version 8.3*, Rev. 2), the H3 gravel and CCU gravel are both represented by the high conductivity zone making up the Hanford paleochannel (see also response to RAI 2-16) and have similar hydraulic characteristics.

The cross sections presented in Figures 2-14-6 and 2-14-7 illustrate that the saturated thickness of the CCU gravel thins to the east and south of the IDF in a similar fashion as the saturated thickness of the H3 gravel thinned in the IDF PA GFM (see RPP-RPT-59958 Figure 3-52). To

illustrate this, an isopach of the saturated thickness of the CCU gravel near the IDF has been developed from the hydrostratigraphic contacts in the current version of the CPVZ GFM (ECF-HANFORD-18-0035, Rev. 0) by taking the difference between the long-term water table elevation (119.5 m asl) and the top of the Rwie (Figure 2-14-8). Consistent with the cross section, the CCU gravel saturated thickness decreases to the east and south of the IDF and decreases to 0.0 m where the long-term water table (at an elevation of 11.9.5 m asl) is below the top of the Rwie.

Figure 2-14-5. Location of Cross-Sections through the Central Plateau Vadose Zone Geologic Framework Model near the Integrated Disposal Facility.

Source: Derived from ECF-HANFORD-18-0035, *Central Plateau Vadose Zone Geoframework.*

IDF = Integrated Disposal Facility

Note: Green circles indicate those boreholes that have identified the presence of Rwie. Borehole 299-E17-56 was drilled in 2019 and is not included in the current version of ECF-HANFORD-18-0035.

Current Interpretation of the Hydraulic Conductivity of HSUs near the IDF
In addition to evaluating the revised interpretation of the HSUs near the IDF documented in updates to the GFMs (both the Hanford South GFM and the CPVZ GFM) to address this RAI, it is also important to evaluate updates to the groundwater flow models of the saturated sediments near the IDF. The basis for the base case hydraulic conductivity for the sediments beneath the IDF is the subject of RAI 2-16. The response to RAI 2-16 notes that since the completion of the

IDF PA, updates to the groundwater flow models have been completed which are relevant to the response to RAI 2-16. Updates to the GFMs are discussed in this RAI response, while updates to the groundwater models and hydraulic properties of the sediments beneath the IDF are discussed in the response to RAI 2-16.

Figure 2-14-6. North-South Cross-Sections through the Central Plateau Vadose Zone Geologic Framework Model near the Integrated Disposal Facility, Section B (top) and Section C (bottom).
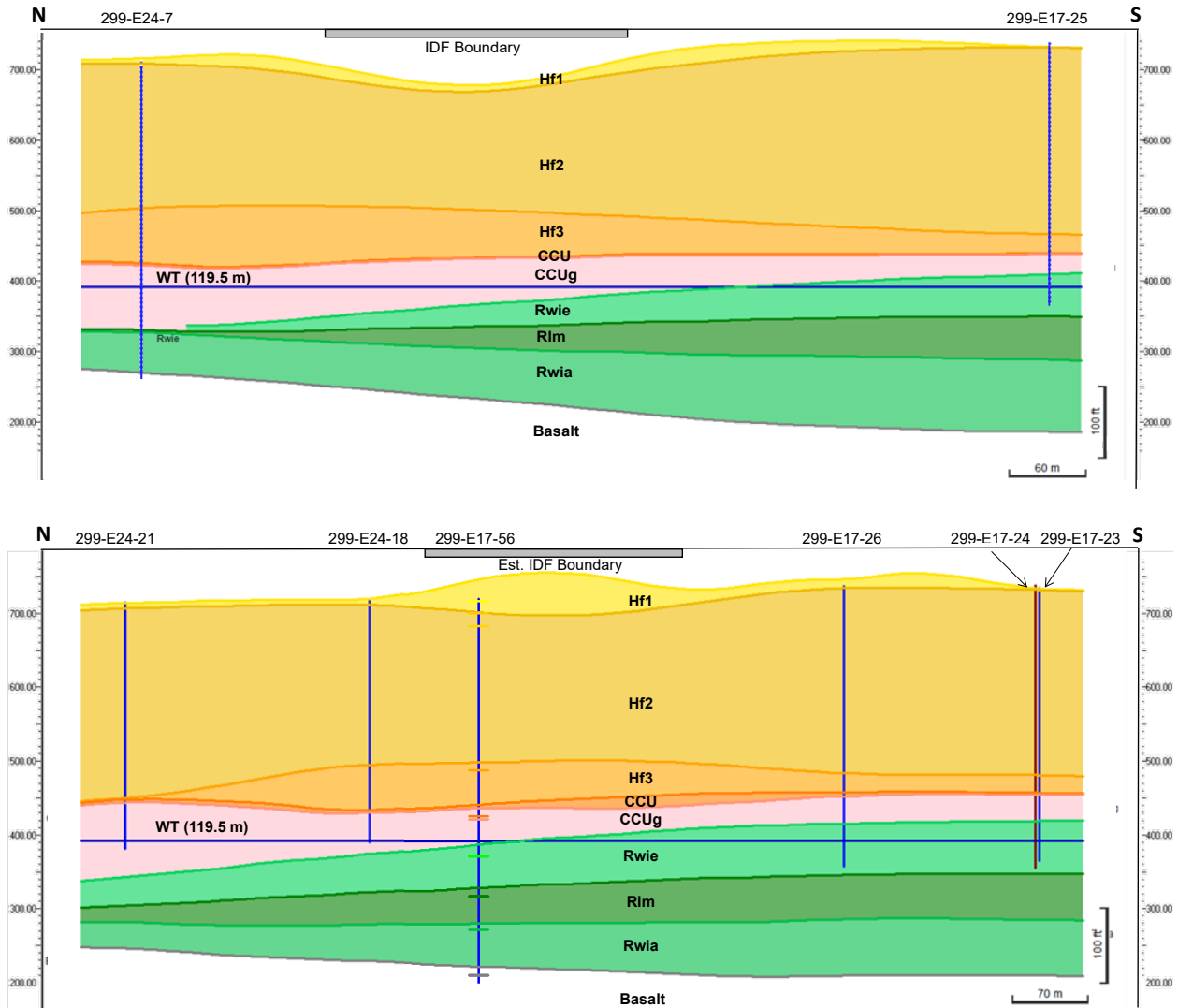
Source: Derived from ECF-HANFORD-18-0035, *Central Plateau Vadose Zone Geoframework*.

Note: The HSU contacts for borehole 299-E17-56 are based on SGW-63813, *Borehole Summary Report for the Installation of Six M-24 Wells in the 200-PO-1, 200-UP-1 and 300-FF-5 Operable Units, FY2019*. Borehole 299-E17-56 was drilled in 2019 and is not included in the Central Plateau Vadose Zone Geologic Framework Model Rev. 1 (ECF-HANFORD-18-0035).
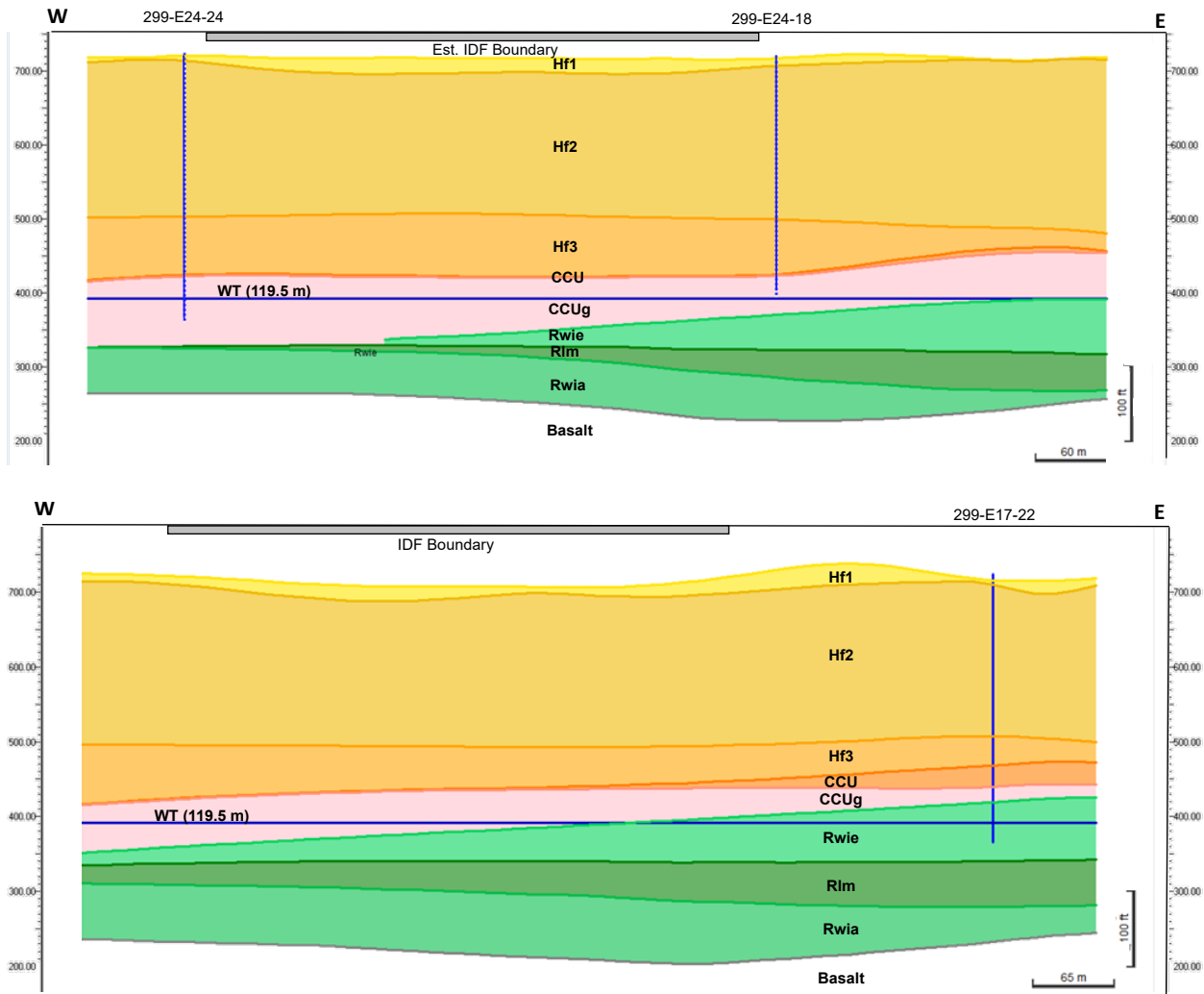
Figure 2-14-7. West-East Cross Sections of Central Plateau Vadose Zone Geologic Framework Model near the Integrated Disposal Facility, Section D (top) and Section E (bottom).

Source: Derived from ECF-HANFORD-18-0035, *Central Plateau Vadose Zone Geoframework*.

Note: The long-term average water table elevation of 119.5 m asl is in the Cold Creek unit (CCU) gravel (CCUg) over most of the Integrated Disposal Facility (IDF) footprint. In comparing these cross sections with the cross section based on the IDF geologic framework model (GFM) (Figure 3-61 of RPP-RPT-59958, *Performance Assessment for the Integrated Disposal Facility, Hanford Site, Washington*), it is apparent that Central Plateau Vadose Zone GFM Rev. 1 has included a thin CCU layer (comprised of sand) between the Hanford formation unit 3 (Hf3) gravel and the CCUg gravel while the IDF GFM interpreted the entire section above the Ringold Unit E (Rwie) as the Hf3 gravel. This revised GFM does not significantly affect the fate and transport of radionuclides in the vadose zone as the CCU sand and CCUg have hydraulic properties similar to those modeled for the Hanford sand (Hanford formation unit 2 [Hf2]) and Hanford gravel (Hf3).

Figure 2-14-8. Saturated Thickness of the Cold Creek Gravel Unit near the Integrated Disposal Facility.
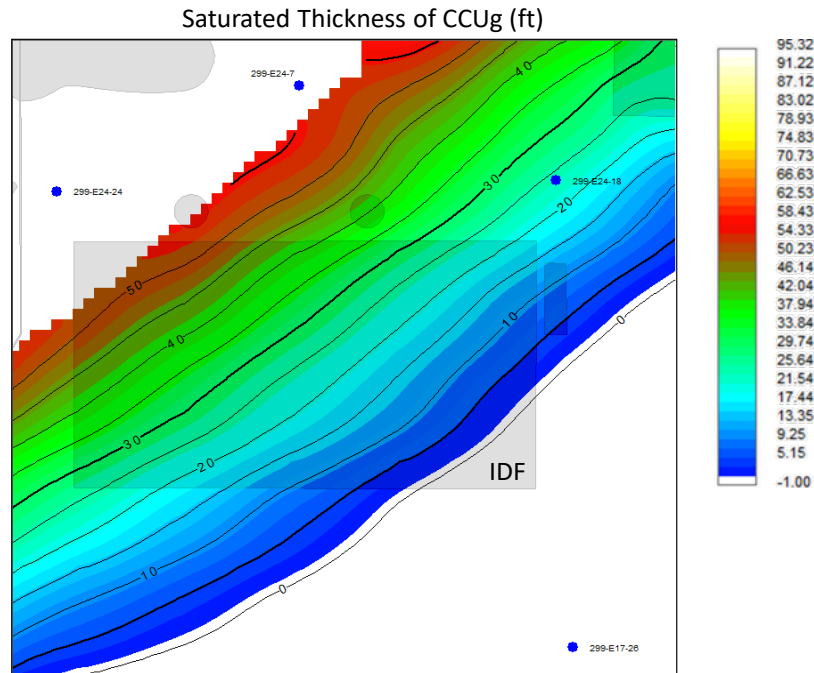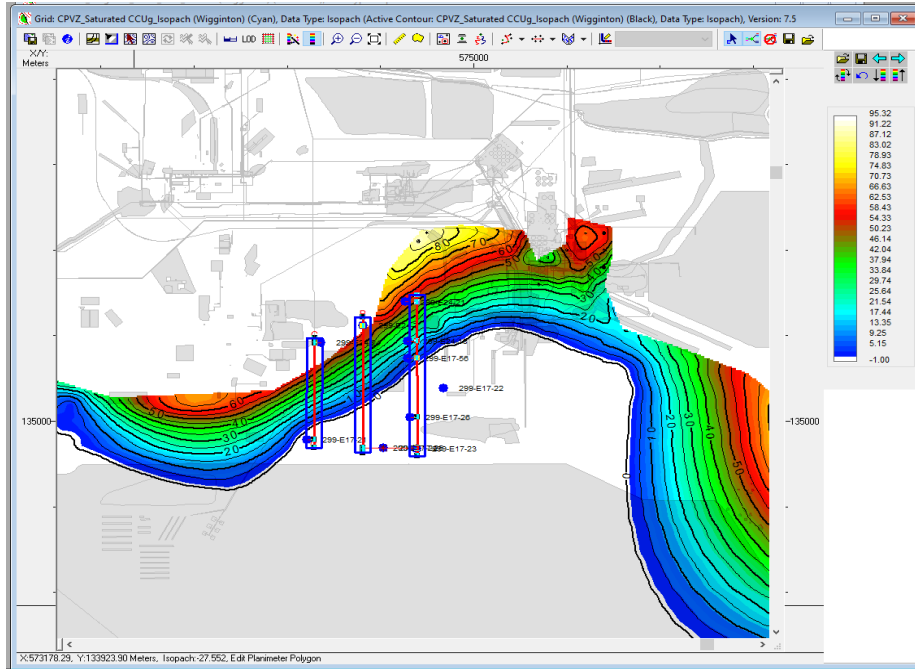
Source: Derived from ECF-HANFORD-18-0035, *Central Plateau Vadose Zone Geoframework.*

Note: Contours are in feet. Saturated thickness calculated by subtracting the elevation of the top of the Ringold Unit E (Rwie) from the long-term average steady-state water table elevation of 119.5 m above sea level. Based on the cross sections, the long-term steady-state water table is in the Cold Creek unit gravel (CCUg) in all except the southeast corner of the Integrated Disposal Facility (IDF) where it is in the Rwie. The saturated thickness of the CCUg thins to the southeast similar to the thinning of the Hanford formation unit 3 gravel in the IDF GFM (see Figure 3-52 of RPP-RPT-59958, *Performance Assessment for the Integrated Disposal Facility.*).

At the time of the development of the models and calculations used in the IDF PA, the available groundwater flow model was based on Central Plateau Groundwater Model (CPGWM) Version 6.3.3 documented in CP-47631, Rev. 2. The HSUs included in this groundwater flow model were based on a predecessor to the Hanford South GFM and included the Hanford formation and Rwie near the IDF. The calibrated hydraulic conductivities of the Hanford formation and the Rwie in the CPGWM Version 6.3.3 were 17,000 and 5 m/day, respectively. These values were used in the local-scale model of groundwater flow beneath the IDF as documented in RPP-CALC-61032, *Vadose Zone and Saturated Zone Flow and Transport Calculations for the Integrated Disposal Facility Performance Assessment* and summarized in RPP-RPT-59958. The calculated groundwater flow direction and flow rate in the Hanford formation beneath the IDF were controlled by the contrast in hydraulic conductivity between the Hanford formation and Rwie (defined by the results of the CPGWM Version 6.3.3) combined with the lateral continuity of the Hanford formation and Rwie defined in the Hanford South GFM and IDF GFM.

As summarized in the response to RAI 2-16, subsequent to the completion of the IDF PA updates to the groundwater flow model were completed. The most recent models are the CPGWM Version 8.4.5 (CP-47631, Rev. 4) and P2R Version 8.3 (CP-57037, Rev. 2). Both of these models modified the characteristics of the HSUs near the IDF by replacing the Hanford and Rwie HSUs directly beneath the IDF with a single HSU that represents sediments in the Hanford channel and is conceptualized as extending from Gable Gap through the 200 East Area in a northwest to southeast trend following the ancestral Columbia River channel. The extent and orientation of this Hanford channel HSU (called the high conductivity zone (HCZ) in the P2R model) is based on the low hydraulic gradients in the central and eastern portions of the 200 East Area as well as the trend of historic tritium plumes in the area. Figure 2-14-9 illustrates the extent of the HCZ modeled in the CPGWM Version 8.4.5 and P2R Versions 7.1 and 8.2 as well as the highly conductive Hanford formation modeled in Appendix L of the TC&WM EIS (DOE/EIS-0391).[80]

Based on the interpreted extent of the Hanford channel and the HCZ in the recent groundwater flow models (CPGWM Version 8.4.5 and P2R Version 8.3), the HSUs beneath the IDF footprint are comprised of the high-hydraulic conductivity Hanford/Cold Creek sediments and there is no evidence of the presence of the lower hydraulic conductivity Rwie. As noted in P2R Version 8.3 (CP-57037, Rev. 2), two explanations are possible for this inconsistency: either (a) the Rwie is not present as mapped in the GFMs, including the most recent CPVZ GFM (illustrated in Figures 2-14-6 to 2-14-8) or (b) the Rwie hydraulic properties have been significantly altered by the presence of the Hanford channel, resulting in the Rwie having a greater hydraulic conductivity in the channel area then in other areas of the model domain. In either case, the hydraulic conductivity of the sediments beneath the IDF is characterized by the Hanford channel deposits rather than the Hanford formation or Rwie away from the Hanford channel.

---

[80] As summarized in the response to RAI 2-16, the current version of the P2R model (version 8.3), did not fix the location of the HCZ but instead allowed the parameter estimation routine used in the model calibration to identify the model cells with a high-hydraulic conductivity within an area called the HCZ analysis area. The calibrated hydraulic conductivity values near the IDF are above 10,000 m/day.

Figure 2-14-9. Location of the High Conductivity Zone (Hanford Channel) Modeled in Central Plateau Groundwater Model Version 8.4.5 and Plateau to River Groundwater Model Version 8.3 and the Tank Closure and Waste Management Environmental Impact Statement.
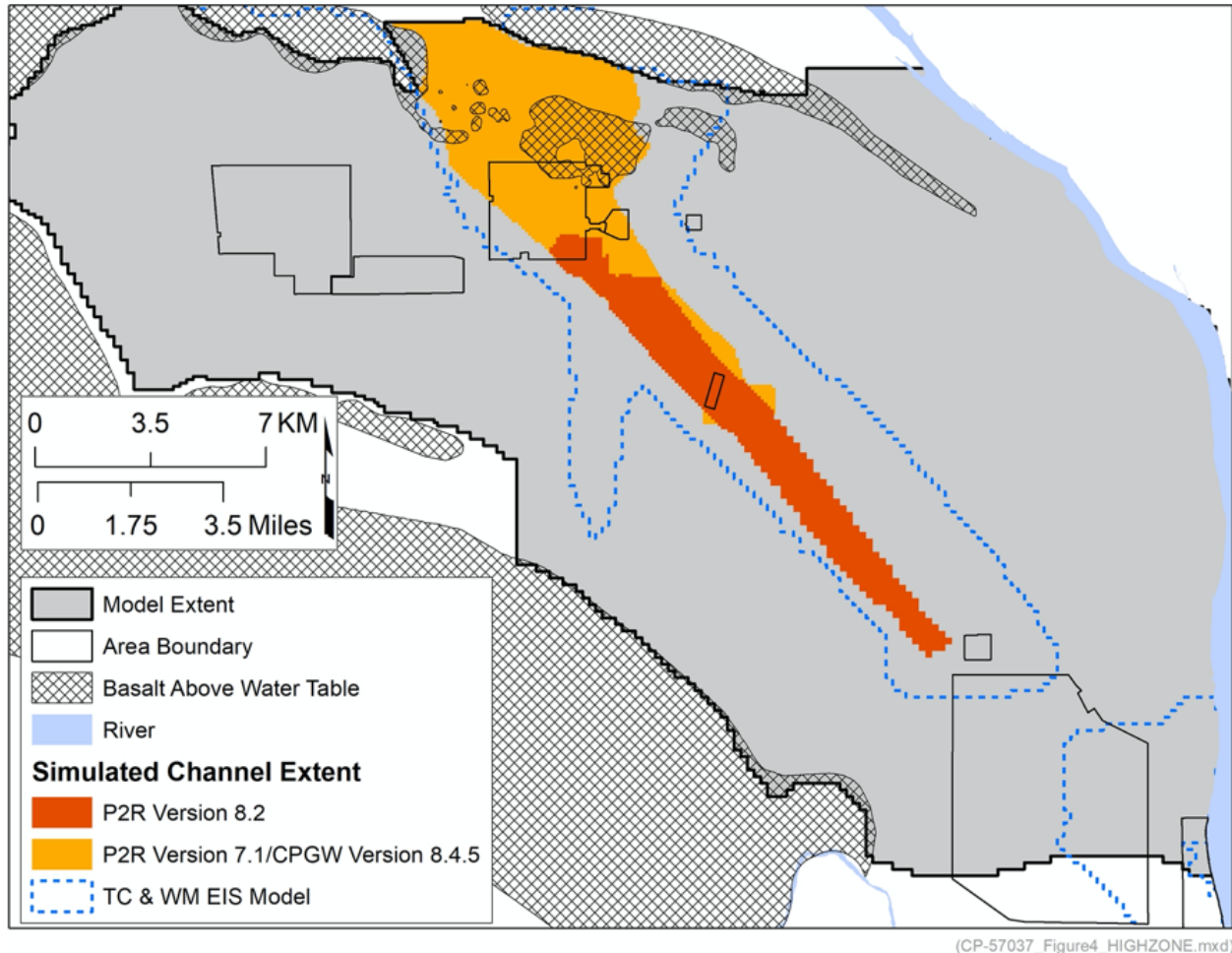
Source: CP-57037, *Model Package Report: Plateau to River Groundwater Model Version 8.3*, Rev. 2, Figure 4-4.

References:
CP-47631, *Model Package Report: Central Plateau Groundwater Model, Version 8.4.5*, Rev. 4.
DOE/EIS-0391, *Final Tank Closure and Waste Management Environmental Impact Statement for the Hanford Site, Richland, Washington*.

Note: The simulated channel extent in these models extends beneath the Integrated Disposal Facility footprint in the southcentral part of the 200 East Area.

Summary

The presence of the Rwie and the location of the Rwie/Hanford (or Rwie/Cold Creek) contact have changed over time as additional information has been developed and interpreted (or reinterpreted) by subject matter experts. Groundwater protection standards are applied at the point of highest concentration at a distance that is at least 100 meters from the disposed-of waste. If the point of highest concentration occurs in an unit that is re-interpreted to be Rwie, then the standards would be applied in the Rwie. In addition, the interpreted hydraulic characteristics of

the sediments in the southeastern part of the 200 East Area, including the area encompassing the footprint of the IDF, have changed over time with improved groundwater flow model calibrations. The current interpretation is that the high-energy gravel deposits in the Hanford channel (the HCZ in P2R Versions 8.2 and 8.3) comprise the HSU underlying the IDF. The calibrated hydraulic conductivity of these deposits is discussed in the response to RAI 2-16.

References

CP-47631, 2015, *Model Package Report: Central Plateau Groundwater Model Version 6.3.3*, Rev. 2, INTERA, Inc., Richland, Washington. Available at: https://pdw.hanford.gov/document/0077133H

CP-47631, 2018, *Model Package Report: Central Plateau Groundwater Model, Version 8.4.5*, Rev. 4, CH2M HILL Plateau Remediation Company, Richland, Washington. Available at: https://pdw.hanford.gov/document/0066449H.

CP-57037, 2020, *Model Package Report: Plateau to River Groundwater Model Version 8.3*, Rev. 2, CH2M HILL Plateau Remediation Company, Richland, Washington. Available at: https://pdw.hanford.gov/document/AR-03674.

CP-60925, 2018, *Model Package Report: Central Plateau Vadose Zone Geoframework Version 1.0*, Rev. 0, CH2M HILL Plateau Remediation Company, Richland, Washington. Available at: https://pdw.hanford.gov/arpir/index.cfm/viewDoc?accession=0065500H.

DOE/EIS-0391, 2012, *Final Tank Closure and Waste Management Environmental Impact Statement for the Hanford Site, Richland, Washington*, U.S. Department of Energy, Washington, D.C.

DOE/ORP-2000-24, 2001, *Hanford Immobilized Low-Activity Waste Performance Assessment: 2001 Version*, U.S. Department of Energy, Office of River Protection, Richland, Washington. Available at: https://www.osti.gov/servlets/purl/807263.

DOE/RL-97-69, 1998, *Hanford Immobilized Low-Activity Tank Waste Performance Assessment*, U.S. Department of Energy, Richland, Washington. Available at: https://www.osti.gov/servlets/purl/10148305.

ECF-200PO1-09-2074, 2010, *200-PO-1 Groundwater Operable Unit Remedial Investigation Report - Geologic Cross Sections*, Rev. 0, prepared by Freestone Environmental Services for CH2M HILL Plateau Remediation Company, Richland, Washington. Available at: https://pdw.hanford.gov/document/0084350.

ECF-HANFORD-13-0029, 2014, *Development of the Hanford South Geologic Framework Model, Hanford Site Washington*, Rev. 0, prepared by INTERA, Inc. for CH2M HILL Plateau Remediation Company, Richland, Washington. Available at: https://pdw.hanford.gov/document/0072753H.

ECF-HANFORD-13-0029, 2015, *Development of the Hanford South Geologic Framework Model, Hanford Site, Washington*, Rev. 1, prepared by INTERA, Inc. for CH2M HILL Plateau Remediation Company, Richland, Washington. Available at: https://pdw.hanford.gov/document/0080813H.

ECF-HANFORD-13-0029, 2015, *Development of the Hanford South Geologic Framework Model, Hanford Site, Washington*, Rev. 2, prepared by INTERA, Inc. for CH2M HILL Plateau Remediation Company, Richland, Washington. Available at: https://pdw.hanford.gov/document/0072751H.

ECF-HANFORD-13-0029, 2017, *Development of the Hanford South Geologic Framework Model, Hanford Site, Washington*, Rev. 3, prepared by INTERA, Inc. for CH2M HILL Plateau Remediation Company, Richland, Washington. Available at: https://pdw.hanford.gov/document/0072750H.

ECF-HANFORD-13-0029, 2017, *Development of the Hanford South Geologic Framework Model, Hanford Site, Washington Fiscal Year 2016 Update*, Rev. 4, prepared by INTERA, Inc. for CH2M HILL Plateau Remediation Company, Richland, Washington. Available at: https://pdw.hanford.gov/document/0072357H.

ECF-HANFORD-13-0029, 2018, *Development of the Hanford South Geologic Framework Model, Hanford Site, Washington*, Rev. 5, prepared by INTERA, Inc. for CH2M HILL Plateau Remediation Company, Richland, Washington. Available at: https://pdw.hanford.gov/document/0064943H.

ECF-HANFORD-18-0035, 2020, *Central Plateau Vadose Zone Geoframework*, Rev. 0, CH2M HILL Plateau Remediation Company, Richland, Washington. Available at: https://www.osti.gov/servlets/purl/1603767.

PNNL-14586, 2002, *Geologic Data Package for 2005 Integrated Disposal Facility Waste Performance Assessment*, Rev. 1, Pacific Northwest National Laboratory, Richland, Washington. Available at: https://www.pnnl.gov/main/publications/external/technical_reports/PNNL-14586Rev1.pdf.

PNNL-15237, 2005, *Geology of the Integrated Disposal Facility Trench*, Pacific Northwest National Laboratory, Richland, Washington.

PNNL-17913, 2009, *Hydrogeology of the Hanford Site Plateau – A Status Report for the 200 West Area*, Rev. 1, Pacific Northwest National Laboratory, Richland, Washington.

RPP-CALC-61032, 2018, *Vadose Zone and Saturated Zone Flow and Transport Calculations for the Integrated Disposal Facility Performance Assessment*, Rev. 0A, prepared by INTERA Inc. for Washington River Protection Solutions, LLC, Richland, Washington.

RPP-RPT-59343, 2016, *Integrated Disposal Facility Model Package Report: Geologic Framework*, Rev. 0, prepared by INTERA, Inc. for Washington River Protection Solutions, LLC, Richland, Washington.

RPP-RPT-59958, 2019, *Performance Assessment for the Integrated Disposal Facility, Hanford Site, Washington*, Rev. 1A, Washington River Protection Solutions, LLC, Richland, Washington.

SGW-63813, 2019, *Borehole Summary Report for the Installation of Six M-24 Wells in the 200-PO-1, 200-UP-1 and 300-FF-5 Operable Units, FY2019*, prepared by Freestone Environmental, Inc. for CH2M HILL Plateau Remediation Company, Richland, Washington. Available at: https://pdw.hanford.gov/document/AR-03916.

RAI 2-15 (Vadose Zone Parameters)

Comment
The log-normal fit of the van Genuchten alpha parameter for the H2 unit does not appear to represent the data well at the tails of the distribution..

Basis
To develop uncertainty distributions of unsaturated flow parameters the empirical data were fit with statistical distributions. The van Genuchten alpha parameter for the H2 unit was assigned a log-normal distribution. The fit of the equation to the data showed deviations at the tails of the distributions (See Figure 4-56 from the PA document provided below).

Figure 2-15-1. Fitted Log-Normal Distribution to the van Genuchten "Alpha" Parameter Data Set Used for the H2 Unit.
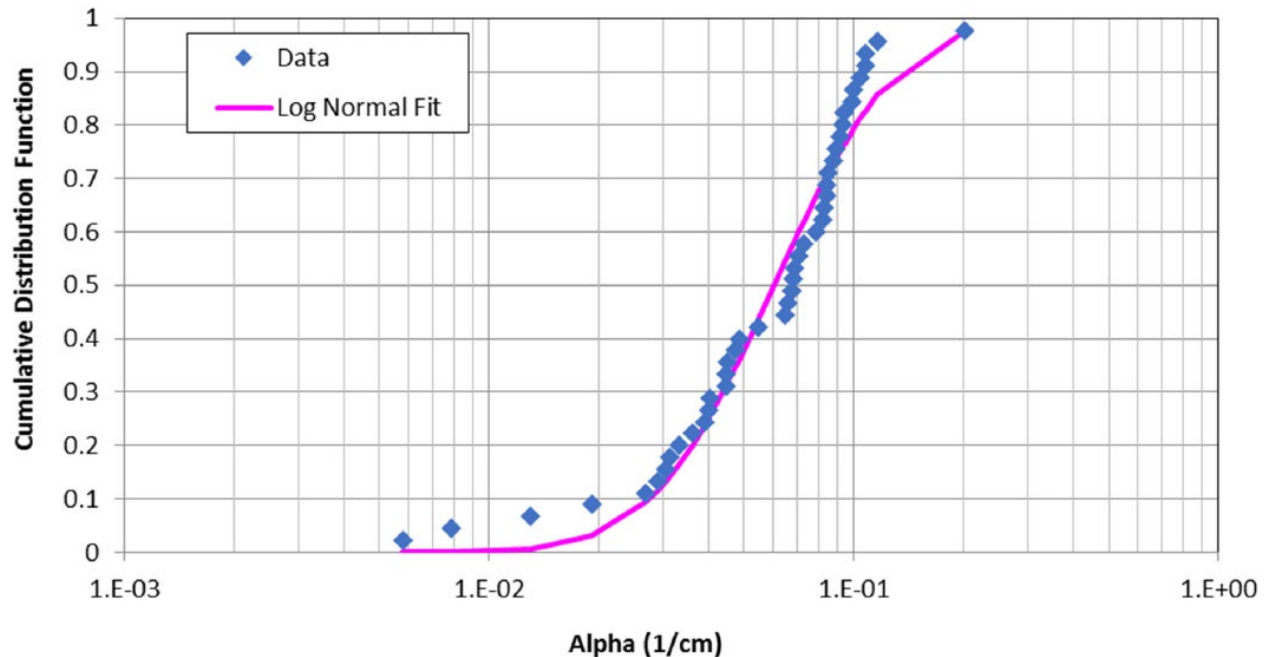
Source: Figure 4-56 of RPP-RPT-59958, *Performance Assessment for the Integrated Disposal Facility, Hanford Site, Washington*.

Path Forward
Please discuss the implications of the deviation in the fitted distributions from the underlying data..

DOE Response
The vadose zone hydraulic (van Genuchten-Mualem) parameter values used to evaluate the fate and transport of radionuclides released from the base of the IDF to the water table are uncertain. The parameter uncertainty is represented in the range of laboratory-measured moisture retention

curves for 44 samples of the H2 sand illustrated in Figures 3-76 and 3-77 of RPP-RPT-59958[81]. The range of moisture retention curves is the result of a range of values for the following van Genuchten-Mualem parameters presented in Table 3-5 of RPP-RPT-59958:

- Saturated moisture content (porosity)

- Residual moisture content

- van Genuchten parameter alpha

- van Genuchten parameter n (correlated to alpha as discussed in RPP-RPT-59958, Section 4.4.2.1.6)

- Saturated hydraulic conductivity (correlated to alpha as discussed in RPP-RPT-59958, Section 4.4.2.1.6).

Although the RAI specifically addresses the adequacy of fit for the van Genuchten parameter alpha, this RAI response discusses the adequacy of all five parameters to represent the underlying data because these parameters are used together to evaluate the uncertainty for the vadose zone hydraulic properties and the implication of this uncertainty on simulated groundwater concentrations and dose in the all-pathways exposure scenario. These five parameters and Equations 4.4.2.1-2 and 4.4.2.1-3 in RPP-RPT-59958 are used to estimate moisture content in the sediments below the IDF. This RAI response looks at how uncertainty in the underlying parameters translates to uncertainty in the predicted moisture content and then compares the predicted moisture content to observed values from boreholes near the IDF.

The response to this RAI is comprised of three parts: first, an evaluation of the impact the sampled uncertain H2 sand hydraulic parameter distributions have on the predicted moisture content in the H2 sand for a given estimate of the net infiltration rate near the IDF; second, an evaluation of the predicted moisture contents in the H2 sand using the H2 sand hydraulic parameter values compared to observed moisture contents in the H2 sand near the IDF; and third, an evaluation of the impact of using alternative vadose zone hydraulic property sets that are representative of the observed moisture contents in the H2 sand near the IDF.

Based on the result of the presented evaluations, it is concluded that: (a) the sampled distributions provide an adequate range of moisture retention parameter sets to capture the expected uncertainty in the performance of the vadose zone as a barrier on the predicted performance, and (b) the sampled distributions provide a reasonable match to moisture contents observed in sediment samples taken from boreholes drilled near the IDF.

---

[81] The discussion in this RAI response focuses on the vadose zone hydraulic parameter values of the H2 sand beneath the IDF and the approach used to evaluate the impact of the uncertainty in the H2 sand hydraulic parameter values in the IDF PA. A similar approach was applied to the H3 gravel; however, because the H3 gravel beneath the IDF is assumed to be analogous to the H3 gravel beneath WMA C, the range of uncertainty in the H3 gravel hydraulic parameter values is the same as that adopted for the WMA C PA (RPP-ENV-58782) as summarized in Section 4.4.2.1.6 of RPP-RPT-59958. Therefore, the uncertainty in the H3 gravel hydraulic parameter values is not discussed in this response.

Evaluation of Uncertain Moisture Retention Relationships to Define the Range of Uncertain Moisture Contents and Pore Velocities

The base case value for each of these five van Genuchten-Mualem parameters (along with the parameter L and the power averaged tensorial-connectivity-tortuosity (PA-TCT) parameter p used to define the moisture-dependent anisotropy (MDA) of the vadose zone sediments) was based on an upscaling of the 44 individual laboratory measured data sets as described in PNNL-23711 and summarized in Section 4.4.2.1.5 and Table 4-24 of RPP-RPT-59958.

To evaluate the uncertainty in the vadose zone hydraulic property values, the approach taken in the IDF PA (similar to the approach adopted in the WMA C PA documented in RPP-ENV-58782) was to fit empirical relationships to each of the five uncertain van Genuchten-Mualem parameter values using the 44 laboratory measured data sets for the H2 sand.

As noted in the RAI, the fitted relationships truncated the distributions at the lowest and highest observed values for each of the five van Genuchten-Mualem parameters. This truncation may affect the developed fitted relationships that are used to identify discrete van Genuchten-Mualem parameter values that are used to represent predicted moisture contents and pore velocities that encompass the range of possible outcomes.

The purpose of developing the fitted distributions to the laboratory-measured van Genuchten-Mualem parameter values is to evaluate the impact that the uncertainty in the vadose zone hydraulic parameter values has on the fate and transport of radionuclides released from engineered features of the IDF through the natural system beneath the IDF. This impact is realized by a change in the predicted moisture content which in turn impacts the interstitial pore water velocity. This velocity impacts the time it takes radionuclides released from the engineered barriers to be transported through the vadose zone to the underlying water table.

Although the RAI comments on one specific distribution for the vadose zone hydraulic property set, this response takes a holistic approach to address uncertainty in all of the parameters in the hydraulic property sets. Transport rates through the vadose zone are not all correlated to the alpha parameter mentioned in the RAI.[82]

The approach taken in the IDF PA was to sample the five uncertain fitted distributions (like the example of the fitted distribution for the van Genuchten alpha parameter illustrated in Figure 4-46 [included in the RAI basis]) 200 times and then to calculate the moisture content for an assumed vertical unsaturated hydraulic conductivity and the resulting pore velocity for each of the 200 sampled realizations. The resulting distribution of pore velocities was used to develop an abstraction to account for uncertainty in the hydraulic parameters in the uncertainty analysis. The vertical unsaturated hydraulic conductivity chosen for this calculation was 1.7 mm/yr

---

[82] Due to the relationship between alpha and the matric potential in the equations used to determine the moisture content for the assumed vertical hydraulic conductivity (RPP-RPT-59958 Equations 4.4.2.1-2 and 4.4.2.1-3), any change to the alpha value will result in a proportional but opposite change in the corresponding matric potential necessary to match the assumed vertical hydraulic conductivity. Consequently, the predicted moisture content computed using Equation 4.4.2.1-2 does not change when the estimate for alpha is overestimated in the uncertainty analysis.

because this is representative of the net infiltration rate in undisturbed areas near the IDF and is close to the mode of the net infiltration rate distribution in the uncertainty analysis in the IDF PA[83]. After sorting the 200 realizations by the pore velocity as represented in Figure 2-15-2, it was then assumed that the uncertainty in the hydraulic property set could be represented in the uncertainty analysis by using a flow field abstraction developed from process model simulations using the parameter values used to generate the 95th, 50th and 5th percentiles of the pore velocity (which correspond to the 5th, 50th, and 95th percentiles of the predicted moisture content, respectively). These cases were called cases Vzp04, Vzp03 and Vzp05, respectively, if the properties are assumed to be isotropic and cases Vzp14, Vzp13 and Vzp12, respectively, if the properties are assumed to have a low anisotropy when using the PA-TCT representation of MDA. The van Genuchten-Mualem parameter values for these cases are reproduced from RPP-RPT-59958 Table 5-47 in Table 2-15-1.

The resulting pore velocity distribution for the 200 realizations developed to evaluate the impact of vadose zone hydraulic property uncertainty is illustrated in Figure 2-15-2. The predicted moisture content for these same 200 realizations is illustrated in Figure 2-15-3. The sampled values for the realizations corresponding to the 5th-, 50th, and 95th percentiles of the vertical pore velocity were used in simulations to develop the moisture profile and Darcy flux in the vadose zone that are used for fate and transport calculations.

---

[83] The net infiltration rate through undisturbed surface soils near the IDF is uncertain. Different values of net infiltration have been recommended by previous researchers. Net infiltration values typically used for the types of soils present near the IDF (Burbank Loamy Sand and Rupert Sand) with mature shrub-steppe vegetation are 3.0 mm/yr and 4.0 mm/yr (PNNL-14702, *Vadose Zone Hydrogeology Data Package for Hanford Assessments*), respectively, with a typical average recommended value of 3.5 mm/yr. This was the value adopted in the TC&WM EIS (DOE/EIS-0391) for the Central Plateau and the value used for the post-barrier design life net infiltration rate base case in the IDF PA (see Tables 2-9, 2-12 and 2-13 and Section 4.4.1.1 of RPP-RPT-59958). Near the IDF, PNNL-14744, *Recharge Data Package for the 2005 Integrated Disposal Facility Performance Assessment* noted that the designation of the soil type is complicated by the presence of silt layers near the surface and recommended that the soil type be classified as a combined Rupert Sand/Burbank Loamy Sand with a best-estimate net infiltration rate of 0.9 mm/yr (with a lower estimated bound of 0.16 mm/yr and an upper estimated bound of 2.1 mm/yr). The value of 0.9 mm/yr was also used for the post-barrier design life net infiltration rates through the IDF-East surface barrier in the TC&WM EIS (DOE/EIS-0391) based on agreements documented in DOE, 2005, *Technical Guidance Document for Tank Closure Environmental Impact Statement Vadose Zone and Groundwater Revised Analyses*. Based on the range of 0.9 mm/yr to 3.5 mm/yr, the IDF PA used a nominal value of 1.7 mm/yr (about a factor of 2 times greater than recommended 0.9 mm/yr value and about a factor of 2 times less than the agreed-to 3.5 mm/yr value) which is close to the mode of 1.9 mm/yr of the uncertainty distribution of post-barrier design life net infiltration rate. The value of 1.7 mm/yr also corresponds to the value used for the ERDF PA (WCH-520, *Performance Assessment for the Environmental Restoration Disposal Facility, Hanford Site, Washington*).

Figure 2-15-2. Cumulative Distribution Function of Vertical Pore Velocity Assuming a Vertical Darcy Flux of 1.7 mm/yr.
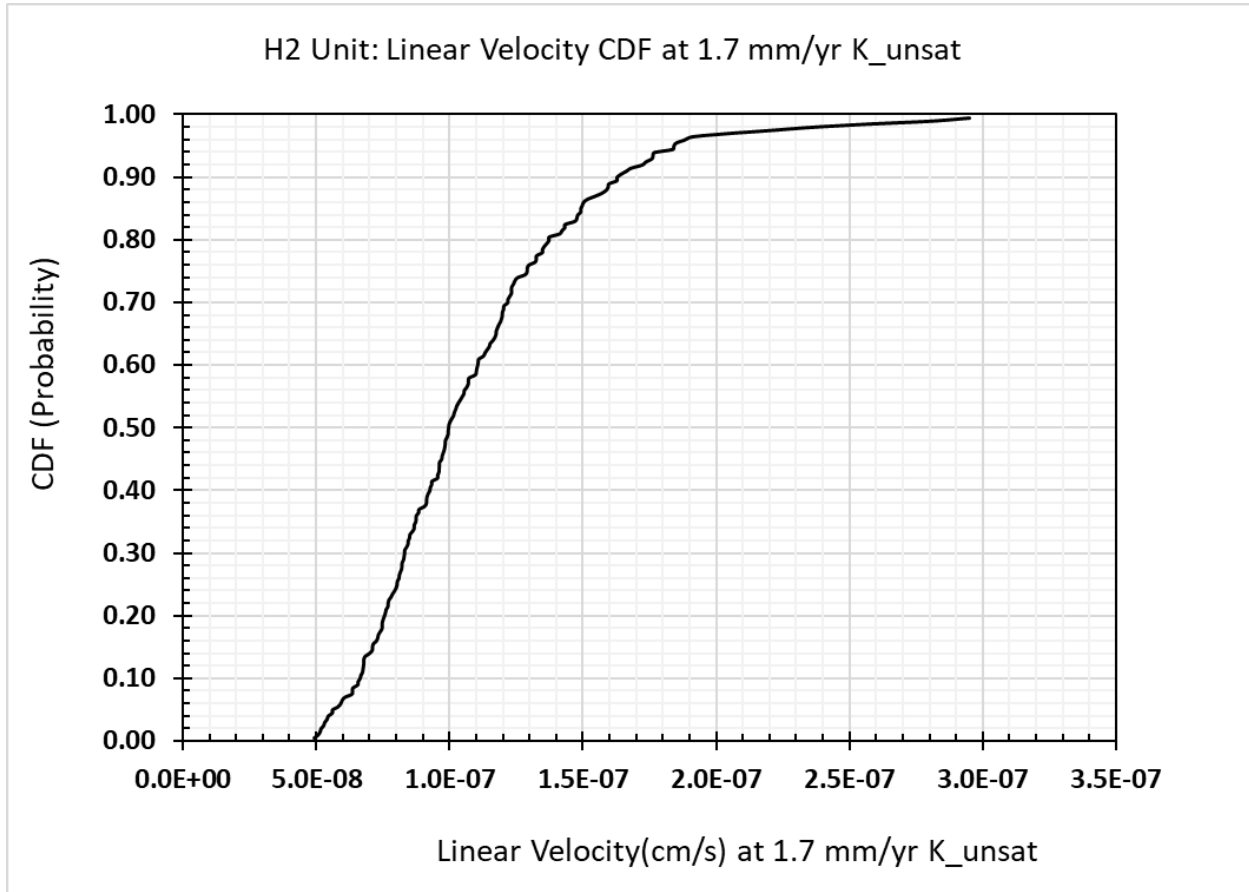
Source: RPP-RPT-59958, *Performance Assessment for the Integrated Disposal Facility, Hanford Site, Washington*, Figure 4-65.

Note: Cumulative Distribution Function (CDF) is based on 200 realizations of sampled values of H2 sand hydraulic (van Genuchten-Mualem) parameter values: (1) saturated moisture content, (2) residual moisture content, (3) van Genuchten alpha, (4) van Genuchten n and (5) saturated vertical hydraulic conductivity. Linear velocity is the vertical velocity assuming the vertical Darcy flux is 1.7 mm/yr and a unit hydraulic gradient. The 95th, 50th and 5th percentile linear pore velocity values are 1.85E-07 cm/s, 1.00E-07 cm/s and 5.62E-08 cm/s, respectively.

The numerical value labels on the x-axis have been edited to reflect two digits; these labels displayed incorrectly when just a single digit was shown.

To evaluate the impact of the sampled distributions of the uncertain van Genuchten-Mualem parameter values (i.e., the saturated moisture content, residual moisture content, van Genuchten alpha, van Genuchten n and saturated vertical hydraulic conductivity) on the predicted moisture content for an assumed vertical Darcy flux of 1.7 mm/yr (corresponding to a vertical hydraulic conductivity of 1.7 mm/yr given a unit vertical hydraulic gradient), five cross plots are presented in Figure 2-15-4. Cross plots provide an indication of how strongly each uncertain

van Genuchten-Mualem parameter influences the predicted moisture content calculated using RPP-RPT-59958 Equations 4.4.2.1-2 and 4.4.2.1-3. These plots illustrate the following.

- The predicted moisture content is most affected by the sampled values of the residual moisture content and the van Genuchten n parameter values and to a lesser extent by the saturated vertical hydraulic conductivity.

- The predicted moisture content is not significantly affected by the sampled values of the saturated moisture content or the van Genuchten alpha parameter values.

- The predicted moisture content decreases with a decrease in the sampled residual moisture content value. The minimum residual moisture content in the assumed uniform distribution is 0.0 and several realizations with values close to 0.0 were sampled from the distribution. The sampled residual moisture content value for the 95th percentile realization is 0.0077.

- The predicted moisture content decreases with an increase in the van Genuchten n parameter value. The maximum observed value in the 44 laboratory-measured samples was 3.182 but this sample also had the maximum laboratory-measured residual moisture content of 0.046 (see Sample 110U in Table 3-5 of RPP-RPT-59958). The sampled van Genuchten n parameter value for the 95th percentile realization is 2.398.

Table 2-15-1. van Genuchten-Mualem Parameter Values used for Base Case and Sensitivity Analyses.

Case or Realization	H2 Vadose Zone Hydraulic Property Sets						
	Ksat (cm/s)	Saturated Moisture Content (-)	Residual Moisture Content (-)	Alpha (1/cm)	n (-)	m (1-1/n)	L
Base Case (Vzp00)	6.20E-03	0.384	0.029	0.0642	1.698	0.411	0.5
121 (Vzp03)	1.40E-03	0.337	0.0183	0.0288	1.814	0.449	0.5
73 (Vzp04)	5.95E-04	0.320	0.00766	0.0366	2.398	0.583	0.5
(Vzp05)	4.84E-04	0.414	0.0317	0.0390	1.694	0.410	0.5

Ksat = Vertical saturated hydraulic conductivity

Case Vzp04 represents one of the 200 realizations used to evaluate the effect of uncertainty in van Genuchten-Mualem parameter values on vadose zone transport and represents the 95th percentile of the vadose zone pore velocity (equivalent to the 5th percentile of the moisture content) for a vertical Darcy flux of 1.7 mm/yr.
Case Vzp03 represents one of the 200 realizations used to evaluate the effect of uncertainty in van Genuchten-Mualem parameter values on vadose zone transport and represents the 50th percentile of the vadose zone pore velocity (equivalent to the 50th percentile of the moisture content) for a vertical Darcy flux of 1.7 mm/yr.
Case Vzp05 represents one of the 200 realizations used to evaluate the effect of uncertainty in van Genuchten-Mualem parameter values on vadose zone transport and represents the 5th percentile of the vadose zone pore velocity (equivalent to the 95th percentile of the moisture content) for a vertical Darcy flux of 1.7 mm/yr.

Figure 2-15-3. Distribution of Predicted H2 Sand Volumetric Moisture Content for 200 Realizations of Uncertain Vadose Zone Property Sets.
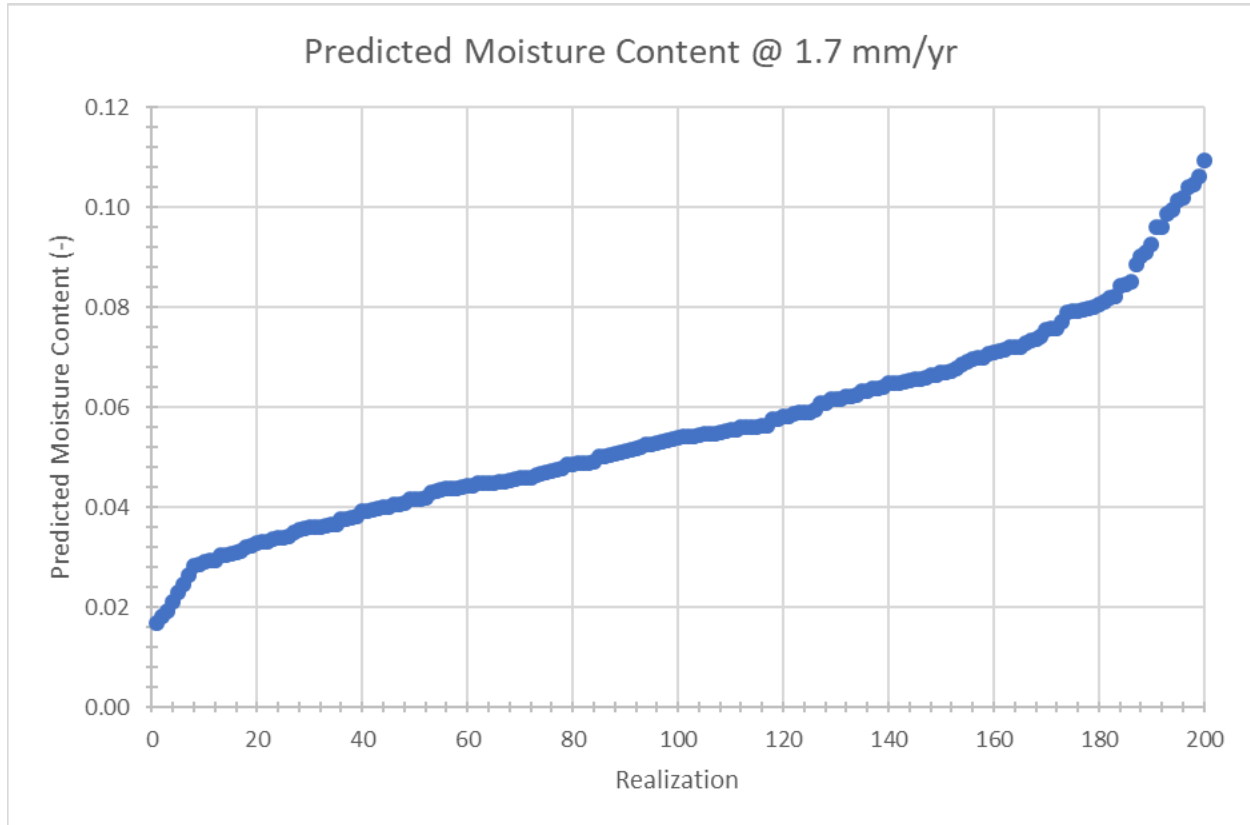
Note: Predicted moisture content distribution assuming a vertical Darcy flux of 1.7 mm/yr for the 200 realizations used to calculate the 5th, 50th and 95th percentile pore velocity distribution. The 200 realizations are sorted from the minimum moisture content of 0.0167 to the maximum value of 0.1093. The 95th percentile of pore velocity corresponds to the 5th percentile of moisture content. The 95th, 50th and 5th percentile pore velocity values are 1.85E-07 cm/s, 1.00E-07 cm/s and 5.62E-08 cm/s, respectively. The corresponding 5th, 50th and 95th percentile moisture contents are 0.0292, 0.0540 and 0.0960, respectively. For comparison purposes, the moisture content predicted for the base case parameter values (case Vzp00) for 1.7 mm/yr is 0.063.

The range of predicted moisture contents in the H2 sand from about 0.016 to 0.11 for an assumed net infiltration rate (and corresponding vertical Darcy flux and vertical unsaturated hydraulic conductivity for a unit hydraulic gradient) of 1.7 mm/yr is representative of the uncertainty in the van Genuchten-Mualem parameter values. For the purpose of identifying discrete cases that represent the range of possible moisture contents based on uncertain van Genuchten-Mualem parameter values, the selection of the 95th, 50th-, and 5th percentile pore velocity cases (i.e., cases Vzp04, Vzp03, and Vzp05 or cases Vzp14, Vzp13, and Vzp12, respectively) is appropriate.

Figure 2-15-4. Cross-Plots of Predicted H2 Sand Volumetric Moisture Content versus Uncertain Vadose Zone Parameter Values for a Vertical Darcy Flux of 1.7 mm/yr. (sheet 1 of 2)
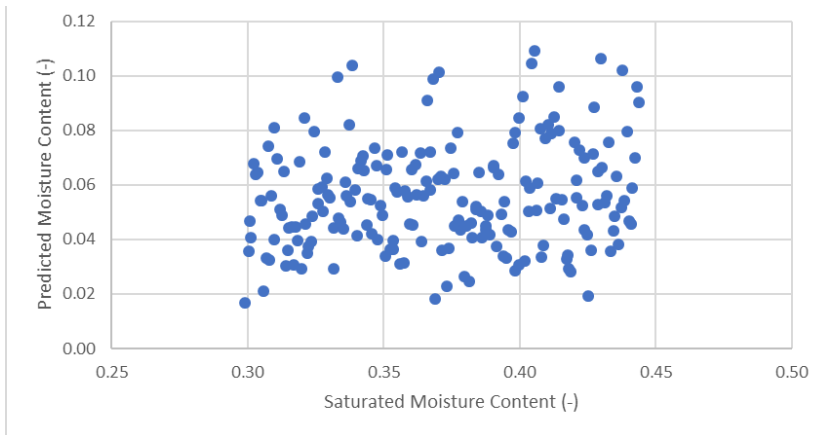
Saturated Moisture Content
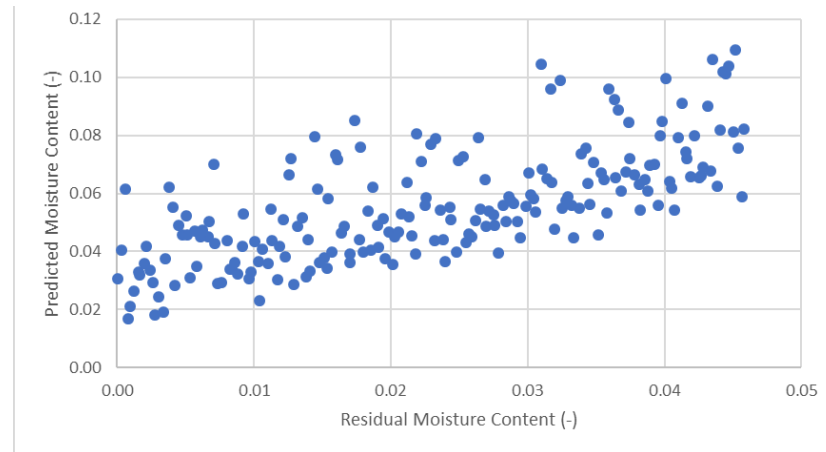
Residual Moisture Content
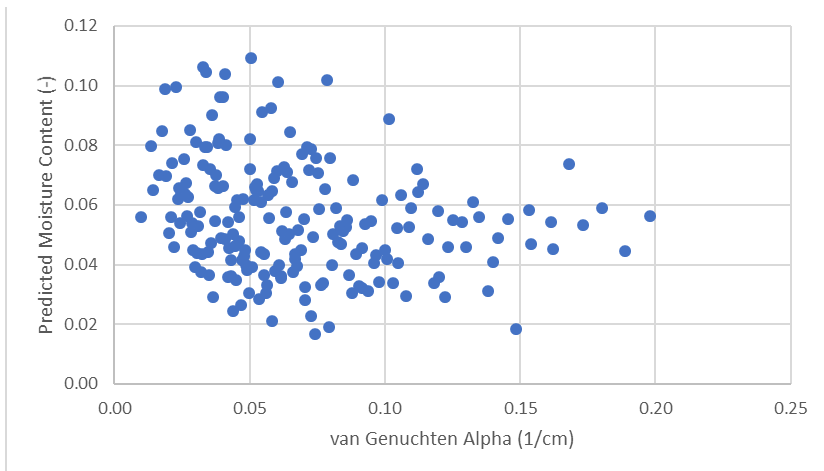
van Genuchten Alpha
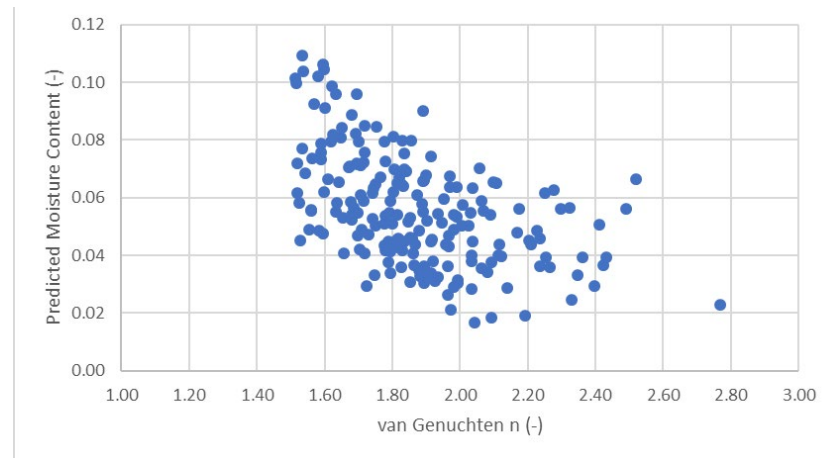
van Genuchten n

Figure 2-15-4. Cross-Plots of Predicted H2 Sand Volumetric Moisture Content versus Uncertain Vadose Zone Parameter Values for a Vertical Darcy Flux of 1.7 mm/yr. (sheet 2 of 2)
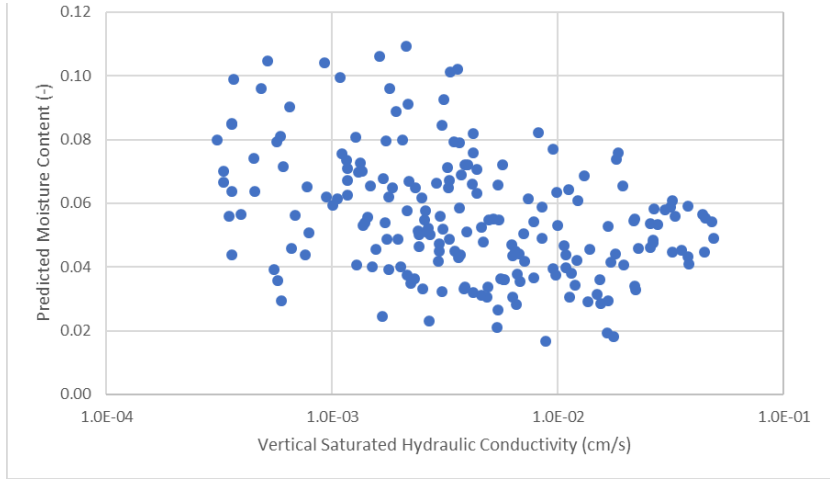
Saturated Hydraulic Conductivity

Note: Derived from Excel® (a registered trademark of Microsoft Corporation in the U.S. and other countries) file used to create the distributions and results used in Figure 4-65 of RPP-RPT-59958, *Performance Assessment for the Integrated Disposal Facility, Hanford Site, Washington.*

The hydraulic property sets for the discrete cases developed to represent the uncertainty in the vadose zone hydraulic parameter values are illustrated in Figure 2-15-5 in comparison to the base case property set (Vzp00) recommended in PNNL-23711. The resulting vertical moisture content profiles calculated using STOMP for these cases are illustrated in Figure 2-15-6 for an assumed net infiltration rate of 1.7 mm/yr[84]. For comparison purposes, Figure 2-15-6 also includes a case using the vadose zone hydraulic property set used in the TC&WM EIS (DOE/EIS-0391). As expected, the 50th percentile case (Vzp03) produces moisture content results that are similar to the base case (Vzp00). As will be discussed in the next section, the van Genuchten-Mualem parameter values represented by case Vzp04 or Vzp14 produce predicted moisture contents that are representative of observed moisture contents in sediment samples taken from boreholes near the IDF.

Evaluation of Alternative Moisture Retention Relationships Compared to Observed Moisture Contents in the H2 Sand near the IDF

The uncertainty in vadose zone hydraulic (van Genuchten-Mualem) parameter values was evaluated using process model sensitivity cases and an abstraction developed from these sensitivity cases. The process model sensitivity cases applied parameter values that reproduced the 95th, 50th and 5th percentile of the pore velocity distribution assuming either an isotropic MDA (cases Vzp04, Vzp03 and Vzp05, respectively) or a low anisotropy MDA (cases Vzp14, Vzp13 and Vzp12, respectively). The complete range of predicted moisture contents for an assumed net infiltration rate (and corresponding vertical Darcy flux) of 1.7 mm/yr illustrated in Figure 2-15-3 is captured by using the discrete cases that supplement the calculations using the base case (Vzp00) property set recommended by PNNL-23711.

The impact of using the different vadose zone property sets was evaluated in different vadose zone sensitivity analyses summarized in Section 5.2.4.3 of RPP-RPT-59958. These vadose zone sensitivity cases were run to define the uncertainty in the predicted moisture content as summarized in Section 5.2.4.8 of RPP-RPT-59958. Additional vadose zone sensitivity cases that were not summarized in RPP-RPT-59958 were performed and documented in RPP-CALC-61032. These sensitivity analyses provide information that can be used to compare the predicted moisture content in the H2 sand for a range of vadose zone property sets and recharge (i.e., net infiltration) conditions to observed moisture content in the H2 sand near the IDF[85].

---

[84] The selection of 1.7 mm/yr for this comparison was based on the observation that it is a about a factor of 2 times greater than the base case of 0.9 mm/yr used for most of the calculations of the IDF-East in the TC&WM EIS (DOE/EIS-0391) and about a factor of 2 times less than the base case assumed value of 3.5 mm/yr used for the IDF PA (RPP-RPT-59958). It also is close to the 1.9 mm/yr value used for the mode of the uncertainty distribution of net infiltration rate used in the uncertainty analyses (Section 6.0) of the IDF PA (RPP-RPT-59958).

[85] Observations of moisture content in the H2 sand have been reported in several PNNL reports based on laboratory analyses of sediment samples taken during drilling of nearby wells. This information is supplemented by neutron probe measurements and neutron moisture logging results of other wells. There are no observations of moisture content in the H3 gravel near the IDF due to the difficulty in retrieving samples from the H3. Therefore, this discussion focuses on comparing the observed H2 sand moisture contents with the predicted moisture contents using estimated net infiltration rates (and corresponding vertical Darcy fluxes) near the boreholes with observed moisture contents.

Figure 2-15-5. Comparison of Vadose Zone Hydraulic Parameter Sets for the H2 Sand.
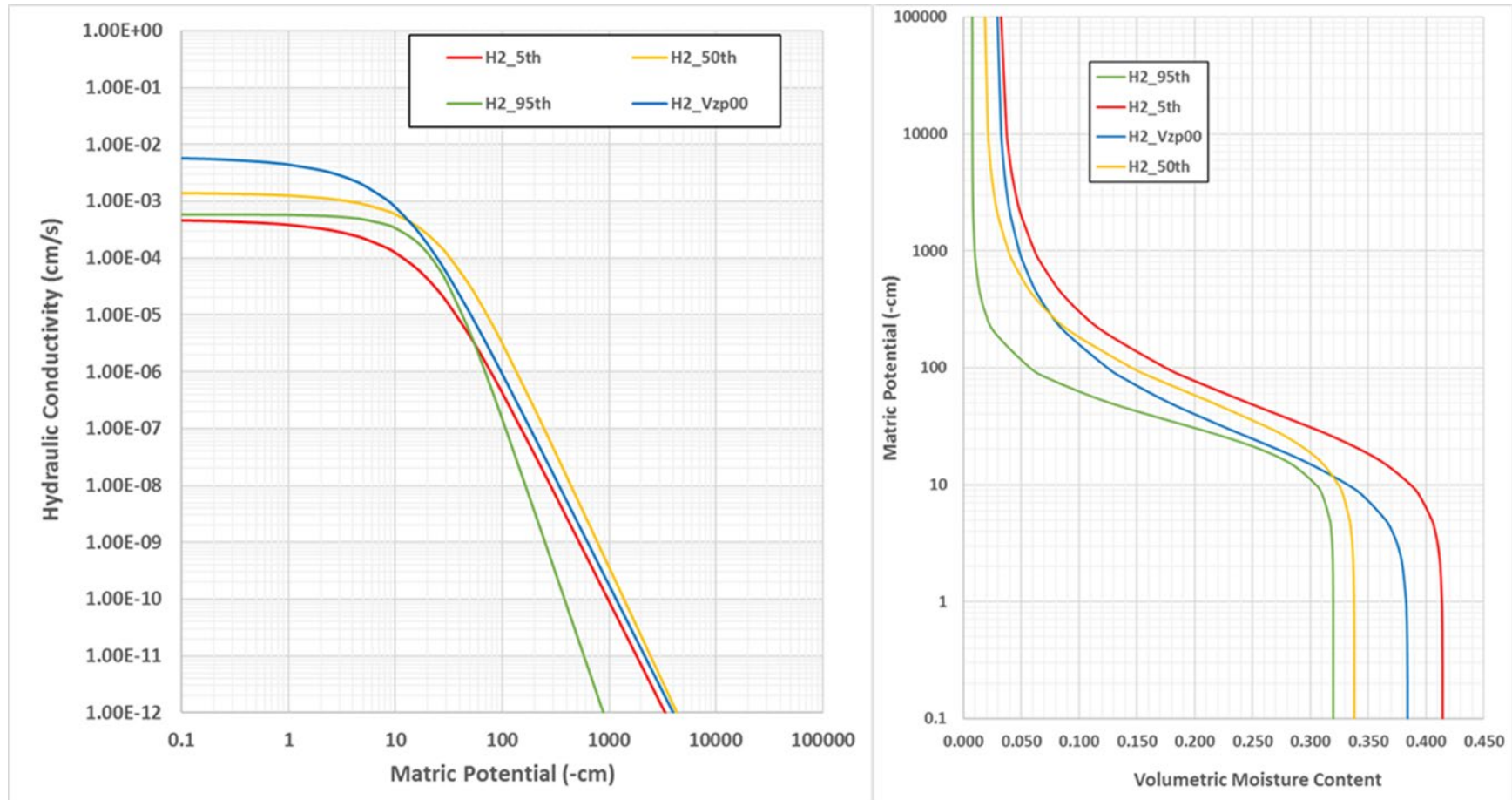
Source: RPP-CALC-61032, *Vadose Zone and Saturated Zone Flow and Transport Calculations for the Integrated Disposal Facility Performance Assessment*, Figure B-25.

Note: Case Vzp00 corresponds to the base case vadose zone hydraulic parameter set for the H2 sand used in the Integrated Disposal Facility Performance Assessment. The 5th, 50th and 95th cases represent hydraulic parameter sets that correspond to the 5th, 50th and 95th percentiles of the pore velocity distribution assuming a vertical Darcy flux of 1.7 mm/yr. They correspond to cases Vzp05, Vzp03 and Vzp04, respectively, for the isotropic moisture-dependent anisotropy.

Figure 2-15-6. Predicted Vertical Moisture Profile Under Integrated Disposal Facility for Different Hydraulic Parameter Sets.
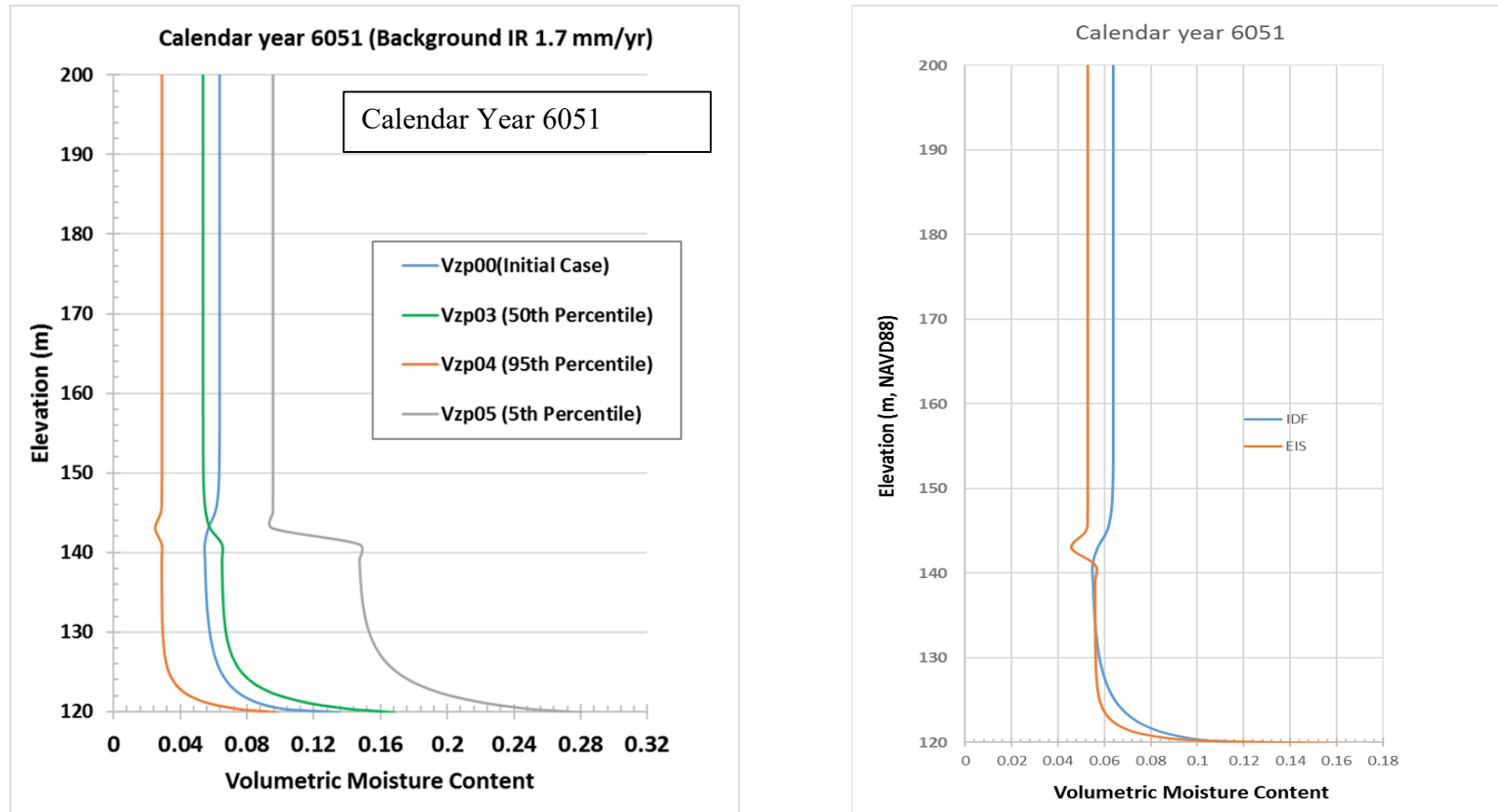
Source: RPP-RPT-59958, *Performance Assessment for the Integrated Disposal Facility, Hanford Site, Washington*, Figures 4-71 and 5-149, derived from RPP-CALC-61032, *Vadose Zone and Saturated Zone Flow and Transport Calculations for the Integrated Disposal Facility Performance Assessment*, Figures B-29 and 7-123.

Note: Vzp00 corresponds to the base case vadose zone hydraulic property set used in the Integrated Disposal Facility (IDF) Performance Assessment. Vzp03, Vzp04 and Vzp05 correspond to the vadose zone hydraulic property sets that result in 50th, 95th and 5th percentiles of the pore velocity (or 50th, 5th and 95th percentiles of the moisture content) assuming a 1.7 mm/yr net infiltration rate and a unit hydraulic gradient. The environmental impact statement (EIS) case corresponds to the base case vadose zone hydraulic property set used in DOE/EIS-0391, *Final Tank Closure and Waste Management Environmental Impact Statement for the Hanford Site, Richland, Washington*. The results assume a uniform net infiltration rate of 1.7 mm/yr through the surface barrier and IDF starting after the assumed 500-year design life of the surface barrier. The selected time (calendar year 6051) corresponds to a time close to the peak [129]I release rate from the vadose zone to the saturated zone.

NAVD88 = *North American Vertical Datum of 1988*

Example plots illustrating the range of predicted moisture contents for different vadose zone property sets are presented in Figure 2-15-7 for long-term average net infiltration rates of 3.5 mm/yr, 1.7 mm/yr and 0.9 mm/yr. These plots illustrate the temporal evolution of the moisture content at a point beneath the IDF liner system that is at an elevation of 169 m asl. This elevation corresponds to the middle of the H2 sand beneath the IDF as the base of the IDF liner system is about at an elevation of 204 m asl and the H2 sand is about 70 m thick beneath the base of the IDF liner system. The three different net infiltration rates are selected for the following reasons.

- 3.5 mm/yr represents the long-term steady-state net infiltration rate assumed for the post-design life of the IDF surface barrier. It represents the base case value assumed in the IDF PA. It also represents an average of the net infiltration rate in the undisturbed Burbank Loamy Sand and Rupert Sand soils with mature shrub-steppe vegetation (with best-estimate net infiltration rates of 3.0 mm/yr and 4.0 mm/yr, respectively, based on PNNL-14702) in other areas of the Central Plateau of the Hanford Site. This value was used for the net infiltration rate through surface barriers after their design life for other areas on the Central Plateau in the TC&WM EIS (DOE/EIS-0391).

- 1.7 mm/yr is the average value for Rupert Sand with mature shrub-steppe vegetation in the Central Plateau recommended in PNNL-16688, *Recharge Data Package for Hanford Single-Shell Tank Waste Management Areas*. This also represents a value about 2 times less than the 3.5 mm/yr case and 2 times greater than the 0.9 mm/yr case. This value was also used for the base case net infiltration rate in the ERDF PA (WCH-520, *Performance Assessment for the Environmental Restoration Disposal Facility, Hanford Site, Washington*). This value is also close to the 1.9 mm/yr used as the mode of the uncertainty distribution of post-design life net infiltration rates used in the IDF PA uncertainty analysis (Section 6.0 of RPP-RPT-59958).

- 0.9 mm/yr represents the best-estimate value of average net infiltration rate in undisturbed surface soils near the IDF recommended in PNNL-14744. This value was based on an average of seven discrete estimates of net infiltration rate using the chloride mass balance approach discussed in PNNL-14744 and recognizes the unique characteristics of the surface soils near IDF and the role that eolian silt deposits near the IDF can have on net infiltration in the area[86]. This value was also used for the post-design life infiltration rate through the surface barrier for most of the calculations of IDF-East in the TC&WM EIS.

---

[86] As summarized in PNNL-14744, the range of net infiltration rates in undisturbed area near the IDF is estimated to be between 0.16 mm/yr and 2.1 mm/yr. In addition, PNNL-14744 notes that the net infiltration rate through the layered soils near IDF can be significantly affected by the contrasting textures of the sediments in nearly horizontal layers of alternating sands, gravels, and fines observed near the IDF that can create capillary breaks that impede infiltration: "The water storage capacity of the eolian material residing above the layers will influence the potential deep drainage rate. Depths of eolian material between 1.0 and 2.0 m may be ideal for storing all precipitation till it can be removed by evapotranspiration, thus significantly reducing deep drainage rates. If thinner than 1.0 m, the eolian material may not be able to store all winter precipitation. If thicker than 2.0 m, the eolian material can store the precipitation, but the water stored near the deep capillary break may be too deep to be removed by evapotranspiration. In either case, the result is an increased potential for higher drainage rates."

Figure 2-15-7. Calculated Moisture Content in the Middle of H2 Sand at 169-meter Elevation with Different Vadose Zone Hydraulic Parameter Sets and Background Infiltration Rates. (sheet 1 of 3)

(a) Background Infiltration Rate of 3.5 mm/yr
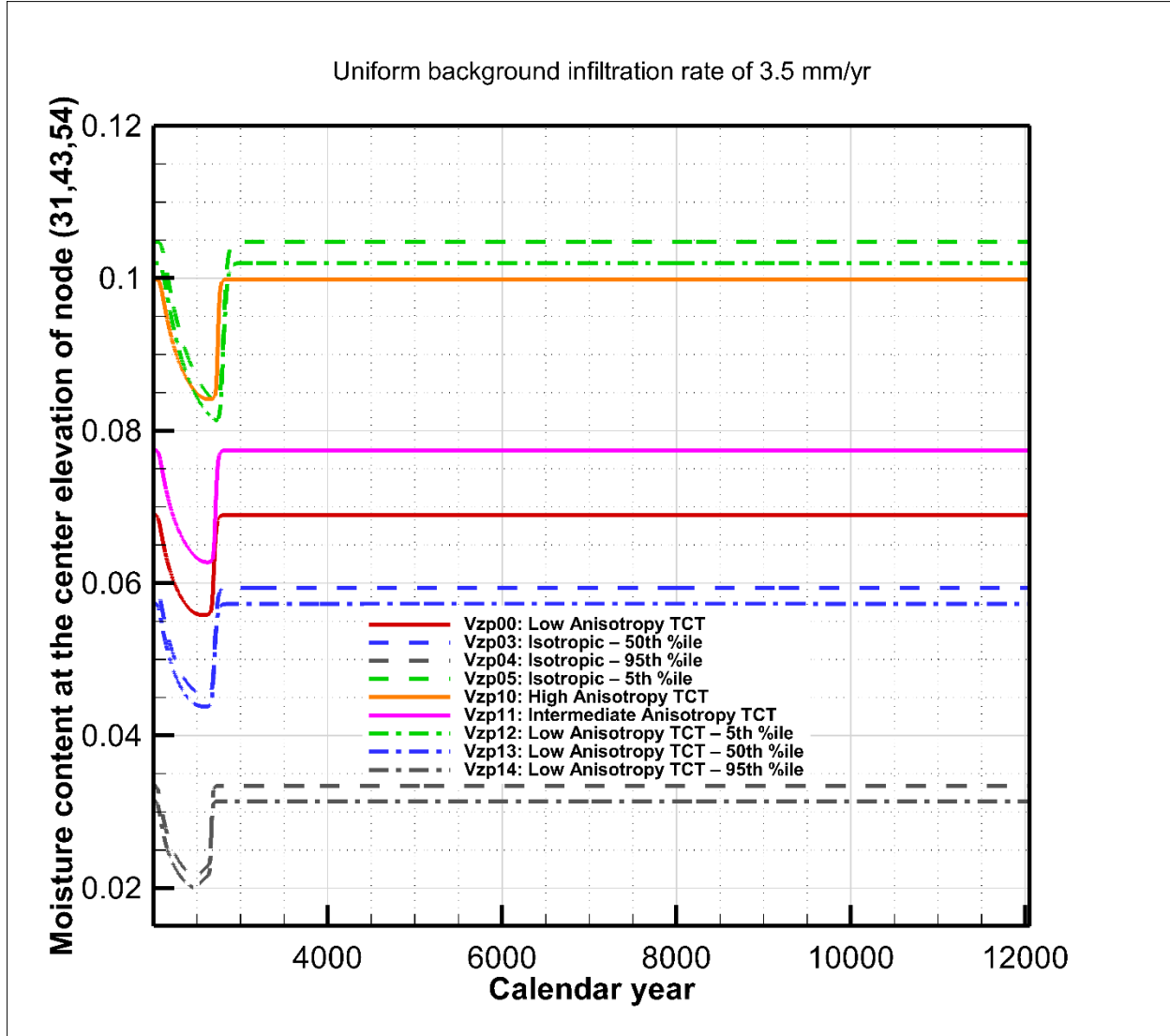
Source: RPP-CALC-61032, *Vadose Zone and Saturated Zone Flow and Transport Calculations for the Integrated Disposal Facility Performance Assessment*, Figure 7-170.

Note: The uniform background infiltration rate of 3.5 mm/yr is applied through the surface barrier after the 500-year design life of the surface barrier, i.e., starting in calendar year (CY) 2551. From CY 2005 to 2151, the vertical Darcy flux through the liner system is 0.0 mm/yr due to the operations of the leachate recovery system. From CY 2151 to 2551, the vertical Darcy flux through the liner system is assumed to be 0.5 mm/yr. The steady-state moisture content for the base case property set (Vzp00) is about 0.069. The steady-state moisture content for the 95th percentile pore velocity case (Vzp04) is about 0.034.

TCT = tensorial-connectivity-tortuosity

**Figure 2-15-7. Calculated Moisture Content in the Middle of H2 Sand at
169-meter Elevation with Different Vadose Zone Hydraulic Parameter
Sets and Background Infiltration Rates. (sheet 2 of 3)**

(b) Background Infiltration Rate of 1.7 mm/yr

Source: RPP-CALC-61032, Figure 7-182.

Note: The uniform background infiltration rate of 1.7 mm/yr is applied through the surface barrier after the 500-year design life of the surface barrier, i.e., starting in CY 2551. From CY 2005 to 2151, the vertical Darcy flux through the liner system is 0.0 mm/yr due to the operations of the leachate recovery system. From CY 2151 to 2551, the vertical Darcy flux through the liner system is assumed to be 0.5 mm/yr. The steady-state moisture content for the base case property set (Vzp00) is about 0.063. The steady-state moisture content for the 95th percentile pore velocity case (Vzp04) is about 0.029.

TCT = tensorial-connectivity-tortuosity

**Figure 2-15-7. Calculated Moisture Content in the Middle of H2 Sand at
169-meter Elevation with Different Vadose Zone Hydraulic Parameter
Sets and Background Infiltration Rates. (sheet 3 of 3)**

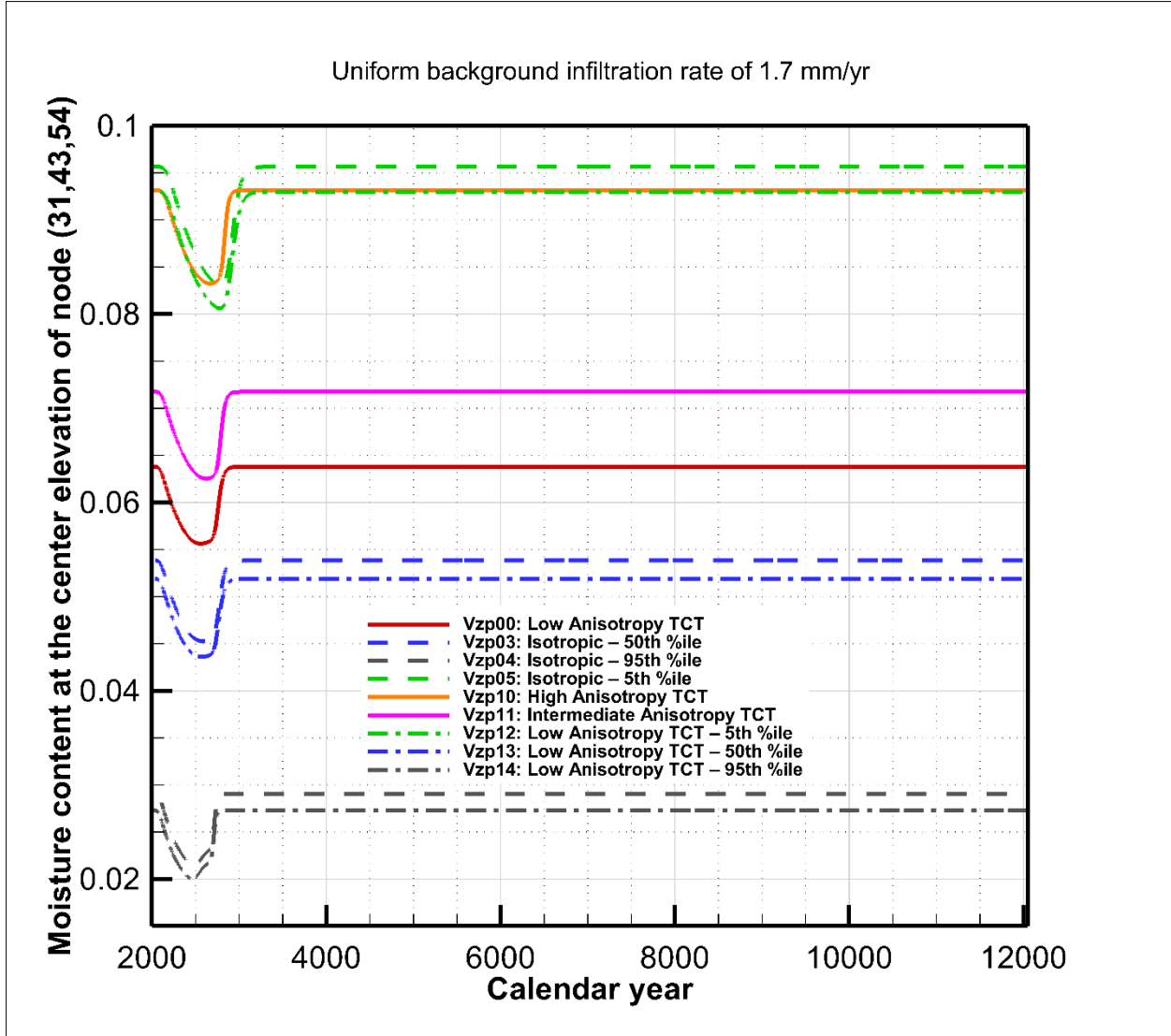**(c) Background Infiltration Rate of 0.9 mm/yr**
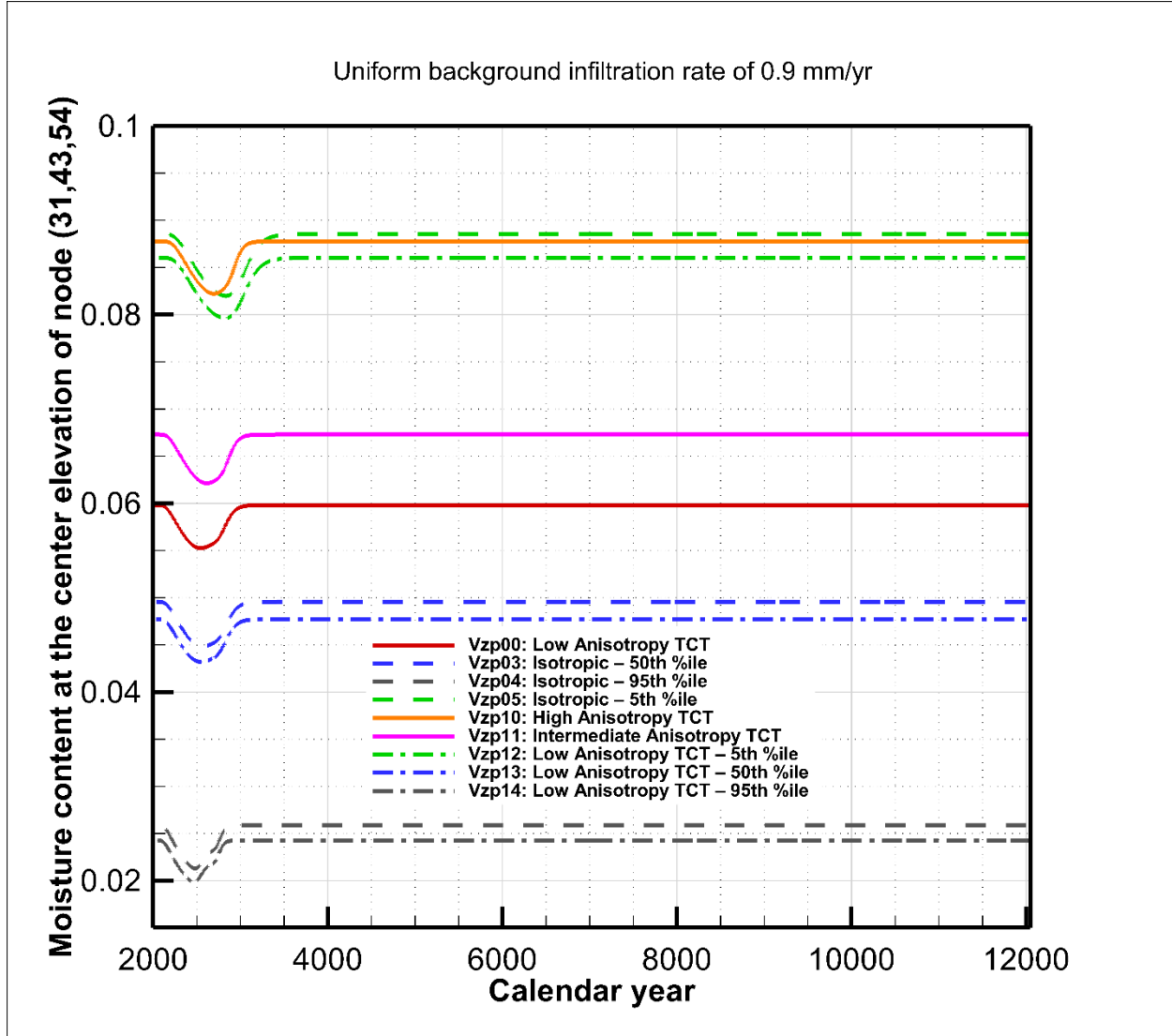
Source: RPP-CALC-61032, Figure 7-188.

Note: The uniform background infiltration rate of 0.9 mm/yr is applied through the surface barrier after the 500-year design life of the surface barrier, i.e., starting in CY 2551. From CY 2005 to 2151, the vertical Darcy flux through the liner system is 0.0 mm/yr due to the operations of the leachate recovery system. From CY 2151 to 2551, the vertical Darcy flux through the liner system is assumed to be 0.5 mm/yr. The steady-state moisture content for the base case property set (Vzp00) is about 0.060. The steady-state moisture content for the 95th percentile pore velocity case (Vzp04) is about 0.026.

TCT = tensorial-connectivity-tortuosity

The predicted moisture contents for the three long-term average steady-state net infiltration rates modeled illustrate the following.

- As the assumed net infiltration rate increases from 0.9 to 1.7 to 3.5 mm/yr, the predicted moisture content increases from 0.060 to 0.063 to 0.069 for case Vzp00, from 0.026 to 0.029 to 0.034 for case Vzp04 and from 0.024 to 0.027 to 0.032 for case Vzp14.

- Case Vzp04 results in lower predicted moisture contents than case Vzp00 by about a factor of two. This is expected because this case represents the 95th percentile pore velocity (or 5th percentile moisture content) for the 1.7 mm/yr net infiltration case.

- Case Vzp14 results in a slightly lower predicted content (by about 0.002) compared to case Vzp04 due to the lateral flow caused by the anisotropy in the vadose zone sediments.

The predicted moisture contents developed over the range of estimated net infiltration rates can be compared to observed moisture contents in the H2 sand.

Available moisture content information for the H2 sand developed from sediment samples and other indirect methods (neutron probes or neutron moisture logging) in undisturbed areas near the IDF is summarized in Table 2-15-2. Based on the sediment samples collected from boreholes drilled near the IDF, the average H2 sand moisture content is about 0.032. This average moisture content is representative of the steady-state vertical Darcy flux through the H2 sand near the IDF which is assumed to be equal to the long-term average net infiltration rate (and thus long-term average recharge rate) in the undisturbed surface conditions with mature shrub-steppe vegetation prior to the surface-disturbing activities resulting from the construction of the IDF[87].

The area near the IDF where boreholes have been drilled and sampled to determine the average *in situ* moisture content of about 0.032 is characterized as being an undisturbed surface (native soil with mature shrub-steppe vegetation), where the net infiltration rate is assumed to be equal to the steady-state vertical Darcy flux. At steady state, the vadose zone model and associated hydraulic (van Genuchten-Mualem) parameter values should be able to calculate moisture contents that are in the range of the observed moisture contents when using a representative net infiltration rate. However, determining what is a representative net infiltration rate is uncertain. To address this uncertainty, a range of values from 0.9 to 3.5 mm/yr have been used for most of the calculations presented in the IDF PA (RPP-RPT-59958) and the examples discussed above. However, it is possible that the net infiltration rate is as low as 0.16 mm/yr (the lower bound recommended in PNNL-14744) or even lower if one considers the possibility that the presence of

---

[87] This assumption may not be applicable in the area around the Sisson and Lu test site (boreholes 299-E24-76 to 299-E24-107), which is located next to an area with disturbed surface conditions which includes an unused waste disposal crib. However, the interpreted moisture content in the Sisson and Lu boreholes was not used to develop the average value of 0.032.

eolian silts in the upper few meters of the vadose zone at the IDF could significantly reduce the net infiltration rate as hypothesized in PNNL-14744[88].

In addition to the moisture contents measured in areas of undisturbed surface conditions, additional moisture content has been measured in areas near the IDF in the 200 East Area that have disturbed surfaces since Hanford operations began in 1944. Examples of these areas include the tank farm areas associated with WMA C and WMA A-AX located about a kilometer north of the IDF. The observed moisture content in sediment samples collected from boreholes drilled in these areas with disturbed surfaces averages about 0.052 (see Table 3-3 and Figure B-2a of RPP-ENV-58782).

The best-estimate net infiltration rate in the disturbed surface areas in the tank farm areas for the time period since the surfaces were disturbed is about 100 mm/yr (PNNL-14702). Although it would take some time for the effects of the surface disturbance and resulting increase in the net infiltration rate (from the pre-disturbance value of 0.9 to 3.5 mm/yr to the post-disturbance value of about 100 mm/yr) to propagate to the depth of the H2 sand beneath the disturbed surfaces, there has been sufficient time between the time the surfaces were disturbed (about calendar year [CY] 1944) to the time when moisture contents were measured (CY 2003 to CY 2013 for WMA C and CY 2014 for WMA A-AX) to allow the moisture regime to reach a quasi-steady state to the depth of the H2 sand. Therefore, it is possible to also use the observed moisture contents in the H2 sand in disturbed surface areas along with the best estimate of the net infiltration rate in these areas to evaluate the representativeness of the vadose zone hydraulic parameter values.

The 200 realizations of vadose zone hydraulic parameter values of the H2 sand were developed to evaluate the impact of the vadose zone hydraulic parameter uncertainty on predicted moisture contents (and thus pore velocity and vadose zone transport times) for the IDF PA. These same 200 hydraulic parameter realizations have been used to compare predicted moisture contents to observed average moisture contents.

Figure 2-15-8 presents the results of the 200 realizations of predicted moisture contents for the best-estimate net infiltration rate in undisturbed surface areas near the IDF of 0.9 mm/yr (based on PNNL-14744) and the best-estimate net infiltration rate in disturbed surface areas near the IDF of 100 mm/yr (based on PNNL-14702). Considering that the average observed H2 sand moisture content for the 0.9 mm/yr case is about 0.032 and the average observed H2 sand moisture content for the 100 mm/yr case is about 0.052, it is apparent that few realizations of the sampled vadose zone hydraulic parameter values can reproduce the observed average moisture contents.

---

[88] The eolian silt deposits that are capable of reducing recharge in the vicinity of the IDF relative to other areas of the Hanford Site are shallow and were removed during IDF excavation. Consequently, the IDF PA base case does not account for these layers when developing the base case long-term recharge rate for the post-closure analysis.

Table 2-15-2. H2 Sand Moisture Content Data in Boreholes Drilled near the Integrated Disposal Facility. (2 sheets)

Monitoring Well ID	Borehole ID	Location	Drilling Date	Moisture Content Data (Depth Range, m bgs)	Number of Sediment Samples	Volumetric Moisture Content (-) Average (min, max)	Reference
299-E24-161	B2428	~ 35 m north of 299-E24-162	1995	Sediment cores (0 – 15 m)	30	0.023 (0.018, 0.035)	PNNL-13033, Table B.3
299-E24-162	B2429	~Northeast corner of Integrated Disposal Facility (IDF) trench	1995	Sediment cores (0 – 15 m)	30	0.024 (0.016, 0.030)	PNNL-13033, Table B.4
Not applicable	C4071	Western cell (cell 1) of IDF trench	1995	Sediment cores (0 – 4.6 m)	7	0.026 (0.020, 0.032)	PNNL-13033, Table B.5
299-E17-21	B8500	~ 400 m south of southwest corner of IDF trench	1998	Sediment cores (14 – 73 m) Sediment cores (3 – 107 m) Neutron log (0 – 100 m)	20 85	0.034 (0.020, 0.061) 0.028 (0.017, 0.065)	RPP-20621, App. A, Table 3 PNNL-13033, Table B.6 PNNL-11957, Figure D.2
Not applicable	B8501	~ 30 m north of B8500	1998	Sediment cores (0 – 14.7 m)	72	0.030 (0.010, 0.071)	PNNL-13033, Table B.7
Not applicable	B8502	~ 30 m east of B8500	1998	Sediment cores (0 – 13.3 m)	70	0.035 (0.016, 0.087)	PNNL-13033, Table B.8
Not applicable	B8503	~ 25 m northeast of B8500	1998	Sediment cores (0 – 8.4 m)	44	0.044 (0.026, 0.061)	PNNL-13033, Table B.9
299-E24-21	C3177	~ 350 m north of northeast corner of IDF trench	2001	Sediment cores (5 – 255 ft) (1.5 – 77.7 m)	37	0.036 (0.008, 0.108)	PNNL-14289, Table 4.3
299-E17-22	C3826	~ 200 m east of IDF	2002	Sediment cores (2.7 – 67.9 m)	16	0.030 (0.020, 0.041)	PNNL-14744, Table B.3

Table 2-15-2. H2 Sand Moisture Content Data in Boreholes Drilled near the Integrated Disposal Facility. (2 sheets)

| Monitoring Well ID	Borehole ID	Location	Drilling Date	Moisture Content Data (Depth Range, m bgs)	Number of Sediment Samples	Volumetric Moisture Content (-) Average (min, max)	Reference
299-E24-76 to 299-E24-107	Not reported	~ 200 m east of northeast corner of IDF trench	2000-2001	Neutron probes (0 m – 18 m)	1,376	0.035 (0.016, 0.167)	PNNL-15443, Tables 2.7 - 2.8
299-E24-164	D0040	~ 120 m north of northeast corner of IDF trench	August 2019	Neutron log (0 – 97.5 m)	Not applicable	~ 0.03	SGW-63813, Appendix D

Note:
a) The sediment samples included in the summary exclude the upper 3 m (3.5 m in the case of B8503) of samples from these boreholes because the shallow moisture contents are likely impacted by short-term transient infiltration events and finer-grained sediments that are not representative of the average *in-situ* conditions.
b) Neutron probes of boreholes 299-E24-76 to 299-E24-107 were conducted prior to, during and after injecting water and tracers as part of the Sisson and Lu field experiment. Different neutron probes and different calibration methods were used during the course of the experiment to convert the neutron measurements (counts per second) to volumetric moisture content. The results of these tests are summarized in PNNL-15443. The moisture contents summarized here are associated with the neutron probe measurements conducted prior to injection tests performed on June 2, 2000 and March 30, 2001.
c) Volumetric moisture contents interpreted from the neutron log conducted after drilling at borehole D0040 (299-E24-164) represent the interval between a depth of 20 and 80 ft below ground surface (bgs). The values above 20 ft bgs were impacted by infiltration from a rainfall event which occurred about 3 weeks prior to the neutron log. The values below 80 ft bgs were likely impacted by water added during drilling below depths of 80 ft bgs.

References:
PNNL-11957, *Immobilized Low-Activity Waste Site Borehole 299-E17-21*
PNNL-13033, *Recharge Data Package for the Immobilized Low-Activity Waste 2001 Performance Assessment*
PNNL-14289, *Geochemistry of Samples from Borehole C3177 (299-E24-21)*
PNNL-14744, *Recharge Data Package for the 2005 Integrated Disposal Facility Performance Assessment*
PNNL-15443, *Vadose Zone Transport Field Study Summary Report*
RPP-20621, *Far-Field Hydrology Data Package for the Integrated Disposal Facility Performance Assessment*
SGW-63813, *Borehole Summary Report for the Installation of Six M-24 Wells in the 200-PO-1, 200- UP-1 and 300-FF-5 Operable Units, FY2019*

Figure 2-15-8. Predicted H2 Sand Moisture Content for Uncertain Vadose Zone Hydraulic Parameter Values for Vertical Darcy Fluxes of 0.9 mm/yr and 100 mm/yr.
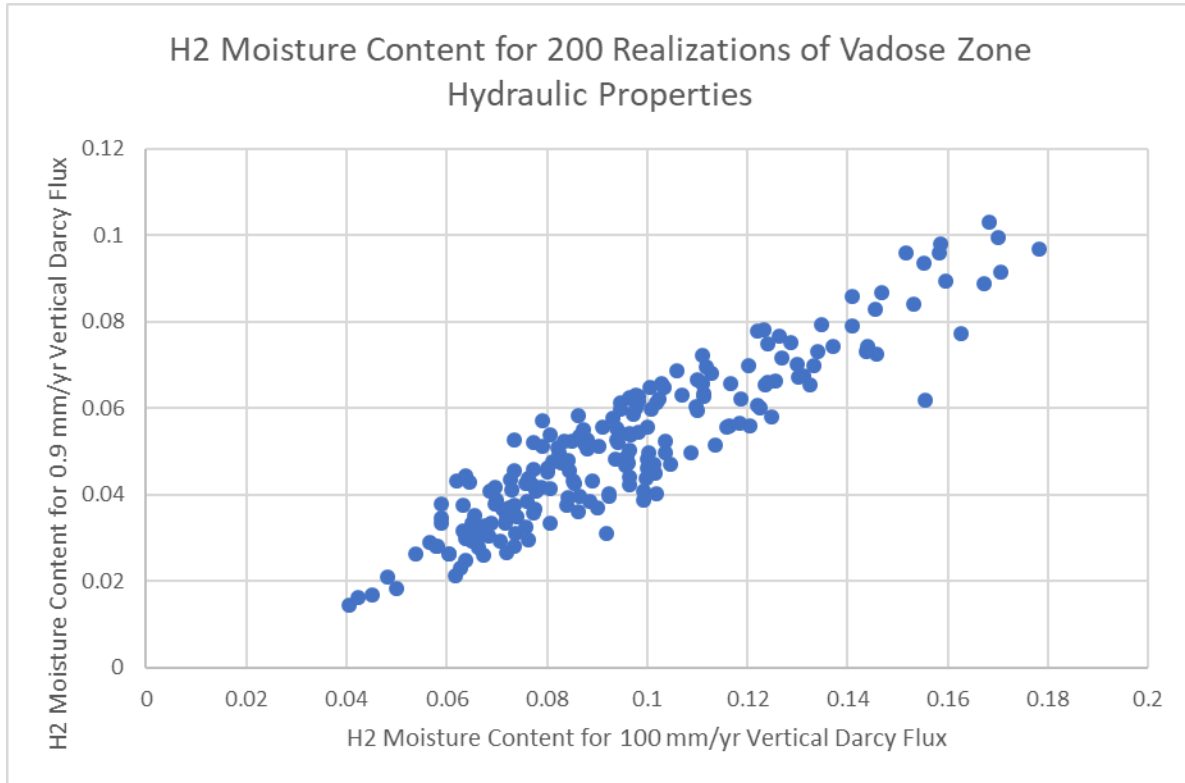
Source: Derived from Excel® (a registered trademark of Microsoft Corporation in the U.S. and other countries) spreadsheet used to develop vadose zone property sets corresponding to the 5th, 50th and 95th percentile of pore velocity (or 95th, 50th and 5th percentile of moisture content).

Note: The observed moisture content for a recharge rate (and corresponding vertical Darcy flux) of 0.9 mm/yr is 0.032. The observed moisture content for a recharge rate (and corresponding vertical Darcy flux) of 100 mm/yr is 0.052. Five realizations result in an under prediction of observed moisture contents for both the disturbed (100 mm/yr) and undisturbed (0.9 mm/yr) surface conditions; i.e., for these five realizations the predicted moisture contents are less than 0.032 and 0.052 for the undisturbed (0.9 mm/yr) and disturbed (100 mm/yr) surface condition, respectively. The 30 realizations with lowest predicted moisture content for both undisturbed and disturbed surface conditions are presented in Table 2-15.3.

The results for individual realizations that come closest to reproducing the observed moisture contents for both infiltration cases are summarized in Table 2-15-3. These are the realizations with the lowest predicted moisture contents for an undisturbed infiltration (and vertical Darcy flux) of 0.9 mm/yr (representative of undisturbed surface conditions near the IDF) and 100 mm/yr (representative of disturbed surface conditions in areas near the IDF such as the WMA C and WMA A-AX tank farm areas). Although there is no unique realization that matches the observed average moisture contents for both the undisturbed and disturbed surface conditions, there are several realizations that produce representative results.

Table 2-15-3. Comparison of Vadose Zone Hydraulic Parameter Realizations with Lowest Predicted Moisture Contents for Best-Estimate Undisturbed and Disturbed Recharge Rates.

Percentile	Undisturbed Surface Recharge (0.9 mm/yr)		Disturbed Surface Recharge (100 mm/yr)	
	Realization #	Predicted Moisture Content	Realization #	Predicted Moisture Content
1	59	0.0145	59	0.0405
	6	0.0161	6	0.0422
2	112	0.0170	112	0.0452
	4	0.0184	46	0.0483
3	46	0.0209	4	0.0499
	189	0.0213	43	0.0539
4	132	0.0232	55	0.0567
	80	0.0250	138	0.0578
5	73	0.0260	13	0.0581
	169	0.0263	140	0.0590
6	129	0.0263	93	0.0590
	43	0.0264	173	0.0590
7	177	0.0267	169	0.0604
	71	0.0277	129	0.0604
8	138	0.0280	189	0.0617
	13	0.0280	181	0.0619
9	168	0.0282	132	0.0627
	55	0.0290	19	0.0633
10	108	0.0294	49	0.0634
	78	0.0294	11	0.0637
11	79	0.0297	124	0.0637
	124	0.0299	80	0.0639
12	128	0.0303	35	0.0644
	192	0.0305	108	0.0651
13	29	0.0308	91	0.0651
	26	0.0310	151	0.0656
14	28	0.0312	29	0.0659
	49	0.0317	128	0.0662
15	96	0.0325	71	0.0664
	84	0.0329	73	0.0673

Note:
Realization 73 is the 95th percentile case used in the IDF PA (RPP-RPT-59958, *Performance Assessment for the Integrated Disposal Facility, Hanford Site, Washington*) (cases Vzp04 or Vzp14) based on an assumed recharge rate of 1.7 mm/yr.

Highlighted realizations are those that result in the lowest predicted moisture contents for both the undisturbed (best-estimate recharge rate of 0.9 mm/yr) and disturbed (best-estimate recharge rate of 100 mm/yr) surface conditions.

Realizations #43, #138, #13 and #55 are representative of cases that reproduce both the observed average moisture content of 0.032 for a best-estimate undisturbed net infiltration rate of 0.9 mm/yr as well as the observed average moisture content of 0.052 for a best-estimate disturbed net infiltration rate of 100 mm/yr.

For several realizations that yield predicted moisture contents that are representative of observed average moisture contents for both undisturbed and disturbed surface conditions, it is possible to evaluate the predicted moisture contents for other assumed net infiltration rates, including an infiltration rate of 3.5 mm/yr that is assumed to be representative of net infiltration through the surface barrier at IDF after the surface barrier's 500-yr design life. This comparison is presented in Table 2-15-4. Compared to the 95th percentile case (realization #73, case Vzp04 or Vzp14) used in the IDF PA (RPP-RPT-59958), the other realizations that yield representative predicted moisture contents for undisturbed and disturbed surface conditions (realizations #55, #138, #43 and #13) produce similar predicted moisture contents for the 3.5 mm/yr base case post-design-life net infiltration rate assumed in the IDF PA. Therefore, these different realizations would be expected to produce similar predicted vadose zone performance predictions to those resulting from realization #73 (cases Vzp04 and Vzp14) if they were implemented in the IDF vadose zone model.

Realization #73 (case Vzp04 or Vzp14) provides a case that is consistent with observed moisture contents in the H2 sand near the IDF when the long-term average undisturbed net infiltration rate is in the range of 0.9 to 3.5 mm/yr. If the undisturbed net infiltration rate is in the range of 0.9 to 3.5 mm/yr, then the vadose zone hydraulic parameter values used in case Vzp04 or case Vzp14 can reproduce the observed H2 sand average moisture content (Table 2-15-4). If the undisturbed infiltration rate is less than 0.16 mm/yr, then the base case (Vzp00) property set provides a representative case that can reproduce the observed moisture contents. Based on these comparisons, it can be concluded that the range of vadose zone hydraulic parameter sets used in the IDF PA encompasses the observed moisture contents given the uncertainty in the assumed undisturbed net infiltration rate.

Impact of Alternative Moisture Retention Relationships on IDF Performance

Sensitivity analyses presented in the IDF PA (Section 5.2.4.3 and 5.2.4.8 of RPP-RPT-59958) on effects of uncertain vadose zone hydraulic parameter values can be used to examine the significance of the uncertain vadose zone hydraulic parameter values on the performance of the IDF disposal facility. Some example results are reproduced as Figure 2-15-9. The following observations can be made from these results.

- Cases Vzp04 and Vzp14[89] result in earlier radionuclide arrival at the water table than the base case (Vzp00) due to the lower predicted moisture content (and higher predicted pore velocity) for a given long-term average steady-state net infiltration rate. For the distributed flow case, this can result in peak arrival times for unretarded radionuclides (e.g., ^{99}Tc) occurring prior to 1,000 years after the facility is closed.

---

[89] Cases Vzp04 and Vzp14 represent the 95th percentile pore velocity (equivalent to the 5th percentile moisture content) for an assumed net infiltration rate of 1.7 mm/yr for both the H2 sand and the H3 gravel. Comparisons between predicted and observed moisture contents are only possible for the H2 sand as there are no relevant observations of moisture content in the H3 gravels in undisturbed surface areas near the IDF. Observations of moisture content in H3 gravels in disturbed surface areas near WMA C and WMA A-AX are available. Cases VZp04 and Vzp14 have also modified the hydraulic property values of the H3 gravel to represent the 95th percentile pore velocity.

- Cases Vzp00 and Vzp04 (and other vadose zone parameter sets) result in similar peak release rates to the water table, albeit at different times.

Table 2-15-4. Predicted Moisture Content in the H2 Sand for Different Vadose Zone Hydraulic Property Sets and Recharge Rates.

Recharge Rates (mm/yr)	H2 Vadose Zone Hydraulic Property Sets (Realization #)							Observed Average Moisture Content
	Base Case (Vzp00)	# 121 (Vzp03)	# 73 (Vzp04)	# 55	# 13	# 138	# 43	
140	NC	0.106	0.072	0.060	0.062	0.061	0.057	0.052
100	0.103	0.100	0.067	0.057	0.058	0.058	0.054	
60	NC	0.092	0.060	0.052	0.053	0.053	0.049	
3.5	0.069	0.060	0.034	0.034	0.034	0.034	0.032	0.032
1.7	0.063	0.054	0.029	0.031	0.031	0.030	0.029	
0.9	0.060	0.050	0.026	0.029	0.028	0.028	0.026	
0.16	0.050	0.040	0.019	0.024	0.022	0.023	0.022	

Note:
The different vadose zone property sets are:
Case Vzp00 is the base case in the IDF PA (RPP-RPT-59958, *Performance Assessment for the Integrated Disposal Facility, Hanford Site, Washington*).
Case Vzp03 (realization #121 of the 200 realizations used to evaluate the effect of uncertainty in van Genuchten-Mualem parameter values on vadose zone transport) represents the 50th percentile for a vertical Darcy flux of 1.7 mm/yr.
Case Vzp04 (realization #73) represents the 95th percentile for a vertical Darcy flux of 1.7 mm/yr.
Realizations #55, #13, #138 and #43 represent cases that come closest to reproducing both the observed moisture content of 0.032 for a best-estimate undisturbed net infiltration rate of 0.9 mm/yr as well as the observed average moisture content of 0.052 for a best-estimate disturbed net infiltration rate of 100 mm/yr (see Table 2-15-3).
The different recharge rates represent the following:
- 100 mm/yr is the recharge rate in areas with disturbed surface conditions with a gravel surface and no vegetation as recommended in PNNL-14702, *Vadose Zone Hydrogeology Data Package for Hanford Assessments* and used in ECF-HANFORD-15-0019, *Hanford Site-wide Natural Recharge Boundary Condition for Groundwater Models*, Rev. 2. This includes the disturbed surfaces in the WMA C and WMA A-AX areas.
- 140 and 60 mm/yr represent the upper and lower limits of the estimated recharge rates in areas with disturbed surface conditions as recommended in PNNL-14702.
- 3.5 mm/yr is the average of the net infiltration rate into the Rupert Sand and Burbank Loamy Sand in areas with mature shrub-steppe vegetation near the IDF as reported in PNNL-14702. 3.5 mm/yr is also the long-term average flux into the IDF after the assumed 500-year design life of the surface cap.
- 1.7 mm/yr is the average value for Rupert Sand with mature shrub-steppe vegetation in the Central Plateau recommended in PNNL-16688, *Recharge Data Package for Hanford Single-Shell Tank Waste Management Areas*. This value is also close to the mode (1.9 mm/yr) of the uncertainty distribution used in the IDF PA. This value was the vertical Darcy flux value used to develop the statistics on moisture content and pore velocity used to define the 95th, 50th and 5th percentile cases in the IDF PA.
- 0.9 mm/yr is the best-estimate recharge rate for the IDF recommended in PNNL-14744, *Recharge Data Package for the 2005 Integrated Disposal Facility Performance Assessment* based on the interpreted chloride mass balance average of seven boreholes near the IDF.
- 0.16 mm/yr is the minimum bounding recharge rate recommended in PNNL-14744 based on the interpreted chloride mass balance in borehole 299-E24-161 located near the IDF.

Average observed moisture contents for the IDF undisturbed recharge conditions are based on about 400 observations in boreholes near the IDF (the same boreholes with measured chloride mass used to estimate the average net infiltration rate in PNNL-14744). Average observed moisture contents for disturbed recharge conditions are based on observations made in WMA C and WMA A-AX for disturbed surface conditions.

Figure 2-15-9. Technetium-99 Breakthrough at Water Table from Solid Secondary Waste Sources for Different Vadose Zone Conceptual Models and Property Sets – Distributed Infiltration 3.5 mm/yr.
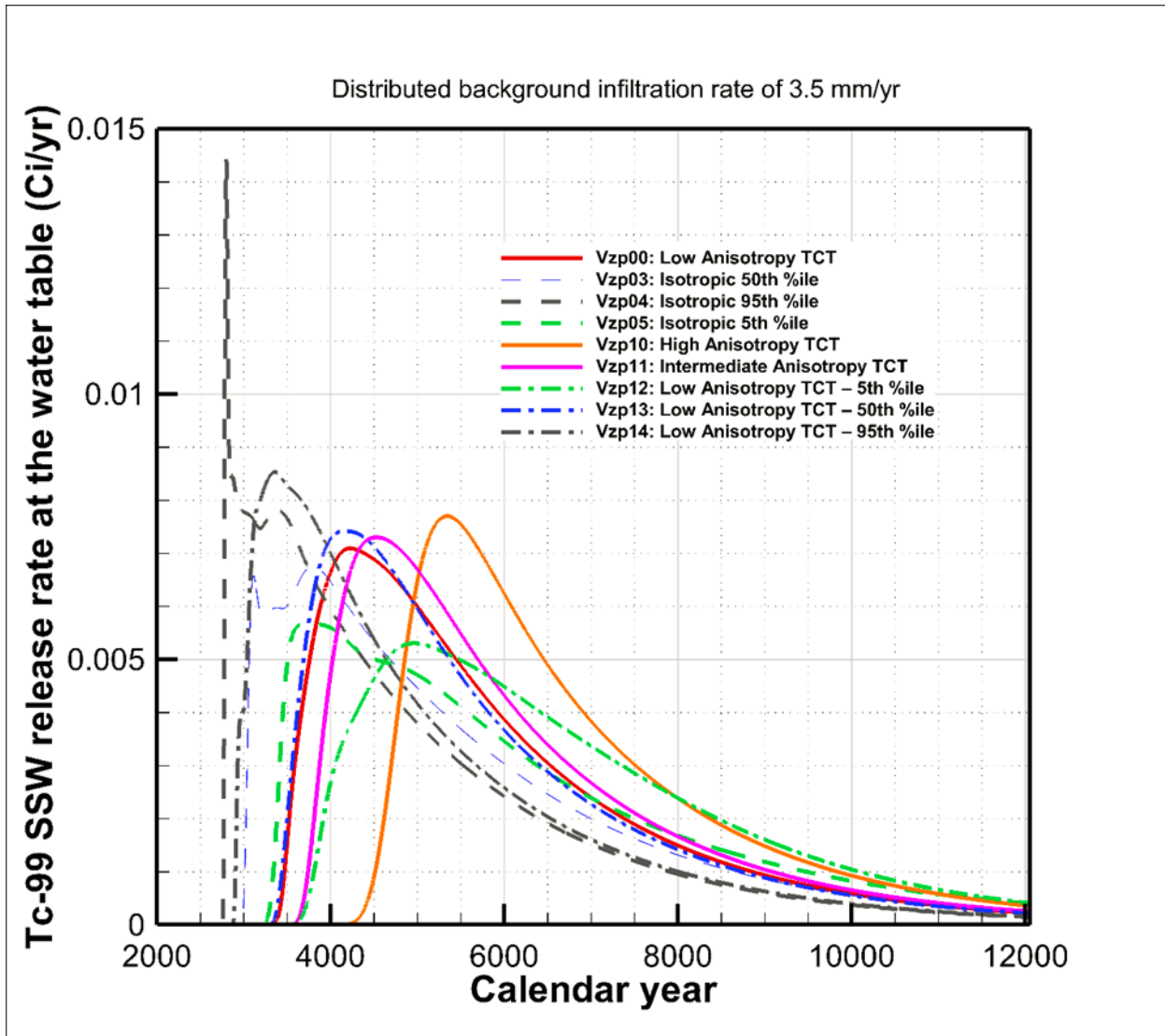
SSW = solid secondary waste   TCT = tensorial-connectivity-tortuosity

Source: RPP-RPT-59958, *Performance Assessment for the Integrated Disposal Facility, Hanford Site, Washington*, Figure 5-147 (derived from RPP-CALC-61032, *Vadose Zone and Saturated Zone Flow and Transport Calculations for the Integrated Disposal Facility Performance Assessment*, Figure 7-154).

As noted in RPP-RPT-59958, many of the detailed process-model sensitivity analyses performed focused on only one component of the disposal system. This is a result of the long computational times for running some of the models. For example, Section 5.2.4 presents the results of sensitivity analyses using only the vadose zone feature of the combined vadose zone/saturated zone flow and transport model because the vadose zone-only STOMP model took only 12 hours to complete while the combined vadose zone/saturated zone flow and transport model took almost 2 weeks to complete.

Because there are no combined vadose zone/saturated zone model runs that correspond to case Vzp04 or Vzp14 with best-estimate values of radionuclide sorption, to evaluate the impact of case Vzp04 and Vzp14 on the predicted groundwater concentration at the 100-m point of assessment boundary, additional calculations were performed to support this RAI response that will be included in future updates to the PA according to the PA change management process. The results of these additional sensitivity analyses are presented in Figures 2-15-10 to 2-15-13. These figures include the base case results presented in Figures 5-98 and 5-99 of RPP-RPT-59958. These figures also contain a secondary axis that converts the groundwater concentration to a dose using the All-Pathways Groundwater Dose conversion factor value of 0.69 mrem/yr per pCi/L for ^{129}I and 3.76E-03 mrem/yr per pCi/L for ^{99}Tc. The following observations can be drawn from these sensitivity analyses.

- The peak concentrations for ^{129}I and ^{99}Tc in the groundwater are not significantly affected by the uncertainty in the vadose zone hydraulic parameter values. This is analogous to the observation made in comparing the peak release rates from the vadose zone to the saturated zone.

- The timing of the peak concentration arrival at the 100-m point of assessment boundary is reduced when using the alternative vadose zone property sets. This is also analogous to the observation made in comparing the time of the peak release rate from the vadose zone to the saturated zone.

- The timing of the peak concentration arrival at the 100-m point of assessment is less for the isotropic case (Vzp04) than the low anisotropic case (Vzp14).
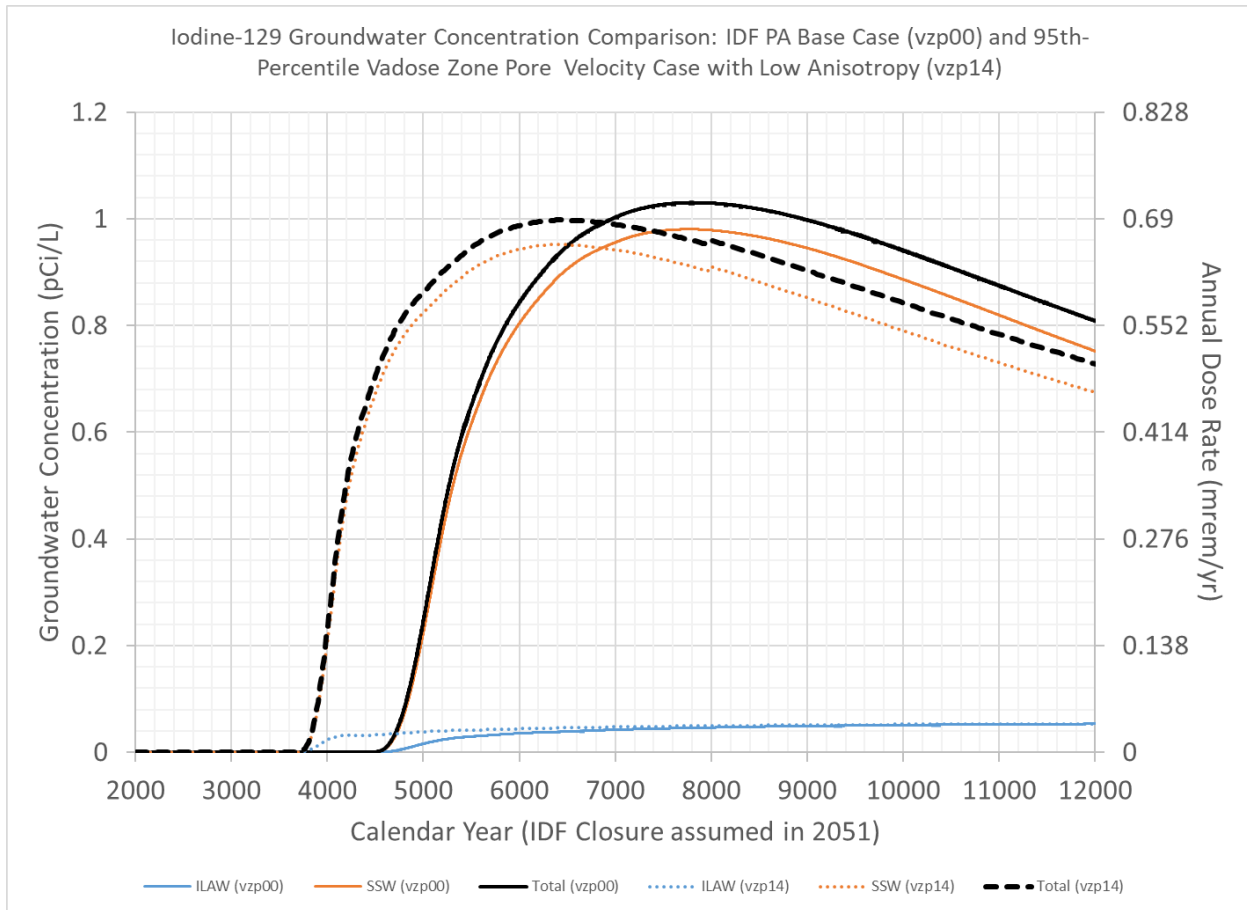
The results of the base case and alternative vadose zone hydraulic property sets are summarized in Table 2-15-5.

Summary

The vadose zone hydraulic (van Genuchten-Mualem) parameter values affect the fate of radionuclides released from the IDF as they are transported through the vadose zone to the underlying saturated zone. The uncertainty in these parameter values can affect the timing of the release of radionuclides to the underlying saturated zone and thus the timing of the radionuclide plume arrival at the point of assessment in the groundwater located 100-m from the edge of the IDF footprint. The IDF PA analyzed the effect of this uncertainty using the existing data on vadose zone hydraulic parameter values from 44 samples of the H2 sediments. Although it is possible that the parameter value uncertainty could be broader than that represented by the 44 samples, the range of values used in the analysis captures the range of predicted moisture contents and thus the expected range of predicted pore velocities and transport times.

The IDF PA noted that the vadose zone was a significant feature due to both the low net infiltration rate and the hydraulic properties of the Hanford sand and gravel units which directly determine whether radionuclides released from the IDF will reach the water table (and hence compliance boundary) within 1,000 years (RPP-RPT-59958, Table 8-6). This importance was highlighted in the discussion of key assumptions presented in RPP-RPT-59958, Section 8.4.2.

Figure 2-15-10. Iodine-129 Breakthrough Curves for Cases Vzp00 and Vzp14 at Location of Peak Impact Along the 100-meter Buffer Boundary for Release from Immobilized Low-Activity Waste Glass and Solid Secondary Waste.
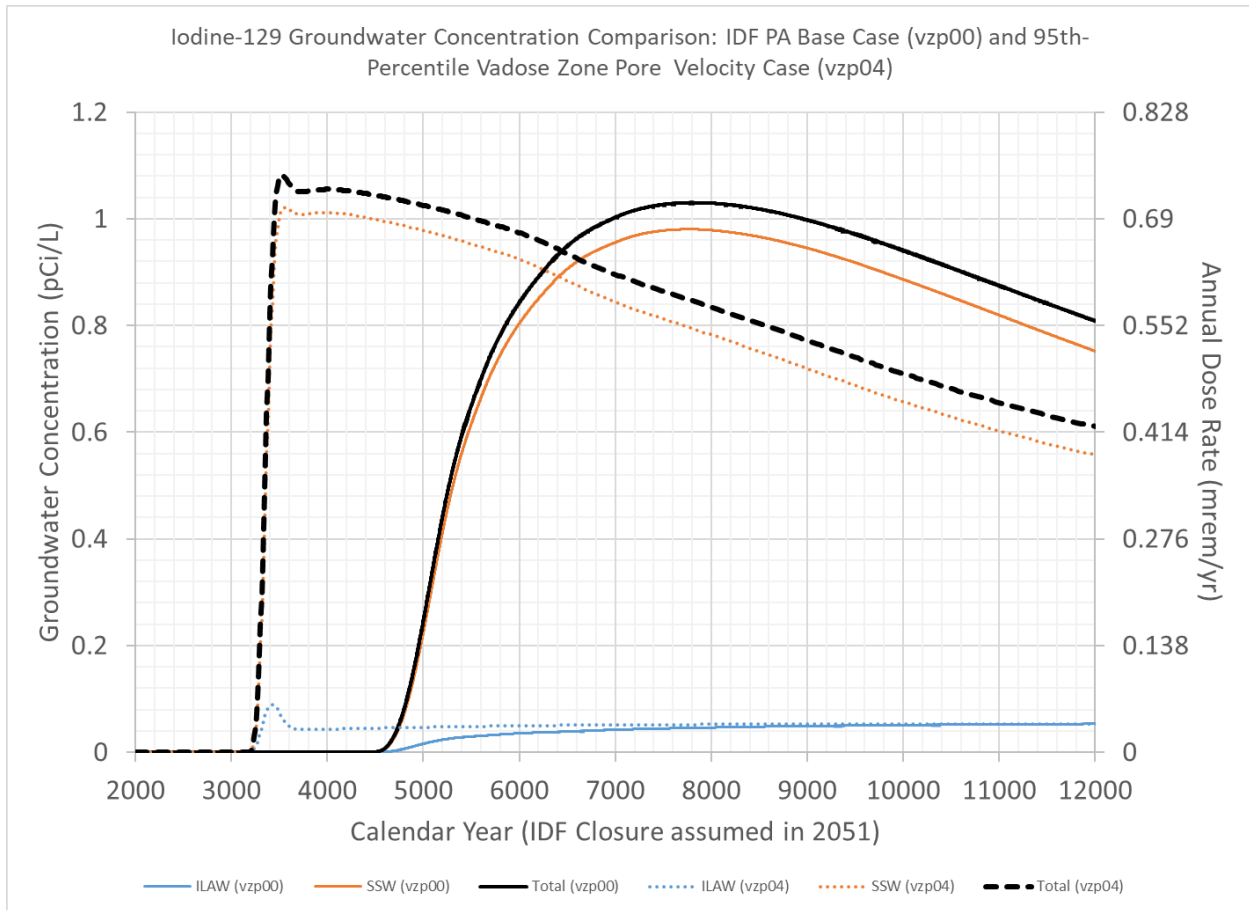

PA = Performance Assessment

Note: Time is in calendar year, the Integrated Disposal Facility (IDF) is assumed to be closed in calendar year 2051. Assumes base case distributed flow recharge rate of 3.5 mm/yr (case Infd06) and base case immobilized low-activity waste (ILAW) and solid secondary waste (SSW) release rate of RPP-RPT-59958, *Performance Assessment for the Integrated Disposal Facility, Hanford Site, Washington.* The total for vzp00 includes a small contribution from Effluent Treatment Facility liquid secondary waste (see RPP-RPT-59958 Figure 5-99), the total for VZP14 does not. The dose is converted from the groundwater concentration to a dose using the All-Pathways Groundwater Dose conversion factor value of 0.69 mrem/yr per pCi/L.

In addition to the transport velocity, and hence transport time, in the vadose zone being affected by the assumed recharge rate and recharge distribution at the top of the vadose zone (e.g., the base of the IDF liner), the transport velocity is also strongly dependent on the assumed van Genuchten-Mualem vadose zone property set and the assumed anisotropic conceptual model for flow in the vadose zone, which in turn affect the calculated moisture content in the vadose zone under future hydrologic conditions. The range of feasible moisture contents is roughly a factor of two greater than or less than the nominal or expected moisture content. This factor of two translates into a factor of two lower or higher pore velocity and therefore a factor of two longer or shorter transport times to the water table. The nominal moisture content at IDF, about 0.07, is about the same as the nominal value at WMA C under similar recharge conditions. There are limited relevant soil moisture measurements in boreholes in the IDF. Future boreholes

in the area should be considered in developing a more robust data set on expected moisture contents. It is noted that these moisture contents represent average values (i.e., the scale of meters), as local scale heterogeneities (i.e., silt lenses and paleosols) can alter the moisture content locally (at the scale of centimeters) (RPP-RPT-59958, Section 8.4.2).

Figure 2-15-11. Iodine-129 Breakthrough Curves for Cases Vzp00 and Vzp04 at Location of Peak Impact Along the 100-meter Buffer Boundary for Release from Immobilized Low-Activity Waste Glass and Solid Secondary Waste.
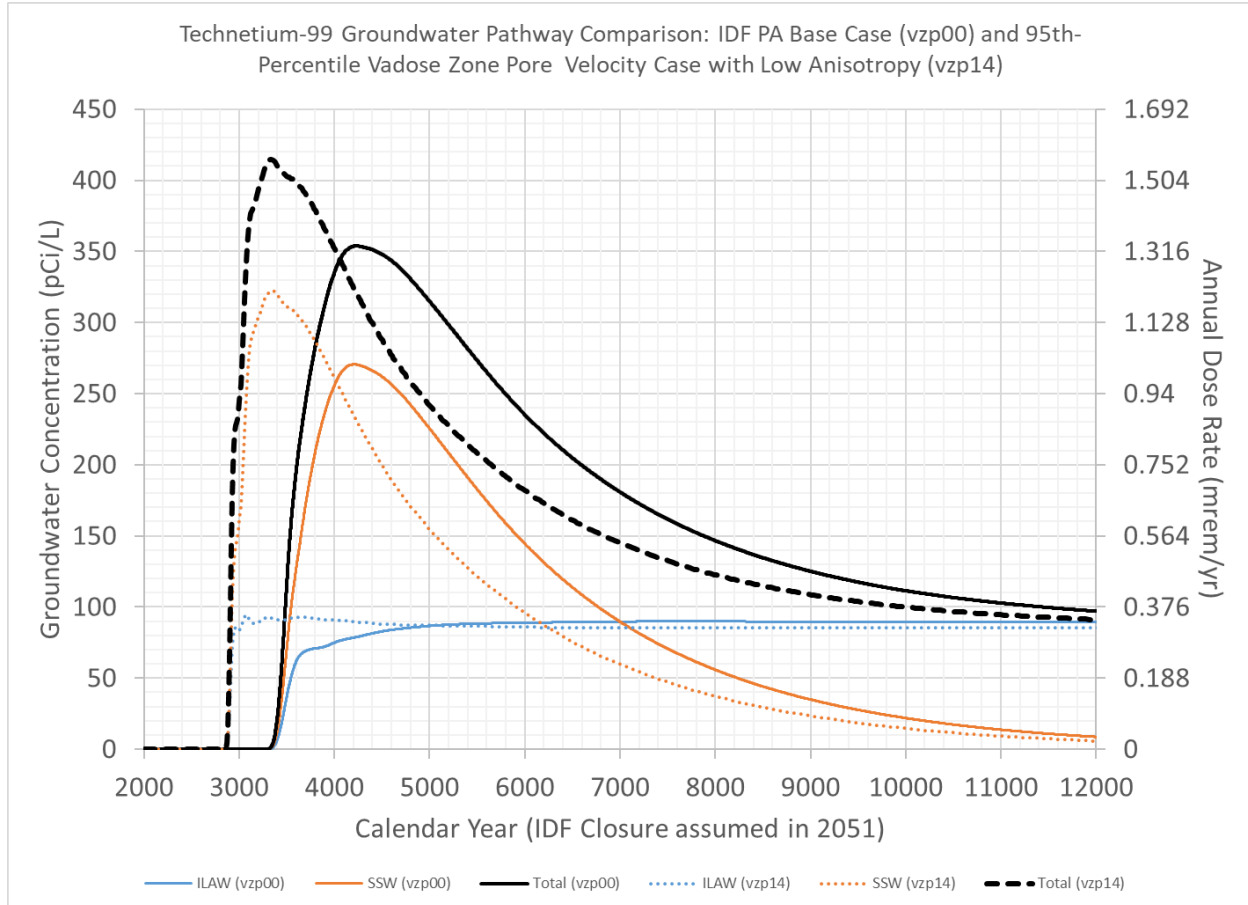

PA = Performance Assessment

Note: Time is in calendar year, the Integrated Disposal Facility (IDF) is assumed to be closed in calendar year 2051. Assumes base case distributed flow recharge rate of 3.5 mm/yr (case Infd06) and base case immobilized low-activity waste (ILAW) and solid secondary waste (SSW) release rate of RPP-RPT-59958, *Performance Assessment for the Integrated Disposal Facility, Hanford Site, Washington*. The total for vzp00 includes a small contribution from Effluent Treatment Facility liquid secondary waste (see RPP-RPT-59958 Figure 5-99), the total for VZP04 does not. The dose is converted from the groundwater concentration to a dose using the All-Pathways Groundwater Dose conversion factor value of 0.69 mrem/yr per pCi/L.

Based on the identified significance of the vadose zone hydraulic property set on the predicted performance, specifically related to the time it takes radionuclides released from the base of the IDF liner system to reach the water table and thus the point of assessment, Table 8-8 of RPP-RPT-59958 recommended including moisture profile measurements in boreholes drilled near the IDF. This recommendation was implemented in Section 4.7 of the IDF Maintenance Plan (CHPRC-03348), where the need to evaluate undisturbed present-day soil moisture profiles

for areas near the IDF was identified and it was noted that one of the few locations with ambient moisture information is at well 299-E17-21.

Figure 2-15-12. Technetium-99 Breakthrough Curves for Cases Vzp00 and Vzp14 at Location of Peak Impact along the 100-meter Buffer Boundary for Release from Immobilized Low-Activity Waste Glass and Solid Secondary Waste.

PA = Performance Assessment

Note: Time is in calendar year, the Integrated Disposal Facility (IDF) is assumed to be closed in calendar year 2051. Assumes base case distributed flow recharge rate of 3.5 mm/yr (case Infd06) and base case immobilized low-activity waste (ILAW) and solid secondary waste (SSW) release rate of RPP-RPT-59958, *Performance Assessment for the Integrated Disposal Facility, Hanford Site, Washington*. The ^{99}Tc release rate to the water table for this vadose zone property set (Vzp14) is illustrated in Figure 5-147 of RPP-RPT-59958. The total for vzp00 includes a small contribution from Effluent Treatment Facility liquid secondary waste (see RPP-RPT-59958 Figure 5-99), the total for VZP14 does not. The dose is converted from the groundwater concentration to a dose using the All-Pathways Groundwater Dose conversion factor value of 3.76E-03 mrem/yr per pCi/L.

Moisture contents observed in H2 sand sediment samples taken from boreholes drilled near the IDF, including new wells installed in FY 2019, have been reviewed to determine that an average value of 0.032 is representative of undisturbed surface conditions near the IDF while a value of 0.052 is representative of disturbed surface conditions near the IDF. These values are within the range of values predicted with the uncertain vadose zone hydraulic property sets used in the IDF PA, which provides confidence in the range of results presented in the IDF PA.

Figure 2-15-13. Technetium-99 Breakthrough Curves for Cases Vzp00 and Vzp04 at Location of Peak Impact along the 100-meter Buffer Boundary for Release from Immobilized Low-Activity Waste Glass and Solid Secondary Waste.
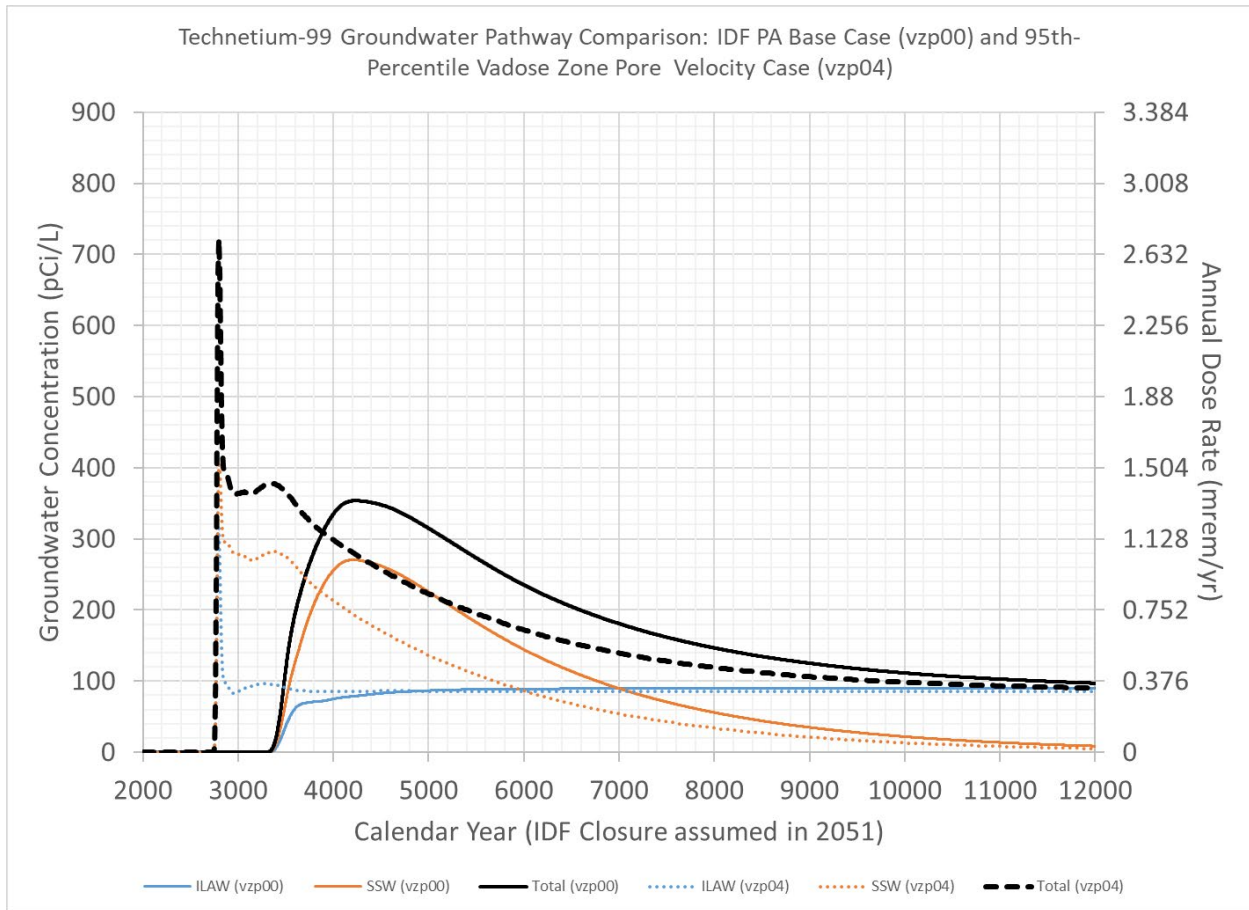

PA = Performance Assessment

Note: Time is in calendar year, the Integrated Disposal Facility (IDF) is assumed to be closed in calendar year 2051. Assumes base case distributed flow recharge rate of 3.5 mm/yr (case Infd06) and base case immobilized low-activity waste (ILAW) and solid secondary waste (SSW) release rate of RPP-RPT-59958, *Performance Assessment for the Integrated Disposal Facility, Hanford Site, Washington*. The ^{99}Tc release rate to the water table for this vadose zone property set (Vzp04) is illustrated in Figure 5-147 of RPP-RPT-59958. The total for vzp00 includes a small contribution from Effluent Treatment Facility liquid secondary waste (see RPP-RPT-59958 Figure 5-99), the total for VZP04 does not. The dose is converted from the groundwater concentration to a dose using the All-Pathways Groundwater Dose conversion factor value of 3.76E-03 mrem/yr per pCi/L.

Using representative vadose zone hydraulic property set cases that reproduce the observed moisture contents for disturbed and undisturbed surface conditions illustrates that the peak groundwater concentrations for risk-significant radionuclides (i.e., ^{99}Tc and ^{129}I) do not exceed groundwater protection standards or DOE's dose limit performance objectives for the All-Pathways scenario. However, the timing of the peak groundwater concentration is earlier than predicted with the base case vadose zone property set used in the IDF PA. Continued maintenance activities to confirm the observed moisture content and to develop better estimates of undisturbed infiltration rates remain as important activities within the IDF maintenance program.

Table 2-15-5. Comparison of Peak Groundwater Concentration for Base Case (Vzp00) and Alternative Vadose Zone Hydraulic Property Set (Vzp04 and Vzp14).

Radionuclide	Waste Source	Peak Concentration (pCi/L)			Time of Peak Concentration (Calendar Year)		
		Case Vzp00	Case Vzp14	Case Vzp04	Case Vzp00	Case Vzp14	Case Vzp04
^{99}Tc	SSW	270	322	408	4208	3346	2801
	ILAW	90	95	321	7663	3073	2794
	SSW+ILAW	350	415	721	4224	3336	2797
^{129}I	SSW	0.980	0.952	1.021	7727	6362	3561
	ILAW	0.053	0.054	0.089	>12051	12036	3421
	SSW+ILAW	1.0	0.998	1.082	7809	6403	3526

ILAW = immobilized low-activity waste   SSW = solid secondary waste

Note: Peak concentrations rounded to nearest pCi/L for ^{99}Tc and 0.001 pCi/L for ^{129}I. Case Vzp00 represents the base case presented in RPP-RPT-59958, *Performance Assessment for the Integrated Disposal Facility, Hanford Site, Washington*, Table 5-43 and illustrated in Figures 5-98 and 5-99 of RPP-RPT-59958. Cases Vzp14 and Vzp04 represent the 95th percentile pore velocity cases developed for the low anisotropy and isotropic moisture dependent anisotropy, respectively.

Note: The *Safe Drinking Water Act of 1974* Maximum Concentration Levels yielding a drinking-water dose of 4 mrem/yr are 900 pCi/L for ^{99}Tc and 1.0 pCi/L for ^{129}I. The peak drinking water dose may be calculated as the peak groundwater concentration times the unit concentration yielding 4 mrem/yr drinking water dose, i.e., 4.444E-04 mrem/yr per pCi/L of ^{99}Tc and 4 mrem/yr per pCi/L of ^{129}I.

Note: The peak groundwater exposure pathway dose of the all-pathways dose may be calculated as the peak groundwater concentration times the base case unit concentration dose factors presented in Table 4-46 of RPP-RPT-59958, i.e., 3.76E-03 mrem/yr per pCi/L of ^{99}Tc and 0.690 mrem/yr per pCi/L of ^{129}I.

References

CHPRC-03348, 2019, *Performance Assessment Maintenance Plan for the Integrated Disposal Facility*, Rev. 1, INTERA, Inc./CH2M HILL Plateau Remediation Company, Richland, Washington.

DOE, 2005, *Technical Guidance Document for Tank Closure Environmental Impact Statement Vadose Zone and Groundwater Revised Analyses*, Final Rev 0, U.S. Department of Energy, Richland, Washington.

DOE/EIS-0391, 2012, *Final Tank Closure and Waste Management Environmental Impact Statement for the Hanford Site, Richland, Washington*, U.S. Department of Energy, Washington, D.C.

ECF-HANFORD-15-0019, 2020, *Hanford Site-wide Natural Recharge Boundary Condition for Groundwater Models*, Rev. 2, INTERA, Inc., CH2M HILL Plateau Remediation Company, Richland, Washington.

NAVD88, *North American Vertical Datum of 1988*, National Geodetic Survey, U.S. Department of Commerce, National Oceanic and Atmospheric Administration, Silver Spring, Maryland.

PNNL-11957, 1998, *Immobilized Low-Activity Waste Site Borehole 299-E17-21*, Pacific Northwest National Laboratory, Richland, Washington. Available at: https://www.osti.gov/servlets/purl/665973.

PNNL-13033, 1999, *Recharge Data Package for the Immobilized Low-Activity Waste 2001 Performance Assessment*, Pacific Northwest National Laboratory, Richland, Washington. Available at: https://www.pnnl.gov/main/publications/external/technical_reports/13033.pdf

PNNL-14289, 2003, *Geochemistry of Samples from Borehole C3177 (299-E24-21)*, Pacific Northwest National Laboratory, Richland, Washington. Available at: https://www.pnnl.gov/main/publications/external/technical_reports/PNNL-14289.pdf.

PNNL-14702, 2006, *Vadose Zone Hydrogeology Data Package for Hanford Assessments*, Rev. 1, Pacific Northwest Laboratory, Richland, Washington. Available at: https://www.pnnl.gov/main/publications/external/technical_reports/PNNL-14702rev1.pdf.

PNNL-14744, 2004, *Recharge Data Package for the 2005 Integrated Disposal Facility Performance Assessment*, Pacific Northwest National Laboratory, Richland, Washington. Available at: https://www.pnnl.gov/main/publications/external/technical_reports/PNNL-14744.pdf.

PNNL-15443, 2006, *Vadose Zone Transport Field Study Summary Report*, Pacific Northwest National Laboratory, Richland, Washington. Available at: https://www.pnnl.gov/main/publications/external/technical_reports/PNNL-15443.pdf.

PNNL-16688, 2007, *Recharge Data Package for Hanford Single-Shell Tank Waste Management Areas*, Pacific Northwest National Laboratory, Richland, Washington. Available at: https://www.pnnl.gov/main/publications/external/technical_reports/PNNL-16688.pdf.

PNNL-23711, 2015, *Physical, Hydraulic, and Transport Properties of Sediments and Engineered Materials Associated with Hanford Immobilized Low-Activity Waste*, RPT-IGTP-004, Rev. 0, Pacific Northwest National Laboratory, Richland, Washington. Available at: https://www.pnnl.gov/main/publications/external/technical_reports/PNNL-23711.pdf.

RPP-20621, 2004, *Far-Field Hydrology Data Package for the Integrated Disposal Facility Performance Assessment*, Rev. 0, CH2M HILL Hanford Group, Inc., Richland, Washington.

RPP-CALC-61032, 2018, *Vadose Zone and Saturated Zone Flow and Transport Calculations for the Integrated Disposal Facility Performance Assessment*, Rev. 0A, prepared by INTERA Inc. for Washington River Protection Solutions, LLC, Richland, Washington.

RPP-ENV-58782, 2016, *Performance Assessment of Waste Management Area C, Hanford Site, Washington*, INTERA, Inc./CH2M HILL Plateau Remediation Company/Ramboll Environ, Inc./Washington River Protection Solutions, LLC/TecGeo, Inc., Richland, Washington.

RPP-RPT-59958, 2019, *Performance Assessment for the Integrated Disposal Facility, Hanford Site, Washington*, Rev. 1A, Washington River Protection Solutions, LLC, Richland, Washington.

Safe Drinking Water Act of 1974, 42 USC 300, et seq.

SGW-63813, 2019, *Borehole Summary Report for the Installation of Six M-24 Wells in the 200-PO-1, 200-UP-1 and 300-FF-5 Operable Units, FY2019*, CH2M HILL Plateau Remediation Company, Richland, Washington. Available at: https://pdw.hanford.gov/document/AR-03916.

WCH-520, 2013, *Performance Assessment for the Environmental Restoration Disposal Facility, Hanford Site, Washington,* Rev. 1, Washington Closure Hanford, Richland, Washington. Available at: https://pdw.hanford.gov/document/0083701.

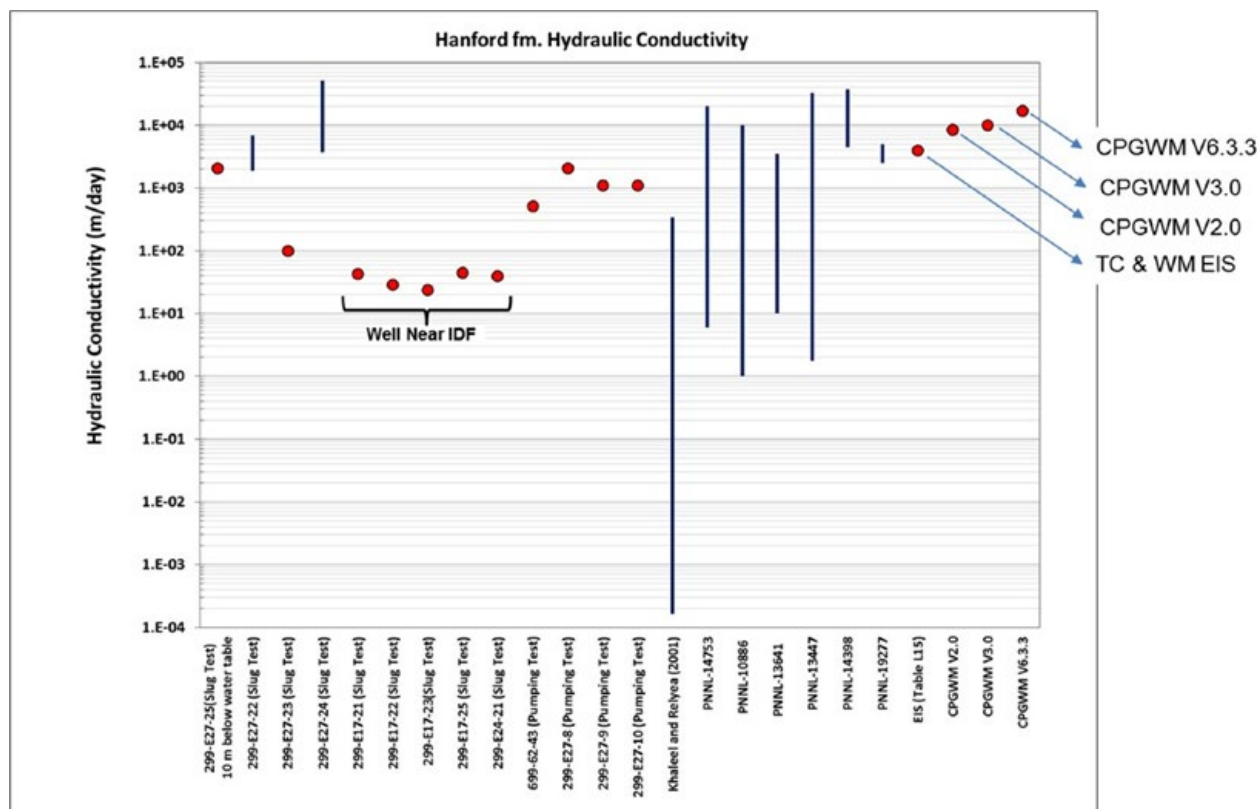## RAI 2-16 (Saturated Zone Hydraulic Conductivity)

Comment
The changes to the estimated hydraulic conductivity values for the saturated zone over time suggest the base case value best estimate may not be reliable.

Basis
The saturated zone hydraulic conductivity, or rather the product of the saturated zone hydraulic conductivity and the gradient, is a key factor with respect to the reduction of risk at the Hanford site. Flux rates of water through the unsaturated zone are relatively low whereas the flow rate of water through the saturated zone are comparably high. This creates a large dilution effect on contaminant fluxes thereby reducing risk to an offsite receptor. DOE has investigated the saturated hydraulic conductivity over numerous decades and produced the very detailed figure (Figure 4-94 in the PA document) shown below. The figure highlights two important features.

First, that the local values can deviate significantly from the global values and secondly, that the estimated values have been highly volatile over time. Since completion of the TC & WM EIS the values have increased almost an order of magnitude. While the specific discharge values may have increased by a lessor amount than estimates of the saturated zone hydraulic conductivity, it isn't apparent why the base case value is thought to be reliable and unlikely to change given the past changes as more data has been collected and additional modeling has been completed.

Figure 2-16-1. Hanford Formation Hydraulic Conductivity Based on Slug Tests, Pumping Tests, and Groundwater Flow Models.

Source: Figure 4-94 of RPP-RPT-59958, *Performance Assessment for the Integrated Disposal Facility, Hanford Site, Washington.*

Path Forward

Please discuss confidence building activities to support the base case saturated zone hydraulic conductivity values assigned. Please discuss plans to verify the base case saturated zone hydraulic conductivity.

DOE Response

DOE acknowledges that there is uncertainty in the hydraulic conductivity of the aquifer sediments underneath the IDF and included an evaluation of this uncertainty in the IDF PA uncertainty analysis. The uncertainty analysis demonstrated that the impact to the environment and dose consequences to a member of the public in the future are very sensitive to the applied value of the aquifer hydraulic conductivity (or Darcy velocity).

The base case hydraulic conductivities of the saturated sediments beneath and downgradient of the IDF are based on the calibrated groundwater models of the Central Plateau. The model basis was the most current available Central Plateau Groundwater Model (CPGWM Version 6.3.3, CP-47631, *Model Package Report: Central Plateau Groundwater Model, Version 6.3.3*, Rev. 2), at the time the IDF-specific groundwater flow model was developed for the IDF PA. The

best-estimate hydraulic conductivity of the gravels of the Hanford formation from CPGWM Version 6.3.3 is 17,000 m/day. This value has evolved with time. This evolution is based on field measurements and model calibrations that are based on additional hydraulic testing information as well as enhancements in the model calibration approach. That evolution is not related to the reliability of the model result, but instead represents the natural evolution of the understanding of the groundwater flow regime in the saturated zone in the 200 East Area of the Central Plateau of the Hanford Site as the area is characterized during ongoing remediation activities related to groundwater operable unit 200-PO-1.

As noted in the RAI basis and the IDF PA, the hydraulic conductivity as well as the related specific discharge in the groundwater regime beneath the IDF are key factors in reducing the groundwater concentration of any radionuclides released from the facility and transported through the vadose zone. As a result, the uncertainty in the groundwater flow regime was identified as a highly significant assumption in Table 8-6 and Section 8.4.3 of the IDF PA (RPP-RPT-59958) and potential monitoring approaches that could be used to confirm the base case values were recommended in Table 8-8 of RPP-RPT-59958.

This RAI response first summarizes the results of the two CPGWMs that were used to define the base case saturated zone hydraulic conductivity and hydraulic gradient. The response then addresses the confidence-building activities that were planned as part of the IDF PA maintenance plan to verify the base case groundwater flow characteristics. Finally, the response concludes with a summary of the most recent information available based on the maintenance activities conducted since the completion of the IDF PA models and calculations.

Summary of Groundwater Flow Model Results used in the IDF PA (RPP-RPT-59958)
Two groundwater flow models of the 200 East Area of the Central Plateau, which encompass the area upgradient and downgradient of the IDF, were available at the time of the development of the IDF PA saturated zone model and associated calculations (RPP-RPT-59344, *Integrated Disposal Facility Model Package Report: Vadose and Saturated Zone Flow and Transport* and RPP-CALC-61032, *Vadose Zone and Saturated Zone Flow and Transport Calculations for the Integrated Disposal Facility Performance Assessment*, respectively). The available groundwater flow models were the TC&WM EIS groundwater flow model (Appendix L of DOE/EIS-0391, *Final Tank Closure and Waste Management Environmental Impact Statement for the Hanford Site, Richland, Washington*) and the CPGWM Version 6.3.3 (CP-47631, Rev. 2). The results of these two flow models were compared in RPP-CALC-61016, *Saturated Zone Flow – Sensitivity Analyses Using the 3-D EIS Groundwater Flow Model and the Central Plateau Groundwater Flow Model in the Vicinity of the Integrated Disposal Facility* and presented as Figures 4-76, 4-77, 4-92 and 4-93 in RPP-RPT-59958.

The groundwater model comparisons illustrate several relevant aspects of the groundwater flow regime near the IDF, as follows.

- Both groundwater flow models include a high-hydraulic conductivity zone that runs from northwest to southeast through the central part of the 200 East Area and is under the IDF footprint. Both models ascribe this high-hydraulic conductivity zone to the presence of a paleochannel of an ancestral Columbia River at the time of the deposition of the Hanford

and Cold Creek units.

- Both groundwater flow models predict low hydraulic gradients within the high-hydraulic conductivity zone.

- The base case calibrated hydraulic conductivity of the high-hydraulic conductivity zone in the TC&WM EIS was 3,973 m/day and in the CPGWM Version 6.3.3 was 17,000 m/day.

- The specific discharge in the high-hydraulic conductivity zone for both calibrated groundwater flow models is about 0.3 m/day, which was used as the base case specific discharge in the saturated zone in the IDF PA.

As concluded in the IDF PA, the similarity in the predicted specific discharge between the two groundwater flow models provided confidence that the base case value used for the IDF PA was reasonable and representative of the groundwater flow beneath the IDF. Uncertainty in the saturated zone flow velocity along the flow path generating the highest groundwater concentrations at the 100-m boundary was evaluated to account for the differences in the hydraulic conductivity values used in the TC&WM EIS and in CPGWM Version 6.3.3 flow models.

Summary of Planned Maintenance Activities to Verify the Groundwater Flow Model Results
Confidence-building activities to support the assumed base case hydraulic conductivity and specific discharge used in the IDF PA were identified in the IDF PA Maintenance Plan (CHPRC-03348). These activities were identified to confirm the base case values used in the IDF PA (RPP-RPT-59958).

As summarized in CHPRC-03348 Section 4.7, the planned maintenance activities include:

- Evaluate saturated zone flow models and parameter values developed for use in other Central Plateau remediation or related activities

- Evaluate assumptions and analyses used in the Hanford Site Composite Analysis (CA) and other planned and ongoing PAs (including the WMA A-AX PA)

- Evaluate saturated zone flow properties and hydrostratigraphy at the IDF.

The description of each of these activities presented in Section 4.7 of CHPRC-03348 consists of the following.

"The Hanford Site is an area of ongoing characterization and modeling of the groundwater flow domain in the Central Plateau area. These groundwater investigations and models could extend and include the 200 East Area and other areas around the IDF. These studies are expected to be of relevance to IDF, specifically with respect to analyses of the present trends in the water table surface in the 200 East Area as well as the hydraulic conductivity of the Hanford

formation. Although the IDF groundwater flow model uses a projected groundwater flow field after the end of Hanford Site operations (calendar year 2200), understanding the transient behavior of the groundwater flow system near the IDF supports the development of the groundwater flow rates used in the IDF PA."

"The Hanford Site CA is expected to be completed in 2019 after which it will be reviewed by the LFRG. Until the DOE O 435.1 compliant CA is complete, the TC&WM EIS (DOE/EIS-0391, Section 6.0 and Appendix U) serves as the Hanford site-wide assessment of cumulative impacts. These impacts include impacts from sources immediately upgradient of the IDF, notably the US Ecology site and the BC cribs and trenches. Analyses of COPCs released from these facilities significantly affects the forecast concentration of technetium-99 and iodine-129 beneath the IDF; therefore, these results should be evaluated to determine their impact on the IDF PA monitoring program."

"The magnitude of dilution for COPCs which reach the saturated zone beneath the IDF is dependent on the hydraulic properties and hydraulic gradient of the hydrostratigraphic units beneath the IDF. While the current site characterization indicates that the present-day and long-term average water table is in the Hanford formation beneath the IDF, this unit is mapped as thinning to the east and south of the IDF and the contact with the Ringold Formation member of Wooded Island – unit E is uncertain. In addition, the single-hole slug tests conducted in the observation wells near the IDF provide only a minimum estimate of the hydraulic properties of the Hanford formation in the small volume stressed around the test wells and are not believed representative of the average hydraulic properties of the Hanford formation at the IDF. Although the properties and extent of the Hanford formation do not affect the PA results during the 1,000-year compliance period, they significantly affect the concentrations in the 1,000-year to 10,000-year sensitivity analysis period. Therefore, opportunities will be explored to conduct larger scale pump tests in the Hanford formation near the IDF."

<u>Summary of Current Groundwater Flow Models and Results</u>
The following section summarizes the recent groundwater flow modeling and related activities conducted since the PA model was completed that are related to confirming the base case hydraulic conductivity values used in the IDF PA.

Confidence-building activities to verify the representativeness of the hydraulic conductivity of the saturated sediments beneath the IDF used in modeling groundwater flow include pumping tests conducted in 2015, the calibration of hydraulic conductivity parameters in the groundwater models using a tritium plume, and a drawdown test performed on two wells near the IDF.

Pumping Tests at 299-E33-268:
Although no additional site-specific information on the hydraulic conductivity of the saturated sediments near IDF has been collected, constant-rate pumping tests have been performed as part of the 200-BP-5 treatability test in the Hanford/Cold Creek gravels in borehole 299-E33-268.

This well is located about 2 km north of the IDF and is part of the same high conductivity zone that runs under the IDF[90]. Two constant rate tests were performed by pumping from 299-E33-268 over a 3-day period and a 27-day period and observing the water level response at nearby wells 299-E33-31 (9 m away), 299-E33-267 (4.5 m away), and 299-E33-342 (130 m away). As summarized in Tables 3-3 and 3-4 of DOE/RL-2015-75, *Aquifer Treatability Test Report for the 200-BP-5 Groundwater Operable Unit*, the hydraulic conductivity interpreted from the 3-day constant rate pumping test at 299-E33-268 ranged from 15,800 to 21,300 m/day with an average value of 18,800 m/day, while that from the 27-day constant rate pumping test at 299-E33-268 ranged from 15,100 to 21,100 m/day, with an average value of 18,200 m/day. These values support the base-case value of 17,000 m/day derived from the CPGWM Version 6.3.3. An additional pumping test is being planned to support field investigations for remediation of the groundwater operable units near the IDF.

Central Plateau Groundwater Model Updates:
The CPGWM has been updated multiple times since the IDF PA simulations were completed. The updates include the development of a successor groundwater flow model called the Plateau to River (P2R) model. The recent updates to these models include:

- July 2015 – CPGWM Version 6.3.3 (CP-47631, *Model Package Report: Central Plateau Groundwater Model Version 6.3.3*, Rev. 2) – used as the basis for the IDF PA

- July 2015 – P2R Version 7.1 (CP-57037, *Model Package Report: Plateau to River Groundwater Transport Model Version 7.1*, Rev. 0)

- November 2016 – CPGWM Version 8.3.4 (CP-47631, *Model Package Report Central Plateau Groundwater Model Version 8.3.4*, Rev. 3)

- January 2018 – CPGWM Version 8.4.5 (CP-47631, *Model Package Report: Central Plateau Groundwater Model, Version 8.4.5*, Rev. 4)

- May 2019 – P2R Version 8.2 (CP-57037, *Model Package Report: Plateau to River Groundwater Model Version 8.2*, Rev. 1)

- February 2020 – P2R Version 8.3 (CP-57037, *Model Package Report: Plateau to River Groundwater Model Version 8.3*, Rev. 2).

The modeling updates are summarized below with particular focus on the updates to the calibrated hydraulic conductivity in the suprabasalt sediments beneath the IDF.

Updates to CPGWM Version 6.3.3 (used for the IDF PA) were made in CPGWM Version 8.3.4 and CPGWM Version 8.4.5 completed in November 2016 and January 2018, respectively. The update in CPGWM Version 8.3.4 was relatively minor and the calibrated hydraulic conductivity of the Hanford channel deposits near the IDF was unchanged from the 17,000 m/day value

---

[90] The suprabasalt sediments in the boreholes near 299-E33-268 are characterized as being part of the Hanford/Cold Creek paleochannel. As noted in the response to RAI 2-14, it is difficult to distinguish between the gravels of the Hanford formation and the gravels of the Cold Creek Unit (CCUg).

developed in CPGWM Version 6.3.3. The update in CPGWM Version 8.4.5 was more significant; this update included a modification to the boundary between the Hanford highly conductive channel and the Hanford formation in the western part of the 200 East Area and the lateral extent of the Hanford channel in the southeastern part of the 200 East Area. The new boundary extended the highly conductive channel to be under the IDF, as illustrated in Figure 2-16-2. The revision to the location of the Hanford channel in the southeastern part of the 200 East Area effectively replaced the Hanford formation and Rwie gravels near the IDF with Hanford channel deposits[91]. The calibrated hydraulic conductivity for the Hanford channel deposits near the IDF was reduced to 15,000 m/day (CP-47631, Rev. 4 Table 4-4).

A successor groundwater flow model to the CPGWM was developed by expanding the extent of the model to the Columbia River. This model is called the Plateau to River (P2R) groundwater flow model. The initial version of this model (P2R Version 7.1, July 2015) was developed concurrently with CPGWM Version 6.3.3 and is documented in CP-57037, Rev. 0. Because the initial version was based on the calibration of the CPGWM Version 6.3.3, it had the same calibrated hydraulic conductivity of the Hanford channel sediments of 17,000 m/day.

Consistent with the changes made to CPGWM Version 8.4.5, a revised version of the P2R model (Version 8.2, May 2019) was developed that changed the modeled extent of the Hanford channel from the representation in Version 7.1. Adjustments to the extent of Hanford channel sediments were made in the calibration of P2R Version 8.2 as illustrated in Figure 2-16-3. These adjustments were made during the calibration to the observed historic tritium plume within and downgradient of the 200 East Area.

The calibrated hydraulic conductivity of the Hanford channel deposits from the P2R Version 8.2 is illustrated in Figure 2-16-4. The hydraulic conductivity of the Hanford channel deposits near the IDF is ~15,000 m/day while downgradient of the IDF the calibrated hydraulic conductivity is between 20,000 and 25,000 m/day.

The most current model of groundwater flow in the Central Plateau is the P2R Version 8.3. The approach used to define the extent of the Hanford channel in P2R Version 8.3 differs significantly from the approach adopted in earlier groundwater flow models. In the earlier models, including the TC&WM EIS model, CPGWM Version 8.4.5 and P2R Version 8.2, the Hanford channel was treated as a fixed feature, called the high conductivity zone (HCZ). The extent of the Hanford channel for the various models is shown in Figure 2-16-3.

---

[91] In addition to presenting the updated calibrated hydraulic conductivity of the suprabasalt aquifer beneath the IDF from revisions to the groundwater flow models, it is appropriate to consider the relevant HSUs beneath and downgradient of the IDF. The identification of the relevant HSUs has evolved with revised interpretations and improved groundwater model calibrations over the past few years. As a result, this RAI is closely related to RAI 2-14 which addresses uncertainty in the presence of the Rwie and the contact between the Rwie and the overlying CCU gravels and the Hanford formation near the IDF. Since the completion of the models and calculations supporting the IDF PA, there have been updates to the GFMs and groundwater flow models that are relevant to address in the responses to RAIs 2-16 and 2-14. Updates to the groundwater flow models are discussed in this RAI response while updates to the GFMs are discussed in the response to RAI 2-14.

Figure 2-16-2. Adjustments to the Hanford Channel Zonation in Layers 1, 2 and 3 of the Central Plateau Groundwater Model Version 8.4.5 in the 200 East Area of the Central Plateau (a) Initial, (b) Modified in Central Plateau Groundwater Model Version 8.4.5.
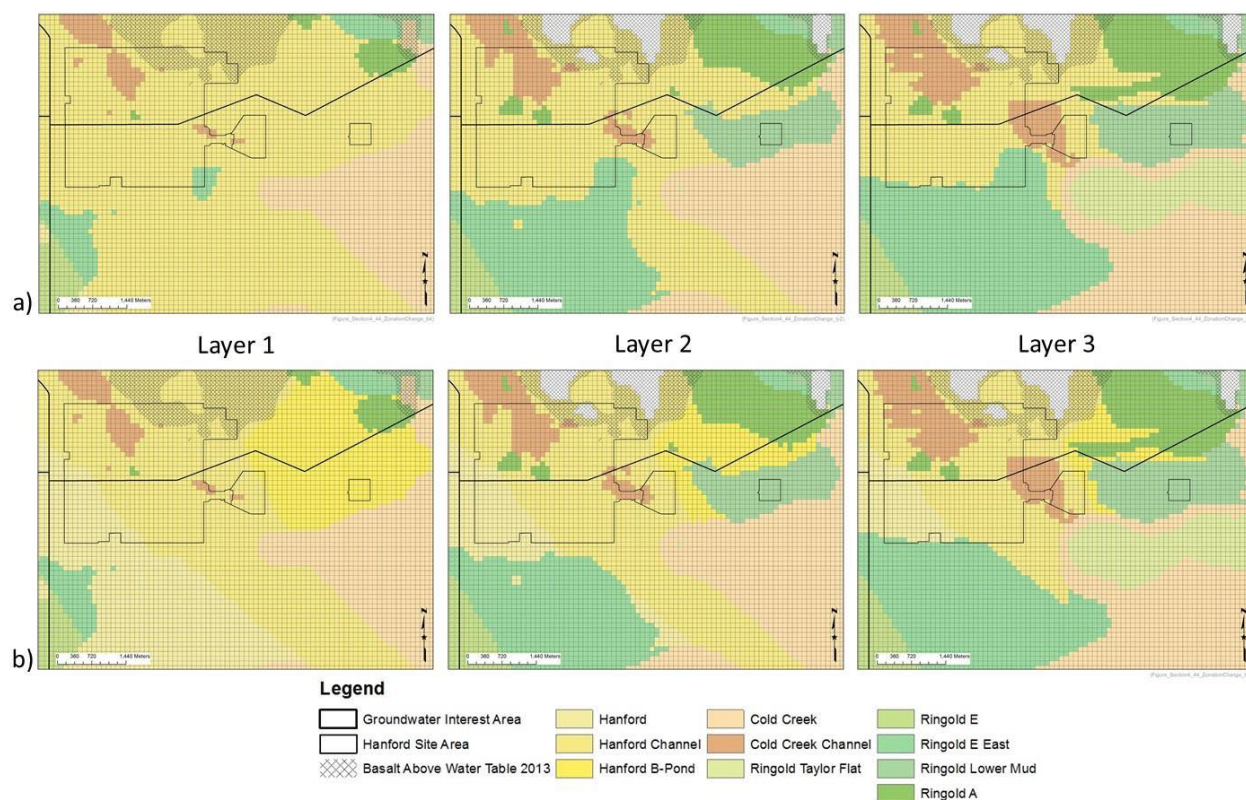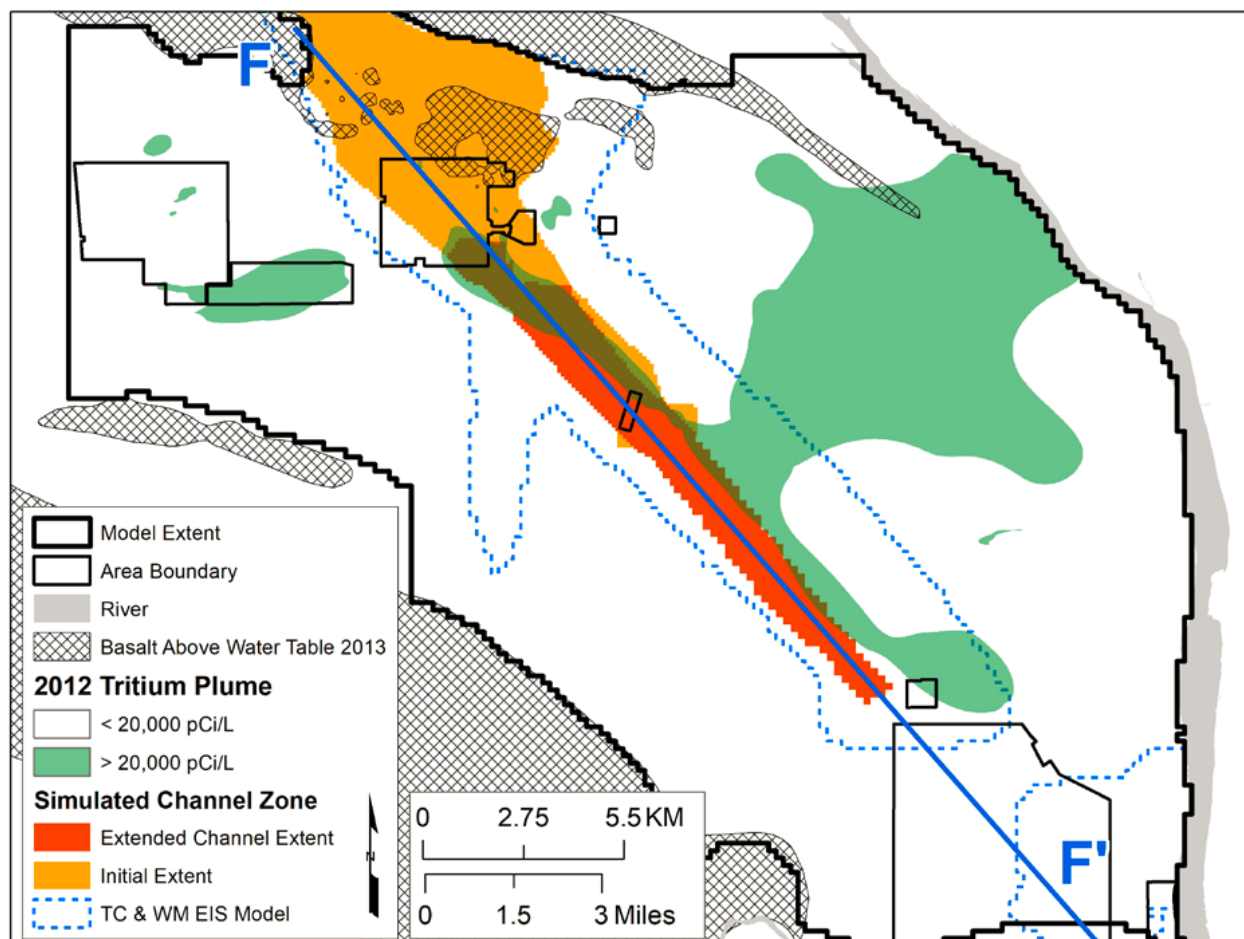

Source: CP-47631, *Model Package Report Central Plateau Groundwater Model Version 8.4.5*, Rev. 4, Figure 4-43.

Note: The initial hydrostratigraphic unit (HSU) zonation is based on a predecessor to the Hanford South geologic framework model (GFM) (ECF-HANFORD-13-0029, *Development of the Hanford South Geologic Framework Model, Hanford Site, Washington*, Rev. 2) and is the same as used in CPGWM Version 6.3.3 (CP-47631, *Model Package Report: Central Plateau Groundwater Model Version 6.3.3*). The modified HSU zonation used in CPGWM Version 8.4.5 (CP-47631, Rev. 4) replaced the Ringold E East in the southeast portion of the 200 East Area, including the area beneath the Integrated Disposal Facility, with the Hanford Channel HSU.

In P2R Version 8.3, the approach taken to calibrate the hydraulic conductivity in the Hanford channel deposits was to first identify an area of the model domain that may contain the Hanford channel, called the HCZ analysis area, and then let the calibration and parameter-estimation process identify the high-hydraulic conductivity within the HCZ analysis area that result in calibrated properties of the Hanford channel deposits to match historical water levels and an existing tritium plume. The location of the HCZ analysis area is illustrated in Figure 2-16-5. Within the HCZ analysis area, the four upper HSUs (i.e., the Hanford formation, CCU, Ringold Taylor Flats unit [Rtf], and Rwie) were treated as a single unit and divided into five separate layers in the model grid.

Figure 2-16-3. Location of the Hanford Channel Included Prior to and After Calibration of the Plateau to River (P2R) Groundwater Flow Model Version 8.2.

Source: CP-57037, *Model Package Report: Plateau to River Groundwater Model Version 8.2*, Rev. 1, Figure 4-29.

Note: The initial extent of the channel zone is the extent modeled in the CPGWM Version 8.4.5 (CP-47631, *Model Package Report: Central Plateau Groundwater Model, Version 8.4.5*, Rev. 4) and P2R Version 7.1 (CP-57037, *Model Package Report: Plateau to River Groundwater Transport Model Version 7.1*, Rev. 0). The extended channel extent is the result of calibrating the P2R Version 8.2 (CP-57037, Rev. 1) to the observed tritium plume. The extent of the channel zone modeled in the TC & WM EIS (DOE/EIS-0391, *Final Tank Closure and Waste Management Environmental Impact Statement for the Hanford Site, Richland, Washington*) is shown for comparison purposes.

The calibrated hydraulic conductivity of the high conductivity zone (comprised of the paleochannel deposits of the Hanford/Cold Creek unit as well as the Rtf and Rwie[92]) in P2R

---

[92] Although there have been no hydraulic tests performed in wells in the southern 200 East Area, evaluation of well development data from monitoring wells drilled in the area indicate that the high-conductivity sediments are not restricted to the Hanford formation and CCU. WMP-27008, *Borehole Summary Report for Wells 299-24-24 (C4647) and 299-E17-26 (C4648), Integrated Disposal Facility*, provides a description of drawdown in wells screened in the Hanford formation and Rwie, respectively. In each case, WMP-27008 noted at least 20 minutes of pumping above 68.1 L/min (18 gal/min) and recorded no measurable drawdown. The hydraulic response of the well screened exclusively in the Rwie supports the results of the DOE/EIS-0391 and P2R Model Version 8.2 that assigned HCZ properties to locations that the Hanford South GFM (ECF-HANFORD-13-0029) assigns to the Rwie.

Version 8.3 are illustrated in Figures 2-16-6 to 2-16-10 for layers 1 to 5 of the model domain. A transmissivity map illustrated in Figure 2-16-11 also shows the location of the modeled HCZ.

Figure 2-16-4. Calibrated Hydraulic Conductivity of Hanford Channel – Plateau to River Groundwater Model Version 8.2.
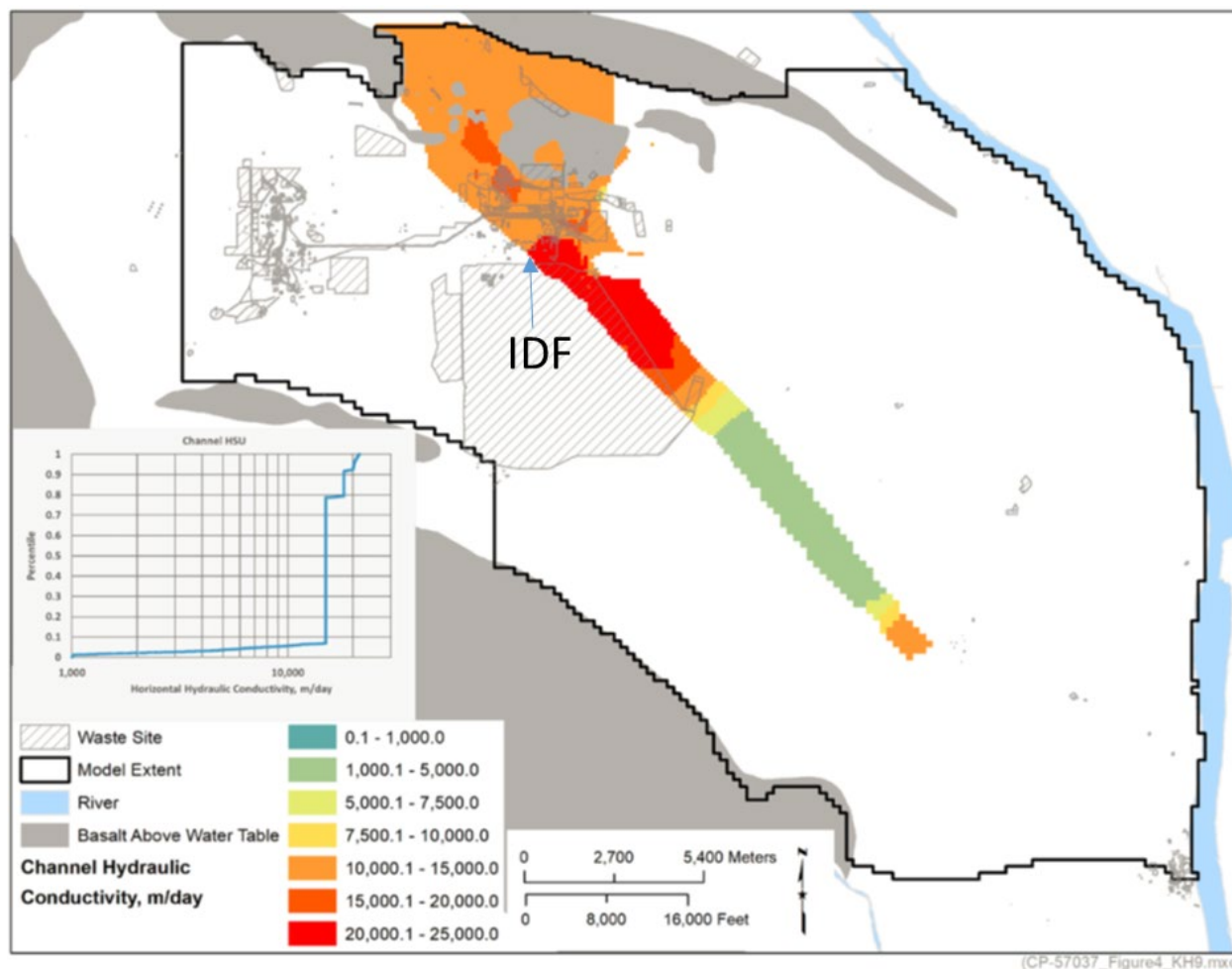
Source: CP-57037, *Model Package Report: Plateau to River Groundwater Model Version 8.2*, Rev. 1, Figure 4-43.

Note: The Hanford channel extends beneath the Integrated Disposal Facility (IDF) footprint and has a calibrated hydraulic conductivity of between 15,000 and 25,000 m/day.

To provide a more detailed representation of the calibrated hydraulic conductivity of the Hanford channel deposits and the HCZ near the IDF, the results of the P2R Version 8.3 in the area near the IDF have been extracted from the model file and this information is presented alongside each regional scale figure.

Summary

As noted in the RAI, the lateral extent and hydraulic conductivity of the Hanford channel sediments beneath the IDF are an important component of the IDF PA, given the role of the saturated zone in diluting radionuclides that may be released from the engineered facility and transported to the water table. This importance was recognized in the IDF PA and resulted in

planned maintenance activity to confirm the base case values used in the IDF PA. The maintenance activities conducted to date have confirmed the hydraulic conductivity value used in the IDF PA base case. Continued maintenance activities will be performed in the future.

Figure 2-16-5. Location of the High Conductivity Zone Analysis Area used in the Plateau to River Version 8.3.
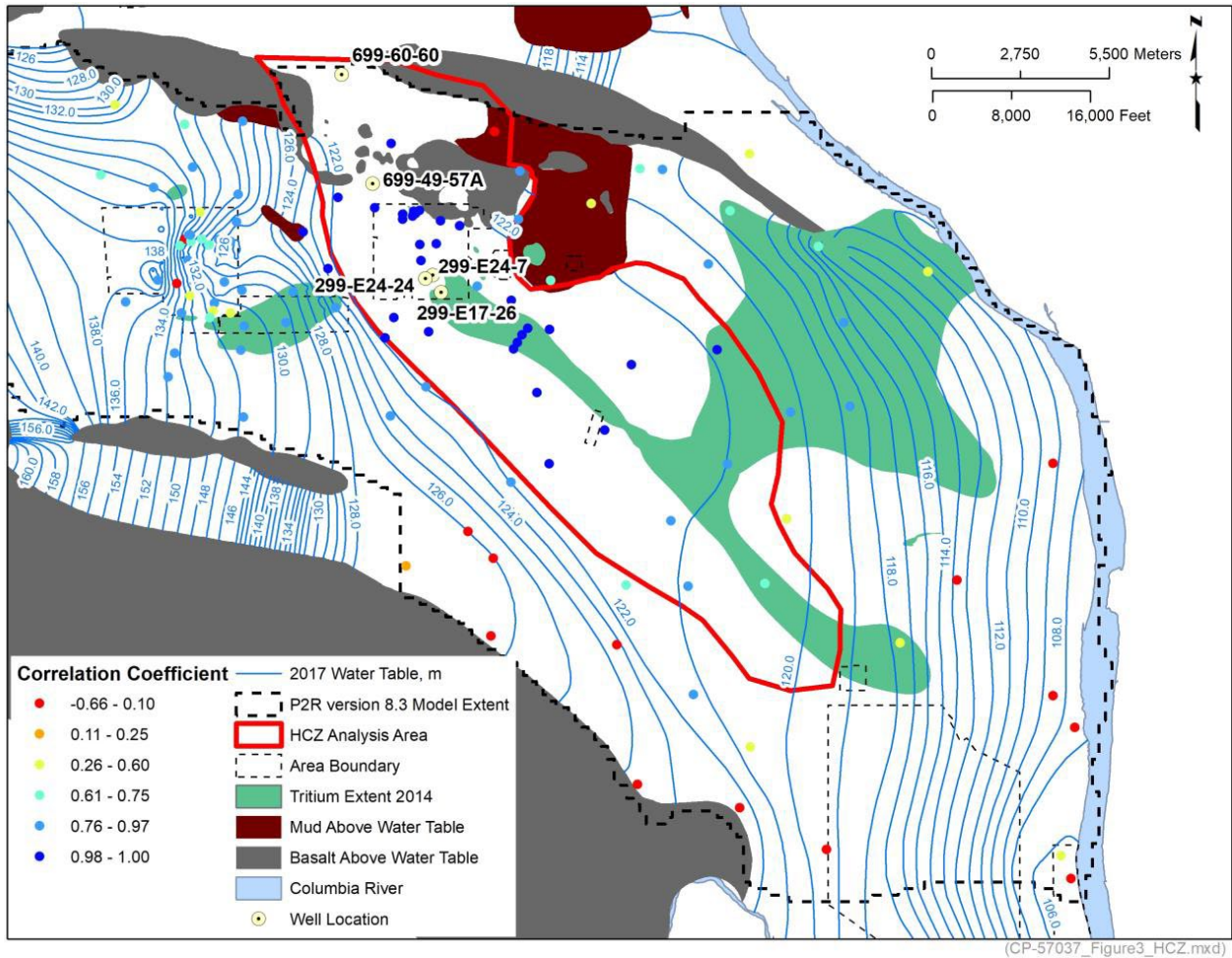
Source: CP-57037, *Model Package Report: Plateau to River Groundwater Model Version 8.3*, Rev. 2, Figure 3-9.

Note: The location of the high conductivity zone (HCZ) analysis area is based on wells that exhibit a similar water level response to anthropogenic water discharges. The HCZ analysis area defines an area that is expected to contain the HCZ; however, the HCZ extent is determined during the model calibration process and is illustrated by the calibrated hydraulic conductivity for Layers 1 to 5 of the Plateau to River (P2R) model in Figures 2-16-6 to 2-16-10 as well as the calibrated transmissivity illustrated in Figure 2-16-11.

Figure 2-16-6. Calibrated Hydraulic Conductivity for Plateau to River Version 8.3 Model Layer 1.
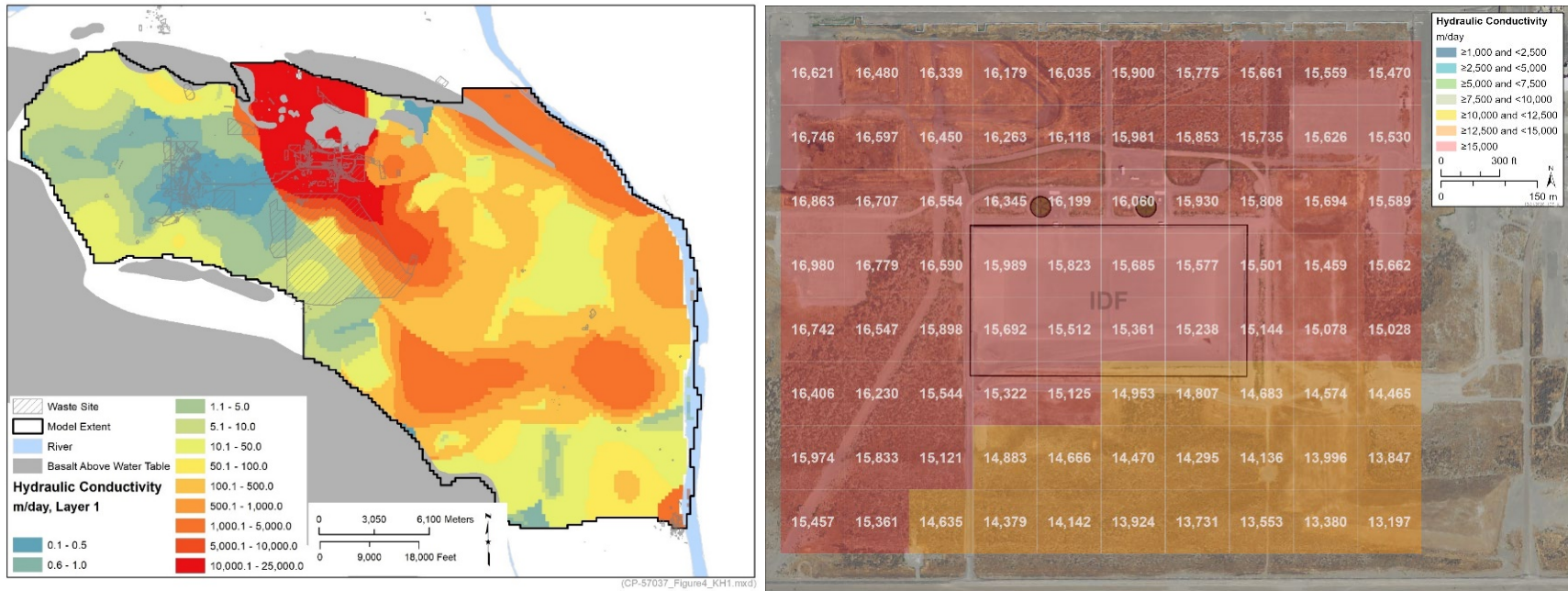
Source: CP-57037, *Model Package Report: Plateau to River Groundwater Model Version 8.3*, Rev. 2, Figure 4-36.

Figure 2-16-7. Calibrated Hydraulic Conductivity for Plateau to River Version 8.3 Model Layer 2.

Source: CP-57037, *Model Package Report: Plateau to River Groundwater Model Version 8.3*, Rev. 2, Figure 4-37.

Figure 2-16-8. Calibrated Hydraulic Conductivity for Plateau to River Version 8.3 Model Layer 3.

Source: CP-57037, *Model Package Report: Plateau to River Groundwater Model Version 8.3*, Rev. 2, Figure 4-38.

Figure 2-16-9. Calibrated Hydraulic Conductivity for Plateau to River Version 8.3 Model Layer 4.
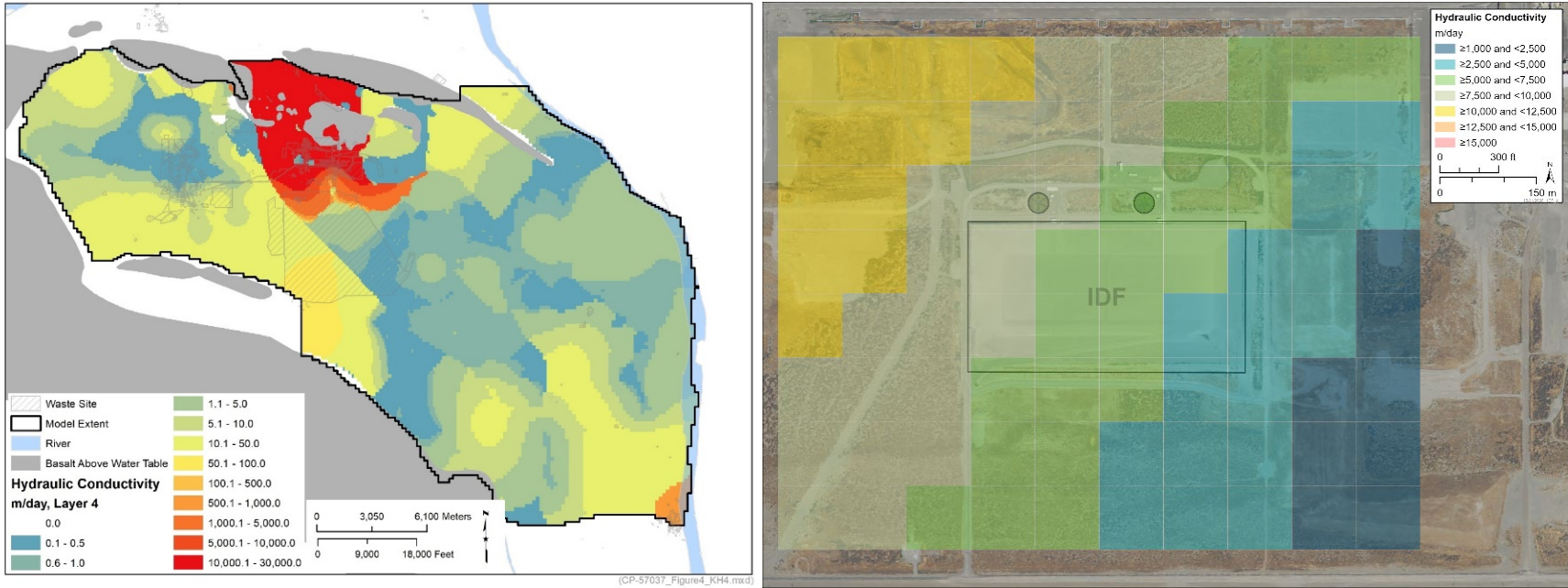
Source: CP-57037, *Model Package Report: Plateau to River Groundwater Model Version 8.3*, Rev. 2, Figure 4-39.

Figure 2-16-10. Calibrated Hydraulic Conductivity for Plateau to River Version 8.3 Model Layer 5.
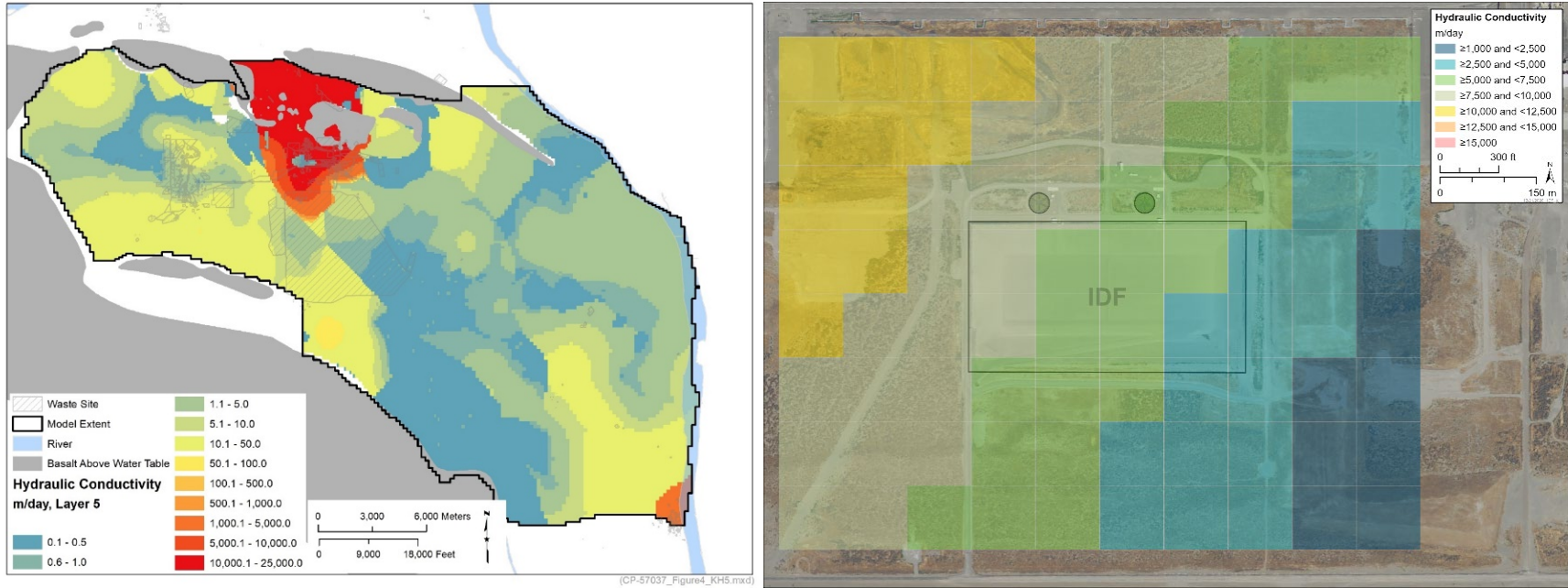
Source: CP-57037, *Model Package Report: Plateau to River Groundwater Model Version 8.3*, Rev. 2, Figure 4-40.

Figure 2-16-11. Calibrated Transmissivity for Plateau to River Version 8.3.

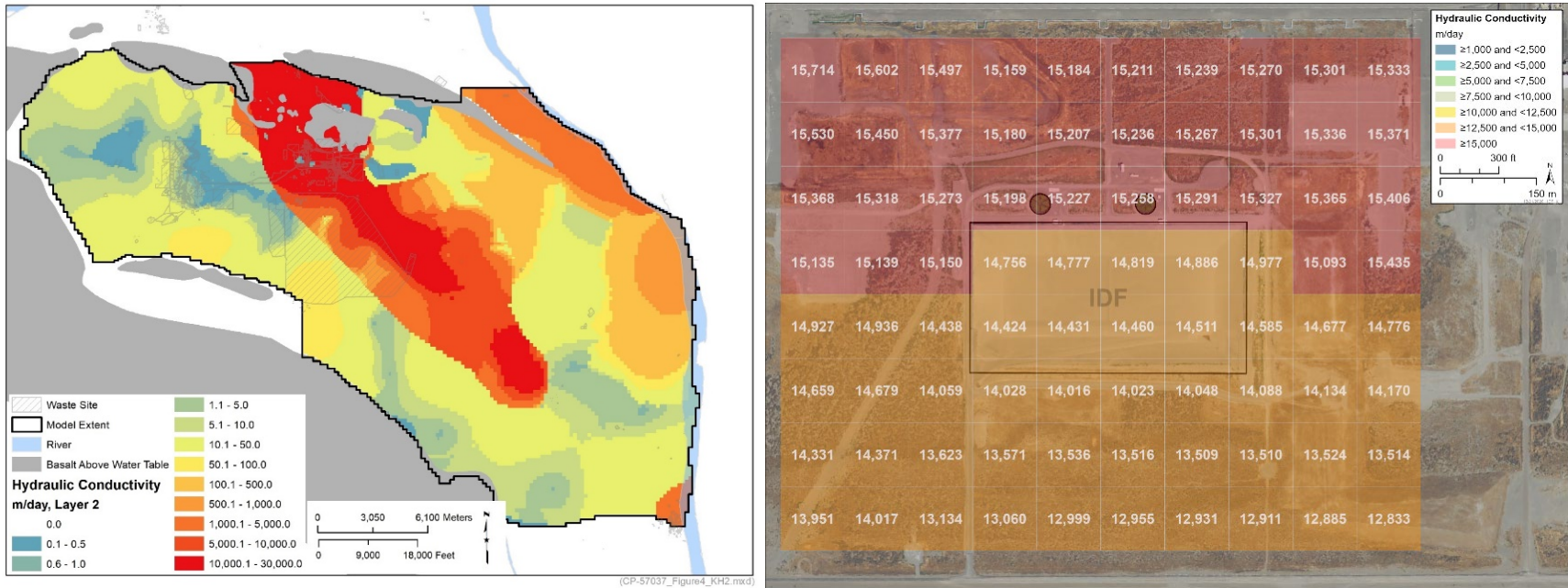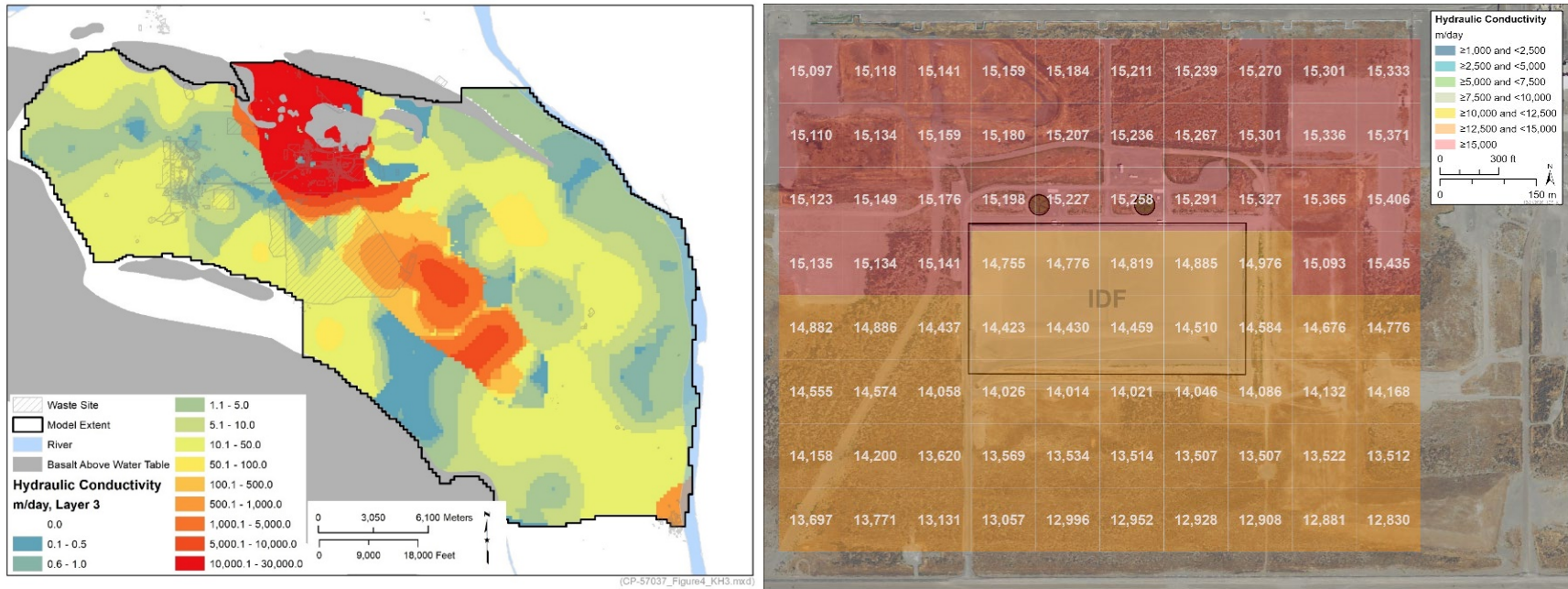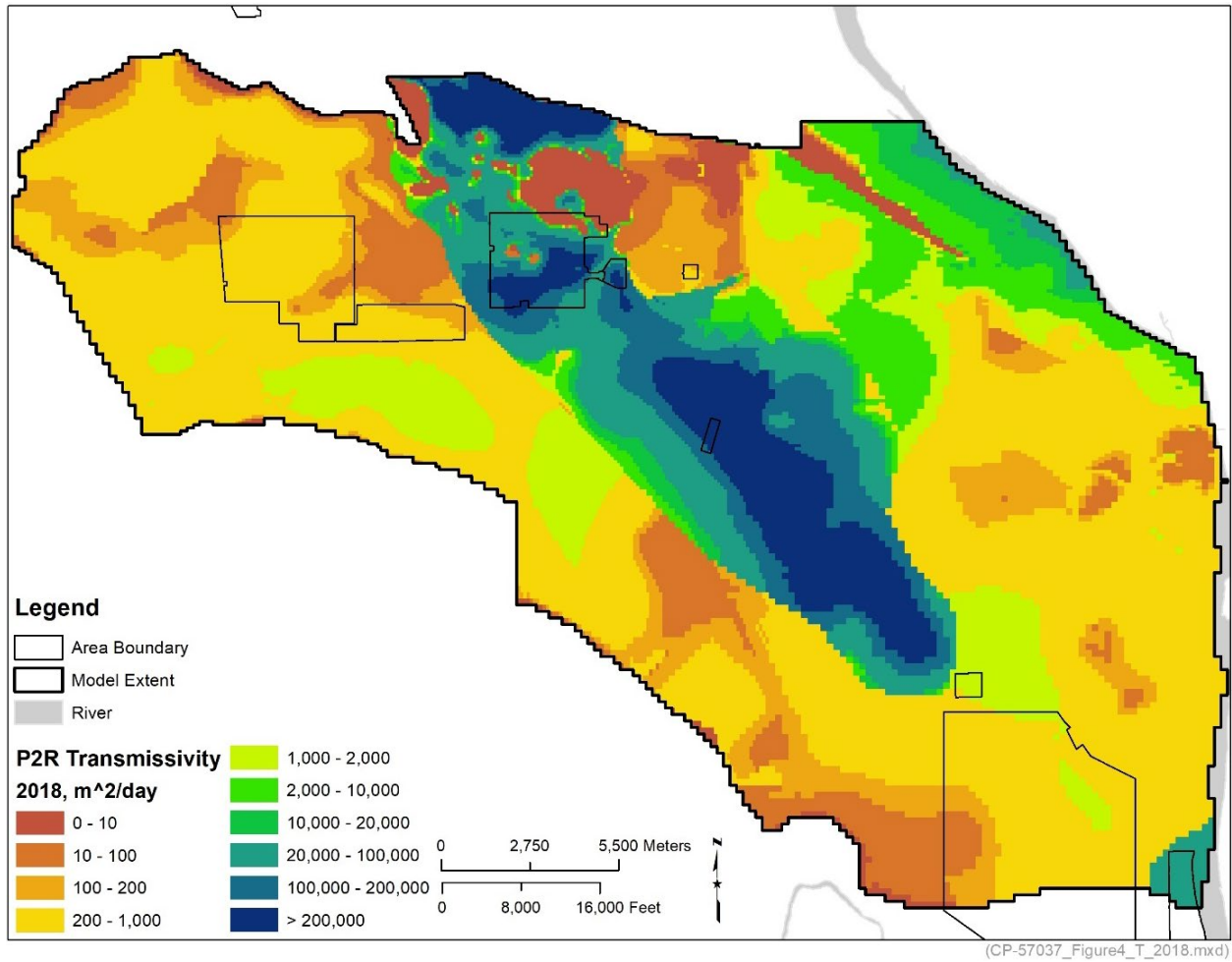Source: CP-57037, *Model Package Report: Plateau to River Groundwater Model Version 8.3*, Rev. 2, Figure 4-44.

Note: The upper surface of the suprabasalt aquifer is assumed to be the modeled 2018 water table surface. The area with transmissivity greater than 20,000 m^2/day represents the high conductivity zone (HCZ). Near the Integrated Disposal Facility (in the southcentral part of the 200 East Area) the calibrated transmissivity is about 100,000 m^2/day representing the HCZ of the Hanford channel in that area.

References

CHPRC-03348, 2019, *Performance Assessment Maintenance Plan for the Integrated Disposal Facility,* Rev. 1, CH2M HILL Plateau Remediation Company, Richland, Washington.

CP-47631, 2015, *Model Package Report: Central Plateau Groundwater Model Version 6.3.3*, Rev. 2, INTERA, Inc., Richland, Washington. Available at: https://pdw.hanford.gov/document/0077133H.

CP-47631, 2017, *Model Package Report: Central Plateau Groundwater Model Version 8.3.4*, Rev. 3, INTERA, Inc./CH2M HILL Plateau Remediation Company, Richland, Washington. Available at: https://pdw.hanford.gov/document/0069098H.

CP-47631, 2018, *Model Package Report: Central Plateau Groundwater Model, Version 8.4.5*, Rev. 4, CH2M HILL Plateau Remediation Company, Richland, Washington. Available at: https://pdw.hanford.gov/document/0066449H.

CP-57037, 2015, *Model Package Report: Plateau to River Groundwater Transport Model Version 7.1*, Rev. 0, CH2M HILL Plateau Remediation Company, Richland, Washington. Available at: https://pdw.hanford.gov/document/0080149H.

CP-57037, 2019, *Model Package Report: Plateau to River Groundwater Model Version 8.2*, Rev. 1, CH2M HILL Plateau Remediation Company, Richland, Washington. Available at: https://pdw.hanford.gov/document/AR-01336.

CP-57037, 2020, *Model Package Report: Plateau to River Groundwater Model Version 8.3*, Rev. 2, CH2M HILL Plateau Remediation Company, Richland, Washington. Available at: https://pdw.hanford.gov/document/AR-03674.

DOE/EIS-0391, 2012, *Final Tank Closure and Waste Management Environmental Impact Statement for the Hanford Site, Richland, Washington*, U.S. Department of Energy, Washington, D.C.

DOE O 435.1, 2011, *Radioactive Waste Management*, Change 2, U.S. Department of Energy, Washington, D.C.

DOE/RL-2015-75, 2016, *Aquifer Treatability Test Report for the 200-BP-5 Groundwater Operable Unit*, Rev. 0, U.S. Department of Energy, Richland Operations Office, Richland, Washington. Available at: https://pdw.hanford.gov/document/0074649H.

ECF-HANFORD-13-0029, 2015, *Development of the Hanford South Geologic Framework Model, Hanford Site, Washington*, Rev. 2, prepared by INTERA, Inc. for CH2M HILL Plateau Remediation Company, Richland, Washington. Available at: https://pdw.hanford.gov/document/0072751H.

RPP-CALC-61016, 2017, *Saturated Zone Flow – Sensitivity Analyses Using the 3-D EIS Groundwater Flow Model and the Central Plateau Groundwater Flow Model in the Vicinity of the Integrated Disposal Facility*, Rev. 0, INTERA, Inc. prepared for Washington River Protection Solutions, LLC, Richland, Washington.

RPP-CALC-61032, 2018, *Vadose Zone and Saturated Zone Flow and Transport Calculations for the Integrated Disposal Facility Performance Assessment*, Rev. 0A, prepared by INTERA Inc. for Washington River Protection Solutions, LLC, Richland, Washington.

RPP-RPT-59344, 2019, *Integrated Disposal Facility Model Package Report: Vadose and Saturated Zone Flow and Transport*, Rev. 0A, prepared by INTERA Inc. for Washington River Protection Solutions, LLC, Richland, Washington.

RPP-RPT-59958, 2019, *Performance Assessment for the Integrated Disposal Facility, Hanford Site, Washington*, Rev. 1A, Washington River Protection Solutions, LLC, Richland, Washington.

WMP-27008, 2005, *Borehole Summary Report for Wells 299-24-24 (C4647) and 299-E17-26 (C4648), Integrated Disposal Facility*, Fluor Hanford Company, Richland, Washington. Available at: https://pdw.hanford.gov/document/DA01417799

RAI 2-17   (Intruder)

Comment
DOE provided the dose result to an inadvertent intruder resulting from the average waste but did
not provide the range of potential intruder doses that could be anticipated. NRC provided a
number of comments and recommendations associated with intruder analyses for WMA-C that
DOE was not able to address in this draft WIR evaluation due to timing differences.

Basis
DOE communicated the dose to an inadvertent intruder resulting from unanticipated future
intrusion into a particular waste type. However, DOE did not communicate the range of
inadvertent intruder doses that could be anticipated for each waste stream.

The waste will be disposed in the IDF which is a near-surface disposal facility. However, the
IDF is a "deep" near-surface disposal facility such that an excavation scenario is highly unlikely.
The intruder scenario evaluated was a drilling scenario where the installation of a well to recover
resources results in the extraction of geologic materials and some waste in the drill cuttings. The
amount of waste potentially disturbed is much lower than what is expected in an excavation
scenario. Whereas in the excavation scenario, the concentration of radionuclides in the disturbed
waste may more closely approximate the average concentration, for a discrete event like drilling
the concentration in the disturbed waste is likely to reflect the variability of radionuclide
concentrations in the waste. The risk is a product of probability and consequence, and the
probability goes down as drilling at locations of less likely concentrations occur (e.g., the most
highly concentrated waste). NRC and most other regulators impose limits that reflect the average
concentration of the waste but also impose requirements as to how much averaging can be used
(e.g., the NRC's Branch Technical Position on Concentration Averaging and Encapsulation
(ML12254B065)).

NRC issued the technical evaluation report (TER) for review of the draft waste evaluation for
WMA-C in May 2020 (ML20128J832). In that report, NRC provided recommendations and
comments on the inadvertent intruder analyses. The inadvertent intruder analyses for VLAW
used essentially an identical approach, but the VLAW analyses were completed prior to the NRC
TER, and therefore, DOE could not address NRC comments. In addition, those comments were
not risk-significant in the context of WMA-C but could be risk-significant with respect to the
VLAW analyses.

Path Forward
Please provide the range of dose impacts to an inadvertent intruder from each waste stream
disposed in the IDF that is within the scope of the draft waste evaluation as discussed previously
in this document. The assessment should consider risk-significant comments made on the WMA-
C intruder assessment, if applicable to the intruder assessment for VLAW.

DOE Response
The Draft WIR Evaluation addresses the WIR criteria for VLAW produced using the DFLAW
approach. Other wastes are outside the scope of the Draft WIR Evaluation, including
non-reprocessing secondary waste (see DOE response [Section 2.0]) and vitrified waste assumed

to potentially be produced by supplemental LAW treatment (for which DOE has made no decision to pursue).[93] To bound the analysis, the IDF PA correctly includes all wastes potentially disposed of in the IDF, including the DFLAW-produced VLAW as well as potential additional VLAW,[94] and all SSW which may be disposed at IDF. The approach to ensuring that all waste packages are acceptable for disposal at the IDF is described in this RAI response and is the same for all waste streams.

DOE's estimate of long-term consequences from the IDF are based on computer models for: 1) estimating radionuclide inventory in the waste and 2) calculating potential post-closure dose consequences to a member of the public in the future. DOE acknowledges that there will be variability in the DFLAW feed stream to the WTP LAW Vitrification Facility. Because of this variability, the vitrified LAW disposed of in the IDF is expected to have variable compositions.

DOE's hypothetical intruder analysis described in RPP-CALC-61254, *Inadvertent Intruder Dose Calculation Update for the Integrated Disposal Facility Performance Assessment* did not evaluate the variability in the radionuclide concentrations in the VLAW or secondary wastes. Instead, all waste in the IDF was simulated using an average concentration computed using the total inventory in a particular waste stream (e.g., VLAW, SSW, or solidified LSW) and the total as-disposed volume of that waste stream. The total as-disposed volume accounted for debris compaction and any solidification material necessary to encapsulate or stabilize the waste.[95] To address inventory uncertainty, DOE did evaluate alternative inventory scenarios to demonstrate that the dose to the hypothetical intruder from each radionuclide in the waste was proportional to the radionuclide inventory in the waste. Thus, inventory uncertainty would always be identified as a significant parameter in an importance analysis and potentially could mask the importance of other parameters.

In addition, the intruder dose model was used to compute the concentration of each radionuclide in the impacted waste that would yield a dose to the intruder that is equal to 500 mrem for an acute 40-hour exposure or 100 mrem/yr for a chronic annual exposure, consistent with DOE's

---

[93] Information concerning supplemental LAW is provided in this RAI response for additional information and completeness only, and is outside the scope of both the Draft WIR Evaluation and DOE decisions concerning supplemental LAW treatment. DOE has not made decisions concerning the potential path forward for supplemental LAW treatment, as explained in footnote 7 of the Draft WIR Evaluation and 78 FR 75913, "Record of Decision: Final Tank Closure and Waste Management Environmental Impact Statement for the Hanford Site, Richland, Washington." As explained in Section 1.2 of the Draft WIR Evaluation, the Draft WIR Evaluation does not address or include in its scope supplemental LAW. To bound the IDF PA analysis, the IDF PA assumed that supplemental LAW may potentially be vitrified and disposed of in the IDF, although, as explained above, DOE has made no decisions concerning the potential path forward for supplemental LAW treatment.

[94] See footnote 93.

[95] RPP-CALC-61254 Rev. 1 evaluated the intruder dose for the eight SSW streams discussed in the PA. The chronic dose after intruding into eight containers of compacted HEPA filters (190 mrem/yr) or eight containers of non-CERCLA, non-tank waste (1,390 mrem/yr) exceeded DOE's performance measure (100 mrem/yr) when the intrusion occurred 100 years after closure. Placing two stacked containers of these low-volume waste streams directly over one another in four separate disposal lifts was not probable. To better represent the mix of waste that will be placed into the IDF over 30 to 50 years of disposal operations, the calculation approach was changed to include an average SSW waste instead of separate waste streams in RPP-CALC-61254 Rev. 2. In addition, WAC were developed to determine concentrations limits for SSW to minimize the placement of waste containers with high intruder consequences above one another.

performance measures for protection of the human intruder in DOE M 435.1-1. Because the IDF waste is disposed of in four lifts, with each lift containing one vitrified waste container or two stacked SSW or solidified LSW containers, the resulting concentration limit is the average concentration in the impacted containers, and is not a limit for each container. The resulting waste concentrations were incorporated into the IDF WAC, IDF-00002, Table G-1. The disposal limits for short-lived radionuclides are sensitive to the time of the inadvertent intrusion. In this analysis, the time of intrusion (2278) was equated to the minimum time that DOE must retain excavation restrictions (through institutional controls) on the Hanford Site to provide reasonable expectation that the dose to an inadvertent intruder would not exceed DOE's performance measures. The recommended institutional control period for the entire Hanford Site is the latest institutional control date specified for a waste site on the Hanford Site in DOE/RL-2001-41, *Sitewide Institutional Controls Plan for Hanford CERCLA Response Actions and RCRA Corrective Actions.* Using this date for intruder analyses is the recommendation from DOE-0431, *Recommendations for Institutional Control Time Period for Conducting DOE Order 435.1 Performance Assessments at the Hanford Site.*

Using a sum of fractions approach (Equation 2.17-1), the waste concentration limits in Table G-1 of the WAC are intended to protect the inadvertent intruder from an acute or chronic dose that exceeds DOE performance measures once intruder protections are assumed lost.

$$SOF = \sum_i^n \frac{C_i}{C_{LIMIT,i}} = \sum_i^n \frac{M_i \times SpAct_i \times \frac{1}{V_{WP}}}{C_{LIMIT,i}} \qquad (2.17\text{-}1)$$

Where:

SOF	=	total sum of fractions with respect to WAC limits
C_i	=	certified waste profile activity concentration of radionuclide i
$C_{LIMIT,i}$	=	waste acceptance criteria concentration limit of radionuclide i (Table G-1 of IDF-00002)
M_i	=	mass of radionuclide i in a container in the waste profile
$SpAct_i$	=	specific activity of radionuclide i
V_{WP}	=	as-disposed volume of the container in the waste profile.

Each waste package destined for IDF will have a certified waste profile that is screened against the WAC concentration limits by the IDF waste acceptance team to ensure that each package is not a hot spot for the facility that could result in a dose to the intruder that exceeds DOE's performance measures. Section 2.0 of IDF-00002 describes the waste acceptance process. Waste generators will prepare a certified waste profile for each waste stream prior to shipping waste to the IDF. The IDF waste acceptance team will review the certified waste profile to ensure each profile meets the requirements in the WAC, including calculating the sum of fractions to ensure protection of an inadvertent intruder. In addition, the sum of fractions is calculated for each shipment of waste to the IDF. The concentrations in the shipment cannot exceed concentrations in the certified waste profile. If all waste shipped to the IDF meets the sum of fractions test, then there is not likely to be a hot spot in the facility that would lead to a dose to an intruder that exceeds DOE's performance measures.

Furthermore, the waste acceptance process could permit disposal of VLAW with a sum of fractions with respect to IDF WAC concentration limits that is greater than 1. However, this requires an evaluation and is done on a case-by-case basis. This allowance occurs because the intruder scenario calculations assume that the intrusion intercepts four VLAW containers, each having one-fourth the inventory that causes the dose. If the drilling event impacts fewer than four VLAW containers or impacts at least one VLAW container with a sum of fractions that is less than one, then it would be possible for one (or more) of the impacted VLAW containers to have a sum of fractions greater than 1 but a dose following an intrusion that is still less than the DOE performance measure. In the event that a forecasted VLAW waste profile has a sum of fractions that is greater than 1, a case-by-case WAC acceptance process will be invoked through the change management process IDF-PRO-EN-54165, *IDF Unreviewed Disposal Question* to ensure that the VLAW container can be safely disposed of in the IDF and to determine if it is necessary to impose any additional constraints on where it can be placed or how much inventory can be placed above it. Although outside the scope of the Draft WIR Evaluation, the same case-by-case evaluation can be performed for SSW and LSW containers that have a sum of fractions greater than 1.

To explore how variability would contribute to the possibility of hot spots in the IDF, the Hanford flowsheet model for LAW vitrification generated a monthly forecast for the amount of each radionuclide that will be incorporated into VLAW and the volume of VLAW produced in that month. This information is reported in RPP-RPT-57991, Rev. 3. The monthly forecasted inventory and volumes were used to compute a monthly average concentration in the VLAW. This monthly average illustrates the variability in the VLAW because of variability in the LAW feed. The resulting concentrations were compared to the concentration limits and a sum of fractions for each month was computed using Equation 2-17-1. The results are shown in Figure 2-17-1 for the WTP LAW Vitrification Facility that includes the DFLAW mission and vitrification in the WTP LAW Vitrification Facility following pre-treatment at the WTP Pre-Treatment Facility after the DFLAW mission is completed. Consistent with the PA that assumes that any LAW exceeding the processing capability of the first vitrification facility will be vitrified in a second vitrification plant, Figure 2-17-2 shows the sum of fractions result for potential supplemental LAW vitrification for additional information and completeness, although DOE has not made decisions concerning the path forward for Supplemental LAW treatment. In no month did the monthly-average concentration yield a sum of fractions that exceeded 1. Individual radionuclides that exceeded 1% of the disposal limit concentration in any month are also plotted separately to illustrate their contribution to the total sum of fractions. There were only six radionuclides that exceeded 1% of the disposal limit concentration in at least one month: [63]Ni, [90]Sr[96], ^{99}Tc, [126]Sn, [239]Pu, and [241]Am. The variability in the fraction of the disposal limit for a single radionuclide shown in Figures 2-17-1 and 2-17-2 demonstrate the flowsheet variability in the product concentration. The plotted fraction is the product concentration divided by a fixed value for the disposal concentration limit according to Equation 2-17-1. For the six radionuclides that have a peak concentration that is at least 1% of the disposal limit, either the chronic rural pasture scenario or chronic suburban garden scenario have the most restrictive

---

[96] The decontamination factor for ^{90}Sr in the Tank-Side Cesium Removal unit is zero in the flowsheet model that produced the input to this calculation. If ^{90}Sr is also captured and retained during the Tank-Side Cesium Removal treatment, ^{90}Sr in the VLAW product will be lower than simulated with a decontamination factor of zero.

concentration limits. The results shown in Figures 2-17-1 and 2-17-2 can be converted to a dose value by multiplying the fractions by 100 mrem/yr.

Figure 2-17-1. Monthly Radionuclide Sum of Fractions for Vitrified Low-Activity Waste.
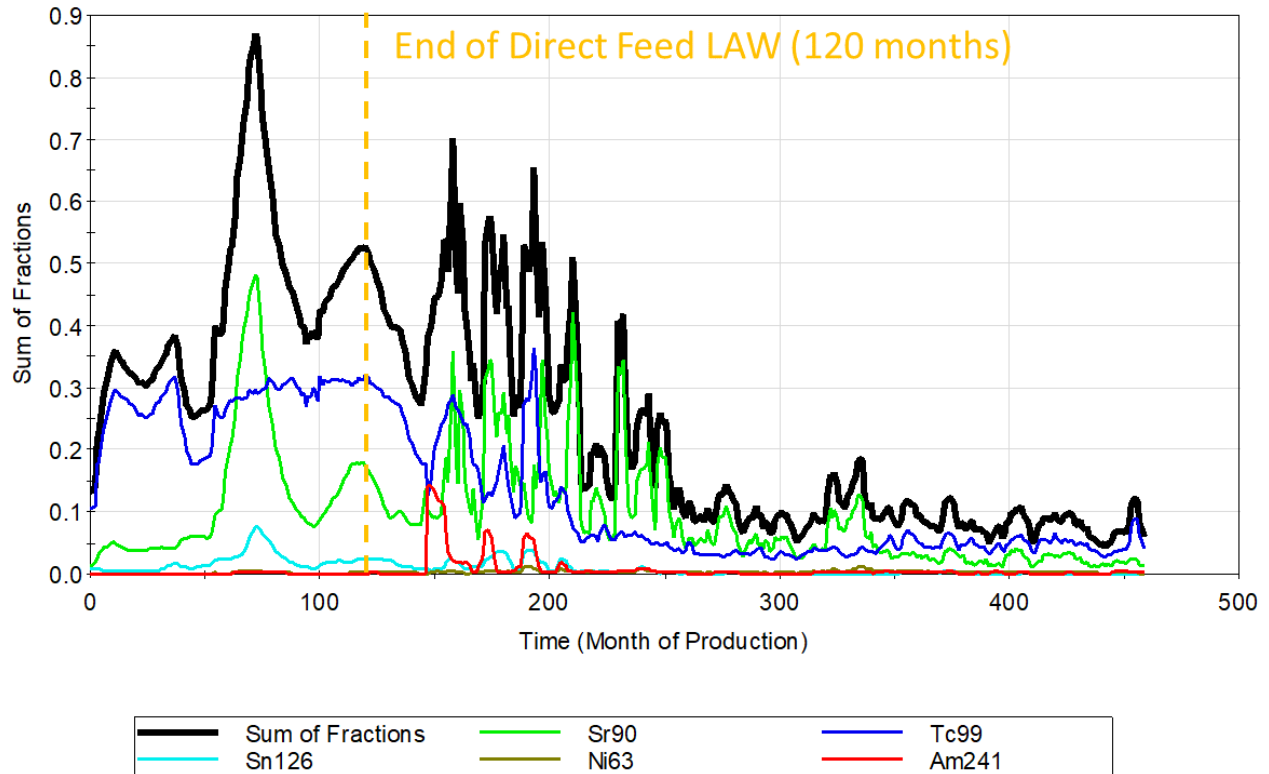
Note: Low-activity waste (LAW) vitrification after the end of Direct Feed LAW is outside the scope of the Draft WIR Evaluation.

The highest sum of fractions is 0.87, which means that an intrusion into any vitrified waste container is not expected to result in a chronic dose to the intruder that exceeds 100 mrem/yr or an acute dose that exceeds 500 mrem.

DOE believes that the site-wide institutional control plan, WAC concentration limits, and evaluations comparing the contents of waste packages to the concentration limits will provide reasonable expectation that the performance measures will be met for protection of the hypothetical human intruder at the IDF.

DOE has reviewed NRC's comment on the intruder analysis performed for Hanford WMA C made in their Technical Evaluation Report (TER) (ML20128J832 referred to as WMA C TER). DOE was not able to address NRC's intruder scenario and exposure factor recommendations for the latest revision of the IDF intruder analysis because the recommendations were provided after that IDF intruder analysis was completed. The following list identifies the NRC

comments/recommendations on the WMA C intruder analysis presented in the WMA C TER and a response concerning VLAW in the IDF PA.

- A quantitative basis should be developed that engineered components will deter modern drilling methods for hundreds of years (WMA C TER Recommendation #43). Although the WMA C PA credited the robustness of the tank dome for deterring an inadvertent intrusion into the tank for 500 years, the IDF PA inadvertent intruder calculations do not credit any engineered components for deterring an inadvertent intrusion beyond 100 years of institutional controls after IDF closure.

Figure 2-17-2. Monthly Radionuclide Sum of Fractions for Supplemental Vitrified Low-Activity Waste (after Direct Feed Low Activity Waste Mission).
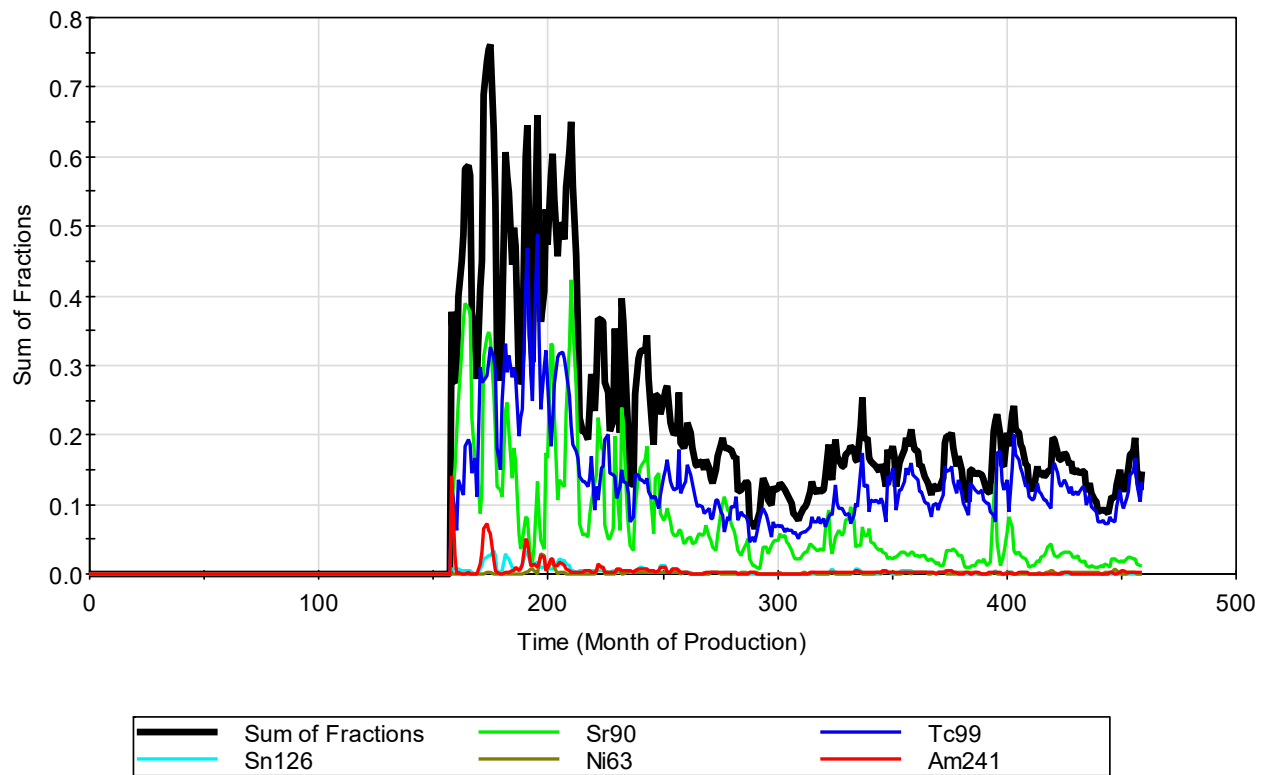
Note: See footnote 93.

- The drill cuttings are spread over a large area and tilled deep into the soil surface (15 cm) achieving a large amount of dilution. Unless the entire property is tilled, such a deep depth is not consistent with natural phenomenon. Tillage depth should be consistent with future land and exposure scenario assumptions (WMA C TER Recommendation #44). One of the main uses of the inadvertent intruder analyses documented in the IDF PA is the development of disposal concentrations limits that are published in the IDF WAC. According to RPP-CALC-61254 Rev. 3 Table 6-6, there are only six radionuclides in VLAW with mission-averaged concentrations that are greater than 0.5% of the disposal limit calculated for an intrusion that occurs 100 years after closure: ^{241}Am (0.7%), ^{137}Cs (0.6%), ^{239}Pu (0.8%), ^{126}Sn (1.5%), ^{90}Sr (29.8%), and ^{99}Tc (10.5). When the intrusion is

mitigated by DOE's presence on the site and institutional controls until 2278 (as recommended in DOE-0431), the disposal limits increase for short-lived radionuclides so that the projected ^{90}Sr inventory in VLAW drops to 9% of the disposal limit (RPP-CALC-61254 Rev. 3 Table 6-7). When the tillage depth outside the garden area in the Suburban Garden scenario is reduced from 15 cm to 5 cm, the disposal limits reported in RPP-CALC-61254 Rev. 3 Table 6-6 for ^{241}Am, ^{137}Cs, ^{239}Pu, and ^{126}Sn drop by 20 to 44%. Based on the projected inventory of these radionuclides in VLAW relative to the concentration limits reported above, a 20% to 44% reduction in the inventory limit indicates that the intruder dose in these scenarios would not exceed the DOE dose limit set forth in the performance measures for acute or chronic exposures. The disposal limits for ^{90}Sr and ^{99}Tc are unchanged because these limits are determined by the Rural Pasture scenario, which continues to use a 15-cm tillage depth for the pasture. Generally, a reduction in the tilling depth of the pasture will have an inversely proportional change (i.e., increase) on the dose to the intruder and a proportional reduction in the disposal limit concentrations when the rural pasture scenario is the concentration limiting scenario for a radionuclide. The predominant exposure pathway for ^{90}Sr and ^{99}Tc in the Rural Pasture scenario is the milk ingestion pathway. Dairy cow ingestion of fodder is the primary (>99%) bioaccumulation route from the soil for these radionuclides. HNF-SD-WM-TI-707, *Exposure Scenarios and Unit Factors for Hanford Tank Waste Performance Assessment*, Rev. 5, which is the source for the tilling depth value used in the PA, selected 15-cm tillage depths to be consistent with the root depth of garden vegetables (HNF-SD-WM-TI-707 Section 2.1.2). HNF-SD-WM-TI-707 acknowledges that shallower tilling depths would lead to less dilution in the soil after mixing, but would be offset by roots that might extend below the contaminated zone and would ultimately provide the same amount of bioaccumulation. This position was developed for the garden scenarios and was carried over into the pasture scenario without adjustment. The bioaccumulation factors for pasture scenarios were selected for sparsely-vegetated pastures, but the pasture area is computed assuming a heavily-vegetated pasture (crop yield was 1.5 wet kg of fodder per square meter). Due to the differences in the assumed vegetation state for the pasture area and the bioaccumulation factors, the pasture area or bioaccumulation factors may overestimate milk dose by a factor of two or more. Therefore, it is believed that the tilling depth of 15 cm, although it may not be typical of natural mixing, is adequate for this hypothetical analysis and offsets other "conservatisms" included in other parameters used in the dose calculation. The exposure scenario data package providing the scenario-specific inputs is under revision. This recommendation will be added to the list of changes being considered for the data package update.

- The consumption rates between the intruder and on-site receptor are inconsistent. The fruit and vegetable consumption rates used are more applicable to an average member of the public rather than a gardener. (WMA C TER Recommendation #45) The exposure scenario data package providing the scenario-specific inputs is under revision. This recommendation will be added to the list of changes being considered for the data package update.

- Site-specific values for biosphere parameters should be used when available (WMA C TER Recommendation #46). DOE agrees that site-specific data should be used for all parts of the performance assessment when available. In the absence of site-specific information for a representative future person in the hypothetical intruder scenario, the biosphere parameters developed in HNF-SD-WM-TI-707 Rev. 5 that were used in the PA were developed using generalized exposure factors and in some cases were modified to accommodate regional influences (see example below from HNF-SD-WM-TI-707 Rev. 5 page A-17).

  > "The column labeled "USDA" *[in Table A4 titled Food and Water Consumption Rates]* comes from indirect estimates of average per capita food consumption based on food production in the United States .... Losses from exports, industrial uses, and end-of-year stocks were taken into account. The other and fruit consumption rates do not include bananas, pineapples, or citrus fruits, because they are not grown in southeastern Washington."

- Plot sizes are arbitrary. If a gardener is gardening, they would size the garden to provide all the family needs (WMA C TER page 3-139, related to WMA C TER Recommendation #46). The size of the garden and pasture are developed in HNF-SD-WM-TI-707. The garden size is assumed to be ¼ the size necessary to grow all the fruits and vegetables consumed based on exposure factors in EPA/600/P-95/002Fa, *Exposure Factors Handbook Volume 1: General Factors*. The exposure scenario data package providing the scenario-specific inputs is under revision. The size of the contaminated areas will be added to the list of changes being considered for the data package update.

- Site-specific values for exposure parameters should be used when available, such as Hanford mass loading factors from BNWL-2081, *Radioactive Particle Resuspension Research Experiments on the Hanford Reservation*. Mass loading for driller should be re-evaluated (WMA C TER Recommendation #47). DOE anticipates taking a risk-informed approach to potential data collection of mass loading factors. The only application of this data collection effort would be to support calculations in the hypothetical intruder scenarios. For this RAI response, the disposal concentration limits were recalculated using a mass loading factor that is 10 times higher than the base case value, a value consistent with the maximum discussed by the NRC in the WMA C TER, and the tillage depth was changed to 5 cm for the area outside of the garden in the Suburban Garden scenario. The sum of fractions for the projected inventory that includes VLAW, SSW and ETF-LSW reported in RPP-CALC-61254 Rev. 3 Table 6-6 increased from 0.675 to 0.773.

- Recommended including radon in dose calculations to increase transparency with stakeholders as it could be a hidden impact when it is excluded even though a separate standard is used for compliance (WMA C TER Recommendation #48). Consistent with DOE M 435.1-1, the dose to the inadvertent intruder should exclude the dose from radon in air. Therefore, radon contributions to dose are excluded in the inadvertent intruder

dose assessment. Radon release is simulated and compared to the radon flux performance objective, which limits radon releases to 20 pCi/m^2/s at the surface of the disposal facility. Therefore, the NRC's TER recommendation is inconsistent with DOE M 435.1-1, and DOE Technical Standard DOE-STD-5002-2017, *Disposal Authorization Statement and Tank Closure Documentation*.

References

78 FR 75913, 2013, "Record of Decision: Final Tank Closure and Waste Management Environmental Impact Statement for the Hanford Site, Richland, Washington," *Federal Register*, Vol. 78, pp. 75913–75919 (December 13).

BNWL-2081, 1977, *Radioactive Particle Resuspension Research Experiments on the Hanford Reservation*, Battelle Pacific Northwest Laboratories, Richland, Washington.

DOE-0431, 2019, *Recommendations for Institutional Control Time Period for Conducting DOE Order 435.1 Performance Assessments at the Hanford Site*, Rev. 0, U.S. Department of Energy, Office of River Protection, Richland, Washington.

DOE M 435.1-1, 2011, *Radioactive Waste Management Manual*, Change 2, U.S. Department of Energy, Washington, D.C.

DOE/RL-2001-41, 2019, *Sitewide Institutional Controls Plan for Hanford CERCLA Response Actions and RCRA Corrective Actions*, Rev. 9, U.S. Department of Energy, Richland Operations Office, Richland, Washington.

DOE-STD-5002-2017, 2017, *Disposal Authorization Statement and Tank Closure Documentation*, U.S. Department of Energy, Washington, D.C.

EPA/600/P-95/002Fa, 1997, *Exposure Factors Handbook Volume 1: General Factors*, U.S. Environmental Protection Agency, National Center for Environmental Assessment, Washington, D.C.

HNF-SD-WM-TI-707, 2007, *Exposure Scenarios and Unit Factors for Hanford Tank Waste Performance Assessment*, Rev. 5, CH2M HILL Hanford Group, Inc., Richland, Washington.

IDF-00002, 2019, *Waste Acceptance Criteria for the Integrated Disposal Facility*, Rev. 0, CH2M HILL Plateau Remediation Company, Richland, Washington.

IDF-PRO-EN-54165, 2019, *IDF Unreviewed Disposal Question*, Rev. 1, CH2M HILL Plateau Remediation Company, Richland, Washington.

ML20128J832, 2020, *Technical Evaluation Report, Draft Waste Incidental to Reprocessing Evaluation for Closure of Waste Management Area C, Hanford Site, Washington*, U.S. Nuclear Regulatory Commission, Rockville, Maryland.

RPP-CALC-61254, 2017, *Inadvertent Intruder Dose Calculation Update for the Integrated Disposal Facility Performance Assessment*, Rev. 1, Washington River Protection Solutions, LLC, Richland, Washington.

RPP-CALC-61254, 2018, *Inadvertent Intruder Dose Calculation Update for the Integrated Disposal Facility Performance Assessment*, Rev. 2, Washington River Protection Solutions, LLC, Richland, Washington.

RPP-CALC-61254, 2019, *Inadvertent Intruder Dose Calculation Update for the Integrated Disposal Facility Performance Assessment*, Rev. 3, Washington River Protection Solutions, LLC, Richland, Washington.

RPP-RPT-57991, 2019, *River Protection Project Integrated Flowsheet*, 24590-WTP-RPT-MGT-14-023, Revision 3, Washington River Protection Solutions, LLC, Richland, Washington.

RAI 2-18   (^{90}Sr Inventory Uncertainty)

Comment
Additional information is needed regarding the uncertainty in the ^{90}Sr inventory estimate and how the inventory uncertainties are propagated into the GoldSim model.

Basis
Strontium-90 is a key radionuclide, especially for the intruder scenario. The projected chronic dose to the hypothetical human intruder 100 years after IDF closure under the rural pasture resident scenario is 43.3 mrem/yr (as compared to DOE's performance metric of 100 mrem/yr). The peak dose is driven by the milk ingestion pathway (40.5 mrem/yr). The total dose is principally due to ^{90}Sr and ^{99}Tc, which contribute 29.8 mrem/yr and 10.4 mrem/yr, respectively, to the total dose (page 7-38 of the PA document).

There is uncertainty in the inventory of ^{90}Sr within the Best Basis Inventory (BBI). The PA document (page 3-232) indicates that ^{90}Sr estimates in the BBI could be off by as much as 80 percent. However, it is unclear how uncertainty in ^{90}Sr inventory coming from the BBI model is included and propagated into the GoldSim model. In a public teleconference with DOE on September 28, 2020 (ML20311A202), DOE indicated that because of the direct correlation between inventory and dose they intentionally did not include inventory uncertainty in the GoldSim model to be able to see the effects of other aspects of uncertainty more readily. Instead, DOE indicated that they evaluate uncertainty in risk with inventory in RPP-CALC-63176. Specifically, the PA results are scaled to forecast the impact to groundwater in this tool instead of using GoldSim model. DOE also indicated that for the intruder analysis, in RPP-CALC-61254 Rev 3, DOE analyzed different ^{90}Sr levels and how it influences the need for intruder barriers.

Path Forward
Please provide a description of how ^{90}Sr inventory uncertainty impacts the dose to the inadvertent intruder. Please provide the reference RPP-CALC-61254, Rev 3.

DOE Response
The BBI uncertainty estimate discussed on page 3-232 of the IDF PA (RPP-RPT-59958) refers to the uncertainty in the total estimate of the waste in the single- and double-shell tanks at Hanford. The uncertainty estimate is derived from tank waste samples in the BBI database that have an estimate of sample uncertainty. The BBI database includes samples from every waste phase, not just waste phases that will provide feed to the WTP LAW Vitrification Facility. The greatest ^{90}Sr activity and highest uncertainty is from samples from the sludge phase (see Figure 2-18-1), which is not a phase that will be fed through the LAW vitrification process. To provide an estimate for the uncertainty in the ^{90}Sr concentrations that might be present in the LAW feed, the BBI uncertainty analysis discussed in Appendix B of RPP-CALC-62058, *Waste Stream Inventory Calculations for the Integrated Disposal Facility Performance Assessment*, Rev. 1 and discussed in Section 3.3.2.4 of the IDF PA was repeated with just the BBI data for the supernatant phase in 19 double-shell tanks. The uncertainty in the supernatant samples is more representative of the sample uncertainty for staged feed to the WTP LAW Vitrification Facility during DFLAW operations as well as vitrification in the WTP LAW Vitrification Facility

following pre-treatment at the WTP Pre-Treatment Facility after the DFLAW mission is completed[97] and vitrification for supplemental LAW[98] .

Figure 2-18-1. Strontium-90 Inventory in All Waste Phases in the Best-Basis Inventory with Estimates of Sample Uncertainty.

---
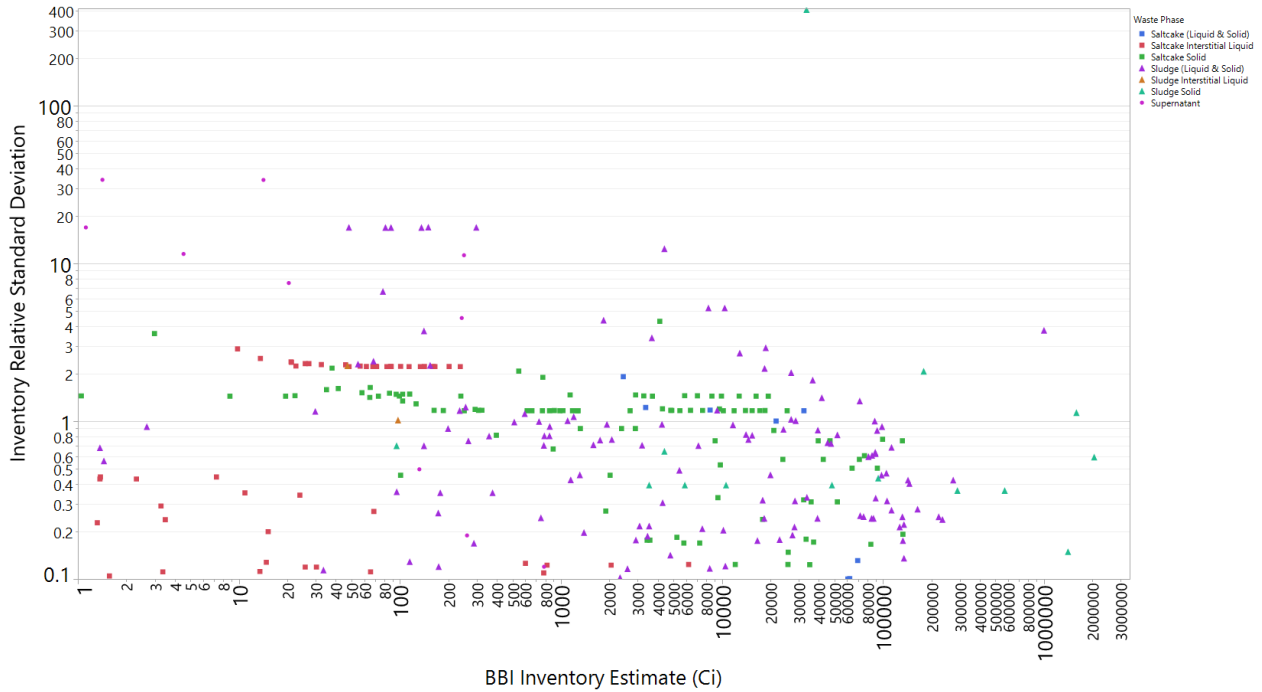
[97] Vitrification in the WTP LAW Vitrification Facility following pre-treatment at the WTP Pre-Treatment Facility after the DFLAW mission is completed provided for additional information and completeness, and is outside the scope of the Draft WIR Evaluation.

[98] Information concerning supplemental LAW is provided in this RAI response for additional information and completeness only, and is outside the scope of both the Draft WIR Evaluation and DOE decisions concerning supplemental LAW treatment. DOE has not made decisions concerning the potential path forward for supplemental LAW treatment, as explained in footnote 7 of the Draft WIR Evaluation and 78 FR 75913, "Record of Decision: Final Tank Closure and Waste Management Environmental Impact Statement for the Hanford Site, Richland, Washington." As explained in section 1.2 of the Draft WIR Evaluation, the Draft WIR Evaluation does not address or include in its scope supplemental LAW. To bound the IDF PA analysis, the IDF PA assumed that supplemental LAW may potentially be vitrified and disposed of in the IDF, although, as explained above, DOE has made no decisions concerning the potential path forward for supplemental LAW treatment.

When the inventory uncertainty analysis[99] is rerun with just the supernatant samples in the BBI database, the ^{90}Sr inventory uncertainty is much lower than the ^{90}Sr inventory uncertainty with the other waste phases. When all phases were sampled using the relative sample deviations in the BBI database, the 95th-percentile of the total ^{90}Sr inventory in all of the tank waste was 71% higher than the BBI inventory without uncertainty (Table 3-24 in the IDF PA). When only the supernatant samples from double-shell tanks are used in the same evaluation, then the total activity of ^{90}Sr included in the BBI uncertainty analysis is 3.45E05[100] Ci and the 95th-percentile value is 3.57E05 Ci. The 95th-percentile of the total ^{90}Sr inventory is only 3.5% higher than the total ^{90}Sr inventory without uncertainty (see Figure 2-18-2). When the analysis is re-run using an untruncated normal distribution, the 95th-percentile inventory is lower.

The uncertainty estimate is determined by the relative standard deviation in the BBI database for each waste phase. Supernatant concentrations are determined by laboratory analysis of liquid grab samples collected from different depths in the tank. The number of samples collected from each tank, including duplicates, is determined by the Data Quality Objectives in tank-specific sampling plans. Two of 21 tanks with a supernatant phase contain 91% (3.15E05 Ci of 3.45E05 Ci) of the total ^{90}Sr activity in the supernatant phase. The reported uncertainty for these tanks drives the uncertainty in the total uncertainty estimate. The relative standard deviation for the inventory estimate of 1.80E05 Ci of ^{90}Sr in tank 241-AN-107 supernate is 0.0223. The relative standard deviation in the inventory estimate of 1.35E05 Ci of ^{90}Sr in tank 241-AN-102 supernate is 0.0311. The low relative standard deviations of the grab samples for the ^{90}Sr concentrations in the supernate suggests that there will be little uncertainty in the LAW feed once characterization samples are collected and analyzed.

The sum of fraction results for ^{90}Sr presented in the response to RAI 2.17 illustrate the variability in the LAW feed and the potential impact to an inadvertent intrusion into four containers of VLAW. The results show that the peak impact to an intruder from just ^{90}Sr after drilling into four containers of VLAW is roughly 48% of DOE's dose limits for an intruder, which are 500 mrem for an acute exposure and 100 mrem/yr for a chronic annual exposure[101]. An additional 3.5% inventory uncertainty in the VLAW feed propagated to the VLAW would

---

[99] In the inventory uncertainty analysis, the BBI records were queried to find all double-shell tanks that have ^{90}Sr in the supernatant phase. Only the sample records that also had relative standard deviations to characterize the uncertainty in the sample estimate were used. Each estimate and relative standard deviation were used to create a triangular distribution for each sample record. The bounds of the distribution were determined by adding or subtracting three standard deviations from the sample estimate. The mode of the distribution was set equal to the sample estimate without uncertainty. The distributions were sampled and all the values were added together to get the total inventory with uncertainty. The 95th-percentile of 10,000 Monte Carlo realizations was compared to the total inventory without uncertainty to estimate the uncertainty in the total inventory of ^{90}Sr in sampled LAW feed.

[100] Due to radionuclide decay and processing in the WTP HLW Vitrification Facility, the BBI inventory in supernatant phase of the double-shell tanks is not necessarily the same inventory in the feed stream to the WTP LAW Vitrification Facility. The total ^{90}Sr inventory in the BBI supernate can be different from the inventory in the VLAW simulated in the IDF PA.

[101] The radionuclide concentration limit is the radionuclide concentration in the waste that results in a dose to the intruder that is equal to either DOE's acute dose limit or chronic dose limit. The concentration limits are determined for acute and chronic dose scenarios and the more restrictive concentration is set as the disposal limit. For ^{90}Sr, a chronic scenario has a more restrictive concentration limit. Therefore, a waste concentration that is 48% of the ^{90}Sr concentration limit yields a chronic dose to the intruder that is 48 mrem/yr from ^{90}Sr.

not cause the sum of fractions to exceed 1, so it would also not cause the dose to an inadvertent intruder to exceed DOE performance measures.

Figure 2-18-2. Estimate of Strontium-90 Inventory Uncertainty in Supernate from Best-Basis Inventory Records.
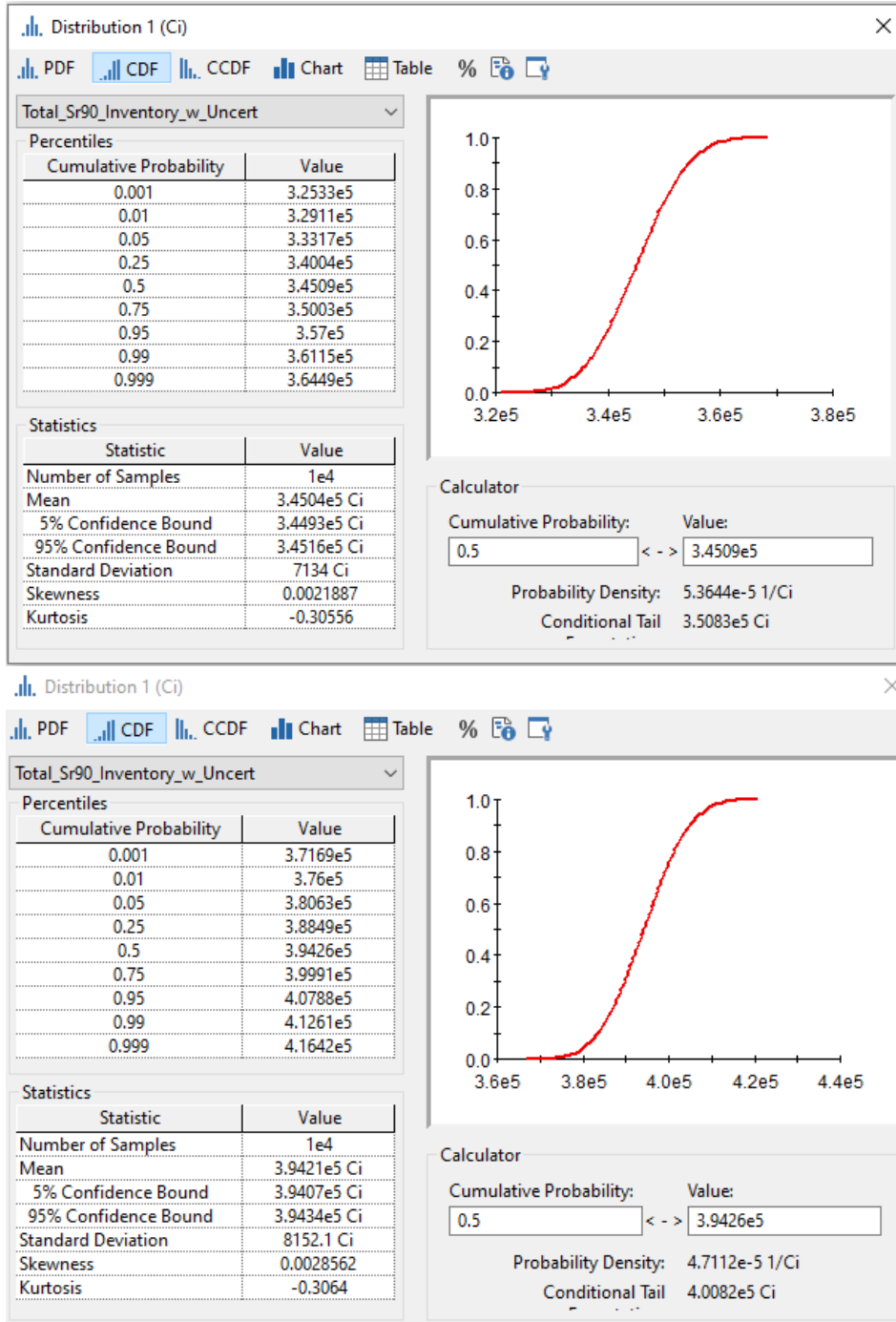
The IDF disposal limit for ^{90}Sr is derived from the inadvertent intruder analysis (RPP-CALC-61254, *Inadvertent Intruder Dose Calculation Update for the Integrated Disposal*

Facility Performance Assessment, Rev 3). Subsequent to completion of the IDF PA, the DOE Office of River Protection and DOE Richland Operations Office provided guidance (DOE-0431, *Recommendations for Institutional Control Time Period for Conducting DOE Order 435.1 Performance Assessments at the Hanford Site*) that all Hanford Site intruder analyses should consider that inadvertent intrusion would be mitigated by mandated institutional controls until 2278. A *Comprehensive Environmental Response, Compensation, and Liability Act of 1980* (CERCLA) Record of Decision for a waste site on the Hanford Site requires DOE to maintain institutional controls at Hanford to prevent excavation into that waste site until 2278. Consistent with the recommendation in DOE-0431, IDF disposal limits for all radionuclides were reevaluated in RPP-CALC-61254 Rev. 3 assuming potential intrusion occurs no sooner than 2278. Table 6-5 in RPP-CALC-61254 Rev. 3 shows how the disposal limits for all radionuclides vary with the duration of credited intruder protections, with dates ranging from 100 years after closure (2151) out to calendar year 2278. Disposal limits for short-lived fission products (primarily ^{90}Sr and ^{137}Cs) were very sensitive to the duration of institutional controls used to provide intruder protections; disposal limits for longer-lived radionuclides were not as sensitive to the duration of intruder protections.

The analysis was carried out until 2278 because the analysis included in the previous revision of the IDF PA that assumed institutional controls until 2151 was not sufficient to protect the intruder when VLAW concentrations of ^{90}Sr were as high as the WTP maximum allowable concentration of 20 Ci ^{90}Sr /m^3. The results of the analysis revealed that intruder protections until 2242 were necessary to keep doses below DOE performance measures when the VLAW contained 20 Ci ^{90}Sr /m^3. However, intruder protections until 2176 were needed to keep doses below DOE performance measures when the VLAW contained an average ^{90}Sr concentration forecasted for the entire DFLAW mission in Table C-7 of RPP-RPT-57991, *River Protection Project Integrated Flowsheet*. When additional radionuclides are disposed of with ^{90}Sr, the duration to protect the intruder must be extended beyond these dates. The sum of fractions calculation in the response to RAI 2-17 calculates disposal limits for ^{90}Sr assuming institutional controls on the Hanford Site until 2278.

Furthermore, the waste acceptance process could permit disposal of VLAW with a sum of fractions with respect to IDF WAC concentration limits that is greater than one. However, this requires an evaluation and is done on a case-by-case basis. This allowance occurs because the intruder scenario calculations assume that the intrusion intercepts four VLAW containers, each having one-fourth the inventory that causes the dose. If the drilling event impacts fewer than four VLAW containers or impacts at least one VLAW container with a sum of fractions that is less than one, then it would be possible for one (or more) of the impacted VLAW containers to have a sum of fractions greater than one but a dose following an intrusion that is still less than the DOE performance measure. In the event that a forecasted VLAW waste profile has a sum of fractions that is greater than 1, a case-by-case WAC acceptance process will be invoked through the change management process in IDF-PRO-EN-54165, *IDF Unreviewed Disposal Question* to ensure that the VLAW container can be safely disposed of in the IDF and determine if it is necessary to impose any additional constraints on where it can be placed or how much inventory can be placed above it. Although outside the scope of the Draft WIR Evaluation, the same case-by-case evaluation can be performed for SSW and LSW containers that have a sum of fractions greater than one.

References

78 FR 75913, 2013, "Record of Decision: Final Tank Closure and Waste Management Environmental Impact Statement for the Hanford Site, Richland, Washington," *Federal Register*, Vol. 78, pp. 75913–75919 (December 13).

Comprehensive Environmental Response, Compensation, and Liability Act of 1980, 42 USC 9601 et seq.

DOE-0431, 2019, *Recommendations for Institutional Control Time Period for Conducting DOE Order 435.1 Performance Assessments at the Hanford Site*, Rev. 0, U.S. Department of Energy, Office of River Protection, Richland, Washington.

IDF-PRO-EN-54165, 2019, *IDF Unreviewed Disposal Question*, Rev. 1, CH2M HILL Plateau Remediation Company, Richland, Washington.

ML20311A202, 2020, *Public Teleconference between the Nuclear Regulatory Commission and the Department of Energy on the Hanford Draft WIR Evaluation for Vitrified Low Activity Waste*, September 28, 2020.

RPP-CALC-61254, 2017, *Inadvertent Intruder Dose Calculation Update for the Integrated Disposal Facility Performance Assessment*, Rev. 1, Washington River Protection Solutions, LLC, Richland, Washington.

RPP-CALC-61254, 2018, *Inadvertent Intruder Dose Calculation Update for the Integrated Disposal Facility Performance Assessment*, Rev. 2, Washington River Protection Solutions, LLC, Richland, Washington.

RPP-CALC-61254, 2019, *Inadvertent Intruder Dose Calculation Update for the Integrated Disposal Facility Performance Assessment*, Rev. 3, Washington River Protection Solutions, LLC, Richland, Washington.

RPP-CALC-62058, 2018, *Waste Stream Inventory Calculations for the Integrated Disposal Facility Performance Assessment*, Rev. 1, Washington River Protection Solutions, LLC, Richland, Washington.

RPP-CALC-63176, 2020, *Integrated Disposal Facility Risk Budget Tool Analysis*, Rev. 0A, Washington River Protection Solutions, LLC, Richland, Washington.

RPP-RPT-57991, 2019, *River Protection Project Integrated Flowsheet*, 24590-WTP-RPT-MGT-14-023, Rev. 3, Washington River Protection Solutions, LLC, Richland, Washington.

RPP-RPT-59958, 2019, *Performance Assessment for the Integrated Disposal Facility, Hanford Site, Washington*, Rev. 1A, Washington River Protection Solutions, LLC, Richland, Washington.

RAI 2-19   (Releases from the ETF-LSW Waste)

Comment
Additional information is needed on the modeled release of ^{129}I and ^{99}Tc from the ETF-LSW waste.

Basis
Several aspects of the modeling used for the release from the ETF-LSW waste could result in the underestimation of the potential release. The ETF-LSW waste originates from the treatment of liquid waste from WTP operations, including the liquid effluent from the melter primary off-gas treatment system and the LAW vitrification secondary off-gas/vessel vent treatment system. As described above in RAI 1-3, there is uncertainty in how much of key radionuclides, such as ^{129}I and ^{99}Tc, will end up in the ETF-LSW waste stream due to uncertainty in how well these radionuclides will be incorporated into the glass. For example, in Case 7, the inventories of ^{129}I and ^{99}Tc in the ETF-LSW waste are assumed to be a small percentage of the total, while in Cases 10A and 10B, the inventories of ^{129}I and ^{99}Tc are assumed to be much higher. In the GoldSim model, the calculated fractional release rates of ^{129}I and ^{99}Tc from the ETF waste on a unit inventory basis (i.e., "fractional_release_rate_all") are approximately an order of magnitude less than the release rates from other waste streams, such as the ion exchange waste stream and the waste streams that are encapsulated in cementitious mortar or paste.

The basis for the best-estimate parameter values assumed for the release from the solidified ETF-LSW waste is provided in PNNL-25194 (2016) and is summarized in the PA document. One key modeling assumption for the release from the ETF-LSW stream, that appears to be non-conservative, is the assumed probability distribution of the effective diffusivity coefficient. A log-uniform distribution with a range of 1.8x10-13 cm2/s to 5.5x10-8 cm2/s was assumed for the ETF-LSW waste, while the probability distribution assumed for the diffusivity for the other cementitious materials was higher. The data cited in PNNL-25194 includes effective coefficient data for iodine and technetium, which are expected to sorb slightly, as well as data from sodium, nitrate, and nitrite. The measured diffusivity coefficients at the low end of the observed range were for iodine and technetium and likely include sorption. This item was also identified by the Low-Level Waste Disposal Facility Federal Review Group (LFRG) as Issue Number IDF-S19-PA12-05. The corrective action stated for this item was to add a clarifying discussion to Section 6.3.2.3 of the PA document. This discussion acknowledges that the effective diffusivities include sorption and states that the minimum value of the distribution was based on the assumption that the Kd of the species in question (iodine and technetium) is equal to 0. The assumption that the Kd values for these elements is equal to 0 is inconsistent with the assumed Kd values in the model. Additionally, the response to the LFRG comment stated that "the ETF-LSW waste form is a negligible contributor to dose as shown in Figure 6-63". This figure reference appears to be incorrect. However, Figure 6-58 does show the dose contribution from the ETF-LSW waste being less when the Case 7 inventory is assumed. This figure does not provide any information as to the relative dose contribution of the ETF-LSW waste if a higher inventory of ^{129}I and ^{99}Tc end up in this waste stream.

Additionally, the diffusive length assumed in the GoldSim model for the ETF-LSW waste (0.2 m) is approximately an order of magnitude longer than the diffusive lengths for the other waste

forms, but it is not clear what the basis is for this waste length being longer. It also is not clear what effect this assumption has on the modeled diffusive fluxes of the radionuclides out of the wasteform and the potential dose from this release.

Path Forward
Please provide additional information on the expected fractional release rate for ^{129}I and ^{99}Tc for the ETF-LSW wasteform and describe whether the modeled performance is consistent with this wasteform's expected performance as compared to the other cementitious wasteforms included in the PA. Consider providing an evaluation of the potential fractional release and the dose from the ETF waste using an effective diffusion coefficient value that does not include sorption. Also consider providing an evaluation of the potential dose if the inventory in this waste stream is higher than assumed in Case 7 (i.e., a Case 10A/10B inventory) using a revised effective diffusion coefficient value. Please provide additional information on the basis for the diffusive length assumed for the ETF-LSW waste. If this diffusive length was an error, provide an updated evaluation of the fractional release rate from the ETF-LSW waste that incorporates a corrected value for the diffusive length. Consider providing an updated value for the diffusive length, if appropriate, in the evaluation requested above.

DOE Response
The Draft WIR Evaluation addresses the WIR criteria for VLAW produced during the DFLAW operations only. As such, vitrified waste assumed to be produced after DFLAW operations and all SSW and LSW, assumed during DFLAW operations or assumed after DFLAW operations, is outside the scope of this WIR evaluation. See DOE response (Section 2.0). However, DOE recognizes the importance of the IDF PA, which is a reference for the Draft WIR Evaluation, and is providing the information below in response to the RAI, including a discussion of the full potential treatment mission, SSW, and LSW for additional information. The approach to ensuring that all waste packages are acceptable for disposal at the IDF is described in this RAI response and is the same for all waste streams.

The grout used to solidify LSW from the Hanford ETF is different from the grout used to encapsulate debris and solidify other non-debris waste streams from the WTP such as carbon adsorption media, ion-exchange resin, and silver mordenite. The grout used in the PA calculations to solidify ETF-LSW was specifically designed for the expected composition of the secondary waste from the treatment of liquid waste streams at the ETF. The grout formulation was designed to achieve specific performance requirements. Specifically, the hydrated lime was added to sequester sulfate in ettringite [Ca6Al2(SO4)3(OH)12•26(H2O)] early in the curing phase, avoiding late ettringite formation that can lead to undesired swelling and cracking of the waste form and to increase the pH to activate the blast furnace slag to maintain reducing conditions to help immobilize ^{99}Tc (PNNL-25194, *Secondary Waste Cementitious Waste Form Data Package for the Integrated Disposal Facility Performance Assessment* and PNNL-26443, *Updated Liquid Secondary Waste Grout Formulation and Preliminary Waste Form Qualification*). Consequently, compared to an encapsulating or void fill grout, DOE believes that it is appropriate to assign different properties to the grouted ETF-LSW waste form. DOE continues to evaluate alternative grout formulations for ETF-LSW waste streams. An alternative formulation to that used in the PA has been specified by the ETF Modular Grout Project. This grout formulation results in a low-pH, sulphur-activated blast furnace slag waste form with

upfront struvite precipitation to prevent release of ammonia gas. Laboratory studies evaluating the necessary properties to use in PA calculations are expected to be published in a research report in FY 2021. Once completed, DOE will use its change control process to evaluate the new grout formulation for possible implications on the conclusions of the PA.

In the process models used to determine compliance with DOE performance objectives, radionuclide releases from containers of solidified LSW were simulated using an effective diffusion coefficient for non-sorbing species and accounted for sorption using a radionuclide-specific distribution coefficient (K_d) (RPP-CALC-61030, *Cementitious Waste Form Release Calculations for the Integrated Disposal Facility Performance Assessment*, Section 4.2.2). The effective diffusion coefficient used in the compliance case simulations of ETF-LSW with hydrated lime was 1.6E-09 cm^2/s (RPP-CALC-61030 Table 6-10), which is the geometric average value for sodium reported in PNNL-25194 Table 3.1. The geometric average for the apparent diffusion coefficient for ^{99}Tc, which accounts for sorption and redox conditions, was 1.8E-13 cm^2/s (PNNL-25194 Table 3.1). No apparent diffusion coefficient value was reported in PNNL-25194 for ^{129}I in a hydrated lime-based waste form; the laboratory work developing the values for technetium, sodium, and nitrate did not include iodine (PNNL-25194 Section 3.1.2).

In a subsequent report that was not available in time to support the PA calculations, additional tests with hydrated lime grout for the ETF-LSW were reported in PNNL-26443. This report included a diffusion coefficient for iodine in the different tests that were performed. The results are compared to diffusion coefficients for sodium in Figure 2-19-1. The results indicate that iodine has some affinity for the grout solids since the diffusion coefficients are lower than for non-sorbing sodium. When the K_d is backed out of the reported diffusion coefficient using Equations 4-5 and 4-6 in RPP-CALC-61030, the K_d values for iodine without getters range from 0.2 to 4 mL/g with an arithmetic average equal to 1 mL/g[102]. However, it is noted that the effective diffusion coefficients for sodium reported in PNNL-26443 increased by a factor of up to 18 over the values reported in PNNL-25194. The reported diffusion coefficients in PNNL-26443 for iodine including sorption were comparable to the effective diffusion coefficient for non-sorbing species in PNNL-25194 (equal to 1.6E-09 cm^2/s).

Simulations treating iodine as non-sorbing in the grouted waste form were performed in the sensitivity analyses described in RPP-CALC-61030. In addition, the initial and updated values for the apparent iodine diffusion coefficient in ETF-LSW are within the range of values included in the uncertainty analysis that are computed from sampled values using Equations 4-5 and 4-6 in RPP-CALC-61030 (Figure 2-19-2).

Simulations in RPP-CALC-61030 for the compliance case used a grout K_d of 0.8 mL/g for ^{99}Tc and 4.0 mL/g for ^{129}I (RPP-CALC-61030 Tables 6-10 and 6-11). RPP-CALC-61030 Figure 7-56 shows the ETF-LSW release rates that are used to compute the dose in the groundwater pathway analysis and provide the basis for comparison of alternative cases. In addition to the compliance case, sensitivity cases evaluated the release of iodine and technetium to the vadose zone from ETF-LSW using alternative values for K_d, effective diffusion coefficients, saturated hydraulic

---

[102] Distribution coefficient estimates assume a porosity of 0.5 and saturation of 1 from Table 3.4 in PNNL-25194 because these properties were not reported in PNNL-24463.

conductivity, cement type, waste package type, net infiltration rate, and inventory (RPP-CALC-61030 Tables 6-12 through 6-15). The compliance case and sensitivity cases for ETF-LSW in RPP-CALC-61030 include 77 process model simulations. Multiple simulations reported in RPP-CALC-61030 included simulations with the diffusion coefficient derived for sodium and no iodine or technetium sorption to the grout. The results reported in RPP-CALC-61030 are limited to releases rates and cumulative amounts released at 1,000 and 10,000 years of simulation time; additional results from select simulations are presented and discussed in this RAI response. The simulated results presented in RPP-CALC-61030 Table 7-22 reveal that the FRRs and cumulative fraction released in 1,000 and 10,000 years for Case 7 and Case 10A inventories are the same. Thus, the FRRs are independent of initial inventory and simulated results can be scaled to consider uncertainties in inventories. The results presented below are expressed as fractional values.

Figure 2-19-1. Comparison of Laboratory Measured Effective Diffusion Coefficients for Iodine and Sodium.
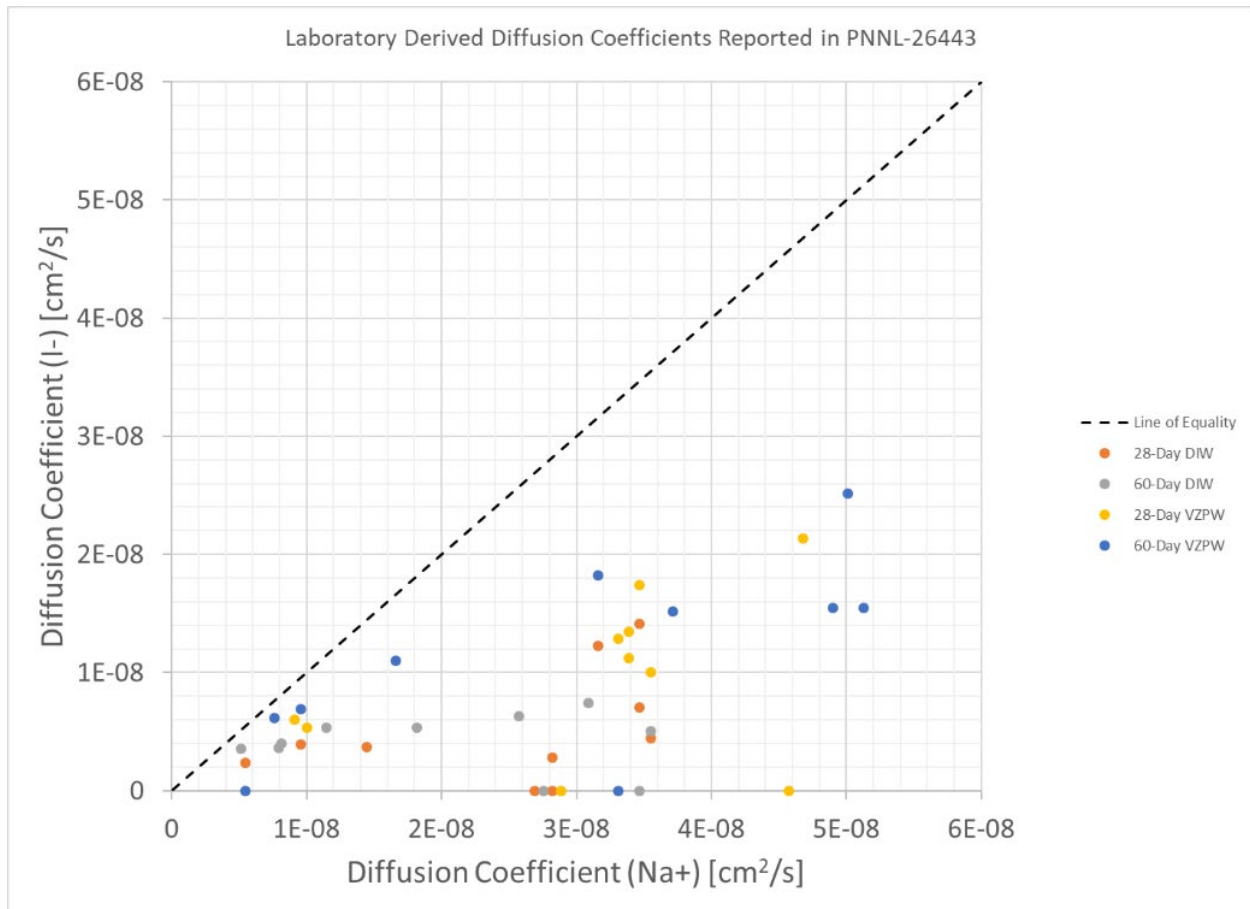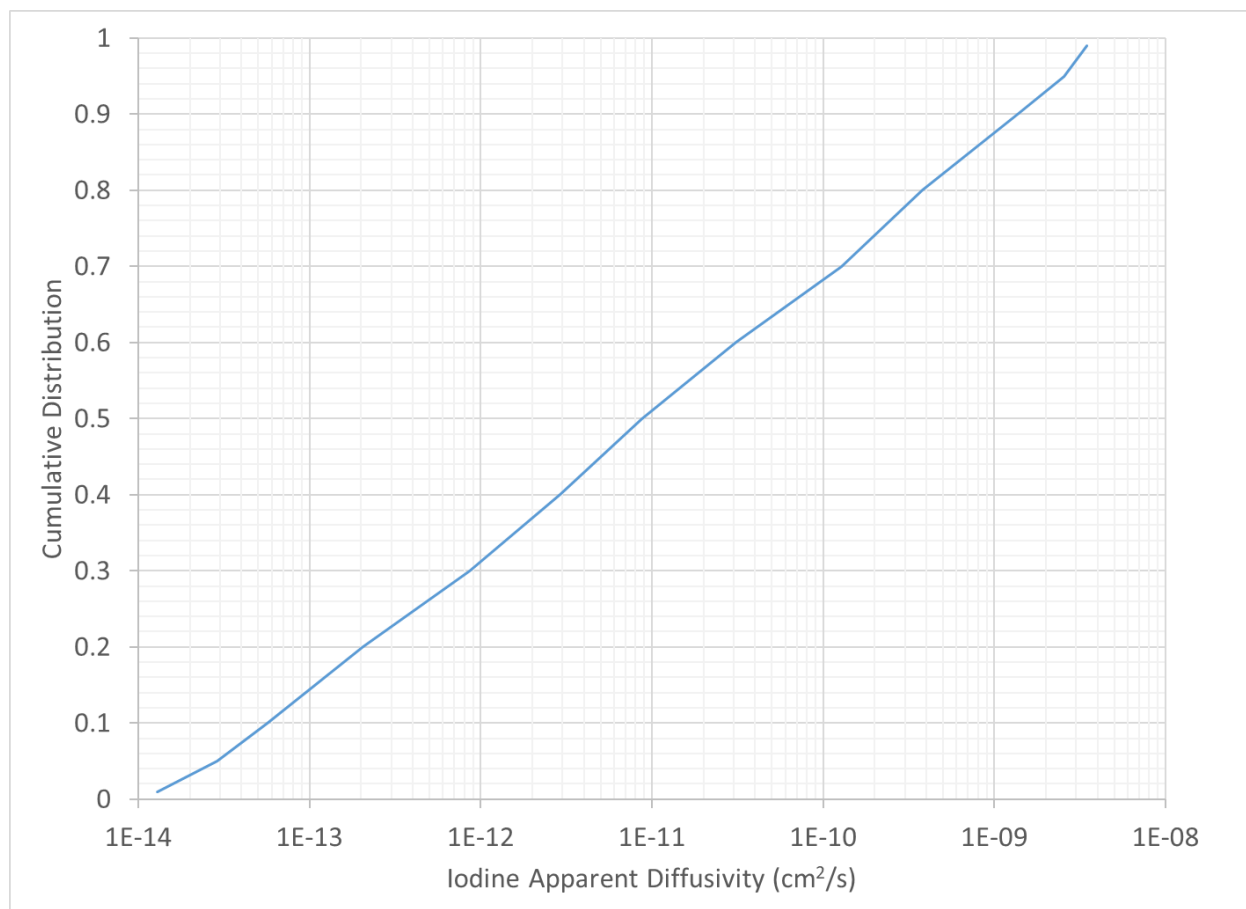

DIW = de-ionized water   VZPW = vadose zone pore water

Values from PNNL-26433, *Updated Liquid Secondary Waste Grout Formulation and Preliminary Waste Form Qualification*, Tables 6.6 and 6.7.

Figure 2-19-2. Distribution of Iodine Apparent Diffusion Coefficients in Integrated Disposal Facility Performance Assessment Uncertainty Analysis.

Reference: RPP-RPT-59958, *Performance Assessment for the Integrated Disposal Facility, Hanford Site, Washington.*

Iodine:

The IDF PA compliance case simulated [129]I releases from the ETF-LSW stream using a grout distribution coefficient of 4 mL/g and an effective diffusion coefficient of 1.6E-09 cm^2/s. Measured values for the apparent diffusion coefficient of iodine in PNNL-26443 suggest that the applied K_d may underestimate iodine release rates. RPP-CALC-61030 simulated iodine release from ETF-LSW without sorption onto the grout and reported cumulative fractions released at 1,000 and 10,000 years. Time histories of the releases rates with and without sorption to the grout are compared in Figures 2-19-3 and 2-19-4. The peak release rate, which is roughly proportional to the peak impact to groundwater and peak [129]I dose result from this waste stream, increases by a factor of 8 for the case with no sorption and a factor of 17 for the case with no sorption and an effective diffusion coefficient that is a factor of three higher than the base case.

Knowing that the peak impact to groundwater and the peak dose are proportional to the peak release rate from the waste form because of the linear transport processes imposed in the vadose and saturated zones, an estimate of the peak dose can be inferred by scaling the base case results by 8 or 17 to estimate doses for these release conditions. In the base case the peak groundwater

concentration from ^{129}I in ETF-LSW, which included 0.064 Ci ^{129}I in 18,900 m^3 of grouted waste, is approximately 0.016 pCi/L (RPP-RPT-59958, Figure 1-7). Using a unit dose conversion factor of 0.69 mrem/yr per pCi/L, this yields a dose at the 100-m buffer zone of 0.011 mrem/yr. Scaling this dose result by a factor of up to 17 to evaluate higher apparent diffusivity values yields a dose rate of 0.2 mrem/yr from ^{129}I in ETF-LSW. If 0.282 Ci of ^{129}I (1% of all the tank waste) ended up in ETF-LSW with an apparent diffusion coefficient equal to 5E-9 cm^2/s and a K_d of 0 mL/g, then the peak dose rate from ^{129}I in ETF-LSW would be approximately 3.5 mrem/yr.

Figure 2-19-3. Comparison of Fractional Release Rates to Vadose Zone from Solidified Liquid Secondary Waste for Background Infiltration Rates of 1.7 mm/yr: Iodine-129.
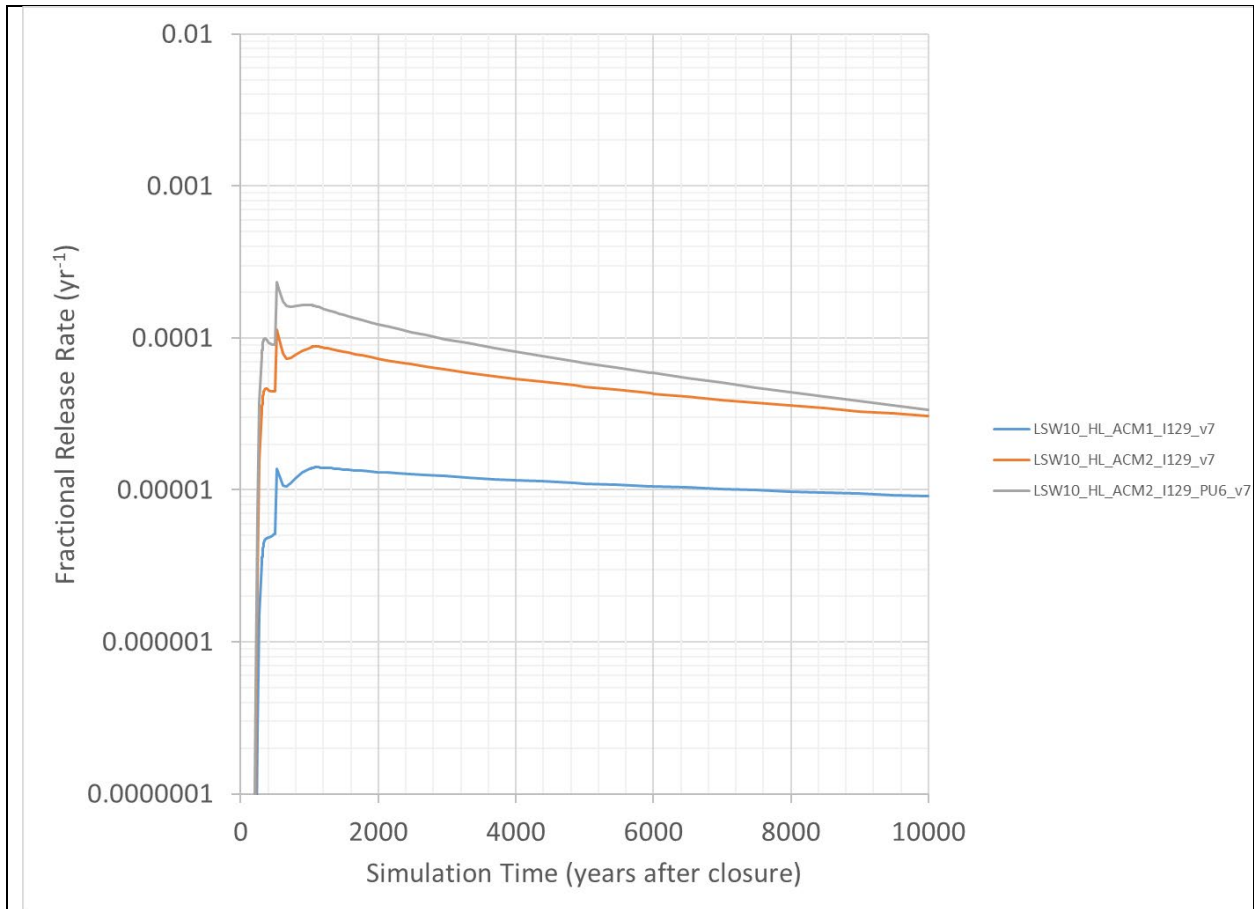
General Conditions:	Stacked B-25 boxes; long-term net infiltration rate = 1.7 mm/yr; saturated hydraulic conductivity = 1.5E-09 cm/s
LSW10 HL ACM1 129 v7	K_d = 4 mL/g, D_{eff} = 1.6E-09 cm^2/s
LSW10 HL ACM2 129 v7	K_d = 0 mL/g, D_{eff} = 1.6E-09 cm^2/s
LSW10 HL ACM2 129 PU6 v7	K_d = 0 mL/g, D_{eff} = 5.0E-09 cm^2/s

Figure 2-19-4. Comparison of Fractional Release Rates to Vadose Zone from Solidified Liquid Secondary Waste for Background Infiltration Rates of 3.5 mm/yr: Iodine-129.

General Conditions:	Stacked B-25 boxes; long-term net infiltration rate = 3.5 mm/yr; saturated hydraulic conductivity = 1.5E-09 cm/s
LSW10_HL_ACM1_129_v7	K_d = 4 mL/g, D_{eff} = 1.6E-09 cm^2/s (Performance Assessment compliance case)
LSW10_HL_ACM2_129_v7	K_d = 0 mL/g, D_{eff} = 1.6E-09 cm^2/s
LSW10_HL_ACM2_129_PU6_v7	K_d = 0 mL/g, D_{eff} = 5.0E-09 cm^2/s
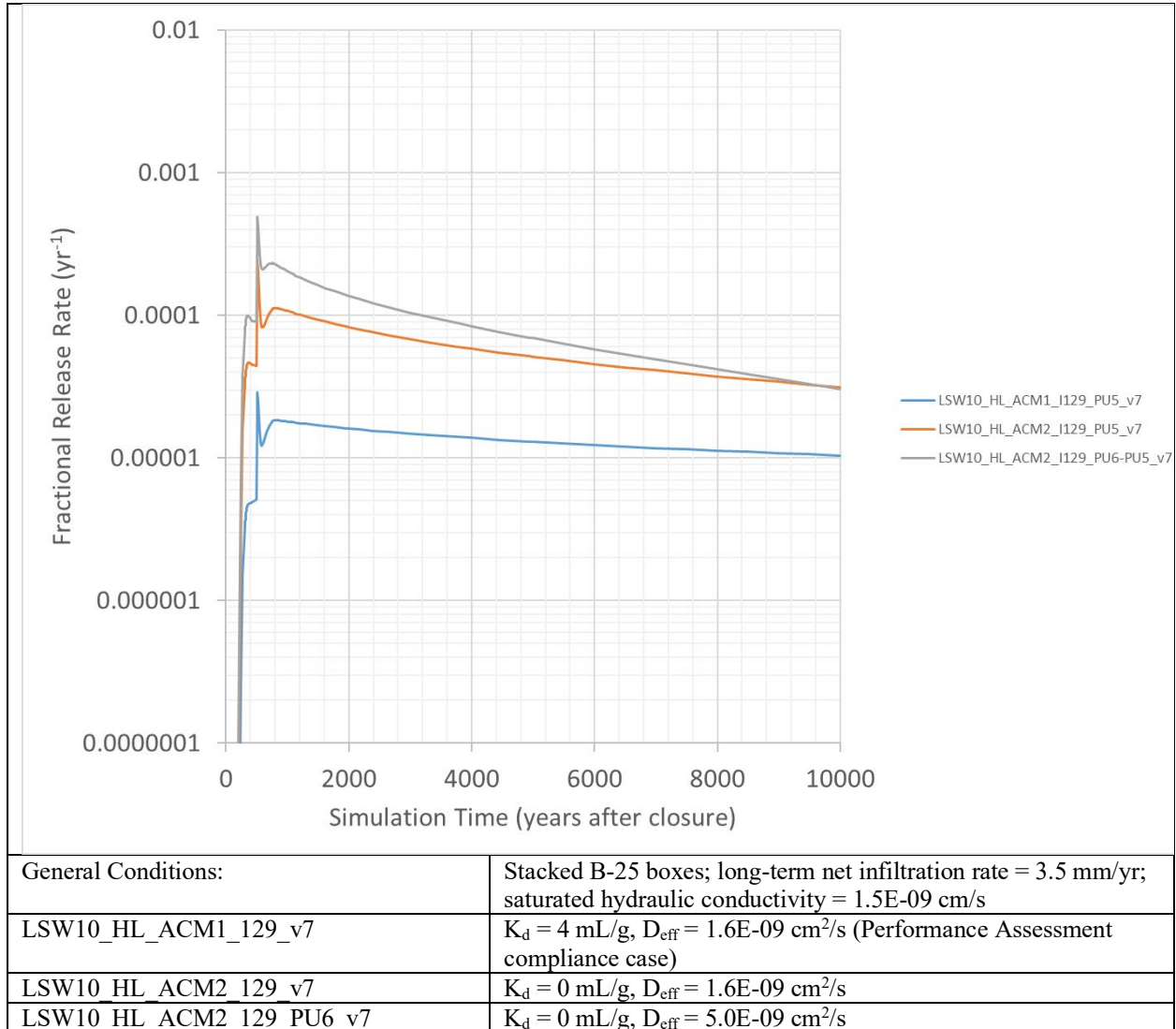
Technetium:

The applied K_d for ^{99}Tc (0.8 mL/g) in the PA compliance case assumes oxidizing conditions for the grout; the simulation does not account for the strong reducing capability of the engineered grout that could have been simulated using a K_d value greater than 1,000 mL/g as long as the reducing capacity of the grout remains. As a result, DOE believes that the simulations for ^{99}Tc overestimate release and are appropriate for simulating this designed waste form in the PA dose assessment.

In addition, the only simulated difference between iodine and technetium when the waste form K_d is set to zero for both radionuclides is the decay rate and molecular weight. The primary transport parameters would be the same so that FRRs for both would be similar. This is verified by comparing the cumulative fractions released for process model simulations

LSW10_HL_ACM2_I129_PU6-PU5_v7 and LSW10_HL_ACM1_Tc99_PU6-PU5_v7. In both of these cases the simulated conditions are the same: two stacked B25 boxes; D_{eff}=5E-9 cm^2/s; K_d=0 mL/g; long-term net infiltration rate=3.5 mm/yr; and K_{sat}=1.5E-9 cm/s. In these runs 80.1% of the ^{129}I is released to the vadose zone in 10,000 years compared to 79.2% of the ^{99}Tc (RPP-CALC-61030 Tables 7-23 and 7-24). For the cases with D_{eff}=1.6E-9 cm^2/s and K_d=0 mL/g the percentage of each radionuclide released to the vadose zone are 53.9% for ^{129}I and 53.1% for ^{99}Tc (RPP-CALC-61030 Tables 7-23 and 7-24).

System Model Representation:

The implementation of the cementitious waste release model in the compliance case calculations and the abstracted model included in the system model are described in RPP-CALC-61030 and RPP-RPT-59726, *Integrated Disposal Facility Model Package Report: System Model*, respectively. Of particular distinction between the two models is the treatment of diffusion in the backfill surrounding the waste containers and how it influences diffusion out of a breached container. In the process model simulation (referred to in RPP-CALC-61030 as the Advective Diffusive Transport [ADT] model), the backfill diffusivity was artificially increased above the value that would be determined from the Millington-Quirk model for partially saturated media (see RPP-RPT-59958 Section 4.4.1.3.3 for discussion of the Millington-Quirk model for these waste forms). The diffusivity was increased by setting the tortuosity of the backfill to 1. Consequently, the effective diffusivities differ only by the different porosity and saturation in the waste form and the backfill[103]. These changes were implemented to minimize the influence of harmonic averaging of the diffusive conductance between adjacent nodes representing the waste form and backfill. Owing to the low saturations in the backfill surrounding the waste containers, the Millington-Quirk model would have predicted very low tortuosity in the backfill, which due to harmonic averaging of the diffusive conductance between adjacent nodes in the computational grid, would have limited diffusion into the backfill from the waste form. This was verified using an alternate representation of waste form release referred to in DOE/EIS-0391 as the Shrinking Core Diffusion Model for cementitious waste forms. Because the backfill also has an advective component to transport and this component was previously shown to be the dominant transport mechanism in the backfill in DOE/EIS-0391, it was decided to equate the effective diffusion coefficient for the backfill to the diffusion coefficient of the waste and set the tortuosity in the backfill to unity to minimize the influence of harmonic averaging that would constrain releases from the ETF-LSW waste package. When this change was made, the releases to the vadose zone had much better agreement with results reported in DOE/EIS-0391. An alternate method to increase the node discretization by using smaller grid block sizes near the waste form / backfill interface was considered. However, the amount of discretization necessary to minimize harmonic average affects would have made computational times excessively long to represent a minor transport pathway in the backfill.

---

[103] By setting the tortuosity of the backfill to 1, the backfill has the same effective diffusivity as the LSW, because the diffusion coefficient specified in STOMP is per species (i.e., ^{99}Tc or ^{129}I), not material. Thus, the only difference arises from the porosity and saturation assigned to the backfill and LSW (in Stomp the measured diffusivity is multiplied by porosity and saturation). For SSW, the tortuosity of the backfill was also set such that the diffusivity of the grout and backfill was the same.

In the process model, separate simulations are performed for each waste form and contaminant; therefore, it is possible to specify different backfill properties for SSW and LSW to account for the condition specified above. However, in the system model the effective diffusion coefficient for the backfill (and the tortuosity) is shared by the LSW and SSW release models. Therefore, it was not possible to impose the same manipulation of backfill properties for LSW releases that was used in the process model without defining two different media elements to represent the same backfill material. To ensure that waste form releases from the LSW were still controlled by diffusion across the waste form / backfill interface, the diffusive length was adjusted until the simulated releases using the system model abstraction had good agreement with the process model result. Examples of system model calculations evaluating different diffusive lengths for a comparison to the process model results are shown in Figures 2-19-5 and 2-19-6. Note that these are new calculations developed for this RAI response; however, a similar analysis was performed during system model development but those results have not been reported previously. A good agreement was determined by comparing peak release rates to the vadose zone and total cumulative releases in 10,000 years. Faster releases in the system model were acceptable when both metrics could not be obtained within 5%.

Figure 2-19-5. System Model Development of the Diffusive Length in the Backfill near Packages of Liquid Secondary Waste: Iodine-129.
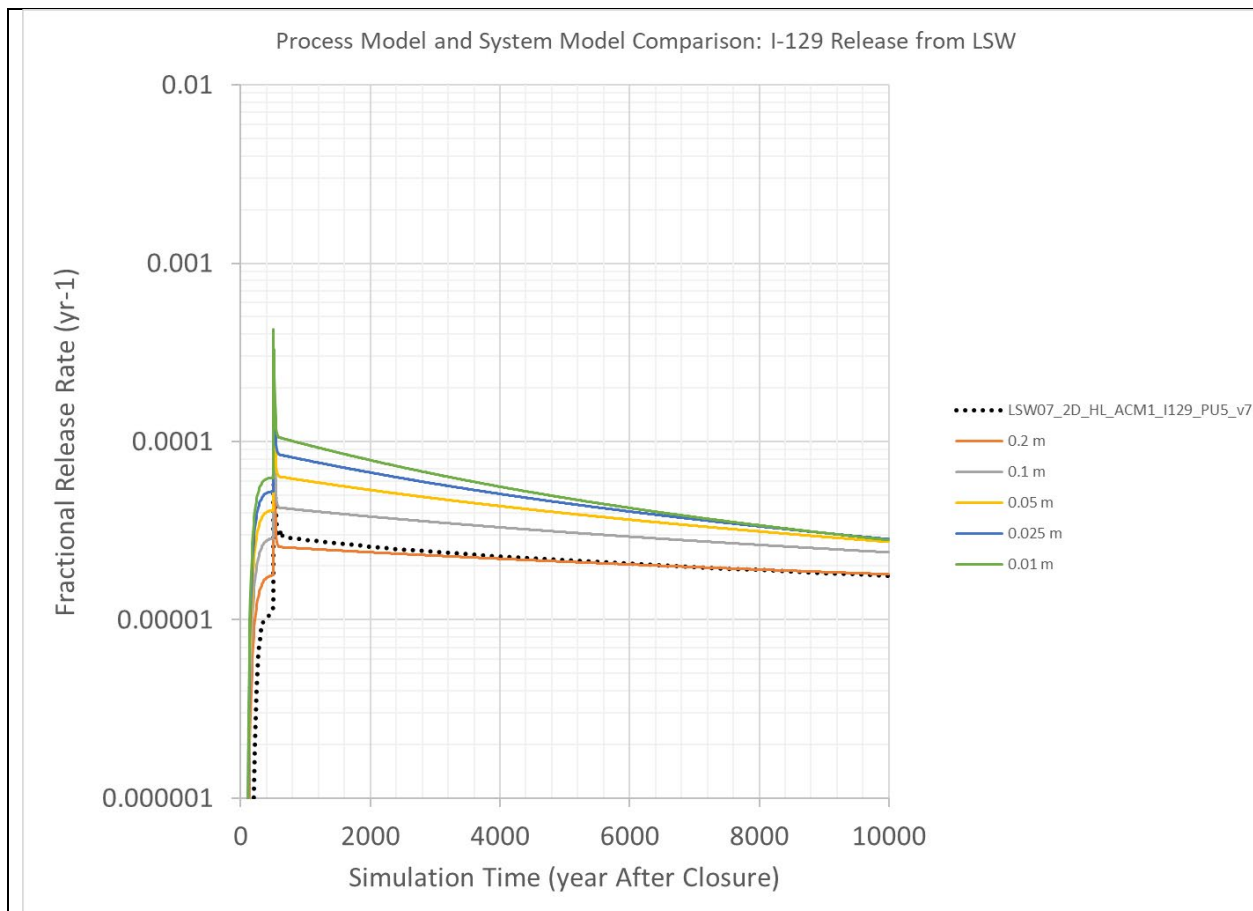
LSW = liquid secondary waste

Figure 2-19-6. System Model Development of the Diffusive Length in the Backfill near Packages of Liquid Secondary Waste: Technetium-99.
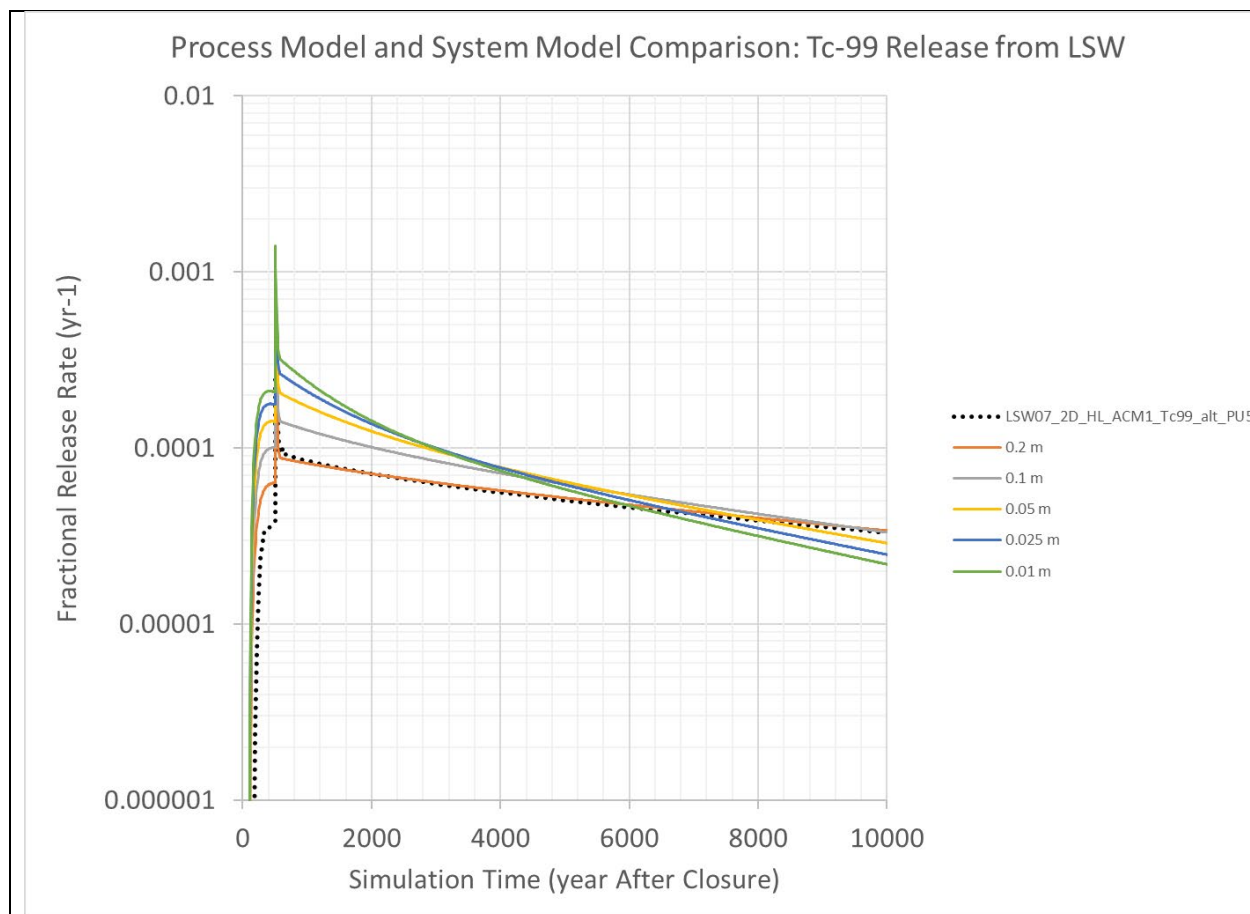
LSW = liquid secondary waste

When the diffusive length was set to the maximum anticipated spacing between waste containers (0.2 m), the peak release rates, which drive groundwater impacts and dose in the groundwater pathway scenario, were 63% and 77% higher in the system model than in the process model for [129]I and ^{99}Tc, respectively. The cumulative releases of [129]I and ^{99}Tc from LSW in the two models had better agreement. The total [129]I released in the process model was 21.1% of the initial inventory (RPP-CALC-61030 Table 7-29) compared to 20.9% of the initial inventory in the system model. The cumulative release of ^{99}Tc from LSW was 51.0% of the initial inventory (RPP-CALC-61030 Table 7-29) in the process model and 53.6% of the initial inventory in the system model. These system model results were considered acceptable for the intended use of the system model to evaluate parameter uncertainty and perform other sensitivities knowing that the peak impacts to groundwater and a member of the public in the future occur in the sensitivity analysis period that follows DOE's time of compliance.

References

DOE/EIS-0391, 2012, *Final Tank Closure and Waste Management Environmental Impact Statement for the Hanford Site*, Richland, Washington, U.S. Department of Energy, Washington, D.C.

PNNL-25194, 2016, *Secondary Waste Cementitious Waste Form Data Package for the Integrated Disposal Facility Performance Assessment*, RPT-SWCS-006, Rev. 0, Pacific Northwest National Laboratory, Richland, Washington.

PNNL-26443, 2017, *Updated Liquid Secondary Waste Grout Formulation and Preliminary Waste Form Qualification*, RPT-SWCS-009, Rev. 0, Pacific Northwest National Laboratory, Richland, Washington.

RPP-CALC-61030, 2017, *Cementitious Waste Form Release Calculations for the Integrated Disposal Facility Performance Assessment*, Rev. 0, INTERA, Inc. for Washington River Protection Solutions, LLC, Richland, Washington.

RPP-RPT-59726, 2017, *Integrated Disposal Facility Model Package Report: System Model*, Rev. 0, INTERA, Inc. for Washington River Protection Solutions, LLC, Richland, Washington.

RPP-RPT-59958, 2019, *Performance Assessment for the Integrated Disposal Facility, Hanford Site, Washington*, Rev. 1A, Washington River Protection Solutions, LLC, Richland, Washington.

RAI 2-20   (I Sorption on the SSW-GAC and SSW-AGM Wasteforms)

Comment
Additional information is needed for the assumed sorption of [129]I on the SSW-GAC (Granular Activated Carbon) and SSW-AgM (Silver Mordenite) wasteforms.

Basis
The modeled release of [129]I from the SSW-GAC and SSW-AgM wasteforms is significantly reduced by the assumed sorption of the [129]I onto these wasteforms. The assumed distributions of the distribution coefficient (Kd) values for [129]I on the SSW-GAC and SSW-AgM wasteforms are much larger than the distributions assumed for the other cementitious wasteforms in this model and are much larger than typically observed Kd values for [129]I on cementitious materials.

The Kd values assumed for [129]I for the SSW-GAC and the SSW-AgM wasteforms are based on an average of a Kd value for sorption of [129]I onto a typical cementitious material and the sorption of [129]I onto GAC or AgM. Although the sorption of the [129]I onto the GAC and AgM contained in these wasteforms could improve the overall sorption of [129]I on these wasteforms compared to typical cementitious wasteforms, the sorption on the combined material might not be equal to the average sorption of its components due to changes in the chemical environment in the wasteform. It is not clear what support exists for the Kd values assumed in the GoldSim Model, and it is not clear if analytical measurements of the [129]I sorption on simulated wasteforms comparable to the SSW-GAC and SSW-AgM wasteforms have been performed.

The sorptive capacity of [129]I on the waste forms for the SSW-GAC and the SSW-AgM waste streams was identified during the LFRG review as issue number ISF-S09-PA03-02. As a corrective action/resolution for this issue, a sensitivity case was performed for the air pathway that used Kd values that were lower than were previously assumed but were still much higher than for typical cementitious materials. However, a sensitivity analysis was not performed to evaluate the potential effect of less sorption of [129]I on these wasteforms on the dose. The corrective action/resolution states that the "full range of uncertainty in the Kd values was considered in the probabilistic analysis" for the groundwater pathway. However, the entire range of Kd values included in the GoldSim model is high and this range does not appear to capture the potential for the sorption of [129]I to be much lower than assumed. The corrective action/resolution to this issue also stated that R&D activities were expected to be performed in the future to characterize the Kd on the carbon media and silver mordenite waste forms.

Path Forward
Please provide additional information to support the assumed Kd values for [129]I on the SSWGAC and the SSW-AgM wasteforms, and if any R&D activities have taken place on this topic to date, provide the results of those activities. Alternatively, provide a sensitivity analysis showing the effect on the release rates and potential dose from [129]I from these two wasteforms if the sorption on these wasteforms is lower than assumed in the model.

DOE Response
The Draft WIR Evaluation addresses the WIR criteria for VLAW produced using the DFLAW approach. Other wastes are outside the scope of the Draft WIR Evaluation, including secondary

waste and vitrified waste produced after the DFLAW mission is completed. Vitrified waste produced after the DFLAW mission is completed includes vitrification at the WTP LAW Vitrification Facility following pre-treatment at the WTP Pre-Treatment Facility [104] and vitrification at a potential WTP Supplemental LAW Facility (for which DOE has made no decision to pursue).[105] To bound the analysis, the IDF PA correctly includes all wastes potentially disposed of in the IDF, including the DFLAW-produced VLAW as well as additional VLAW,[106] and all SSW which may be disposed at IDF. DOE recognizes the importance of the IDF PA to the WIR evaluation and provides the following response for additional information only on this RAI that addresses the SSW included in the PA.

DOE acknowledges that there is uncertainty in the capability of the cement waste forms for carbon adsorption media (SSW-GAC) and silver mordenite (SSW-AgM[107]) to retain iodine. In the PA models, enhanced retention of iodine was simulated in these two waste forms relative to other cementitious waste forms to be consistent with the known enhanced sorptive characteristics of the types of pure media included in these waste forms. The enhanced sorptive characteristics of these two media are the reason that they are used in the operation of the off-gas treatment systems. Iodine sorption onto SSW-GAC was simulated in the base case with a sorption coefficient of 302 mL/g and a range of values from 70 mL/g to 989 mL/g in the uncertainty analysis. Iodine sorption onto SSW-AgM was simulated in the base case with a sorption coefficient of 502 mL/g and a range of values from 96 mL/g to 4,750 mL/g in the uncertainty analysis. As discussed in the RAI, these distribution coefficients are the arithmetic average of values for grout and the media. These values do not account for any chemical change to the waste form environment or loss of performance over time. These assumed values in the IDF PA were noted as a critical assumption requiring confirmation in Section 1.5.5 of the IDF PA (RPP-RPT-59958). As a critical assumption that needs to be verified, laboratory research to

---

[104] After DFLAW operations are completed, vitrification of additional LAW in the WTP LAW Vitrification Facility will follow pre-treatment at the WTP Pre-Treatment Facility. The Draft WIR Evaluation only includes vitrified LAW produced using the DFLAW approach; therefore, vitrification at the WTP LAW Vitrification Facility after DFLAW is outside the scope of the Draft WIR Evaluation. The discussion of the PA results for WTP-vitrified LAW generated during this post-DFLAW time period is provided for additional information and completeness, and is outside the scope of the Draft WIR Evaluation.

[105] Information concerning the secondary waste associated with the supplemental LAW is provided in this RAI response for additional information and completeness only, and is outside the scope of both the Draft WIR Evaluation and DOE decisions concerning supplemental LAW treatment. DOE has not made decisions concerning the potential path forward for supplemental LAW treatment, as explained in footnote 7 of the Draft WIR Evaluation and the 78 FR 75913, "Record of Decision: Final Tank Closure and Waste Management Environmental Impact Statement for the Hanford Site, Richland, Washington." As explained in Section 1.2 of the Draft WIR Evaluation, the Draft WIR Evaluation does not address or include in its scope supplemental LAW. To bound the IDF PA analysis, the IDF PA assumed that supplemental LAW may potentially be vitrified and disposed of in the IDF, although, as explained above, DOE has made no decisions concerning the potential path forward for supplemental LAW treatment.

[106] See footnotes 104 and 105105.

[107] Silver mordenite columns are part of the off-gas treatment system in the WTP HLW Vitrification Facility, which will not be operational during the DFLAW time period covered by the Draft WIR Evaluation.

collect data to verify the assumed values was included in the Research and Development section of the PA Maintenance Plan (CHPRC-03348).

> "Evaluate bulk (i.e., average) transport properties (notably distribution coefficient [K_d]) of solidified nondebris waste streams, with special focus on the retention of iodine-129 on the granular activated carbon (GAC) and silver mordenite substrate materials".

Beginning in FY 2019, DOE began collecting data to support this critical assumption. The most recent work to develop data to support this critical assumption was completed in September 2020 in PNNL-28545, *Development and Characterization of Cementitious Waste Forms for Immobilization of Granular Activated Carbon, Silver Mordenite, and HEPA Filter Media Solid Secondary Waste.*

The report concluded that grout formulations that were used in the IDF PA to solidify non-debris waste streams such as spent carbon adsorption media and AgM are capable of stabilizing the media. The research report included results from sorption experiments and EPA 1315 leaching experiments with stabilized GAC and AgM. For the carbon adsorption media stabilized with a typical Hanford grout formulation (like Hanford Grout Mix 5 used as the representative grout in the IDF PA), the iodide diffusivities were lower than the best-estimate and optimistic values reported for a mobile species from a mortar in the SSW data package that developed input values for the PA (SRNL-STI-2016-00175, *Solid Secondary Waste Data Package Supporting Hanford Integrated Disposal Facility Performance Assessment*). Releases from the waste form decrease with decreases in diffusivities. The stabilized AgM grout samples using a typical Hanford grout formulation did not produce measurable iodide in the leachates, and only "maximum" diffusivity values could be reported[108]. These values were more than four orders of magnitude lower than the mobile species value in the data package. The diffusivity values reported in PNNL-28545 for a typical Hanford grout formulation were used to estimate a K_d value for these waste forms that is consistent with the disposal conditions. The K_d is estimated from the measured properties using RPP-RPT-59958, Equations 4.4.1.3-10 and 4.4.1.3-11, which are combined in Equation 2.20-1. The apparent or observed diffusion coefficient is a lumped parameter that accounts for diffusion and sorption. In contrast, the effective diffusion coefficient in the following equations does not account for sorption and is estimated in the laboratory using a non-sorbing species.[109]

$$D_{app} = \frac{D_{eff}}{\left[1 + \frac{(1-n)\rho_s K_d}{Sn}\right]} \qquad (2.20\text{-}1a)$$

---

[108] The values are referred to as "maximum" values but are very low. The values are determined using leachate concentrations that are higher than observed in the leachate, which means they overestimate the diffusivity.

[109] These definitions of effective and apparent diffusion coefficients are consistent with the usage in the SSW data package (SRNL-STI-2016-00175) and the IDF PA. PNNL-28545 uses laboratory experiments to measure the diffusion coefficient, but these measurements determine the lumped parameter that accounts for diffusion and sorption. PNNL-28545 refers to the lumped parameter as the observed or effective diffusivity; however, the lumped value that accounts for sorption is consistent with the term apparent diffusivity used in the PA and SSW data package and in this RAI response.

Or,
$$K_d = \left[\frac{D_{eff}}{D_{app}} - 1\right]\left[\frac{Sn}{(1-n)\rho_s}\right] = \left[\frac{D_{eff}}{D_{app}} - 1\right]\left[\frac{Sn}{\rho_b}\right] \qquad (2.20\text{-}1b)$$

Where:

D_{app}	=	"apparent" or "observed" diffusion coefficient
D_{eff}	=	"effective" diffusion coefficient
n	=	porosity
ρ_s	=	solid density
ρ_b	=	dry bulk density ($= (1-n)\rho_s$)
K_d	=	distribution coefficient
S	=	saturation

Distribution Coefficient Estimation

For carbon adsorption media stabilized using a typical Hanford grout (SSW-GAC) contacted by a simulant representing Hanford pore water, the apparent diffusivity from the EPA 1315 leachate test (performed in duplicate) was 4.80E-10 cm²/s (PNNL-28545 Table 7-2). The measured value leached with de-ionized water (DIW) was 1.1E-09 cm²/s (PNNL-28545 Table 7-2). The measured porosity of a 30% GAC/grout mixture was 0.388 (PNNL-28545 Table 5-4). The average bulk density of a 30% GAC/grout mixture was 1.509 g/cm³ (PNNL-28545 Table E.6). Saturation and the diffusivity for a non-sorbing species were not reported in PNNL-28545. A saturation for the leaching test of 99% was assumed. The diffusivity for a non-sorbing contaminant used in the PA was assumed for the calculation to estimate the K_d observed in the leaching tests.

$$K_d = \left[\frac{5.4E-08\ \frac{cm^2}{s}}{4.8E-10\ \frac{cm^2}{s}} - 1\right]\left[\frac{0.99 \times 0.388}{1.509\ \frac{g}{cm^3} \times 1\ \frac{cm^3}{ml}}\right] = 28.4\ ml/g$$

Following the same methodology for the experiment conducted in DIW, the estimated K_d value for SSW-GAC with an average reported density of 1.482 g/cm³ leached by DIW is 12.5 mL/g. These estimated values are lower than the PA base case and lower than the range of values considered in the uncertainty analysis. The values are similar to the adsorption K_d for iodine and GAC in a pore water equilibrated with grout (16 mL/g reported in PNNL-28545 Table 6-3). A process model simulation reported in RPP-CALC-61030 evaluated a distribution coefficient as low as 50 mL/g. Although this result was not carried forward to dose, the cumulative releases to the vadose zone were reported and can be quantitatively compared. In this sensitivity case, the cumulative fractions released to the vadose zone in 1,000 and 10,000 years increased by factors of 5.9 and 5.5, respectively, compared to the equivalent case that used a 302 mL/g for the distribution coefficient[110]. This comparison uses the cumulative fractions released in case

---

[110] Although the increase is nearly proportional to the change in distribution coefficients, the relationship between cumulative fraction released and distribution coefficient is non-linear. Disproportionally higher releases would be expected using distribution coefficient values that are lower than 50 mL/g.

GAC_ACM1_I129_v7 that are reported in RPP-CALC-61030 Table 7-4 and the fractions released in case GAC_ACM2_I129_PU7_v7 reported in RPP-CALC-61030 Table 7-15.

Because the effective diffusion coefficient for a non-sorbing species in SSW-GAC was not reported in PNNL-28545, there is uncertainty in this value, which means there is uncertainty in the K_d determined using this value. If the effective diffusion coefficient for a non-sorbing species is an order of magnitude lower than the value used from the PA for a mortar, then the K_d value decreases to 2.6 g/mL, a value that is consistent for cementitious material without accounting for any sorption onto the spent media that was used to capture it by sorption in the off-gas treatment system.

$$K_d = \left[\frac{5.4E - 09\ \frac{cm^2}{s}}{4.8E - 10\ \frac{cm^2}{s}} - 1\right]\left[\frac{0.99 \times 0.388}{1.505\frac{g}{cm^3} \times 1\frac{cm^3}{ml}}\right] = 2.6\ ml/g$$

Following the same methodology for the experiment conducted in DIW, the estimated K_d value for SSW-GAC with a reported density of 1.482 g/cm^3 leached by DIW is 1.0 mL/g.

The second part of this RAI response evaluates the dose using these revised parameter values for SSW-GAC.

For AgM stabilized using a typical Hanford grout (SSW-AgM) contacted by a simulant representing Hanford pore water, the apparent diffusivity from the EPA 1315 leachate test (performed in duplicate) was 4.90E-13 cm^2/s (PNNL-28545 Table 7-2 and page 7.5). This value is determined by detection limits because iodine was not measured in the leachate. The average bulk density of the stabilized AgM was 1.169 g/cm^3 (PNNL-28545 Table E.8). Porosity, saturation and the effective diffusivity for a mobile species were not measured in PNNL-28545. Therefore, the values used in the PA are substituted into Equation 2.20-1b to estimate the K_d observed in the leaching tests.

$$K_d = \left[\frac{5.4E - 08\ \frac{cm^2}{s}}{4.9E - 13\ \frac{cm^2}{s}} - 1\right]\left[\frac{0.99 \times 0.24}{1.169\frac{g}{cm^3} \times 1\frac{cm^3}{ml}}\right] = 22,400\ ml/g$$

The estimated value is much greater than the PA base case and greater than the range of values considered in the uncertainty analysis. Even when the diffusivity for a non-sorbing species is reduced by a factor of 10 and the porosity is changed to values between 0.1 and 0.6, the calculated K_d values are still above what was simulated in the PA. Based on this analysis, SSW-AgM does not warrant a re-evaluation following DOE's change control process.

Re-Evaluation of SSW-GAC

The IDF PA system model was re-run with iodine distribution coefficients in SSW-GAC set to 28.4 mL/g, 12.5 mL/g, and 2.6 mL/g. The initial inventory of iodine sorbed to the GAC prior to disposal was unchanged despite the observation in this report that iodine retention on GAC is

lower than previously thought. The effective diffusivity for a non-sorbing species was also reduced to 5.4E-09 cm^2/s in the latter sensitivity case. Figure 2-20-1 and Figure 2-20-2 show the comparable release rates and cumulative releases from the IDF to the vadose zone and Figure 2-20-3 shows the simulated groundwater concentrations and corresponding dose results. Consistent with the dose results presented in the PA, the system model dose for SSW sources includes all SSW sources. Therefore, the dose results shown in Figure 2-20-3 include other SSW sources, but the dose from the other SSW sources are computed using the base case conditions for those waste streams.

The iodine release rates to the vadose zone from SSW-GAC shown in Figure 2-20-1 illustrate that release rates using the new acquired K_ds for the SSW-GAC waste stream are higher than the PA reference case. These release rates have a similar shape, with a release rate that slowly increases as iodine released from the waste containers reaches the bottom of the IDF. There is a sudden increase in the release rate 500 years after closure when the surface barrier performance degrades and a greater amount of water flows into the IDF. At this time all of the mass that was in the process of being transported to the bottom of the IDF before the increase in flow occurred is rapidly transported to the bottom of the IDF with the increased flow. After this sharp increase the rates drop and releases are governed by the diffusive release from the waste package. The release rates are generally higher for lower K_d values, which is expected for the diffusive release model with some sorption.

Figure 2-20-2 shows the cumulative release to the vadose zone when the rates applied in Figure 2-20-1 are integrated. The cumulative release in 10,000 years is about 9 times higher for the 28.4 mL/g case than it is in the system model base case. This can be compared with the STOMP simulations that showed a 5.5 to 6 factor increase for a 50 mL/g case (the integrated rates shown in Figure 2-20-1b). In the case with the highest releases, the cumulative amount released in 10,000 years amounts to about 20% of the initial inventory allocated to the SSW-GAC.

Figure 2-20-3 shows the simulated groundwater concentrations from all SSW waste streams for the different sensitivity cases. All of the difference is attributed to the change in iodine retention in SSW-GAC. Due to sorption in the vadose zone, iodine reaches the groundwater after the DOE time of compliance has passed. After this time, the iodine concentrations in the groundwater increase to levels that exceed the safe drinking water level, which is 1 pCi/L. However, the simulated concentrations are all lower than the concentration that results in a 4 mrem/yr drinking water dose using conversion factors from DOE-STD-1196-2011, *Derived Concentration Technical Standard*. The peak iodine dose from all SSW sources increased by a factor of 3.2 from 1.1 mrem/yr to 3.5 mrem/yr when the SSW-GAC distribution coefficient for iodine decreased from 302 mL/g to 28.4 mL/g. The peak dose was 6.3 mrem/yr when the SSW-GAC k_d is reduced to 12.5 mL/g. In both cases the peak dose occurred more than 7,000 years after closure. The peak dose occurs after the DOE time of compliance and is lower than DOE's All-Pathways dose limit (25 mrem/yr).

**Figure 2-20-1. Iodine-129 Release Rate to Vadose Zone from Carbon Adsorption Media:
Solid Secondary Waste-Granular Activated Carbon Sensitivity Studies
a) System Model, b) Process Model (fractional release rate).**
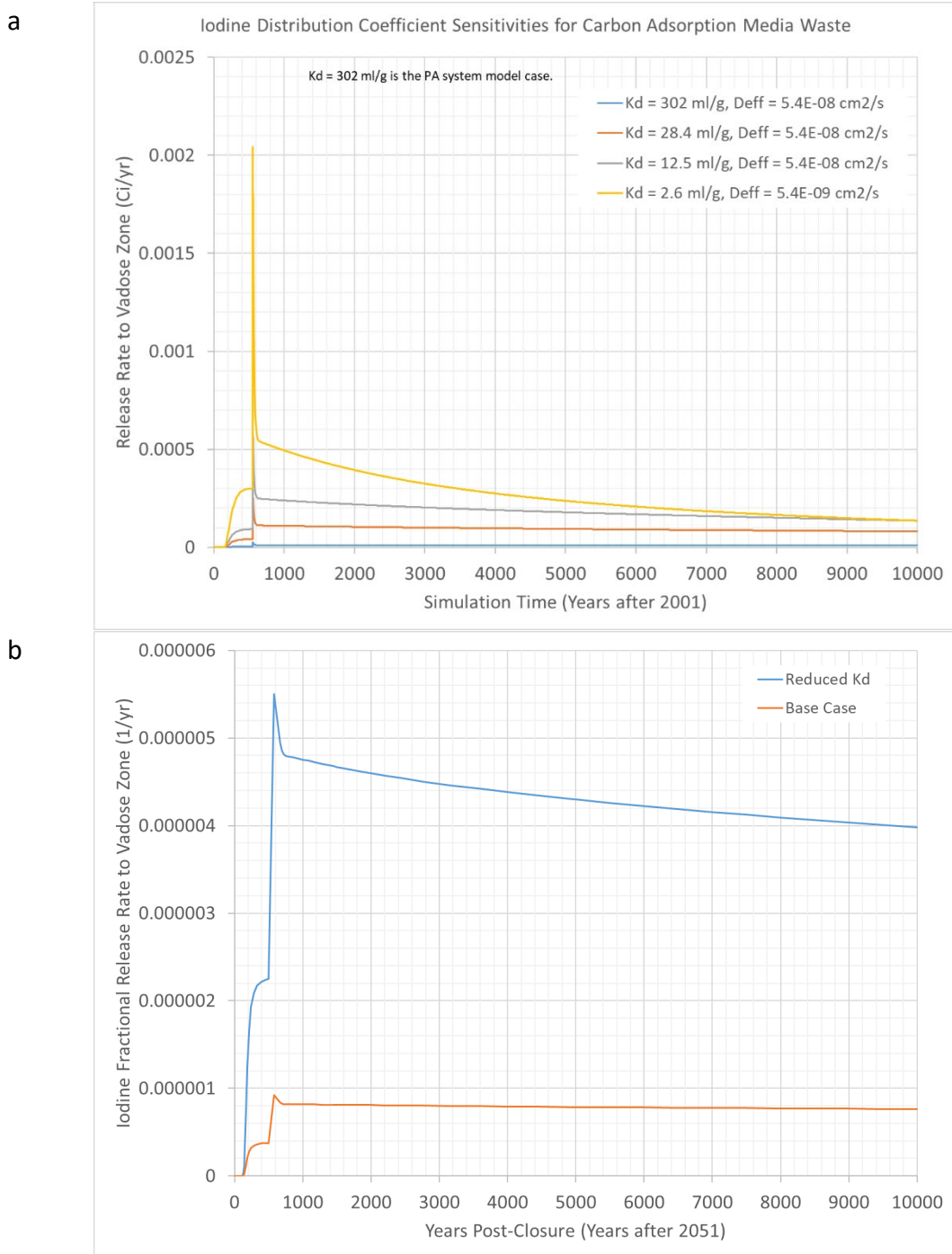
Note: In the Performance Assessment system model, some inventory is provided with a decay date in 2001. This inventory is decayed within the model until the time of assumed Integrated Disposal Facility closure in 2051. Therefore, time zero in the simulations shown in Figure 2-20-1a is 2001. For Figure 2-20-1b, closure was assumed to be 30 years after the start of low-activity waste vitrification in 2021.

Figure 2-20-2. Iodine-129 Cumulative Release to Vadose Zone from Solidified Carbon Adsorption Media: Solid Secondary Waste-Granular Activated Carbon Sensitivity Studies.
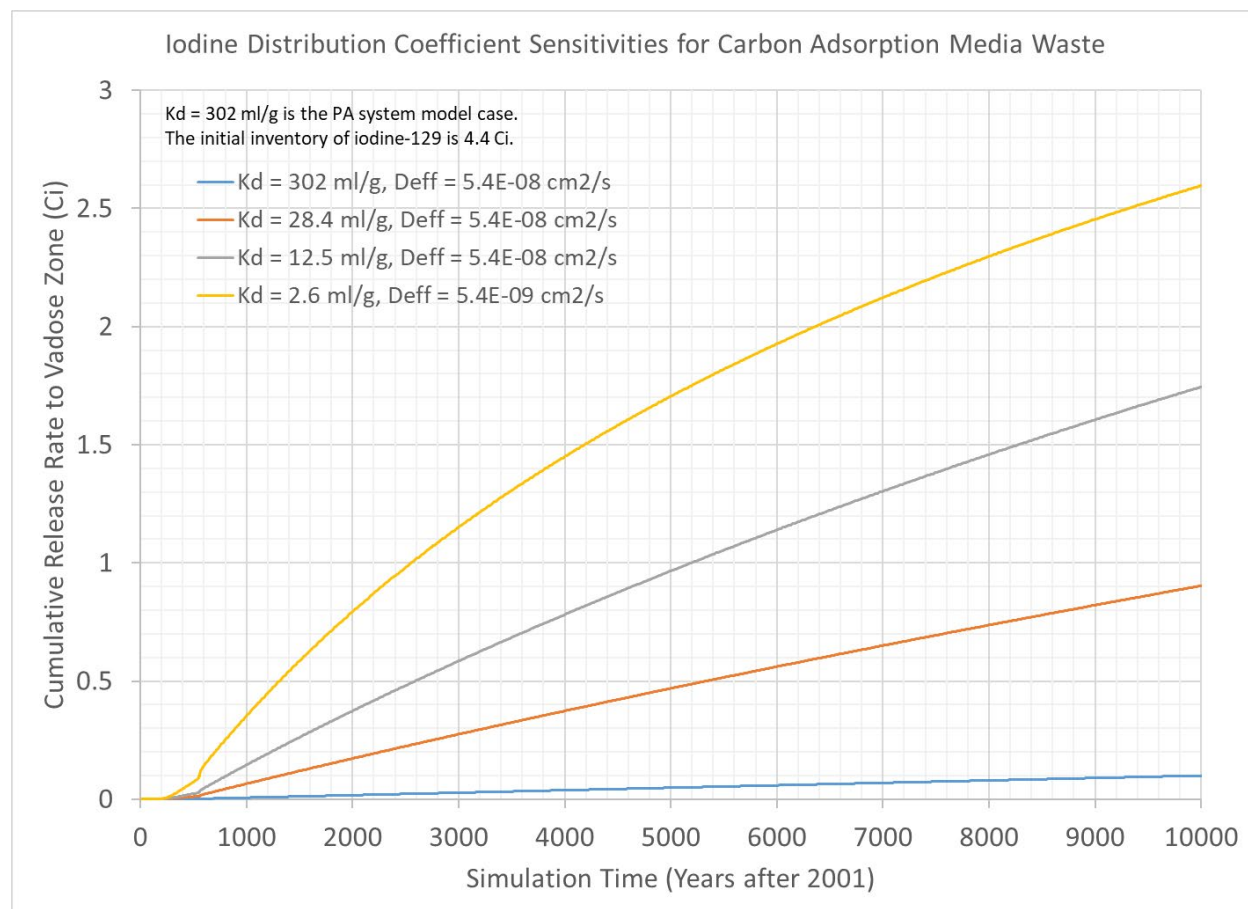

Note: In the Performance Assessment (PA) system model, some inventory is provided with a decay date in 2001. This inventory is decayed within the model until the time of assumed Integrated Disposal Facility closure in 2051. Therefore, time zero in the simulations is 2001.

When the SSW-GAC distribution coefficient for iodine decreased from 302 mL/g to 2.6 mL/g and the effective diffusion coefficient for a non-sorbing species is reduced from 5.4E-08 cm^2/s to 5.4E-09 cm^2/s, the peak dose increased to 10.5 mrem/yr, but occurred more than 6,300 years after closure.

Additional Information

The new data collection effort completed in September 2020 includes new parameter values for SSW other than the distribution coefficients that are the subject of this RAI response, which has been provided as additional information because SSW is outside the scope of the Draft WIR Evaluation. These other measured SSW properties include: porosity, density, and saturated hydraulic conductivity. The new information will be evaluated using the established PA change control process later this year.

Figure 2-20-3. Iodine-129 Groundwater Concentration and Annual Dose Solidified Carbon Adsorption Media: Solid Secondary Waste-Granular Activated Carbon Sensitivity Studies.
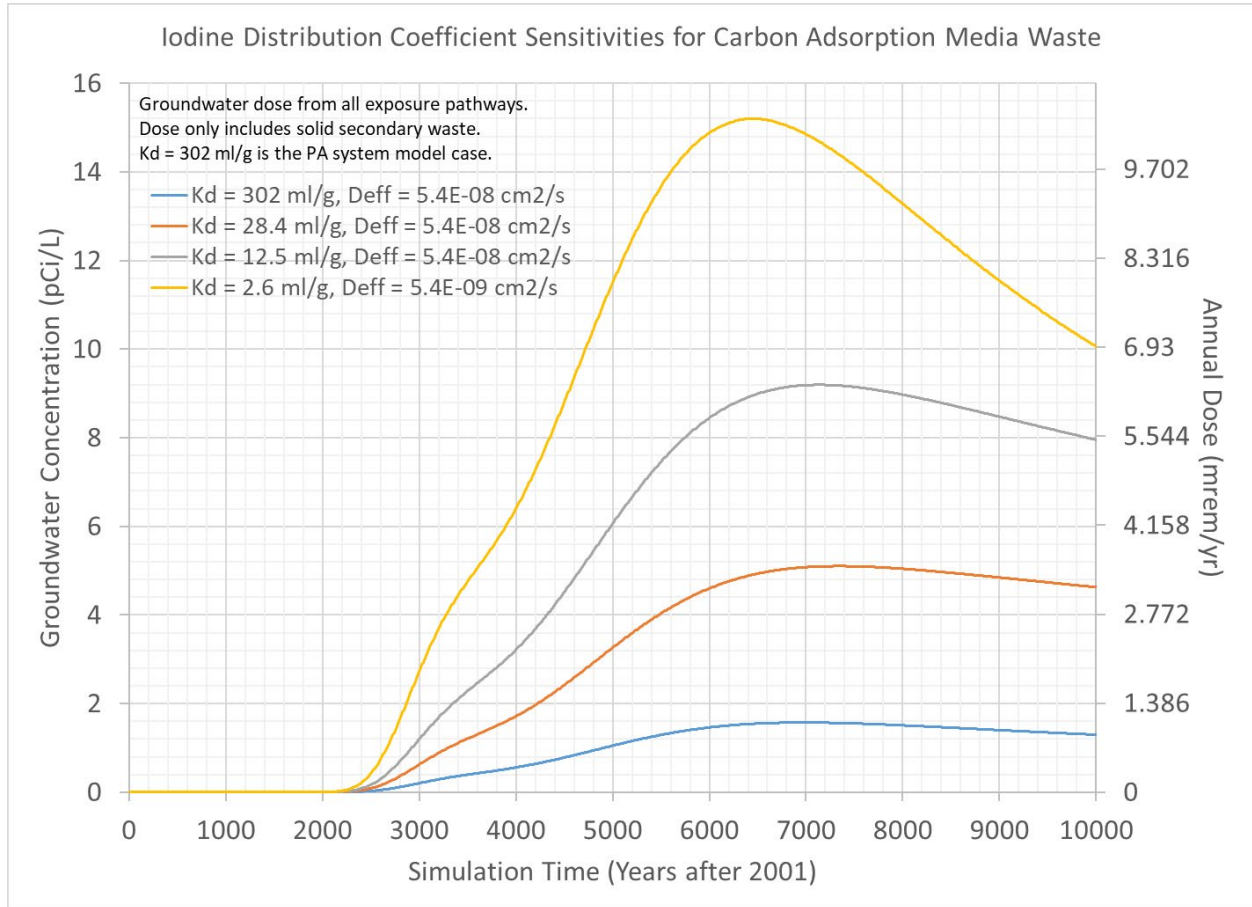
Note: The groundwater concentration can be converted to an annual dose using the conversion factor 0.69 (mrem/yr) / (pCi/L).

Note: The inventory of [129]I simulated in the carbon adsorption bed waste is 4.4 Ci, which is 15% of the [129]I estimated to be in the tank farm tanks. More recent flowsheets indicate 96% of the [129]I estimated to be in the tank farm tanks is vitrified. This means that the amount of [129]I expected to be in this waste stream will be much lower than 4.4 Ci.

The initial results presented in this RAI response will be formally evaluated in a Special Analysis that becomes part of the IDF PA technical basis. However, because the peak dose impact is less than the DOE performance objective and occurs more than 1,000 years after closure, the conclusions of the PA will not change. An evaluation of other parameters reported in PNNL-28545 will also be included in the forthcoming Unreviewed Waste Disposal Question analysis.

References

78 FR 75913, 2013, "Record of Decision: Final Tank Closure and Waste Management Environmental Impact Statement for the Hanford Site, Richland, Washington," *Federal Register*, Vol. 78, pp. 75913–75919 (December 13).

CHPRC-03348, 2019, *Performance Assessment Maintenance Plan for the Integrated Disposal Facility*, Rev. 1, INTERA, Inc./CH2M HILL Plateau Remediation Company, Richland, Washington.

DOE-STD-1196-2011, 2011, *Derived Concentration Technical Standard*, U.S. Department of Energy, Washington, D.C.

PNNL-28545, 2020, *Development and Characterization of Cementitious Waste Forms for Immobilization of Granular Activated Carbon, Silver Mordenite, and HEPA Filter Media Solid Secondary Waste*, Rev. 1, RPT-SWCS-014, Rev. 1.0, Pacific Northwest National Laboratory, Richland, Washington.

RPP-CALC-61030, 2017, *Cementitious Waste Form Release Calculations for the Integrated Disposal Facility Performance Assessment*, Rev. 0, INTERA, Inc. for Washington River Protection Solutions, LLC, Richland, Washington.

RPP-RPT-59958, 2019, *Performance Assessment for the Integrated Disposal Facility, Hanford Site, Washington*, Rev. 1A, Washington River Protection Solutions, LLC, Richland, Washington.

SRNL-STI-2016-00175, 2016, *Solid Secondary Waste Data Package Supporting Hanford Integrated Disposal Facility Performance Assessment*, Rev. 0, Savannah River National Laboratory, Savannah River Nuclear Solutions, Aiken, South Carolina.

RAI 2-21   (Releases from Cementitious Wasteforms)

Comment
More information is needed on the process for determining and evaluating the final cementitious grout specifications for waste streams stabilized with cementitious grout.

Basis
In the PA document, DOE indicated that secondary waste streams generated as the result of WTP operations will be solidified or encapsulated using cementitious materials. The PA document states that the "final specification of the solidification and encapsulation matrices, however, are currently uncertain and will eventually be selected on the bases of several performance factors: adequate mechanical strength for handling, transportation and emplacement; compatibility with other engineered barriers and waste forms in the IDF; [and] limited rates of release of COPCs into the IDF." The PA document further states "[b]ecause the details of the SSW cementitious grout mix specification(s) and final disposal configuration for SSW have not been defined, the SSW data package relied on available information from existing studies of cementitious materials considered representative of mixes that may be used for SSW encapsulation and/or solidification". It is not clear if any further information on the proposed specifications for the cementitious matrices has been developed since the PA document was written.

Additionally, in the LFRG review, one of the key issues identified was that the Waste Acceptance Criteria (WAC) for the current PA has not been developed to protect key assumptions and limits. The corrective action/resolution for this item is that a WAC document will be developed based on the analysis documented in this revision of the PA. It is not clear if this document has been developed yet and/or if any other documents have been prepared that describe the methodology that will be used to ensure that the performance of the selected grout mixtures is consistent with the performance assumed in the PA for key parameters (e.g., parameters related to the chemical and hydraulic performance of the wasteform).

Path Forward
Please provide additional information, if any, that has been developed on the planned specifications for the cementitious grout mixes to be used to stabilize waste generated as part of WTP operations. Provide the WAC for the current PA, if available. Provide a description of the process that will be used to design and the cementitious grout mixes to ensure that the performance of the grout mixtures will be consistent with the performance assumed in the PA for all of the expected compositions of the waste streams.

DOE Response
The Draft WIR Evaluation addresses the WIR criteria for VLAW produced using the DFLAW approach. Other wastes are outside the scope of the Draft WIR Evaluation, including secondary waste and vitrified waste assumed to potentially be produced by supplemental LAW treatment (for which DOE has made no decision to pursue).[111] To bound the analysis, the IDF PA

---

[111] Information concerning SSW generated from supplemental LAW is provided in this RAI response for additional information and completeness only, and is outside the scope of both the Draft WIR Evaluation and DOE decisions concerning supplemental LAW treatment. DOE has not made decisions concerning the potential path

correctly includes all wastes potentially disposed of in the IDF, including the DFLAW-produced VLAW as well as, potentially, additional VLAW,[112] and all SSW which may be disposed at IDF. However, DOE recognizes the importance of the PA, which is a reference for the Draft WIR Evaluation, and is providing the information below in response to the RAI, including a discussion of the full potential treatment mission, SSW, and LSW for additional information. The approach to ensuring that all waste packages are acceptable for disposal at the IDF is described in this RAI response and is the same for all waste streams.

A copy of the WAC was uploaded to the NRC share site on December 8, 2020.

The grout used in the PA to solidify or encapsulate SSW, referred to as Hanford Grout Mix 5, is a commercially-available product from a local concrete supplier. For other waste, this mix was developed in the early 1990s[113] (see Figure 2-21-1). The grout mix and variations of the mix used onsite were studied in the laboratory to develop the necessary parameters for simulating releases in a computer model. The developed parameters are reported in SRNL-STI-2016-00175.

At the time the PA data collection effort was performed to establish the inputs that were used in modeling SSW, waste generation from WTP operations was still five or more years away. At that time, no decisions were being made about the expected grout formulation for SSW. For this reason, the PA assumed that the disposal practice that was being used at the time was appropriate for waste form release modeling and identified this as a key assumption. Since the PA had been completed, no decision has been made to develop and use an alternative to Hanford Grout Mix 5. Therefore, the use of Hanford Grout Mix 5 is still the expected path forward for disposal in the IDF. Any variations to the proposed grout mix, including the addition of sand, would be subject to change management controls to ensure that key assumptions in the PA are protected. For different grout formulations, laboratory measurements for the grout density, porosity, saturation, saturated hydraulic conductivity, and effective diffusion coefficients would be required to perform the evaluations. The response to RAI 2-20 identifies data collection efforts in PNNL-28545 to evaluate these properties for the three SSW streams included in the IDF PA.

---

forward for supplemental LAW treatment, as explained in footnote 7 of the Draft WIR Evaluation and 78 FR 75913, "Record of Decision: Final Tank Closure and Waste Management Environmental Impact Statement for the Hanford Site, Richland, Washington." As explained in Section 1.2 of the Draft WIR Evaluation, the Draft WIR Evaluation does not address or include in its scope supplemental LAW. To bound the IDF PA analysis, the IDF PA assumed that supplemental LAW may potentially be vitrified and disposed of in the IDF, although, as explained above, DOE has made no decisions concerning the potential path forward for supplemental LAW treatment.

[112] See footnote 111.

[113] This mix is the basis for what is currently used by an offsite treatment vendor to prepare containerized waste for disposal on the Hanford Site. Variations of this mix add sand as an aggregate. Certain other waste destined for disposal onsite is sent offsite for treatment prior to disposal; the waste generator has the opportunity to specify a grout mix or rely upon the treatment contractor to select the treatment method and use a grout formulation that ensures the treated product meets both the disposal facilities WAC and also land disposal requirements in the State of Washington.

Figure 2-21-1. Mix Design Worksheet for Hanford Grout Mix 5.

MIX DESIGN WORKSHEET

MIX NO: ___5___   CALCULATED BY: Jerry L. England   DATE: 3-11-93

GEL: __11__   DATE ISSUED: ___.___   LAB NOTEBOOK NO: N/A   PAGE: N/A

CEMENT TYPE: ASH GROVE I-II   W/C: 0.30

	SIZE	SPECIFIC GRAVITY
AGGREGATE		
SAND	FLY ASH	
CENTRALIA		

	DESCRIPTION	ABSOLUTE VOLUME (FT^3)	SSD WEIGHTS (LB)
CEMENT	I-II	3.00	588
WATER	TAP	11.33	706
AIR	N/A		
AGGREGATE	N/A		
SAND	FLY ASH	12.53	1706
WRA			
OTHER			
OTHER			
OTHER	0.5%	0.14	

REMARKS   Add 8 oz. WRA per 100 lbs of cement material. Add 1.5 lbs fiber per

cubic yard (PRO MESH).

MIXING

INSTRUCTIONS   Water cure 73°F ± 3°F for 28 Days.

CHECKED BY: _H. Benny_   DATE: 8/12/93

Section 4.6 in CHPRC-03348 (referred to as the IDF PA Maintenance Plan) identifies activities to continually evaluate national and international research on grout properties and release models to see if useful insights can be learned and used to compare with conceptual and numerical model assumptions and parameter values used in the IDF PA. PNNL-28545 illustrates this data collection effort to protect key assumptions in the IDF PA. Another research opportunity identified ultra-high performance cementitious composites as a possible candidate to encapsulate SSW at Hanford. DOE and WRPS Chief Technology Office awarded two contracts to investigate this material for treatment of SSW prior to disposal at IDF. Initial studies showed promise for this material having very low leaching characteristics (Hasan et al. 2019). Subsequently, in FY 2020 Savanah River National Laboratory began investigating the application of Ultra-High Performance Cementitious Composites to encapsulate waste streams. The final report for this work is expected to be completed mid-FY 2021.

References

78 FR 75913, 2013, "Record of Decision: Final Tank Closure and Waste Management Environmental Impact Statement for the Hanford Site, Richland, Washington," *Federal Register*, Vol. 78, pp. 75913–75919 (December 13).

CHPRC-03348, 2019, *Performance Assessment Maintenance Plan for the Integrated Disposal Facility*, Rev. 1, INTERA, Inc./CH2M HILL Plateau Remediation Company, Richland, Washington.

Hasan, T. W., S. Allena, L. Gilbert, and M. R. Choma, 2019, *Investigating Ultra-High-Performance Cementitious Composite (UHPCC) as a Possible Encapsulation Grout for Hanford Solid Secondary Waste – FY2018 Report*, Washington State University Tri-Cities, Richland, Washington.

PNNL-28545, 2020, *Development and Characterization of Cementitious Waste Forms for Immobilization of Granular Activated Carbon, Silver Mordenite, and HEPA Filter Media Solid Secondary Waste*, Rev. 1, RPT-SWCS-014, Rev. 1.0, Pacific Northwest National Laboratory, Richland, Washington.

SRNL-STI-2016-00175, 2016, *Solid Secondary Waste Data Package Supporting Hanford Integrated Disposal Facility Performance Assessment*, Rev. 0, Savannah River National Laboratory, Savannah River Nuclear Solutions, Aiken, South Carolina.

5.0   ASSESSMENT OF WASTE CONCENTRATION AND CLASSIFICATION

No RAI Responses fall into this categorization.

6.0 REFERENCES

10 CFR 61, "Licensing Requirements for Land Disposal of Radioactive Waste,"
Subpart C—Performance Objectives, *Code of Federal Regulations*, as amended.

10 CFR 61.55, "Waste Classification," *Code of Federal Regulations*, as amended.

Atomic Energy Act of 1954, 42 USC 2011, et seq., as amended.

DOE M 435.1-1, 2011, *Radioactive Waste Management Manual*, Change 2, U.S. Department of Energy, Washington, D.C.

DOE O 435.1, 2011, *Radioactive Waste Management*, Change 2, U.S. Department of Energy, Washington, D.C.

DOE/ORP-2020-01, 2020, *Draft Waste Incidental to Reprocessing Evaluation for Vitrified Low-Activity Waste Disposed Onsite at the Hanford Site, Washington*, U.S. Department of Energy, Office of River Protection, Richland, Washington.

DOE-ORP-PPD-EM-50168, 2020, *Waste Incidental to Reprocessing Determinations*, Rev. 2, U.S. Department of Energy, Office of River Protection, Richland, Washington.

IDF-00002, 2019, *Waste Acceptance Criteria for the Integrated Disposal Facility*, Rev. 0, CH2M HILL Plateau Remediation Company, Richland, Washington.

Interagency Agreement 89304019SEM000003/P0000, 2020, *Consulting Services concerning DOE WIR evaluations on Vitrified Low Activity Waste*, U.S. Department of Energy, Office of River Protection, Richland, Washington/U.S. Nuclear Regulatory Commission, Rockville, Maryland.

MR-50461-00, 2019, *2019 Flowsheet Integration Joint Scenarios*, Rev. 3, Washington River Protection Solutions, LLC, Richland, Washington.

NRC, 2020, "Request for Additional Information on the Draft Waste Incidental to Reprocessing Evaluation for Vitrified Low-Activity Waste Disposed Onsite at the Hanford Site, (Docket Number PROJ0736)" (letter from C. McKenney to M. Gilbertson, U.S. Department of Energy, Office of Environmental Management, November 06), U.S. Nuclear Regulatory Commission, Washington, D.C.

Nuclear Waste Policy Act of 1982, 42 USC 10101, et seq.

NUREG-1854, 2007, *NRC Staff Guidance for Activities Related to U.S. Department of Energy Waste Determinations – Draft Final Report for Interim Use*, U.S. Nuclear Regulatory Commission, Office of Federal and State Materials and Environmental Management Programs, Washington, D.C.

RPP-RPT-57991, 2019, *River Protection Project Integrated Flowsheet*, 24590-WTP-RPT-MGT-14-023, Rev. 3, Washington River Protection Solutions, LLC, Richland, Washington.

RPP-RPT-59958, 2019, *Performance Assessment for the Integrated Disposal Facility, Hanford Site, Washington*, Rev. 1A, Washington River Protection Solutions, LLC, Richland, Washington.

Waste Isolation Pilot Plant Land Withdrawal Act, Public Law 102-579, as amended.

This page intentionally left blank.

ATTACHMENT A

Reserved